REGIONAL AND BASIN SCALE MODELLING OF HYDRO-ECOLOGY: POTENTIAL IMPACTS OF CLIMATE CHANGE FROM A CONSERVATION PERSPECTIVE



JONATHAN N W DAVID

JESUS COLLEGE

UNIVERSITY OF OXFORD

A THESIS SUBMITTED FOR THE DEGREE OF

DOCTOR OF PHILOSOPHY

TRINITY 2018

The work described in this Thesis was carried out in the School of Geography and the Environment, University of Oxford from October 2012 to September 2018, under the supervision of Professor Paul G. Whitehead. All of the work is my own unless otherwise stated and has not been submitted previously for any other degree at this or any other university.

JONATHAN DAVID

SEPTEMBER 2018

ACKNOWLEDGEMENTS

I am very grateful to the many people who have helped and supported me over the course of this research; it would not have been possible without your insight and knowledge.

I would like express my sincere gratitude to my supervisor, Prof. Paul Whitehead, for his extensive insight into hydro-ecology and for guidance throughout this doctorate. Your support and understanding has been very much appreciated. Special thanks must also go to Dr Jill Crossman for her expert opinion on all matters INCA and for her input into the development of the Thames Basin methodology. Furthermore, I gratefully acknowledge NERC for funding to undertake this research.

I would also like to thank Dr Russ Money, Dr Paul Jepson, Prof. Simon Dadson and Dr Rich Grenyer for their insight into the early drafts of this work and for their helpful feedback and suggestions. The thesis is better for it! I would also like to thank all those in the OUCE Water Room for lending a listening ear and to Dr Giamba Bussi, in particular, for his help with the Thames INCA models.

Special thanks must go to my friends from all walks of life for their kind words and support throughout this journey and in particular to our home-group for all of the meals! My family, as ever, have been brilliant. To my Mum, siblings and in-laws, your thoughts and words have been a source of inspiration and helped me press on through the hard times.

I wish to especially thank my Dad, Prof. Bill David, for our long discussions and for stepping up and helping me to push forward. Were it not for you, I fear I would never have finished! For your insights through the latter stages of the DPhil, and particularly for the herculean task of proof-reading, I am truly thankful.

Finally, my greatest thanks go to Frances, my wife. Although I have worked on this thesis our entire married life, it has very much been a shared experience. Your constant love, support and understanding throughout have been invaluable and have spurred me on to the end. I will forever be grateful.

DEDICATION

To Frances, my wonderful wife. For the constant encouragement, love and patience that you have shown me throughout this journey we've shared.

To my beautiful daughter, Tabitha. Your arrival at the end of this journey has brought us so much joy and we eagerly begin this new chapter of our lives together.

It is to you both that I dedicate this thesis.

ABSTRACT

REGIONAL AND BASIN SCALE MODELLING OF HYDRO-ECOLOGY: POTENTIAL IMPACTS OF CLIMATE CHANGE FROM A CONSERVATION PERSPECTIVE

JONATHAN N W DAVID

JESUS COLLEGE, UNIVERSITY OF OXFORD

D. PHIL. THESIS – TRINITY TERM, 2018

The principal objective of this thesis has been to assess the potential impacts of climate change on hydro-ecology at the regional and basin scale, with particular reference to the associated effects these may have on conservation efforts. Different methodologies are required when considering climate-change impact at regional and basin scales. At the regional scale, the vulnerability of European HydroBasins was determined through the application of a 'top-down' methodology to climate assessment and incorporation of novel approaches in determining both catchment and species sensitivity and resilience to climate change. The congruence between existing European protected areas and catchments most vulnerable to climate change was explored, suggesting fewer than 25% of these catchments are currently adequately included. At the basin scale, a 'scenario-neutral' approach was adopted, and the sensitivity of four key hydro-ecological variables to perturbed climatic drivers identified on a catchment-by-catchment basis in the Thames Basin, UK. Linking these responses to Water Framework Directive thresholds of environmental quality and the application of UKCP09 probabilistic scenarios generated quantifiable estimates of potential ecological alteration under climate change. Protocols were developed to further aggregate these into whole basin summary maps, and congruence between existing protected areas and potential ecological alteration under climate change was explored. The results presented in this thesis should be used to a) re-design the European protected area network to better account for projected climate change, and b) explore the most effective management strategies in mitigating climate change within existing protected areas of the Thames Basin and identify high impact Priority River Habitats for conservation and restoration.

TABLE OF CONTENTS

INTRODUCTION AND SUMMARY **1**

CHAPTER 1 LITERATURE REVIEW **4**

1.1 THE EVIDENCE FOR ANTHROPOGENIC CLIMATE CHANGE 4

1.1.1 Trajectories of climate change *6*

1.2 THE IMPORTANCE OF FRESHWATER SYSTEMS 7

1.3 CLIMATE CHANGE AND ITS IMPACT ON FRESHWATER ECOSYSTEMS 10

1.3.1 Impacts on freshwater ecosystems *11*

1.4 CONSERVING FRESHWATER ECOSYSTEMS – THE STATUS QUO 12

1.4.1 Integrated River Basin Management (IRBM) *13*

1.4.2 Systematic Conservation Planning *14*

1.4.3 Environmental Flow Assessments *16*

1.5 MODELLING CLIMATE CHANGE FOR WATER MANAGEMENT AND ADAPTATION 18

1.6 VULNERABILITY – A FRAMEWORK FOR CLIMATE CHANGE ASSESSMENT 19

1.7 THESIS AIMS AND OBJECTIVES 22

CHAPTER 2 REGIONAL ASSESSMENT: VULNERABILITY OF EUROPEAN CATCHMENTS TO CLIMATE CHANGE **24**

2.1 INTRODUCTION AND OBJECTIVES 24

2.2 METHODOLOGY 25

2.2.1 Species data *25*

2.2.2 Climate and hydrological data *26*

2.2.3 Protected areas *28*

2.2.4 Exposure assessment *30*

2.2.5 Sensitivity assessment *32*

2.2.6 Resilience assessment *36*

2.2.7 Climate change vulnerability assessment *38*

2.3 RESULTS 40

2.3.1 Exposure *40*

2.3.2 Sensitivity *40*

2.3.3 Resilience *41*

2.3.4 Climate change vulnerability *43*

2.4 DISCUSSION 50

CHAPTER 3 THAMES BASIN: MODEL CALIBRATION 54

3.1 INTRODUCTION AND OBJECTIVES 54

3.2 INTRODUCTION TO THE INTEGRATED CATCHMENT (INCA) MODELS 58

3.3 CALIBRATION OF PERSIST MODEL FOR USE IN INCA 62

3.4 DELINEATION OF SUB-CATCHMENTS AND DEVELOPMENT OF RIVER NETWORK 64

3.5 CALIBRATION OF INCA MODELS FOR THE THAMES CATCHMENT 65

3.6 SUB-CATCHMENT CHARACTERISTICS 67

3.6.1 Velocity-discharge parameters *67*

3.6.2 Base Flow Index *71*

3.6.3 Land use data and fertiliser loadings *72*

3.6.4 Atmospheric deposition *73*

3.6.5 Effluent and abstraction data *74*

3.6.6 Observed discharge and chemistry data *76*

3.7 CALIBRATION RESULTS 81

CHAPTER 4 THAMES BASIN: METHODOLOGY 85

4.1 INTRODUCTION 85

4.2 SCENARIO-NEUTRAL CLIMATE CHANGE METHODOLOGY 86

4.3 SELECTION OF STANDARDS TO ASSESS CHANGES IN KEY HYDROLOGICAL AND NUTRIENT VARIABLES UNDER CLIMATE CHANGE 92

4.4 BIOLOGICAL STANDARDS 96

4.4.1 Introduction *96*

4.4.2 Data *97*

4.4.3 Methodology *99*

4.5 PHYSICAL STANDARDS 117

4.5.1 Flow Regime as determined by application of the Dundee Hydrological Regime Alteration Method (DHRAM) *117*

4.5.2 Temperature *121*

4.6 CHEMICAL STANDARDS 124

4.6.1 Typology for nutrient conditions for rivers *125*

4.6.2 Ammonia standards *126*

4.6.3 Phosphorus standards *127*

4.7 SUMMARY MAPS FOR USE IN CONSERVATION EFFORTS: QUANTIFICATION OF ECOLOGICAL RISK WITH REFERENCE TO CLIMATE CHANGE 129

CHAPTER 5 THAMES BASIN: RESULTS 139

5.1 OUTLINE OF RESULTS AND SELECTION OF EXEMPLAR CATCHMENTS 139

5.2 EXEMPLAR CATCHMENTS DETAILED RESULTS 146

5.2.1 Soluble Reactive Phosphorus (SRP) *146*

5.2.2 Ammonia *158*

5.2.3 Water Temperature *168*

5.2.4 Dundee Hydrological Regime Alteration Method (DHRAM) *177*

5.3 MACROINVERTEBRATE MODEL RESULTS 189

5.4 MAPS OF THE THAMES BASIN FOR HYDRO-ECOLOGICAL INDICATORS 197

5.4.1 Introduction and description of basin maps *197*

5.4.2 Soluble Reactive Phosphorus *199*

5.4.3 Ammonia *206*

5.4.4 Water Temperature *213*

5.4.5 DHRAM *221*

5.5 QUANTIFYING CLIMATE RISK: THAMES BASIN SUMMARY MAPS 228

CHAPTER 6 THAMES BASIN: DISCUSSION 232

6.1 CLIMATE CHANGE AND SOLUBLE REACTIVE PHOSPHORUS 232

6.2 CLIMATE CHANGE AND AMMONIA 236

6.3 CLIMATE CHANGE AND WATER TEMPERATURE 238

6.4 CLIMATE CHANGE AND CHANGES TO THE FLOW REGIME (DHRAM) 240

6.5 Climate Change and Macroinvertebrates 243

6.6 Resilience to climate change at the basin-scale 245

6.7 The potential impacts of climate change on freshwater conservation in the Thames Basin 246

6.8 Uncertainties in the modelling process 253

6.9 Limitations of methodology 256

CHAPTER 7 CONCLUDING REMARKS AND SUGGESTIONS FOR FURTHER WORK 260

REFERENCES 266

APPENDIX I 285

APPENDIX II 299

APPENDIX III 327

INTRODUCTION AND SUMMARY

Climate change is predicted to become a major and increasing threat to biodiversity in the 21st Century, with many species already altering their ranges and phenological responses to the relatively small perturbations that have occurred over the past few decades (Parmesan, 2006, Comte et al., 2013). Furthermore, existing levels of greenhouse gas emissions will commit Earth to substantial climatic alterations in the coming decades, and therefore the potential for loss of biodiversity, termination of evolutionary potential and disruption of ecological services and processes are highly likely to occur (Solomon et al., 2009).

This is particularly true for freshwater ecosystems, since changes in precipitation, temperature and evaporation directly determine the distribution of river flows and groundwater recharge over space and time (Kundzewicz et al., 2008). Thus, alterations in the magnitude, frequency, duration, timing and variability of thermal and hydrological attributes to a freshwater ecosystem can have dramatic effects on its associated biodiversity, productivity and function (Bates et al., 2008a, Heino et al., 2009, Woodward et al., 2010, Poff and Zimmerman, 2010). Moreover, current evidence suggests that freshwater biodiversity is in significant decline globally (Jenkins, 2003, Revenga and Kura, 2003), predominantly due to anthropogenic disturbance and overutilisation of freshwater resources, further compounded by the high intrinsic vulnerability of freshwater ecosystems and biodiversity to such threats (Dudgeon et al., 2006). Therefore, the cumulative effect of these synergistic factors and the non-substitutional nature of freshwater for human development suggest that freshwater ecosystems and the biodiversity they support are, and will remain, among the most endangered globally (Sala et al., 2000, Palmer et al., 2008).

Given this double jeopardy, conservation and management actions are urgently required if this downward trend of functionally intact freshwater ecosystems is to be reversed and accurate accounting systems for freshwater protected areas are to be established. However, to date, few protected areas outside the Ramsar network have been identified and strategically designed specifically for freshwaters (Abell et al., 2007). Consequently, these ecosystems are often only

protected through their incidental incorporation into terrestrial protected areas (Saunders et al., 2002). Significant advances have been made in defining a freshwater-specific protected area vocabulary (Abell et al., 2007), and the development of complementarity-based optimisation algorithms to account for the complex inter-connected nature of freshwaters for use within systematic conservation planning (Linke et al., 2008, Amis et al., 2009, Linke et al., 2011, Nel et al., 2011a). The successful application of Systematic Conservation Planning (SCP) approaches (a well-established scientific approach for identifying priority areas for conserving biodiversity (Margules and Pressey, 2000)) to aquatic settings marks a milestone in the development of protected areas designed specifically for freshwaters (Kingsford, 2011).

However, despite these major advances, very few studies have explicitly incorporated the potential impacts of climate change on conservation planning in freshwater systems (Nel et al., 2011b, Turak et al., 2011b, Laizé et al., 2014). Consideration of these impacts would signify a significant step forward in conservation planning for freshwaters, as it would be possible to identify more resilient protected areas by accounting for temporal changes in climate and associated spatial shifts of species (Walther et al., 2002). Additionally, mitigation and restoration strategies can be identified, and their efficacy tested using scenario modelling to prioritise management actions now and further refine the protected area network.

Key to the development of these conservation plans and restoration strategies are the assessment of the potential effects of climate change on freshwater biodiversity. However, to date, these have been restricted to the application of the niche-based species distributions models (for example Comte et al., 2013, Domisch et al., 2013, Markovic et al., 2014b). Such models relate current conditions to existing species distributions and project these using climate change models, thus only considering exposure to climate change. However, as outlined by Dawson et al. (2011), one must consider all aspects of vulnerability to assess the biodiversity consequences of climate change: exposure, sensitivity and adaptive capacity (or resilience). These vulnerability assessments have now become the framework of choice when assessing impacts of climate change and provide

opportunities for integration across multiple disciplines (Smit and Wandel, 2006, IPCC, 2007). In an ecological context, this vulnerability framework has predominantly been applied to terrestrial and marine species and ecosystems (Chin et al., 2010, Foden et al., 2013). Conversely, comprehensive vulnerability assessments to climate change in a freshwater setting are still lacking. Utilising such vulnerability assessments should provide an innovative conceptual framework to complement existing conservation planning methodologies for freshwaters.

This thesis explores novel approaches for assessing the vulnerability of freshwater systems to climate change, with the aim of demonstrating proof-of-concept methodologies at both the regional and basin scales. Specifically, this research adopts a holistic approach to identifying priority areas for incorporation into conservation and management plans based on the 'vulnerability principle' and its three core components; sensitivity, resilience and exposure (Dawson et al., 2011, Brown et al., 2012). The regional scale assessment focusses on utilising freshwater species ranges and large-scale datasets for over 18,000 European sub-catchments. The basin scale assessment focusses on high resolution datasets and locally downscaled climate data for 292 sub-catchments within the Thames region (situated in SE England). This research goes beyond the existing literature, by demonstrably assessing the impact of climate change through the application of a vulnerability framework and generating outputs applicable to future freshwater conservation and management plans at multiple spatial scales.

Chapter 1 LITERATURE REVIEW

1.1 THE EVIDENCE FOR ANTHROPOGENIC CLIMATE CHANGE

Anthropogenic climate change and our collective failure to properly address its challenges together pose the greatest threat not only to the current distribution and fitness of ecosystems and their associated biodiversity at the global scale but even to the persistence of human society. Earth's climate system has perpetually gone through periods of warming and cooling, with at least 5 major glaciation periods over Earth's history, due primarily to changes in solar energy due to subtle variations in the Earth's orbit (Eyles and Young, 1994). The current climate is on average 10°C cooler than the beginning of the tertiary period (50-60 million years ago), yet 5°C warmer than the Pleistocene period (12,000 - 2 million years ago) (McManus et al., 2004). However, physical evidence (ice cores, oceanic sediments and layers of sedimentary rocks) demonstrates that the climate system also responds to variations in atmospheric greenhouse gas (GHG) concentrations, such as carbon dioxide, CO_2; methane, CH_4; nitrous oxide, N_2O (Petit et al., 1999). These gases induce climatic warming by affecting the transfer of infrared energy through the atmosphere, with higher concentrations of atmospheric GHGs leading to increased temperatures. Over the period from 1880 to 2012, increased anthropogenic GHG emissions, driven largely by economic and population growth, have increased atmospheric CO_2 concentrations from 275ppm (parts per million) to 408ppm (IPCC, 2014b). Concurrently, globally averaged combined land and ocean surface temperature data, as calculated by a linear trend, show an average warming of 0.85°C (IPCC, 2014b). This rate of change in both atmospheric CO_2 concentrations and globally averaged temperatures is unprecedented in at least the last 800,000 years (Gillett and Thompson, 2003). The effects of these GHG emissions, along with other anthropogenic drivers, have been observed throughout the climate system and are extremely likely to have been the dominant cause of global warming since the mid-20th-century. Furthermore, total anthropogenic emissions have continued to increase from 1970 to present day; most of the warming has occurred over this same period with five of the warmest years on record taking place since 2010 (IPCC, 2014a). Significantly, at the time of writing, 2016 was the warmest

year on record to date, with eight of the 12 months (from January through September, with the exception of June) the warmest on record for those respective months (GISTEMP, 2018). This strongly indicates that the rate of anthropogenic climate change is continuing to increase despite many countries introducing mitigation strategies. These effects are likely to become more severe with time (IPCC, 2014a).

Increases in atmospheric GHG emissions have also impacted other components of the earth-climate system. Of the energy accumulated due to increasing temperatures between 1971 and 2010, only about 1% has been stored in the atmosphere, with over 90% transferred to the world's oceans manifesting in increased water temperatures (IPCC, 2014b). Globally, ocean warming is largest near the surface, with the upper 75 m warmed by 0.44°C since 1971. Furthermore, since the beginning of the industrial era, oceanic uptake of CO_2 has resulted in a 26% increase in acidity (a decrease in pH of 0.1) of ocean surface water (Feely et al., 2009). This rapid increase in both temperature and acidification has seen a catastrophic decline in the extent and health of coral reefs, with a mass bleaching event in 2016-2017 causing a 50% die-off in the Great Barrier Reef, the world's largest reef (Heron et al., 2017). Increases in surface water temperatures have also shown a 30-year trend towards an increase in the frequency and severity of major ocean circulation systems (such as El Nino), leading to increasingly severe flooding events (Meehl et al., 2000) and more frequent category 4-5 hurricanes (Elsner et al., 2008). The global water cycle has also been impacted, with an increase in precipitation since 1901 when averaged over the mid-latitude land areas of the Northern Hemisphere. Extreme precipitation events have been increasing in intensity, with both an increase in the frequency and severity of major flood events (IPCC, 2007). Over the period 1992 to 2011, the Greenland and Antarctic ice sheets have been losing mass and glaciers have continued to shrink across the planet (IPCC, 2014b). In response to increased surface temperature and changing snow cover, Northern Hemisphere spring snow cover has continued to decrease in extent and permafrost temperatures have increased in most regions since the early 1980s (Brown, 2000). Over the period of 1979 to 2012, the annual Arctic sea-ice extent has decreased in every season and in every successive decade since 1979, at a rate of 3.5-4.1% per decade (Stroeve et al., 2012). Finally, due to the thermal

expansion of water and increased ice-sheet and glacial melt, global mean sea level rose by 0.19m over the period 1901 to 2010 (Nicholls and Cazenave, 2010). The rate of sea level rise since the mid-19th century has been larger than the mean rate during the previous three millennia (Gillett et al., 2013). This increase in sea-level has led to more severe storm surges and increased ingress of saline water into coastal freshwaters (Michener et al., 1997).

1.1.1 TRAJECTORIES OF CLIMATE CHANGE

The effects of climate change will manifest themselves in three different trajectories: a gradual change in mean climate, changes in variability around a mean value and 'state-level' or 'modal' changes in climate (Bates et al., 2008b). Most climate models have a bias toward depicting climate change as a gradual shift in mean variables. However, whilst variables such as air temperature, mean precipitation, or even mean monthly extreme precipitation may shift in a relatively even way in some regions (IPCC, 2007), a gradual adjustment is likely to be the least characteristic way in which these changes will manifest in freshwater ecosystems (Kernan et al., 2010).

In most regions the frequency and degree of extreme weather events are shifting (Katz, 2010). From a freshwater perspective this results in both more droughts and more floods, often with longer duration and greater severity (or intensity) (Bates et al., 2008b). For ecosystems, species, and people, this type of climate change is probably far more significant than changes in mean climate, even when both types of changes are occurring simultaneously (Aldous et al., 2011). However, no climate model is currently capable of predicting changes in climate variability to a sufficient degree of confidence (Pielke and Wilby, 2012).

Finally, 'state-level' or 'modal' change is the shift of climate from a period of relative climatic stability, to a period of rapid shifts in many climate variables (passing a climate tipping point or "threshold"), followed by another period of relative stability (IPCC, 2007). The paleo-climatic record shows many instances of these stability-transition-stability climate shifts and current examples of this type of modal change include the rapid disappearance of glaciers in Glacier National Park (glacier to snowpack to tundra to grasslands and forest) (Hall and Fagre, 2003). Other examples include the

sudden initiation, cessation, or spatial shifting of ocean currents (Hoegh-Guldberg and Bruno, 2010), and major shifts in cyclical timing of global climate engines such as El Niño or the North Atlantic oscillation (Gergis and Fowler, 2009). Modal change is extremely difficult to model and predict, though it is this trajectory that is likely to form the context in which serious ecological and economic shocks are triggered (Alley et al., 2003).

In conclusion, climate change is predicted to become a major threat to biodiversity in the 21st century, with many ecosystems already experiencing alterations in key functional processes and changes to species community structure and dynamics in response to perturbations that have occurred over the past few decades (Parmesan, 2006, Comte et al., 2013). Furthermore, existing levels of greenhouse gas emissions will commit Earth to substantial climatic alterations in the coming decades, and therefore the potential for loss of biodiversity, termination of evolutionary potential and disruption of ecological services and processes are all highly likely to occur (Solomon et al., 2009).

1.2 THE IMPORTANCE OF FRESHWATER SYSTEMS

Freshwater biodiversity is a highly valuable natural resource, providing economic, cultural, aesthetic, scientific and educational goods and services (Dudgeon et al., 2006). Despite comprising only 0.01% of the global water balance, and covering a mere 0.8% of the Earth's surface, freshwater ecosystems support disproportionately high levels of biodiversity and endemism (Groombridge and Jenkins, 2002). Approximately 6% of all described species, including one third of all vertebrate species and some 40% of global fish diversity, are confined to freshwaters (Hawkesworth and Kalin-Arroyo, 1995, Lundberg et al., 2000, Balian et al., 2008). These are likely to be conservative figures, as there is a paucity of knowledge regarding freshwater species diversity, particularly in tropical latitudes that support the majority of the world's species and specifically amongst invertebrates and microbes (Stiassny, 2002, Revenga and Kura, 2003). However, current evidence suggests that freshwater biodiversity is in significant decline globally (Jenkins, 2003, Revenga and Kura, 2003, Dudgeon et al., 2006, Heino et al., 2009). For North America alone, the projected extinction risk for freshwater fauna

is five times that of terrestrial fauna, a rate comparable to species loss in tropical rainforest (Ricciardi and Rasmussen, 1999). Furthermore, due to the scarcity of data and assessments of freshwater biodiversity status and trends, many species may become extinct before they are taxonomically classified (Revenga et al., 2005).

The cause of this alarming decline is predominantly due to the anthropogenic disturbance and overutilization of freshwater resources, compounded by the high intrinsic vulnerability of freshwater ecosystems and biodiversity to such threats (Dudgeon et al., 2006). These threats can be grouped into five interacting categories: overexploitation of freshwater fisheries, degradation and destruction of freshwater ecosystems, water pollution, flow alterations, and invasion and deliberate introduction of exotic species.

Overexploitation of freshwater fisheries has thus far received little attention yet poses a major threat to specific freshwater species and increasingly whole ecosystems. In 2002 alone, approximately 8.7 million tonnes of wild fish were caught, a fourfold increase since the 1950s (Food and Agriculture Organization of the United, 2002). This systematic overfishing of freshwaters is likely to continue to rise because of the importance of inland fisheries as an income and food source for millions of communities worldwide (Allan et al., 2005). Whilst overexploitation primarily affects vertebrates, the other four threat categories have consequences for freshwater biodiversity from microbes to megafauna (Dudgeon et al., 2006).

The degradation and destruction of freshwater ecosystems can occur through direct impacts, such as the extraction of river sand for construction purposes, and through indirect impacts in the drainage basin such as the clearance of forests near rivers (Malmqvist and Rundle, 2002). This clearance results in increased runoff and sediment loads, which in turn can lead to major habitat alterations, such as shoreline erosion and the clogging of river beds (Datry et al., 2015).

Water pollution is a threat of pandemic proportions (Ricciardi and Rasmussen, 1999). Though many countries have made significant progress in reducing domestic and industrial pollution point sources, threats from agricultural runoff, nutrient enrichment and other chemicals continue to rise globally

(Smith et al., 2006). Additionally, the position of rivers and lakes in the landscape (invariably in valley bottoms) causes them to become sinks to wastes, pollutants and sediment runoff. However, unlike seas and oceans, rivers and lakes typically lack sufficient volumes of water to dilute these contaminants and mitigate other impacts (Vercruysse et al., 2017).

Flow alterations are ubiquitous in running waters, but tend to be most severe in locations of highly variable flow regimes due to the need for flood protection or water storage for human populations (Nilsson et al., 2005). A study by Nilsson and Berggren (2000) suggests that existing dams retain approximately 10,000 km^3 of water, or five times the volume of all the worlds rivers, whilst water retention by dams in the Northern Hemisphere alone is sufficient to cause measurable geodynamic changes in the Earth's rotation and gravitational field (Chao, 1995). Flow modifications are so severe in places that some of the world's largest rivers, including the Yellow in China and the Colorado in the USA, regularly fail to reach the sea (Pearce, 2006). These extreme flow modifications are likely to be exacerbated further by climate change due to increased flooding and droughts and the respective water-engineering responses (White et al., 2006, Stakhiv, 2011). Since freshwater systems are defined largely by their hydrology (the supply and movement of water), then the aforementioned alterations of flow regimes have severe negative impacts on freshwater species and ecosystems that will continue to worsen if current trends persist (Xenopoulos and Lodge, 2006).

Invasion and deliberate introduction of exotic species to freshwater ecosystems poses a highly significant threat to native biodiversity (Saunders et al., 2002). Though the effects of these introductions vary, their establishment has frequently been to the detriment of native species. This is the case for widespread areas of both Britain and the western United States (Olden et al., 2010). Exotic terrestrial species may also affect freshwater ecosystems, as demonstrated by the introduction of *Tamarix* species altering the water regime in riparian soils and thus affecting stream flows in Australia and North America (Tickner et al., 2001).

However, the single most decisive factor driving the threats to freshwater ecosystems is the necessity of fresh water for human populations. This need is so strong that, in many parts of the

world, fresh water is subject to severe competition between multiple human stakeholders, occasionally to the point of armed conflict (Poff et al., 2003a). As such, the allocation of water to maintain freshwater biodiversity is typically of low priority globally.

These well-documented, synergistic stressors are so ubiquitous that 65% of freshwater habitats globally are impacted to a moderate to high degree (Vorosmarty et al., 2010). Indeed, such anthropogenic alteration of rivers, lakes and wetlands has persisted throughout human history, to the point that it is likely that few water bodies now exist that have not been irreversibly altered from their original state by human activities (Lévêque and Balian, 2005). In addition, anthropogenic climate change threatens to exacerbate the effects of these threats (particularly in highly impacted basins) to the future detriment of freshwater biodiversity and human water security, prompting costly and extensive interventions (Palmer et al., 2008). The cumulative effect of these interacting factors and the non-substitutional nature of freshwater for human development implies that freshwater ecosystems and the biodiversity they support are, and will remain, among the most endangered globally (Sala et al., 2000).

1.3 CLIMATE CHANGE AND ITS IMPACT ON FRESHWATER ECOSYSTEMS

It is widely accepted that long-term observations and model projections indicate that freshwater ecosystems are both highly vulnerable and directly affected by anthropogenic climate change (Sala et al., 2000, Scholze et al., 2006, Bates et al., 2008b, Heino et al., 2009, Moss et al., 2009, Knouft and Ficklin, 2017, Markovic et al., 2017, Koutroulis et al., 2018). Changes in precipitation, temperature and evaporation determine the distribution of river flows and groundwater recharge over space and time (Kundzewicz et al., 2008). Although there are significant regional differences, both global annual temperatures and precipitation are predicted to increase during the 21st century (IPCC, 2007). A review of papers summarising the effects of climate change on the thermal and hydrological regimes of freshwater ecosystems suggests that a range of changes are anticipated. These include, amongst others, more extreme floods and droughts, increased sediment and nutrient transport, higher water temperatures, longer ice-free seasons, increased water body stratification, earlier snowmelt, lower

dissolved oxygen and increased salinity (Wilby et al., 2010). These are complemented by biotic effects, including changes in species physiology, dispersal, phenology, predation and, ultimately, ecosystem structure, productivity and nutrient cycling (Walther et al., 2002).

1.3.1 IMPACTS ON FRESHWATER ECOSYSTEMS

Responses of freshwater ecosystems to climate change can broadly be described in terms of three different but inter-related components: water quantity (volume), water timing and water quality. A change in one of these components often leads to shifts in the others (Poff and Zimmerman, 2010).

Water quantity refers to the water volume of a given ecosystem, which is controlled through the balance of inflows (precipitation, runoff, groundwater seepage) and outflows (water abstractions, evapotranspiration, natural outflows). The most striking changes in water quantity may well occur through precipitation extremes leading to floods and droughts (Arthington et al., 2006). However, lake and wetland levels may also change radically due to slight changes in the balance between precipitation and evaporation rates. The occurrence of extreme precipitation events is expected to continue to increase globally, as is the severity of extreme events themselves (Bates et al., 2008b).

Water timing, often described as the 'flow regime', is the variation in water quantity over some period (usually a single year). The flow regime is considered as the primary determinant (or "master variable") for sustaining biodiversity and ecological integrity in lotic (riverine) systems (Poff et al., 1997). It acts as a 'clock' for species and ecosystems, and thus changes in the timing of any given event (e.g. date of maximum flow) can have profound ecological responses. The range and variation of flows over recent historical time, referred to as the natural flow regime (Richter et al., 2006), sets a template for contemporary ecological processes, evolutionary adaptations and native biodiversity maintenance (Arthington et al., 2006). Consequently, the behaviour, physiology, and developmental processes of many terrestrial and almost all aquatic organisms are adapted to particular water timing regimes, such as fish spawning during spring floods or accelerated metamorphosis from tadpole to adult frog in a rapidly drying wetland (Poff and Zimmerman, 2010). Shifts in flow patterns due to climate change may result in detrimental mismatches between behaviour and the aquatic habitat.

Frameworks exist that seek to form quantitative relationships between ecological responses and types of flow alteration, and can be very useful in determining ecosystem changes due to future climate change (Poff et al., 2010). Indeed, whilst many regions globally are seeing increases in climate variability, the seasonality of precipitation and evapotranspiration regimes is changing universally; even in the absence of changes in the mean annual precipitation (IPCC, 2007). Since changes in water timing result in changes in water quantity and quality, shifts in the timing of freshwater flows have become a leading driver in global declines in freshwater biodiversity, as a result of a range of anthropogenic impacts. Therefore, as the pace of climate change quickens, this pressure is also likely to accelerate.

Water quality refers to how appropriate the water of an ecosystem is for some 'use', whether biological or economic. Many fish species, for instance, have narrow habitat quality preferences for dissolved oxygen, water temperature, dissolved sediment, and pH (Xenopoulos et al., 2005). Water quality is typically altered by changes in water timing or quantity. Changes in intense precipitation events impact the rate at which materials are flushed to rivers and groundwater and changes in flow volumes affect dilution of loads. In addition, shifts in water temperature alter the operational rate of key chemical processes in water (e.g. dissolved oxygen) (Kundzewicz et al., 2008).

The consequences of climate change are predicted to vary substantially between different freshwater ecosystems. For example, due to the close relationship between air temperature and water temperature, smaller streams are likely to be affected more strongly than larger streams (Baattrup-Pedersen et al., 2018). Additionally, smaller streams are more vulnerable to low-flow and flood episodes than larger streams (Schindler, 1997). Furthermore, smaller ponds are more susceptible to thermal stress than larger lakes, with cold-adapted species lacking cold-water refugia in shallower ponds (Heino et al., 2009).

1.4 CONSERVING FRESHWATER ECOSYSTEMS – THE STATUS QUO

Governments across the globe have made commitments to establish protected area systems that contain viable representations of every terrestrial, freshwater and marine ecosystem (IUCN 2003).

This goal has been realised extensively throughout terrestrial systems and to a lesser, but increasing extent over the past two decades, in the marine realm (Lubchenco et al., 2003, Phillips, 2007). However, to date, few protected areas outside of the Ramsar (or Wetlands of International Importance) network have been identified and strategically designed specifically for freshwaters. Furthermore, several studies have highlighted significant gaps in the representation and ecological viability and integrity of protected area systems for freshwater ecosystems (Yip et al., 2004, Abellán et al., 2007, Nel et al., 2007, Carrizo et al., 2017), with these ecosystems often only protected through their incidental incorporation into terrestrial protected areas (Saunders et al., 2002). The predominant emphasis within these protected areas has been the management of terrestrial biodiversity, and this has often resulted in a negative impact on included freshwater ecosystems that have been deliberately altered through the construction of dams, bridges and tourist lodges (Nel et al., 2009a). Consequently, the protection afforded to populations of freshwater species within such protected areas is often severely compromised (Driver et al., 2005, Amis et al., 2009). This occurs for a number of reasons, which include the extension of species ranges outside the protected area or the presence of invasive species within them (Keith, 2000, Impson et al., 2002, Abellán et al., 2007). This is particularly pertinent to many freshwater fish, whose medium to long-distance movements between habitats make place-based strategies for conservation, such as protected areas, particularly challenging (Fausch et al., 2002). Additionally, rivers are often viewed as delineators of protected area boundaries, rather than unique habitats meriting protection. In conclusion, effective conservation and management action is urgently required if the downward trend of functionally intact freshwater ecosystems is to be reversed and accurate accounting systems for freshwater protected areas are to be established.

1.4.1 Integrated River Basin Management (IRBM)

Full protection of a freshwater system requires conserving both its entire upstream catchment as well as the downstream habitats of focal species (Saunders et al., 2002). However, several major challenges face the use of such approaches. Firstly, as a result of human pressure, very few large

catchments remain intact worldwide with the lower reaches of rivers, deltas and estuaries being particularly disturbed (Abell et al., 2007). Therefore, opportunities for managing entire catchments in their pristine state are now practically impossible. Secondly, balancing the interests of multiple stakeholders and aquatic species in a catchment area of finite resources poses significant ethical, social and economic problems. Integrated River Basement Management (IRBM) schemes hold potential for conserving and restoring freshwater ecosystems, whilst also maximising the economic and social benefits derived from water resources in an equitable manner (Jones et al., 2003). IRBM schemes offer a robust platform for addressing the goals of freshwater conservation and climate change adaptation (Nel et al., 2011b). Within this framework, protected areas could in principle mitigate site-specific threats to freshwaters, and proactively prevent specific cases such as pollution and invasive species (Abell et al., 2007). Both systematic conservation planning and environmental flow assessment are central principles to the conservation of freshwaters within the IRBM framework. These methodologies and the latest developments in their application within freshwater conservation are outlined below.

1.4.2 SYSTEMATIC CONSERVATION PLANNING

Systematic conservation planning (SCP) is a well-established scientific approach for identifying priority areas for conserving biodiversity (Margules and Pressey, 2000). The majority of systematic conservation plans address four key principles; Comprehensiveness, Adequacy, Representativeness and Efficiency ('CARE' principles) (Nel et al., 2011b). '*Comprehensiveness'* details that the full range of species, processes and ecosystems must be included when planning in a study region, whilst '*Representativeness'* ensures that the full range of biodiversity is represented within the regions chosen for comprehensiveness through choosing suitable surrogates to serve as proxies for all biodiversity attributes (Linke et al., 2011). This principle acknowledges that conservation action areas are only a sample of the total landscape. '*Adequacy'* deals with how a conservation area network should be designed to ensure the persistence of all biodiversity attributes. This is typically the most challenging principle in conservation plans (particularly freshwaters) and the most common

quantitative conservation targets are set (i.e. species occurrences or percentage of remnant ecosystem type) through measures such as expert opinion (Desmet and Cowling, 2004), population viability analysis (Araújo and Williams, 2001) or by conserving processes that support the persistence of biodiversity (Pressey et al., 2007). Finally, '*Efficiency*' recognises that conservation resources are limited and thus plans must minimise costs and impacts on stakeholders.

A central feature of the systematic conservation planning framework is the use of complementarity-based algorithms to promote efficiency by selecting planning units that contain the most unrepresented features (Pressey, 1994). Areas are chosen to complement, and not duplicate, each other's biodiversity. Incorporating social and economic constraints for the planning units also improves the cost efficiency of conservation planning mechanisms and remains a relatively recent development that deserves more research, particularly in freshwater contexts (Klein et al., 2008, Lira-Noriega et al., 2015). There are two key outputs generated by conservation planning tools: an 'irreplaceability' map and a 'minimum set' map (Nel et al., 2011b). The 'irreplaceability' map is a relative index that details the likelihood to meet conservation target for each planning unit, where units with high 'irreplaceability' have few options for replacement but those with low values may be replaced (Ferrier et al., 2000). The 'minimum set' map outlines the most efficient spatial solution for achieving conservation targets at the lowest possible cost (Ferrier, 2002).

Originally developed in the terrestrial realm, recent advances in systematic conservation planning, coupled with the alarming decline in freshwater biodiversity, have led to its increased application in freshwater ecosystems (Nel et al., 2009b, Linke et al., 2011, Lira-Noriega et al., 2015, Carrizo et al., 2017, Hermoso et al., 2018). Systematic conservation planning in freshwaters delineate sub-catchments as the planning unit, in order to manage both the water resource and associated catchment (Thieme et al., 2007). Most also incorporate a river network topology that facilitates consideration of upstream-downstream linkages between candidate sub-catchments (Moilanen et al., 2008, Hermoso et al., 2018). There are several key issues to consider when developing a freshwater conservation plan: choosing surrogate features as indicators of freshwater biodiversity

(Turak and Koop, 2008), selecting suitable target levels for conservation (Linke et al., 2011), considering longitudinal (upstream-downstream), lateral (wetlands), vertical (groundwater) and temporal connectivity in freshwater ecosystems (Turak and Linke, 2011), and the use of multiple zones as management options (Abell et al., 2007).

1.4.3 ENVIRONMENTAL FLOW ASSESSMENTS

Changes to the flow regime of rivers invariably results in a loss of ecosystem function and resilience, with greater divergences from the natural flow regime (both volume and timing) causing greater ecosystem changes (Arthington et al., 2006, Poff and Zimmerman, 2010). Environmental flow assessments evaluate the extent to which a river ecosystem changes with alterations to its natural flow regime, with the resultant environmental-flow recommendations outlining the flow regime necessary to sustain key ecological and societal values (Tharme, 2003).

Three key developments over the past two decades have enabled environmental flow assessments to become a highly useful tool for informing Integrated River Basin Management (Nel et al., 2011b). Firstly, the development of holistic methodologies has enabled environmental flow assessments to encompass the whole aquatic ecosystem, including riparian zones, floodplains and estuaries. These comprehensively assess the set of social and economic benefits derived from the ecosystem, which is especially important for the livelihoods of dependent rural communities (King et al., 2003). Secondly, a shift towards scenario-based assessments means a suite of outcomes can be considered, rather than single, prescriptive flow-regime recommendations. Scenario construction is aided by establishing flow-response relationships that enable the prediction of response indicators to changes in the flow regime. Biophysical response indicators have also been supplemented with indicators relevant to social and economic consequences, ensuring trade-offs between the three can be assessed in a stakeholder-driven negotiation process (Dollar, 2010). Finally, conceptual frameworks and tools have been developed for flow-assessments across large geographical scales (e.g. catchments and bioregions), allowing for the configuration of rivers at different levels of ecological condition (natural to highly modified) based on societal values. The scale of these approaches

necessitates a methodology that can be applied with limited existing data, achieved through combining empirical measurements with modelled data and expert opinion. Additionally, a key premise is that rivers in a specific hydro-geomorphological class (e.g. stable groundwater streams) have similar flow-ecological responses that can be applied across the class without requiring data for all rivers (Arthington et al., 2006, Kennard et al., 2010).

Recent advances have outlined theories of integrating environmental flow assessments with conservation plans for freshwaters (Nel et al., 2011b, Kingsford, 2011, Pittock and Finlayson, 2011). This involves the use of decision-support frameworks and tools (i.e. the Ecological Limits Of Hydrological Alteration tool (ELOHA)) for scenario-based, regional environmental flow assessment (Tharme, 2003, Richter et al., 2006, Dollar, 2010, Poff et al., 2010). Within this theory, future ecological, social and economic costs and consequences are assessed through scenarios of catchment development and flow alterations (Dollar, 2010, Poff et al., 2010). The outputs from systematic conservation planning (i.e. 'irreplaceability' and 'minimum-set' maps) are then used to produce different conservation scenarios that can be used in assessing these costs and identify priority areas for protection that achieve both conservation and flow targets simultaneously (Nel et al., 2011b).

Despite these recent developments in the discipline of freshwater conservation planning, failure to incorporate uncertainty and dynamic threats, such as climate change, remains a substantial gap in the development of these strategies (Pittock et al., 2008, Nel et al., 2009b). The integration of freshwater conservation planning with environmental flow assessments represents a promising step forward for the discipline of freshwater conservation, as it presents an opportunity to incorporate the analysis of climate change impacts in conservation plans for freshwater ecosystems (Kingsford, 2011). Although general approaches have been explored for assessing freshwater conservation plans in the context of climate change (Nel et al., 2011b, Pittock and Finlayson, 2011, Turak et al., 2011b), these would benefit from being integrated into new ideas on climate change adaptation in freshwaters (Palmer et al., 2008, Comer et al., 2012, Mantyka-Pringle et al., 2016).

1.5 MODELLING CLIMATE CHANGE FOR WATER MANAGEMENT AND ADAPTATION

The dominant approach to climate change impact analysis uses ocean-atmosphere general circulation models (GCMs) as the driver of the assessment (Brown and Wilby, 2012). This current suite of 'top down' models was originally intended to assess the global consequences of different emission scenarios and develop a set of policies to mitigate against future impacts (Kundzewicz and Stakhiv, 2010). More recently, GCMs and scenarios (e.g. IPCC SRES A1, B2 etc.) have now been widely applied in scientific research to generate plausible future climates and derive quantitative estimates of future consequences at both regional and basin scales (Cox and Stephenson, 2007).

However, despite significant advances in model construction, GCMs remain limited in their ability to forecast much beyond broad scale climate patterns, primarily due to the complexity and non-linearity of the Earth-climate system (Wilby, 2010, Pielke and Wilby, 2012). Additionally, scenario-led approaches are unsuitable for exploring the full range of uncertainty in key variables of a system relevant to decision makers, as they only consider a minimum range of uncertainty that excludes possible climate outcomes (Brown and Wilby, 2012). Indeed, precipitation, the principal input to freshwater systems, remains inadequately modelled in present climate models (Kundzewicz et al., 2008, Maraun et al., 2010, Bock et al., 2018). Due to these uncertainties, recent studies have moved towards employing a diverse range of GCMs, driven by plausible emission scenarios, to generate quantitative measures of uncertainty (Taye et al., 2011, Bae et al., 2011). However, the successful transfer between these models and climate adaptation decisions remains limited, with seemingly more effort invested in quantifying the uncertainty of model outcomes than determining appropriate adaptation strategies (Prudhomme et al., 2010).

Therefore, climate risk analysis in a decision-making context must consider analyses other than climate projections (Brown and Wilby, 2012). There is a growing body of literature informing adaptation to climate change through 'bottom-up' approaches, which do not rely on the use of predictive, scenario-based 'top-down' approaches (Smit and Wandel, 2006). Sensitivity analyses have

been developed that provide information on how a system would respond to perturbations in climatic variables (Brown et al., 2012). These 'scenario-neutral' approaches can be termed 'bottom-up meets top-down', as they initially focus on the issues of concern for a system and then on how climate information may add value to the analysis (Prudhomme et al., 2010, Brown et al., 2012). This statistical technique is a time and cost-effective approach to climate downscaling (when compared to scenario-led assessments and dynamical downscaling methods), which establishes empirical relationships between GCM-resolution climate variables and local climate (e.g. at the catchment scale) (Stakhiv, 2011).

Furthermore, this approach facilitates the inclusion of an ensemble of GCMs in the analysis, thereby enabling a fuller understanding of future uncertainties (Bastola et al., 2011b). Methodologically there are three main steps: 1) identify the problem and define objectives and performance measures, 2) conduct a sensitivity analysis to identify hazards and evaluate performance of system under a broad range of climatic and non-climatic variability and change, and 3) use climate information (including projections) to evaluate risk (Bastola et al., 2011b). The key advantages of this 'scenario-neutral' approach to climate change risk analysis are that the sensitivity domain can cover the entire spectrum of possible future values to plan for surprise and extreme projections (Prudhomme et al., 2010) and it is flexible to the emergence of new climate change projections, changes in the planning time horizon and to evolving societal attitudes to risk (Brown and Wilby, 2012). In addition, the scenario-neutral approach explicitly incorporates the concept of exposure and sensitivity, meaning it is highly applicable to the emerging field of climate change vulnerability analyses outlined below.

1.6 VULNERABILITY – A FRAMEWORK FOR CLIMATE CHANGE ASSESSMENT

Current assessments of the impact of climate change on freshwater biodiversity have largely been restricted to the application of niche-based species distributions models (e.g. Comte et al., 2013, Domisch et al., 2013, Markovic et al., 2014b). These models vary in sophistication and scope, but in general, they examine the current conditions that species are exposed to and then consider the extent that these conditions will change in the future. Such approaches have been criticised as only

considering one aspect of the effect of climate change on species; that of exposure (Wilby and Dessai, 2010). Within the literature, exposure is defined as the extent of climate change likely to be experienced by a species or locale (Williams et al., 2008, Foden et al., 2013, Pacifici et al., 2015). The extent of exposure typically depends on the rate and magnitude of climate change in habitats and regions occupied by a species. However, two other important aspects also influence the impact of climate change on species and ecosystems: sensitivity and resilience. Firstly, sensitivity is defined as the degree to which the survival, persistence, performance or regeneration of a species, population or ecosystem is dependent on the prevailing climate (Williams et al., 2008, Foden et al., 2013, Pacifici et al., 2015). Secondly, resilience is defined as the capacity of a species or population to cope with climate change by persisting *in situ*, by shifting to more suitable local microhabitats, or by migrating to more suitable regions (Williams et al., 2008, Foden et al., 2013, Pacifici et al., 2015). In the context of ecosystems, resilience is the capacity of a habitat to maintain functionality in response to perturbation through adaptation, reorganisation and evolution of key processes and structures (Willis et al., 2018). Within the new integrated science of climate-change biodiversity assessment the combination of these three aspects provide an indication of the vulnerability of species; defined as the extent to which a species or population is threatened (Foden et al., 2013, Pacifici et al., 2015, Willis et al., 2018).

However, there is a qualitative difference between exposure (the external component of vulnerability) and coping (the internal components; sensitivity and resilience) (Adger, 2006). Unlike sensitivity and resilience, exposure is an attribute of the relationship between the system and the perturbation (climate change), rather than that of the system itself. Instead, vulnerability is a function of system sensitivity and resilience (IPCC, 2014b). The transformation, or potential impact, suffered by a system is a function of its vulnerability, the properties of the perturbation, and the exposure of the system to the perturbation (Gallopín, 2006). From this perspective, a system may be very vulnerable to a certain perturbation but persist without problems in-so-far as it is not exposed to it. From the perspective that includes exposure as a component of vulnerability, a system that is not exposed to a perturbation would be defined as non-vulnerable. This decision of including or not

including exposure as a component of vulnerability has consequences (IPCC, 2014a). In the latter instance, vulnerability becomes a property of the relationship between the system and its environment (specifically between the system and the perturbation), rather than a property of the target system (Gallopín, 2006). The tangible characterisation of vulnerability (indices, maps, etc.) needs to consider the full set of possible combinations of situations and must be changed if the distribution of exposure changes (for instance, when alternative climate scenarios are examined). Conversely, if exposure is externalised from vulnerability, exposure is a relational property, and vulnerability is a property of the system, becoming expressed or revealed when the system is exposed to the perturbation (Gallopín, 2006). Vulnerability from this viewpoint is an attribute of the system existing prior to the disturbance, although it is often related to the history of disturbances to which the system was exposed in the past. If the vulnerability of different target systems could be characterised based on their sensitivity and resilience, their exposure to a perturbation could be independently determined, and the harm or outcome of the resulting transformation of the system could be estimated from the composition of the two factors. Using a climate change example, only one map of vulnerability would be needed, which could be overlaid with different maps of exposure resulting from diverse models or scenarios.

Therefore, how exposure is considered within a vulnerability framework is crucial in determining research outputs and their usefulness in a conservation context. Ideally, the conceptual framework of vulnerability should be determined prior to the application of methodological aspects. However, in real world scenarios, the scale and complexity of the study region and availability of critical data sources typically determine which approach to vulnerability is utilised (IPCC, 2014a). The scale of the study region will often determine the resolution and nature of data already available, alongside the feasibility of collecting new data to fill in the gaps (Margules and Pressey, 2000). In the context of vulnerability analyses and freshwater conservation planning, scale determines critical methodological components, such as the choice of biological and environmental surrogates selected (e.g. species richness or complex macroinvertebrate indices) or type of hydrological model used to simulate flows and nutrients (e.g. coarse-scale distributed/gridded models or complex, process-based models)

(Poiani et al., 2000). Secondly, the context of the study region can provide clear constraints in terms of existing policy and management efforts, alongside influencing conservation targets for the region. In a freshwater setting, major national or regional water policies (e.g. the Water Framework Directive (WFD) in Europe) stipulate legal guidelines for flows, water quality and abstractions and outline conservation targets for the region of interest. Furthermore, existing national bodies, utility companies and other stakeholders have vested interests and management strategies for the study region that would need to be considered when developing and implementing a climate change vulnerability assessment.

1.7 THESIS AIMS AND OBJECTIVES

The primary aim of this thesis is to address the concept of scale and context in the creation of climate change vulnerability analyses used to inform existing and future freshwater conservation and management plans and restoration priorities. To this end, two novel and distinct methodologies were developed and applied in two case studies; one at the regional scale for over 18,000 catchments throughout Europe and the other at the basin scale for 292 catchments within the Thames Basin, UK. Both approaches apply varying interpretations of the vulnerability framework outlined above to assess the potential impact that climate change may have throughout the study region. It is envisioned that the outputs of both case studies can further be used to identify priority areas for inclusion in conservation, management and restoration plans.

Conceptually, at the regional scale, catchments are prioritised based on preserving maximum species richness under multiple climate change scenarios. In brief, exposure was internalised within the vulnerability framework, with changes in key hydro-ecological indicators providing a quantitative measure of expected climate change within a catchment. Furthermore, sensitivity was defined at the catchment scale through the summation of present species whose traits defined them as particularly sensitive to alteration in climate. Finally, resilience was defined as the potential conferred by landscape features within and between catchments to mitigate adverse effects on species due to climate change. The combination of these three components thus provides an assessment of

vulnerability to climate change for catchments at the European scale. The methodology, results and discussion of this regional approach form the first part of this thesis.

Contextually, unlike regional-scale studies, basin-scale management cannot focus on maximising species richness using future species distribution modelling. This is because most species exist outside of the local context, meaning the full range of a species' environmental tolerances cannot be accurately elucidated at the local scale (Araújo et al., 2011). Thus conceptually, at the basin scale, the aim of this research is to test the application of a vulnerability framework in determining the sensitivity of key Water Framework Directive (WFD) indicators of ecosystem health to perturbations in two key climatic variables: mean annual precipitation and temperature. Critically, exposure is externalised from the vulnerability framework using a scenario-neutral, 'bottom-up' approach to assessing climate change. The potential impact of climate change can be determined through the incorporation of any predictive GCM outputs, generating a probabilistic envelope of future risk for each catchment. Finally, the concept of resilience is explored in the discussion of results, through outlining several management strategies identified from the resilience literature (such as stream shading, adding meanders (Wilby et al., 2010)) aimed at reducing the impact of alterations in each of the WFD indicators. The detailed methodology, results and discussion of this local approach form the second part of this thesis.

Chapter 2 REGIONAL ASSESSMENT: VULNERABILITY OF EUROPEAN CATCHMENTS TO CLIMATE CHANGE

2.1 INTRODUCTION AND OBJECTIVES

Conceptually, at the regional scale, the aim of this research is to provide prioritisation of catchments for different management strategies based on the preservation of maximum species richness under multiple climate change scenarios. This chapter aims to assess the vulnerability of European freshwater ecosystems to climate change at the regional scale. The study region encompasses all major European countries, covers over 10 million km^2 and supports a population of approximately 742.5 million people (UN, 2015). In addition, the region contains numerous major international rivers vital to infrastructure, fisheries and power generation. In particular, the Danube River flows through ten countries and is one of the most heavily obstructed river basins worldwide (Liermann et al., 2012). The planning units chosen for the study are HydroBasin level 8 resolution catchments (Lehner & Grill, 2013), which delineate European river and lake systems into 18,783 catchments (average area of 536.3 km^2). Following the vulnerability terminology of Turner et al. (2003), as adopted for freshwater ecosystems by Poff et al. (2012), the three climate change vulnerability dimensions utilised are: 1) extrinsic *exposure* to climate change (i.e. the extent to which environmental conditions in each catchment will change); 2) intrinsic *sensitivity* to altered environmental conditions (i.e. the lack of potential for freshwater species to persist in a catchment), and 3) *resilience* (i.e. the aspects of a catchment that enable freshwater species to cope under climate change). The exposure, sensitivity and resilience estimates were combined to provide comprehensive assessments of the vulnerability of European river and lake catchments to a range of climate change scenarios. Finally, based on vulnerability category and coverage by the European protected areas network, priority catchments were identified that may facilitate the development of broad-scale climate change conservation management strategies.

2.2 METHODOLOGY

2.2.1 SPECIES DATA

Distribution maps were obtained for 1,685 European freshwater species including 323 plants, 508 fishes, 657 molluscs, 134 odonates, 54 amphibians, 5 crayfish and 4 turtles (www.iucn.org/species_BioFresh). This dataset includes native portions of species ranges throughout Europe that were compiled by the IUCN Global Species Programme as part of the Red List assessment process. The non-native portions were excluded due to missing information on their impact on resident communities. The data were mapped to the HydroBasins level 8 resolution catchments (Lehner & Grill, 2013), hereafter called 'catchments'; see Figure 2-1). Given the dendritic, hierarchical structure of river and stream networks, the catchment resolution is more appropriate for mapping freshwater species occurrences than grid cell mapping, and ensures compatibility between the analysis and management scales (Luck et al., 2009).

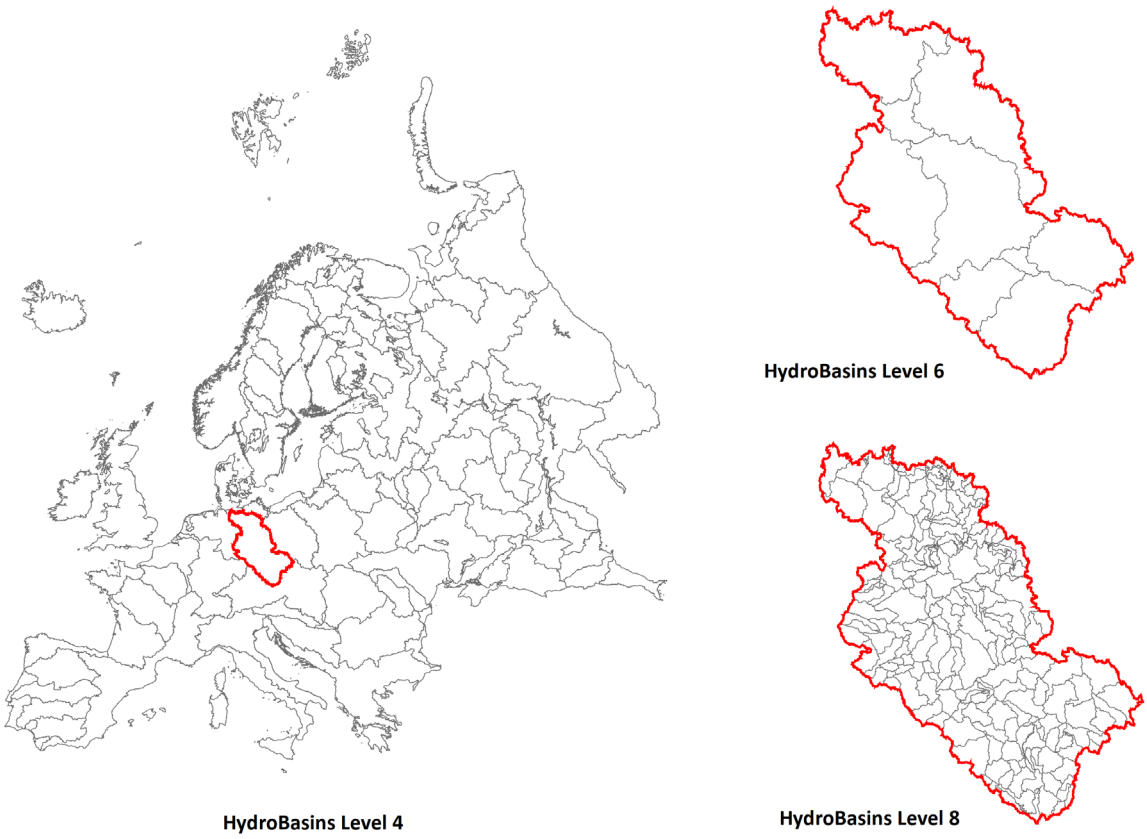


Figure 2-1: A comparison of different HydroBasins dataset resolutions for the Elbe River Basin (blue). The average catchment area at the HydroBasins level 8 resolution is 536.3 km^2.

2.2.2 CLIMATE AND HYDROLOGICAL DATA

The climatic and hydrological data describing the thermal and hydrological regimes across Europe for the 20th and 21st century were derived from the global gridded 0.5° by 0.5° (~50km by ~50km) WATCH (Water and Global Change) dataset (https://gateway.ceh.ac.uk/). The WATCH project is a European Union funded initiative (FP6) that brought together scientists from 25 EU institutions (including those from the USA and Japan) to improve the understanding of the terrestrial water cycle (Hagemann et al., 2011). The central focus of the project was to develop a common modelling framework that enabled the linkage of a diverse group of spatial datasets with existing hydrological and water resource models. Two important datasets were developed (comprising eight key climatic variables) that enable the consistent application of climate data at the European and global scale; The WATCH Forcing Data, covering the period 1901-2001 and the WATCH Driving Data, covering the period 2001-2100 (Weedon et al., 2011). These datasets were generated using three well-established General Circulation Models (GCMs), ECHAM5, CNRM and IPSL, with each following the A2 and B1 emission scenarios. A2 and B1 storylines describe a world with continuously increasing global population and regionally oriented economic growth (A2), and a world where global population peaks mid-century and declines thereafter and introduces clean and resource-efficient technologies (B1) (Nakicenovic et al., 2000). Furthermore, the compilation of over 400 hydrological stations throughout Europe have facilitated the validation of a Water Model Inter-comparison Project (WaterMIP), which provides fit-for purpose estimation of river flows at global, continental and regional scales via the application of WATCH Forcing and Driving data through an ensemble of hydrological models (Weedon et al., 2011). The specific details of these models and how they are utilised in this research are outlined below.

This research utilises the bias corrected (Piani et al., 2010) daily data for air temperature and naturalised flows generated by WaterGAP (Döll et al., 2003), GWAVA (Meigh et al., 1999) and LPJmL (Bondeau et al., 2007) hydrological models (HMs) for three time periods: 1971-2000 (hereafter called ‘baseline’), 2021-2050 (hereafter called ‘2030s’) and 2071-2100 (hereafter called ‘2080s’). Only

naturalised flows obtained from running the hydrological component of the hydrological models only (i.e. without the water usage component) were used in this research. This decision was made due to the substantial differences between how each hydrological model methodologies in representing anthropogenic and social impacts on river flow (Haddeland et al., 2011). Consequently, the results will mainly consider the climate related changes in hydrological regimes. Therefore, the climatic data includes 18 distinct sets (3 GCMs × 2 scenarios × 3 time periods) and the hydrological data includes 54 distinct sets (3 HMs × 3 GCMs × 2 scenarios × 3 time periods; see Figure 2-2 for details). The WorldClim 30 arc-second (approximately 1 km×1 km) dataset (Hijmans et al. (2005); www.worldclim.org) was used to derive the catchment specific average and maximum temperatures over the period 1960-2000 (hereafter called 'extended baseline'). All climatic and hydrological data were mapped to the HydroBasins level 8 scale, providing consistency with species data. The scale of the planning units (HydroBasins) and exposure data were very similar (~50km^2), leading to a roughly equivalent 1:1 ratio between datasets (i.e. one exposure grid cell mapped to one catchment). In cases where multiple exposure grid cells were present in a catchment, the average data value was interpolated from the relevant grid cells using the Spatial Analysis toolset in ArcGIS©. Figure 2-2 provides a clear flow chart for the derivation of climatic and hydrological datasets comprising the exposure component of this regional vulnerability analyses.

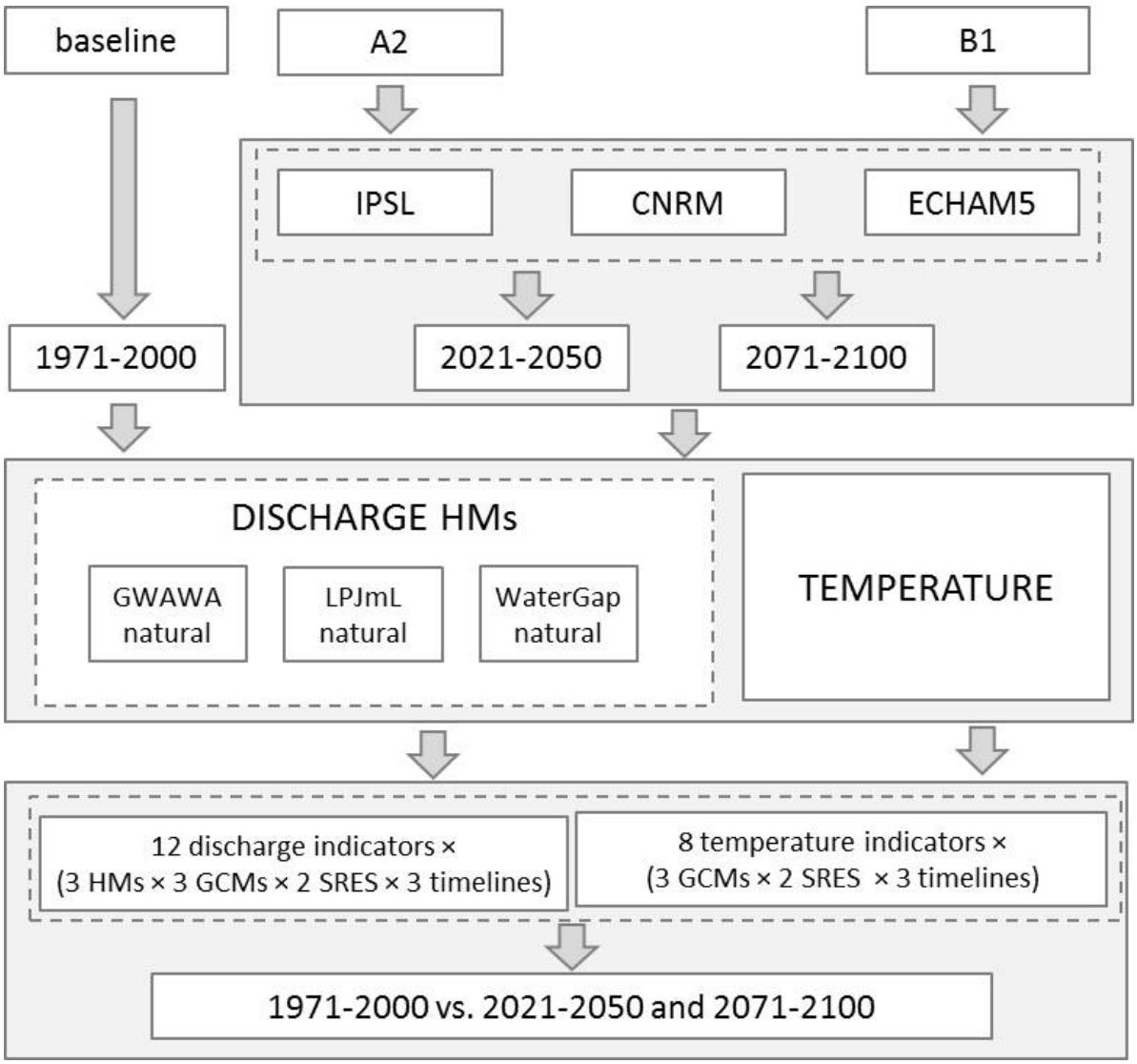


Figure 2-2: Flow chart for the derivation of climatic and hydrological change indicators.

2.2.3 PROTECTED AREAS

The protected areas used in this analysis include data obtained from the World Database on Protected Areas (WDPA, www.wdpa.org) and the NATURA 2000 database (www.eea.europa.eu) (Figure 2-3). From the WDPA dataset, only protected areas with IUCN categories I-IV were considered, corresponding to strict nature reserves, wilderness areas, ecosystem conservation and protection areas, conservation areas for natural features and areas with conservation through active management. All Natura 2000 sites were used, as they comprise Special Protected Areas (SPA) and adopted Sites of Community Importance (SCI), designated by EU Member States under the Birds Directive (79/409/EEC) and the Habitats Directive (92/43/EEC) with the aim of long-term protection

of Europe's most valuable and threatened species and habitats. The total area considered protected (hereafter referred to as PA) within each individual catchment was calculated by overlaying the union of the WDPA and Natura 2000 layers with the catchments layer using the Spatial Analysis toolset in ESRI ArcGIS© (Figure 2-4).

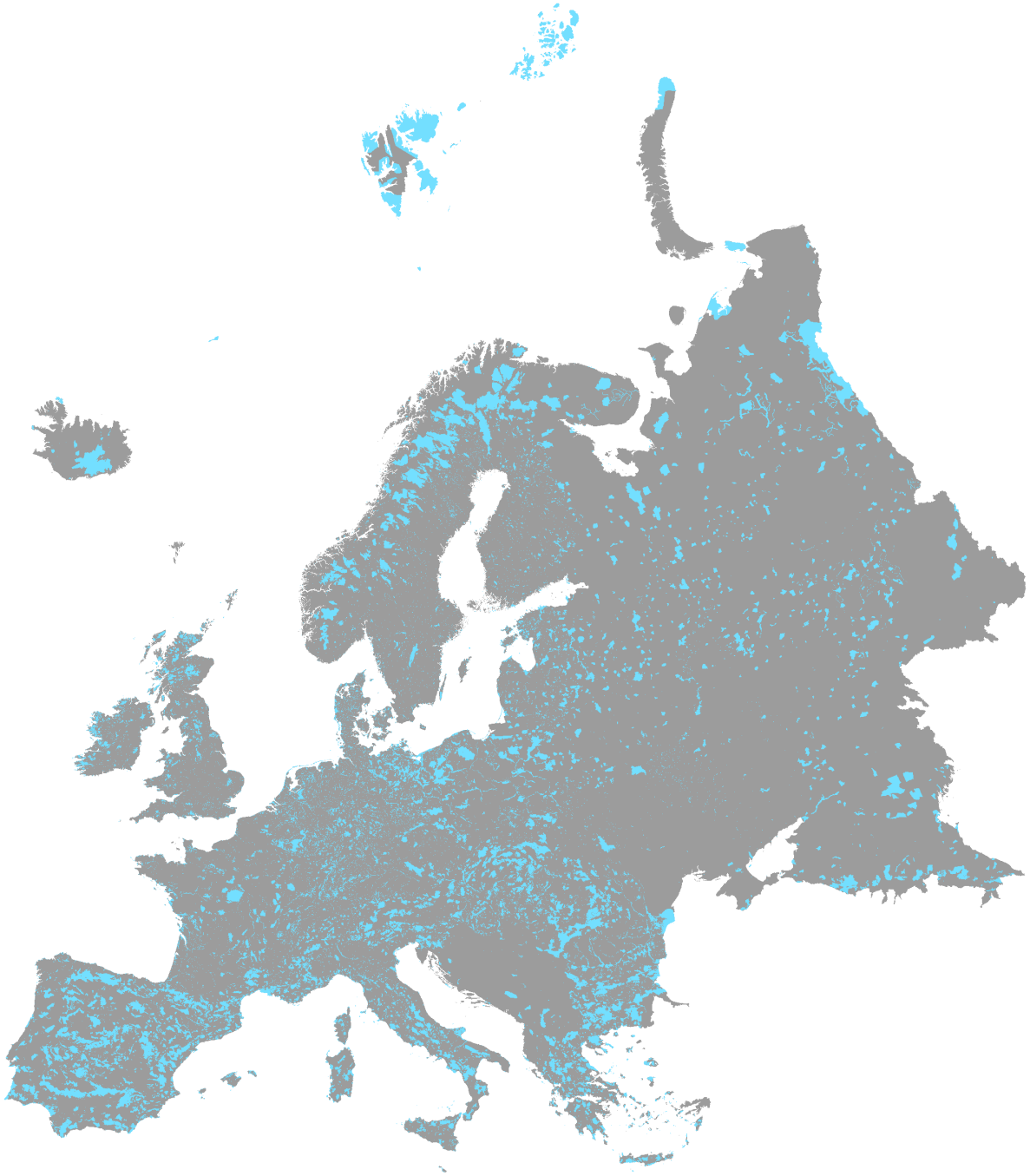


Figure 2-3: European protected area network (Natura 2000 and WDPA data with IUCN categories I-IV). Total area of protected areas is 1,221,230km².

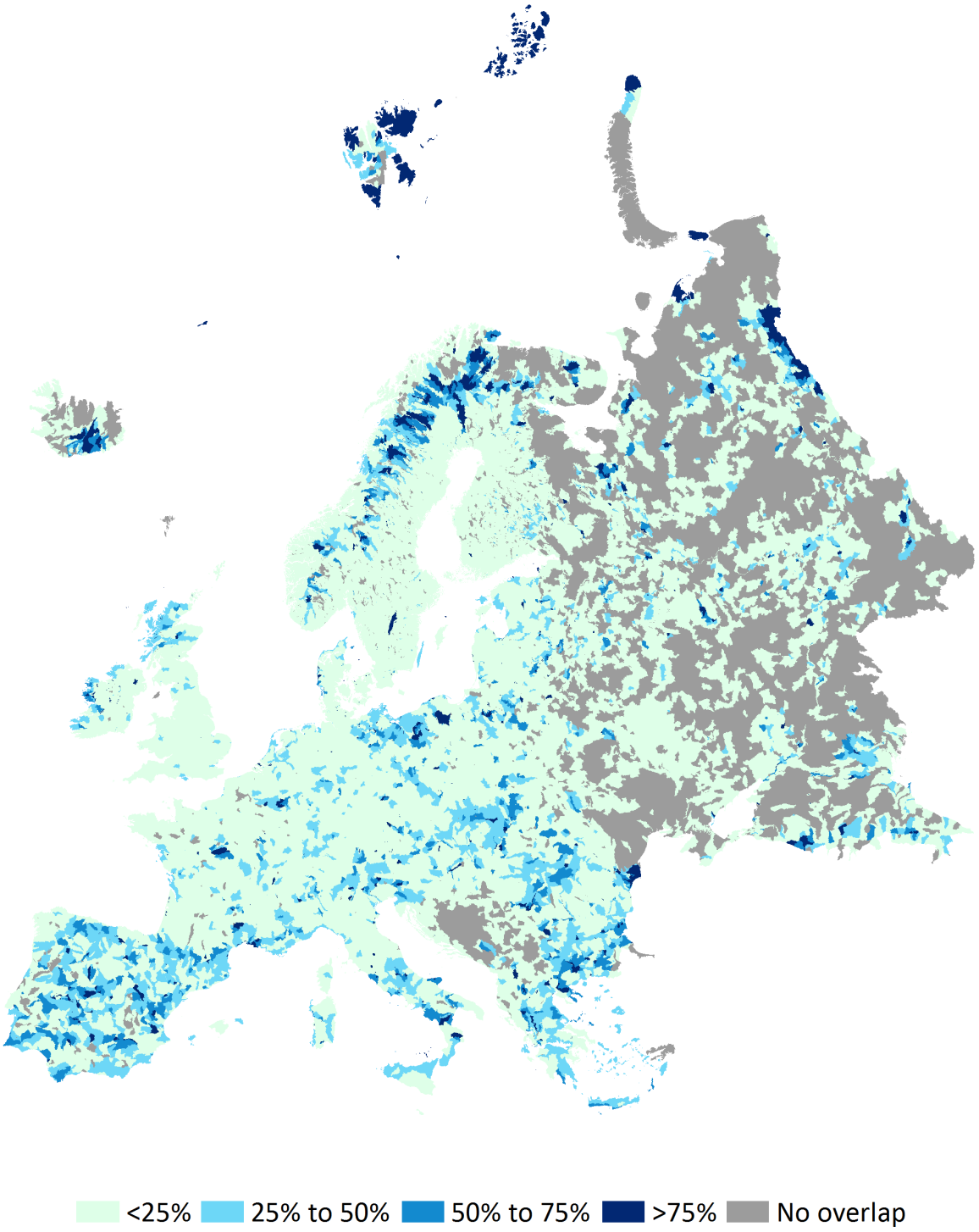


Figure 2-4: Percentage area per catchment overlapped by the European protected area network in Figure 2-3.

2.2.4 EXPOSURE ASSESSMENT

Due to the stochastic nature of environmental processes, both hydrological and thermal regimes have a non-stationary character, with temperature and river flow patterns varying substantially from catchment to catchment. However, climate change is expected to magnify these naturally occurring changes, thus exacerbating current threats to freshwater ecosystems. In the following section, a brief

summary of the potential consequences of changes in the regime attributes of freshwater ecosystems are outlined. The conceptual framework for calculation of the exposure indicators is based on the Indicators of Hydrological Alteration (IHA) approach introduced by Richter et al. (1996 & 1997) and further refined for application at the monthly time-scale by Laizé et al. (2014). Underlying these approaches is the assumption that ecologically relevant hydrological and thermal regime alterations are best described by changes to the 1) magnitude, 2) frequency, 3) duration, 4) timing and 5) variability of regime attributes. Some relevant ecological impacts of these alterations are briefly summarised below and considered in more depth in the introductory chapter of this thesis:

Magnitude. The magnitude of hydrological and thermal events reflects the availability of the freshwater habitat for both in-stream and riparian species. In addition, the magnitude of thermal events plays a fundamental role on the water quality and distribution of aquatic species (Caissie, 2006, Comte et al., 2013).

Frequency. The frequency of events occurrence, in particular high and low extremes (such as floods and droughts or heat and cold waves), affects population dynamics through impacts on species reproduction or increases in mortality (Richter et al., 1996).

Duration. The events duration, in particular increases in the duration of droughts and summer heat stress, may lead to significant distortions in community structure and composition and poses elevated, potentially lethal risks, for cold-water species (Markovic et al., 2013) .

Timing. The timing of events, particularly the timing of annual extremes, may impair ecological success of a specific life-stage. Thus, changes in event timing may result in weakening or breaks in trophic interactions (Woodward et al., 2010).

Variability. The variability of hydrological and thermal regimes strongly affects food-web synchrony. Changes in regime variability may affect habitat availability and lead to disruption of established patterns in food-web synchrony (Kishi et al., 2005).

To address the climate change related alterations of hydrological and thermal regimes, a set of indicators were developed as specified in Table 2-1. Firstly, for each indicator, the change between baseline and future conditions was determined (2030s vs. baseline and 2080s vs. baseline). Secondly, the results for each GCM and emission scenario were merged by averaging the corresponding indicator values per grid cell, and across all HMs for discharge related indicators. Thirdly, for each grid cell, the related hydrological and thermal alterations were calculated by counting the number of indicators exceeding the corresponding thresholds (Table 2-1), selected following van Vliet et al. (2013) and Laizé et al. (2014). Fourthly, the catchment related hydrological and thermal alterations were calculated from the corresponding gridded layers using the ESRI ArcGIS zonal statistics tool. Finally, the exposure to climate change was calculated by merging the catchment related hydrological and thermal alterations and then normalising to a 0-1 scale.

2.2.5 SENSITIVITY ASSESSMENT

Freshwater ecosystems dominated by threatened, restricted-range species and those with narrow environmental tolerances are more likely to suffer greater impacts from climate change than ecosystems containing only more common and/or widespread species (Markovic et al., 2014b). The sensitivity assessment applied here combines various concepts including the threat, range-restricted and ecoregion-restricted criteria of freshwater Key Biodiversity Areas (KBA) (Holland et al., 2012), the irreplaceability of the Alliance for Zero Extinction concept (Ricketts et al., 2005) and the species traits approach (Foden et al. (2013). Specifically, the following attributes of sensitivity are incorporated into the assessment:

2.2.5.1 PRESENCE OF THREATENED SPECIES

This criterion reflects species' risk of extinction following the IUCN Red List of Threatened Species™, which classifies threatened species into categories 'Critically Endangered' (CR), 'Endangered' (EN), or 'Vulnerable' (VU) based on a globally accepted set of quantitative criteria (IUCN, 2014). Given that CR, EN and VU species are at extremely high risk or very high risk of extinction in the wild (IUCN, 2014), climate change is considered an additional threat to increasing their extinction risk.

Table 2-1: Exposure indicator methodologies and thresholds. Q and T, respectively represents a specific discharge and temperature value or percentile i.e. Q_{max}/T_{max} - maximum discharge/temperature value; Q_{90}/T_{90} - 90th percentile value; NMQ_{90}/NMT_{90} – number of months above baseline Q_{90}/T_{90}; NMQ_{10} - number of months below baseline Q_{10}; MM – modal month over 30 years; $NCMQ_{90}/NCMT_{90}$– annual mean number of consecutive months above baseline Q_{90}/T_{90}; $NCMQ_{10}$ - annual mean number of consecutive months above baseline Q_{10}; QR– flow range ($Q_{max} – Q_{min}$); TR- temperature range ($T_{max} – T_{min}$); *i* – month; std – standard deviation.

Indicator	Type	Methodology	Threshold
Hydrological indicators			
Average monthly flows	Magnitude	$\lvert Q_{50,future}-Q_{50,baseline}\rvert / Q_{50,baseline}$	>30%
High flows	Magnitude	$(Q_{90,future}-Q_{90,baseline}) / Q_{90,baseline}$	>30%
Low flows	Magnitude	$(Q_{10,future}-Q_{10,baseline}) / Q_{10,baseline}$	<-30%
Frequency of high flows	Frequency	$(NMQ_{90,future}-36) / 36$	>30%
Frequency of low flows	Frequency	$(NMQ_{10,future}-36) / 36$	>30%
Timing of maximum flow	Timing	$\lvert MMQ_{max,future}-MMQ_{max,baseline}\rvert$	≥1 month
Timing of minimum flow	Timing	$\lvert MMQ_{min,future}-MMQ_{min,baseline}\rvert$	≥1 month
Duration of high flows	Duration	$(NCMQ_{90,future}-NCMQ_{90,baseline}) / NCMQ_{90,baseline}$	>30%
Duration of low flows	Duration	$(NCMQ_{25,future}-NCMQ_{25,baseline}) / NCMQ_{25,baseline}$	>30%
Flow range	Variability	$\lvert QR_{future}-QR_{baseline}\rvert / QR_{,baseline}$	>30%
Flow annual cycle	Variability	$\frac{1}{12}(\sum_{i=1}^{12} \lvert Q_{i,future} - Q_{i,baseline}\rvert / Q_{i,baseline})$	>30%
Flow seasonality	Variability	$\lvert std(Q_{future}) - std(Q_{baseline})\rvert / std(Q_{50,baseline})$	>30%
Thermal indicators			
Average monthly temperatures	Magnitude	$(T_{50,future} - T_{50,baseline})$	>2 °C
Temperature extremes	Magnitude	$(T_{90,future} - T_{90,baseline})$	>2 °C
Frequency of high temperatures	Frequency	$(NMT_{90,future}-36)/ 36$	>30%
Duration of heat stress	Duration	$(NCMT_{90,future}-NCM\ T_{90,baseline}) / NCM\ T_{90,baseline}$	>30%
Timing of maximum temperature	Timing	$\lvert MMT_{max,future}-MMT_{max,baseline}\rvert$	≥1 month
Temperature range	Variability	$\lvert TR_{future}-TR_{baseline}\rvert$	>2 °C
Temperature annual cycle	Variability	$\frac{1}{12}(\sum_{i=1}^{12} \lvert T_{i,future} - T_{i,baseline}\rvert$	>2 °C
Temperature seasonality	Variability	$\lvert std(T_{future}) - std(T_{baseline})\rvert / std(T_{50,baseline})$	>30%

Normalised scores were assigned based on the total number of species classified in any of the three categories (i.e. 0 for a catchment with no threatened species and 1 for a catchment with the maximum number of threatened species across the study region).

In addition, a 'conservative catchment scoring' approach was adopted, whereby the presence of at least one threatened species triggered catchment classification as 'sensitive to climate change' (i.e. catchment containing CR, EN or VU species was assigned the score 1, otherwise, 0). Two estimates of this sensitivity component were calculated, with one using the European species' Red List Status and the other using the global species' Red List Status.

2.2.5.2 PRESENCE OF SPECIES WITH RESTRICTED RANGES

Species with small (restricted) ranges generally have higher extinction risk than widespread species (Purvis et al., 2000). As such, the inherent vulnerability of restricted-range species to external pressures is compounded by climate change related effects. For a species to have a restricted range, a threshold value for the Extent Of Occurrence (EOO) of 50,000 km^2 for odonates and 20,000 km^2 for other taxa groups was adopted following Holland et al. (2012). Thus, the total range size for each species was derived by summing the total area of catchments with known species occurrences. Normalised scores were obtained by calculating the total number of restricted range species per catchment relative to the catchment with the highest number of restricted range species (i.e. 0 for a catchment with no species of restricted range and 1 for the catchment with the maximum number of such species). In addition, for the 'conservative catchment scoring' approach, the presence of a single restricted-range species triggered catchment classification as 'sensitive to climate change' (i.e. a catchment with a single restricted range species was assigned the score 1, otherwise, 0).

2.2.5.3 PRESENCE OF SPECIES CONFINED TO A SINGLE BIOGEOGRAPHIC UNIT

Regions with unique species assemblages are generally sensitive to environmental change, with climate change likely to compound this effects (Malcolm et al., 2006). To assess this component of sensitivity, the Freshwater Ecoregions Of the World (FEOW) developed by Abell et al. (2008), were used as biogeographic units whose boundaries typically corresponded to drainage basins with

distinct evolutionary history and/or ecological processes. Thus, for each catchment, the proportions of species that occur in a single freshwater ecoregion were identified. Thresholds for the proportion of ecoregion-restricted species relevant to classify any catchment as 'sensitive to climate change' impact are 25% for fish and 5% for all other taxa groups. These were adapted from thresholds used in Holland et al. (2012) to identify Key Biodiversity Areas (KBAs) based on ecoregion-restricted assemblages. For each catchment, if the given thresholds were exceeded for any of the taxa groups, this sensitivity attribute was assigned the score 1, otherwise, 0.

2.2.5.4 UNIQUE CATCHMENTS

If a catchment represents the entire known range of any species then it was considered unique and particularly sensitive to climate change (Linke et al., 2008). The uniqueness value of all catchments was calculated for each species ('$Uval_s$') as the ratio between the catchment area occupied by a species (0 if the species is not currently present, otherwise the size of the catchment area) and the total species' range area. Therefore, the uniqueness value of a catchment for a species is between 0 (for a catchment that does not belong to species range) and 1 (for a catchment representing the entire species range). The final catchment specific uniqueness score ('Uscore') was then calculated as the maximum of a catchment's uniqueness values based on the total species composition of that catchment using the following: $\mathrm{Uscore\,(c)} = \max(\mathrm{IRval}_s), \mathrm{s} = 1, \ldots, s_c$, where s_c denotes the species inhabiting catchment *c*.

2.2.5.5 SPECIES WITH NARROW ENVIRONMENTAL TOLERANCE

Tolerance to a wide range of climatic conditions is tightly linked to the ability of a species to resist and recover from environmental change (Poff et al., 2012). Therefore, species with narrow environmental tolerances are highly likely to be more sensitive to climate change than those with broad environmental tolerances (Williams et al., 2008). The temperature range (maximum-minimum) over the extended baseline period (1960-2000) across a species current range was used as a proxy for species environmental Tolerance Breadths ('TB') (Angilletta, 2009). A cumulative distribution function of unique species' tolerance breadths was created, and each species was assigned a

normalised score such that TBn_s=1-(TB_s-TB_{min})/(TB_{max}-TB_{min}) (i.e. 0 for species with the highest tolerance ('TB_{max}'), and 1 for species with the lowest ('TB_{min}')). The catchment specific score for this sensitivity attribute ('TB_{score}') was then calculated following $\mathrm{TB_{score}(c) = max\,(TBn_s), s = 1,..,s_c}$, where s_c denotes the species inhabiting the catchment *c*.

Catchment specific sensitivity was then calculated as an average across the individual scores of the five sensitivity attributes. The sensitivity assessments based on the standard and conservative catchment scoring are hereafter referred to as 'standard' and 'conservative' approach respectively.

2.2.6 RESILIENCE ASSESSMENT

Habitat connectivity and availability of diverse freshwater environments (e.g. from mountainous streams to lowland rivers) are one of the key factors influencing the recolonisation ability of species, and thus species resilience to climate change. As such, the resilience concept of Poff et al. (2012) was adopted as the conceptual framework, which considers resilience more broadly as a feature of the landscape and not as a species' trait.

A lack of hydrological catchment connectivity due to natural dispersal barriers (such as drainage divides of the 'major' basins i.e. basins with sea or ocean outlet) and anthropogenic barriers (such as dams and weirs), reduces species success at tracking spatial shifts in suitable habitats (Hein et al., 2011). Therefore, to account for hydrological catchment connectivity, both natural dispersal barriers (drainage divides of the major basins were estimated using the Pfafstetter coding feature of HydroBasins) and anthropogenic barriers (dams and obstacles) were considered as contributing towards the disruption of connectivity. The geographic location of about 5,500 dams and obstacles (referred to hereafter as 'dams') across the European catchments was extracted from the ECRINS (European Catchments and Rivers Network System) database (http://www.eea.europa.eu/data-and-maps/data/european-catchments-and-rivers-network). Two dispersal scenarios were considered: 1) a scenario with dams and, 2) an optimistic scenario without dams. Consequently, the set of hydrologically connected upstream and downstream catchments for an individual HB8 catchment is

different for most catchments between the two dispersal scenarios. The following resilience attributes were considered:

2.2.6.1 ALTITUDINAL RANGE

Altitudinal range provides an indirect measure of the basin-specific differences in the opportunities available to freshwater species to escape thermal stress, where basins with a small altitudinal range provide less opportunity than those with alpine streams (e.g. Comte et al., 2013). For each catchment, the maximum altitudinal range across the connected catchments was used.

2.2.6.2 LATITUDINAL GRADIENT

Many freshwater species are already expanding their ranges to higher latitudes in response to climate change (Hickling et al., 2005, Domisch et al., 2013). Consequently, a catchments latitudinal range can be used as a proxy for resilience to adverse effects of climate change. To assess the opportunity for species to move northwards as a response to increasing temperatures, the maximum latitudinal range for each catchment was calculated. This was defined as the difference between latitudes of the northernmost border of the northernmost connected catchment and southernmost border of the southernmost connected catchment.

2.2.6.3 NETWORK DENSITY

The density of a river network represents a natural source of resilience for freshwater species within a catchment, since more numerous, smaller rivers are more likely to provide refugia from climate change impacts than single, larger rivers (Campbell Grant et al., 2007). This was quantified as the ratio between the total length of river network in a catchment and the catchment area and provides a perspective of refugia options available to species within a catchment (intrinsic refugia).

2.2.6.4 NETWORK COMPLEXITY

The complexity of a river network represents a natural source of resilience for freshwater species, as better connected catchments provide more refugia options than those that are isolated (Poff et al., 2012). This was quantified as the total number of connected catchments to each catchment within

the study area, providing a perspective of refugia options available to a species outside the catchment (extrinsic refugia).

For each resilience attribute, all catchments were sorted by score and then normalised to the 0-1 scale (i.e. 0 for a catchment with the smallest and 1 for a catchment with the largest value for the resilience attribute). Finally, catchment specific resilience was calculated as an average of the corresponding values for the resilience attributes. Resilience scores were then redefined as 1-resilience to enable comparison with the exposure and sensitivity components.

2.2.7 CLIMATE CHANGE VULNERABILITY ASSESSMENT

Each of the three dimensions that make up the vulnerability of freshwater ecosystems to climate change, namely exposure, sensitivity and 1–resilience, were assigned a category of 'low' (<0.25), 'medium' (0.25-0.49), 'high' 0.5-0.74) or 'very high' (≥0.75); similar to van Vliet et al. (2013). Given that vulnerability is considered here as a combination of all three dimensions, each having four categories, the three-dimensional logical matrix has 64 score combinations (Table 2-2).

The numerous score combinations can be mapped to 'low', 'medium', 'high' or 'very high' climate change vulnerability in a variety of ways (e.g. Chin et al., 2010, Comer et al., 2012). To account for the variability in these options, four distinct methods were used (see Table 2-2 for details): Vulnerability Assessment Method 1 (VAM_1) is the most pessimistic approach, with the climate change vulnerability calculated as the mean value of the individual dimension scores and classified as 'low' (<0.25), 'medium' (0.25-0.49), 'high' (0.5-0.74) or 'very high' (≥0.75). As such, VAM_1 has 7 score sets in the category 'low', 22 in 'medium', 25 in 'high' and 10 in 'very high'. VAM_2 is based on the symmetric cumulative distribution function, with 10 score combinations in the category 'low', 22 in 'medium', 22 in 'high' and 10 in 'very high'. VAM_3 is based on a positively skewed cumulative distribution function, with 19 score combinations in the category 'low', 19 in 'medium', 16 in 'high' and 10 in 'very high'. VAM_4 is the most optimistic approach and employs the rule that categories are assigned to score combinations based on the single lowest dimension score; e.g. 'low' score in any vulnerability dimension must lead to a 'low' vulnerability classification and so forth, with the 'very

high' vulnerability category only assigned if all three vulnerability dimensions scored 'very high'. This results in 37 score combinations in the category 'low', 19 in 'medium', 7 in 'high' and 1 in 'very high'.

Table 2-2: Different methods for the climate change vulnerability estimation.

Score combinations for vulnerability components			Number of Permutations	VAM_1	VAM_2	VAM_3	VAM_4
very high	very high	very high	1	very high	very high	very high	very high
high	very high	very high	3	very high	very high	very high	high
high	high	very high	3	very high	very high	very high	high
very high	very high	medium	3	very high	very high	very high	medium
high	high	high	1	high	high	high	high
very high	high	medium	6	high	high	high	medium
high	high	medium	3	high	high	high	medium
very high	medium	medium	3	high	high	high	medium
very high	very high	low	3	high	high	high	low
low	high	very high	6	high	high	medium	low
high	medium	medium	3	high	medium	medium	medium
medium	medium	medium	1	medium	medium	medium	medium
high	high	low	3	medium	medium	medium	low
low	medium	very high	6	medium	medium	medium	low
high	medium	low	6	medium	medium	low	low
very high	low	low	3	medium	medium	low	low
medium	medium	low	3	medium	low	low	low
low	low	high	3	low	low	low	low
medium	low	low	3	low	low	low	low
low	low	low	1	low	low	low	low

To help inform and facilitate the development of climate change conservation management strategies, the number of catchments within the European protected areas network (Natura 2000 and WDPA) was assessed for each of the vulnerability assessment methods (VAM_1 to VAM_4) and for the consensus patterns (VAM_1 to VAM_3 and VAM_1 to VAM_4). Within the consensus patterns, a catchment was assigned a vulnerability category only if the same category was assigned for all considered approaches, otherwise it was categorised as 'no consensus'. This 'gap' analysis identified catchments with <25 % of surface area protected by the European protected area networks and predicted to have 'high' to 'very high' vulnerability to climate change

2.3 RESULTS

To explore the vulnerability of European freshwater to climate change at the catchment scale, each vulnerability dimension (exposure, sensitivity and 1-resilience) was analysed separately and in combination with all others. The absolute Pearson correlations between the three vulnerability dimensions are below 0.1 for all combinations of scenarios (A2, B1), time periods and dispersal scenarios, indicating very little statistical dependence. [Note: figures references with a preceding 'A' can be found in the attached appendix (i.e. Figure A1)].

2.3.1 EXPOSURE

Catchments characterised by a combination of large predicted changes in both thermal and hydrological regimes are mainly located in Spain, the Balkan countries and Baltic Sea countries (Figure 2-5a-b). For example, changes to hydrological regimes will mainly affect southern Europe by the 2030s yet are predicted to increase by the 2080s and affect the Pechora, Northern Dvina and Mezen River basins in Russia and northern Scandinavian catchments. Whilst there is little variability between the scenarios for the 2030s (Figure 2-5a-b, Figure A1), variability increases with time so that the percentage area of categories 'high' and 'very high' increases from 33.6 % for 2030s to 84.8 % for 2080s B1 scenario and from 25.2 % to 92.6 % for 2080s A2 scenario (Figure A1).

2.3.2 SENSITIVITY

The sensitivity patterns based on the European Red List are almost identical to those based on the Global Red List (Figure 2-5c-d, Figure A2), and thus only the latter is considered in further analyses. The highest numbers of threatened, restricted range or ecoregion-restricted species were found in catchments along the Croatian Adriatic Sea coastline, for the Balkan Lakes Ohrid and Prespa and the Duero, Tajo and Guadiana River basins in Spain (Figure A2). Lake Ladoga, the only habitat of the fish species *Coregonus ladogae* and the West Highlands of Scotland were found to be highly unique with respect to species' composition. Additionally, warm adapted species in the southernmost parts of Europe appear to be less sensitive to climate warming than species in central and northern Europe (Figure A2f).

The number of globally threatened species per catchment is generally below 5 (84 % of the study area). However, for 21 catchments it is between 15 and 60. As a result, when using the relative species numbers to calculate the individual sensitivity attributes the majority of catchments were assigned 'low' sensitivity (Figure 2-5, Figure A3a-b). In contrast, when applying the conservative approach, most catchments (> 90 %) are in the sensitivity categories 'medium' to 'high' (Figure A3c-d).

2.3.3 RESILIENCE

The degree of a catchments' connectivity appears to have a prevailing influence on all resilience components. Owing to numerous dispersal barriers, resilience is low for most catchments (Figure 2-5e-f). Consequently, the natural potential of the basins' altitudinal range, latitudinal gradient or river network complexity to provide species the opportunity to cope with climate change is considerably low, except for the Northern Caucasus region in Russia and the Piedmont region in Italy (Figure A4). Without dams, the Danube, Neva, Dnieper and the Volga basins could provide 'high' to 'very high' resilience potential due to their high altitudinal range and latitudinal gradient (Figure A4). Consequently, for the dispersal scenario considering dams, resilience scores only fall into categories 'low' (90.2%) and 'medium' (9.8 %), whilst for the dispersal scenario without dams, catchments are distributed across the 'low' (44.5%), 'medium' (27.7%), 'high' (20.6%) and 'very high' (7.3%) categories. It is important to note that these values are inverted (1-resilience) in Figure 2-5 for direct comparison with exposure and sensitive components (i.e. a 'low' 1-resilience scores correspond to a 'very high' resilience classification).

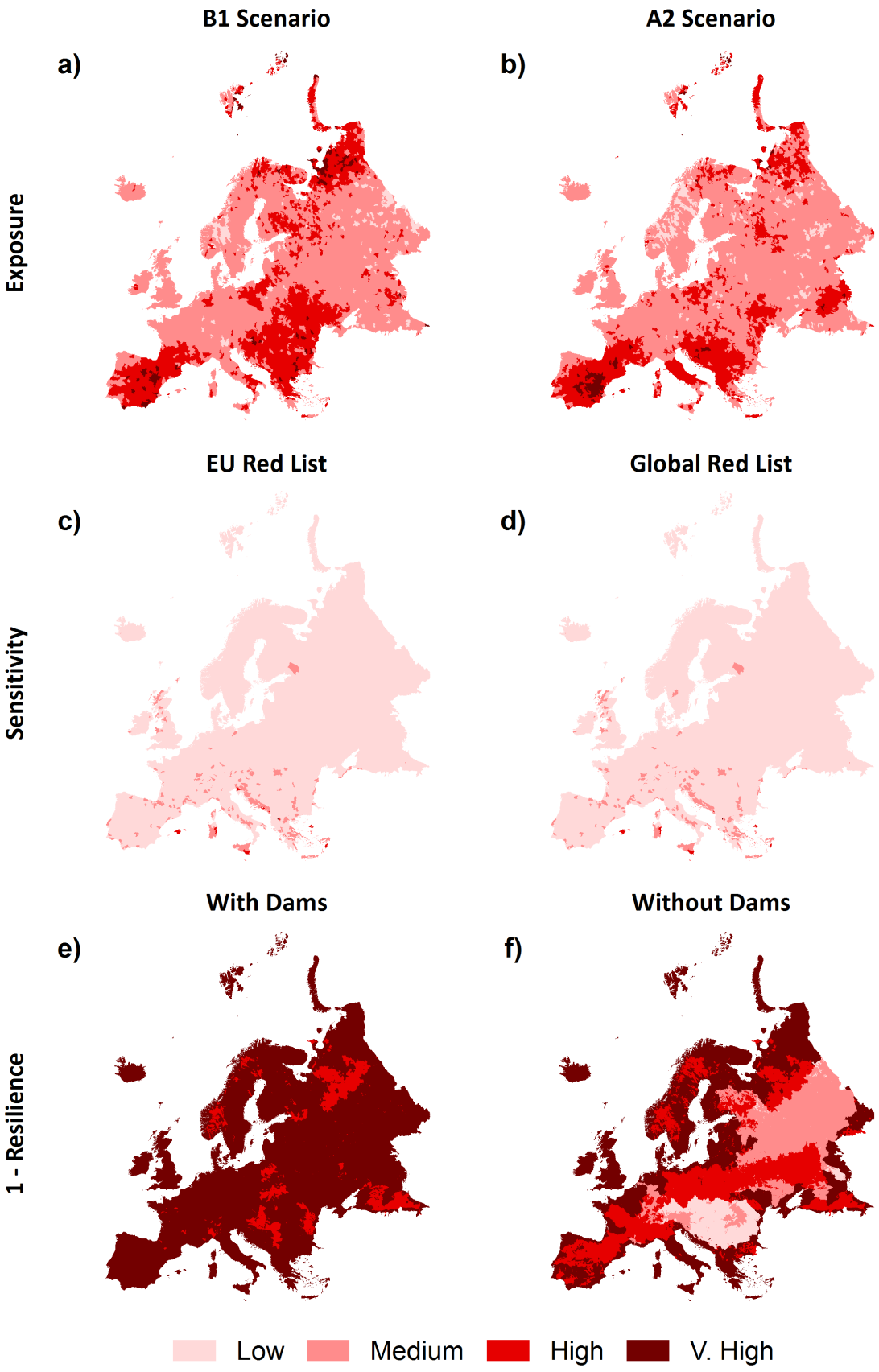


Figure 2-5: The final scores for the exposure (a, b), sensitivity (c, d), and 1- resilience (e, f) following different scenarios: a) the exposure for 2030s following B1 scenario; (b) the exposure for 2030s following A2 scenario; c) the sensitivity based on all five sensitivity dimensions with the 'presence of threatened species' using the European Red List and d) using species' global Red List Category; (e, f) shows 1- resilience score with (e) and without (f) consideration of dam influence.

2.3.4 CLIMATE CHANGE VULNERABILITY

Table 2-3 and Table A1-5 provide summary statistics for the number of catchments, percentage surface area and percentage protected area for each climate change vulnerability category and each vulnerability method, whilst Table 2-4 and Table A5 provide summary statistics for the consensus methods. A comparison between the vulnerability estimates based on the 'standard' and the 'conservative' sensitivity approaches is provided for the most pessimistic VAM (VAM_1, Table 2-3 vs. Table A1 and Figure 2-6 vs. Figure A5). Specifically, the 'conservative' sensitivity approach predicted 'medium' to 'high' sensitivity to climate change for most catchments (Figure A5), since the presence of a single threatened or restricted range species was enough to register sensitivity. As such, the 'conservative' sensitivity approach generally predicted higher vulnerabilities than the 'standard' approach (e.g. for 2030s B1 scenario with dams, 66.5 % of area with 'high' vulnerability for the 'conservative' approach vs. 71.9 % of area with 'medium' vulnerability for the 'standard' approach). Consequently, within all further analyses the 'standard' sensitivity approach was used, as it provides a relative sensitivity for a given species composition and is thus more appropriate to characterise vulnerability of the freshwater ecosystems at the catchment scale than the 'conservative' approach that considers individual species.

Overall, there are considerable variations in the spatial distribution of vulnerability categories across different vulnerability methods. For the most optimistic method (VAM_4), irrespective of the scenario and timeline, more than 95% of European river and lake catchments are predicted to be in the 'low' vulnerability category. Such vulnerability predictions are highly unrealistic given predicted shifts in climate and widespread impoundment of rivers. Therefore, following the precautionary principle (Myers, 1993), only VAM_1, VAM_2 and VAM_3 were included in further analyses (for completeness, results for VAM_1 to VAM_4 can be found in: Table A5, Figure A9).

Table 2-3: Summary statistics for the VAM_1 based climate change vulnerability categories using the 'standard' sensitivity assessment. No. catchments are the number of catchments in each vulnerability category ('low', 'medium', 'high' and 'very high'). Surface area denotes the percentage of the total study area (10,073,990 km^2), and protected area denotes the percentage of the surface area found within the European protected area networks (Natura 2000 and WDPA for IUCN categories I-IV). Note that for 13 catchments the climate change vulnerability could not be estimated due to missing data on the resilience components.

	Scenario/ category	2030s B1 dams	2030s A2 dams	2080s B1 dams	2080s A2 dams	2030s B1 no dams	2030s A2 no dams	2080s B1 no dams	2080s A2 no dams
No. catchments	low	0	0	0	0	1087	1080	9	12
	medium	13161	14243	6333	4166	14501	15098	11342	9531
	high	5600	4515	12411	14536	3174	2581	7397	9176
	very high	9	12	26	68	8	11	22	51
surface area [%]	low	0.0	0.0	0.0	0.0	6.0	5.9	0.0	0.0
	medium	71.9	76.9	38.9	25.8	77.2	80.2	63.6	54.2
	high	28.0	22.9	60.8	73.3	16.7	13.8	36.1	45.2
	very high	0.1	0.1	0.3	0.9	0.1	0.1	0.3	0.5
protected area [%]	low	0.0	0.0	0.0	0.0	7.8	12.5	0.0	64.0
	medium	10.1	10.1	9.4	8.4	11.0	10.5	10.4	10.2
	high	16.1	17.2	13.6	13.2	17.4	18.8	15.2	14.4
	very high	58.2	32.8	36.4	26.0	53.7	35.0	34.5	32.0

Table 2-4: Summary statistics for the VAM_1, VAM_2 and VAM_3 consensus-based climate change vulnerability categories using the 'standard' sensitivity assessment. No. catchments are the number of catchments according to all of the major vulnerability estimation methods (VAM_1, VAM_2 and VAM_3) in the vulnerability categories ('low to medium' and 'high to very high', with 'no consensus' denoting catchments where the three vulnerability estimation methods did not agree on the vulnerability category. Surface area denotes the percentage of the total study area (10,073,990 km^2), and protected area denotes the percentage of the corresponding surface area that is within the European protected area networks (Natura 2000 and WDPA for IUCN categories I-IV). Note that for 13 catchments the climate change vulnerability could not be estimated due to missing data on the resilience components.

	Scenario	2030s B1 dams	2030s A2 dams	2080s B1 dams	2080s A2 dams	2030s B1 no dams	2030s A2 no dams	2080s B1 no dams	2080s A2 no dams
No. catchments	low to medium	13280	14481	6768	4125	15706	16279	11925	9948
	high to very high	573	548	1098	2942	459	373	768	1703
	no consensus	4930	3754	10917	11716	2618	2131	6090	7132
surface area [%]	low to medium	69.8	75.0	38.4	23.9	82.9	84.9	66.0	56.1
	high to very high	5.2	4.9	8.1	15.9	4.0	3.3	5.7	9.9
	no consensus	25.0	20.1	53.5	60.1	13.1	11.8	28.3	34.0
protected area [%]	low to medium	10.4	10.4	9.5	8.3	11.0	10.9	10.4	10.2
	high to very high	23.4	23.1	25.3	19.7	23.8	26.0	25.6	21.3
	no consensus	14.7	15.9	12.0	11.6	15.5	16.9	13.3	12.7

For dispersal scenarios with dams, vulnerability is generally one category more severe than for those without dams. The differences between dispersal scenarios are particularly pronounced in the Danube, Neva, Dnieper and the Volga basins (Figure 2-7 and Figure A6-8). For the 2030s, there is a consensus among the applied methods that the majority of catchments have 'low' to 'medium' vulnerability to climate change (>60 % of the study area, Table 2-4, Figure 2-7), with up to 573 lake and river catchments predicted to have 'high' to 'very high' vulnerability for methods VAM_1 to VAM_3 (Table 2-4, Figure 2-7). For the 2080s, the consensus between the vulnerability methods is lower than for 2030s, suggesting considerable uncertainty. However, most methods indicate vulnerability increases for the 2080s compared to 2030s across southern Europe (Spain, Italy, Balkan countries) and northern Europe (Scandinavia and northernmost parts of Russia).

Lake Ohrid (shared by the Republic of Macedonia and Albania) and Lake Prespa (shared by Albania, Greece and the Republic of Macedonia) are predicted to have 'very high' vulnerability to climate change for VAM_1 to VAM_3 and all scenarios and timelines. Similarly, 'high' to 'very high' vulnerability to climate change is predicted in Lake Skadar (shared between Albania and Montenegro), Lake Ladoga (Russia), the Greek islands of Rhodes and Lesbos, the Spanish island of Mallorca, the Italian islands of Sardinia and Sicily and for catchments along the Adriatic Sea coast, eastern Spain, southern Greece, western Italy, northern Russia and Finland, Crimea and in the north-west of England and highlands of Scotland (Figure 2-7). Furthermore, catchments with 'high' to 'very high' vulnerability to climate change for VAM_1 to VAM_3 (Table 2-4) have, on average, less than 25% of their area covered by the European protected areas network. A gap analysis was conducted to analyse the congruence between vulnerability maps for the 2030s and 2080s (using the most pessimistic scenario (B1) with dams) and the existing European PA network, identifying priority catchments for future management actions (Figure 2-8).

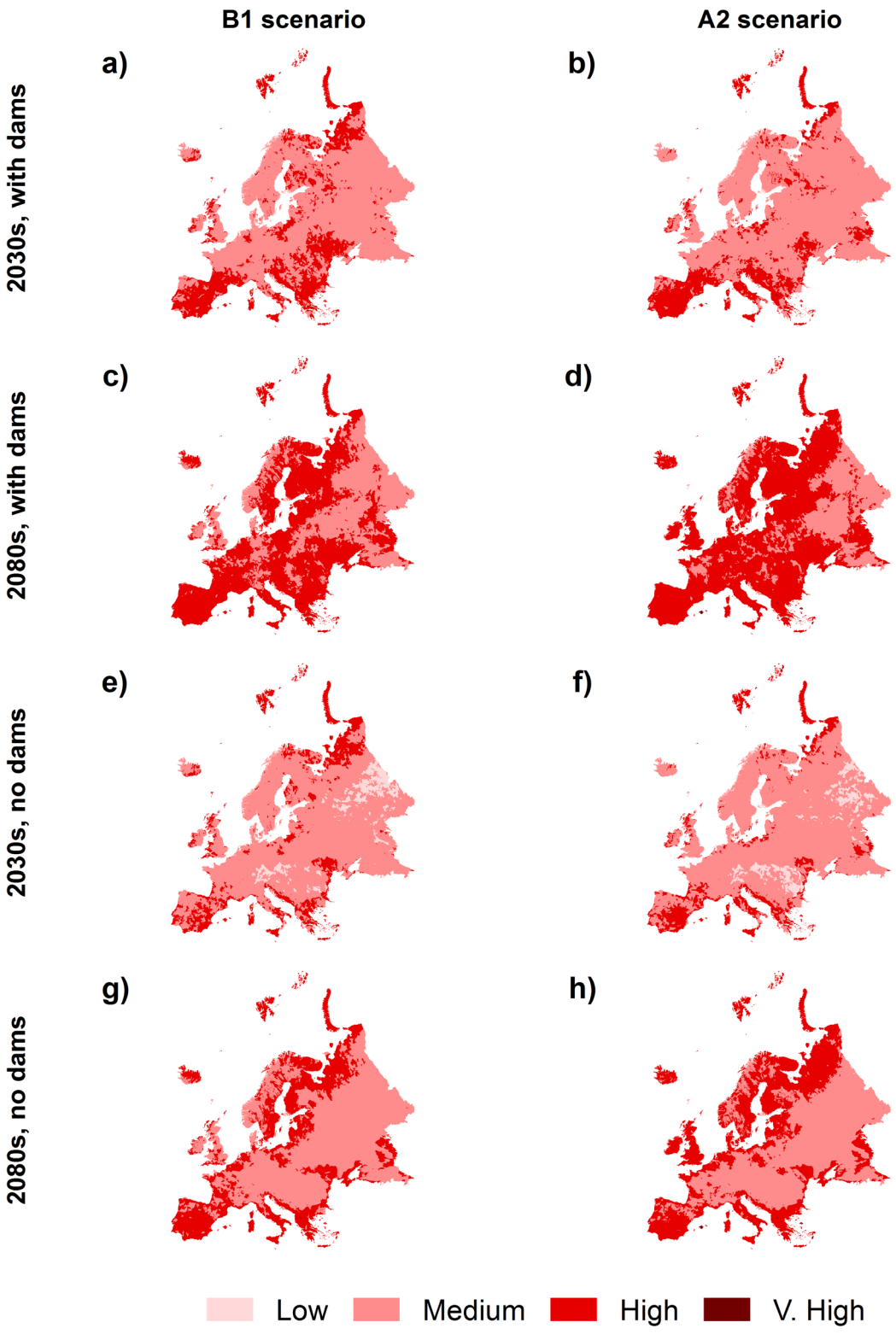


Figure 2-6: The vulnerability to climate change for European freshwater ecosystems at the catchment scale: a) 2030s exposure, B1 scenario, with dams; b) 2030s exposure, A2 scenario, with dams; c) 2080s exposure, B1 scenario, with dams; d) 2080s exposure, A2 scenario, with dams; e) 2030s exposure, B1 scenario, without dams; f) 2030s exposure, A2 scenario, without dams; g) 2080s exposure, B1 scenario, without dams; h) 2080s exposure, A2 scenario, without dams; The sensitivity dimension is based on the species Global Red List Category and adopts the 'standard' assessment. The vulnerability calculation is based on the method VAM_1 (see Table 2-2). Summary statistics are provided in Table 2-3.

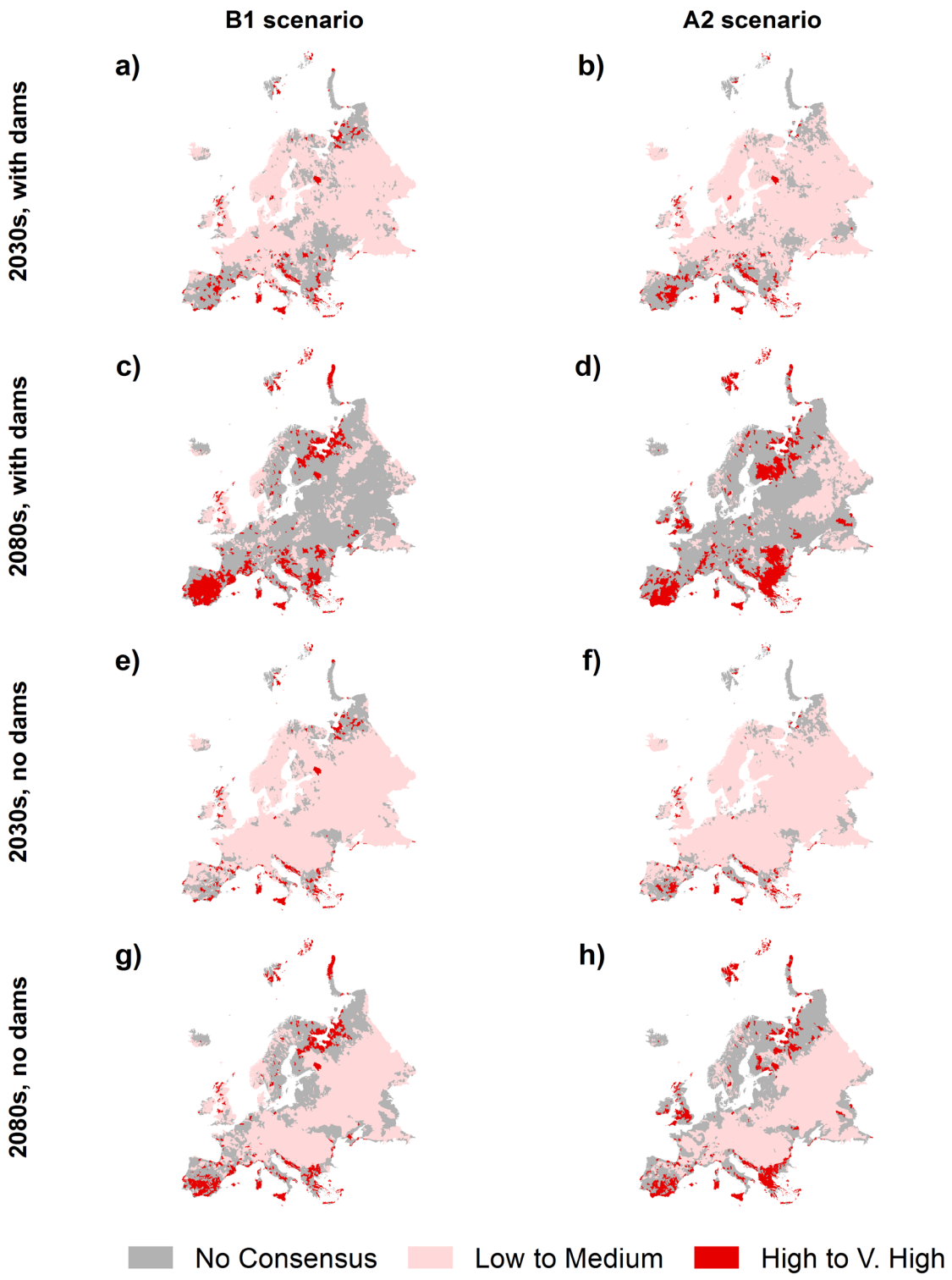


Figure 2-7: Consensus pattern of the vulnerability to climate change for the scenario with dams (a-d) and without dams (e-h): a) 2030s exposure, B1 scenario, with dams; b) 2030s exposure, A2 scenario, with dams; c) 2080s exposure, B1 scenario, with dams; d) 2080s exposure, A2 scenario, with dams; e) 2030s exposure, B1 scenario, without dams; f) 2030s exposure, A2 scenario, without dams; g) 2080s exposure, B1 scenario, without dams; h) 2080s exposure, A2 scenario, without dams. Within the consensus approach, a catchment was assigned the category 'low to medium' or 'high to very high' only if the same category was assigned for VAM_1, VAM_2 and VAM_3 methodologies; otherwise it was assigned 'no consensus'. All VAM used the 'standard' sensitivity assessment. Summary statistics are provided in Table 2-4.

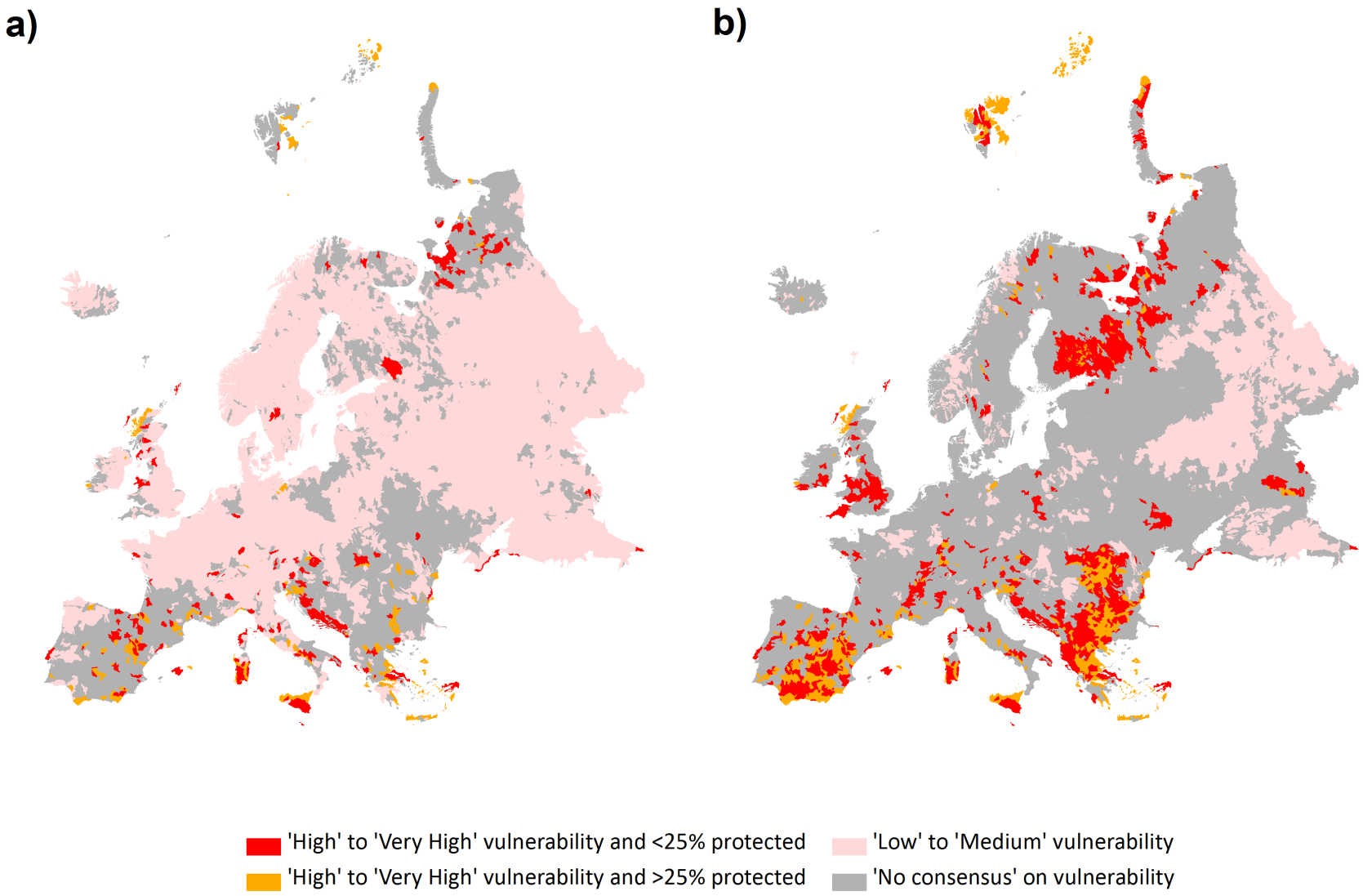


Figure 2-8: Gap analysis of Protected Areas and Climate Change Vulnerability. The most pessimistic scenarios were chosen for the 2030s and 2080s from the consensus of VAM_1, VAM_2 and VAM_3 methodologies to highlight catchments most in need of management actions (< 25 % of their area protected by the current European protected area network and *'high'* to *'very high'* climate change vulnerability) a) 2030s exposure, B1 scenario, with barriers; b) 2080s exposure, A2 scenario, with barriers. Summary statistics found in Table 2-4.

2.4 DISCUSSION

The results highlight the Ebro basin in Spain, Garonne in France, Pechora in Russia and catchments along the Adriatic coast and northern Scandinavia as likely to experience the highest levels of exposure to climate change, confirming and refining the findings of van Vliet et al. (2013) and Laizé et al. (2014). The biodiversity rich ancient lakes of Ohrid and Prespa, situated in the central Balkans, are also shown to be particularly sensitive to climate change. This is primarily due to their large numbers of restricted-range and endemic species; Lake Ohrid alone supports 212 known endemic species and is probably the most diverse lake in the world given its size (358 km^2) (Albrecht and Wilke, 2009). The resilience of freshwater ecosystems to climate change was shown to be strongly impaired by the anthropogenic disruption of hydrologic habitat connectivity by dams. The effect of dams was highest in the basins of the Danube, Neva, Dnieper and Volga Rivers, significantly reducing species' dispersal potential. Specifically, strictly aquatic species such as diadromous fishes (those that migrate between sea and freshwaters to complete their life cycle) and endemic fishes, like most of the sculpins (Cottus spp.), are among the most impacted by this connectivity loss (Liermann et al., 2012). Most of the European diadromous fish species are now endangered, signifying that climate change paired with connectivity loss needs to be considered within current conservation plans (Lassalle et al., 2008).

The consensus vulnerability maps show the Balkan Lakes and Mediterranean islands to be most vulnerable to climate change, along with up to 573 lake and river catchments predicted to have *'high'* to *'very high'* vulnerability scores by the 2030s and 2,942 by the 2080s. Of these, less than 25% (by area) are situated within current protected areas, which generally have been designated for terrestrial conservation and thus do not protect freshwater biodiversity (Nel et al., 2009b, Nel et al., 2011a). This, coupled with pollution due to poor land use practices and unsustainable water abstraction (Woodward et al., 2010), present a strong argument for review of the current protected area network to ensure persistence of freshwater ecosystems and the services they provide. The most vulnerable catchments identified in this study and the catchments identified in the gap analysis provide a practical starting point for future planning and mitigation strategies.

Uncertainty in the climate change vulnerability estimates were reduced through the application of this framework by using a variety of taxonomic groups (plants, fishes, molluscs, amphibians, crayfish and turtles) coupled with the high spatial resolution of the planning units (>18,000 European lake and river catchments). Specifically, consideration of the magnitude and direction of change in the hydrological and thermal regimes for multiple GCMs and hydrological models has provided more refined estimates of climate change exposure for freshwater ecosystems than has been possible at this spatial scale before. In addition, Key Biodiversity Areas (of which AZEs are a subset) are defined as the most important areas for the global persistence of biodiversity. The inclusion of KBA criteria in the vulnerability framework enabled identification of the KBAs that are most at threat from climate change, complementing the study by (Carrizo et al., 2017) and providing an additional means of prioritising catchments for management. Furthermore, by explicitly including upstream and downstream connectivity, this framework has overcome the major limitation of most commonly used bioclimatic methods (see Poff et al. (2012)). Finally, the combination of different vulnerability assessment methods to form consensus maps helped reduce uncertainties related to each of the individual methods.

Despite this comprehensive framework, estimates of the vulnerability of European river and lake catchments to climate change are affected by several limitations. For example, the methodology does not account for the variability in the dispersal capacity amongst the species studied. Also, the capacity for lake-dwelling species to seek refugia within lake ecosystems has not been included (Angilletta, 2009). More importantly, in addition to climatic factors, a complex interplay of other issues, including shifts in phenology, evolutionary adaptation, pollution, over-abstraction of water and biotic interactions, determine species success in dealing with climate change. Also, the effects of climate change could be amplified by synergies with other stressors. For example, elevated temperatures during summer droughts could intensify the impacts of eutrophication and toxins by increasing pollutant concentrations (Woodward et al., 2010). Consequently, further research is required to improve the 'proof-of-concept' vulnerability estimates presented here. Specifically, there is a need to further understand the role that hydrological catchment connectivity plays in species-

specific ability to cope with climate change, how species evolutionary history confers adaptive potential and the effectiveness of current protected area networks in ensuring persistence of freshwater biodiversity. Furthermore, protected area planning will also need to facilitate species dispersal to more suitable habitats (Linke et al., 2011, Nel et al., 2011a, Bagchi et al., 2013), including options that enable species' movement across dispersal barriers, or ultimately, options for assisted colonisation (Hoegh-Guldberg et al., 2008).

In summary, climate change is expected to amplify existing threats within catchments, alongside causing novel shifts in the hydrological, thermal and biotic components of freshwater ecosystems. The ability of species and communities to adapt to climate change, together with the availability of in-stream refugia and options for species to move across natural and artificial barriers will become increasingly important as time progresses. Additionally, an important and typically overlooked factor is the human response to climate change through management actions and mitigation strategies (Stein et al., 2013). Specifically, strong cross-sector cooperation among government and industry stakeholders to implement Integrated River Basin Management (IRBM) is required. This should be supported by systematic conservation planning and monitoring across catchments. A shift in thinking from terrestrial management approaches to one of focal areas, critical management zones and catchment management zones (Abell et al., 2007) will provide the framework for freshwater management at the regional scale. Within this framework immediate action should include: i) a review of management plans by catchment management authorities and protected area managers to ensure that freshwater systems are both targets for conservation and to raise awareness of the climate change vulnerability of the catchment to promote cooperation among all stakeholders; ii) catchment-scale risk assessments based on current and planned industry practices and developments both within the vulnerable catchments identified here and in other catchments to ensure their resilience is not degraded and; iii) identification of opportunities to increase catchment resilience by restoring and enhancing functions such as ecological flows and connectivity for species dispersal, for instance with fish passes in dams.

Therefore, to sustain freshwater biodiversity in the future, a proactive, strategic and holistic management approach is needed to reconcile the needs of all ecosystem actors. This research redresses the current paucity of integrated climate change assessments for freshwater ecosystems by presenting an overview of climate change vulnerability at the European scale that offers a basis for informing these new management approaches.

Chapter 3 THAMES BASIN: MODEL CALIBRATION

3.1 INTRODUCTION AND OBJECTIVES

Conceptually, at the basin scale, the aim of this research is to test the application of a vulnerability framework in determining the sensitivity of key Water Framework Directive indicators of ecosystem health to perturbations in two key climatic variables; mean annual precipitation and temperature. Critically, exposure is externalised from the vulnerability framework using a scenario-neutral, 'bottom-up' approach to assessing climate change. The potential impact of climate change can be determined through the incorporation of any predictive GCM outputs (exposure), generating a probabilistic envelope of future risk for each catchment. Finally, the concept of resilience is explored through outlining several management strategies identified from the resilience literature (e.g. stream shading, adding meanders (Wilby et al., 2010)) aimed at reducing the impact of alterations in each of the WFD indicators.

The local-scale study focuses on the non-tidal portion of the Thames Basin (all catchments upstream of Teddington Weir, London). The River Thames is a major river in southern and south-eastern England, draining 9,927km^2 and providing freshwater to approximately 14 million people (Gardiner et al., 1994), the majority of whom live downstream within London. The Thames receives treated wastewater from approximately 3 million people, with major sewage treatment plants typically concentrated in the lower reaches near London (Kinniburgh and Barnett, 2010). The river is sourced in Cricklade, Gloucestershire and flows through major cities such as Oxford, Reading and London before discharging into the North Sea below Teddington. The basin geology is dominated by high permeability chalk, with limestone in the headwaters and low permeability clay/mudstone present both up-stream and downstream of the chalk area (Bloomfield et al., 2011) (see Figure 3-1). Furthermore, water quality is dominated by high pH and high base cation water where chalk aquifers are present (Neal et al., 2000). The basin is also heavily farmed, with 35.5% of the basin used for intensive agriculture. The upper part of the basin is predominantly arable land interspersed with grassland, with very little urban land in the headwaters. The proportion of urban land increases into

the eastern part of the basin, becoming the predominant land-use type in the lower-most catchments around London. Approximately 13% of the entire basin is wooded, with wetlands (floodplains and marshes) encompassing 4% (see Figure 3-2). The climate is temperature, with both Atlantic and continental influences. The mean annual precipitation is 730 mm (1960–2014, with a minimum of 538 mm in 1973 and a maximum of 974 mm in 2000) and the annual average temperature is 10.7°C (1960–2014, minimum: 8.6°C in 1963, maximum 12.1°C in 2014), with a difference of around 1.5–2°C between the interfluve and the valleys. The average summer temperature is 16.5°C and the average winter temperature is 4.7°C (Bussi et al., 2016c). The average daily flow is 67 m^3s^{-1}, with a daily Q_5 (discharge exceeded only 5% of the time) of 206 m^3s^{-1} (measured at the most downstream reach, Teddington Weir) (CEH, 2015). Average daily flow in the Thames varies considerably throughout the year, with high flows in winter from October to February of 82.3 m^3s^{-1} (50th percentile) to lower flows in summer from March to September of 42.2 m^3s^{-1} (50th percentile) (Jin et al., 2012, Crossman et al., 2013c).

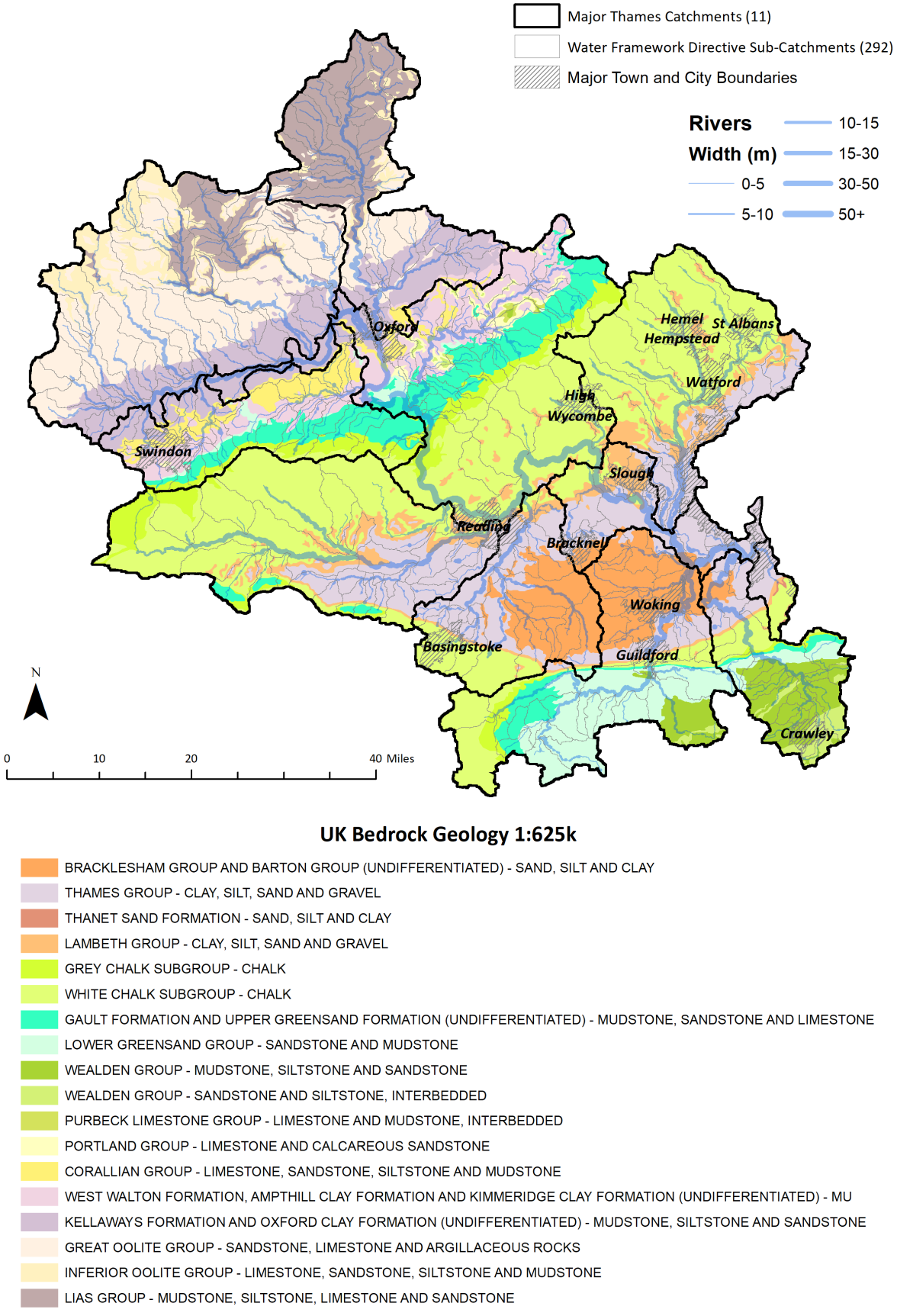


Figure 3-1: Geology within the Thames Basin. Data from UK bedrock geology map 1:625k scale, used under Open Government Licence.

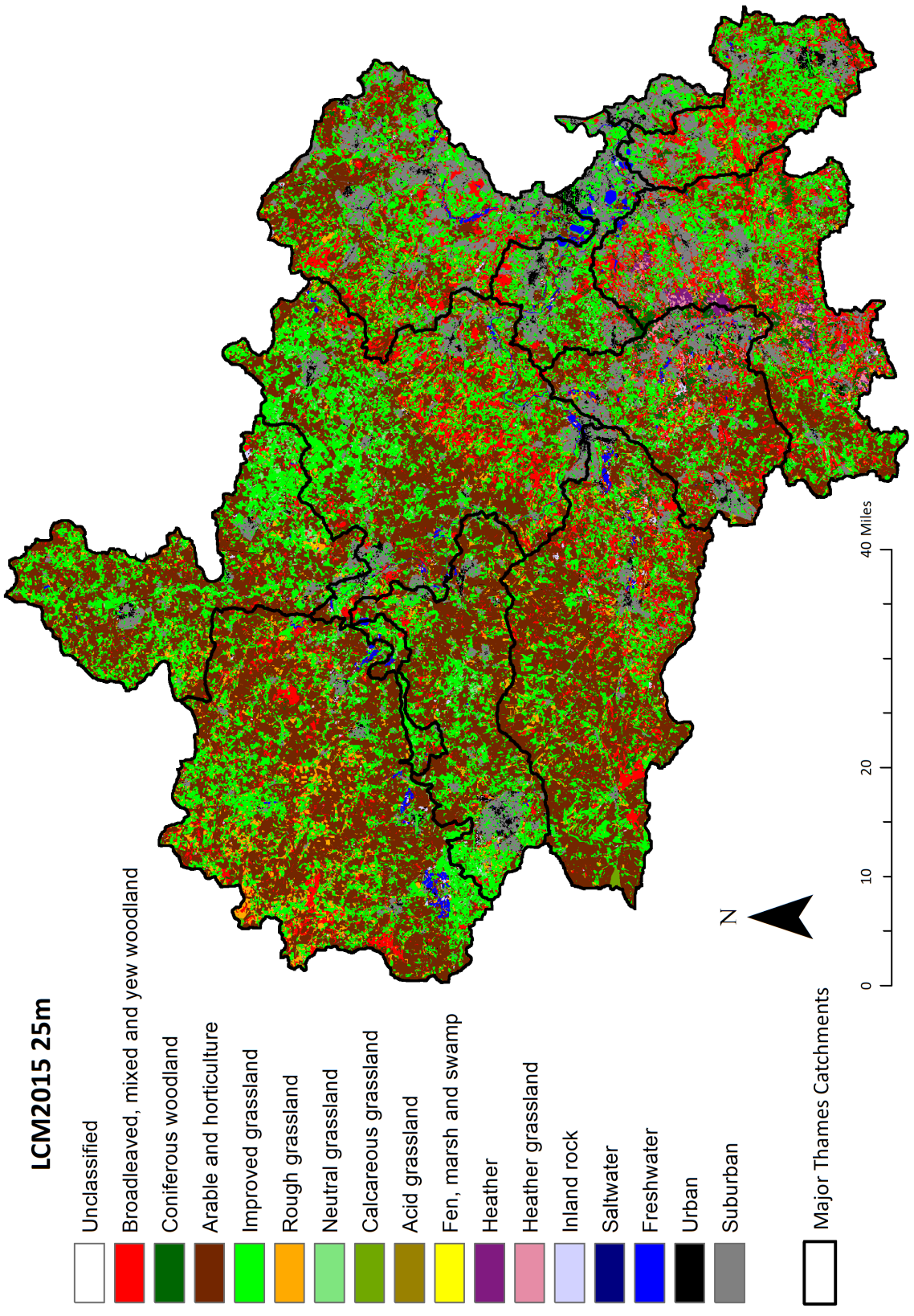


Figure 3-2: Land Cover within the Thames Basin. Data from LCM15 used under licence from CEH.

3.2 INTRODUCTION TO THE INTEGRATED CATCHMENT (INCA) MODELS

The suite of dynamic, process-based Integrated Catchment (INCA) models were used in this study to simulate baseline and future daily river discharge and water quality (Whitehead et al., 1998b). INCA is a well-established model framework, having been implemented in over 40 catchments across the UK and EU, in addition to individual cases in North and South America, Asia and Australia. The models produce daily estimates of stream discharge and water quality, analysing inputs from both diffuse and point sources (Whitehead et al., 2009), through the simulation of flow pathways and pollutant fluxes in terrestrial and aquatic environments. The model is spatially distributed, enabling user-specified variation in reach lengths, rate coefficients, land use, velocity flow relationships, and deposition. The model has been recently modified to simulate fully branched river networks, where there are no restrictions on tributary inputs, or stream orders (Whitehead et al., 2011). Two fully branched versions of INCA are used in this study; INCA-P, to simulate phosphorus and sediment, and INCA-N, to simulate nitrogen. Within the models, information flows from the individual process equations, through the sub-catchment comprised of five land use types, to a hierarchical network of multiple reaches and tributaries. A mass balance is imposed at all sub-catchment and river reach boundaries, operating on multiple scales: the cell level for each individual land use, the sub-catchment level for multiple land use inputs and transport of nutrient fluxes along reaches, and at the network scale for total loads from all sub-catchments (Whitehead et al., 2011).

Specifically, the hydrological component of INCA models flow moving through the soil zone, the groundwater zone and river system. This is formulated as a simple two box system, with hydrologically effective rainfall moving through the soil system and either recharging groundwater or leaching into the river reach. Groundwater flows are also routed to river reaches after a suitable delay controlled by residence time. A series of differential equations, outlined below, explain (i) the flow of water through the land-components (buckets) within a reach and; (ii) the flow of water between reaches. In each instance, the equations are solved using a fourth order Runge-Kutta

method of solution with a Merson variable step length integration routine (Whitehead et al., 1998b). This method enables the stable integration of equations thus minimising numerical problems.

The flow models for the two zones in the plant/soil system are given as:

Soil zone: $$\frac{dx_1}{dt} = \frac{1}{T_1}(U_1 - x_1)$$

Groundwater zone: $$\frac{dx_2}{dt} = \frac{1}{T_2}(U_s x_1 - x_2)$$

Where x_1 and x_2 are output flows (m^3s^{-1}) for the two zones and U_1 is the input driving hydrologically effective rainfall (HER). T_1 and T_2 are time constants associated with the zones and U_s is the baseflow index (i.e. proportion of water being transferred to the lower groundwater zone).

The river flow model is based on the mass balance of flow between a multi-reach river system. Within each reach, flow variation is determined by a non-linear reservoir model, as described in terms of the relationship between inflow, (I) outflow (Q), and storage (S) as given by:

$$\frac{ds(t)}{dt} = I(t)Q(t)$$

Where, $S(t) = T(t) \times Q(t)$, with T a travel time parameter, which can be expressed as:

$$T(t) = \frac{L}{v(T)}$$

Where L is the reach length and v, the mean flow velocity in the reach (ms^{-1}), is related to discharge, Q, through:

$$v(t) = aQ^b(t)$$

Where, a and b are constants to be estimated from tracer experiments or derived theoretically from Manning's formula using known river reach parameters. This hydrological model forms the basis for all INCA models and, whilst relatively simple, is effective in simulating flows along rivers.

Simultaneously, whilst solving flow equations it is possible to solve mass balance equations for nitrate-nitrogen, ammonium-nitrogen and various forms of phosphorus in both the soil and groundwater compartments. INCA-N models the following key processes in the soil zone using a series of generalised differential equations that account for both temperature and soil moisture-dependent reaction kinetics: plant uptake for NH_4-N and NO_3-N, ammonia nitrification, denitrification of NO_3-N, ammonia mineralisation, ammonia immobilisation and N fixation. Furthermore, the land phase model accounts for all the inputs affecting each land use, including dry and wet deposition of NH_4-N and NO_3-N and fertiliser addition for both NH_4-N and NO_3-N (e.g. as ammonium nitrate). The specifics of differential model structure and process equations for INCA-N are detailed in Whitehead et al. (2006) and Wade et al. (2007). Similarly, INCA-P uses a series of interconnected differential equations to model key processes in the soil, groundwater, water column and stream bed. These include reaction kinetics, nutrient recycling, exchange with the sediments and sediment diagenesis. Furthermore, INCA-P accounts for stocks of inorganic and organic P in the soil (in readily available and firmly bound forms), and Total Phosphorus (TP) in groundwater and stream reaches (Dean et al., 2009). The input fluxes accounted for in INCA-P include atmospheric deposition, inorganic fertilizer, plant residue, livestock waste and slurry application. Stream output is calculated by subtracting various output fluxes, such as plant uptake and movement to firmly bound P, from these inputs (Whitehead et al., 2009). The details of differential model structure about the process equations for INCA-P are described in Wade et al. (2002a), (2002b) and Whitehead et al. (2009), (2011). These key inputs, outputs and process within both INCA-N and INCA-P are outlined in Figure 3-3.

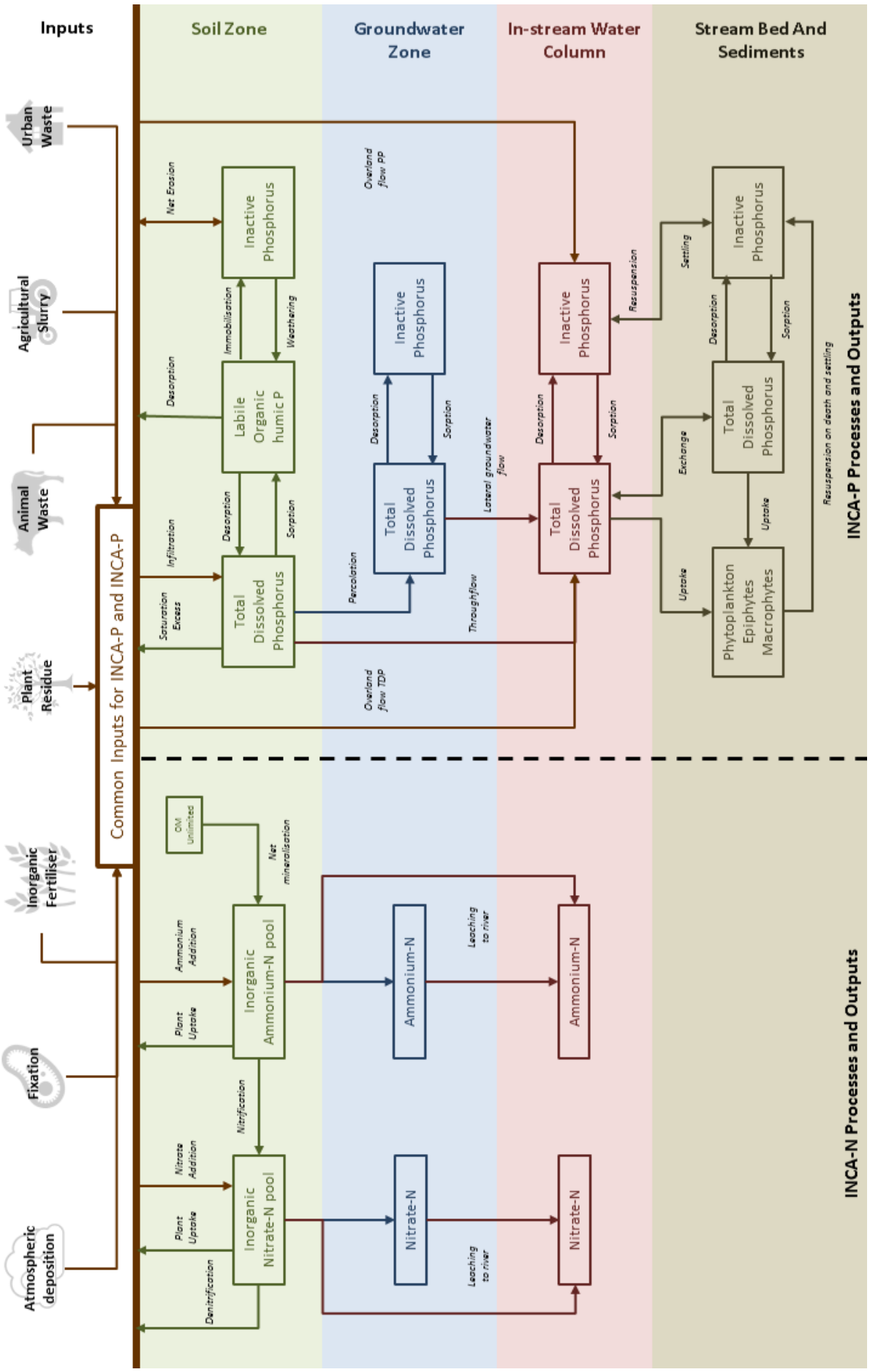


Figure 3-3: Overview of the inputs, processes and outputs considered in both INCA-N and INCA-P models.

3.3 CALIBRATION OF PERSiST MODEL FOR USE IN INCA

INCA requires time series of precipitation, temperature, Hydrologically Effective Rainfall (HER) and Soil Moisture Deficit (SMD) as inputs. These are provided through the Precipitation, Evapotranspiration and Runoff Simulator for Solute Transport (PERSiST) watershed-scale hydrological model, which has been specifically designed for use with the INCA family of models (Futter et al., 2014). PERSiST requires daily time-series of observed precipitation and air temperature from one or more sites within the catchment as driving data. PERSiST conceptualises a watershed as a series of sub-catchments consisting of one or more landscape units. Each unit consists of interconnected water stores (or 'buckets') that control hydrologic response and simulate water fluxes through the terrestrial part of a catchment and into rivers and streams (Lindström et al., 1997).

Observed daily time-series of precipitation (mm) and temperature (°C) were obtained from the British Atmospheric Data Centre for 45 meteorological sites across the Thames catchment (where meteorological data existed for the period 1961-present). These were combined to form a single time-series of average precipitation and temperature values across the whole Thames catchment. The PERSiST model was run using this input time-series as driving data and calibrated against existing observed flow data provided by the Environment Agency over the 30-year time period of 1984-2013. An existing study by Futter et al. (2014) implemented a Monte Carlo-based approach to sensitivity and parameter uncertainty analysis for the Thames Basin. This determined that model results were particularly sensitive to evapotranspiration parameters and residence times (Futter et al., 2014). Therefore, catchment information and parameters were adapted from Futter et al. (2014) for the application of PERSiST in the Thames catchment in this thesis. During the calibration process, the feasible space of model parameters for evapotranspiration and residence times was sampled randomly and 10,000 parameter-sets were generated. The PERSiST model was subsequently run using each of these parameter sets over the 1984-2013 period, and model performance was compared with observed daily stream flow values using the Nash Sutcliffe Co-efficient and R^2 value (Nash and Sutcliffe, 1970). A simulated-annealing algorithm was used to estimate the global

minimum (in terms of modelled/observed ratio of NSE and R^2) of the multivariate parameter sets, whilst disregarding extraneous local minima (Sumner et al., 1997, Madsen et al., 2002). This combination of model calibration based on the use of generic search routine and user-specified calibration priorities generated a best-fit PERSiST model with an average R^2 value of 0.812 and a Nash Sutcliffe Co-efficient of 0.802 for each of the reaches. This suggests a 'very high' level of model performance in reproducing observed flows following the model evaluation guidelines given by Moriasi et al. (2007) (see Figure 3-4). A daily time-series containing HER and SMD for the period 1984-2013 was subsequently produced for input into the INCA models.

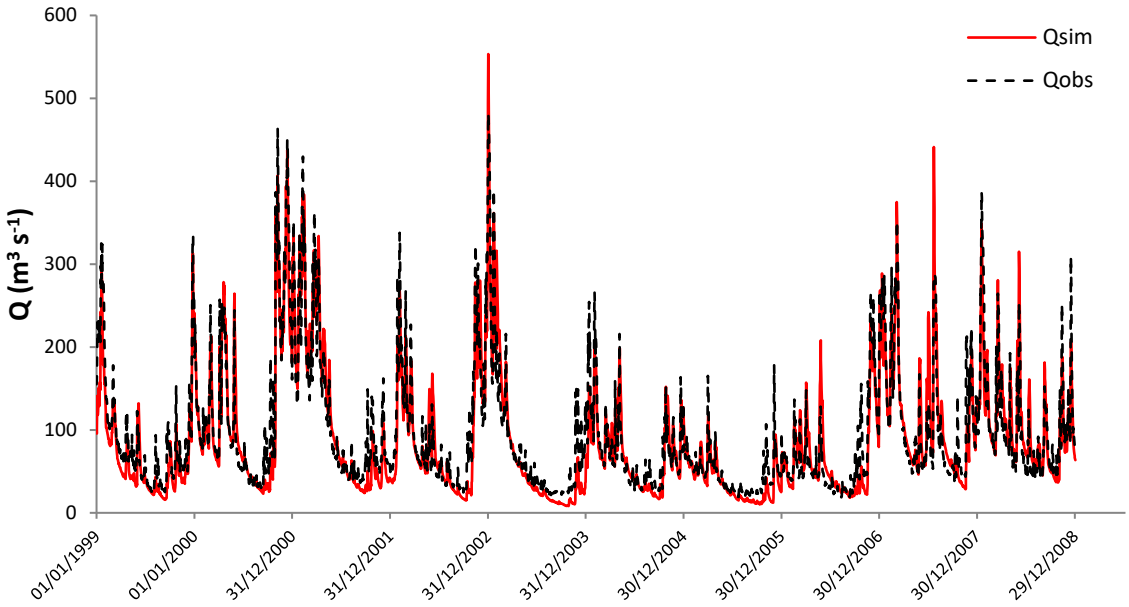


Figure 3-4: Observed and predicted discharge (m^3s^{-1}) from calibrated PERSiST model for Teddington Weir (furthest downstream catchment) over a 10-year period (1999-2008). This reach has an R^2 = 0.875 and NSE = 0.866.

3.4 DELINEATION OF SUB-CATCHMENTS AND DEVELOPMENT OF RIVER NETWORK

Existing applications of INCA on the Thames Basin divided the catchment into 22 reaches (average length 9,893m) and sub-catchments (average area 454km^2) from the source at Cricklade to the lowest weir on the freshwater downstream boundary at Teddington (Jin et al., 2010, Crossman et al., 2013c, Bussi et al., 2016a, Bussi et al., 2016c, Bussi et al., 2017). Such coarse resolution is of limited use in the development of management strategies and conservation plans, as management decisions are frequently made at a significantly finer scale. Thus, to provide meaningful planning units for the study, the WFD sub-catchment data layer used by the Environment Agency to implement monitoring and management plans was chosen (EA, 2014b). This divides the Thames Basin into 292 sub-catchments and provides an order of magnitude improvement in terms of resolution over existing applications of INCA in the region. In addition to this, a high resolution dendritic river network was created for the Thames region based on the Digital River Network (DRN) (used under the Open Government Licence (2015)), providing the reach structure for each sub-catchment (see Figure 3-5) (used under licence A2975 from the EA). Combining these data layers enabled the creation of a fully branched INCA model of the Thames Basin that accurately simulated the flow of water through all 292 sub-catchments. However, the INCA models were unable to simulate all 292 catchments combined for the calibration period of 1984-2013 due to the processing constraints of the model. Therefore, it was necessary to split the Thames Basin into 11 sub-basins (each comprised of sub-catchments) and model them individually. Thus, in total, 22 INCA models were developed that simulated the entire region of interest (Figure 3-5).

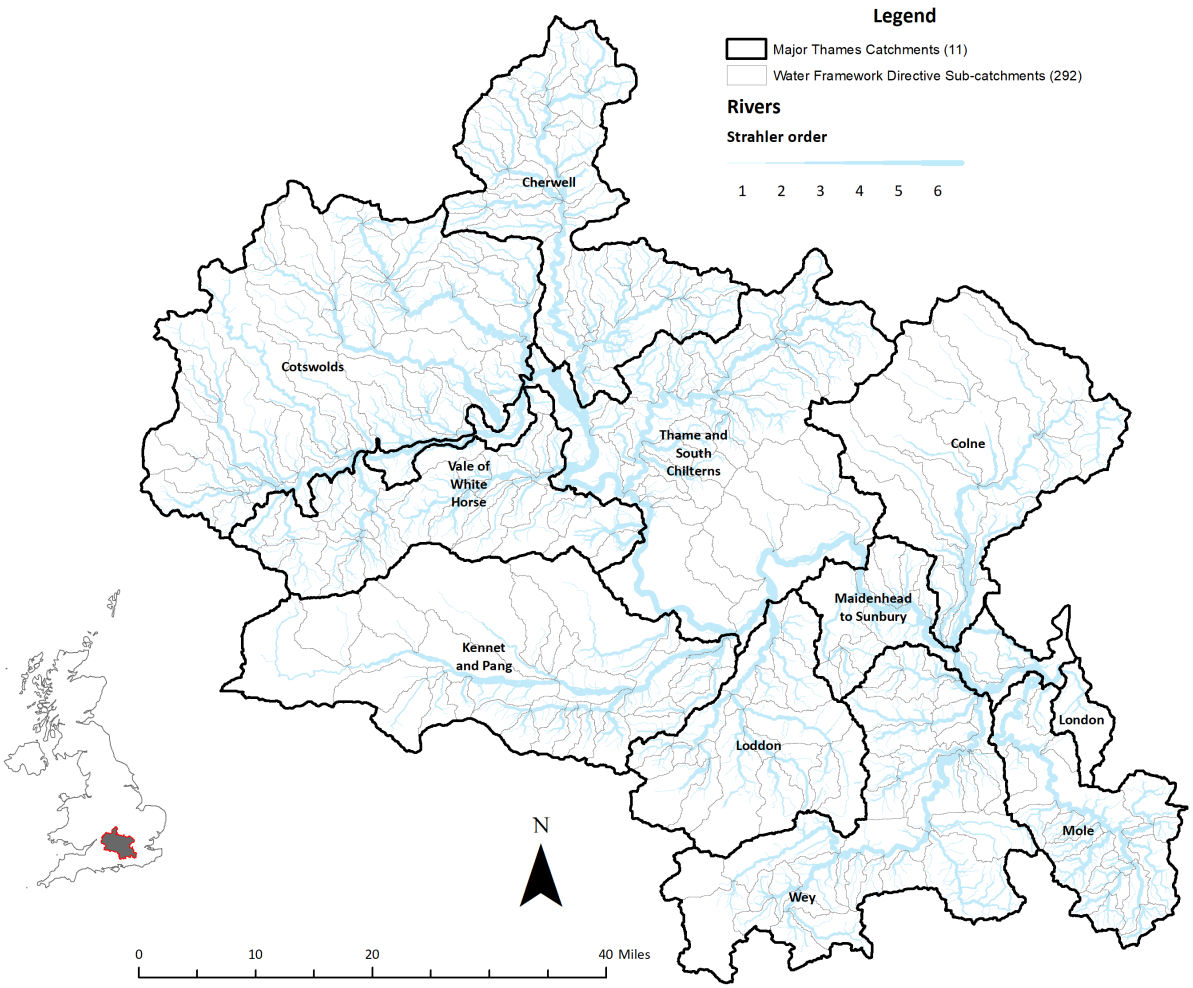


Figure 3-5: Map detailing the 11 major catchments of the study region and constituent sub-catchments. In total there are 292 minor sub-catchments in the planning region. The dendritic river network is depicted based on Strahler order.

3.5 CALIBRATION OF INCA MODELS FOR THE THAMES CATCHMENT

A large volume of information is required to set up both INCA-N and INCA-P models. Full descriptions of these input parameters are provided in Wade et al. (2002a) and Wade et al. (2002b) for INCA-N and INCA-P respectively. Based on a prior general sensitivity analysis of the INCA model in Thames Basin (Whitehead et al., 2015, Bussi et al., 2016a) and author's knowledge, the following 20 parameters were identified as the most influential:

1. Hydrological parameters (Jackson-Blake and Starrfelt, 2015, Bussi et al., 2016a)
    1.1. Rainfall excess proportion (proportion of excess rain converted to runoff)
    1.2. Soil water and groundwater residence times (i.e. flow velocity for sub-superficial flow and base flow)

1.3. Maximum infiltration rate

1.4. Flow-velocity coefficient (coefficient of a power law, $v = aQ^b$, used to calculate channel flow velocity from discharge)

1.5. Flow threshold for saturation excess direct runoff

2. Nitrogen parameters (Wade et al., 2002a, Jin et al., 2012)

2.1. Soil denitrification coefficient,

2.2. Nitrification

2.3. Mineralisation and immobilisation rates in soil

2.4. Nitrogen uptake rate by crops

2.5. Groundwater nitrate concentration

2.6. Instream nitrification rate

2.7. Instream denitrification rate

3. Sediment parameters (Lazar et al., 2010, Crossman et al., 2013a, Bussi et al., 2016a)

3.1. Splash and flow erosion parameters (defining erodibility of soils)

3.2. Flow erosion direct runoff threshold (threshold above which flow erosion occurs)

3.3. Transport capacity scaling factor (adjusts transport capacity on hillslopes)

3.4. Transport capacity non-linear coefficient (adjusts transport capacity on hillslopes)

3.5. Instream sediment transport parameters (adjusts channel transport capacity)

4. Phosphorus parameters (Crossman et al., 2013b, Jackson-Blake and Starrfelt, 2015, Bussi et al., 2017)

4.1. Soil matrix sorption coefficient (adjusts sorption capacity of soils)

4.2. Water column sorption coefficient (adjusts sorption capacity of water column)

4.3. Stream bed sorption coefficient (adjusts sorption capacity of bed sediment)

Where appropriate, input parameters were taken from existing Thames Basin INCA models (see Jin et al. (2012), Crossman et al. (2013c), Jackson-Blake and Starrfelt (2015), Bussi et al. (2016a) and Bussi et al. (2016c)). However, these previous studies implemented INCA models for 22 reaches within the Thames Basin. As outlined above, this research divides the Thames Basin into 11 sub-basin models

containing a total of 292 catchments. Consequently, such a significant increase in resolution necessitated the calculation of a wide range of key parameters. The methodology for calculating these is given below and a summary of all key input parameters is provided in Table 3-2.

3.6 SUB-CATCHMENT CHARACTERISTICS

Sub-catchment characteristics such as area and reach length are important aspects of INCA. The land-phase component of INCA model hydrology and chemistry in a 1km^2 parcel of land, the results of which are then multiplied by the actual area of the sub-catchment. Furthermore, reach length and width are important modifiers of how INCA calculates water volume and residence time. These parameters were calculated using the Zonal Statistics tool in ESRI ArcGIS© from data layers calculated using a drainage network derived from a 50m resolution Digital Elevation Model (British National Grid) (used under the Open Government Licence (2015)). Average sub-catchment area is 34.1km^2 and average reach length per sub-catchment is 11,965m.

3.6.1 VELOCITY-DISCHARGE PARAMETERS

Hydrology in each corresponding reach is also characterized by specifying the 'a' and 'b' parameters of the velocity–flow relationship, $v = aQ^b$ (where v is velocity (m/s) and Q is discharge (m^3/s)). These parameters are used to calculate water velocity and residence times within each reach and directly affect instream processes such as nutrient transformation rates. Typically, values are derived from tracer experiments conducted in-stream (Leopold and Maddock Jr, 1953). However, such information was not available in the Thames Basin at the resolution required for the sub-catchments used in this study. Therefore, a two-step process was developed that provided estimates for the 'a' parameter at the scale of each individual reach. In all reaches, the 'b' parameter was set at 0.67 (corresponding to an open channel river) following Leopold and Maddock Jr (1953).

Two critical sets of data were necessary for calculating the velocity-flow parameters. Firstly, the average reach length (l; m), width (w; m) and slope (S; m/m) were extracted from the digital river network using ArcGIS© for all sub-catchments. Secondly, both the mean typical river depth (d; m)

and average discharge (Q) for each of the 170 river levels stations and 72 NRFA stations in the Thames Basin were manually extracted from the associated CEH websites (CEH, 2015) and stored in a geo-located database. Mean typical river levels were extrapolated for sub-catchments without river level stations by attributing values from the nearest, connected sub-catchment of equal Strahler order containing a river level station.

For the 72 sub-catchments where average discharge was known (those that contained an NRFA station), the continuity equation, $Q = Av$, (where A corresponds to the cross-sectional area of flow ($w \times d$; m^2)), was used to determine velocity (v) values. For the remaining sub-catchments in which only width, slope and river depth were known, the Manning formula ($v = \frac{k}{n} {R_h}^{2/3} S^{1/2}$) was used in conjunction with the continuity equation to determine velocity (v) and discharge (Q) values. The Manning formula is an empirical formula that estimates the average velocity of open channel flow (Manning, 1891). The hydraulic radius (R_h) is a measure of channel flow efficiency and is defined as the ratio of the channel's cross-sectional area of flow (A) to the wetted perimeter (P), or $R_h = \frac{A}{P}$. The wetted perimeter (P; m) can be defined as the sum of all surfaces in contact with the river, which is simplified in this study to $w + 2d$. The slope (S) is a ratio of the altitudinal drop (in meters) between the point furthest upstream and downstream in a catchment and the reach length between those two points (in metres). The Manning coefficient, n; $m^{1/3}/s$, is an empirically derived measure of channel smoothness and is dependent on a variety of factors, such as sinuosity of channel, river bed composition and presence of vegetation (Chow, 1959). As such, the Manning coefficient varies throughout the Thames Basin from 0.015 in artificial and dredged channels to 0.1 in deep, weedy reaches. Values were assigned to categories based on the predominant land-use type, Strahler order and river morphology within a sub-catchment, which were then matched to descriptions given in Chow (1959) (see Table 3-1 for details). The conversion factor k equalled 1, as metric units were used in all calculations.

Table 3-1: River type and associated Manning's coefficients (*n*).

River type	Estimated Manning's coefficients (*n*)
Headwater streams	0.03 – 0.05
Floodplain – intermediate river – predominantly grassland/agriculture	0.025-0.45
Floodplain – intermediate river – predominantly wetland/forest	0.055-0.085
Floodplain – large river – predominantly grassland/agriculture	0.045-0.065
Floodplain – large river – predominantly wetland/forest	0.075-0.1
Artificial/dredged - urban	0.015-0.025
Artificial/dredged – non-urban	0.025-0.04

It is thus possible to derive the a parameter for each sub-catchment by substituting the values calculated above into the rearranged velocity-flow relationship: $a = vQ^{-b}$. The accuracy of the above methodology in predicting flow-velocity parameters was tested by calculating velocity values using the Manning formula in sub-catchments where actual discharge is known and correlating this against velocities calculated using the continuity equation for the same catchments. Regression analysis demonstrated an R^2 valued of 0.7201, indicating very good overall model performance (see Figure 3-6).

Table 3-2: Key input parameters for INCA calibration, including a brief description and source of the data.

Data	Data description	Data source
Physical sub-catchment properties		
Area (km²), reach length/width (m) and slope	Derived from GIS layers	Environment Agency
Hydrological inputs		
Flow-velocity parameters *a* and *b*	Parameter *a* Derived from physical sub-catchment parameters and NRFA gauging stations. Parameter *b* from Leopold and Maddock Jr (1953)	Environment Agency and Centre for Ecology and Hydrology
Base Flow Index	Measurements for flow rating derived from each flow gauge and extrapolated to other tributaries (Wade et al., 2002b)	Environment Agency
Residence times	Measurements for groundwater residence time for each sub-catchment)	Calculated from hydrological response curves (Soulsby et al., 2006)
Water abstraction	Discharge abstracted by major water companies in Thames Basin	Environment Agency
Observed Data		
Nitrate, Ammonium, SRP	Routine water chemistry sampling (2-4 times per month) and event sampling for 116 sites in Thames Basin	Environment Agency
Discharge	Daily time series of flow for 76 sites in Thames Basin	Centre for Ecology and Hydrology
Precipitation and temperature	Daily time series created from averaging all weather station data in Thames Basin	Met Office
Soil moisture deficit and hydrological effective rainfall	Daily time series generated from precipitation and temperature time series	Derived from PERSiST model
Land use data and nutrient inputs		
Land use data	Ecological land classification and land use classifications GIS layer	LCM2007 land coverage map (Centre for Ecology and Hydrology)
Nutrient inputs to non-intensive agriculture	Grazing inputs	Cattle and sheep populations (DEFRA, 2015a) combined with associated nutrient input rates (Withers and Lord, 2002)
	Manure and fertiliser inputs	Estimated from soil nutrient balances (DEFRA, 2015b)
Nutrient inputs to intensive agriculture	Grazing inputs	Pigs and poultry populations (DEFRA, 2015a) combined with associated nutrient input rates (Withers and Lord, 2002)
	Manure and fertiliser inputs	Estimated from soil nutrient balances (DEFRA, 2015b)
Nutrient inputs to whole catchment	Atmospheric deposition	Phosphorus deposition taken from nearest monitoring site (DEFRA, 2015b). Nitrogen deposition calculated from UK deposition maps (DEFRA, 2015c)
Point source nutrient inputs	Direct effluent inflow calculated from major sewage treatment works in Thames Basin	Environment Agency

3.6.2 Base Flow Index

The Base Flow Index (BFI) is used in the land phase of INCA to differentiate between soil water and groundwater, with values ranging between 0 and 1. Higher BFI values increase the proportion of groundwater transferred to river runoff and decrease the response of the hydrograph, with the opposite occurring for lower values. Measurements for flow rating were derived from the National River Flow Archive for each of the 77 flow gauges in the Thames Basin (see Table 3-4) (CEH, 2015). BFI values were extrapolated to sub-catchments without flow gauges following the methodology in Wade et al. (2002b).

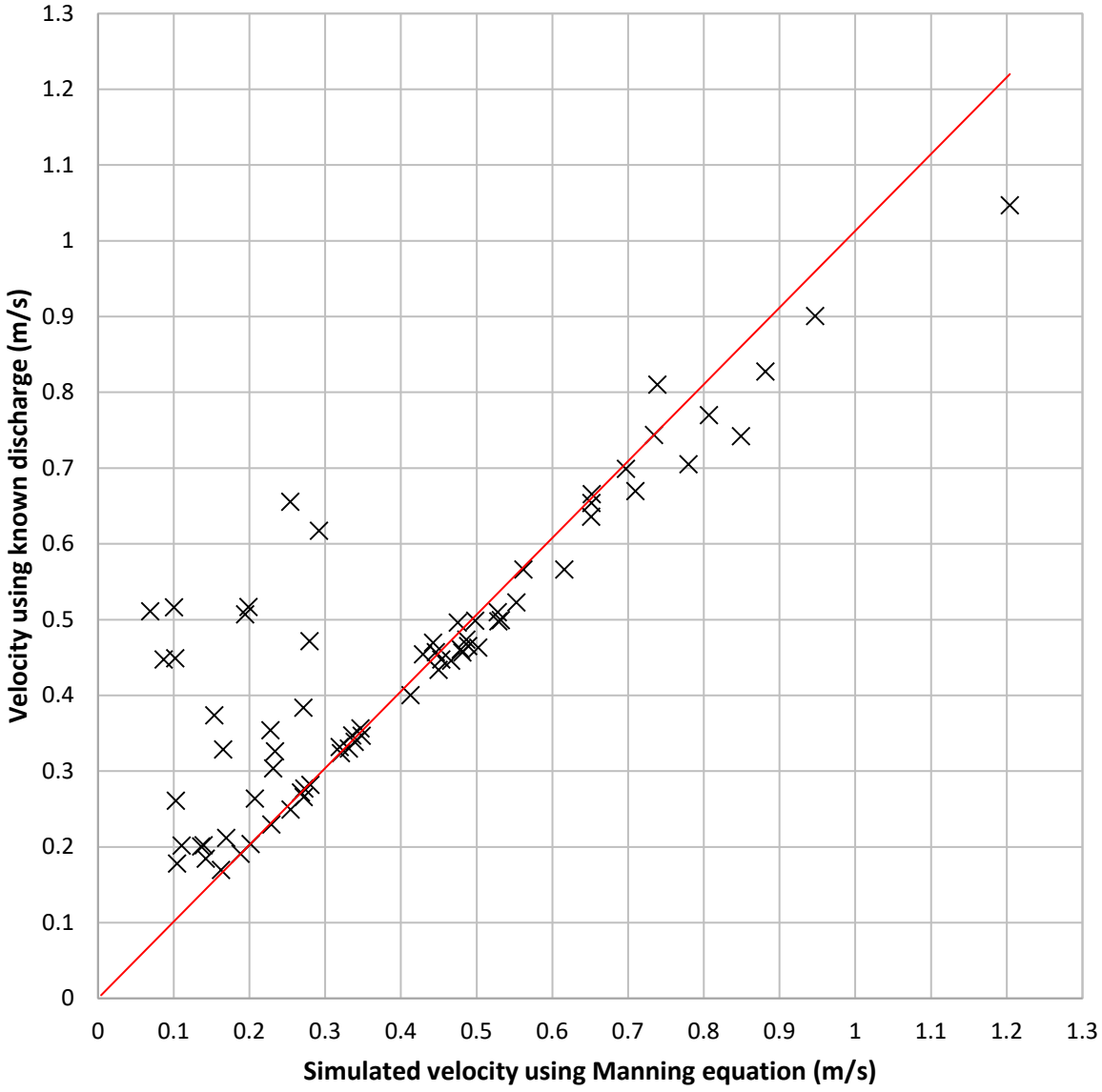


Figure 3-6: Regression analysis demonstrating the correlation between observed velocity value and those simulated using the Manning equation (R^2 = 0.72).

3.6.3 LAND USE DATA AND FERTILISER LOADINGS

Land use data is a key component of INCA, as land phase parameters directly affect the flow and nutrient concentrations and process fluxes in soils and, by extension, in-stream flow and chemistry (Whitehead et al., 2011). Multiple land-use types, each having its own unique set of parameters, can be modelled in INCA. The 25m resolution 2015 Land Cover Map of the UK and NI (LCM15, used under licence from CEH (NERC, 2011)) and Zonal Statistics tool in ArcGIS© were used to calculate the percentage of each land-cover class for all sub-catchments in the Thames Basin. These land-cover classes were then grouped into five land-use categories for use in INCA (see Table 3-3 for details); Urban, Intensive Agriculture, Non-intensive Agriculture, Wetlands and Forest. Land-phase parameters for each land-use type were calculated following Jin et al. (2012) and Crossman et al. (2013c) for INCA-N and INCA-P respectively.

Daily application rates of nitrogen and phosphorus from fertiliser and grazing animals to agricultural lands were calculated using a) current Department for Environment Food and Rural Affairs (DEFRA) farming statistics for the Thames Basin (DEFRA, 2015a) and b) previously identified nutrient application rates for vegetation types (DEFRA, 2011). Application rates were multiplied by sub-catchment land use area to attain land use-specific annual application loads (kg N $year^{-1}$ and kg P $year^{-1}$). Daily application rates (kg N ha^{-1} day^{-1} and kg P ha^{-1} day^{-1}) were then calculated by first ascertaining the monthly distributions of the annual load based upon the survey of land use and fertiliser practice in the River Ant catchment (Wade et al., 2004), and then dividing the monthly load by the number of days per month and the land class area within each sub-catchment. Likewise, nutrient applications to the land from livestock were calculated using individual input rates derived from Withers and Lord (2002). These input rates were then multiplied by the total number of livestock in each reach (DEFRA, 2015a). The sub-groups of DEFRA land-use types were combined into INCA-compatible categories (Table 3-3). Since cows and sheep predominantly graze grassland (Wade et al., 2004), livestock application rates for cattle and sheep were assigned to the “grassland” land

use classification, and pigs and poultry to "other arable" (Table 3-3). Following Wade et al. (2007), P inputs from applications of fertiliser and grazing animals comprised 70% inorganic and 30% organic P.

Table 3-3: Summary table showing the conversion between LandSFACS and INCA land-use types and their associated fertiliser loadings derived from DEFRA farm statistics.

Defra farming statistics, 2015	INCA land use type	LandSFACS	Nutrient inputs from fertilisers			
			Organic P (kg P/ha/day)	Inorganic P (kg P/ha/day)	Nitrate (kg N/ha/day)	Ammonium (kg N/ha/day)
-	Urban	Urban	-	-	-	-
Cereal Other arable Pigs Poultry	Intensive agriculture	Arable and horticulture	0.260	0.600	0.600	0.350
Permanent grassland Semi-permanent grassland Fallow Grazing Cows Sheep	Non-intensive agriculture	Improved grasslands Semi-natural grasslands	0.032	0.072	0.500	0.250
Orchard	Wetlands	Mountain heath and bog Standing open water	-	-	-	-
Forest	Forest	Broad-leaved/mixed woodland Coniferous woodland	-	-	-	-

3.6.4 ATMOSPHERIC DEPOSITION

Atmospheric deposition of N was calculated using 5km^2 resolution deposition maps provided by DEFRA (DEFRA, 2015c). Maps of nitric acid dry deposition (HNO_3), nitrate wet deposition (NO_3), dry ammonia deposition (NH_3) and wet ammonium (NH_4) were downloaded for 2004-2011. Average concentrations were then calculated over this period for each sub-catchment, using the Zonal Statistics tool in ArcGIS©. Atmospheric deposition of P was taken from the nearest monitoring site to the Thames and applied catchment-wide (DEFRA, 2015b).

3.6.5 EFFLUENT AND ABSTRACTION DATA

Point source nutrient input data for INCA is incorporated through the effluent discharge of Sewage Treatment Works (STW). In total, 252 major STW (those operated by large water/waste companies) were identified in the Thames Basin and geo-located in ArcGIS© (see Figure 3-7). The associated effluent time-series were then extracted directly from databases held by the Environment Agency at Red Kite House in Wallingford. INCA requires daily averages of flow (m^3/s) and concentrations of phosphorus, nitrate and ammonium (mg P/litre) (depending on INCA model used) to simulate effluent discharge in a reach, which is applied every day for the whole simulation period (Whitehead et al., 2009). Custom scripts in Matlab© were created to extract the daily mean discharge for each STW and convert the resulting values to the appropriate units (m^3/s). These scripts also extracted concentrations of soluble reactive phosphorus (surrogate for total phosphorus), nitrate and ammonium from Environment Agency chemistry datasets for each STW over the entire monitoring period. Average daily nutrient concentration values for each STW were then calculated from the resulting time-series and grouped by sub-catchment based on location. Finally, effluent data was combined in sub-catchments that contained multiple STW using the following methodology: 1) nutrient concentrations (mg/litre) were multiplied by their respective discharge values (converted to litres/sec), 2) the resulting nutrient weights are summed and then divided by the summed discharge for all STW in the sub-catchment (litres/sec). This gives a total nutrient concentration for the catchment that accounts for varying discharge and effluent concentrations in each STW.

The Thames catchment provides potable water to approximately 14 million people, in addition to irrigating arable land throughout much of its catchment. As such, there is substantial water abstraction throughout the entire Thames Basin, and it is therefore necessary to incorporate these effects in to the model. Abstraction is incorporated into INCA as an average discharge (m^3/s), which is then deducted from the total discharge of the reach on a daily timescale over the whole simulation period (Whitehead et al., 2009). Abstraction data were obtained for the Thames from information held by the Environment Agency. In total, 47 major abstraction facilities (those operated by large

water companies) were mapped in ArcGIS© and assigned to the relevant sub-catchment (see Figure 3-7). Average discharge (m^3/s) was calculated from annual abstraction statistics, and where multiple sites were present in a catchment, amalgamated to provide total average daily abstraction for each reach. These values do not account for the variation in abstraction throughout the year depending on river level and groundwater availability (i.e. greater in winter than summer months). However, it does provide estimates of abstraction throughout the Thames, which is an essential component to accurately model discharge and nutrient concentrations through the catchment. Note that effluent and abstraction data were unavailable in both the Colne and Mole catchments due to logistical complications with the governing body (Environment Agency NW Thames).

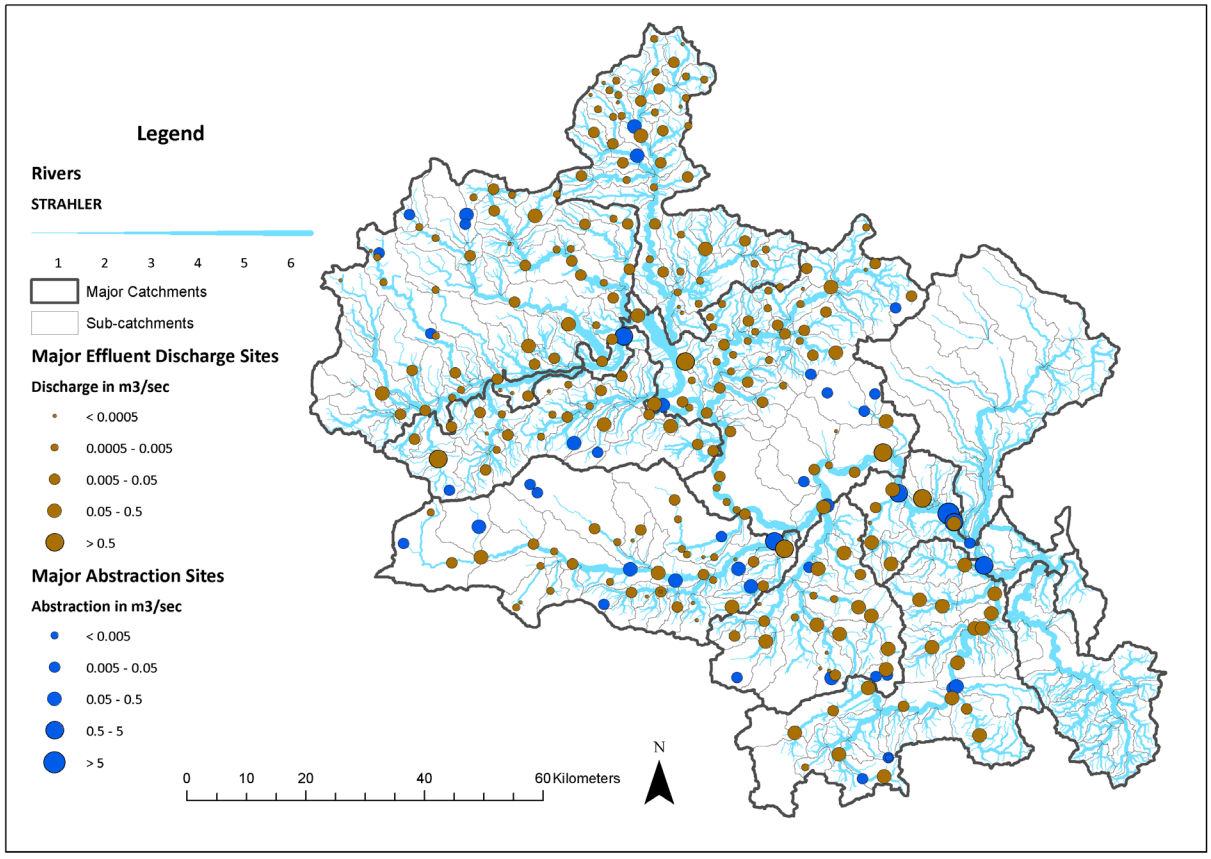


Figure 3-7: Location of major effluent and abstractions sites in the Thames catchment

3.6.6 OBSERVED DISCHARGE AND CHEMISTRY DATA

Observed discharge and nutrient data is required to calibrate and validate INCA models. Observed daily time-series of discharge (m^3/s) were collected from the National River Flow Archive (NRFA) for 76 stations in the Thames Basin (CEH, 2015). Stations are well distributed throughout all major catchments and where multiple occurred in a sub-catchment, the furthest downstream station was chosen. On average, 97% of daily records exist for a period of 41 years for each station (continuous records exist at Teddington Weir dating back to 1883 or 132 years). See Table 3-4 and Figure 3-8 for description and location of gauging stations. Observed concentrations of soluble reactive phosphorus (SRP), nitrate and ammonium were extracted directly from the Environment Agency Water Chemistry Monitoring Network database held at Red Kite House in Wallingford. In total, 116 sample points furthest downstream in each given sub-catchment were chosen throughout the Thames Basin (see Figure 3-8 for locations). The frequency of nutrient concentration data collection and monitoring period varies across the Thames region, although most sites have been sampled on at least a monthly basis for the calibration period of 1984-2013. Note that observed chemistry data were unavailable in both the Colne and Mole catchments due to logistical complications with the governing body (Environment Agency NW Thames).

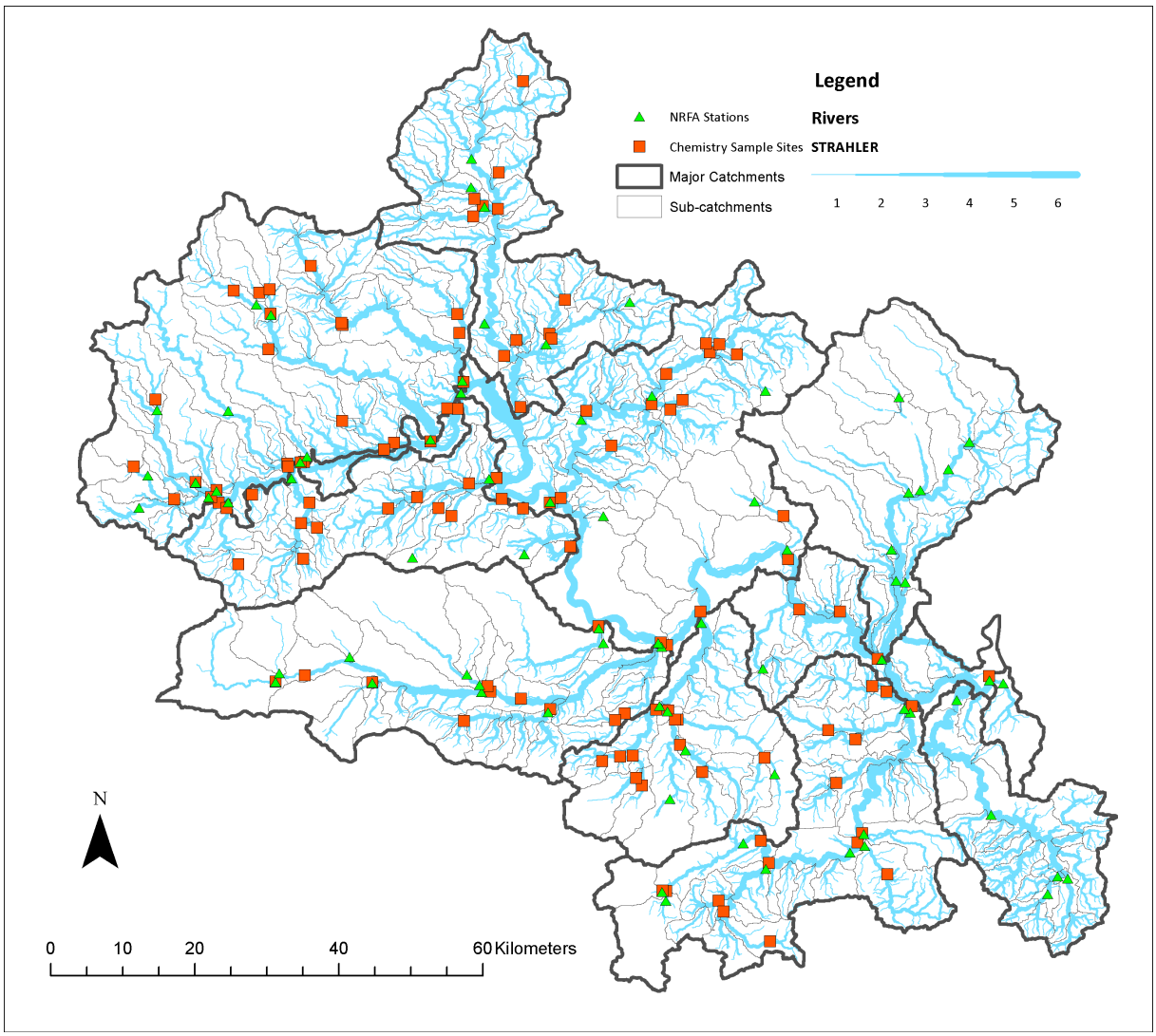


Figure 3-8: Location of flow gauging stations and chemistry sample sites in the Thames catchment

Table 3-4: Flow station data for all sites within the Thames Basin (n = 76).

Location	River	Upstream area (km²)	Station Level (m)	Station Type	Data Period	Percent complete	BFI	Mean Q (m3/s)	Q95 (m3/s)	Q70 (m3/s)	Q50 (m3/s)	Q10 (m3/s)
Kingston	Thames	9948	4.7	Ultrasonic	1883-2015	100	0.63	65.409	7.54	22.1	40.5	161
Days Weir	Thames	3444.7	45.8	Miscellaneous	1938-2015	100	0.64	28.515	3.26	8.86	16.8	69
Newbridge	Windrush	362.6	63.4	Compound broad-crested weir	1950-2015	100	0.86	3.341	0.737	1.62	2.63	6.68
Swallowfield	Blackwater	354.8	42.3	Compound broad-crested weir	1952-2015	100	0.67	3.116	1.03	1.67	2.29	5.81
Eynsham	Thames	1616.2	59.7	Miscellaneous	1951-2015	100	0.67	14.032	1.14	4.28	8.94	33
Denham	Colne	743	34.1	Broad-crested weir	1952-2015	100	0.87	4.105	1.83	2.902	3.68	6.62
Tilford	Wey	396.3	47.8	Crump weir	1954-2015	100	0.72	3.226	1.3	1.87	2.42	5.48
Kingston upon Thames	Hogsmill	69.1	6.1	Broad-crested weir	1956-2015	98	0.74	1.063	0.552	0.756	0.891	1.64
Berrygrove	Colne	352.2	54.7	Compound Crump weir	1934-2015	99	0.68	0.825	0.159	0.382	0.564	1.63
Hansteads	Ver	132	62.3	Compound Crump weir	1956-2015	100	0.88	0.431	0.084	0.257	0.366	0.816
Lodge Farm	Whitewater	44.6	71.5	Crump weir	1927-2015	100	0.94	0.375	0.169	0.263	0.33	0.612
Theale	Kennet	1033.4	43.4	Crump weir	1961-2015	100	0.88	9.802	3.78	5.83	8.04	17.5
Grendon Underwood	Ray	18.8	65.7	Flat V	1962-2015	94	0.16	0.098	0	0.002	0.012	0.237
Shaw	Lambourn	234.1	75.6	Crump weir	1962-2015	100	0.97	1.743	0.76	1.13	1.48	2.95
Enslow Mill	Cherwell	551.7	65	Compound Crump weir	1965-2015	100	0.65	3.909	0.654	1.4	2.49	9.15
Sheepbridge	Loddon	164.5	42.4	Crump weir	1965-2015	99	0.76	2.236	0.97	1.33	1.72	3.82
Hedsor	Wye	137.3	26.8	Crump weir	1964-2015	100	0.93	0.994	0.477	0.747	0.95	1.51
Brimpton	Enborne	147.6	59.4	Compound Crump weir	1967-2015	100	0.52	1.309	0.161	0.379	0.724	2.89
Banbury	Cherwell	199.4	88.7	Compound Crump weir	1966-2015	97	0.4	1.125	0.018	0.148	0.42	2.88
Pangbourne	Pang	170.9	39.6	Crump weir	1968-2015	100	0.87	0.648	0.193	0.371	0.534	1.17
Hungerford	Dun	101.3	99	Crump weir	1968-2015	100	0.95	0.704	0.269	0.419	0.559	1.3
Shalford	Tilling Bourne	59	31.7	Crump weir	1968-2015	100	0.89	0.532	0.314	0.421	0.489	0.745
Croxley Green	Gade	184	49.7	Compound Crump weir	1970-2015	100	0.88	0.998	0.371	0.706	0.92	1.64
Bagnor	Winterbourne Stream	49.2	80.5	Crump weir	1962-2015	100	0.96	0.174	0.05	0.096	0.137	0.33
Cassington Mill	Evenlode	430	60.2	Compound Crump weir	1970-2015	100	0.71	3.826	0.624	1.36	2.52	8.88
Cerney Wick	Churn	124.3	82.2	Compound Crump weir	1969-2015	100	0.83	0.891	0.01	0.231	0.58	2.235
Marlborough	Kennet	142	126.5	Crump weir	1972-2015	100	0.94	0.886	0.073	0.301	0.565	2.13
High Wycombe	Wye	67.7	76.9	Rectangular thin-plate weir	1997-2015	99	0.94	0.242	0	0.107	0.19	0.517
West Mill Cricklade	Thames	185	78.5	Compound Crump weir	1972-2015	100	0.68	1.408	0.066	0.259	0.754	3.73
Priory Mill Lechlade	Leach	76.9	71.7	Crump weir	1972-2015	99	0.79	0.761	0.068	0.225	0.494	1.87
Bramshill House	Hart	84	49.8	Crump weir	1972-2015	99	0.64	0.787	0.223	0.376	0.553	1.53
Adderbury	Sor Brook	106.4	28.2	Crump weir	1967-1988	99	0.74	0.85	0.184	0.382	0.651	1.71
Binfield	The Cut	50.2	45.6	Miscellaneous	1957-2015	99	0.46	0.396	0.068	0.136	0.234	0.834
Horley	Mole	89.9	51.7	Compound broad-crested weir/Velocity area	1961-2015	96	0.45	1.485	0.27	0.576	0.812	3.01

Location	River	Upstream area (km²)	Station Level (m)	Station Type	Data Period	Percent complete	BFI	Mean Q (m3/s)	Q95 (m3/s)	Q70 (m3/s)	Q50 (m3/s)	Q10 (m3/s)
Gatwick Airport	Mole	31.8	56.7	Ultrasonic	1961-2015	91	0.23	0.336	0.016	0.039	0.096	0.845
Letcombe Bassett	Letcombe Brook	4	105.6	Flat V	1971-2015	99	0.96	0.092	0.012	0.042	0.07	0.2
Ewelme	Ewelme Brook	13.4	65.9	Flat V	1970-2015	89	0.98	0.045	0.006	0.028	0.041	0.083
Castle Mill	Mole	316	39.2	Crump weir	1971-2015	95	0.42	3.726	0.795	1.18	1.76	8.61
Ewen	Thames	63.7	100.5	Miscellaneous	2002-2015	100	0.64	0.581	0	0.037	0.207	1.668
Royal Windsor Park	Thames	7046	13.5	Ultrasonic	1979-2015	100	0.71	59.348	14.9	27.34	41.22	128.7
Sheepen Bridge	Ampney Brook	74.4	78	Flat V	1980-2015	99	0.73	0.743	0	0.166	0.484	1.84
Malborough Poulton Farm	Og	59.2	124.9	Flat V	1980-2015	100	0.95	0.337	0.008	0.091	0.213	0.803
Farnham	Wey (North)	191.1	63.5	Miscellaneous	1978-2015	99	0.73	0.771	0.182	0.362	0.531	1.53
Weybridge	Wey	1008	9.2	Ultrasonic	1979-2015	94	0.65	7.19	2.4	3.88	5.11	13.7
Abingdon	Ock	234	51.4	Compound Crump weir	1962-2015	98	0.64	1.572	0.332	0.562	0.905	3.594
Gatwick Link	Gatwick Stream	33.6	54.7	Crump weir	1975-2015	99	0.61	0.72	0.263	0.357	0.488	1.36
Water Eaton	Ray	84.1	75.9	Ultrasonic	1974-2015	99	0.57	1.367	0.462	0.65	0.877	2.68
Rickmansworth	Chess	105	47.1	Crump weir	1974-2015	99	0.95	0.562	0.177	0.387	0.51	0.95
Bury Mill	Gade	48.2	86.5	Flume	1975-2012	99	0.83	0.154	0.027	0.086	0.126	0.296
Inglesham	Cole	140	72.7	Compound Crump weir	1976-2015	99	0.52	1.239	0.138	0.351	0.643	2.78
Buscot	Thames	997	70.3	Miscellaneous	1980-1998	98	0.71	9.149	1.24	3.33	5.88	21.4
Uxbridge	Pinn	33.3	30.5	Electromagnetic	1984-2003	96	0.21	0.2	0.01	0.026	0.054	0.51
Oaksey	Swill Brook	53.3	87.5	Flat V/Ultrasonic	1984-2010	59	0.36	0.314	0	0.017	0.069	1.01
Ramsbury	Aldbourne	53.1	106.4	Flat V	1982-2015	100	0.96	0.234	0.023	0.056	0.093	0.649
Denham Lodge	Misbourne	94.8	35	Crump weir	1984-2015	99	0.9	0.261	0.062	0.154	0.209	0.487
Newbury	Kennet	548.1	70	Ultrasonic	1989-2015	97	0.93	4.985	1.86	2.82	3.85	9.89
Esher	Mole	469.6	10	Ultrasonic	1984-2015	84	0.5	5.422	1.31	2.16	3.03	11.8
Wheatley	Thame	533.8	50	Ultrasonic	1989-2015	98	0.54	3.816	0.758	1.183	1.782	9.96
Perrott's Brook	Churn	59	120.1	Flat V	1990-2015	98	0.88	0.67	0.038	0.212	0.478	1.59
Fairford	Coln	130	83.7	Electromagnetic	1991-2015	98	0.93	2.116	0.638	1.12	1.76	4.06
Staines	Thames	8120	10	Ultrasonic	1990-2012	95	0.66	54.988	10.6	18.4	33.1	136
Sulham	Sulham Brook	3	42.7	Flat V	1991-2012	99	0.61	0.07	0.003	0.018	0.033	0.154
Kings Pond (Alton)	Wey	45.9	99.3	Rectangular thin-plate weir	1991-2015	99	0.88	0.108	0	0.031	0.073	0.258
Alton	Caker Stream	88.1	99.6	Flat V	1991-2015	100	0.4	0.081	0	0.003	0.015	0.247
Bramley	Cranleigh Waters	109.5	34.9	Ultrasonic	1990-2012	98	0.39	1.13	0.198	0.3	0.447	2.57
Farnborough	Blackwater	35.5	66.8	Electromagnetic	1996-2015	88	0.71	0.516	0.174	0.318	0.404	0.906
Addlestone	Bourne (South)	90.1	10.9	Velocity-area	1992-2012	92	0.67	0.87	0.341	0.511	0.676	1.48
Reading	Thames	4633.7	30	Ultrasonic	1992-2015	99	0.64	38.301	5.14	12.8	23.4	95.7
Twyford	Loddon	751.8	32	Ultrasonic	1995-2006	84	0.69	6.327	2.2	3.45	4.5	12

Location	River	Upstream area (km²)	Station Level (m)	Station Type	Data Period	Percent complete	BFI	Mean Q (m3/s)	Q95 (m3/s)	Q70 (m3/s)	Q50 (m3/s)	Q10 (m3/s)
Islip	Ray	290.1	50	Ultrasonic	1996-2015	92	0.41	2.194	0.148	0.419	0.766	7.2
Guildford	Wey	689.6	30.4	Ultrasonic	1996-2015	94	0.67	5.982	2.25	3.27	4.18	11.3
Bourton on the Water	Windrush	65.5	132.1	Crump weir	1995-2015	100	0.94	0.737	0.325	0.48	0.628	1.25
Bourton on the Water	Dikler	90.7	123.9	Crump weir	1995-2015	100	0.82	0.971	0.201	0.44	0.733	2.04
Bodicote	Sor	87.7	90.5	Crump weir	1995-2015	99	0.74	0.686	0.139	0.279	0.476	1.498
Blewbury	Mill Brook	2	59.8	Flat V	1996-2015	99	0.96	0.109	0.025	0.067	0.095	0.201
Wendover	Wendover Springs	9.5	120.1	Rectangular thin-plate weir	1963-2012	87	0.96	0.078	0.03	0.053	0.07	0.13

3.7 CALIBRATION RESULTS

The INCA-N and P models were then calibrated over the 30-year time period 1984-2013 for the 11 major sub-basins within the Thames Basin (see Appendix II for a detailed summary of model parameters and observed data used for each major catchment). Validation was not considered necessary, given that the models were calibrated against observed data over the same time period (30 years) that they will be used to model baseline and future scenarios. Following the procedure outlined for the PERSiST model, both INCA-N and INCA-P were calibrated following a general sensitivity analysis of the Thames Basin. The feasible ranges of the 20 particularly influential parameters highlighted previously were sampled randomly and 10,000 different parameters sets were generated. Subsequently, both INCA models for each sub-basin were run using each of these parameter sets over the calibration period of 1984-2013. Model performance was assessed through comparison with observed values of flow and water quality in the most downstream catchment of each sub-basin using the R^2 (Nash and Sutcliffe, 1970) and percent bias (PBIAS) values (Gupta et al., 1999). A simulated-annealing algorithm was used to estimate the global minimum (in terms of modelled/observed ratio of R^2 ad PBIAS) of the multivariate parameter sets, whilst disregarding extraneous local minima (Sumner et al., 1997, Madsen et al., 2002). This combination of model calibration based on the use of generic search routine and user-specified calibration priorities generated very good correspondence with observed data for flow, SRP and nitrate simulations. Monthly average R^2 values across all models were 0.61, 0.48 and 0.50 respectively (see Table 3-5 for correlation coefficients for each major catchment and Appendix III for detailed correlation coefficients of each reach with observed data). It is notable that observed chemistry data, in addition to effluent and abstraction calibration data, were unavailable for both the Colne and Mole catchments.

Model performance throughout the entire calibration period (1984-2013) is demonstrated in Figure 3-9A (flow), 3.9B (SRP) and 3.9C (Nitrate), for the furthest downstream sub-catchment of the non-tidal Thames (Teddington Weir). Notably, SRP calibration was effected by the introduction of new,

stricter sewage treatment plant effluent guidelines in 2002 to ensure 100% compliance with the Bathing Water Directive mandatory standards for England and Wales by 2006 (DEFRA, 2002) (as demonstrated in Figure 3-9 by the associated drop in observed SRP concentrations from 2004-2006 to 2007-onwards). Catchments were calibrated to average observed values over the 30-year calibration period (1984-2013). As such, the model slightly underestimates simulated SRP concentrations before 2006 and rather over-estimates concentrations from 2006 onwards. However, by taking a 30-year average over the whole calibration period, these simulated biases are accounted for and provide a good-fit against observed values for the same period.

Model error was evaluated using a percent bias (PBIAS) approach (Gupta et al., 1999). This measures the average tendency of the simulated data to be larger or smaller than their observed counterparts. The optimal value of PBIAS is 0.0, with low-magnitude values indicating accurate model simulation. Positive values indicate model underestimation bias, and negative values indicate model overestimation bias. Model error was calculated using Equation 1, where PBIAS is the deviation of data being evaluated, expressed as a percentage (Moriasi et al., 2007).

$$PBIAS = \left[\frac{\sum_{i=1}^{n}\left(y_i^{obs} - y_i^{sim}\right) * 100}{\sum_{i=1}^{n}(y_i^{obs})}\right] \quad \textbf{Equation 1}$$

Where y_i^{obs} is the observed value at time step i and y_i^{sim} is the simulated value at time step i.

Average error across all models was 18.9%, -30.2% and 22.5% for flow, SRP and nitrate respectively, indicating a tendency for the models to overestimate flow and nitrate values and underestimate values of SRP. Similar to Crossman et al. (2013c), average errors in model flow, SRP and Nitrate were found to be greater in the summer (22.4%, -32.6 %, 27.1% respectively) than in the winter (15.4%, -27.8%, 17.9%). Average model errors for each major sub-basin are provided in Table 3-5.

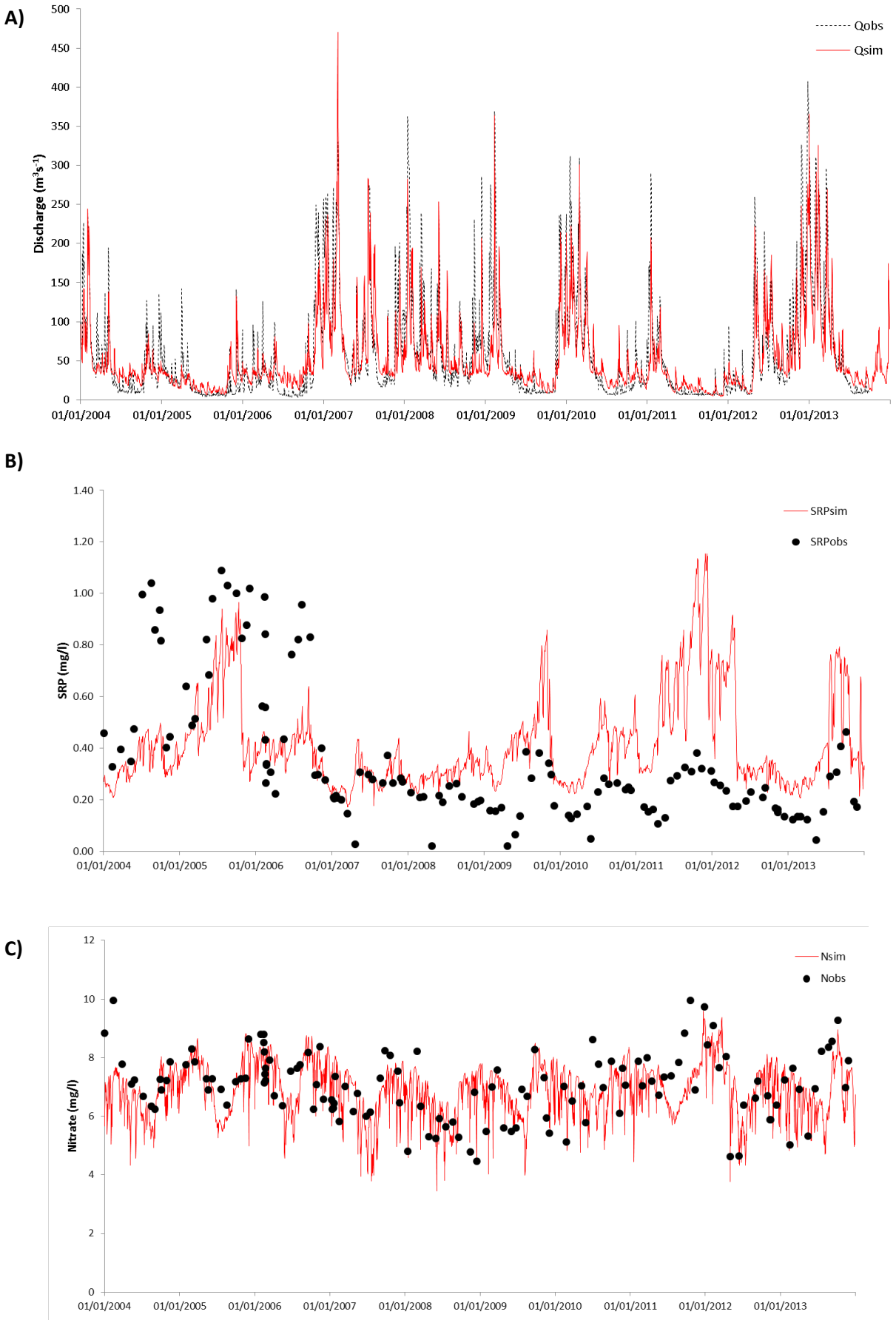


Figure 3-9: Fit of model to observed data in furthest downstream catchment (Teddington Weir) of non-tidal Thames basin, for 10 year period from 2004 to 2013, A) Flow (m^3s^{-1}), B) SRP (mg l^{-1}) and C) Nitrate (mg l^{-1}).

Table 3-5: Average model correlation coefficients and percent bias error for calibration runs of 11 sub-basins

	Model correlation coefficients (R^2)			Model percent bias error (%)		
Major catchment	**Discharge**	**SRP**	**Nitrate**	**Discharge**	**SRP**	**Nitrate**
Main stem of the Thames	0.73	0.51	0.52	13.7	-25.6	19.4
Maidenhead and Sunbury	0.40	0.31	0.43	28.0	-38.5	28.2
Mole	0.47	-	-	25.2	-	-
Wey	0.52	0.47	0.52	21.2	-27.2	21.3
Colne	0.69	-	-	14.5	-	-
Loddon	0.54	0.51	0.50	18.5	-35.2	24.4
Kennet and Pang	0.76	0.50	0.49	13.1	-31.8	25.6
Thame and South Chilterns	0.77	0.48	0.50	13.0	-36.2	20.1
Vale of the White Horse	0.64	0.48	0.54	20.6	-27.4	18.6
Cherwell	0.53	0.48	0.46	22.4	-26.9	27.8
Cotswolds	0.68	0.54	0.56	17.3	-23.4	17.1
Averages	**0.61**	**0.48**	**0.50**	**18.9**	**-30.2**	**22.5**

Chapter 4 THAMES BASIN: METHODOLOGY

4.1 INTRODUCTION

Following the formulation and calibration of INCA models to current conditions, the next phase was to assess climate change impacts in the Thames Catchment. Conventionally, the analysis of climate change impact on water quality and resources follow two complementary methodologies (Singh et al., 2014): the "top-down (scenario-led)" approach and the "bottom-up (scenario-neutral)" approach. The former adopts a cascading methodology; whereby emissions scenarios are used to drive climatic models, which in turn drive hydrological and environmental models (Prudhomme et al., 2010). An advantage of this approach is that fewer scenarios need to be computed, as the range of variability is determined by the scenario utilised. Furthermore, top-down approaches are not limited by the response of a catchment to a limited number of pre-chosen climatic variables, and so can better assess changes in seasonality and extreme events.

However, such an approach tends to end at impact assessment, with few tangible planned adaptation decisions arising from previous studies (Prudhomme et al., 2010). This is due, in part, to the propagation and expansion of uncertainty through the modelling cascade (from emissions, to atmospheric concentrations of greenhouse gases, to climate model sensitivity, etc.), culminating in such a range of outcomes that practical management decisions become impossible (Bastola et al., 2011a). Conversely, in the latter (scenario-neutral) approach, a response surface of environmental vulnerability indicators to changes in some climatic features is built using environmental models (Brown and Wilby, 2012). The likelihood of these climatic changes occurring are then assessed through integration of potential future climate risk (often informed from GCM scenarios) into the results of this methodology (Guo et al., 2018). One clear advantage of a scenario-neutral approach over a top-down approach is that it can be implemented independently from climate scenarios projections, which only account for projected future changes (Bastola et al., 2011b). Consequently, it allows the exploration of climatic alterations that may not be reproduced by the range of available climate models. As such, results can be compared with updated scenarios without repeating the

study, thus providing a practical and usable tool for practitioners and governing bodies (Brown and Wilby, 2012).

In this thesis, a scenario-neutral approach is applied at the catchment-scale, with a top-down methodology having been applied when conducting the continental scale approach in Chapter 2. The scenario-neutral approach is most appropriate for a catchment-specific context, as the high-resolution network of INCA models produced for the Thames outlined in Chapter 3 enable the sensitivity of key environmental variables to climate change to be assessed for each of the 292 sub-catchments of the Thames Basin. This research utilises specific standards developed by UKTAG for the Water Framework Directive (WFD) to assess the status of a catchment, directly linking catchment status with changes in key climatic variables. Furthermore, this approach makes use of UK Climate Projections (UKCP09) for the 2040s (2030-2059), 2060s (2050-2079) and 2080s (2070-2099) to further quantify and assess the risk of a change in the status of key biological and physio-chemical standards and determine appropriate management responses for specific catchments affected by climate change.

4.2 SCENARIO-NEUTRAL CLIMATE CHANGE METHODOLOGY

The aim of a scenario-neutral climate methodology is to identify the sensitivity of a response variable to specific climatic input parameters under a range of synthetic scenarios (Prudhomme et al., 2010). River flow is considered to be the 'master variable' dictating riverine habitats and species distributions (Poff et al., 2003b). Therefore, to assess future changes within a catchment with relation to climate change it is pertinent to identify key climatic stressors that influence river flow. The key climatic parameters influencing river flow are precipitation and temperature (Arthington et al., 2010, Gibson et al., 2005). The quantity and timing of precipitation directly impacts river flow within a catchment, both in the short-term through direct runoff and long-term through replenishment of groundwater resources (Maxwell and Kollet, 2008). In addition to regulating river discharge, air temperature is highly correlated to water temperature, which can have a significant direct impact on riverine habitats and species (Webb et al., 2008). Thus, to create an envelope of

variable hydrological conditions (water discharge and temperature), changes in mean annual precipitation and air temperature were considered in this research.

Alterations to mean annual precipitation and temperature were introduced by means of a uniform "delta change" transformation (Hay et al., 2000) applied to observed daily precipitation and temperature values. Delta change values are calculated by determining the differences of 30-year annual averages between an observed baseline and future climate sets (in percentage change precipitation and degrees Celsius change in temperature). These annual delta values are then applied to the daily values of the baseline, producing observed data that has been 'delta-shifted' to match the amount of change demonstrated by each of the perturbed runs. This ensures that whilst the local climate is accurately represented, the relationship between the climate sets is maintained. The alterations were chosen to cover the projected changes in annual precipitation and temperature by climate models, but also to stress the system further, with the aim of assessing not only future plausible changes but also the response of the system under very extreme conditions. Following Beniston et al. (2007) and Christensen and Christensen (2007), for Northern Europe the annual temperature is expected to increase up to 5.3°C by 2080–2099, while annual precipitation is expected to vary between 0 and +16% (although a decrease in summer precipitation of up to 21% is also forecasted). Consequently, a total of 300 altered climate change series were generated, describing changes in mean annual precipitation from -30% to +40% (15 steps in 5% intervals) and mean annual temperature change from -1c to +8.5°C (20 steps in 0.5°C intervals), as outlined in Table 4-1.

These synthetic climate sets are subsequently used to drive the calibrated PERSiST model for the Thames to obtain soil moisture deficit and hydrologically effective rainfall, which in turn are used to drive each of the 22 calibrated INCA models (11 INCA-P and 11 INCA-N models representing each of the major catchments within the Thames Basin; see section 3.4 for details). This produces a set of altered daily flows, water temperature and nutrient (phosphorus, ammonia and nitrate) concentrations for each of the altered climate series for all 292 sub-catchments within the Thames Basin. Finally, a series of response surfaces were generated for each catchment corresponding to

annual averages of key variables (water flow and temperature, alongside phosphorus and ammonium concentrations) for all altered climate series. In addition to absolute values, the relative change in flow and nutrients, and absolute change in water temperature was determined by calculating the difference between each synthetic climate set and the un-perturbed baseline (highlighted in Table 4-1 in grey). These gridded datasets correspond to the response of a specific catchment variable to a broad range of variation in both annual average precipitation and temperature and represent a sensitivity matrix from which future risk due to climate change can be elucidated using existing probabilistic climate change scenarios.

Table 4-1: Table showing the number matrix of synthetic climate sets used in this research. Un-perturbed (baseline) conditions correspond to the 37th climate set.

		Percentage change in mean annual precipitation														
		-30	**-25**	**-20**	**-15**	**-10**	**-5**	**0**	**5**	**10**	**15**	**20**	**25**	**30**	**35**	**40**
Degrees celsius change in mean annual temperature	**8.5**	286	287	288	289	290	291	292	293	294	295	296	297	298	299	300
	8	271	272	273	274	275	276	277	278	279	280	281	282	283	284	285
	7.5	256	257	258	259	260	261	262	263	264	265	266	267	268	269	270
	7	241	242	243	244	245	246	247	248	249	250	251	252	253	254	255
	6.5	226	227	228	229	230	231	232	233	234	235	236	237	238	239	240
	6	211	212	213	214	215	216	217	218	219	220	221	222	223	224	225
	5.5	196	197	198	199	200	201	202	203	204	205	206	207	208	209	210
	5	181	182	183	184	185	186	187	188	189	190	191	192	193	194	195
	4.5	166	167	168	169	170	171	172	173	174	175	176	177	178	179	180
	4	151	152	153	154	155	156	157	158	159	160	161	162	163	164	165
	3.5	136	137	138	139	140	141	142	143	144	145	146	147	148	149	150
	3	121	122	123	124	125	126	127	128	129	130	131	132	133	134	135
	2.5	106	107	108	109	110	111	112	113	114	115	116	117	118	119	120
	2	91	92	93	94	95	96	97	98	99	100	101	102	103	104	105
	1.5	76	77	78	79	80	81	82	83	84	85	86	87	88	89	90
	1	61	62	63	64	65	66	67	68	69	70	71	72	73	74	75
	0.5	46	47	48	49	50	51	52	53	54	55	56	57	58	59	60
	0	31	32	33	34	35	36	37	38	39	40	41	42	43	44	45
	-0.5	16	17	18	19	20	21	22	23	24	25	26	27	28	29	30
	-1	1	2	3	4	5	6	7	8	9	10	11	12	13	14	15

To determine the risk of forecasted changes in biological and physio-chemical variables due to climate change, this research compares the catchment sensitivity framework with the UKCP09 projections for the 2040s, 2060s and 2080s. UKCP09 are probabilistic projections developed by the UK Met Office to provide climate change projections for the United Kingdom with greater spatial and temporal detail than previous efforts (i.e. UKCIP02). The application of UKCP09 has been widely used in UK water resource planning (Arnell, 2011, Christierson et al., 2012, Hall et al., 2012, Tang and Dessai, 2012) and applied in a set of studies in the Thames Basin (Bussi et al., 2016a, Bussi et al., 2016c, Bussi et al., 2017). These projections are based on the results of the HadCM3 coupled ocean-atmosphere Global Circulation Model (Gordon et al., 2000), run as a perturbed physics ensemble to sample model and parameter uncertainties (Murphy et al., 2007). The resulting HadCM3 projections were downscaled to a 25km grid, based on an ensemble of 11 variants of the regional climate model HadRM3. A multivariate statistical procedure was then applied to build local-scale distributions of changes for various climate variables over seven overlapping 30-year time periods. Due to the significant uncertainty associated with the tails of the probability distribution, change factors below 1% and above 99% were omitted from the research (Kay and Jones, 2012).

UKCP09 provides projections for three scenarios of the Special Report on Emissions Scenarios (see section 1.3 for specific scenario details) (Nakicenovic and Swart, 2000). The scenarios utilised by UKCP09 are A1FI, A1B and B1; considered ‘High’, ’Medium’, and ‘Low’ with regards to future emissions respectively. For the purposes of this research, the A1F1 (‘High’) scenario was chosen to provide results that were conservative in estimate. Among the available outputs from UKCP09 are expected changes in average precipitation and temperature for each emission scenario, obtainable from the online data portal - http://ukclimateprojections-ui.metoffice.gov.uk/ui/start/start.php. For each scenario, a set of 10,000 probabilistic precipitation and temperature change factors were downloaded for the 2040s, 2060s and 2080s, encompassing the Thames Basin. These change factors represent a subset of the variations in precipitation and temperature considered in this research, and consequently define a sub-region of the system response matrix defined in Table 4-1 (as demonstrated in Figure 4-1).

Furthermore, Figure 4-1 shows an increase in uncertainty, associated with a reduction in density and spread in the distribution of change factors, for series further in the future. Notably, the variation in the range of temperature between temporal series (vertical shift) is significantly greater than that of precipitation (lateral shift), indicating potential changes in annual precipitation are likely to remain similar between time-periods, whereas potential annual temperature is likely to vary significantly between time-periods. Values are generated for each change factor from the system response matrix using bicubic interpolation (an extension of cubic spline interpolation for interpolating data points on a regular, two-dimensional grid) (Dierckx, 1995). Bicubic interpolation is constructed of piecewise third-order polynomials that pass through a set of control points, represented by the system response matrices in this research, generating a continuous, smooth surface between these points (Bartels et al., 1998). Bicubic interpolation was chosen, as it gives an interpolated surface that is smoother than bi-linear or nearest-neighbour interpolation, ensuring greater resolution of sample data. Whilst bi-cubic interpolation is most appropriate for continuous distributions (e.g. nutrient concentrations), nearest-neighbour interpolation was used for system response matrices that were discrete in nature (e.g. integer indicator values).

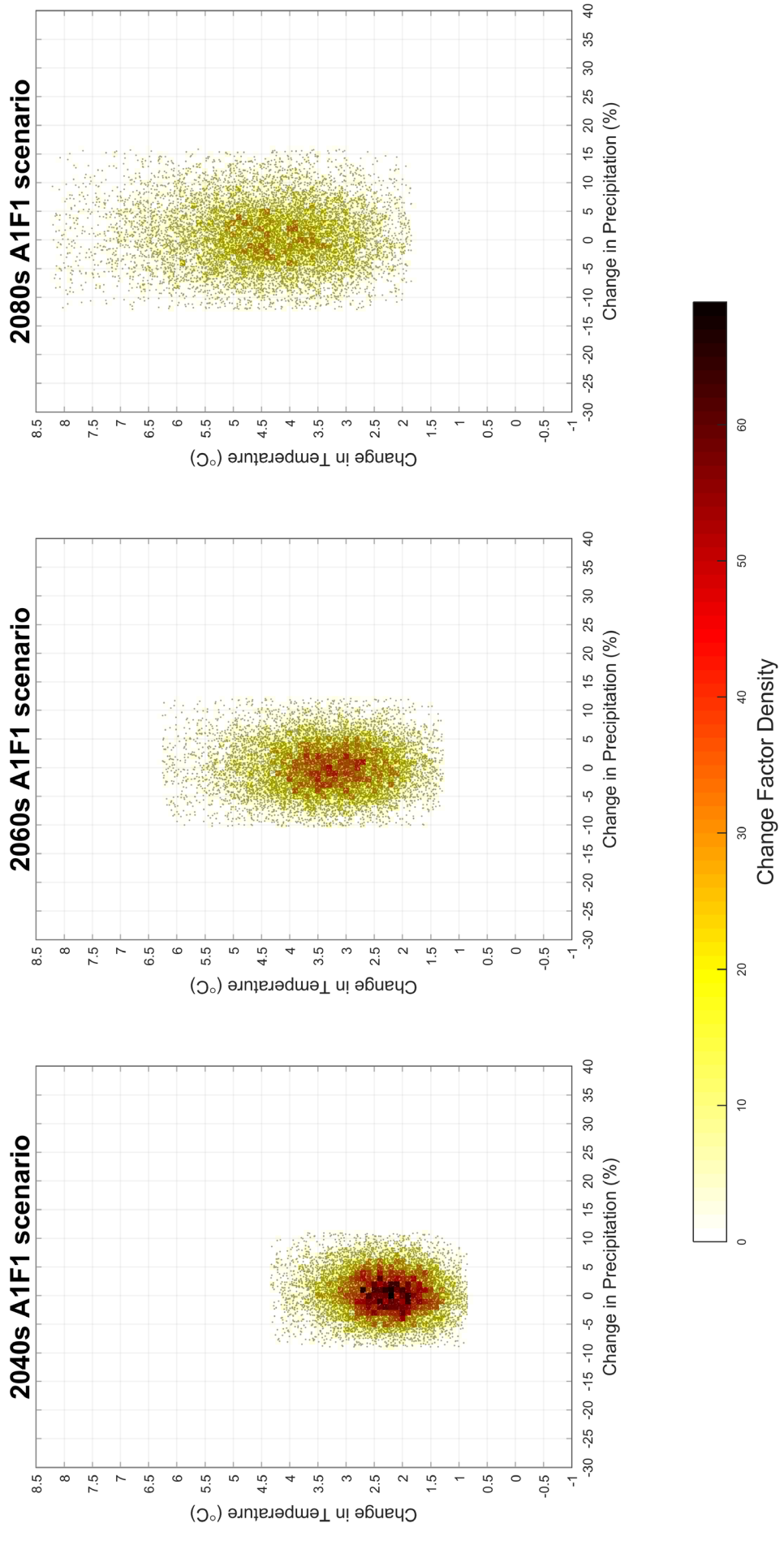


Figure 4-1: Series of annual average precipitation and temperature change factors produced by UKCP09 for the A1F1 (High) scenario for the 2040s, 2060s and 2080s.

4.3 SELECTION OF STANDARDS TO ASSESS CHANGES IN KEY HYDROLOGICAL AND NUTRIENT VARIABLES UNDER CLIMATE CHANGE

The Water Framework Directive (WFD) was established by the European Commission in 2000 with the aim of refining existing fragmented policy by expanding the scope of water protection to all waters, surface waters and groundwater across all member states (European_Commission, 2012). To achieve this, the focus of water management was shifted to the river basin (the natural geographical and hydrological unit), instead of according to administrative or political boundaries. Objectives regarding the status of waterbodies were introduced and environmental standards matched to each objective. Two key objectives are the following:

1) Preventing deterioration in status
2) Restoring water bodies to 'good' status by a set deadlines (2015 in the first cycle, 2021 in the second cycle) (European_Commission, 2012)

The status of water bodies is assigned to one of five classes; 'High', 'Good', 'Moderate', 'Poor' or 'Bad'. Classes are assigned by the environmental agencies of each member state based on an assessment of faunal and floral community condition and specific environmental standards, such as nutrient and pollutant concentrations. The WFD requires that the overall status of a waterbody be determined by the lowest status from all the assessed standards; to have 'High' status, for example, a waterbody must comply with all standards associated with 'High' status. Once all waterbodies have been assessed within a river basin and environmental shortfalls identified, a management plan is developed that seeks to determine the most cost-effective combinations of actions required to meet the WFD objectives.

Key to this process is the development of environmental standards that are used to determine the ecological and chemical status of a waterbody. The UKTAG is the working group of experts drawn from UK environmental agencies and conservation bodies responsible for developing classification tools and rules for the chemical, biological and physical quality standards in UK waterbodies, and how these can be used in River Basin Management planning (UKTAG, 2014b). In deriving standards,

the UKTAG seeks standards that apply to all water bodies of the same type and can lead to and make use of sound monitoring programmes, thus producing unbiased estimates of compliance and national performance. The development of standards is often dependent on the data available. For certain standards, the UKTAG can compare biological data collected from hundreds or thousands of sites with the environmental conditions to which the plants and animals are sensitive. This process can identify standards that correspond directly with the biological definition of 'Good' status, which in turn leads to sensible estimates of compliance and good decisions. For other standards (e.g. flow limits and certain pollutants), there are insufficient data to derive standards in this way. In these cases, the UKTAG uses the current scientific understanding of the causes of ecological change relying on advice from independent experts from a range of scientific disciplines. Estimates of compliance and decisions arising from these standards are to be treated as more circumspect than those derived using observed environmental data. A list of standards was first published in 2006 (UKTAG, 2008) and have been extended and revised several times, as more data has become available from continued monitoring of environmental parameters and efficacy of existing standards in achieving objectives outlined in management plans (UKTAG, 2014b).

This thesis aims to utilise key standards developed for the WFD to assess waterbody status under a suite of climate change scenarios. This research focuses explicitly on lotic waters (i.e. riverine systems), and, as such, only standards associated with lotic systems were considered when developing the methodology. Standards were chosen that could be modelled to an acceptable degree of accuracy using INCA models and were sensitive to changes in annual average precipitation and temperature. Five key standards were chosen that incorporated the breadth of existing biological, physical and chemical standards. These are macroinvertebrate indices (biological), water temperature and indicators of hydrological alteration (physical) and ammonia and phosphorus concentrations (chemical). The specific justification and methodological approach for each standard are outlined in the sections below.

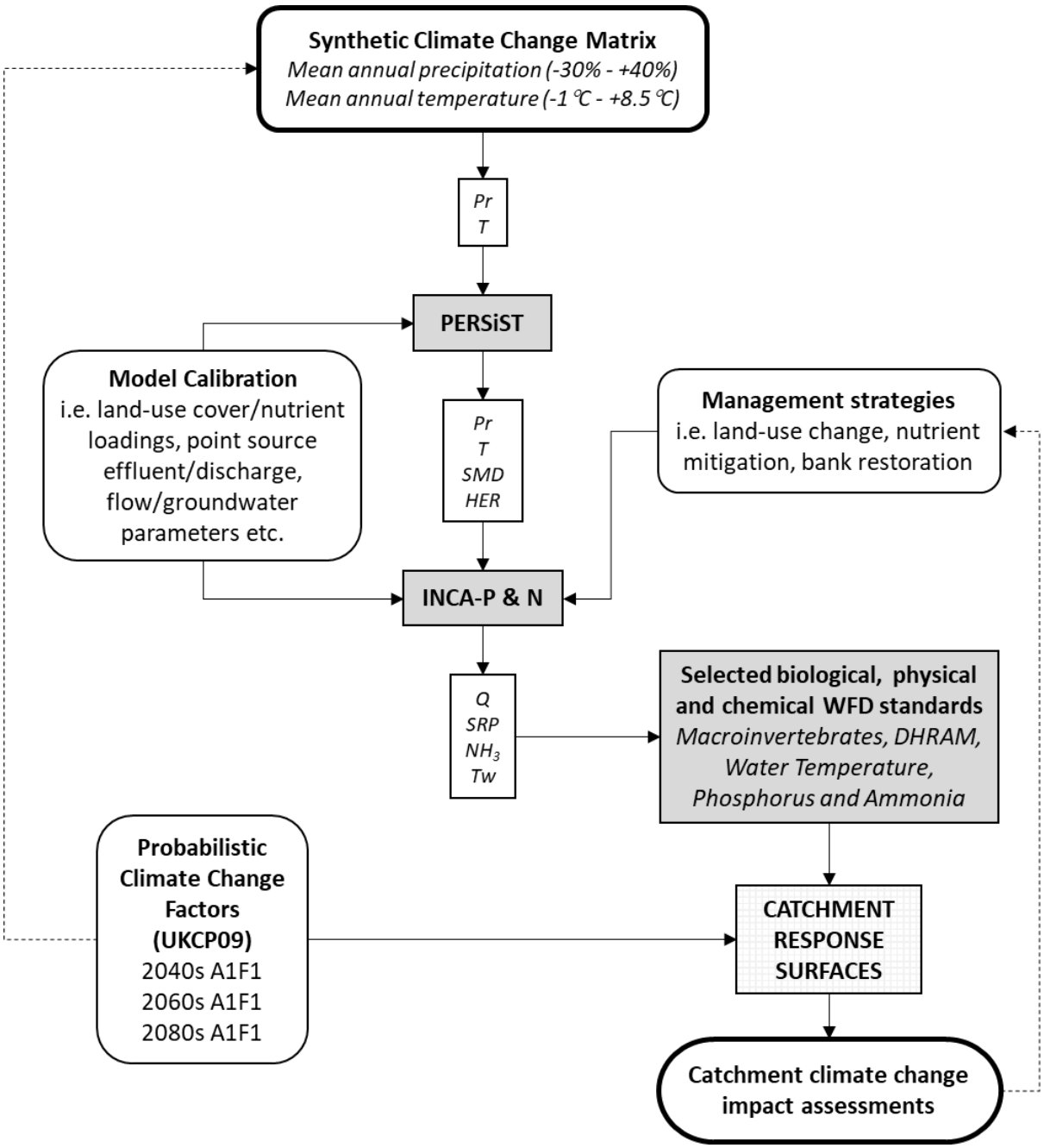


Figure 4-2: Flow diagram of catchment-scale climate change impact methodology. Solid arrows indicate the flow of data through the cascade, with dashed arrows representing feedback loops where outputs can inform input parameters. Rounded boxes indicate data external to the models (e.g. catchment calibration data), shaded square boxes indicate models/equations, and square boxes contain data generated by said models/equations (*Pr* – precipitation, *T* – temperature, *SMD* – soil moisture deficit, *HER* – hydrologically effective rainfall, *Q* – river discharge (m^3/s), *SRP* – soluble reactive phosphorus (mg/l), NH^3 – ammonia (mg/l), T_w – water temperature (°C)). The hatched box represents the catchment response surfaces for all chosen standards and the oblong box contains the catchment impact assessments based on the overlaying probabilistic climate change factors with the response surfaces for the catchment.

In summary, Figure 4-2 provides a flow diagram of the methodology developed and used in this research to assess the impact of climate change at the catchment-scale. The flow of data through the figure is demonstrated by solid arrows, with dashed arrows representing feedback loops where

model outputs can inform input parameters. For example, the probabilistic climate change factors produced by UKCP09 indicate that there is a possibility the upper bounds of annual average temperature over the Thames Basin may increase by as much as 8.25°C. Therefore, the synthetic climate change matrix should include increases in temperature of up to 8.5°C. This 'bottom-up' or 'scenario-neutral' approach to climate change impact assessment (Prudhomme et al., 2010) initially requires the identification of sources of climatic alteration that are likely to affect the variable object of the study (in this instance, specific WFD standards). In this research, annual average temperature and precipitation were identified as sources of climatic alteration and were applied to the observed climate to produce altered climatic series.

Following calibration of both the PERSiST and INCA models to current, observed data, each altered climatic series is used to drive the model hierarchy to produce daily values of discharge, soluble reactive phosphorus, ammonia and water temperature. The sensitivity of the catchment to selected biological, physical and chemical standards is then assessed for each synthetic climate scenario, generating a sensitivity framework composed of catchment response surface matrices for each of the selected standards (Macroinvertebrates, Dundee Hydrological Regime Alteration Method (DHRAM), Water Temperature, Phosphorus and Ammonia). Overlaying currently available probabilistic climate change factors with this sensitivity framework determines the likelihood of impact of future climate change on the catchment. The status of each catchment is then determined by the standard that has the worst predicted status. Those catchments exhibiting shifts in status (either positive or negative) due to changes in climate are highlighted, and recommendations made for the potential management priorities that such catchments should receive.

4.4 BIOLOGICAL STANDARDS

4.4.1 INTRODUCTION

Presently, several biological standards exist for determining the status of river catchments within the UK. These standards focus on different taxa within a riverine ecosystem, and include indicators associated with macrophytes and phytobenthos (diatoms), benthic invertebrates and fish (UKTAG, 2014b). Each standard is typically calculated as the ratio between observed sample data taken from the field using standardised sampling protocols and the predicted 'pristine' condition of the site derived using a modelling framework of environmental variables associated with existing un-impacted sites. Macro-invertebrates (or benthic invertebrates) were chosen as the biological standard for this research, as they are very important 'keystone' organisms in aquatic ecosystems, contributing to many ecosystem processes (e.g. nutrient cycling and acting as food sources for other organisms) (Wallace and Webster, 1996). Macro-invertebrate communities are also particularly sensitive to fluctuations in water temperature (Milner and Petts, 1994), flow velocity (James et al., 2008), dissolved oxygen (Connolly et al., 2004), streambed porosity (Olsen and Townsend, 2003), organic matter abundance (Lepori and Malmqvist, 2007) and the temporal variability of these factors (Hussain and Pandit, 2012). Consequently, macro-invertebrates are used extensively as indicators of ecological conditions in aquatic studies (Crossman et al., 2011, Turak et al., 2011a). Therefore, since macroinvertebrates are useful surrogates for assessing ecological condition, predicting changes in macroinvertebrate indices based on modelled future environmental data can provide ecologically meaningful results (Lawrence et al., 2010, Vaughan and Ormerod, 2012, Guse et al., 2015).

At present, the River Invertebrate Classification Tool (RICT) (Davy-Bowker et al., 2008) is used throughout the UK to classify assessments of the general degradation of macro-invertebrates in rivers according to Water Framework Directive (WFD) requirements. This is achieved through the application of the Whalley Hawkes Paisley Trigg (WHPT) metric to macroinvertebrate samples. The WHPT was primarily developed to assess the quality of macroinvertebrate communities with relation to organic enrichment (Walley and Hawkes, 1996, 1997). However, it has also been demonstrated to

act as an indicator of generalised degradation in rivers, as it is known to be sensitive to both toxic pollution and other combinations of pressures (Paisley et al., 2014). Using these site specific WHPT scores, the RICT is used to determine a WFD probabilistic classification through the River Invertebrate Prediction And Classification System (RIVPACS) (Wright et al., 1998) model, which derives an Ecological Quality Ratio (EQR) between WHPT scores for both an estimated 'pristine' site and observed samples. The detailed methodology of how the current RICT classification method is incorporated into this thesis is outlined below.

4.4.2 DATA

Both the Environment Agency (EA) and Centre for Ecology and Hydrology (CEH) have provided over 7000 macro-invertebrate samples collected throughout the Thames Basin (except for the Colne sub-basin) over the past 20 years, accounting for variations in both spatial and temporal correlations. Samples provided include both species/family abundance data and specific index scores (WHPT, ASPT, NTAXA) and environmental predictor variables used in calculation of WFD standards. Samples were collected using the standard 'kick-sampling' methodology compliant with BS EN 27828:1994, ISO 7828-1985 (EU-STAR, 2004a). Benthic macro-invertebrates are collected from shallow flowing waters by disturbing the substratum with the feet, upstream of a hand-net (standardised mesh size of 1mm) held vertically on the riverbed. All habitats within the chosen sampling site should be sampled within a 3-minute period, with an additional manual search, lasting one minute, performed for macro-invertebrates attached to submerged solid objects (i.e. plant-stems, stones and logs). Rivers too deep to be kick-sampled are sampled by either (i) sweeping a long-handled pond net (standardised mesh size of 1 mm) through any aquatic vegetation within reach of the banks of the river, and (ii) kick sampling in any shallow areas, or by using a naturalist's dredge or air-lit sampler; as compliant with BS EN ISO 9391:1995, BS 6068-5.15:1995 (EU-STAR, 2004b). Samples are then analysed in laboratory conditions to identify the presence of macro-invertebrate taxa to RIVPACS taxonomic-level TL2 (families) (Davy-Bowker et al., 2008). The abundance data for each taxon within a sample should also be logged to values outlined in Table 4-2, section 4.4.3.1. Samples are routinely

collected at the same site in both the Spring (April-May) and Autumn (September-October) to ensure intra-annual consistency and provide an indication of inter-annual variations in species composition.

In order to determine the most appropriate samples for use in the macro-invertebrate model, it was necessary to select specific sites and samples from the over 7000 provided by the EA. As such, a logical ruleset based on a variety of factors was determined to identify the most appropriate sample sites. This ruleset is outlined in bullet points below. In total, 290 sites were identified for use in the development of the macro-invertebrate predictive model, which were spatially distributed throughout the Thames Basin and associated catchment types (see Figure 4-3).

- Only one macroinvertebrate site is selected for each catchment.
- Macroinvertebrate sample sites should be situated at the furthest possible point downstream in catchment, to best represent upstream conditions.
- Macroinvertebrate sites should have samples for at least one complete year (two seasonal samples; Spring and Autumn), with some sites having three complete years (6 samples).
    - These samples should be for the most up-to-date years distributed by the EA (2011, 2012 and 2013) (at time of collection; 2015).
- Macroinvertebrate sites should have both and National River Flow Archive (NRFA) and Chemistry monitoring site within 1km.
    - Furthermore, discharge and water chemistry data should be available at these sites for at least a full 3 months prior to each sample date.
    - This ensures key environmental indicators of discharge and water quality can be linked to specific macroinvertebrate scores for use in the predictive model.
- Macroinvertebrate samples must also have available the associated environmental predictors collated at the time of sample collection.
    - These are used in the RICT methodology to predict ‘pristine’ expected WHPT scores.

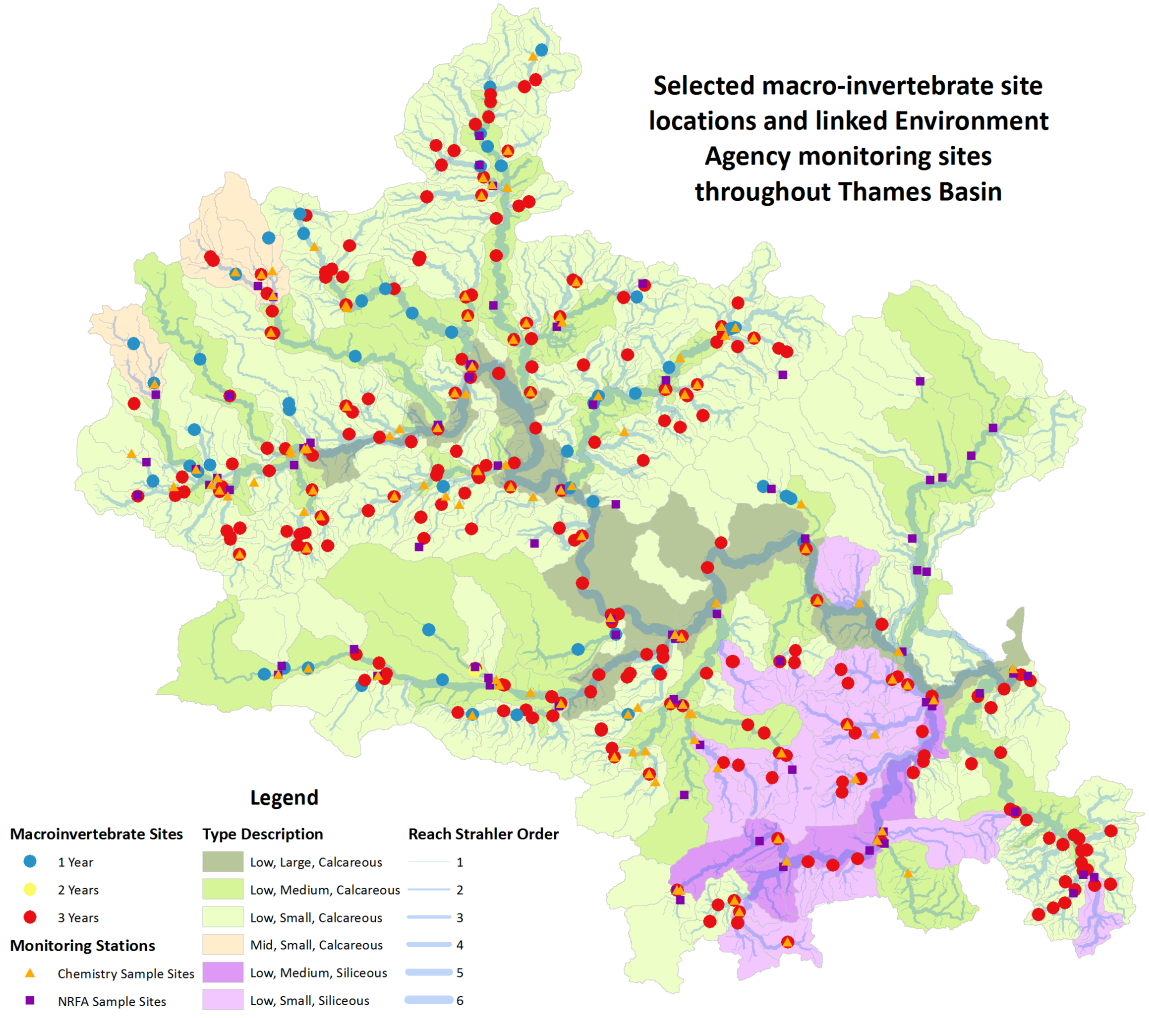


Figure 4-3: Selected macroinvertebrate site locations and linked Environment Agency monitoring sites (Chemistry and Flow) used in this research. Multiple years (2011-2013) of sample data is available for most sites, as colour coded in the legend. Catchment typology is provided for reference.

4.4.3 Methodology

The methodology developed in this research builds upon existing studies that have correlated macro-invertebrate diversity indices with environmental predictor variables (see Adriaenssens et al. (2004), HERING et al. (2006), Monk et al. (2006), Monk et al. (2008), Hoang et al. (2010), Dunbar et al. (2010), Lawrence et al. (2010), Wagenhoff et al. (2012), Domisch et al. (2013), Worrall et al. (2014), Yazdian et al. (2014)) and links climate induced change to alterations in the status of WFD standards. The selection of relevant environmental predictor variables is an essential step in producing a model

that has robust and accurate predictive power. The selection process of these variables for this research is explained in detail in section 4.4.3.2.

4.4.3.1 Generation of macroinvertebrate indices for observed samples

Firstly, the WHPT index and associated NTAXA (number of taxa in sample) and ASPT (Average Score Per Taxon) metrics were calculated for each observed seasonal sample (Spring/Autumn), for each year, at each of the 290 macroinvertebrate sites in the Thames Basin (Figure 4-3). The observed WHPT indices were calculated following the methodology outlined below and in Paisley et al. (2014):

1. Calculate number of taxa (NTAXA)

The observed value of NTAXA is derived from the sum of the number of different taxa listed in Table 4-3 that are present in each of the seasonal samples, for each calendar year. Due to sample sorting and identification errors, the calculated observed NTAXA may be under-estimated and must be bias-corrected. The samples for each season were bias-corrected using a value provided by the EA for each sample, based on an audit of the procedures in place and experience of individual conducting the identification process.

2. Calculate average score per taxon (ASPT)

The first step in deriving the observed ASPT for a sample is by calculating the sum of the pressure sensitivity scores assign to each taxon present in each seasonal sample (P_s). Firstly, count the number of individuals in each taxa list in Table 4-3 and note the relevant abundance code (see Table 4-2). Secondly, for each taxon present, use the associated abundance code to identify the relevant pressure sensitivity score from Table 4-3. Finally, sum all taxon pressure sensitivity scores as derived above to produce the summed pressure sensitivity score for all taxa present in each seasonal sample (P_s). The observed value of ASPT for each seasonal sample is thus derived as P_s divided by NTAXA. The observed value of ASPT derived above must then be bias-corrected to account for identification errors and taxa missed during sample sorting. The estimated ASPT of missed taxa for each seasonal sample is defined as: 4.29 **+** 0.077 **x** observed value of NTAXA. Thus, the bias-corrected value of ASPT

is calculated as follows: [(Observed value of NTAXA **x** observed value of ASPT) **+** (NTAXA bias value **x** estimated ASPT of missed taxa)] **÷** bias-corrected observed value of NTAXA.

Table 4-2: Abundance categories and relevant number of individuals of a species in a sample used in calculation of WHPT metric

Abundance Code	Number of individuals present in each sample
AB1	1 to 10
AB2	11 to 100
AB3	101 to 1000
AB4	>1000

Secondly, reference WHPT-ASPT and WHPT-NTAXA scores were generated for each seasonal sample as per the RICT methodology. This methodology uses 13 Predictive Environmental Variables (PEVs) (Table 4-4) to generate estimated WHPT metrics for each sample using a database of 'pristine' reference samples encompassing all variations in river types throughout the UK between 1978 and 2002 (RIVPACS). However, for certain river types, sites considered to be in reference state do not exist. Consequently, for these river types, the least perturbed of the remaining sites is used to predict the fauna that should occur under reference conditions. As such, in these circumstances, expected scores are adjusted upwards to be more closely aligned with reference conditions (UKTAG, 2014a). RICT was developed as a collaborative, inter-agency project between the regulatory agencies for surface waters in the UK and represents the best practice in determining the ecological health of a river based on macroinvertebrate sampling. The model is complex and subject to regular updates as new data and methods become available. A detailed description of the specific algorithms and processes behind RICT can be found in Easdale (2007), Davy-Bowker et al. (2008) and UKTAG (2014a).

Table 4-3: The WHPT Pressure Sensitivity Scores (PS_S) for each Abundance Category

Taxa Family	AB1	AB2	AB3	AB4
TRICLADA (Flatworms)				
Dendrocoelidae	3.0	2.6	2.6	2.6
Dugesiidae	2.8	3.1	3.1	3.1
Planariidae	4.7	5.4	5.4	5.4
MOLLUSCA (Snails, Limpets and Mussels)				
Neritidae	6.4	6.5	6.9	6.9
Viviparidae	5.2	6.7	6.7	6.7
Unionidae	5.2	6.8	6.8	6.8
Sphaeriidae (Pea mussels)	4.4	3.5	3.4	2.3
Lymnaeidae	3.6	2.5	1.2	1.2
Planorbidae (excl. *Ancylus* group)	3.2	3.0	2.4	2.4
Valvatidae	3.3	3.1	2.7	2.7
Physidae	2.7	2.0	0.4	0.4
Acroloxidae	3.6	3.8	3.8	3.8
Ancylus group (= Ancylidae)	5.8	5.5	5.5	5.5
Bithyniidae	3.6	3.8	3.3	3.3
Dreissenidae	3.7	3.7	3.7	3.7
Hydrobiidae	4.1	4.2	4.6	3.7
OLIGOCHAETA (worms)				
Oligochaeta	3.6	2.3	1.4	-0.6
HIRUDINIA (Leeches)				
Piscicolidae	5.2	4.9	4.9	4.9
Glossiphoniidae	3.4	2.5	0.8	0.8
Erpobdellidae	3.6	2.0	-0.8	-0.8
Hirudinidae	-0.8	-0.8	-0.8	-0.8
CRUSTACEA (Crayfish, Shrimps and Slaters)				
Astacidae (including non-native species)	7.9	7.9	7.9	7.9
Corophiidae	5.7	5.8	5.8	5.8
Asellidae	4.0	2.3	0.8	-1.6
Crangonyctidae	3.8	4.0	3.6	3.6
Gammaridae	4.2	4.5	4.6	3.9
Niphargidae	6.3	6.3	6.3	6.3
EPHEMEROPTERA (Mayflies)				
Siphlonuridae (including Ameletidae)	11.3	12.2	12.2	12.2
Heptageniidae (incl. Arthropleidae)	8.5	10.3	11.1	11.1
Ephemeridae	8.3	8.8	9.4	9.4
Leptophlebiidae	8.8	9.1	9.2	9.2
Ephemerellidae	7.9	8.5	9.0	9.0
Potamanthidae	9.8	10.4	10.4	10.4
Caenidae	6.5	6.5	6.5	6.5

Taxa Family	AB1	AB2	AB3	AB4
Baetidae	3.6	5.9	7.2	7.5
PLECOPTERA (Stoneflies)				
Perlidae	12.6	13.0	13.0	13.0
Chloroperlidae	11.4	12.2	12.2	12.2
Taeniopterygidae	11.0	11.9	12.1	12.1
Perlodidae	10.5	11.5	11.5	11.5
Capniidae	9.7	9.4	9.4	9.4
Leuctridae	9.3	10.6	10.6	10.6
Nemouridae	8.7	10.7	10.7	10.7
ODONATA (Damselflies)				
Calopterygidae (= Agriidae)	5.9	6.2	6.2	6.2
Platycnemididae	6.0	6.0	6.0	6.0
Coenagrionidae (= Coenagriidae)	3.4	3.8	3.8	3.8
ODONATA (Dragonflies)				
Cordulegasteridae	9.8	9.8	9.8	9.8
Aeshnidae	4.7	4.7	4.7	4.7
Libellulidae	4.1	4.1	4.1	4.1
HEMIPTERA (Bugs)				
Aphelocheiridae	8.6	8.5	8.0	8.0
Hydrometridae	4.3	4.3	4.3	4.3
Gerridae	5.2	5.5	5.5	5.5
Mesoveliidae	4.7	4.7	4.7	4.7
Nepidae	2.9	2.9	2.9	2.9
Naucoridae	3.7	3.7	3.7	3.7
Pleidae	3.3	3.3	3.3	3.3
Notonectidae	3.4	3.9	3.9	3.9
Corixidae	3.7	3.9	3.7	3.7
Veliidae	4.5	3.9	3.9	3.9
COLEOPTERA (Beetles)				
Gyrinidae	8.1	9.0	9.0	9.0
Scirtidae (= Helododae)	6.9	6.8	6.8	6.8
Dryopidae	6.0	6.0	6.0	6.0
Elmidae	5.3	7.4	8.3	8.3
Haliplidae	3.6	3.4	3.4	3.4
Paelobiidae (= Hygrobiidae)	3.8	3.8	3.8	3.8
Dytiscidae	4.5	4.8	4.8	4.8
Hydraenidae	8.5	10.5	10.5	10.5
Hydrophilidae	5.8	8.8	8.8	8.8
Noteridae	3.2	3.2	3.2	3.2
MEGALOPTERA				
Sialidae	4.2	4.4	4.4	4.4

Taxa Family	AB1	AB2	AB3	AB4
NEUROPTERA, PLANIPENIA				
Sisyridae	5.7	5.7	5.7	5.7
TRICHOPTERA (Caddis-flies - caseless)				
Philopotamidae	11.2	11.1	11.1	11.1
Polycentropodidae	8.2	8.1	8.1	8.1
Hydropsychidae	5.8	7.2	7.4	7.4
Glossosomatidae	7.8	7.6	7.2	7.2
Psychomyiidae	5.8	5.7	5.7	5.7
Rhyacophilidae	8.1	9.2	8.3	8.3
TRICHOPTERA (Caddis-flies - cased)				
Odontoceridae	11.1	10.3	10.3	10.3
Lepidostomatidae	9.9	10.3	10.2	10.2
Goeridae	8.8	8.8	9.4	9.4
Brachycentridae	9.6	9.5	8.9	8.9
Sericostomatidae	8.9	9.4	9.5	9.5
Beraeidae	8.8	7.3	7.3	7.3
Molannidae	6.5	7.6	7.6	7.6
Leptoceridae	6.7	6.9	7.1	7.1
Phryganeidae	5.5	5.5	5.5	5.5
Limnephilidae (including Apataniidae)	5.9	6.9	6.9	6.9
Hydroptilidae	6.1	6.5	6.8	6.8
DIPTERA (True flies)				
Simuliidae	5.5	6.1	5.8	3.9
Tipulidae (including Cylindrotomidae, Limoniidae & Pedicidae)	5.4	6.9	6.9	7.1
Chironomidae	1.2	1.3	-0.9	-0.9
Athericidae	9.3	9.5	9.5	9.5
Ceratopogonidae	5.4	5.5	5.5	5.5
Chaoboridae	3.0	3.0	3.0	3.0
Culicidae	2.0	1.9	1.9	1.9
Dixidae	7.0	7.0	7.0	7.0
Dolichopodidae	4.9	4.9	4.9	4.9
Empididae	7.0	7.6	7.6	7.6
Ephydridae	4.4	4.4	4.4	4.4
Muscidae	4.0	2.6	2.6	2.6
Psychodidae	4.5	3.0	3.0	3.0
Ptychopteridae	6.4	6.4	6.4	6.4
Rhagionidae	9.6	9.6	9.6	9.6
Sciomyzidae	3.4	3.4	3.4	3.4
Stratiomyidae	3.6	3.6	3.6	3.6
Syrphidae	1.9	1.9	1.9	1.9
Tabanidae	7.1	7.3	7.3	7.3

Table 4-4: Predictive Environmental Variables (PEVs) used in predictive reference WHPT scores within RICT. The details for how to derive these PEVs is also listed.

Predictive Environmental Variable (PEV)	Description	Derivation of PEV
PEV_1	Latitude	Derived from National Grid Reference
PEV_2	Longitude	Derived from National Grid Reference
PEV_3	Altitude	Log10(Altitude (m))
PEV_4	Distance from source	Log10(Distance from source (km))
PEV_5	Stream width	Log10(Stream width (m))
PEV_6	Stream depth	Log10(Stream depth (cm))
PEV_7	Mean substratum	Derived from percentage cover of boulders and cobbles, pebbles and gravel, sand and silt and clay
PEV_8	Discharge Category	Value of Discharge Category (1-9)
PEV_9	Alkalinity	Value of Alkalinity (mg/l $CaCO_3$)
PEV_{10}	Alkalinity (log)	Log10(Alkalinity) (mg/l $CaCO_3$)
PEV_{11}	Slope at site	Log10(Slope at site) (m/km)
PEV_{12}	Mean air temperature	Derived from National Grid Reference
PEV_{13}	Air temperature range	Derived from National Grid Reference

Access to RICT is through a web-portal (accessed at http://rict.sepa.org.uk), to which data is uploaded and calculations processed via a remote server. The WHPT scores and 13 environmental predictor variables for each seasonal sample across all sites were uploaded to the RICT portal and processed using the default values for number of model iterations (10,000) and EQR boundaries (see Table 4-5). (i) Expected WHPT scores were generated for each seasonal sample using the predictive environmental variables for each site. (ii) Mean seasonal WHPT scores were then calculated using the raw index results (ASPT and NTAXA) across 1-3 years at a sample site. (iii) Mean seasonal Ecological Quality Ratios (EQR) were then determined as the difference between estimated and observed mean

seasonal WHPT scores. (iv) The seasonal EQRs are then combined and subjected to a correction factor to form a mean, bias-corrected, multi-season EQI value for each site. (v) Finally, probabilistic classifications relating to WFD standards are produced using these EQR values and the threshold standards outlined in Table 4-5.

Table 4-5: Boundary Ecological Quality Ratio (EQR) values for WHPT

WFD standards	WHPT-ASPT	WHPT-NTAXA
High/Good	0.969	0.80
Good/Moderate	0.860	0.68
Moderate/Poor	0.723	0.56
Poor/Bad	0.585	0.47

4.4.3.2 Development of predictive models to predict macroinvertebrate classification under future climates

In order to generate estimations of changes in EQR values, and thus WFD classification, under altered climates, it was necessary to develop two predictive models that simulated both observed and expected 'pristine' WHPT scores as derived through the RICT methodology above (similar to Glendell et al. (2014)). Essential to this process is determining key physio-chemical and climatic variables that may act as predictors of macroinvertebrate indices. However, the choice of said variables is limited by available outputs from the suite of INCA models calibrated for the Thames Basin in this thesis. For example, dissolved oxygen and alkalinity are important determinants of macroinvertebrate communities (Paisley et al., 2011, Yazdian et al., 2014), yet neither dissolved oxygen concentrations or water pHs are available outputs from the INCA models calibrated and applied in this thesis. Furthermore, local stream attributes, such as percentage cover of various sub-strata, contribute significantly towards the structure of macroinvertebrate communities (HERING et al., 2006, Dunbar et al., 2010). However, such localised environmental parameters are impossible to model under future conditions to the required degree of accuracy (DURANCE and ORMEROD, 2007). As such, meaningful catchment-scale variables that can be modelled with enough accuracy and that impact on the function and structure of macroinvertebrate communities must be elucidated. Over 200

catchment-scale, physio-chemical and hydrological variables known to impact macroinvertebrate communities were compiled from existing literature sources (see HERING et al. (2006), Monk et al. (2006), DURANCE and ORMEROD (2007), Monk et al. (2007), Monk et al. (2008), Dunbar et al. (2010), Paisley et al. (2011), Monk et al. (2012), Wagenhoff et al. (2012), Domisch et al. (2013), Worrall et al. (2014), Glendell et al. (2014), Yazdian et al. (2014), Aazami et al. (2015)) and reduced, based on the availability of outputs from the INCA models, to a selection of 23 variables (see Table 4-6). These variables were utilised in the development of a predictive model for observed WHPT scores for each catchment.

Furthermore, 13 key catchment statistics were compiled for use in the predictive model for expected WHPT scores for each catchment (see Table 4-7). These variables were chosen, as they were both analogous to the PEVs utilised by RICT in determining expected reference metrics, available for all catchments within the Thames Basin (unlike the PEVs) and were temporally and spatially consistent. Both model methodologies are outlined below, along with goodness of fit statistics for both training and validation sets. The use of catchment-scale variables is justified in this instance, as the model seeks to predict changes in combined metrics of macroinvertebrate communities, rather than predict the presence or absence of macroinvertebrates at the species or family level (Statzner et al., 2008, Monk et al., 2012). Taking such a broad-scale modelling approach is necessary, as predictions must be made for all catchments throughout the Thames Basin, despite not every catchment containing a macroinvertebrate sampling site. Furthermore, it was not feasible at the basin-scale to generate predictions of localised stream variables (i.e. percentage sub-strata cover) due to time, data and computational constraints. Local-scale interactions and changes in the presence and abundance of specific species is inherently incorporated into the model using RICT and RICPACS in determining the model's response variable based on observed and expected WHPT metrics.

Table 4-6: The 23 physio-chemical variables, with description, used in predictive macroinvertebrate model to generate observed WHPT scores for each catchment

Predictive Variable	Description
Q_{mean}	Mean flow rate in m^3s^{-1} in 3 months prior to sample collection
Q_{std}	Standard deviation of flow rate in m^3s^{-1} for 3 months prior to sample collection
Q_{min}	Min flow rate in m^3s^{-1} in 3 months prior to sample collection
Q_{max}	Max flow in rate m^3s^{-1} in 3 months prior to sample collection
Q_{10}	Flow rate in m^3s^{-1} which was equalled or exceeded for 10% of flow record in 3 months prior to sample collection. A high flow parameter that provides a measure of the variability of a flow regime
Q_{95}	Flow rate in m^3s^{-1} which was equalled or exceeded for 95% of flow record in 3 months prior to sample collection. A low flow parameter that provides particular relevance to water quality conditions
Q_{low}	Low exceedance flows. Flows exceeded for 95% of flow record divided by mean flow rate for 3 months prior to sample collection. Provides particular relevance to the severity and duration of low flows relative to mean values
SRP_{mean}	Mean, standard deviation, minimum and maximum concentrations (mg/l) of macro-nutrients (SRP, Nitrate and Ammonia) and mean water temperature (°C) at sampling site over 3 months prior to sample collection
$Nitrate_{mean}$	
$Ammonia_{mean}$	
$WaterTemp_{mean}$	
SRP_{std}	
$Nitrate_{std}$	
$Ammonia_{std}$	
$WaterTemp_{std}$	
SRP_{min}	
$Nitrate_{min}$	
$Ammonia_{min}$	
$WaterTemp_{min}$	
SRP_{max}	
$Nitrate_{max}$	
$Ammonia_{max}$	
$WaterTemp_{max}$	

Table 4-7: The 13 catchment variables, with description, used in predictive macroinvertebrate model to generate expected, or reference, WHPT scores for each catchment

Predictive Variable	Description
Catchment Area	Area of catchment in km^2
Catchment Type	WFD UK catchment type
Strahler Order	Strahler Order (1-6) of main river reach in catchment
River Gradient	Gradient (m/km) of main river reach in catchment
River Length	Length (km) of main river reach in catchment
River Width	Average width (m) of main river reach in catchment
Distance from source	Distance from source (km) of main river reach in catchment
Base Flow Index (BFI)	BFI is a measure of the ratio of long-term baseflow to total stream flow, representing the slow continuous contribution of groundwater to surface river flow
Catchment Urban Land-Use	Percentage of land-use in catchment derived from high-resolution, 25m UK Land Cover Map 2015 (LCM15)
Catchment Intensive Agriculture Land-Use	
Catchment Non-Intensive Agriculture Land-Use	
Catchment Wetlands Land-Use	
Catchment Forest Land-Use	

The primary innovation in the modelling framework was the identification and calculation of catchment-scale environmental predictor variables throughout the Thames Basin, and the application of these in determining the sensitivity of the WFD classification for macroinvertebrates to changes in climatic variables based on observed macroinvertebrate classification as calculated by RICT and RIVPACS. To achieve this several methodological steps were developed as outlined below:

1. Customised code written in MatLab™ was used to extract the relevant physio-chemical and hydrological data from both NRFA and chemical sites linked to each of the macroinvertebrate sampling sites involved in the RICT and RIVPACs calculations above. The predictor variables in

Table 4-6 were then generated for each macroinvertebrate seasonal sample (Spring and Autumn) using three months of data prior to the sample being taken. In total, 814 observations were generated for use in the observed model.

2. Customised code written in MatLab™ was used to extract the catchment-specific variables in Table 4-7 for each of the catchments containing a macroinvertebrate sample site. In total, 205 observations were generated for use in the expected model.
3. The observed and estimated values for each seasonal sample, as determined by the RICT and RIVPACs methodology above, were compiled for each of the macroinvertebrate seasonal samples and linked to the predictor variables above.
4. The Regression Learner application in MatLab™ was used to generate two models; observed and expected, using the relevant predictor variables and response variables generated by RICT.

The Regression Learner application in MatLab™ utilises parallel pooling to rapidly cycle through a suite of regression methodologies and select the model methodology with the best-fit using a variety of comparative statistics (e.g. R^2 and Root Mean Squared Error (RMSE)). In, addition, Principal Component Analysis (PCA) was conducted for predictor variables to reduce the complexity of the models and remove collinearity between variables. PCA is a quantitatively rigorous approach to reducing redundancy amongst a large group of variables (Seber, 2009), with the method generating a new set of variables; principal components. Each principal component is a linear combination of all original variables, with all principal components orthogonal to each other, thus eliminating redundant information. In each model, the numbers of principal components kept were those that represented 95% of the total variance of the original predictive variables (8/23 for observed model and 4/13 for expected model). Furthermore, hold-out validation was applied to each of the regression models (25% of data) in order to prevent over-fitting. This data was then used to validate the accuracy of the model in predicting response variables. The regression methodologies fitted in this process include variations of linear models (i.e. stepwise, interactions), Gaussian process regression models (i.e. rational quadratic, Matern 5/2), support vector machines (i.e. linear,

quadratic and Gaussian) and ensembles of trees (i.e. bagged and boosted). In both the expected and observed models, the ensemble of bagged trees regression method provided the best fit against the relevant response variables. Bagged trees regression is a combination of bagging (or **b**ootstrap **agg**regat**ing**), a form of ensemble learning (Breiman, 1996) and decision tree learning, a form of predictive model (Breiman, 1984).

Regression trees uses a decision tree, a flowchart-like structure in which each internal node represents a logical test, each branch an outcome of this test and each leaf node a class label (based on a computation of all attributes), to progress from predictive variables (branches) to response variable values (leaves). The response of a regression tree is predicted by following the tree from the root node to a leaf node. In this process, at each node, a decision is made as to which branch to follow based on a rule associated with that node. This process is repeated until a leaf node is reached, with the value of this leaf node the predicted response of the regression tree. The size and depth, and therefore potential predictive power, of a regression tree may be altered through changing the minimum leaf size component. The minimum leaf size for the observed and expected model was 2 and 3 respectively. Bagging is a machine learning ensemble algorithm used to improve regression classification by combining classifications of randomly generated training sets. In the context of ensemble bagged trees, multiple decision trees are built by repeatedly resampling the training data with replacement. An average response of the trained ensemble can thus be derived by taking an average over all predictions from individual trees. Typically, the number of bootstraps, or learners, can be modified to improve the predictive power of the model; although an optimum number of bootstraps exists for any given regression model. The optimisation of learners was achieved through an iterative approach, whereby multiple models were generated with varying number of learners, and the model providing the best-fit to response variables selected. The number of learners used in the observed and expected models was 81 and 34 respectively.

Model performance was determined through a series of statistics and presented as both regression plots (Figure 4-4 and Figure 4-5) and error histograms (Figure 4-6 and Figure 4-7) for both the

observed model and expected model respectively. It is evident that both models demonstrate strong predictive capacity with regards to training data, with the observed model (R^2 0.908; RMSE 0.312) performing better than the expected model (R^2 0.714; RMSE 0.078). The application of each model to the validation datasets further demonstrates the strong predictive capacity of the models, suggesting that the training data were not over-fitted, with observed model again outperforming the expected model (R^2 0.879 and 0.717 respectively). Model errors, as outlined in the error histograms, suggest that over 90% of both predicted training and validation outputs for both the observed and expected model are within ±0.35 and ±0.14 of target values respectively. Furthermore, both modal error bars are on or within 0.1 of the zero-error lines. The relative weight of these errors between models is similar, as the observed model predicts a broader range of target values (2.7-6.9) than the expected model (4.8-6.15). This is due to the wide range of WHPT observed at sites throughout the Thames Basin and the relatively narrow range of 'reference' WHPT scores expected for the same sites. Finally, there is a slight tendency towards overestimating target values in the validation set of the observed model and underestimating those in the expected model.

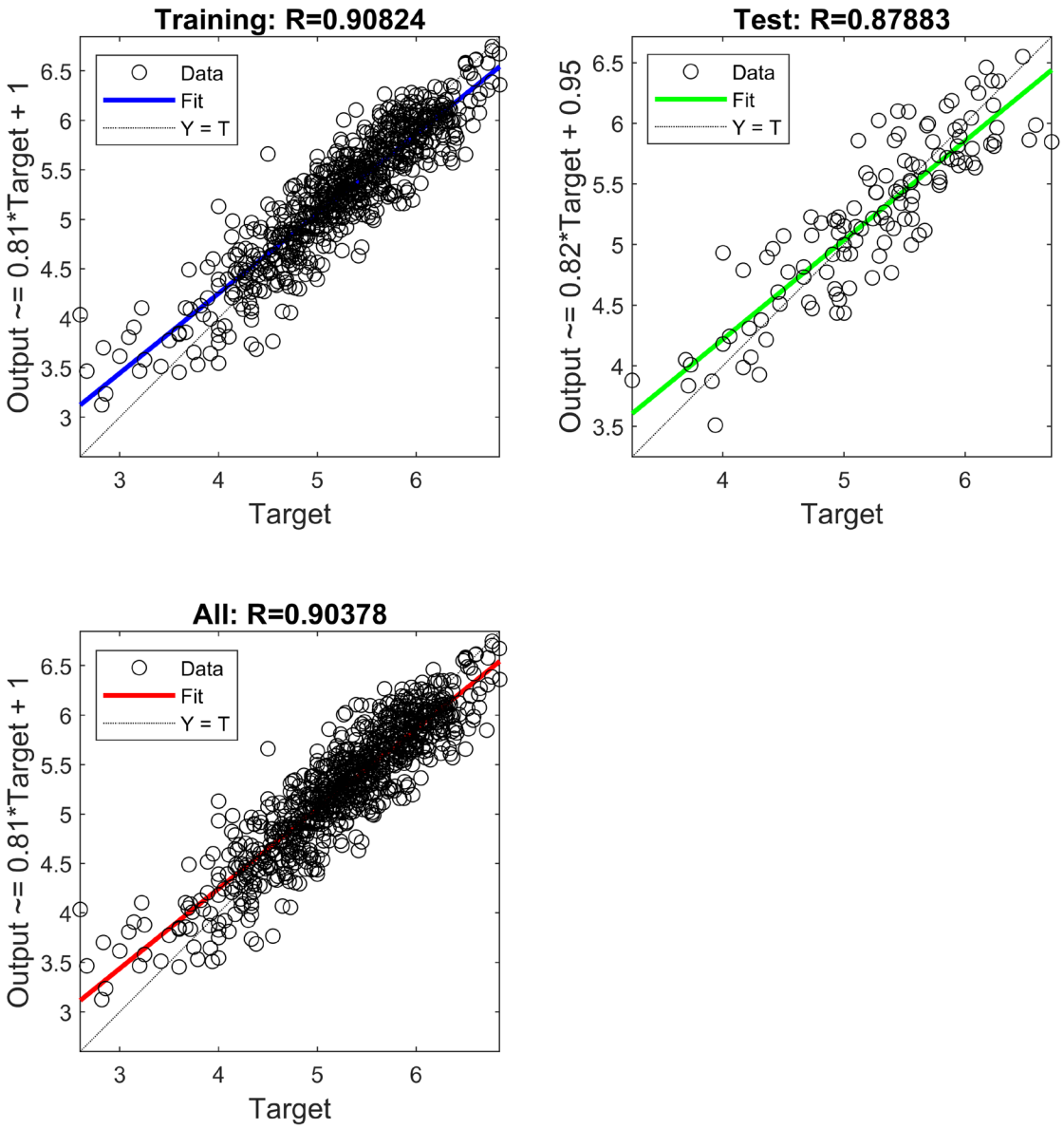


Figure 4-4: Regression plots for the observed macroinvertebrate model, given as target score vs output score. These are provided for the training data (top left), validation data (top right) and combined data (bottom left). A line of best-fit is provided for each plot along with the associated R value (top of plot).

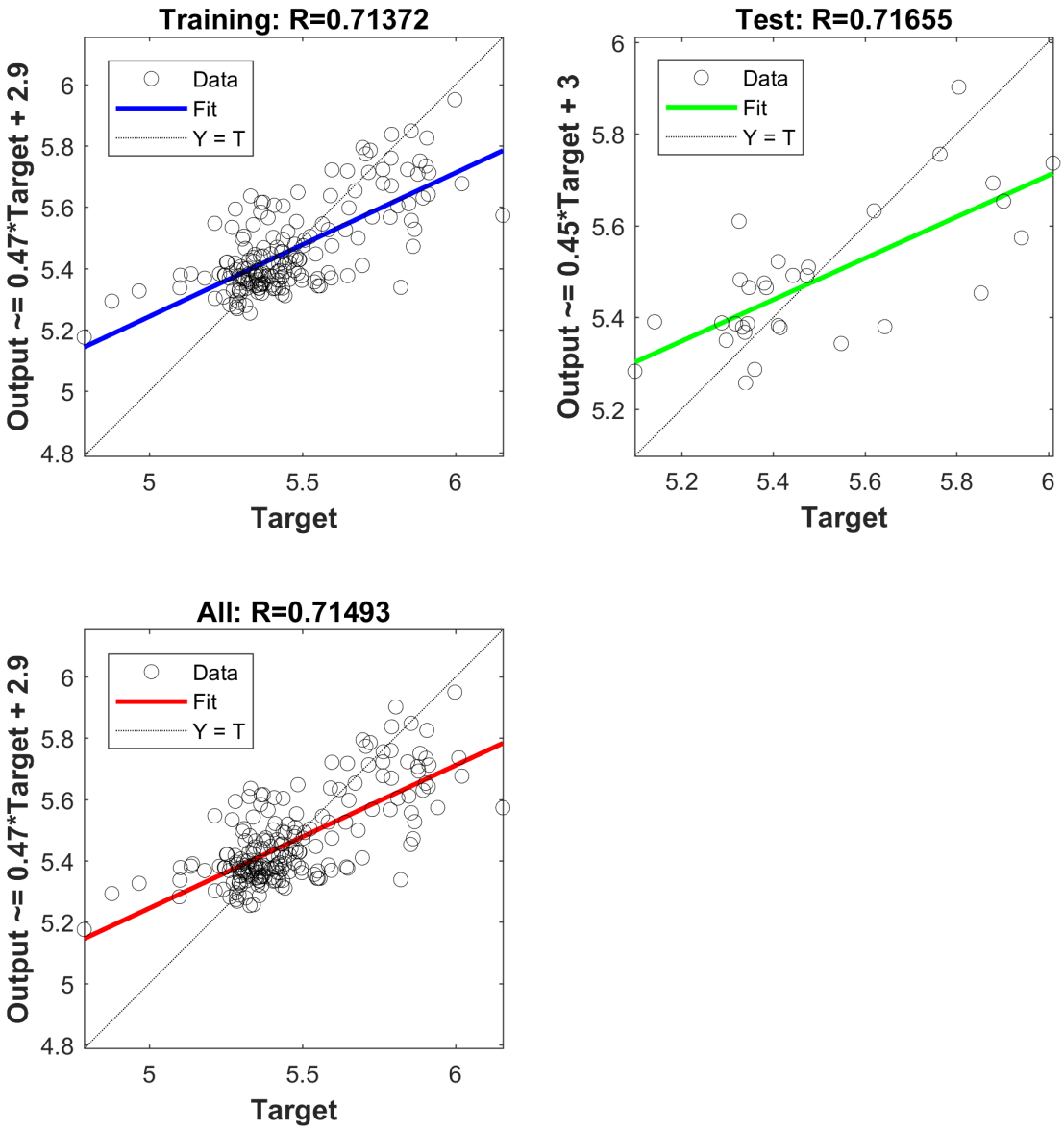


Figure 4-5: Regression plots for the expected macroinvertebrate model, given as target score vs output score. These are provided for the training data (top left), validation data (top right) and combined data (bottom left). A line of best-fit is provided for each plot along with the associated R value (top of plot).

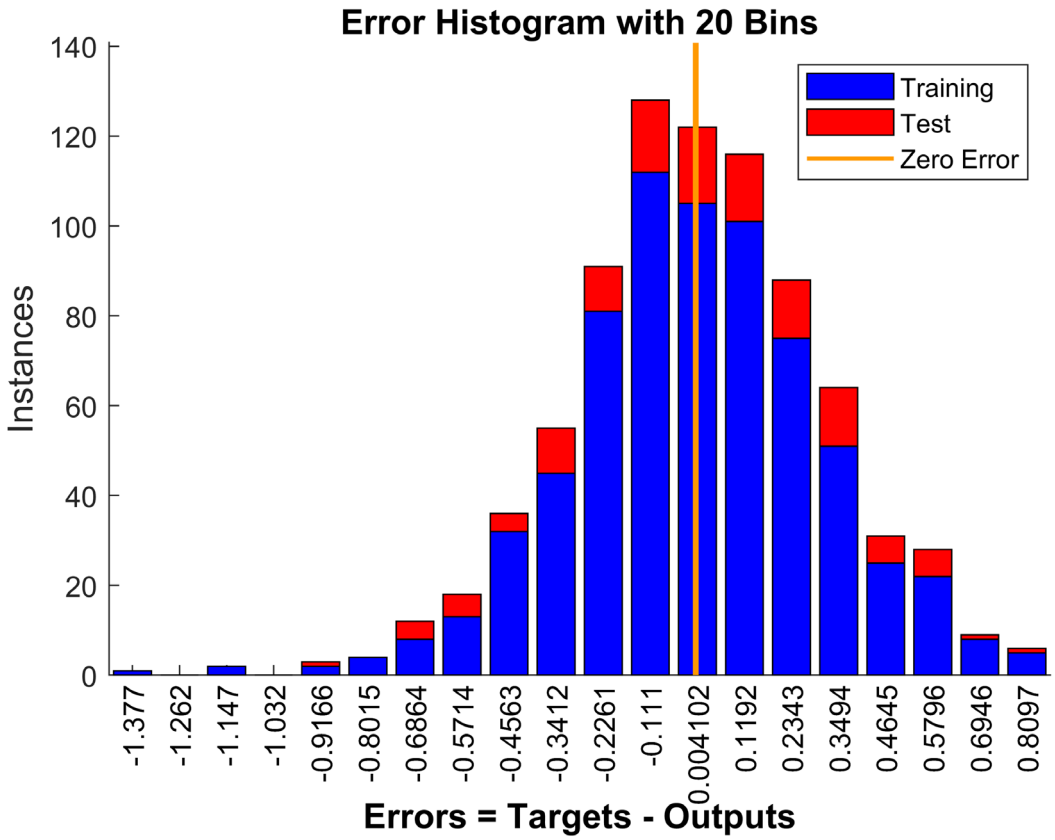


Figure 4-6: Error histogram for the observed macroinvertebrate model. Model deltas (target score-output score) for the training data are binned into categories and represented by blue bars, with those for the validation data represented by the red bars.

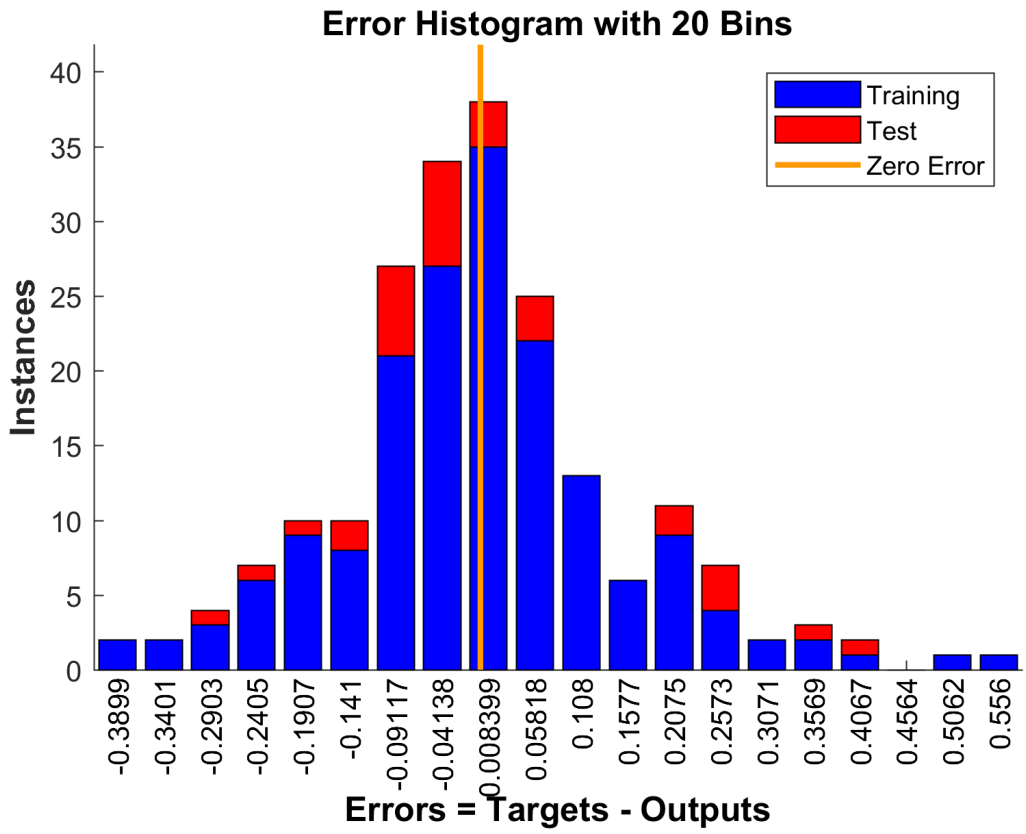


Figure 4-7: Error histogram for the expected macroinvertebrate model. Model deltas (target score-output score) for the training data are binned into categories and represented by blue bars, with those for the validation data represented by the red bars.

4.4.3.3 Application of predictive models to Thames Basin

The final step in determining the sensitivity of biological standards in catchments to changes in climate is the application of both predictive models throughout the Thames Basin. Firstly, the predictor variables in Table 4-6 used for the observed model were calculated for each catchment based on outputs from the INCA models for each season (Spring, Autumn), for each year (30 years) for each of the 300 altered climate sets. Spring values were evaluated using 3 months of data from March to May while autumn values were calculated from September to November. This was achieved through customised code written in MatLab™ and applied to each INCA output file. Secondly, the predictor variables in Table 4-7 used for the expected 'reference' model were collated for each catchment within the Thames basin. Thirdly, to account for predictive errors, 10,000 paired model errors were randomly generated for both observed and expected models. When applied to both the observed and expected models, this produces a probabilistic envelope of potential EQR values for any given seasonal average within any given catchment. Fourthly, using customised code produced in MatLab™, both the observed and expected models were applied to all predictor variables for each catchment, producing both observed and expected WHPT metrics for each season (Spring and Autumn), for each year (30 years) and for all 300 altered climate sets. Subsequently, both these observed and expected WHPT metrics were averaged across seasons and combined to form a single, mean annual 30-year average. Fifthly, utilising the method described in step 3, a probabilistic envelope of 10,000 EQR values were calculated using the mean annual 30-year average values of observed WHPT and expected WHPT as outlined in the RICT methodology above. Finally, the resulting EQR values for each catchment in the Thames Basin were classified as per Table 4-5, providing a percentage probability for macroinvertebrate WFD class for each of the 300 altered climate sets, analogous to those devised using the RICT methodology. Exposure and sensitivity are explicitly incorporated into this linked model of INCA and macroinvertebrate diversity GLM. Changes in macroinvertebrate diversity are calculated using beta-coefficients from the GLM (i.e. sensitivity of the species diversity index to specific changes in their environment), and future modelled physicochemical variables from INCA (i.e. exposure).

4.5 PHYSICAL STANDARDS

According to the WFD, the ecological status of any water body should be determined based on biological data (such as the macro-invertebrate data above). However, for rivers, status assessments also require reference to physical standards such as hydro-morphology and temperature regimes. For the purposes of this research two standards have been selected to represent the physical components of rivers and how these respond to changes in annual precipitation temperature. Firstly, changes to the flow regime are addressed through the application of the Dundee Hydrological Regime Alteration Method (referred from this point on as DHRAM) (Black et al., 2005). Originally developed to link changes in WFD status to the impact of anthropogenic structures (e.g. dams, sewage treatment plants etc.) on river flow-regime, this methodology has been adapted to assess the sensitivity of WFD flow-regime classification to changes in annual precipitation and temperature. Secondly, the WFD standards developed by UKTAG for water temperature in rivers based on fish temperature niches were used (UKTAG, 2014b).

4.5.1 FLOW REGIME AS DETERMINED BY APPLICATION OF THE DUNDEE HYDROLOGICAL REGIME ALTERATION METHOD (DHRAM)

Hydrological processes, or flow regime, represent a 'master' variable in the ecological functioning of river systems (Poff et al., 1997). Alterations to the natural flow regime over annual, seasonal and event-based timescales affect the biodiversity and evolutionary potential of a river ecosystem (Richter et al., 1997, Olden and Poff, 2003). Key features of the hydrological regime essential to ecosystem health are flow magnitude, frequency, duration, timing and rate of change. The magnitude of hydrological and thermal events reflects the availability of the freshwater habitat for both in-stream and riparian species. In addition, the magnitude of thermal events plays a fundamental role on the water quality and distribution of aquatic species (Caissie, 2006, Comte et al., 2013). The frequency of events occurrence, in particular high and low extremes (such as floods and droughts or heat and cold waves), affects population dynamics through impacts on reproduction or increases in species mortality (Richter et al., 1996). The duration of hydrological events, in particular

increases in the duration of droughts and summer heat stress, may lead to significant distortions in community structure and composition and poses elevated, potentially lethal risks, for cold-water species (Markovic et al., 2013). The timing of events, particularly the timing of annual extremes, may impair the ecological success of a specific life-stage. Thus, changes in event timing may result in weakening or breaks in the trophic interactions (Woodward et al., 2010). The rate of change of hydrologic and thermal regimes strongly affects food-web synchrony. Changes in regime variability may affect habitat availability and lead to disruption of established patterns in food-web synchrony (Kishi et al., 2005).

A suite of biologically relevant hydrological indices, the Indicators of Hydrological Alteration (IHA), have been developed that reflect these five broad groups of ecologically important features of natural regimes and form widely adopted practical management framework to analyse both natural and altered hydrological regimes (Richter et al., 1996, 1998). A study by Olden and Poff (2003) used various statistical techniques (including principal component analysis) to demonstrate that the IHA successfully represent all relevant aspects of flow regime alteration and capture much of the data provided by alternative indices of hydrological alteration. The Dundee Hydrological Regime Alteration Methodology (DHRAM) was developed to classify the risk of damage to in-stream ecology using a five-class scheme compatible with the requirements of the EC Water Framework Directive and, as such, utilises these indices of the IHA due to their ability to comprehensively characterise ecologically relevant hydrological regime alteration (Black et al., 2005). Conceptually, it is assumed that the risk of damage to ecosystem structure increases in direct proportion to the cumulative distortion to the hydrological regime. DHRAM uses daily mean flow time-series data, representing un-impacted and impacted situations for the site of interest, in relation to any type of anthropogenic hydrological impact. It compares two sets of flow time series representing un-impacted (or reference) and impacted conditions at the same site, using all 32 IHA indicators (or descriptors) spanning all the features identified by Richter et al. (1996) (see Table 4-8 for details).

Table 4-8: Parameters for the Indicators of Hydrological Alteration

Group	Indicator	Description
Magnitude of monthly water conditions	January mean flow February mean flow March mean flow April mean flow May mean flow June mean flow July mean flow August mean flow September mean flow October mean flow November mean flow December mean flow	Absolute mean and coefficient of variation of monthly average discharge (m^3/s) across all years of sampling period
Magnitude and duration of annual extremes	1-day minimum flow 3-day minimum flow 7-day minimum flow 30-day minimum flow 90-day minimum flow 1-day maximum flow 3-day maximum flow 7-day maximum flow 30-day maximum flow 90-day maximum flow	Absolute mean and coefficient of variation of minimum and maximum discharge (m^3/s) for specified time-period across all years of sampling period
Timing of annual extremes	Julian date of 1-day minimum flow Julian date of 1-day maximum flow	Absolute mean and coefficient of variation of Julian date of 1-day minimum and maximum across all years of sampling period
Frequency and duration of high and low pulses	Annual number of high pulses Annual number of low pulses	Absolute mean and coefficient of variation of annual number of days that flow rises above 75th percentile (high pulses) and falls below 25th percentile (low pulses) across all years of sampling period
	Mean duration of high pulses Mean duration of low pulses	Absolute mean and coefficient of variation of duration in days that flow rises above 75th percentile (high pulses) and falls below 25th percentile (low pulses) across all years of sampling period
Rate and frequency of change in conditions	Mean daily flow increase Mean daily flow decrease	Absolute mean and coefficient of variation of daily rises and falls in discharge (m^3/s) across all years of sampling period
	Number of rises Number of falls	Absolute mean and coefficient of variation of number of daily rises and falls in discharge across all years of sampling period

To calculate DHRAM classifications for a specific site, a series of steps are followed, as outlined here: 1) Means (measures of central tendency) and coefficients of variation (CV; measures of dispersion) are generated for each of these 32 indicators for both un-impacted and impacted conditions at a site,

producing 64 inter-annual statistics in total. 2) The absolute percentage change in means and CVs between the un-impacted and impacted flow series are calculated for each indicator. 3) Averages for all of the absolute changes in mean and all of the absolute changes in CV are calculated for each group of indicators (see Table 4-8), producing five summary indicators for changes in group means (summary indicators 1a–5a) and five for changes in group CVs (summary indicators 1b–5b). Whilst this approach inevitably results in certain summary indicators yielding changes of greater magnitude than others, it is desirable to afford equal weighting to each of the IHA groups in order to present a balanced assessment of change (Olden and Poff, 2003). 4) A system for allocating points to describe the relative severity of change in each summary group was developed by exploring the errors obtained in modelling through review of summary indicator values obtained from 20 natural (reference) catchments and 11 catchments affected by a range of human impacts (Black et al., 2000) distributed throughout Scotland. Three thresholds of increasingly severe impact were determined for each summary group using the following method:

I. The model errors for the 20 natural catchments were used to obtain a lower benchmark score, defined by the mean plus one standard deviation of those 20 errors. This was used to define the summary indicator threshold at which one impact point would be scored.
II. An upper benchmark was defined by the maximum observed summary indicator obtained from the sample of 11 impacted catchments.
III. Two intermediate thresholds were then computed for each summary indicator, obtained by dividing the difference in values between the lower and upper benchmarks by three.
IV. For summary group values exceeding the lower threshold, one point was scored; for the intermediate threshold, two impact points were scored; and for those exceeding the upper intermediate threshold, three impact points were scored.
V. Thus, for any summary indicator, a total of three impact points could be scored. As such, a site could score a theoretical maximum of 30 impact points.

Threshold values for each summary indicator are shown in Table 4-9. In the absence of relevant climate change specific thresholds for low-land UK rivers, these thresholds were used in this

research. This is not unprecedented, as Dyer et al. (2014) have applied a similar methodology in an Australian catchment to assess the impacts of climate change on ecologically-relevant flow regime and water quality attributes.

Table 4-9: Hydrological change thresholds used for allocation of impact points,

IHA summary indicator	Percentage change in IHA group score		
	Lower Threshold (1 impact point)	Intermediate Threshold (2 impact points)	Upper Threshold (3 impact points)
1a (Group 1 means)	19.9	43.7	67.5
1b (Group 1 CVs)	29.4	97.6	165.7
2a (Group 2 means)	42.9	88.2	133.4
2b (Group 2 CVs)	84.5	122.7	160.8
3a (Group 3 means)	7	21.2	35.5
3b (Group 3 CVs)	33.4	50.3	67.3
4a (Group 4 means)	36.4	65.1	93.8
4b (Group 4 CVs)	30.5	76.1	121.6
5a (Group 5 means)	46	82.7	119.4
5b (Group 5 CVs)	49.1	79.9	110.6

Finally, cumulative DHRAM scores were calculated by summing impact points across all IHA summary indicators (minimum 0; maximum 30). These were then mapped to WFD classifications using the thresholds outlined in Table 4-10, as taken from Black et al. (2005).

Table 4-10: DHRAM score thresholds used to allocate WFD classification.

WFD Class	DHRAM Score Upper Range	Description
High	0	Un-impacted condition
Good	4	Low risk of impact
Moderate	10	Moderate risk of impact
Poor	20	High risk of impact
Bad	30	Severely impacted condition

4.5.2 TEMPERATURE

Similarly to river flow-regime, water temperature is recognised as an important and highly sensitive driver of water quality (Webb et al., 2008). Temperature influences aquatic life in a variety of direct and indirect ways. Directly, water temperature influences the distribution (e.g. Boisneau et al. (2008),

growth rates (e.g. Jensen (2003), Imholt et al. (2010), (2011)), timing of life history events (e.g. Harper and Peckarsky (2006)), predator-prey interactions (e.g. Boscarino et al. (2007)), metabolism (e.g. Alvarez and Nicieza (2005)) and ultimately survival (e.g. Wehrly et al. (2007)) of aquatic organisms in river systems. Indirectly, temperature controls in-stream processes such as rates of production and nutrient consumption, further influencing ecological processes of food availability, decomposition (e.g. Ormerod (2009)) and dissolved oxygen concentration (e.g. Sand-Jensen and Pedersen (2005)). Riverine water temperatures are controlled by complex dynamic energy (heat) and hydrological fluxes at the air-water and water-riverbed interfaces (Hannah et al., 2008b), and occur through a combination of radiation, conduction, convection and advection (Webb et al., 2008). Morphological characteristics of the river, such as the shape of the channel and the velocity and depth of the water also contribute towards controlling temperature, alongside localised effects of shading by riparian vegetation and groundwater inputs (Hannah et al., 2008a, Hannah and Garner, 2015). Furthermore, the hierarchical organisation of river systems contributes to the propagation of water temperature downstream, with summer temperatures typically increasing from headwater to estuary (Montgomery, 1999). Diffuse and point source anthropogenic impacts on rivers, such as discharges of effluents, water abstractions and changes in land-use may also significantly contribute towards changes in riverine water temperatures (Caissie, 2006).

Aquatic species sensitivity to water temperature is varied, with certain species able to occupy a broad range of temperatures, whilst others have an extremely narrow tolerance range (Beitinger et al., 2000). However, most species do have some capacity to adapt to changes in water temperature outside of their current ‘niche’ (Heino et al., 2009). It is this temperature tolerance and capacity to adapt, specifically relating to fish species, that UKTAG used to develop temperature standards for UK rivers (UKTAG, 2014b). A basic river typology was derived for water temperature, cool-water and warm-water, based on the salmonid and cyprinid groupings for the Freshwater Fish Directive (see Table 4-11) (UKTAG, 2014b).

Table 4-11: River typology based on fish community

Type	Key species	Complementary Species	Abundance/comments
R1	Brown Trout	Salmon; Bullhead	Very high abundance of Trout
R2	Salmon; Brown Trout	Bullhead; Stone Loach	Very high abundance of Salmon
R3	Brown Trout	Eel; Bullhead; Stone Loach	Very high abundances of minor species and high abundance of Trout
R4	Brown Trout; Eel	Lamprey; Flounder	Relatively high abundance of diadromous species plus some coastal species
R5	Barbel; Chub	Grayling; Stone Loach	Relatively high abundance of Barbel, indicative of main river stem of large rivers
R6	Roach; Bream	Gudgeon; Chub; Dace; Perch	Relatively high abundances of common cyprinid species
R7	Pike; Bleak	Roach	Presence of bleak and relatively high abundances of Pike and Bream indicative of larger lowland rivers
R8	Salmon; Grayling	Brown Trout; Pike	Relatively high abundances of Grayling, Salmon and Pike. Constitutes sites from Hampshire chalk rivers Test and Itchen
River water temperature typology			
Cool Water		**R1, R2, R3, R4, R8**	
Warm Water		**R5, R6, R7**	

Since fish species spend two thirds of their lifetime within 2°C of a preferred temperature, the proposed boundary between 'High' and 'Good' status for rivers is the upper limit of this niche (±2°C of the preferred temperature). Similarly, the boundary between 'Good' and 'Moderate' status is the upper limit of the niche in which most fish will spend their entire lifetime (±5°C of the preferred temperature). The boundary between 'Moderate' and 'Poor' status is the lower limit of the range in estimates of lethal temperatures for fish species. These standards are derived from annual 98th percentiles of water temperature for a site and outlined in Table 4-12.

Table 4-12: Proposed boundaries for water temperature

Water temperature (°C) (Annual 98th percentiles)				
River Type	**High**	**Good**	**Medium**	**Poor**
Cold Water	20	23	28	30
Warm Water	25	28	30	32

4.6 CHEMICAL STANDARDS

Riverine water chemistry is primarily determined by the nature of inputs into the river, and subsequently by the physical, biological and chemical processes that impact these inputs in-stream (Robson and Neal, 1997). These inputs can broadly be defined as from either diffuse (i.e. agricultural, geological or atmospheric) or point sources (i.e. sewage works, industry, local-farm effluent etc.), and can introduce a wide-range of compounds into the river system (e.g. pesticides, heavy metals, macro-nutrients, sediment etc.). The severity and extent of impact that these inputs have on riverine ecosystems vary, though many are associated with a reduction in water quality and detrimental impacts on lotic biodiversity. Specifically, increasing nutrient concentrations in rivers alters the biomass and composition of biological communities (Smith et al., 1999). Enhanced plant and algal production are such an example, which can lead to the physical blockage of river channels and fish kills due to a reduction in dissolved oxygen. Many of these determinants of water quality are monitored throughout UK rivers by the Environmental Agency and, using these data, standards have been developed to assess and classify the chemical status of a river.

Key chemical WFD standards that contribute towards determining riverine status are dissolved oxygen, biological oxygen demand (BOD), pH, phosphorus, ammonia and a range of heavy metals (UKTAG, 2014b). Due to time, financial and computational constraints, not all water quality components could be assessed in this research. However, ammonia and phosphorus were selected, as the INCA models used in this research (INCA-N and INCA-P) produce daily concentrations of both macro-nutrients. Furthermore, excessive anthropogenic inputs of ammonia and phosphorus are key drivers in the eutrophication of freshwaters, a significant environmental problem globally (Elser et al., 2007). Throughout the UK and across Europe, reducing ammonia and phosphorus concentrations in surface waters has become a top priority. Whilst improvements in wastewater treatment and stricter control over fertiliser use has seen a marked decrease in the dissolved nutrient concentrations of rivers in recent decades (Leaf, 2018), many surface waters still suffer from eutrophication due to both sewage effluent and agricultural nutrient inputs (Leaf, 2018). Therefore, a reduction in diffuse and point sources of nutrients to rivers is essential to improving water quality

and biodiversity. However, in-stream nutrient concentration is often a result of a variety of highly variable fluxes and processes, meaning direct management solutions linking changes in diffuse and point sources to in-stream nutrient concentrations is rarely straightforward. Furthermore, the long-term accumulation of nutrients in catchment soils, groundwater and stream bed sediments may continue to affect freshwater ecology long after farm or effluent based remediation has been implemented (Jarvie et al., 2013, Sharpley et al., 2015).

4.6.1 TYPOLOGY FOR NUTRIENT CONDITIONS FOR RIVERS

In developing standards for the nutrient content of rivers in the UK, it is first necessary to classify rivers into different types. Creating this typology allows nutrient thresholds to be elucidated and applied to catchments sharing similar characteristics. The basic typology developed by UKTAG utilises two factors, alkalinity and altitude, both of which have been shown to play important roles in determining the biota of UK rivers (UKTAG, 2014b). Alkalinity is expressed as five divisions of the concentration of calcium carbonate (which cover the range found in UK rivers) and altitude is split into two types – less than or greater than 80 metres. The typology is shown in Table 4-13.

Table 4-13: Basic typology for rivers

Site Altitude	Alkalinity (as mg/l CaCO3)				
	Less than 10	**10 to 50**	**50 to 100**	**100 to 200**	**Over 200**
Under 80 metres	Type 1	Type 2	Type 3	Type 5	Type 7
Over 80 metres			Type 4	Type 6	

The following thresholds of alkalinity and altitude created suitable levels of sensitivity to pressures from ammonia:

• Alkalinity: up to, then above 50 mg/l of calcium carbonate;

• Altitude: up to, then above 80 metres.

Thus, those types with similar ammonia standards were amalgamated to form a simplified typology of two types outlined in Table 4-14.

Table 4-14: Final typology for ammonia in rivers

Upland and low alkalinity	Types: 1, 2, 4 and 6
Lowland and high alkalinity	Types: 3, 5 and 7.

4.6.2 AMMONIA STANDARDS

Ammonia (NH_3) is one of several forms of nitrogen that exist in aquatic environments, but unlike other forms of nitrogen (e.g. nitrates and nitrites) that can cause over-enrichment of a water body at elevated concentrations and indirect effects on aquatic life, ammonia causes direct toxic effects and sub-lethal impacts on fish and macro-invertebrates (de Zwart et al., 2006). Ammonia is primarily a decay product of nitrogenous organic wastes and naturally occurs in rivers due to the decomposition of animal and vegetable waste matter (mineralisation), gas exchange with the atmosphere (volatilisation and dissolution) and nitrogen fixation processes by bacteria (denitrification) (Johnson et al., 2007). Key artificial sources of ammonia in rivers are diffuse agricultural nitrogen-based runoff (such as fertilisers, pesticides and manure) and point-source sewage effluent from water treatment works (Jin et al., 2012). Ammonia has not been shown to adsorb to soil particulates and therefore erosion and lag-effects associated with groundwater do not appear to influence ammonia concentrations in rivers (Johnson et al., 2007).

The standards developed by UKTAG are based on the ammonia concentrations associated with macro-invertebrate communities at 'High' and 'Good' status. Thresholds of status were defined by the concentration of ammonia achieved by 90% of the samples assessed for each river type as outlined in Table 4-14. Catchment classification is determined by the 90th percentile of annual average ammonia concentration (in mg/l), dependent on thresholds determined by catchment type. Standards for ammonia are outline below in Table 4-15.

Table 4-15: Standards for ammonia in rivers

Total Ammonia (mg/l) (90th Percentile)				
Type	**High**	**Good**	**Moderate**	**Poor**
Upland and low alkalinity	0.2	0.3	0.75	1.1
Lowland and high alkalinity	0.3	0.6	1.1	2.5

4.6.3 PHOSPHORUS STANDARDS

Phosphorus (P) is a plant nutrient and is fundamental to the ecological quality of river waters (Jarvie et al., 2002). Elevated concentrations of the soluble reactive portion of phosphorus (SRP) in rivers can lead to eutrophication (Jarvie et al., 2006), with changes in the composition and abundance of plant species leading to a reduction in habitat quality and ultimately in-stream biodiversity (Gardner et al., 2002). It is particularly during periods of ecological sensitivity (i.e. flood events) that the concentration of SRP has the greatest influence upon ecological river quality (Jarvie et al., 2006). Whilst phosphorus occurs naturally in river systems, artificial sources of phosphorus can be from both diffuse (e.g. agricultural runoff) and point (e.g. sewage treatment works) inputs (Whitehead et al., 2013). Agricultural sources, which are applied to the catchment as fertiliser and delivered to rivers in a dissolved or particulate form through runoff following rainfall events, account for a significant proportion of nutrient loads in UK rivers, supplying over 45% of total phosphorus (Gardner et al., 2002). Since phosphorus readily adsorbs to soil particles, bank erosion is a major contributor to riverine phosphorus concentrations, particularly under flood conditions (Gentry et al., 2007). Furthermore, phosphorus migrates with groundwater flows, with the consequence that catchments with groundwater discharge may experience a lag-effect of increased phosphorus concentrations associated with precipitation events long after the event has occurred (Carlyle and Hill, 2001). Thus, changes in the concentration of phosphorus in rivers are likely to be sensitive to increased precipitation events associated with climate change (Wu et al., 2012, El-Khoury et al., 2015).

Standards for phosphorus have undergone several reviews by UKTAG, with the latest iteration involving a regression analysis of a large set of linked biological and chemical data across the UK (UKTAG, 2014b). Phosphorus standards are derived using the ratio between estimated 'reference' conditions and observed concentrations of soluble reactive phosphorus (SRP) for a site, producing standards in the form of annual mean concentrations of reactive phosphorus in µg/l estimated for the lower-class boundary of high, good, moderate and poor ecological status, depending on the value of 'EQR' used. The recommended standard for a site is calculated using the following equation:

$$Standard = 10^{((1.0497 \times log_{10}(EQR) + 1.066) \times (log_{10}(Ref_{SRP}) - log_{10}(3{,}500)) + log_{10}(3{,}500))}$$

Estimated 'reference' or 'natural' conditions are first predicted using values of alkalinity and altitude to represent key geological and geographic factors that determine a site's natural phosphorus concentrations. This is outlined in the equation below:

$$Ref_{SRP} = 10^{(0.454(\log_{10} alk) - 0.0018(altitude) + 0.476)}$$

Where Ref_{SRP} is the predicted soluble reactive phosphorus (SRP) 'reference' concentration of a site in µg/l, alk is alkalinity measure as the concentration of $CaCO_3$ in mg/l at a site and $altitude$ is the altitude of a site above mean sea level in metres. For sites with an alkalinity greater than 250 mg/l, alkalinity is set to 250 mg/l. For sites with an alkalinity less than 2 mg/l, it is set to 2 mg/l. For sites with an altitude greater than 355 metres, altitude is set to 355 metres. Finally, if the predicted value of Ref_{SRP} is < 7 µg/l, Ref_{SRP} is set to 7 µg/l.

A regression equation was developed linking biological data (the worst classed of macrophytes and diatoms) and these phosphorus ratios. Provided the alkalinity and altitude of a site are known, the equation can be used to estimate the likely ranges of phosphorus concentrations at the site associated with each biological status class. The regression equation was re-arranged and used to calculate the most likely phosphorus concentration at the midpoint of each biological class. The ecological quality ratio (EQR) represents the degree of disturbance to diatom and macrophyte status compared with near undisturbed conditions where adjacent classes overlap (i.e. between High & Good, Good & Moderate, Moderate & Poor, Poor & Bad). The values for $'EQR'$ in the standard equation are: 'High', 0.702; 'Good', 0.532; 'Moderate', 0.356; and 'Poor', 0.166. Thus, substituting these values into the generalised equation generates specific equations for each class demonstrated in Table 4-16.

Standards were thus determined for each catchment within the Thames basin using the equations above. 'Reference' phosphorus concentrations were derived using annual average alkalinity concentrations and altitude values extracted from the observed chemistry sites and digital elevation model (DEM) data.

Table 4-16: Standards for phosphorus in rivers

Annual mean reactive phosphorus concentration (in µg/l) is calculated as follows:	
High	$10^{((1.0497\times log_{10}(\mathbf{0.702})+1.066)\times(log_{10}(Ref_{SRP})-log_{10}(3{,}500))+log_{10}(3{,}500))}$
Good	$10^{((1.0497\times log_{10}(\mathbf{0.532})+1.066)\times(log_{10}(Ref_{SRP})-log_{10}(3{,}500))+log_{10}(3{,}500))}$
Moderate	$10^{((1.0497\times log_{10}(\mathbf{0.356})+1.066)\times(log_{10}(Ref_{SRP})-log_{10}(3{,}500))+log_{10}(3{,}500))}$
Poor	$10^{((1.0497\times log_{10}(\mathbf{0.166})+1.066)\times(log_{10}(Ref_{SRP})-log_{10}(3{,}500))+log_{10}(3{,}500))}$

4.7 SUMMARY MAPS FOR USE IN CONSERVATION EFFORTS: QUANTIFICATION OF ECOLOGICAL RISK WITH REFERENCE TO CLIMATE CHANGE

The quantitative assessment of future risk is, by its nature, a difficult task (Ylhäisi et al., 2015). However, where there is a classification of indicator quality, such as the WFD scheme, it is possible to develop a semi-quantitative estimate of risk through the introduction of the concept of an estimated ecological impact or notional fiscal cost for remediation. Outlined below is a novel process, like that employed in section 2.2.7, that is used to produce summary maps highlighting the risk associated with alterations in selected hydro-ecological indices under climate change. These represent the aggregation together of the data and concepts discussed in this thesis and present high-resolution, simplified outputs that consider and illustrate the dynamic threat of climate change on key parameters of riverine health and function. These summary maps are straightforward to interpret and visually and have the potential to be significant in the development of future management plans for the Thames Basin.

The first consideration in aggregating together these indicators is to decide where there is no notional cost and therefore no impact and no associated risk. The concept of a notional impact or weight, is a common method in the derivation of summary indicators used to differentiate between the relative importance that aggregated variables have towards the final discriminators (Turnhout et al., 2007). Conceptually, if it is decided that no action is required for catchments with 'High' and 'Good' indicators then there is no associated notional cost and, consequently, no impact and no related risk. If, however, there is intent to change catchments with 'Good' status to 'High' status then

there will be a cost that can be considered as an associated risk. This latter scenario is considered in the present work, as it is the most stringent indicator of risk. It is to be noted that the most recent revision to River Basin Management plans outlines the requirement that all catchments across the UK should attain an overall ecological classification of 'High' or 'Good' by 2021 (EA, 2015a).

It is reasonable to presume that the worse the indicator then the greater the notional cost and impact, and thus the greater the associated risk (Chin et al., 2010, Comer et al., 2012). If there is no readily available information on the relative severity that WFD classifications have on freshwater communities, the least biased assumption for notional cost is that it becomes an order of magnitude more expensive and impactful on moving from a class to the adjacent poorer class in the WFD scheme (i.e. 'Good' to 'Moderate'). The resulting class magnitudes are listed in Table 4-17. With no remediation required for indicators that are 'High' (following EA (2015a)), then the cost, $C = 0$; for all other classes, as indicated in the table below, $C = \mathrm{u}^m$, where u denotes the base value of the magnitude and m is the order of magnitude.

Table 4-17: Class magnitude and cost used in this methodology for each of the WFD classifications

Class	High	Good	Moderate	Poor	Bad
Class magnitude (m)	0	1	2	3	4
Class 'cost'	0	u	u^2	u^3	u^4

In future scenarios, most indicators are likely to span more than one class, since a percentage likelihood of classification was used to reflect the uncertainty in UKCP09 projections. The fractions, α_m, of each class sum up to unity; i.e. $\sum_{m=0}^{4} \alpha_m = 1$. The summed cost over all the classes are the individual class 'costs' weighted by the class fraction; i.e., $C = \sum_{m=1}^{4} \alpha_m \, u^m$. Note that the summation begins at 1, as there is no cost assigned to a 'High' status. Taking the logarithm (base u) of this cost returns the cost to a scale between 0 and 5. This maps the notional cost, and thus the associated risk, back on to class magnitudes so that the order of magnitude of the risk is $R = \log_{(\text{base u})}(\sum_{m=1}^{4} \alpha_m \, u^m)$ and may be indicated on catchment maps by the familiar class colours associated with WFD standards (UKTAG, 2014b). These equations are explicitly described in Table 4-18.

Table 4-18: A detailed explanation of cost components and order of magnitude risks. The bold integers with subscript, u, indicate numbers expressed in base u; e.g. with u =4, then $\mathbf{1_u}$, $\mathbf{10_u}$, $\mathbf{100_u}$, and $\mathbf{1000_u}$ are respectively: 1, 4, 16 and 64.

Class	High	Good	Moderate	Poor	Bad	Risk
Class % (α)	α_0	α_1	α_2	α_3	α_4	
'Cost" components	0 +	$\alpha_1 \times [\mathbf{1_u}]$ +	$\alpha_2 \times [\mathbf{10_u}]$ +	$\alpha_3 \times [\mathbf{100_u}]$ +	$\alpha_4 \times [\mathbf{1000_u}]$	= Σ
'Risk' = $\log_u$('cost')						= $\log_u(\Sigma)$

The risk, R, expressed as an order of magnitude, provides an intuitive overview of the increased impact associated with climate change, as determined by the UKCP09 projections used in this thesis.

Tables 4-19 to 4-22 show a worked example of the methodology for the order of magnitude risk assessments for SRP and ammonia concentrations, water temperature and flow regime alteration (DHRAM) for the Teddington catchment respectively. Four different base values, namely 2, 4, 16 and 4^{12}, have been selected for the order of magnitude. The SRP and ammonia concentration indicators

for the Teddington catchment are defined within a single class for 2040s, 2060s and 2080s scenarios. Independent of the size of the order of magnitude, the base value, the risk is returned as the same value as the indicator class itself. For SRP and ammonia concentration, the order of magnitude of the risks, are respectively associated with 'Poor' and 'Good'. The risk increases monotonically from u=2 to $u=4^{12}$, as the higher the base value the more disproportionate the cost associated with remediation. Indeed, large base value places a disproportionate emphasis on the worst-case indicators and essentially selects only these worst-case scenarios. Having a factor of two increases in the notional cost of moving from, for example, a 'Good' to 'Moderate' class indicator is likely to be too small. The RGB colour values in the 'Risk' column are determined by a linear interpolation of the RGB values of the classes on either side of the 'Risk' value;

e.g. RGB(0.858) = 0.142×RGB(High) + 0.858×RGB(Green)

RGB(0.858) = 0.142×RGB(0, 0, 255) + 0.858×RGB(0, 255, 0) = RGB(0, 36, 219)

The colour difference, which equates directly to the order of magnitude risk, between u=4 to u=16 are not visibly significant, indicating that a good visual estimate of risk is not too dependent on the order of magnitude of the notional cost change on going from one class to its neighbour. Basin maps for $u=4^2=16$ are shown for all four WFD indicators in Figure 4-8.

Table 4-19: Order of magnitude risk assessments for SRP concentration for the Teddington catchment. The cell colours in the Risk column are determined from the numbers in the Risk column.

SRP (2040/2060/2080)	High		Good		Moderate		Poor		Bad	Risk
class % (α)	0		0		0		1		0	
"cost" components	0	+	0	+	0	+	[100_u]	+	0	
$\log_u$("cost") u=2										3.000
$\log_u$("cost") u=4										3.000
$\log_u$("cost") $u=4^2$										3.000
$\log_u$("cost") $u=4^{12}$										3.000

Table 4-20: Order of magnitude risk assessments for ammonia concentration for the Teddington catchment. The cell colours in the Risk column are determined from the numbers in the Risk column.

ammonia 2040/2060/2080)	High	Good	Moderate	Poor	Bad	Risk
class % (α)	0	1.000	0	0	0	
"cost" components	0 +	$[1_u]$ +	0 +	0 +	0	
$\log_u$("cost") u=2						1.000
$\log_u$("cost") u=4						1.000
$\log_u$("cost") $u=4^2$						1.000
$\log_u$("cost") $u=4^{12}$						1.000

Table 4-21: Order of magnitude risk assessments for water temperature for the Teddington catchment. The cell colours in the Risk column are determined from the numbers in the Risk column.

H_2O temp (2040)	High	Good	Moderate	Poor	Bad	Risk
class % (α)	0.905	0.095	0	0	0	
"cost" components	0 +	0.095×$[1_u]$ +	0 +	0 +	0	
$\log_u$("cost") u=2						0.000
$\log_u$("cost") u=4						0.000
$\log_u$("cost") $u=4^2$						0.151
$\log_u$("cost") $u=4^{12}$						0.858
H_2O temp (2060)	High	Good	Moderate	Poor	Bad	Risk
class % (α)	0.475	0.520	0.005	0	0	
"cost" components	0 +	0.520×$[1_u]$ +	0.105×$[10_u]$ +	0 +	0	
$\log_u$("cost") u=2						0.084
$\log_u$("cost") u=4						0.566
$\log_u$("cost") $u=4^2$						0.817
$\log_u$("cost") $u=4^{12}$						1.683
H_2O temp (2080)	High	Good	Moderate	Poor	Bad	Risk
class % (α)	0.185	0.704	0.105	0.006	0	
"cost" components	0 +	0.704×$[1_u]$ +	0.105×$[10_u]$ +	0.006×$[100_u]$ +	0	
$\log_u$("cost") u=2						0.908
$\log_u$("cost") u=4						1.144
$\log_u$("cost") $u=4^2$						1.495
$\log_u$("cost") $u=4^{12}$						2.693

Table 4-22: Order of magnitude risk assessments for DHRAM for the Teddington catchment. The cell colours in the Risk column are determined from the numbers in the Risk column.

DHRAM (2040)	High		Good		Moderate		Poor		Bad	Risk
class % (α)	0.060		0.858		0.082		0		0	
"cost" components	0	+	0.858×[$\mathbf{1}_u$]	+	0.082×[$\mathbf{10}_u$]	+	0	+	0	
$\log_u$("cost") u=2										1.032
$\log_u$("cost") u=4										1.124
$\log_u$("cost") u=4^2										1.280
$\log_u$("cost") u=4^{12}										1.850
DHRAM (2060)	**High**		**Good**		**Moderate**		**Poor**		**Bad**	**Risk**
class % (α)	0.013		0.826		0.161		0		0	
"cost" components	0	+	0.826×[$\mathbf{1}_u$]	+	0.161×[$\mathbf{10}_u$]	+	0	+	0	
$\log_u$("cost") u=2										1.201
$\log_u$("cost") u=4										1.279
$\log_u$("cost") u=4^2										1.443
$\log_u$("cost") u=4^{12}										1.890
DHRAM (2080)	**High**		**Good**		**Moderate**		**Poor**		**Bad**	**Risk**
class % (α)	0.002		0.670		0.329		0		0	
"cost" components	0	+	0.670×[$\mathbf{1}_u$]	+	0.329×[$\mathbf{10}_u$]	+	0	+	0	
$\log_u$("cost") u=2										1.407
$\log_u$("cost") u=4										1.493
$\log_u$("cost") u=4^2										1.641
$\log_u$("cost") u=4^{12}										1.933

The concept of the order of magnitude of a risk can be extended to multiple indicators. Although the order of magnitude notional costs of different indicators is not likely to be the same and that the remediation associated with different indicators may be correlated, it is assumed, for simplicity, that the orders of magnitude notional ecological impacts for all indicators are the same and that the costs are additive. In Table 4-23, the combined risk impacts, associated with SRP and ammonia concentrations, water temperature and flow regime alteration (DHRAM) for the Teddington catchment, are enumerated and displayed in terms of class colours. Here u=4 has a specific meaning in that if all four indicators are described by the same single class then notional cost and risk will be exactly one class higher. For example, with u=4, then the combination of four indicators with

"Moderate" status moves the risk up to the next order of magnitude. Intuitively, this is not desirable. In contrast, $u=4^2=16$ means that the combined risk of four WFD indicators with identical class status moves half an order of magnitude ($4=16^{1/2}$) towards the next class but remains within the same class. This is more acceptable assessment of risk and thus $u=4^2=16$ has been chosen in preference to $u=4$. For consistency, and in order to provide an indication of the contributions of each WFD indicator, the order of magnitude risk associated with individual indicators is also calculated in base $u=4^2=16$ (if for example, five indicators were under consideration then the order of magnitude, u, should be $5^2=25$). The use of an order of magnitude $u=4^{12}$, or indeed any high power of 4, places emphasis on the worst performing indicators.

Table 4-23: Order of magnitude risk assessments of the combined impact for SRP, water temperature, ammonia concentration and DHRAM for the Teddington catchment. The cell colours in the Risk column are determined from the numbers in the risk column.

Combined (2040)	High	Good	Moderate	Poor	Bad	Risk
class % (α)	0.965	1.953	0.082	1.000	0	
"cost" components	0 +	$1.953\times[\mathbf{1}_u]$ +	$0.082\times[\mathbf{10}_u]$ +	$1.000\times[\mathbf{100}_u]$ +	0	
$\log_u$("cost") u=2						3.613
$\log_u$("cost") u=4						3.096
$\log_u$("cost") $u=4^2$						3.005
$\log_u$("cost") $u=4^{12}$						3.000
Combined (2060)	**High**	**Good**	**Moderate**	**Poor**	**Bad**	**Risk**
class % (α)	0.488	2.346	0.166	1.000	0	
"cost" components	0 +	$2.346\times[\mathbf{1}_u]$ +	$0.166\times[\mathbf{10}_u]$ +	$1.000\times[\mathbf{100}_u]$ +	0	
$\log_u$("cost") u=2						3.740
$\log_u$("cost") u=4						3.124
$\log_u$("cost") $u=4^2$						3.007
$\log_u$("cost") $u=4^{12}$						3.000
Combined (2080)	**High**	**Good**	**Moderate**	**Poor**	**Bad**	**Risk**
class % (α)	0.188	2.374	0.433	1.001	0	
"cost" components	0 +	$2.374\times[\mathbf{1}_u]$ +	$0.433\times[\mathbf{10}_u]$ +	$1.001\times[\mathbf{100}_u]$ +	0	
$\log_u$("cost") u=2						3.861
$\log_u$("cost") u=4						3.168
$\log_u$("cost") $u=4^2$						3.015
$\log_u$("cost") $u=4^{12}$						3.000

In Figure 4-8, the order of magnitudes used to assess risk were assumed to be equal for all four indicators. If, for example, the ecological impact and/or fiscal cost for one indicator are known to be substantially larger than all others, then a larger order of magnitude can be assigned to this indicator. This will be visually reflected in the associated map with colours that are most closely associated with the high-risk indicator. This is demonstrated in Figure 4-9, with the colour values in the combined map including SRP closely following those in the SRP, since the poorest values in most catchments are those associated with SRP. This is reflected in the combined map excluding SRP, demonstrating a scenario where a single indicator does not represent the dominant risk.

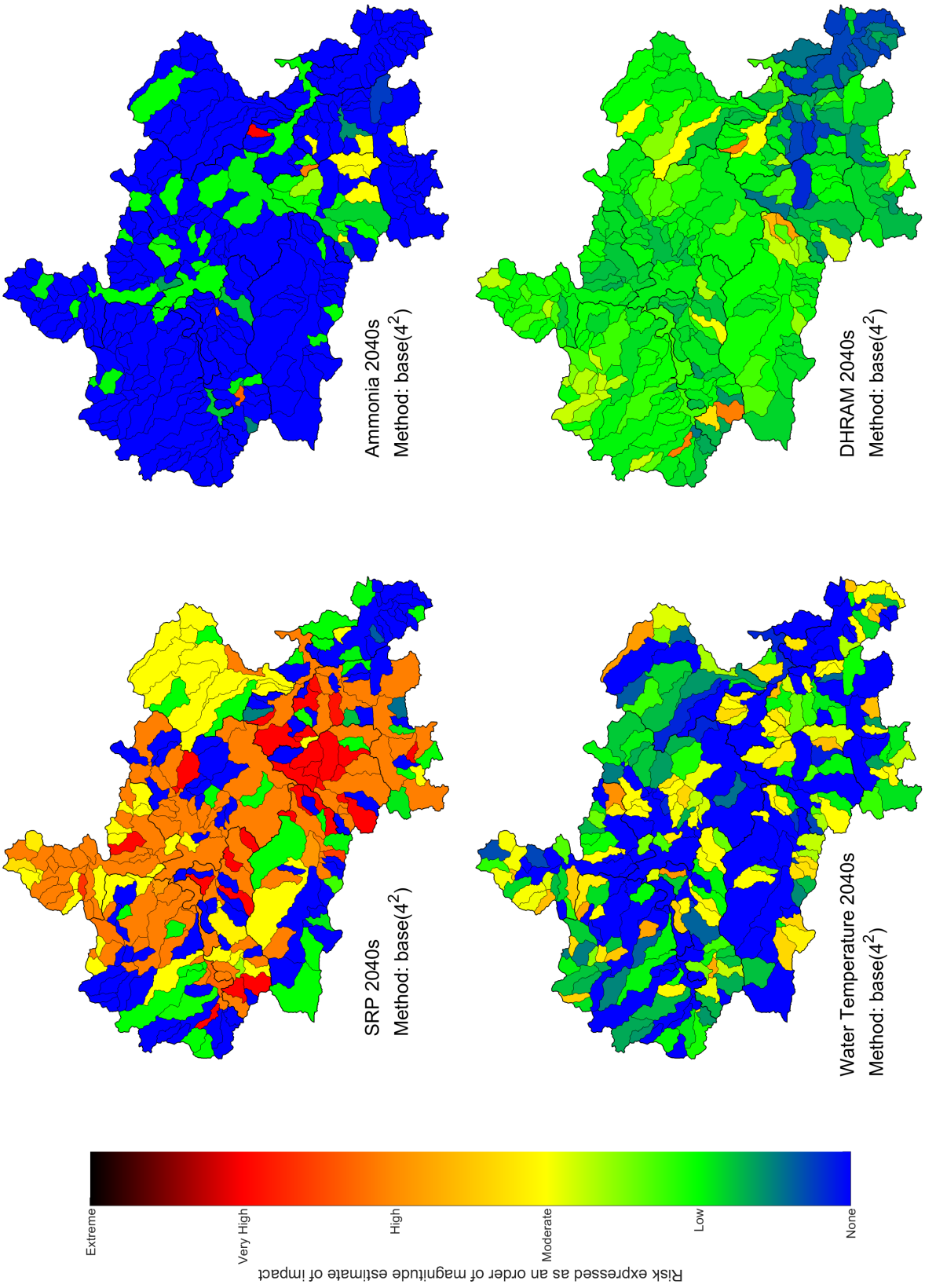


Figure 4-8: 2040 risk assessment Thames catchment maps for SRP, ammonia, water temperature and DHRAM.

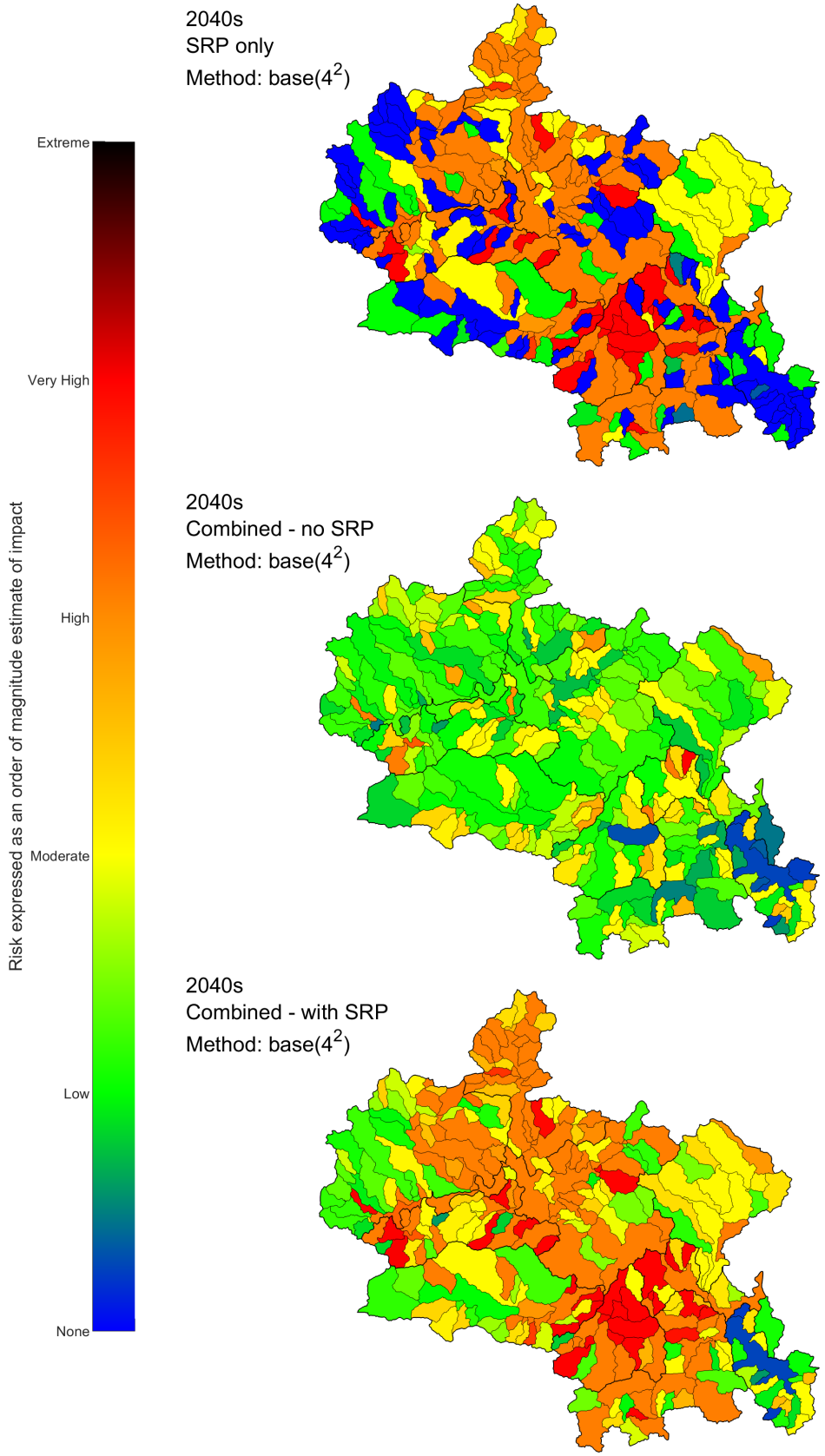


Figure 4-9: Thames Basin maps for 2040s projection of SRP only, combined risk without SRP, and combined risk with SRP for the base 4^2method.

Chapter 5 THAMES BASIN: RESULTS

5.1 OUTLINE OF RESULTS AND SELECTION OF EXEMPLAR CATCHMENTS

The presentation and analysis of results for the Thames Basin has required significant consideration and innovation because of (i) due to the sheer volume of data generated (daily 30 year time-series of 5 key variables for 292 catchments across 300 altered climate sets) and (ii) the complex nature of presenting the aforementioned data in a coherent and spatially explicit manner that acknowledges the levels of uncertainty associated with each stage of calculation. To accommodate these requirements, four key summary graphs have been generated for each variable for all sub-catchments within the Thames basin. A total of 5,840 graphs have been created and are presented in electronic Appendix I as figure palettes (see attached CD). In this chapter, following the criteria outlined below, six catchments were chosen that act as exemplars of the UK River Typologies found within the Thames basin. The detailed analyses of these exemplar catchments for each key variable form the first section of this chapter. The second section of this chapter focuses on summary risk assessment maps, generated using the HadCM3 probabilistic change factors and catchment response surfaces, which provide an overview of the response of all catchments for each variable under multiple plausible climate scenarios. The final section of this chapter focuses on the accumulation of these key physio-chemical variables across each catchment to present a holistic view of future climate induced risk and its potential impact on riverine ecosystem health.

In choosing the catchments to present detailed results, the objective was to select, for each catchment type within the Thames basin, an exemplar that represents the least human impact. This means that the variation in response variables within a catchment and between different catchment types can primarily be attributed to changes in altered climatic stressors. A total of six catchment types are present within the Thames basin from the UK river typology scheme, which utilises Strahler order, elevation and geology to categorise catchment throughout the UK. Table 5-1 outlines the types present within the Thames Basin, along with key statistics for each type.

Table 5-1: Summary statistics for each catchment type within the Thames Basin

Catchment Type	Number in Thames Basin	Average Area	Average Length	Average Width	Average elevation
Low, Large, Calcareous	7	111.81	42.65	40.1	37.5
Low, Medium, Calcareous	41	65.48	24.63	9.8	66.4
Low, Small, Calcareous	141	26.07	8.62	3.8	79.4
Mid, Small, Calcareous	8	29.92	9.16	4.1	154.5
Low, Medium, Siliceous	4	64.84	29.4	10.5	47.7
Low, Small, Siliceous	34	24.81	8.73	3.7	49.2

Several criteria were developed to isolate the most appropriate catchment for each of the six types with the most downstream catchment satisfying the following criteria selected:

1. The catchment must not be designated as heavily modified for artificial (i.e. canals). These are highlighted in red in Figure 5-1.
2. There must be minimal effluent and discharge point sources within the catchment, whilst also considering said sources in upstream catchments
3. There must be NRFA and chemistry sampling points within the catchment, to corroborate modelled results with quantitative sampled data.
4. Urban land-use must be minimal within the catchment
5. When multiple catchments exist conforming to the above criteria, then a geographical balance between types should be sought to gain a more representative sample of the entire Thames basin.

The selected catchments are outlined in bold in Figure 5-1. Due to the nature of the typology, specific catchment types are clustered within areas of the Thames Basin, which in turn are associated with land-cover characteristics (e.g. predominantly agricultural or urban etc.). As such, it is not possible to control for differences in land-use when identifying exemplar catchments and this should be considered when discussing the various responses of the catchments to changes in climate.

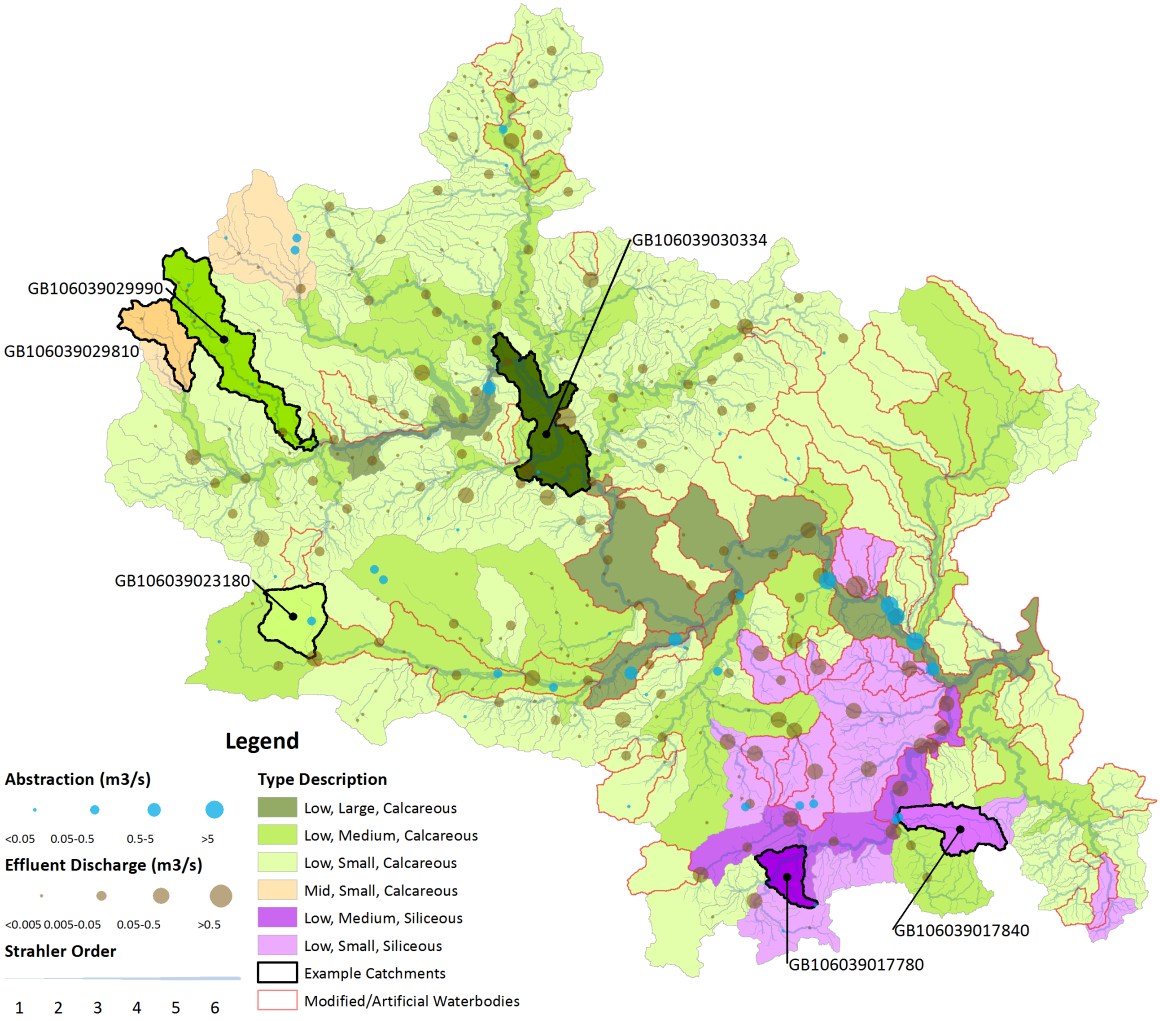


Figure 5-1: Map of the Thames Basin illustrating the exemplar catchments chosen as representative of catchment typology. Exemplar catchments are labelled and outlined in black. Modified/artificial waterbodies are outlined in red. Abstraction and effluent sites are represented by blue and brown circles respectively. UK catchment typologies within the Thames are also presented.

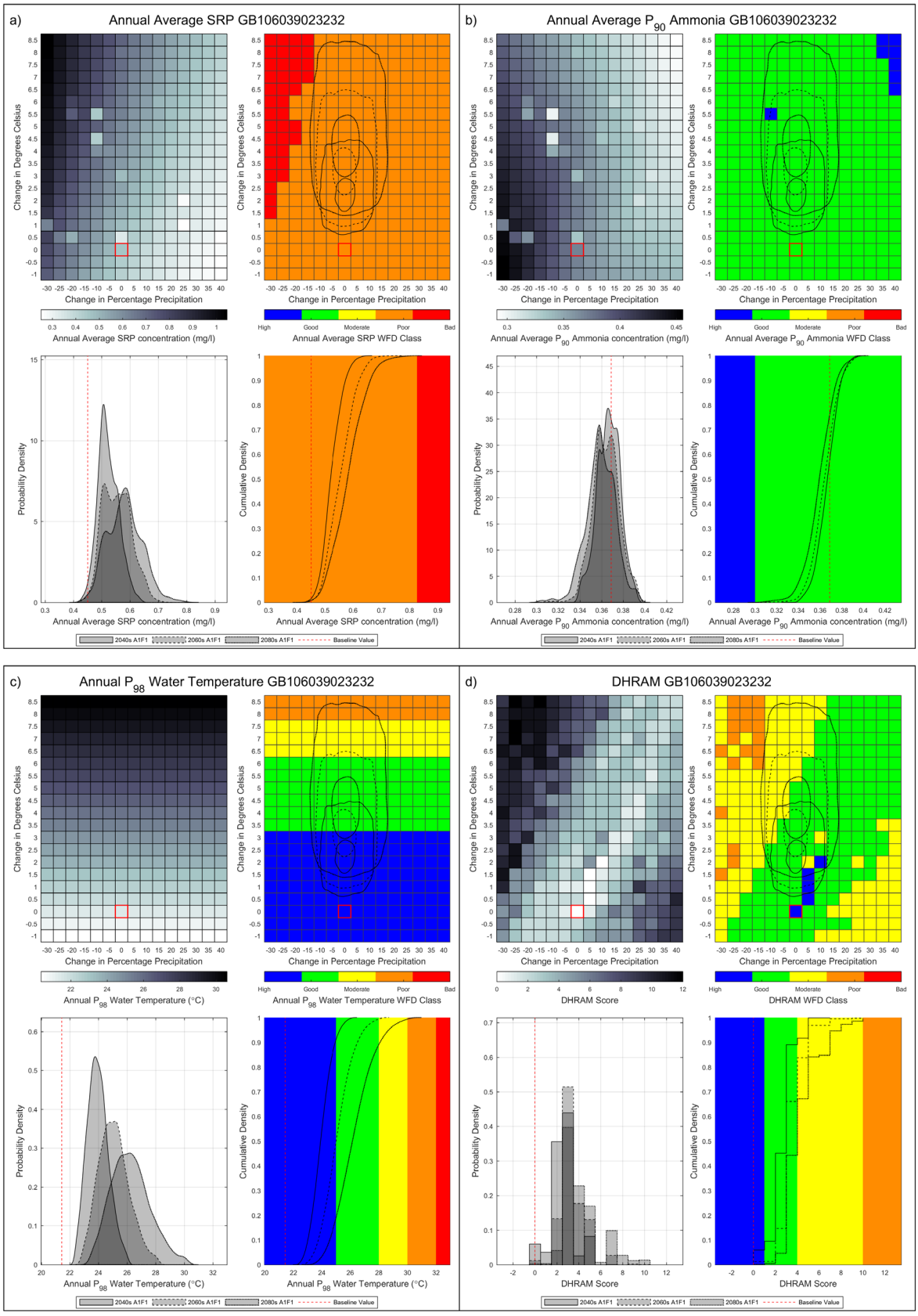


Figure 5-2: Example figure palettes produced for each catchment within the Thames Basin (palette presented is the most downstream catchment in non-tidal Thames at Teddington Weir). Four standards were assessed; a) SRP, b) ammonia, c) water temperature and d) DHRAM. For each parameter, four graphs were produced: top-left - raw data response surface; top-right - class response surface; bottom-left - Probability Distribution Function (PDF) for UKCP09 projections; bottom-right Cumulative Distribution Function (CDF) for UKCP09 projections.

Figure 5-2 provides a demonstration of the figure palette created for each of the catchments throughout the Thames basin, with four graphs produced for each of the key variables (SRP, Ammonia, Water Temperature and DHRAM). The top left graph is a gridded response surface comprised of 300 (15x20) cells representing each of the altered climate sets, with change in precipitation on the x-axis and change in temperature on the y-axis. The data represented on the flattened z-axis (represented by a graduated colour-scheme) are the 30-year annual average data values corresponding to the relevant altered climate set on the x and y axes. The extremities of the colour map are limited by the minimum and maximum values across the whole 300 climate series for each catchment. It is therefore worth noting that it is not possible to compare colour values between catchments. Furthermore, the magnitudes of the data values are often subjected to a power of 10 factorisation in order to improve legibility of the response surface and legend.

The top right graph is a gridded response surface of the WFD environmental quality classes associated with the data values in the top left graph. The specific details and methodology involved in assigning these classes are discussed in sections 4.5 and 4.6. There exists a total of five classes ranging from High (blue), through Good (green), Moderate (yellow), Poor (orange) to Bad (red). These class response surfaces are comparable between catchments, as the WFD standards were developed for use across all catchments within the UK. It is worth noting that, despite a gradient in the underlying data values across the response surface signifying a directional catchment response in the relevant variable to changes in annual average precipitation and temperature, it may be that no change in class occurs across the entire response surface since a threshold standard has not been exceeded. On both response surfaces, there are superimposed solid, dotted and dashed lines (for legibility, red in the data response surface and black in class response surface). These represent the first and third standard deviation contour lines encompassing the 10,000 probabilistic HadCM3 change factors for the 2040s, 2060s and 2080s respectively. Contour lines were plotted to improve legibility of the underlying response surfaces whilst also providing an indication of the range and density of future predicted change factors. The detailed distribution of these probabilistic change factors is presented in Figure 4-1.

These probabilistic change factors are used to assess the future risk of changes in climate associated with any given future scenario predicted using scenario-driven climate-earth system models. To recap, each change factor data point associated with a given predicted precipitation and temperature value is used to interpolate values from the underlying catchment response surface derived from the 300 scenario-neutral altered climates. The detailed methodology of this process can be found in section 4.2, with varying interpolation methods being used (e.g. bi-cubic splines, nearest-neighbour) depending on the underlying data type (e.g. continuous, discrete). The resulting interpolated data are then transformed using both a probability density function (PDF) and cumulative density function (CDF), which form the basis for the final two graphs found in the figure palette.

The bottom left graph represents the probability density functions (PDFs) for each of the future scenarios (2040s, 2060s, 2080s), with line styles consistent with the contour lines found on the response surfaces above. The probability density function is directly related to the gradient of the response surface, and as such, the coarseness of the response surface grid can cause small rounding errors when using bicubic spline interpolation at minimal values (e.g. very small negative of SRP). Negative values of macro-nutrients are impossible and so, when these do occur, they are treated as an artefact of the interpolation methodology and set to zero. The axes of the PDF require explanation; (i) the x-axis indicates the modelled data values represented by the flattened z-axis on the response surfaces and (ii) the y-axis is the probability density, which is a function of the density per unit of x-axis; the integral of the area under the curve and above the horizontal axis is equal to 1. The baseline value, or where changes in precipitation and temperature are 0, is represented on the graph by a vertical red dotted line. PDFs are useful for interpreting the location and trend of a distribution, and the direction of future distributions in relation to the baseline. Furthermore, the shape of the distribution provides important information as to the confidence associated with predicting future values for each future scenario. Narrower distributions indicate there is a closer spread of possible future values, thus giving greater confidence in predicting their value. Conversely, a wider distribution suggests greater uncertainty in predicting future values. The vertical shape of the

distribution is also important in determining whether multiple modal points exist. Unimodal distributions indicate there is a single modal (most frequent) maximum, whereas poly-modal distributions indicate that multiple maxima, and therefore a significant probability of multiple future probable options exists in the response surface.

Further to the above, the projected future scenarios for the six exemplar catchments are presented for each physio-chemical variable using boxplots. This method of data presentation provides a clear summary overview of each physio-chemical variable for all exemplar catchment on a single page. The boxplots are essentially a visual representation of the cumulative probability distribution function data, where the boxes (defined by the lower and upper quartiles; 25^{th} to 75^{th} percentiles) have been coloured with the corresponding WFD environmental quality class colours. Dependent on the distribution of data and relevant WFD standards, some of the boxes have more than one colour. The boundary between the colours represents the transition point between the WFD classes. In this situation, the areas within the box give a clear indication of the relative probabilities for each class. Within this box, the solid red line represents the median data value, and the whiskers at the end of the dotted line on either side of the box are representative of the breadth of the data outside of the interquartile range, neglecting outliers, and give an indication of the shape of the distribution. Finally, the small red crosses represent data values considered to be outliers, as defined by the methodology above.

5.2 EXEMPLAR CATCHMENTS DETAILED RESULTS

5.2.1 SOLUBLE REACTIVE PHOSPHORUS (SRP)

Soluble reactive phosphorus (SRP) plays a key role in the life-cycle of many aquatic species, with current WFD standards derived from specific macroinvertebrate tolerances towards in-stream phosphorus concentrations (UKTAG, 2014b). SRP varies significantly between catchments and within river reaches due to input of phosphorus to the river from diffuse sources (e.g. runoff from agriculture) and point sources (e.g. water treatment effluent) (Whitehead et al., 2013). Such variation in SRP concentrations across and within catchments in the Thames region leads to a variation in the response of catchments under altered climate scenarios, as demonstrated by the exemplar catchments below. All in-text references for this section relate to Figure 5-3, Figure 5-4 and Figure 5-5.

Catchments a) and f) exhibit similar catchment responses under altered climatic conditions, with both showing high concentrations of SRP across the response surface (0.2-0.9mg/l) and a relatively lateral gradient with higher concentrations at negative precipitation change through to lower concentrations at high precipitation change. In addition to the lateral gradient along the precipitation axes of change, there is also a slight diagonal gradient associated with temperature change, with the highest concentrations at the greatest positive temperature change (-30% precipitation) and the lowest concentrations at negative temperatures (40% precipitation). In contrast, catchments b) and d) exhibit very different responses to altered climates, following a diagonal gradient from higher values associated with negative temperature and high precipitation change to lower temperatures found at high temperature and negative precipitation change. Whilst both catchments exhibit very low concentrations across the entire response surface, catchment b) has most of the altered climate cells above the 5°C and 0% precipitation change gradient indicating concentrations essentially approaching zero, with a rapid increase in concentrations along this diagonal gradient to the highest concentration of 0.0025mg/l found at -1°C and 40% precipitation change. Catchment d) has a more gradual gradient of SRP concentrations across the response surface, with a notable reduction in

concentration values to near negligible values along the 0°C and -30% precipitation to 8.5°C and 10% precipitation diagonal; this leads to approximately a third of the response surface exhibiting negligible concentrations. The highest values of 0.008mg/l are associated with -1°C and 40% precipitation change. Catchments c) and e) have similar response surfaces, with very low variation in concentrations (0.01mg/l) across the response surface relative to the magnitude of the values themselves. The response surface for catchment c) follows a vertical gradient along the precipitation change axes from higher concentrations at high precipitation change to lower concentrations at negative precipitation change. Most of the cells are associated with higher concentrations, with a slight diagonal gradient present along the temperature axes, with the highest concentration values found in the top-left (8.5°C and -30%) and lowest in the bottom-right (-1°C and 40%) of the response surface. Catchment e) displays an atypical catchment response surface to changes in annual average precipitation and temperature. There is no clear, single gradient, rather bands and patches of increased concentration levels. Lower concentrations are confined to a patch bounded by the gradient from 3°C and -30% precipitation change to 8.5°C and -10% precipitation change. This is accompanied by a significant increase in concentrations across the remaining response surface, with clear patches of higher concentrations at increased levels of precipitation and lower temperature change.

Despite the various concentration gradients present in the catchment response surfaces, each class response surface is relatively homogeneous in terms of WFD classifications. For both catchment a) and f), the high concentration values in both catchments ensure that much of the response surface is classified as ‘Poor’. For both catchments, there are a small number of cells designated as ‘Bad’, found only at the highest concentrations associated with high temperature and negative precipitation change. Due to the very low concentrations found in catchment b) and d), the entire response surface for both catchments is classified as ‘High’. Catchment c) has low concentration values across much of the response surface, leading to most cells classified as ‘High’. However, a small patch of cells with the highest concentrations are classified as ‘Good’ (bottom-right of the response surface; low temperature and greatest precipitation change). Finally, due to the low variation in

concentrations across this catchment, bar a few patches of increased concentrations and a clear area of low concentrations, most of the catchment is classified as 'Good'. A distinct exception to this is the block of 'High' classification caused by the lower concentrations associated with high temperature and negative precipitation change.

The probability density functions (PDFs) and cumulative density functions (CDFs) for each exemplar catchment are derived by interpolating concentration values from the underlying catchment response surface for 10,000 random probabilistic change factors generated using the HadCM3 model for the 2040s, 2060s and 2080s. As such, the distribution and trends seen in the probability density functions are directly related to the concentration gradients found on the relevant catchment response surface from which they are derived. Thus, catchments with similar response surfaces will have similar PDFs and CDFs.

The PDFs for catchments a) and f) both suggest that annual average SRP concentration will increase under all three potential future scenarios over unperturbed (baseline) values, which are represented by the red dotted line. The PDFs associated with the 2040s (solid black line) display approximately normal distributions centred on modal values of 0.41mg/l and 0.43mg/l respectively for a) and f). The narrow width of the distribution (full width at half maxima of 0.05mg/l and 0.06mg/l for a) and f)) suggests an increased confidence in determining concentrations for the 2040s. For the 2060s (dashed line) and 2080s (dotted line), the PDFs develop into bi-modal and tri-modal distributions respectively. This evolution of the PDF has important consequences, as it indicates that no single concentration is most probable. Rather, there are two more probable concentrations for the 2060s and three for the 2080s. Importantly, when these multi-modal PDF distributions are observed, it is evident that it is inappropriate to use the average or median concentration values. The PDF distributions also become wider the later the projected scenario date, which indicates a generally greater degree of uncertainty as time progresses. The full width at half maximum is a good visible indicator that can be obtained for the PDF of this increased uncertainty. For a) and f) respectively for the 2040s, 2060s and 2080s, these are 0.05mg/l, 0.09mg/l ad 0.14mg/l and 0.06mg/l, 0.10mg//l and

0.14mg/l. These values give a clear indication of the increasing range of possible concentrations as the scenarios progress into the future. This is also reflected in the CDFs for both catchments, due to the change in gradients between scenarios, with increasingly shallower gradients further into the future. The steep gradient associated with the 2040s scenario covers a smaller range of values, in contrast to the shallower gradient of the 2080s, which covers a wider range of values. This divergence between scenarios over increasingly higher cumulative densities suggests a decreased confidence in the detailed prediction of concentration values in future years.

Each of the PDFs and CDFs for catchments b) and d) suggests that the SRP concentration for this catchment will decrease below unperturbed values in all three future scenarios, with increasingly lower values from the 2040s to 2080s. The distributions for catchment b) demonstrate a skew towards lower values, with unimodal peaks at lower values and a tail towards higher values. Notably, predictive confidence increases with an increase in future scenarios, contrary to the most other catchments, indicating that the catchment is reaching an asymptotic threshold point in the future. This is evident from the response surface, as the extremely low concentrations of SRP in the catchment approach zero for most cells covered by the 2080s probabilistic factors. This is further reflected in the CDF, with a steep gradient for the 2080s and shallower for the 2040s that diverge at greater cumulative probability densities. Furthermore, the shapes of all CDFs mirror the skewed nature of the PDFs, with no tail at low cumulative densities and a significant plateau at high densities. The PDF distributions for catchment d) vary between scenarios, with the 2040s demonstrating a unimodal, essentially normal distribution, the 2060s a bimodal distribution and the 2080s a unimodal distribution with a skew towards higher concentration values. The widths of the PDFs are similar for each scenario and are larger than the regular increase in modal values, resulting in a significant overlap between each distribution. This is reflected in the CDFs, with even distance between scenarios for the length of each CDF, and a slight variation in curve shape due to the diagonal gradient of concentrations found in the response surface.

Finally, catchments c) and e) exhibit differing responses in the PDFs to those of the other catchments, due to the difference in concentration gradients on the respective response surfaces. There is substantial overlap between PDFs for each scenario for both catchments, with an overall shift towards lower concentration values further into the future, with all PDFs and CDFs suggesting modal concentrations lower than unperturbed conditions. All PDFs for both catchments exhibit multiple modal values and highly structure distributions. This is a consequence of the narrow range of concentration values and the resultant proportionately larger impact that slight changes in concentration for a response surface cell have on the overall PDF distribution. This is mirrored in the CDFs for both catchments, with all scenarios exhibiting regular changes in gradient along the lengths of the curves. Catchment c) displays a greater overlap between scenarios than those of catchment e), suggesting smaller variation in concentrations into the future for catchment c) over those in catchment e), due to the concentration gradients found on the response surfaces (horizontal and diagonal respectively). This is further reflected in the CDFs, with scenario curves converging at higher cumulative densities in catchment c), whilst those in catchment e) do not.

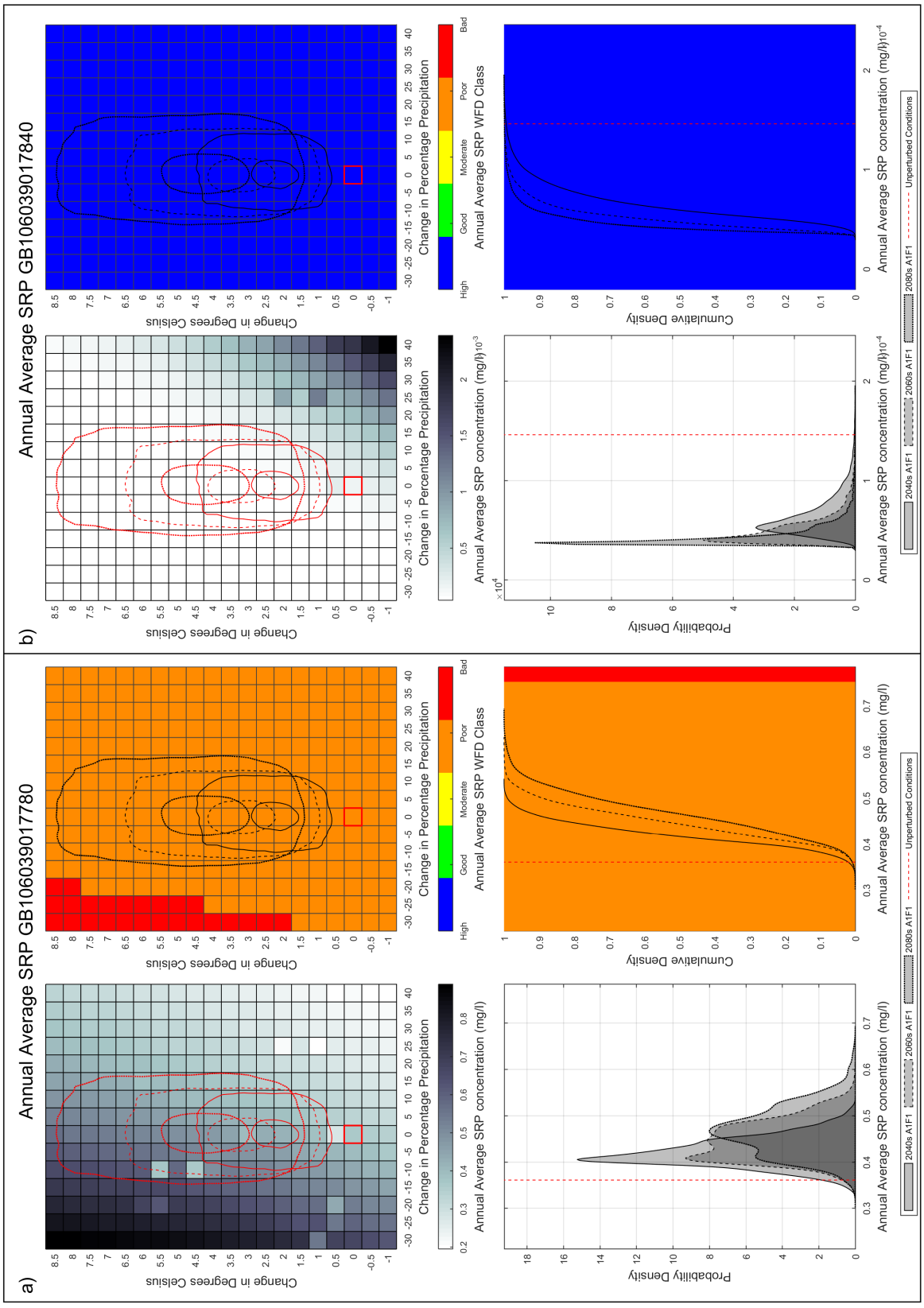


Figure 5-3: Figure palettes of SRP concentration for exemplar catchments 17780 and 17840 (Low, Medium, Siliceous and Low, Small, Siliceous respectively). Four graphs are presented for each catchment: top-left - raw data response surface; top-right - class response surface; bottom-left and bottom-right - Probability Distribution Function (PDF) and Cumulative Distribution Function (CDF) for UKCP09 projections respectively.

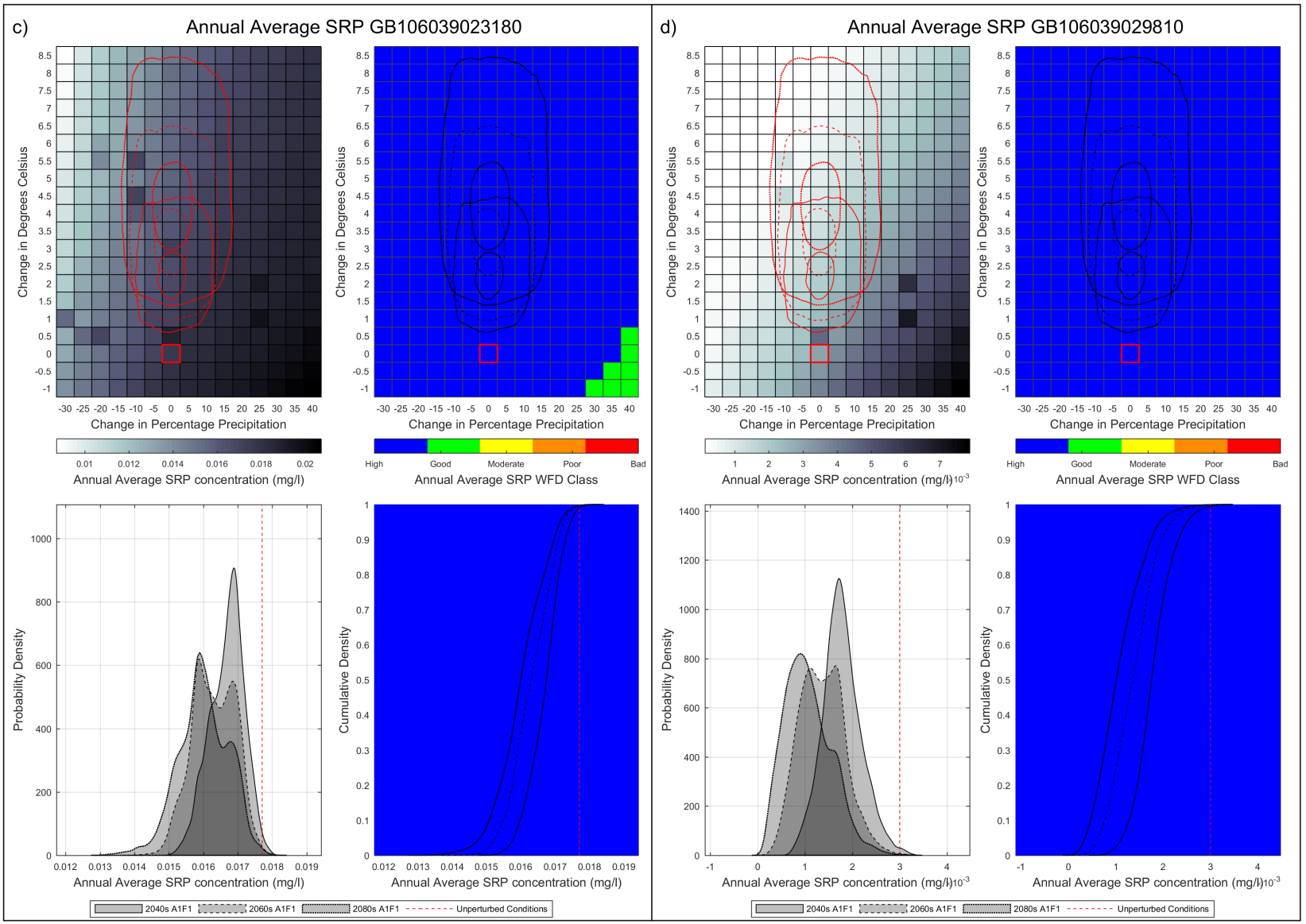


Figure 5-4: Figure palettes of SRP concentration for exemplar catchments 23180 and 29810 (Low, Small, Calcareous and Mid, Small, Calcareous respectively). Four graphs are presented for each catchment: top-left - raw data response surface; top-right - class response surface; bottom-left and bottom-right - Probability Distribution Function (PDF) and Cumulative Distribution Function (CDF) for UKCP09 projections respectively.

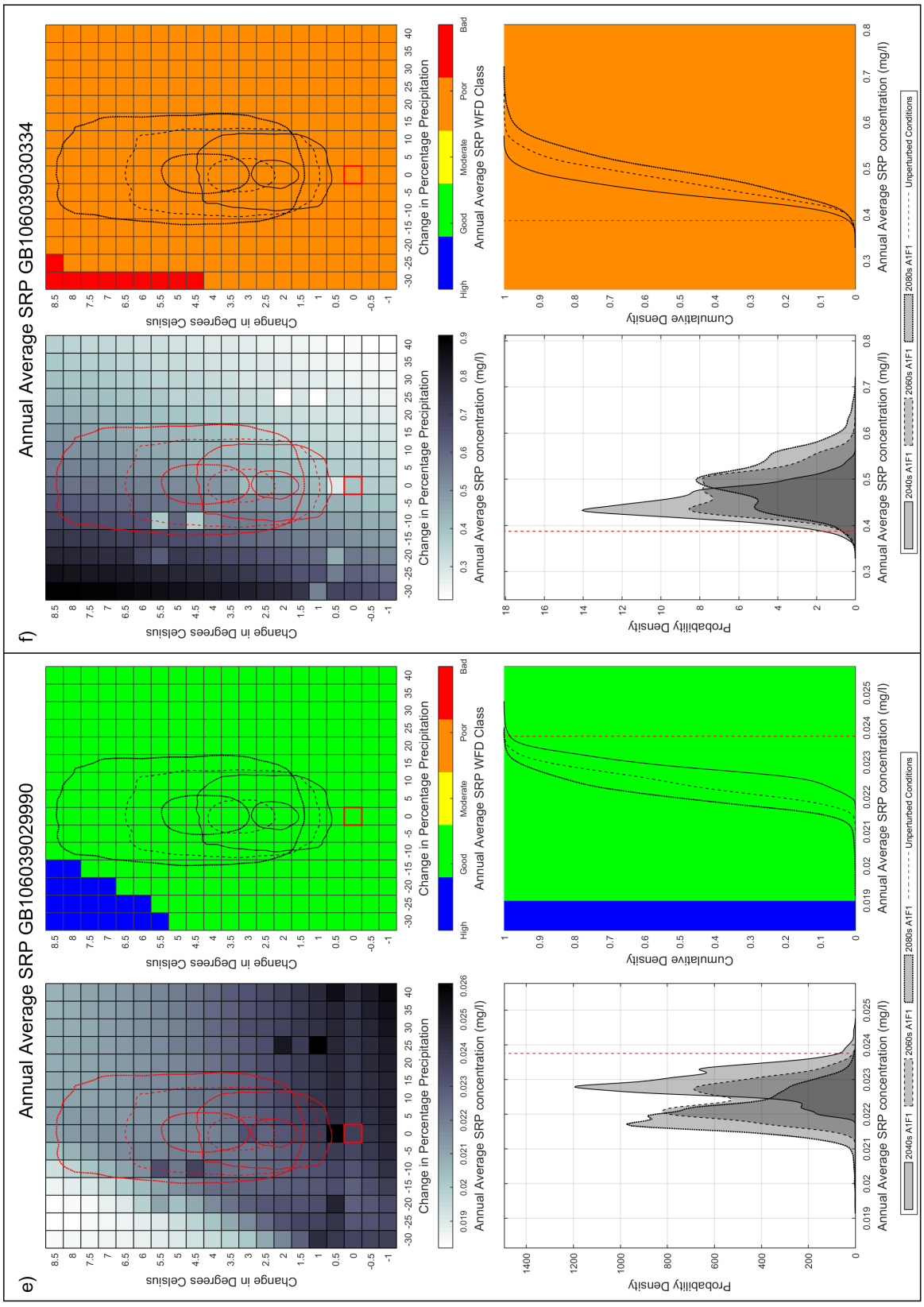


Figure 5-5: Figure palettes of SRP concentration for exemplar catchments 29990 and 30334 (Low, Medium, Calcareous and Low, Large, Calcareous respectively). Four graphs are presented for each catchment: top-left - raw data response surface; top-right - class response surface; bottom-left and bottom-right - Probability Distribution Function (PDF) and Cumulative Distribution Function (CDF) for UKCP09 projections respectively.

Table 5-2: Summary statistics for SRP for each exemplar catchment. Statistics provided for response surfaces and box-plots for each of the UKCP09 projections (2040s, 2060s and 2080s).

	Catchment	GB106039017780	GB106039017840	GB106039023180	GB106039029810	GB106039029990	GB106039030334
SRP Response Surface	Average	0.416	5.22E-05	0.0169	1.53E-03	0.0223	0.446
	Min	0.195	3.56E-05	0.0087	1.28E-04	0.0182	0.213
	Max	0.891	2.39E-03	0.0207	7.87E-03	0.0261	0.907
	% High	0	100	97.67	100	6.33	0
	% Good	0	0	2.33	0	93.67	0
	% Moderate	0	0	0	0	0	0
	% Poor	91.67	0	0	0	0	96.67
	% Bad	8.33	0	0	0	0	3.33
SRP 2040s	Q10	0.383	4.57E-05	0.0160	1.28E-03	0.0224	0.411
	Q50 (Median)	0.417	5.92E-05	0.0167	1.75E-03	0.0229	0.444
	Q90	0.462	9.12E-05	0.0173	2.32E-03	0.0234	0.490
	% High	0	100	100	100	0	0
	% Good	0	0	0	0	100	0
	% Moderate	0	0	0	0	0	0
	% Poor	100	0	0	0	0	100
	% Bad	0	0	0	0	0	0
SRP 2060s	Q10	0.398	3.79E-05	0.0155	7.76E-04	0.0218	0.422
	Q50 (Median)	0.445	4.70E-05	0.0163	1.35E-03	0.0224	0.473
	Q90	0.502	6.89E-05	0.0171	1.95E-03	0.0231	0.531
	% High	0	100	100	100	0	0
	% Good	0	0	0	0	100	0
	% Moderate	0	0	0	0	0	0
	% Poor	100	0	0	0	0	100
	% Bad	0	0	0	0	0	0
SRP 2080s	Q10	0.403	3.62E-05	0.0151	4.76E-04	0.0215	0.428
	Q50 (Median)	0.466	4.06E-05	0.0160	1.01E-03	0.0220	0.495
	Q90	0.534	5.80E-05	0.0170	1.73E-03	0.0228	0.563
	% High	0	100	100	100	0	0
	% Good	0	0	0	0	100	0
	% Moderate	0	0	0	0	0	0
	% Poor	100	0	0	0	0	100
	% Bad	0	0	0	0	0	0

Consider Figure 5-6, which displays boxplots for SRP concentrations in the 2040s, 2060s and 2080s for each exemplar catchment. Each plot clearly shows the trends seen in the cumulative distribution functions for each catchment and provides a concise graphical comparison between future scenarios and a relative comparison between exemplar catchments. The specific concentrations for key statistics of all boxplots, such as the median and interquartile range, can be found in Table 5-2.

Catchments a) and f) show almost identical boxplots, with an increase in median values from the 2040s to the 2080s. All median values fall into the 'Poor' classification for these catchments, suggesting no change in WFD classification for these catchments into the future. The size of the boxes and length of whiskers also increase with time, which is indicative of a wider distribution of concentration values and a concomitant reduction in predictive potential. This is also mirrored in the number of outliers in each boxplot, where most are distributed towards higher concentrations. The shapes of the distributions are uniformly normal, except for the 2040s, where the medians are slightly skewed towards lower concentrations.

The boxplot for catchment b) is unlike all the other exemplars, as the interquartile range (represented by the box heights) decreases and whiskers shorten from the 2040s to the 2080s, indicating an increase in predictive potential into the future. The median values decrease over time, suggesting lower SRP concentrations into the future that all coincide with the 'High' WFD classification for this catchment. This represents no change in classification over unperturbed values. Furthermore, the medians tend towards lower concentrations, with short whiskers at low concentrations and long whiskers at higher concentrations suggesting a distributional skew towards lower concentrations.

The boxplots for catchment c) show a gradual decrease in median concentrations from the 2040s to the 2080s, which are all associated with the 'High' WFD class, indicating no future change in classifications over unperturbed values. The width of the interquartile range and the length of the whiskers also increase over time, indicating a reduction in the predictive potential into the future. The distribution of the 2040s is skewed towards higher concentrations, whereas both the 2060s and

2080s are slightly skewed towards lower concentrations. All outliers are found beyond the lower whisker for each scenario, with a larger number present in the 2080s, consistent with a reduction in predictive capacity.

Catchment d) shows a much clearer decrease in median concentrations from the 2040s to 2080s, in part due to the very low concentrations predicted (between 1 to $2x10^{-3}$ mg/l). These concentrations are all associated with the 'High' WFD class, indicating a high likelihood of no change in classification over unperturbed values. The distributions are relatively normal, except for the 2080s which is skewed towards lower values. Like most other exemplar catchments, the interquartile range and width of the whiskers increases over time, indicating a reduction in predictive potential into the future. The number of outliers remain relatively consistent between scenarios, with all found at higher concentrations except for the 2040s where some are also found beyond the lower whisker.

Finally, catchment e) also has a clear decrease in median concentrations from the 2040s to the 2080s, with a larger reduction seen between the 2040s and 2060s than between the 2060s and 2080s. All median concentrations are associated with a 'Good' WFD class for this catchment, suggesting no change in classification over unperturbed values. The size of the interquartile ranges and width of the whiskers do not change significantly with scenario, apart from the 2060s whose interquartile range in larger than both other scenarios. Furthermore, the interquartile range is comparatively small for each scenario in relation to their median, suggesting reduced variation in the number of potential future concentrations and somewhat consistent predictive power over all scenarios. The distributions are all slightly skewed towards lower concentrations, with the median and lowers whiskers all nearer to the 25^{th} percentile (bottom of the box). Finally, the outliers vary substantially between scenarios, with a small number found above the top whisker for the 2040s, none for the 2060s and a larger number for the 2080s distributed either side of both whiskers.

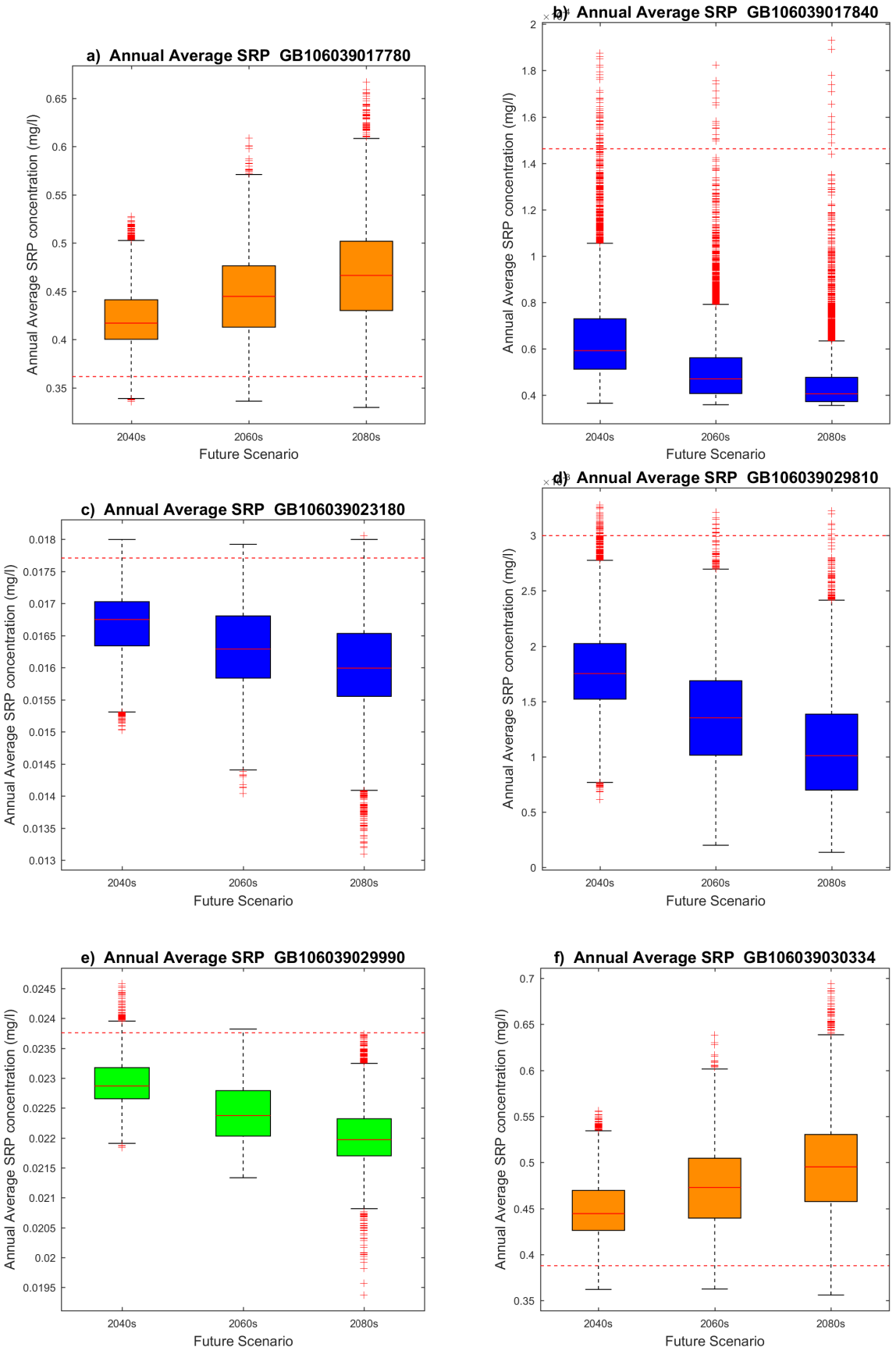


Figure 5-6: Box-plots for SRP for each of the UKCP09 projections (2040s, 2060s and 2080s) for each of the exemplar catchments. Instructions for interpretation are described in section 5.1.

5.2.2 AMMONIA

All in-text references for this section relate to Figure 5-7, Figure 5-8 and Figure 5-9. All response surfaces for the six exemplar catchments demonstrate similar 30-year annual average concentrations of ammonia (in the range between 0.05 to 0.30 mg/l), with the exception of catchment f) that exhibits higher concentrations in the range of 0.35-0.50 mg/l. Catchments a), c), d) and e) exhibit similar diagonal gradients across the response surface, with higher ammonia concentrations associated with higher precipitation and lower temperatures through to lower ammonia concentrations associated with lower precipitation and higher temperatures. Catchment a) exhibits a more gradual gradient and higher percentage of elevated ammonia concentrations than catchments c), d) and e), which all have very similar graduated response surfaces. Catchment b) exhibits a different response of ammonia concentrations to changes in precipitation and temperature from all other exemplar catchments. There is a strong horizontal gradient with a slight flattening at higher temperatures, with higher ammonia concentrations associated with low precipitation values across all temperatures. Concentrations are marginally more elevated at lower temperatures and lower at higher temperatures. Finally, catchment f) displays a diagonal gradient with higher concentrations at low precipitation and lower temperatures and lower concentrations at high precipitation and high temperatures. In addition to this diagonal gradient, high concentrations are present at temperatures below 0°C across all precipitation values, introducing a minor vertical gradient to response surface.

Class response surfaces follow the gradients found in the data response surface, providing that threshold standards are exceeded. For catchments d) and e), the whole response surface classifies as ‘High’ under the WFD ammonia standards, despite the gradients found in the related data response surfaces. For catchments a) and c) most of the cells correspond to ‘High’ status, with a diagonal section of ‘Good’ status found at mid-to-high precipitation and low temperatures for catchment a) and low-to-high precipitation and mid-to-low temperatures for catchment c). Similarly, catchment b) also has many cells corresponding to ‘High’ status, with a significant number also associated with ‘Good’ status. These are restricted to cells associated with negative precipitation change and

temperature changes ranging from -1°C through to 3.5°C. These values follow the gradient of the data response surface and decrease from 3.5°C to 7.5°C with increasingly negative precipitation change. Finally, and conversely, the class response surface for catchment f) corresponds entirely to 'Good' status, despite the gradient in values through the data response surface.

The PDFs and CDFs across all scenarios for catchments a) and c), d) and e) exhibit very similar distribution shapes and trends, with all predicted values lower than unperturbed (baseline) conditions (represented by the vertical red dotted line). In these catchments, the PDF for the 2040s (solid line) has a narrower distribution and higher modal peak than the 2060s (dashed line) and 2080s (dotted line). This is mirrored in the CDFs for each catchment, with decreasingly steep gradients from the 2040s through to the 2080s, indicating a trend towards a greater range of potential future concentration values and thus an increase in the uncertainty of prediction for more distant future scenarios. Furthermore, due to the density and position of probabilistic change factors on the response surfaces, there is significant overlap in predicted future concentrations between future scenarios. However, there is a consistent trend across these catchments towards increasingly lower modal concentrations the further into the future values are predicted and this trend is anticipated to be followed. This is reflected in the CDFs for each catchment, with the scenario curves distinctly separated at lower cumulative densities and converging at higher cumulative densities. For each of these catchments, the PDFs for the 2060s demonstrate a bimodal distribution due to the probabilistic change factors located equally either side of the diagonal gradient of values found in the response surface. These multiple peaks indicate that it is likely that there will be a future bifurcation towards one or other side of the diagonal gradient. It is anticipated that, once this bifurcation is established, future trends are likely to continue to follow the established trend.

Whilst catchment f) typically follows these distribution and trends outlined above, there is not as significant a variation in overlap and height of distribution between scenarios due to the concentration gradient found on the catchment response surface (vertical, rather than diagonal). This is reflected in the greater distance between CDFs for each scenario over other exemplar

catchments, suggesting a larger range in concentrations predicted between future scenarios. One notable difference is the bimodal distribution for the 2040s, caused by a slight diagonal gradient in concentrations at lower temperatures that runs opposite to the gradient found in the other exemplar catchments.

Finally, catchment b) demonstrates a very different response to the other exemplar catchments. The PDFs for all scenarios exhibit almost identical narrow, bimodal distributions that span the unperturbed (baseline) value, with a skew towards slightly lower concentrations. This is due to the gradual horizontal gradient found in the response surface, with the probabilistic change factors for all scenarios (represented by the red contour lines) located on cells spanning a narrow range of concentration values. This is mirrored in the CDFs, with very little distance between scenario curves that have more pronounced tails at lower cumulative densities. Consequently, the predictive capacity across all scenarios is similar, since the catchment would theoretically respond more significantly towards the extremes of the response surface not covered by the probabilistic change factors.

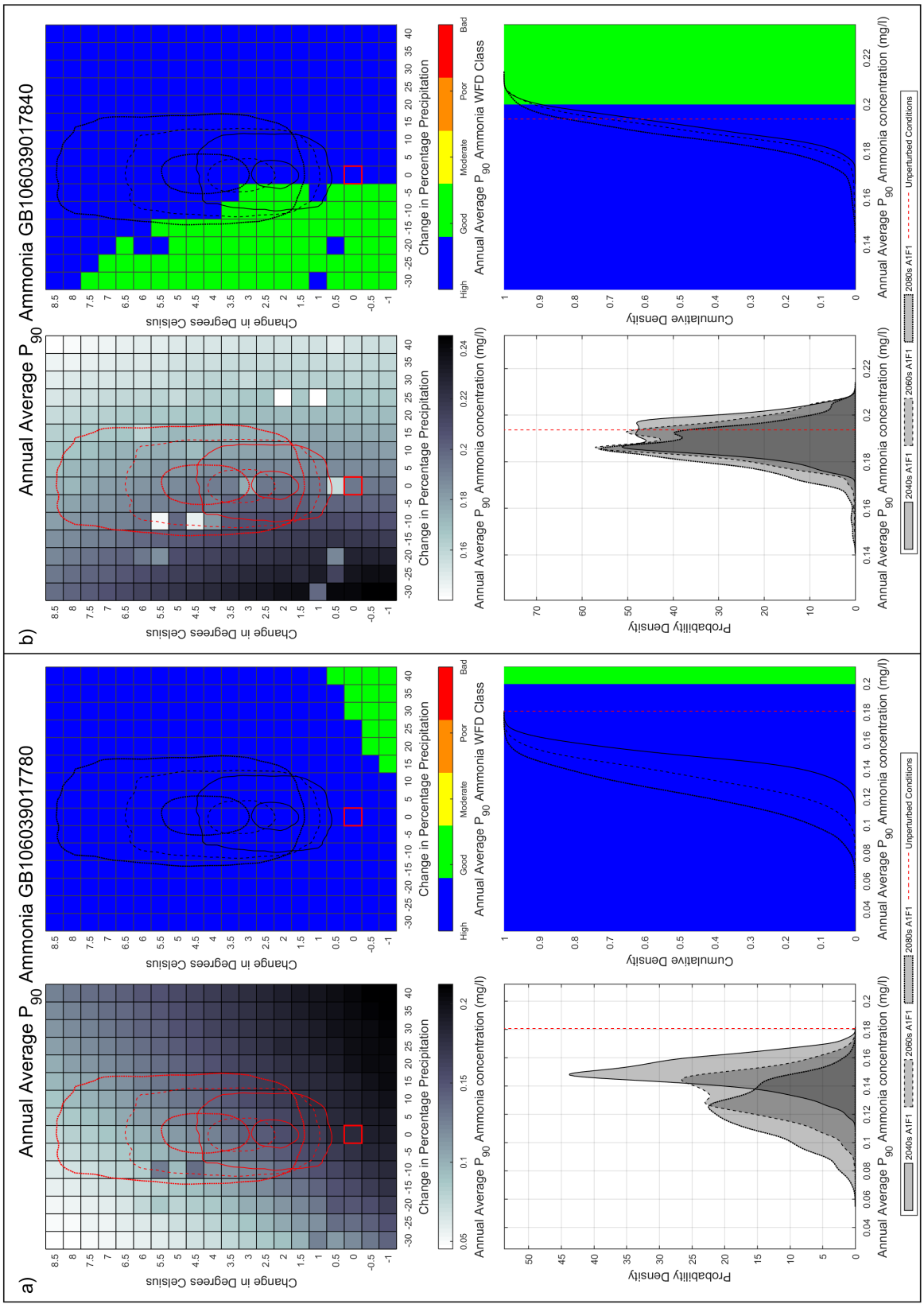


Figure 5-7: Figure palettes of ammonia concentration for exemplar catchments 17780 and 17840 (Low, Medium, Siliceous and Low, Small, Siliceous respectively). Four graphs are presented for each catchment: top-left - raw data response surface; top-right - class response surface; bottom-left and bottom-right - Probability Distribution Function (PDF) and Cumulative Distribution Function (CDF) for UKCP09 projections respectively.

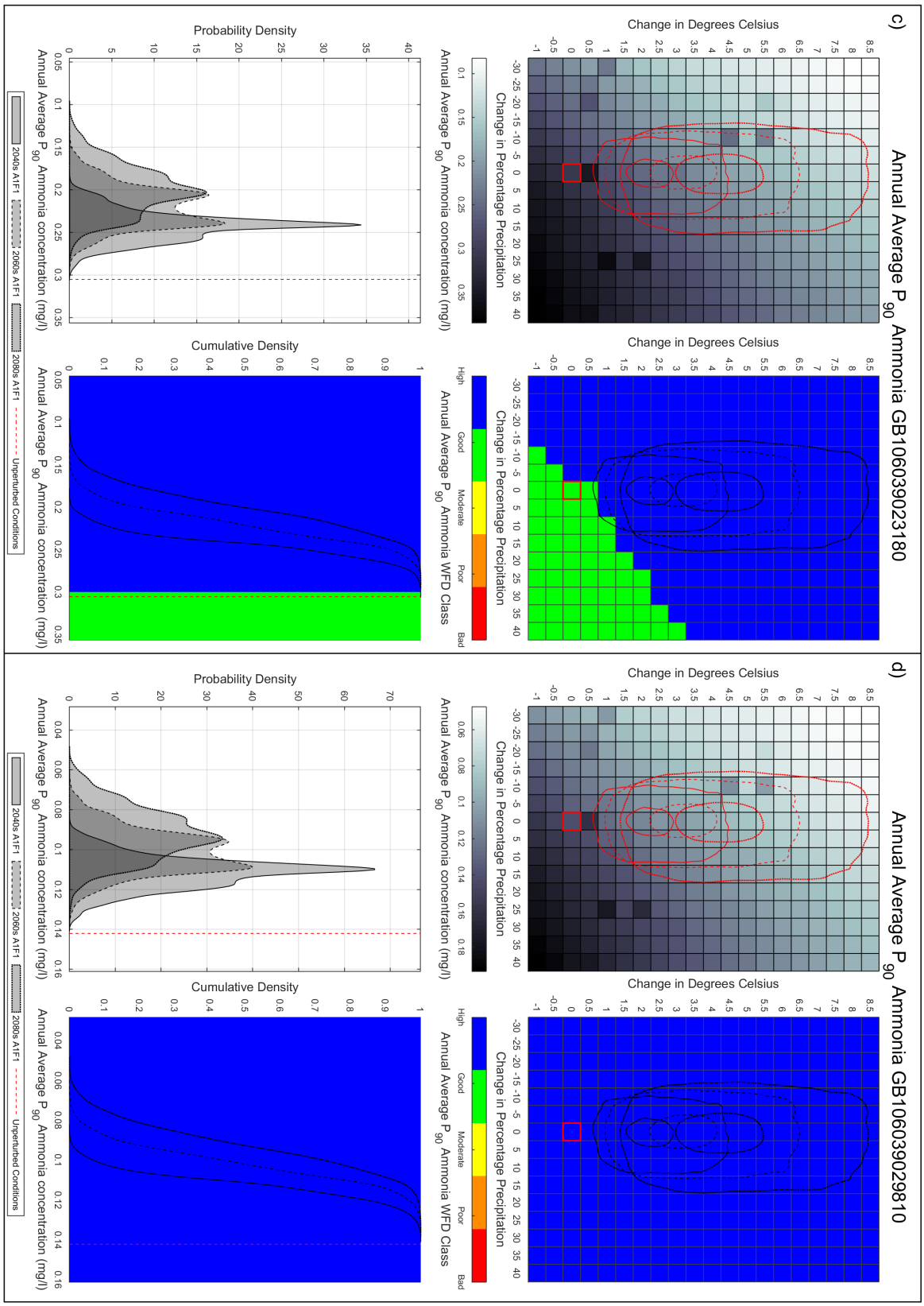


Figure 5-8: Figure palettes of ammonia concentration for exemplar catchments 23180 and 29810 (Low, Small, Calcareous and Mid, Small, Calcareous respectively). Four graphs are presented for each catchment: top-left - raw data response surface; top-right - class response surface; bottom-left and bottom-right - Probability Distribution Function (PDF) and Cumulative Distribution Function (CDF) for UKCP09 projections respectively.

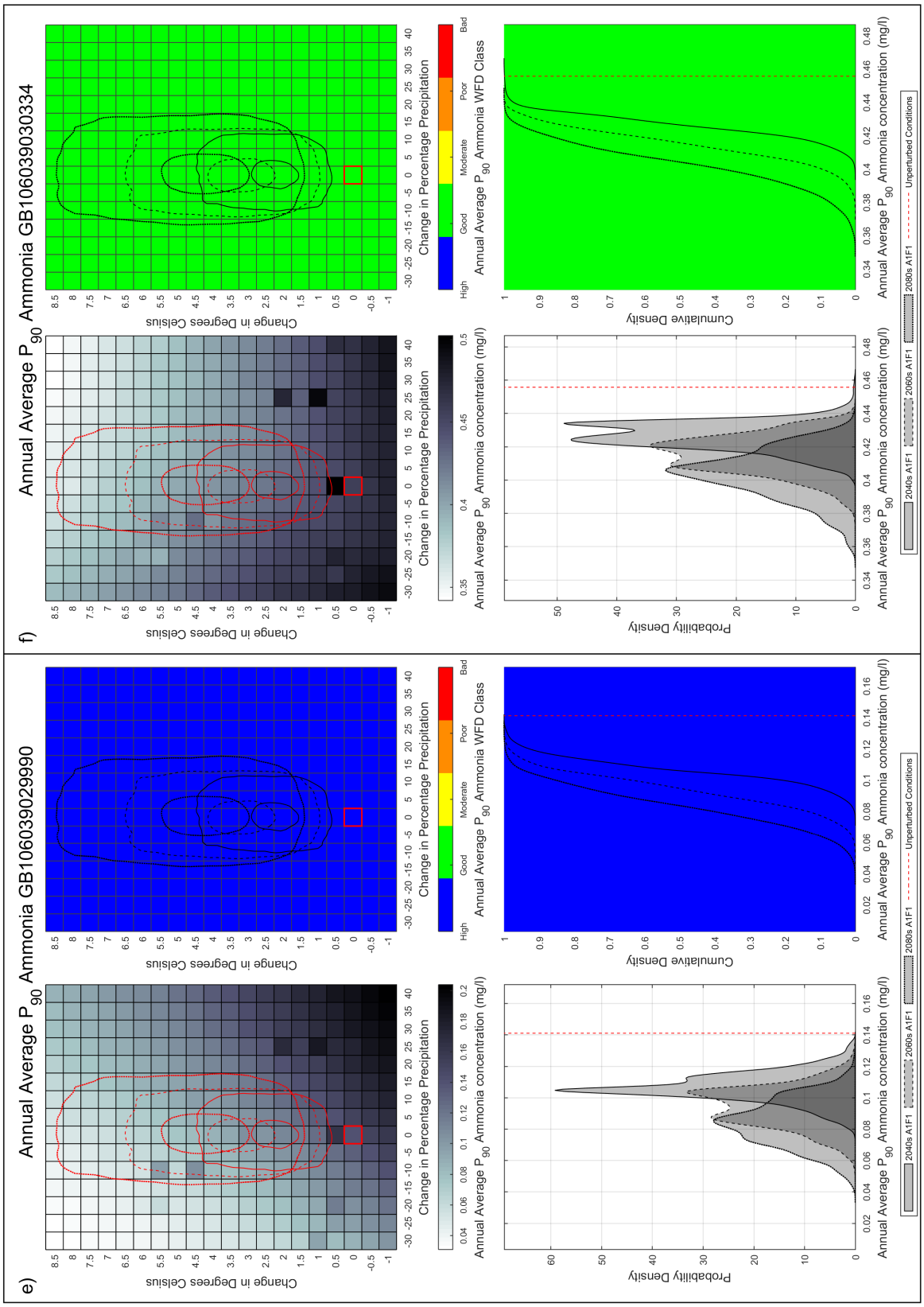


Figure 5-9: Figure palettes of ammonia concentration for exemplar catchments 29990 and 30334 (Low, Medium, Calcareous and Low, Large, Calcareous respectively). Four graphs are presented for each catchment: top-left - raw data response surface; top-right - class response surface; bottom-left and bottom-right - Probability Distribution Function (PDF) and Cumulative Distribution Function (CDF) for UKCP09 projections respectively.

Table 5-3: Summary statistics for ammonia for each exemplar catchment. Statistics provided for response surfaces and box-plots for each of the UKCP09 projections (2040s, 2060s and 2080s).

	Catchment	GB106039017780	GB106039017840	GB106039023180	GB106039029810	GB106039029990	GB106039030334
Ammonia Response Surface	Average	0.135	0.180	0.222	0.102	0.094	0.414
	Min	0.045	0.140	0.083	0.047	0.031	0.342
	Max	0.212	0.245	0.385	0.193	0.204	0.502
	% High	95	73.67	80.67	100	100	0
	% Good	5	26.33	19.33	0	0	100
	% Moderate	0	0	0	0	0	0
	% Poor	0	0	0	0	0	0
	% Bad	0	0	0	0	0	0
Ammonia 2040s	Q10	0.136	0.183	0.222	0.102	0.095	0.416
	Q50 (Median)	0.150	0.191	0.242	0.111	0.106	0.427
	Q90	0.162	0.200	0.265	0.122	0.118	0.436
	% High	100	88.01	99.99	100	100	0
	% Good	0	11.99	0.01	0	0	100
	% Moderate	0	0	0	0	0	0
	% Poor	0	0	0	0	0	0
	% Bad	0	0	0	0	0	0
Ammonia 2060s	Q10	0.116	0.180	0.190	0.088	0.078	0.401
	Q50 (Median)	0.136	0.189	0.221	0.102	0.095	0.416
	Q90	0.153	0.199	0.247	0.114	0.109	0.429
	% High	100	90.86	100	100	100	0
	% Good	0	9.14	0	0	0	100
	% Moderate	0	0	0	0	0	0
	% Poor	0	0	0	0	0	0
	% Bad	0	0	0	0	0	0
Ammonia 2080s	Q10	0.098	0.175	0.163	0.075	0.064	0.384
	Q50 (Median)	0.123	0.186	0.201	0.093	0.084	0.404
	Q90	0.145	0.196	0.237	0.109	0.103	0.422
	% High	100	95.01	100	100	100	0
	% Good	0	4.99	0	0	0	100
	% Moderate	0	0	0	0	0	0
	% Poor	0	0	0	0	0	0
	% Bad	0	0	0	0	0	0

Figure 5-10 outlines the boxplots produced for projected future ammonia concentrations for each of the exemplar catchments. Across all catchments, there is a consistent decreasing trend in median ammonia concentrations from the 2040s through the 2060s to the 2080s. Table 5-3 provides summary statistics for each of the scenarios for all exemplar catchments.

Catchment a) shows a clear reduction in median concentrations from the 2040s to 2080s, each corresponding to a 'High' WFD class for this catchment. Furthermore, the entire interquartile range corresponds to 'High', suggesting no future classification change over unperturbed conditions. The interquartile range and whisker length increase from the 2040s to 2080s, indicating a reduction in predictive potential into the future. Each of the distributions is relatively normal, with a slight skew towards lower values, particularly in the 2040s. Furthermore, outliers are present only below the bottom whisker for each scenario, suggesting a tail in the distribution towards lower concentrations.

The boxplots for catchment b) show only a very slight reduction in median concentrations from the 2040s to 2080s, with significant overlap in concentrations present between all scenario boxplots. All median values and the entire interquartile range correspond to a 'High' class for this catchment, indicating no class change over unperturbed conditions. The interquartile range and whisker length is comparatively consistent between scenarios, suggesting a consistency in predictive potential into the future. Whilst all distributions are reasonably normal, the 2060s and 2080s show a significant tail of outliers at lower concentrations.

Catchments c), d) and e) exhibit very similar boxplots, with the only notable difference being the magnitude of concentrations predicted; catchment c) concentrations are consistently double those of both catchments d) and e). The median concentrations consistently decrease from the 2040s to 2080s, whilst the interquartile range and whisker lengths increase, suggesting a reduction of predictive potential into the future. The median values and entire interquartile ranges for each scenario for all catchments correspond to the 'High' WFD class, suggesting no future change in classification over unperturbed conditions. The distributions for each of the 2060s and 2080s are reasonably normal, with slight tails towards lower concentrations. The median concentration for

each of the 2040s is closer to the 25th percentile (bottom of the box), suggesting a distributional skew towards lower concentrations. The outliers for the 2040s are consistently spread either side of both whiskers, indicating a tail in the distribution towards both high and low concentrations.

Finally, the boxplots for catchment e) demonstrate similar trends and distributions between scenarios to those in catchments c), d) and e), with a gradual reduction in median concentrations and an increase in both the interquartile range and whisker length from the 2040s to 2080s. However, the magnitude of predicted concentrations is significantly higher (between 0.40 to 0.45mg/l), ensuring that the median and entire interquartile range for each scenario corresponds to the 'Good' WFD class for this catchment. This suggests no classification change over unperturbed conditions. There is a slight skew in the 2040s distribution towards lower concentrations and a slight skew in both the 2060s and 2080s towards higher concentrations.

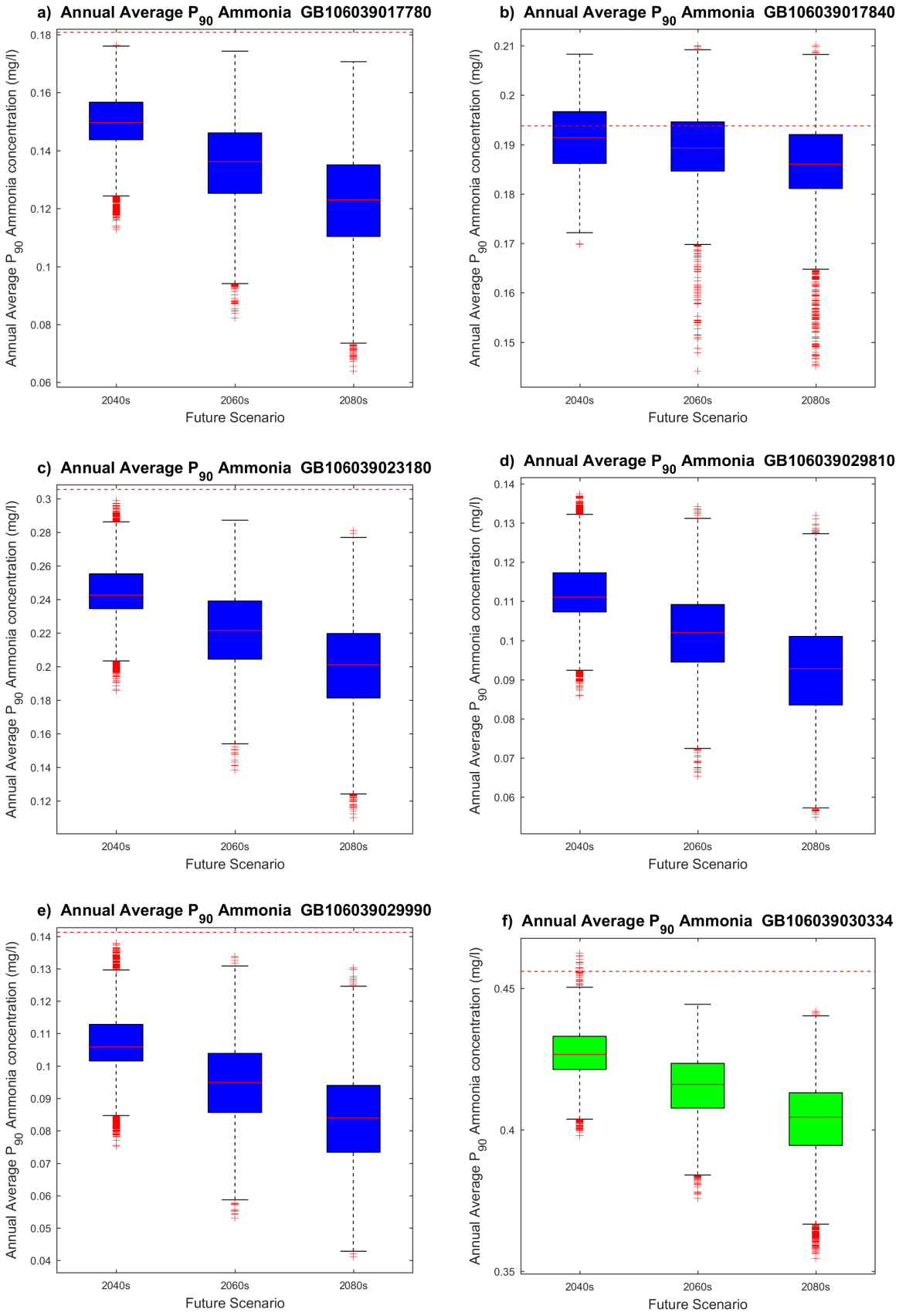


Figure 5-10: Box-plots for ammonia for each of the UKCP09 projections (2040s, 2060s and 2080s) for each of the exemplar catchments. Instructions for interpretation are described in section 5.1.

5.2.3 WATER TEMPERATURE

All in-text references for this section relate to Figure 5-11, Figure 5-12 and Figure 5-13. Whilst average annual P^{98} temperatures for an unperturbed (baseline) climate vary between catchments throughout the Thames basin, the catchment response surfaces for water temperature follow a typically similar pattern and gradient across all catchments due to the strong positive correlation between air temperature and water temperature. As such, all catchments share a gradual vertical gradient in annual average P^{98} temperatures consistent across all precipitation changes, with lower values associated with negative temperature change and high values found at greater temperature change. There is a small variation between the range in temperature values associated with each catchment, with catchments a), b) and e) having water temperatures ranging from 17°C to 27°C, catchments c) and d) with temperatures from 17°C to 25°C and catchment f) from 20°C to 29°C.

Despite consistent trends, these similar temperature gradients do not necessarily correspond to the same classes, due to differences in threshold standards between catchment types. For example, catchments a), b) and e) all exhibit a similar temperature range across the response surface, yet only a) and e) exhibit comparable class patterns, with most cells classified as 'High' and those from 6.5°C upward as 'Good'. Conversely, catchment e) shows most cells as 'Moderate (from 4.5°C upward), with a band of 'Good' cells between 1.5-4°C and 'High' below 1°C. The response of this catchment with regards to WFD classification is much more like catchments c), d) and f), which all span three classifications from 'High' to 'Moderate'. Catchments c) and d) are almost identical in terms of temperature gradient and WFD classifications, with approximately equal numbers of cells corresponding to all three classifications (below 2°C – 'High'; 2.5-5.5°C – 'Good'; above 6°C – 'Moderate'). Catchment f) has most cells corresponding to 'High' (4°C and below), despite the elevated temperatures in this catchment over other catchments, with a band of 'Good' between 4.5-7°C and a small band of 'Moderate' at 7.5°C and above.

The PDFs and CDFs for water temperature across all future scenarios are identical in shape and distribution across all catchments due to the relationship between water temperature and air

temperature. All scenarios are normally distributed around a single modal point; with a trend towards flatter, wider distributions the further in the future values are predicted. This is reflected in the CDFs for each catchment by the divergence between scenario curves and more pronounced tails at higher cumulative densities. There is an overlap in distributions between scenarios with the modal point for the 2040s consistently 2°C higher than the unperturbed baseline across all catchments; with a 3.5°C increase for 2060s and 4.5°C for 2080s. This consistency between catchments is due to the constant gradient across all response surfaces, with the variation between catchments caused by the original unperturbed catchment temperature determining the magnitude of the temperature predicted. Therefore, whilst the shape of the CDFs remains constant between catchments, the quantity and severity of WFD classes they span varies, due to the differing threshold standards between catchment types and magnitude of unperturbed catchment temperature.

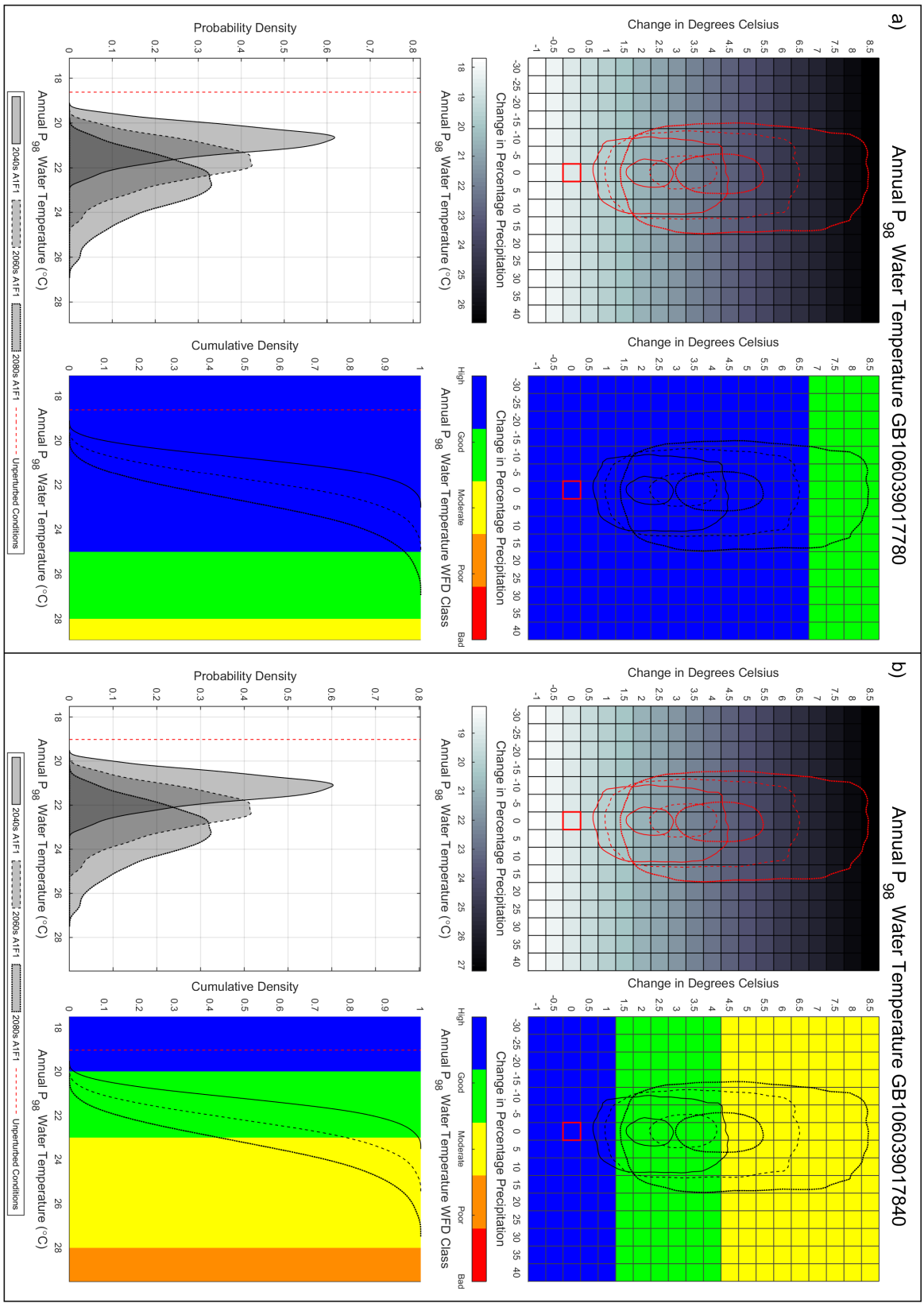


Figure 5-11: Figure palettes of water temperature concentration for exemplar catchments 17780 and 17840 (Low, Medium, Siliceous and Low, Small, Siliceous respectively). Four catchment graphs are presented: top-left - raw data response surface; top-right - class response surface; bottom-left and bottom-right - Probability Distribution Function (PDF) and Cumulative Distribution Function (CDF) for UKCP09 projections respectively.

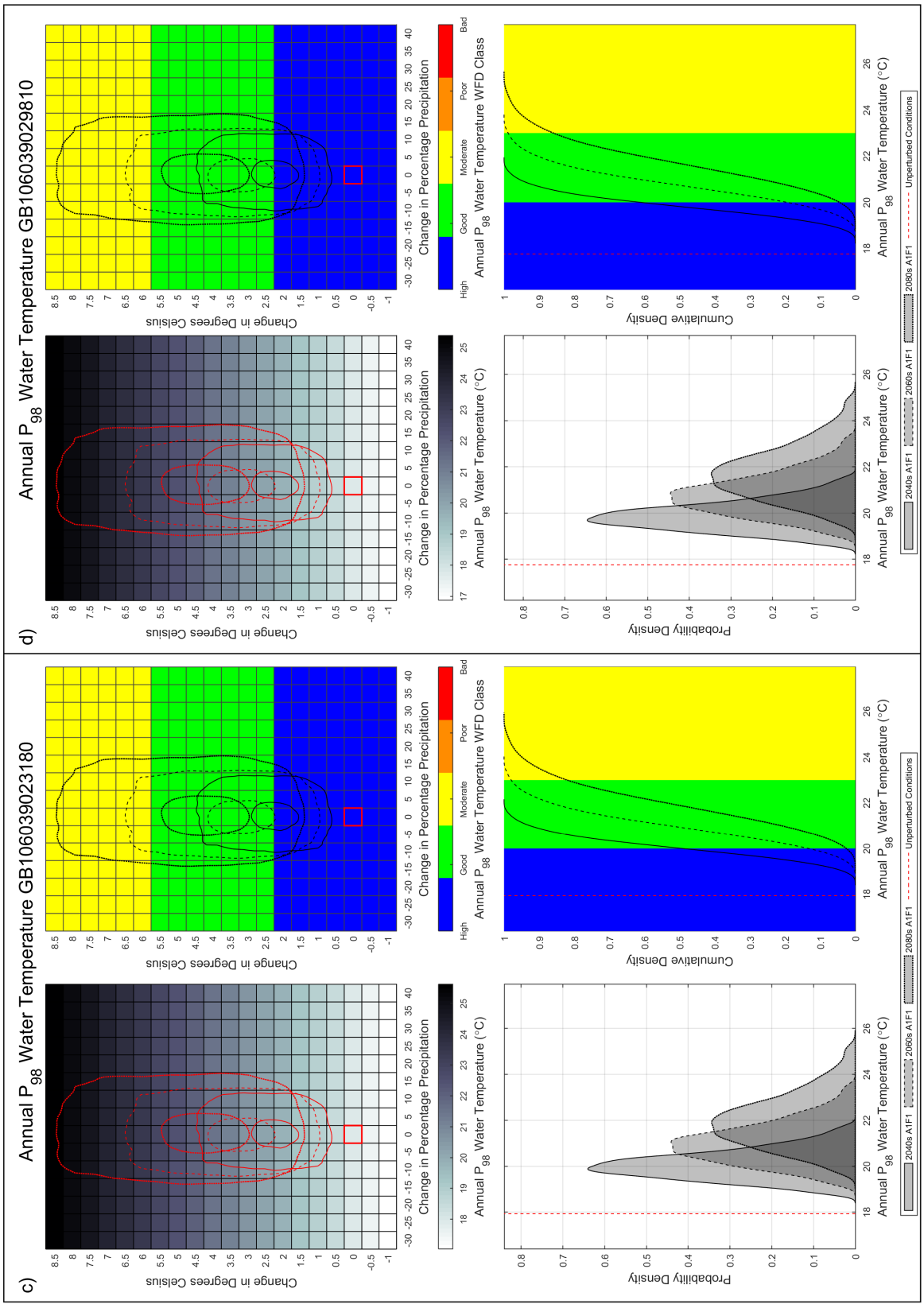


Figure 5-12: Figure palettes of water temperature concentration for exemplar catchments 23180 and 29810 (Low, Small, Calcareous and Mid, Small, Calcareous respectively). Four catchment graphs are presented: top-left - raw data response surface; top-right - class response surface; bottom-left and bottom-right - Probability Distribution Function (PDF) and Cumulative Distribution Function (CDF) for UKCP09 projections respectively.

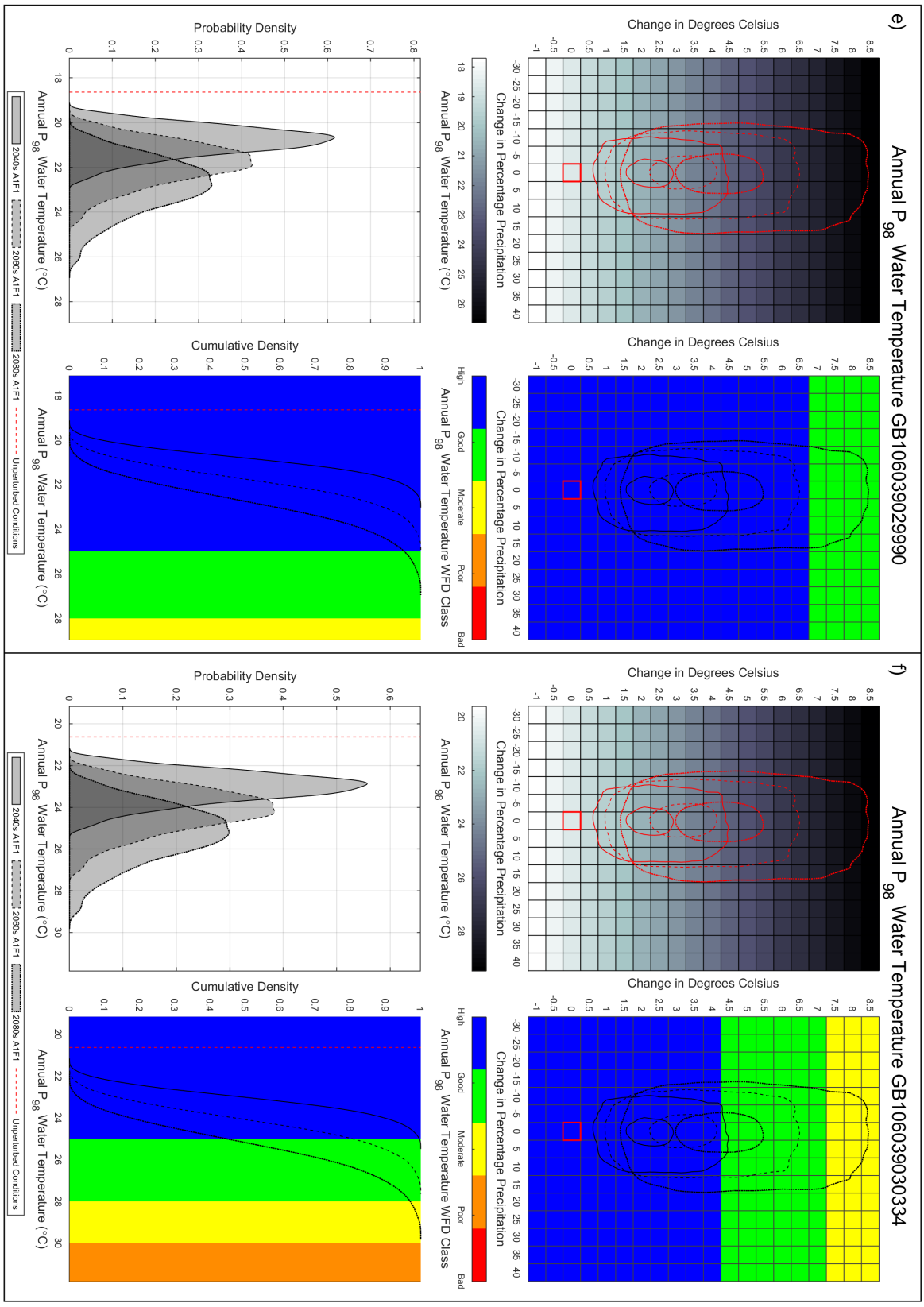


Figure 5-13: Figure palettes of water temperature concentration for exemplar catchments 29990 and 30334 (Low, Medium, Calcareous and Low, Large, Calcareous respectively). Four catchment graphs are presented: top-left - raw data response surface; top-right - class response surface; bottom-left and bottom-right - Probability Distribution Function (PDF) and Cumulative Distribution Function (CDF) for UKCP09 projections respectively.

Table 5-4: Summary statistics for water temperature for each exemplar catchment. Statistics provided for response surfaces and box-plots for each of the UKCP09 projections (2040s, 2060s and 2080s).

	Catchment	GB106039017780	GB106039017840	GB106039023180	GB106039029810	GB106039029990	GB106039030334
Water Temperature Response Surface	Average	22.15	22.63	21.33	21.13	22.17	24.54
	Min	17.69	18.08	17.03	16.87	17.71	19.60
	Max	26.62	27.19	25.63	25.38	26.64	29.48
	% High	80	25	35	35	80	55
	% Good	20	30	35	35	20	30
	% Moderate	0	45	30	30	0	15
	% Poor	0	0	0	0	0	0
	% Bad	0	0	0	0	0	0
Water Temperature 2040s	Q10	20.02	20.46	19.28	19.09	20.04	22.18
	Q50 (Median)	20.78	21.24	20.01	19.82	20.80	23.02
	Q90	21.68	22.15	20.88	20.68	21.70	24.02
	% High	100	0.96	48.85	60.52	100	99.48
	% Good	0	98.36	51.15	39.48	0	0.52
	% Moderate	0	0.68	0	0	0	0
	% Poor	0	0	0	0	0	0
	% Bad	0	0	0	0	0	0
Water Temperature 2060s	Q10	20.66	21.11	19.89	19.70	20.68	22.88
	Q50 (Median)	21.75	22.22	20.94	20.74	21.77	24.09
	Q90	23.03	23.53	22.18	21.96	23.05	25.51
	% High	100	0.01	12.08	18.72	100	79.42
	% Good	0	77.84	85.64	80.11	0	20.58
	% Moderate	0	22.15	2.28	1.17	0	0
	% Poor	0	0	0	0	0	0
	% Bad	0	0	0	0	0	0
Water Temperature 2080s	Q10	21.36	21.82	20.56	20.37	21.37	23.66
	Q50 (Median)	22.74	23.23	21.90	21.69	22.76	25.19
	Q90	24.39	24.92	23.48	23.26	24.41	27.01
	% High	95.28	0	2.06	3.93	95.29	42.76
	% Good	4.71	40.41	78.7	81.88	4.71	54.18
	% Moderate	0	59.59	19.24	14.19	0	3.06
	% Poor	0	0	0	0	0	0
	% Bad	0	0	0	0	0	0

Figure 5-14 shows the scenario boxplots for water temperature for each of the exemplar catchments, with Table 5-4 providing summary statistics. Similarly, to the response surfaces, PDFs and CDFs, the boxplots for water temperature exhibit identical responses over all exemplar catchments. The median temperatures consistently increase over unperturbed conditions by 2.3°C for the 2040s, 3.2°C for the 2060s and 4.3°C for the 2080s for all catchments. The interquartile range (IQR) and length of the whiskers both increase from the 2040s through to the 2080s, indicative of a decrease in predictive potential over time. The distributions for each scenario are all slightly skewed towards lower temperatures, with the upper whisker significantly longer than the lower whisker. Furthermore, outliers are all found beyond the upper whisker, suggesting a longer tail in the distribution towards higher temperatures.

Significantly, however, the magnitude of temperatures predicted and WFD standards vary between exemplar catchments ensuring differences in classifications between scenarios and catchments. For catchment a) and e), temperatures are predicted within the low 20s Celsius for all scenarios, with the median and entire IQR for each scenario corresponding to a 'High' WFD class for this catchment. This suggests no change in future classification over unperturbed conditions. Conversely, whilst catchment b) predicts very similar temperatures for each scenario to catchment a) and e), the WFD standards for this catchment type ensure differences in classification. The medians and entire IQRs for both the 2040s and 2060s both correspond to a 'Good' classification, which is an increase in severity of classification from unperturbed conditions ('High'). The interquartile range for the 2080s spans the threshold between 'Good' and 'Moderate' classes for this catchment, with approximately two thirds of the IQR classified as 'Moderate' and a third as 'Good'. Furthermore, the median is associated with a 'Moderate' class, suggesting a downgrading in classification from 'High' to 'Moderate' is most likely for the 2080s. Catchments c) and d) demonstrate very similar boxplots with respect to the magnitude of predicted temperatures (from high teens to low twenties Celsius) and WFD classifications. The IQR for both 2040s span the threshold between 'High' and 'Good', with catchment c) distributed half 'High', half 'Good' and catchment d) three quarters 'High', a quarter 'Good'. The median value for the 2040s for catchment c) lies on the threshold line between 'High'

and ‘Good’, whilst the median for catchment d) is associated with the ‘High’ class. This suggests that for catchment c) there is an equal probability of a downgrading in classification to ‘Good’ in the 2040s over unperturbed conditions as there is of remaining the same, whilst for catchment d) it is more likely that no classification change will occur (‘High’).

The IQRs and median temperatures for both catchments for the 2060s and 2080s are associated with the ‘Good’ classification, suggesting an increase in severity from ‘High’ to ‘Good’ WFD standards under both scenarios. Finally, catchment e) predicts the highest temperatures out of all exemplar catchments, with temperatures ranging across scenarios from the low-twenties to high-twenties Celsius. However, due to the WFD standards for this catchment type, these high temperatures are not associated with particularly severe classifications. The median temperatures and IQRs for both the 2040s and 2060s are associated with a ‘High’ class for this catchment, suggesting no change in classification over unperturbed conditions for these scenarios. However, the IQR for the 2080s spans the threshold between ‘High’ and ‘Good’ classifications, with the majority classified as ‘Good’. The median is also associated with a ‘Good’ classification, indicating that it is most likely a change of classification will occur from ‘High’ to ‘Good’ over unperturbed conditions for this scenario.

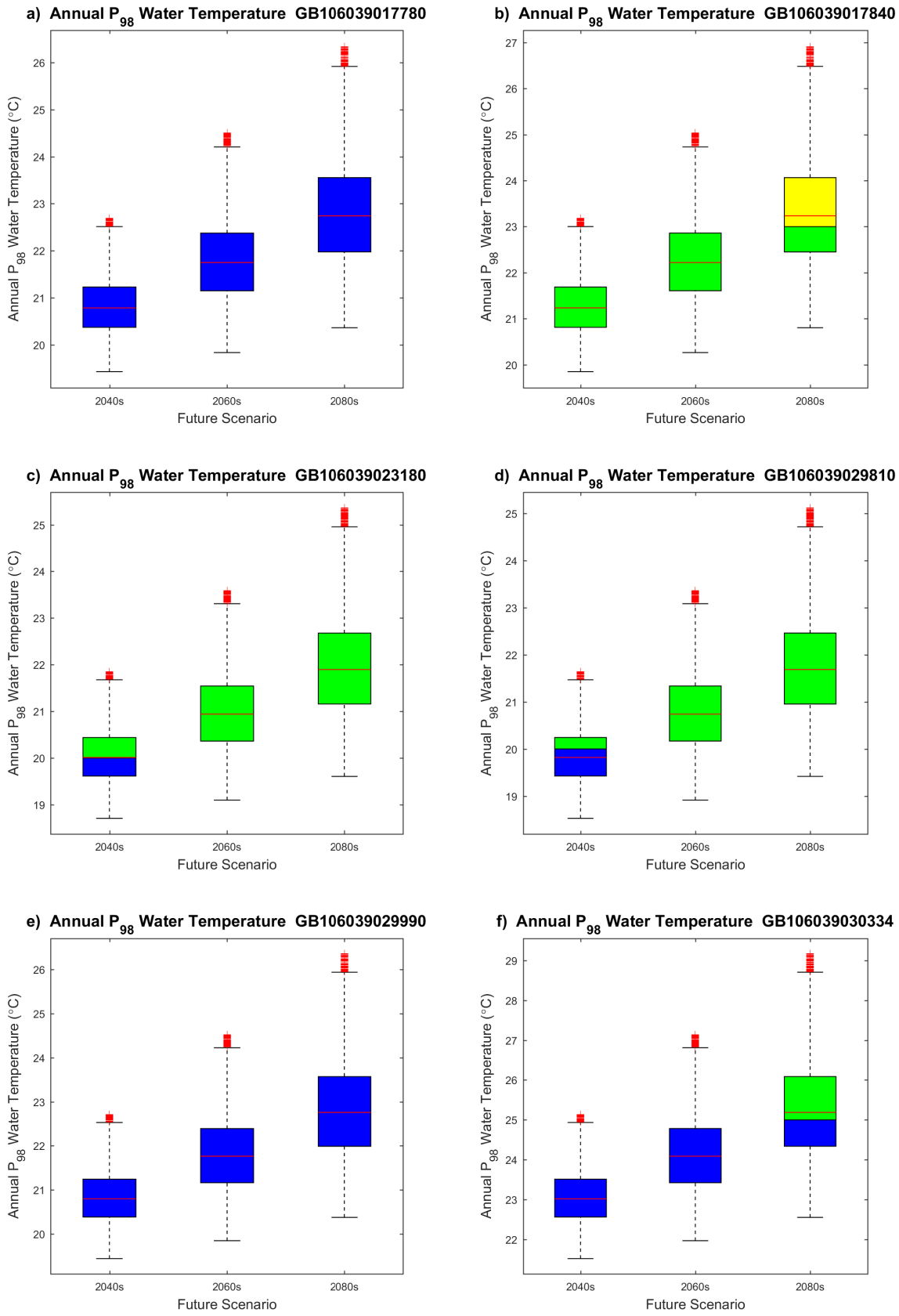


Figure 5-14: Box-plots for water temperature for each of the UKCP09 projections (2040s, 2060s and 2080s) for each of the exemplar catchments. Instructions for interpretation are described in section 5.1.

5.2.4 DUNDEE HYDROLOGICAL REGIME ALTERATION METHOD (DHRAM)

The DHRAM methodology provides a quantitative classification of the extent to which a suite of indicators relating to key aspects of the eco-hydrological regime have altered between an unperturbed (baseline) and perturbed (altered climate set) flow time-series. As outlined in section 4.5.1, DHRAM scores and classifications have been modified for use in this thesis to provide an indication of the response of the hydrological regime of a catchment to changes in precipitation and temperature over a completely naturalised model of the Thames. All in-text references for this section relate to Figure 5-15, Figure 5-16 and Figure 5-17. The response surfaces exhibit significant differences in both the distribution and magnitude of scores between catchments, although there is a persistent trend throughout all response surfaces of a left-to-right diagonal gradient with higher scores generally associated with top-left (high temperature, low precipitation) and bottom-right (low temperature, high precipitation) cells.

Catchments a), d) and e) exhibit similar catchment responses in DHRAM to changes in annual average precipitation and temperature changes. DHRAM scores range from 0-13 in these catchments and follow similar patterns in terms of distribution of scores across their respective response surfaces. Catchment f) also follows a similar pattern but has a reduced range of scores present across the response surface (0-10). A thin band of cells with scores of 0 (corresponding to a 'High' classification) runs diagonally across each catchment from low temperature and middling precipitation change to mid-temperature and mid-precipitation change. This band varies in size across exemplars, with catchment a) having the largest number of cells designated as 'High', and catchments d)-f) having a narrower band and fewer 'High' cells. These bands sit within a band of cells with scores that range from 1-4 (corresponding to 'Good' status) that run in a similar diagonal fashion as above from low temperature and mid-to-low precipitation change through to high temperature and mid-high precipitation change. Typically, these cells form a gradient of increasing

values outward from cells designated as 'High' towards the top-left and bottom-right of the response surface. These cells eventually cross the next WFD classification threshold, forming two bands of cells with scores from 5-11 that correspond to 'Moderate' status. These bands run diagonally and are situated in the top-left and bottom-right of the response surface, with DHRAM scores following a gradient of increasing values towards the extremes of the response surface. In catchment a), there is an equal distribution of these cells in either corner of the response surface, whereas in catchments d-f there is a skew towards more 'Moderate' cells in the top-left of the response surface than the bottom-right. Finally, in catchment a), d) and e) there are a small number of cells with scores of 12-13 corresponding to 'Poor' status. In catchment a), these cells are found at the very extreme top-left of the response surface (7.5-8.5C and -30% precipitation change), whereas in catchment d) they are found at the very extreme bottom-left (-1C and 35-40% precipitation change). Catchment e) varies from these, with a larger number of cells designated as 'Poor' found in both the top-left and bottom-right of the response surface. Catchment b) exhibits less variation in DHRAM scores across the response surface than the other catchments with only scores from 0-8 present (with only a single cell designated as 0). However, the response surface exhibits a similar pattern in distribution of scores to the other exemplar catchments, with increasingly higher scores associated with the top-left (higher temperature and lower precipitation change) and bottom-right (lower temperature and higher precipitation change). Most of the cells have scores 1-4 and are classified as 'Good', with a small number classified as 'Moderate' in the top-left and bottom-right of the response surface. Finally, catchment c) represents the most heavily altered of the exemplar catchments, with scores that range from 1-14 (there are no cells that represent 'High' status). A strong diagonal gradient is present, with the highest scores found in the top-left of the response surface, the lowest scores found in the centre and higher scores found in the bottom-right. A range of scores from 1-4, corresponding to 'Good' status, form the central band across the response surface from low temperature and mid-low precipitation change to high temperature and high precipitation change. A block of scores from 5-11 ('Moderate' status) occupies the bottom-right of the response surface, with another narrow band running diagonally from low temperature and low precipitation change to high temperature and

mid-precipitation change. Finally, a large block of scores from 12-14, corresponding to 'Poor' status, occupies the top-left of the response surface, demonstrating a skew in the highest DHRAM scores towards high temperature and negative precipitation change.

In contrast to the consistency between distributions for water temperature, the PDFs and CDFs for the DHRAM scenarios vary significantly between catchments. Furthermore, the graphs for DHRAM are probability density histograms and cumulative density step graphs, since the predicted scores are integer values. Broadly speaking, DHRAM score distributions fall into 3 categories with respect to unperturbed values; most scores greater, majority the same, and majority lower than the unperturbed score. Catchments a), c), d) and f) fall into the first category, with most scores for each scenario predicted to be greater than the unperturbed value for the catchment, suggesting an increase in hydrological alteration due to changes in precipitation and temperature and further deviation from naturalized conditions. However, there are significant differences in the shape and width of distributions between catchments and between scenarios within catchments themselves. This is due to the variation in scores across the response surfaces for each catchment and overlap between scenario probabilistic change factors. Catchment a) exhibits bimodal distributions for each of the future scenarios, with 2040s peaks at 0 and 3; 2060s at 0 and 3, 4; and 2080s at 0 and 4. In total, the scenarios span a relatively small range of scores (0-5), with an increase in scores chronologically into the future. The CDFs for catchment a) demonstrate a relative similar distribution at lower cumulative densities but diverge at higher densities associated with a change in class from 'Good' to 'Moderate'. The CDFs span three classes ('High', 'Good' and 'Moderate'), with a substantial shift towards more severe classes from the 2040s to the 2080s. Catchments c), d) and f) depict unimodal distributions across all scenarios, with all modal points greater than the baseline score of 2 and 0 respectively. All three catchments demonstrate a consistent skew towards lower scores across all scenarios, with a trend towards flatter, wider distributions into the future. Catchment c) represents the most severely impacted of all the exemplar catchments, with scenario distributions spanning scores from 1 to 13. Both catchment d) and f) exhibit a similar gradient of response to catchment c), except that DHRAM scores across the entire response surface are lower. This gradient

across the response surface for each catchment causes the PDFs and CDFs for the 2040s and 2060s to be associated with low to mid DHRAM scores, whereas the wider distribution of change factors for the 2080s pushes into the higher DHRAM scores associated with high temperature and increasingly negative precipitation change. Consequently, the PDFs and CDFs for the 2080s scenarios across these catchments demonstrate a significant spike in high DHRAM scores in relation to those for the 2040s and 2060s. The shapes of the PDFs for catchments c) and f) have clear modal peak values, with a rapid tapering of the distributions towards the tails across all scenarios. Conversely, catchment d) exhibits flatter distributions across all scenarios, suggesting a less marked gradient of DHRAM scores across the catchment response surface and a decrease in the certainty of predicting any given score.

Catchment e) represents the second category, where the modal value for all scenarios is the same as the unperturbed value (DHRAM score of 1 in this instance). The shape and distribution of PDFs for each scenario are very similar to those of these prior catchments; skewed towards lower DHRAM scores, with higher DHRAM scores and wider distributions predicted into the future. The PDF for the 2040s is unimodal, with a clear modal peak of 1, rapidly tapering towards the tails. The PDFs for both the 2060s and 2080s are bimodal, due to the diagonal gradient of DHRAM scores across the catchment response surface, with peaks scores of 1 and 4.

Catchment b) represents the third and final category, where the modal value for all scenarios is lower than the unperturbed value (DHRAM score of 3 in this instance), suggesting a reduction in hydrological alteration with changes in precipitation and temperature and a return to naturalized conditions. The gradient of response surface for this catchment is less pronounced than other catchments, with relatively homogeneous central cells covered by much of the scenario probabilistic change factors. As such, the PDFs for all scenarios demonstrate a clear modal peak score of 1, with a narrow range of scores (1-6) predicted that shift towards higher DHRAM scores further into the future. Finally, all PDFs and CDFs exhibit a distributional skew towards higher scores.

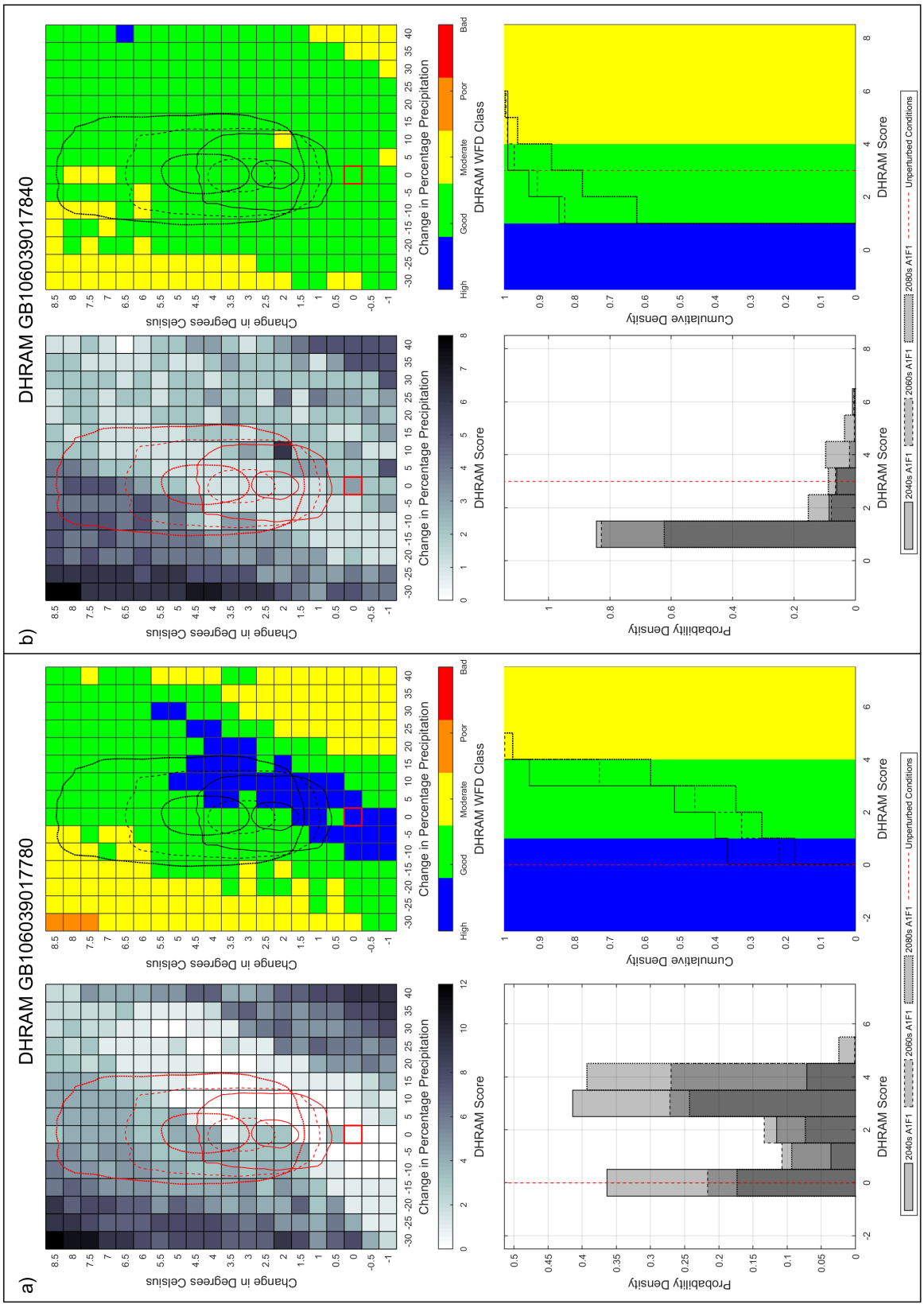


Figure 5-15: Figure palettes of DHRAM concentration for exemplar catchments 17780 and 17840 (Low, Medium, Siliceous and Low, Small, Siliceous respectively). Four catchment graphs are presented: top-left - raw data response surface; top-right - class response surface; bottom-left and bottom-right - Probability Distribution Function (PDF) and Cumulative Distribution Function (CDF) for UKCP09 projections respectively.

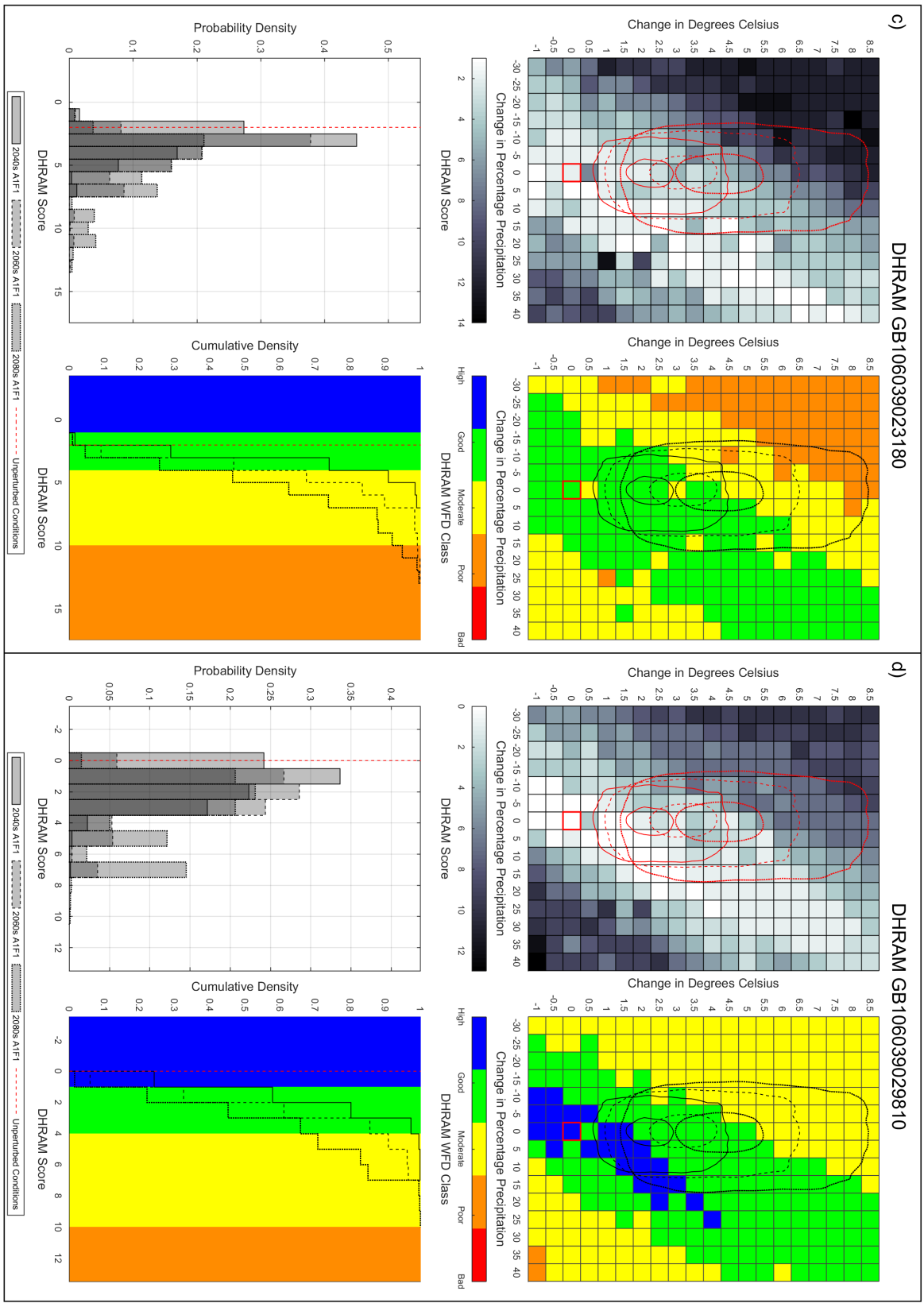


Figure 5-16: Figure palettes of DHRAM concentration for exemplar catchments 23180 and 29810 (Low, Small, Calcareous and Mid, Small, Calcareous respectively). Four catchment graphs are presented: top-left - raw data response surface; top-right - class response surface; bottom-left and bottom-right - Probability Distribution Function (PDF) and Cumulative Distribution Function (CDF) for UKCP09 projections respectively.

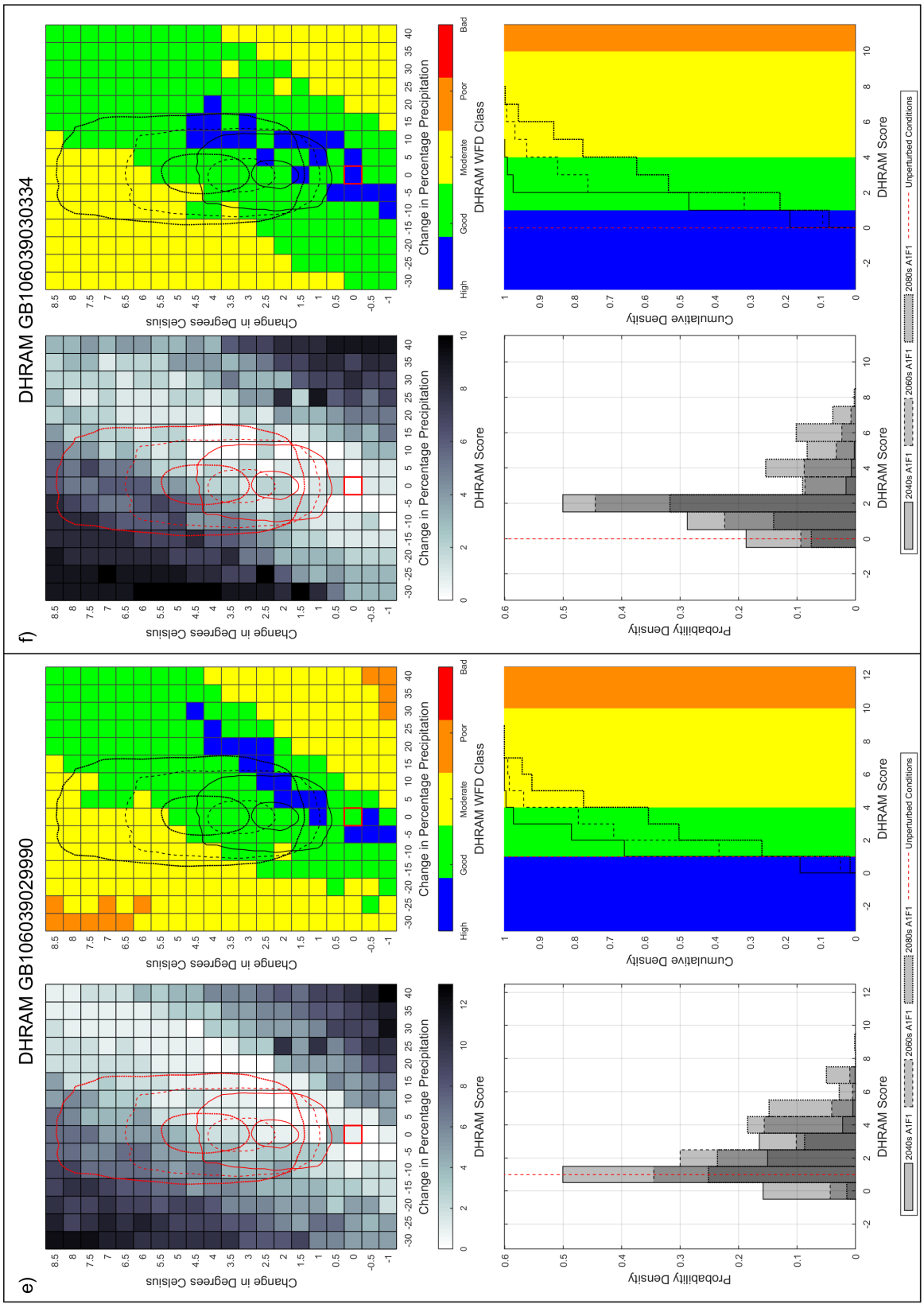


Figure 5-17: Figure palettes of DHRAM concentration for exemplar catchments 29990 and 30334 (Low, Medium, Calcareous and Low, Large, Calcareous respectively). Four catchment graphs are presented: top-left - raw data response surface; top-right - class response surface; bottom-left and bottom-right - Probability Distribution Function (PDF) and Cumulative Distribution Function (CDF) for UKCP09 projections respectively.

Table 5-5: Summary statistics for DHRAM for each exemplar catchment. Statistics provided for response surfaces and box-plots for each of the UKCP09 projections (2040s, 2060s and 2080s).

	Catchment	GB106039017780	GB106039017840	GB106039023180	GB106039029810	GB106039029990	GB106039030334
DHRAM Response Surface	Average	4	2	5	4	5	3
	Min	0	0	1	0	0	0
	Max	12	8	14	13	13	10
	% High	14.33	0.33	0	8.33	6	7.33
	% Good	50	82	44	43	43.33	52.33
	% Moderate	34.67	17.67	36.33	48	46.67	40.33
	% Poor	1	0	19.67	0.67	4	0
	% Bad	0	0	0	0	0	0
DHRAM 2040s	Q10	0	1	2	0	0	0
	Q50 (Median)	2	1	3	1	1	2
	Q90	3	2	4	3	3	2
	% High	36.38	0	0	24.19	15.78	18.67
	% Good	63.62	99.03	90.82	75.34	83.76	81.17
	% Moderate	0	0.97	9.18	0.47	0.46	0.17
	% Poor	0	0	0	0	0	0
	% Bad	0	0	0	0	0	0
DHRAM 2060s	Q10	0	1	3	1	1	1
	Q50 (Median)	3	1	4	2	2	2
	Q90	4	2	7	4	4	4
	% High	21.64	0	0	5.9	4.32	9.32
	% Good	78.25	99.13	67.52	84.9	90.17	84.29
	% Moderate	0.1	0.87	31.69	9.2	5.51	6.39
	% Poor	0	0	0.8	0	0	0
	% Bad	0	0	0	0	0	0
DHRAM 2080s	Q10	0	1	3	1	1	1
	Q50 (Median)	3	1	5	3	2	2
	Q90	4	4	9	7	5	6
	% High	17.33	0	0	1.48	1.45	7.53
	% Good	80.23	96.19	46.45	69.27	75.9	70.06
	% Moderate	2.44	3.81	48.39	29.25	22.65	22.4
	% Poor	0	0	5.16	0	0	0
	% Bad	0	0	0	0	0	0

The boxplots for DHRAM, outlined in Figure 5-18, demonstrate large variation between and within exemplar catchments. Table 5-5 provides summary statistics for the boxplots. Notably, since DHRAM produces integer scores, the boxplots demonstrate some unusual characteristics not found in the figures for previous variables. This is important to understand when interpreting boxplots and determining potential future changes in classification. Furthermore, since DHRAM score is relative to 'natural' conditions and not unperturbed baseline, it is possible for catchments to become more 'naturalised' under future conditions.

The boxplots for catchment a) span very few DHRAM scores over all scenarios (0-5), with the interquartile range (IQR) for 2040s spanning scores from 0-3, and both the 2060s and 2080s spanning 1-4. There is an increase in median values from the 2040s (2) to the 2060s and 2080s (3), all of which are associated with a 'Good' classification. The unperturbed condition of this catchment has a DHRAM score of 0 and is thus considered comparatively natural for the sake of this analysis. As such, all scenarios predict an increase in DHRAM score over unperturbed values and a change in classification from 'High' to 'Good.

Catchment b) depicts unusual boxplots that are a product of using integer score values, with both the 2040s and 2060s having a median score and IQR that are the same value (1), with no whiskers. Similarly, for the 2080s, the median value, 25th percentile and lower whisker all have the same value (1), with the 75th percentile (2) and upper whisker (3) spanning several scores. The presence of outliers in all three scenarios above the upper whiskers indicates that the majority of the DHRAM scores are a single value (1), which is confirmed from viewing the catchment response surface and PDF in Figure 5-15. The DHRAM score under unperturbed conditions is 3 for this catchment, corresponding to a 'Good' classification. Consequently, under all scenarios DHRAM scores are most likely to decrease over unperturbed conditions, indicating a shift towards more 'naturalised' conditions. Notably, no scenario predicts DHRAM scores of 0, and thus no likelihood of classification change under future conditions.

Catchment c) predicts the largest range of DHRAM scores (1-13) out of all exemplar catchments, with higher scores predicted from the 2040s through to the 2080s. Median DHRAM scores increase from the 2040s (3) through the 2060s (4) to the 2080s (5), with a similar shift in IQR towards higher scores over time. The IQR for the 2080s spans double the number of score values than those of the 2040s and 2060s, suggesting a greater range of scores predicted in this scenario. Furthermore, the whiskers suggest a skew towards lower scores, with the lower whisker significantly shorter than the upper across scenarios. The score values for the 2040s IQR all correspond to a 'Good' classification, suggesting no change in classification over unperturbed conditions. Conversely, both the 2060s and 2080s are divided around the threshold between 'Good' and 'Moderate'. The median and majority of the IQR for the 2080s is classified as 'Moderate', suggesting a shift towards more severe classifications further into the future.

The boxplots for catchment d) demonstrate an increase in median values from the 2040s to 2080s, with an associated increase in the size of IQRs between scenarios, suggestive of a reduction in predictive potential over time. The scenarios are skewed towards lower scores, with a longer upper whisker and median values found closer to the 25th percentile. The IQRs and medians for the 2040s and 2060s fully classify as 'Good', with the IQR for the 2080s split between 'Good' and 'Moderate' and the median corresponding to the 'Good' class. Therefore, it is likely a change to a more severe classification will occur in all scenarios in relation to unperturbed conditions ('High'), with a small likelihood of a double classification change occurring in the 2080s.

Catchment e) displays little variation in the median values between boxplots for each scenario, with the 2040s identical to unperturbed conditions (1) and 2060s and 2080s just one higher (2). There is an increase in size and distribution of the IQRs from the 2040s to the 2080s, indicating a greater variation in the number of scores forecast for each catchment and a reduction in the predictive potential over time. The distributions are skewed towards lower DHRAM scores, with the upper whisker longer than the lower. Notably, the lower whisker for each scenario falls on a DHRAM score of 0, suggesting there is an increasingly lower probability that catchments could return to a more

'naturalised' state than current, unperturbed conditions. However, the medians and IQRs for all scenarios fall correspond to the 'Good' class, indicating it is most likely that no future classification change will occur over unperturbed conditions.

Finally, the boxplots for catchment e) exhibit the same median value (2) for each scenario, suggesting a relatively homogenous response surface around central cells covered by these scenarios. For both the 2040s and 2060s, the IQR and distribution of whiskers are identical (skewed towards higher scores), with only an increased number of outliers at higher scores in the 2060s indicative of the higher DHRAM scores predicted at higher temperatures. The shift in the IQR for the 2080s towards higher scores demonstrates the location and change in gradient across the underlying response surface. However, all median values and IQRs for each catchment correspond to the 'Good' class, suggesting a likely change in classification over unperturbed conditions ('High') for all scenarios.

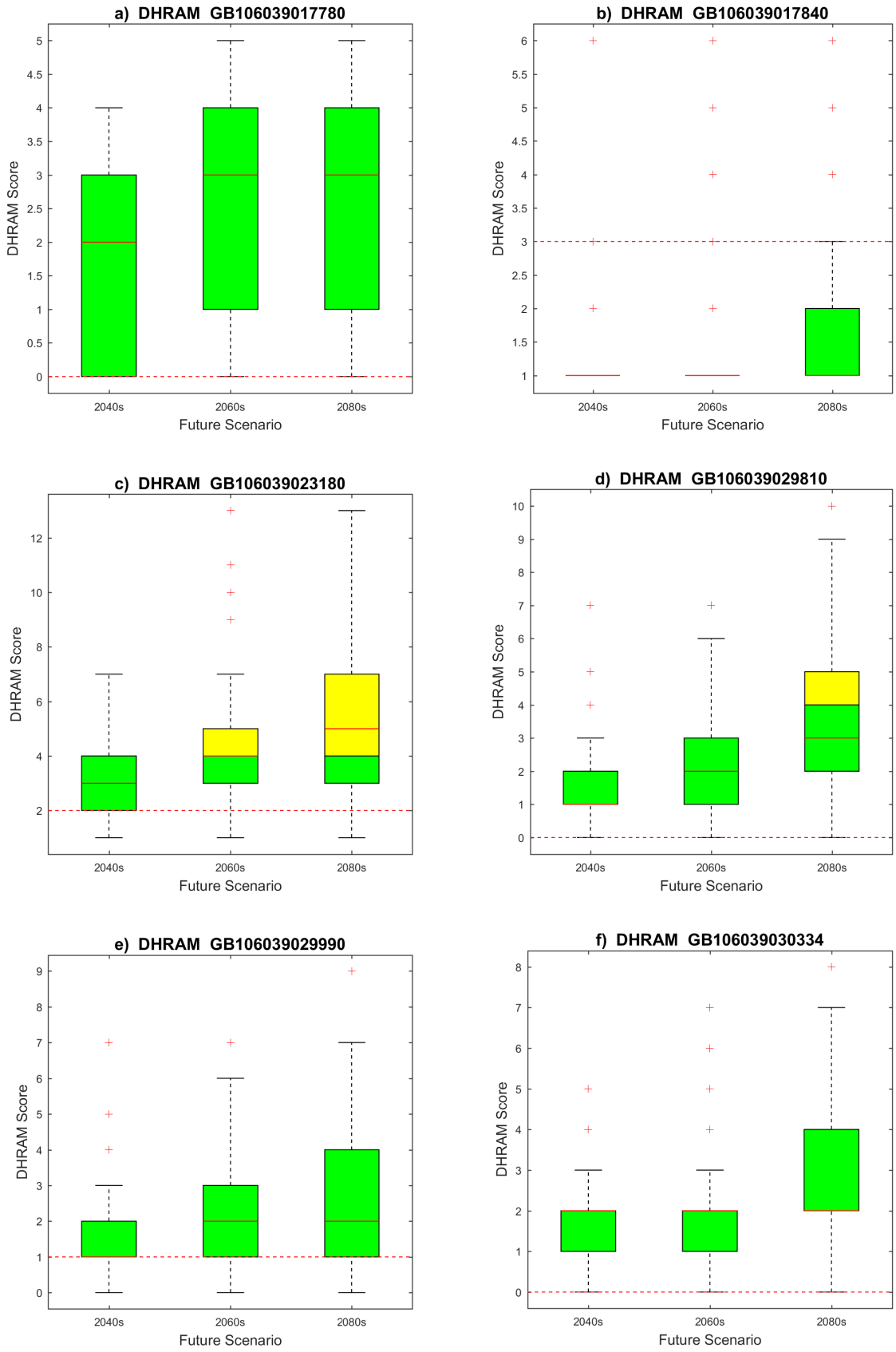


Figure 5-18: Box-plots for DHRAM for each of the UKCP09 projections (2040s, 2060s and 2080s) for each of the exemplar catchments.

Instructions for interpretation are described in section 5.1.

5.3 MACROINVERTEBRATE MODEL RESULTS

The application of both macroinvertebrate models (observed and predicted) to selected model parameters generated from each implementation of both INCA-N and INCA-P for each of the 292 catchments within in the Thames Basin, generated 10,000 EQR values for all 300 altered climate sets. These EQR values were subsequently classified using the WFD standards outlined in Table 4-5 and response surfaces for each of the resulting WFD classifications were generated for each catchment. These outline the sensitivity of the macroinvertebrate model in predicting WFD class due to changes in both mean annual precipitation and temperature and are presented for the six exemplar catchments in Figure 5-19 to Figure 5-24. Similar figures were produced for the remaining 286 catchments and can be found in electronic Appendix II (see attached CD). The predominant classifications for all exemplar catchments, as predicted by the joint macroinvertebrate model, are 'High' and 'Good'. Additionally, there are very low percentages of 'Moderate' classification predicted in catchments c) and f). Due to the nature of the model predictions (i.e. the percentage values across all classification for any given altered climate cell total 100), then typically the response demonstrated in one class surface is inversely related to the response in classes either side (i.e. 'High' and 'Good'). Catchments a) and d) are predominantly classed as 'High' and demonstrate very little variation in the likelihood of class occurrence due to alterations in precipitation and temperature. The reverse is true for catchment f), which demonstrates homogeneously high percentage likelihood across the 'Good' class. However, for catchments b), c) and e) there is a definite split in percentage likelihood between classes 'High' and 'Good', with significant variation shown in distribution across the relevant response surfaces. These patterns are also replicated in catchments a) and d), but to a far lesser extent. Typically, a higher percentage likelihood of classification as 'High' coincides with increased precipitation and lower temperatures. The reverse is true for 'Good' classification, which demonstrates higher percentage likelihood of occurrence with reduced precipitation and higher temperatures.

The boxplots below the response surfaces demonstrate the application of UKCP09 scenarios to each classification to generate estimates of the potential impact from climate change on the percentage

likelihood of occurrence for each classification. This is a somewhat complicated process, since it generates a range of probable outcomes based on the 10,000 UKCP09 delta change points from a response surface itself representing the percentage likelihood of classification. Therefore, when interpreting the box-plots, it is necessary to note that the percentage likelihood of macroinvertebrate classification must always sum to 100% across all classes for each scenario (i.e. taking the 75th percentile (upper box line) for 'High', requires the 25th percentile (lower box line) for 'Good'). This process becomes further complicated if macroinvertebrate classification visibly spans more than two classes (i.e. catchment f)). However, some general trends may be observed from the boxplots as to the potential impact that climate change may have on the percentage likelihood of macroinvertebrate classification. In catchments a) to e), there is a consistent trend towards a reduction in the likelihood of 'High' classification from the 2040s through to the 2080s. Conversely, there is thus an increase in the likelihood of 'Good' classification from the 2040s through to the 2080s. In catchments a), d) and e) these percentage changes are small and have little bearing on the overall likelihood of which class is predicted to occur under each scenario. However, in catchments b) and c), there exists the possibility that changes predicted to occur under all scenarios could shift the overall percentage likelihood of classification from 'High' to 'Good' and 'Good' to 'High' respectively. This shift is more likely to occur in the 2080s than in the 2040s or 2060s. Finally, catchment f) demonstrates predictions that visibly span three classes ('High' to 'Moderate'). There is a trend towards an increased likelihood of 'High' classification occurring from the 2040s to 2080s. However, the observed variation in these changes is very low and therefore has no bearing on the most likely class predicted under all scenarios ('Good').

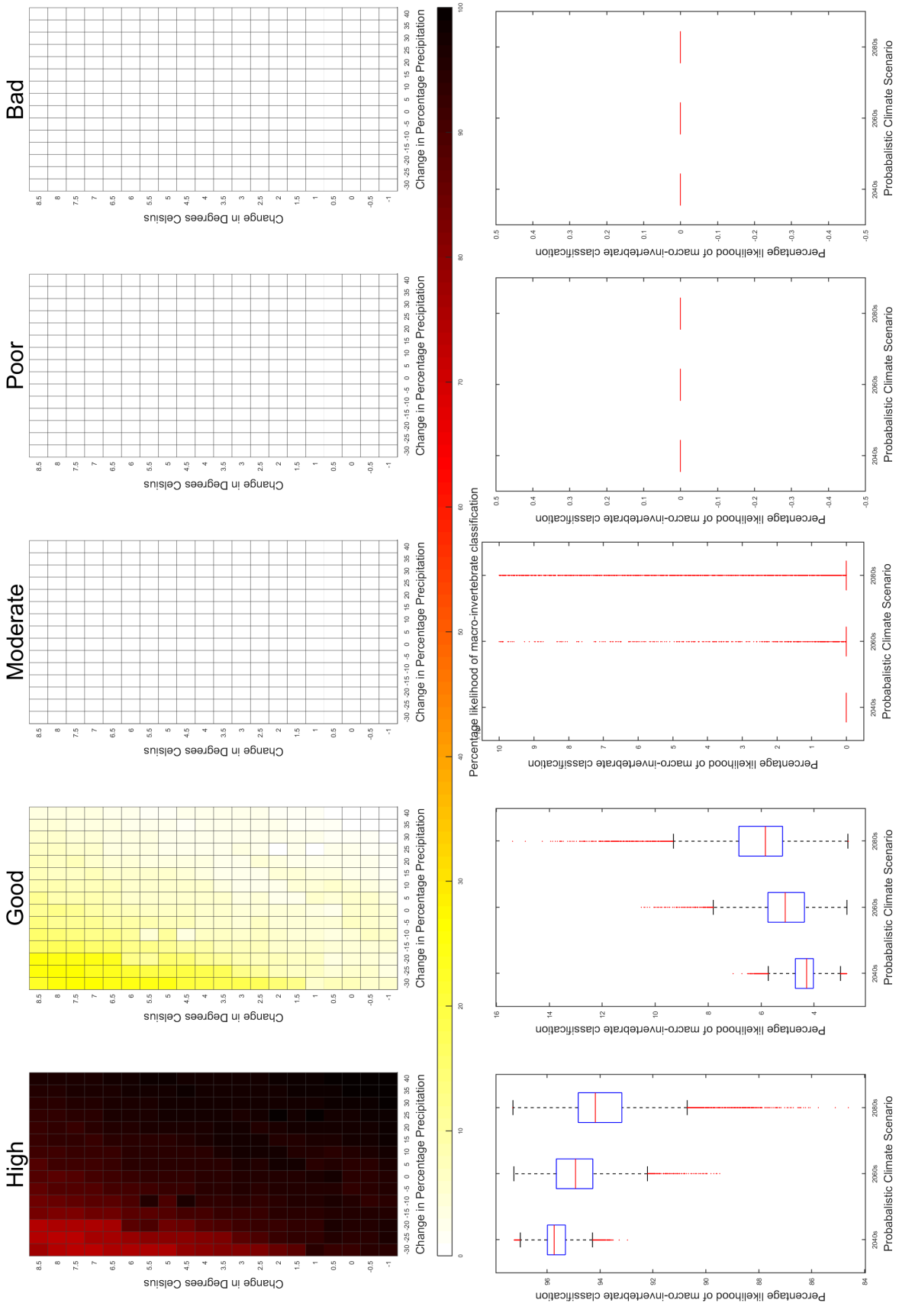


Figure 5-19: Response surface and boxplots for macroinvertebrate classification for exemplar catchment 17780 (Low, Medium, Siliceous).

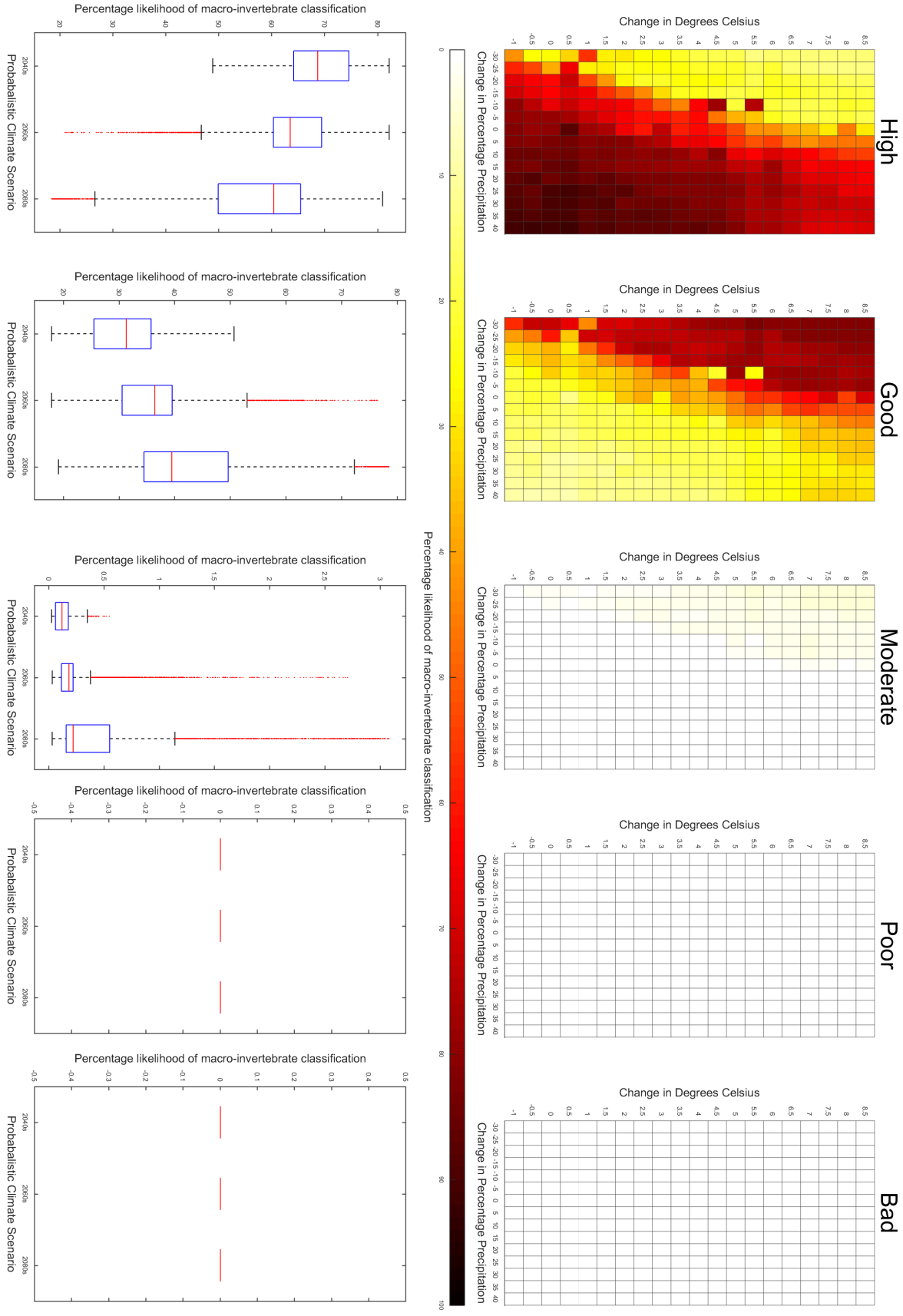


Figure 5-20: Response surface and boxplots for macroinvertebrate classification for exemplar catchment 17840 (Low, Small, Siliceous).

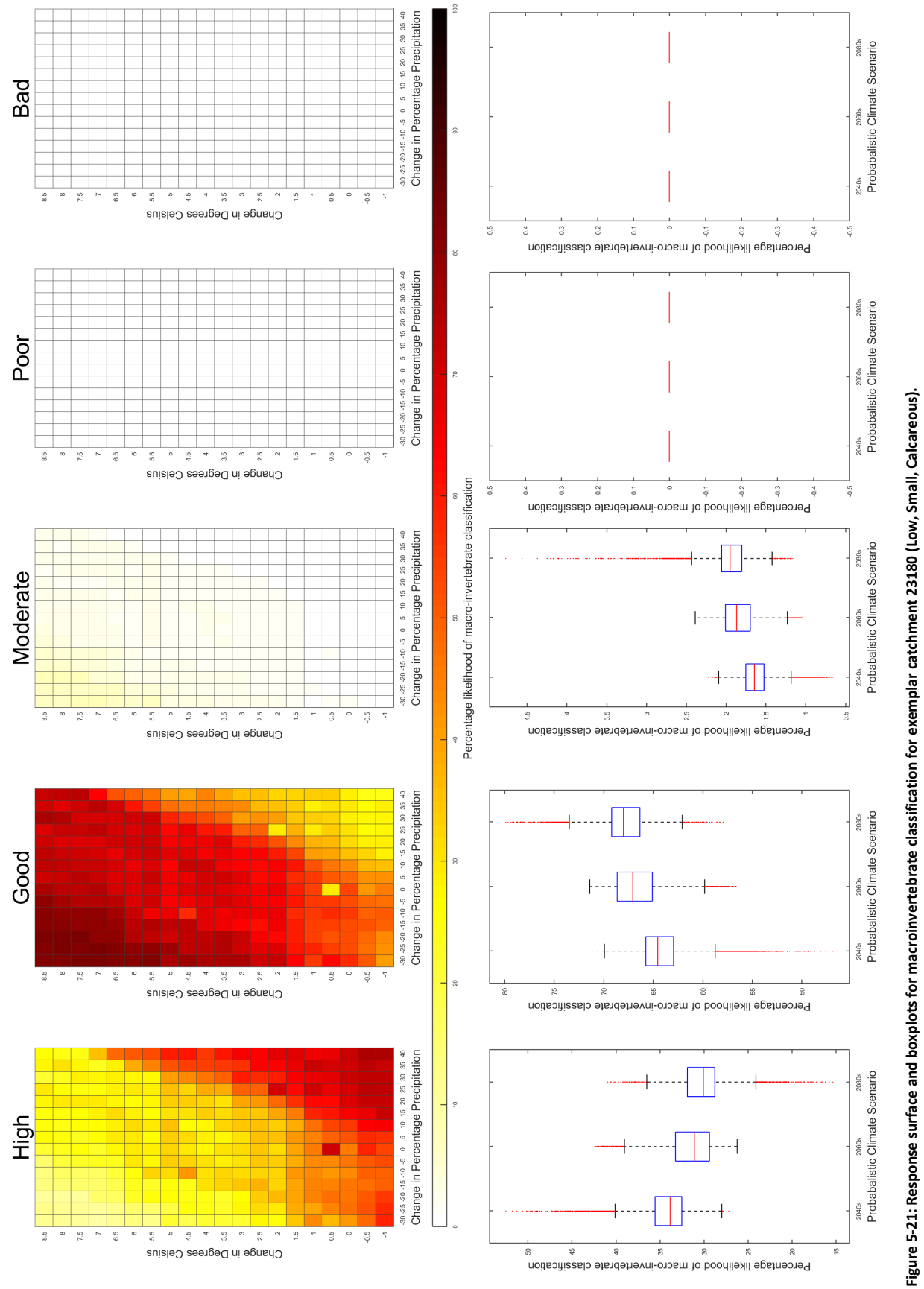


Figure 5-21: Response surface and boxplots for macroinvertebrate classification for exemplar catchment 23180 (Low, Small, Calcareous).

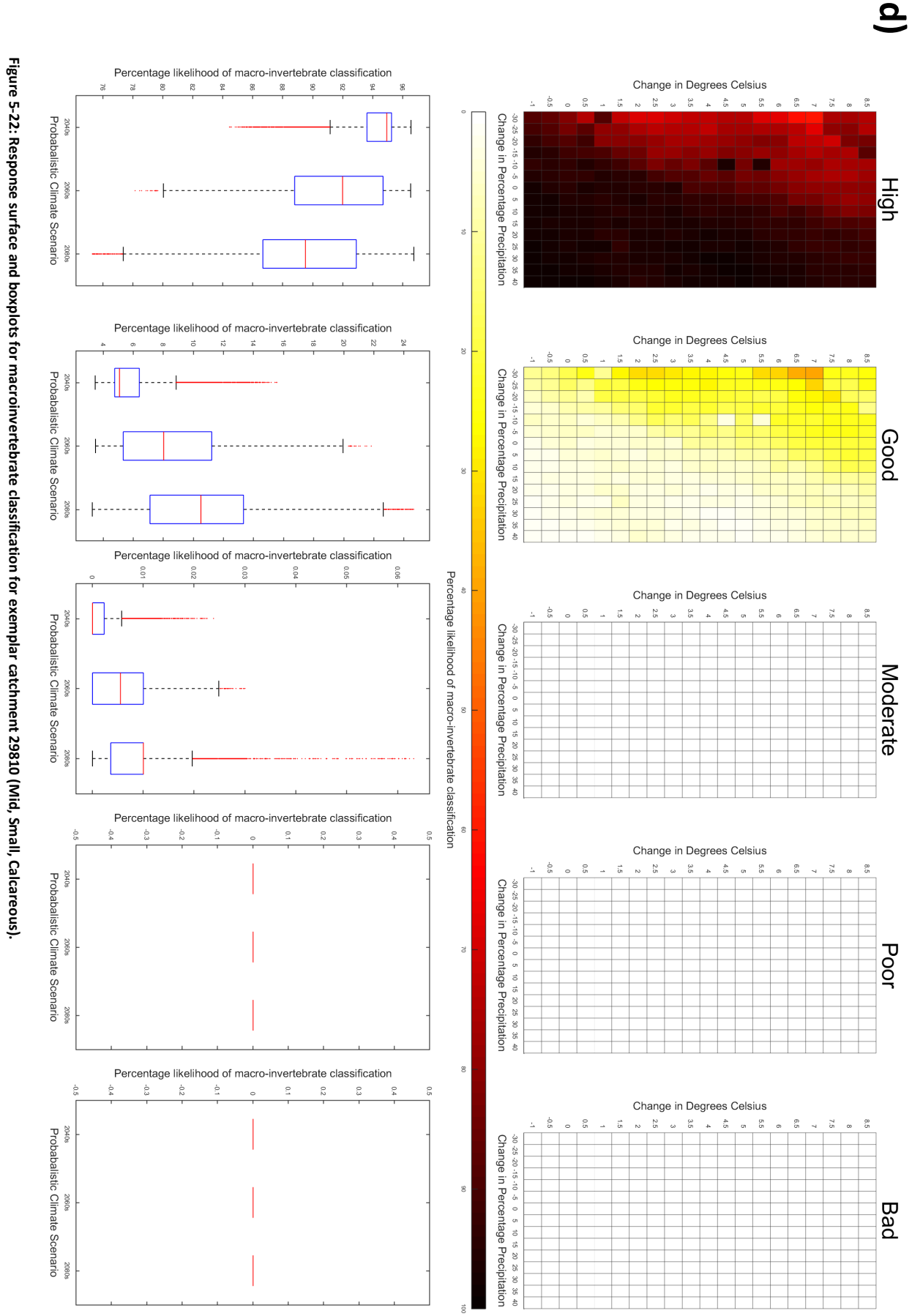


Figure 5-22: Response surface and boxplots for macroinvertebrate classification for exemplar catchment 29810 (Mid, Small, Calcareous).

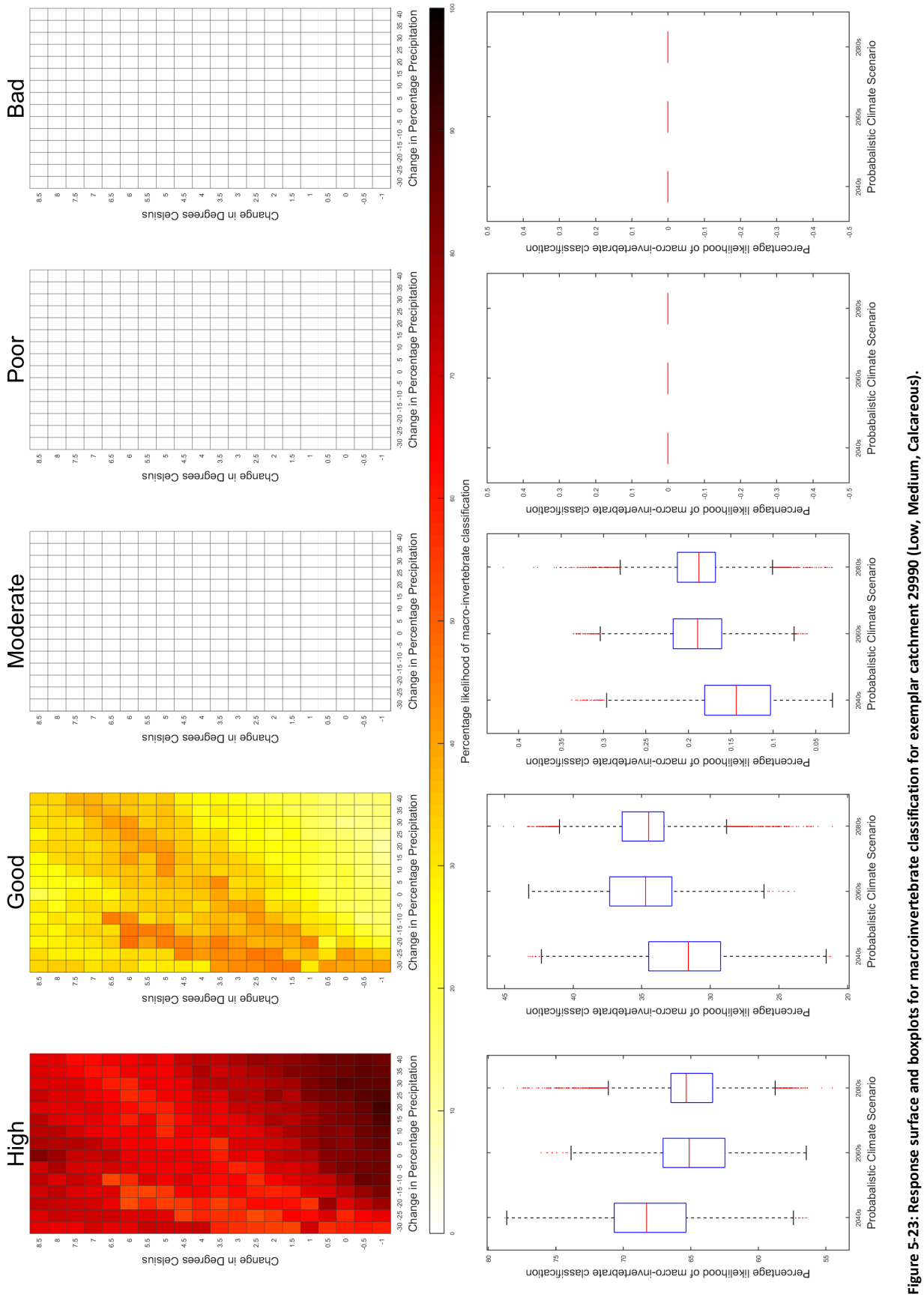


Figure 5-23: Response surface and boxplots for macroinvertebrate classification for exemplar catchment 29990 (Low, Medium, Calcareous).

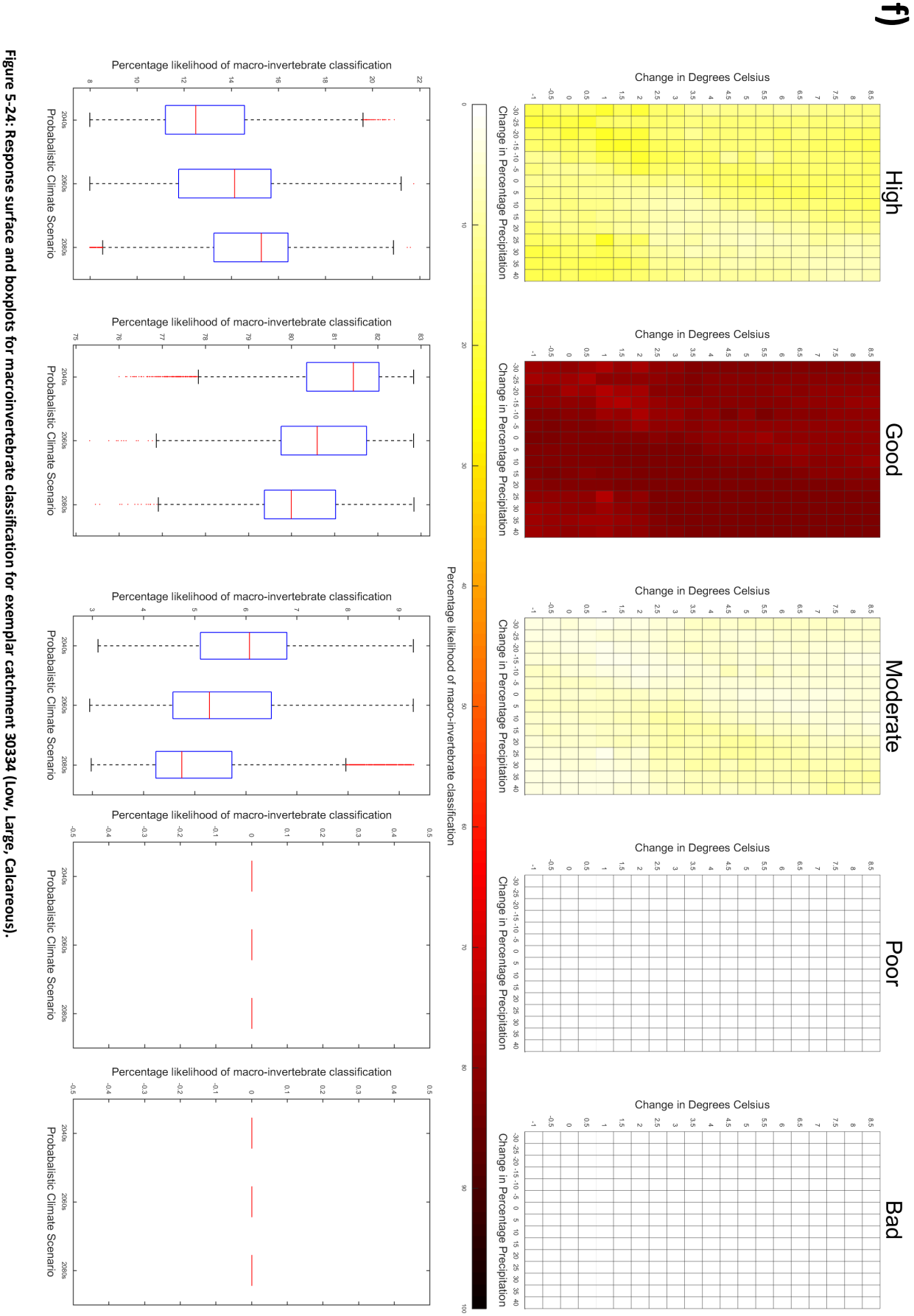


Figure 5-24: Response surface and boxplots for macroinvertebrate classification for exemplar catchment 30334 (Low, Large, Calcareous).

5.4 MAPS OF THE THAMES BASIN FOR HYDRO-ECOLOGICAL INDICATORS

5.4.1 INTRODUCTION AND DESCRIPTION OF BASIN MAPS

The exemplar catchments provide a highly detailed representation and analysis of the data produce for each of the 292 catchments within the Thames Basin. The following section present maps of the Thames Basin that summarise much of this information for each variable and allow the spatial distribution of data throughout the basin to be elucidated. In total, four figures are produced for each variable, resulting in 16 figures in this section of the results. Detailed analysis of the magnitude and spatial variation of both raw data and WFD classification are assessed for each corresponding figure.

The first figure represents the raw data produced for each variable throughout the Thames Basin. In total, 9 maps are included in this figure representing the 10^{th} 50^{th} and 90^{th} percentile of data extracted from the underlying response surface for each catchment using the UKCP09 projections for the 2040s, 2060s and 2080s. The 50^{th} percentile presents values that are as equally likely to occur as to not under each scenario, whilst the 10^{th} and 90^{th} percentiles give an indication as to the spread of the underlying distribution of values. It is important to note that the log of both SRP and ammonia concentrations were taken and displayed in the relevant figure and legends. This is due to the large variation in concentrations for both macro-nutrients found across catchments within the Thames Basin (up to 5 orders of magnitude), thus making it very challenging to demonstrably show changes in values across the distribution of data within each map and between scenarios. Temperature is displayed as degrees Celsius and DHRAM is presented as raw scores. The values were mapped to a greyscale colour-map to maintain consistency with response surface values presented for the exemplars and electronic Appendix I. Values were binned to increase legibility of maps and distinction between colour values. The figures between variables are not comparable, due to the variation in data formats outlined above.

The second figure represents the deviation in raw data values from unperturbed conditions. Again, a total of 9 maps are included in this figure representing the 10^{th}, 50^{th} and 90^{th} percentile of data presented in the first figure as a percentage change (SRP and ammonia) and absolute change (water

temperature and DHRAM) from unperturbed conditions. Unperturbed conditions relate to the climate series that have not been altered and, as such, represent the current, observed data series of precipitation and temperature. The UKCP09 projections for the 2040s, 2060s and 2080s do not include unperturbed (current) conditions. Therefore, the change observed in variables is solely related to the projected distributions of catchment responses for key variables with respect to alterations in climate (annual average precipitation and temperature). As such, these maps provide a better visual representation of the impact climate change is likely to have across the whole basin for each variable, regardless of the magnitude of raw data values. Percentage change was mapped to a colour-map (negative-neutral-positive; blue to white to red) to better highlight the extent of change across the Thames Basin.

The third figure represents the percentage likelihood per class for each of the UKCP09 projections, generating a total of 15 maps per figure. Unlike raw data maps, categorisation into classes enables the full distribution of predicted changes to be presented as a percentage likelihood of occurrence for each scenario. This is represented by the transparency of colour used for each of the five classes; 'High' – blue, 'Good' – green, 'Moderate' – yellow, 'Poor' – range and 'Bad' – red. Since these maps show the spatial cumulative distribution of classes for each UKCP09 scenario (totalling 100% across all classes for any given catchment), it is possible for a catchment to present colour in multiple catchment maps, depending on the magnitude and breadth of underlying class values.

Finally, the fourth figure represented the percentage likelihood of directional change in WFD class relative to unperturbed conditions for each of the UKCP09 projections. The number of maps per figure varies on the magnitude in classes present from unperturbed conditions. The application of WFD standards to categorise raw data into an ecologically meaningful classification system is an essential part of understanding the impact that climate change is projected to have on each individual catchment. Therefore, in keeping with the concept of ecological-integrity, the percentage likelihood of change from unperturbed conditions is presented as either an 'improvement' or 'deterioration' in severity of class predicted. It is worth noting that whilst raw data values may change significantly in proportion to unperturbed conditions under certain scenarios, it is not

necessarily reflected in the class maps, as specific thresholds may not have been exceeded. Therefore, the more severe the change in classification and the higher the probability of occurrence are both vital in identifying catchments most likely to be most at risk of ecological change under UKCP09 scenarios.

5.4.2 Soluble Reactive Phosphorus

Figure 5-25 provides a summary of the raw data for each catchment within the Thames Basin for each of the scenarios derived using the HadCM3 probabilistic change factors for the 2040s, 2060s and 2080s. The 10th, 50th and 90th percentile are presented for the whole basin, with values corresponding to colour bins outlined in the legend. Due to the large variation in SRP concentrations throughout the Thames Basin, it was necessary to log transform the data to enable presentation of results using a single colour gradient. However, despite this, it remains difficult to observe significant colour changes (and thus changes in concentration) along each distribution and between scenarios. One exception to this is the Mole, which shows a definite colour change corresponding to a decrease in concentrations into the future and from lower to higher concentrations across the breadth of the distributions from the 10th to 90th percentiles. This figure has been included for completeness to demonstrate the range of concentrations found throughout the Thames basin and to demonstrate that, whilst change does occur, it is often not discernible.

A more informative and clearer representation of the changes occurring within and between scenarios is presented in Figure 5-26, which shows the percentage change in SRP concentrations for each catchment relative to unperturbed conditions. There is significant change occurring both within and between scenarios across the entire Thames Basin, with shifts towards both more negative and more positive concentrations. Generally, SRP concentrations appear to increase across the majority of the Thames Basin, with notable exceptions being the Mole, Colne, and upper reaches of both the Kennet and Pang and Cotswolds, which all decrease. Specifically, catchments exhibiting the most extreme change in concentrations are scattered throughout the Thames Basin, with higher densities found throughout the Mole and in upper reaches of the Cotswolds, Kennet and Pang and Vale of the

White Horse. There is a trend from the 2040s to the 2080s towards greater changes in SRP concentrations over unperturbed conditions. For example, catchments demonstrating negative changes in the 2040s become more negative through the 2060s to the 2080s; with the reverse being true for positive change (positive becomes more positive). For each scenario, changes in concentration become more positive from the 10th to 90th percentile, with the 50th percentile representing median values of change for each catchment that are as equally likely to occur as not. These distributions become more extreme over time, with a far greater range and magnitude of percentage change in concentrations predicted to occur between the 10th and 90th percentiles in the 2080s than in the 2040s.

Figure 5-27 presents the percentage probability per class for each catchment within the whole Thames Basin under all three future scenarios. These maps directly correlate with those presented in Figure 5-25, with the exception that it is possible, through categorising raw concentrations into five classes, to show the full breadth of future distributions per catchment (using percentage per class). As such, it is notable that catchments may span several classes, dependent on the distribution of raw concentrations and class thresholds. Whilst Figure 5-27 displays significant alterations in SRP concentrations both within and between scenarios over unperturbed conditions, these are rarely reflected in as significant a classification change. Primarily, this is due to the concentration change being insufficient to trigger a threshold change, and when this does occur it is often a fraction of the extremes of the data distribution. Thus, most of the catchment class maps appear very similar to each other across scenarios, with a tendency towards higher percentage probability of class occurrence in extremes over time. The geographical distribution of WFD classes is worth noting. For catchments classified as having both 'High' and 'Good' ecological status, it is evident that the majority of these are headwater streams, except for the entire Mole sub-basin. Similarly, those classified as 'Moderate' are spread throughout the Thames Basin, predominantly in the upper reaches of all catchments, apart from the entire Colne sub-basin. Catchments classified as both 'Poor' and 'Bad' are spread throughout the central region of the Thames Basin and are typically associated with larger, downstream river reaches. The main stem of the Thames from Teddington to

its source are classified as ‘Poor’, along with most of the Cherwell, Wey, Thames and South Chilterns and Vale of the White Horse sub-basins. Additionally, there is a cluster of catchments classified as ‘Bad’ in the lower Loddon and upper Maidenhead and Sunbury sub-basins.

In contrast, Figure 5-28 suggests that alterations in climate appear to have relatively limited impact on the distribution and severity of WFD classes in relation to unperturbed conditions. Many catchments within the Thames Basin display no change in class from unperturbed conditions. However, a minority of catchments do exhibit a single class deviation from unperturbed conditions, with approximately equal numbers of catchments predicting an improvement in class as those predicting deterioration in class. Of these, only half demonstrate a significant shift towards an alternative class (50% probability or higher), with the remaining most likely predicting no change to the status quo. The geographical distribution of these catchments is noteworthy, with most catchments showing significant change categorised as headwater streams. Furthermore, catchments exhibiting an improvement in ecological status are generally found to the South and East of the Thames Basin, with higher densities found in the Maidenhead and Sunbury, Mole and Wey sub-basins. Conversely, catchments exhibiting a change towards deterioration in ecological status are typically located in the North and West of the Thames basin, with particularly high densities found in the Cherwell, Cotswolds and Loddon sub-basins. Finally, there is a trend towards a greater number of catchments exhibiting change over unperturbed conditions from the 2040s through to the 2080s. This is coupled with an increase in the percentage probability of class change over time, regardless of the direction of change.

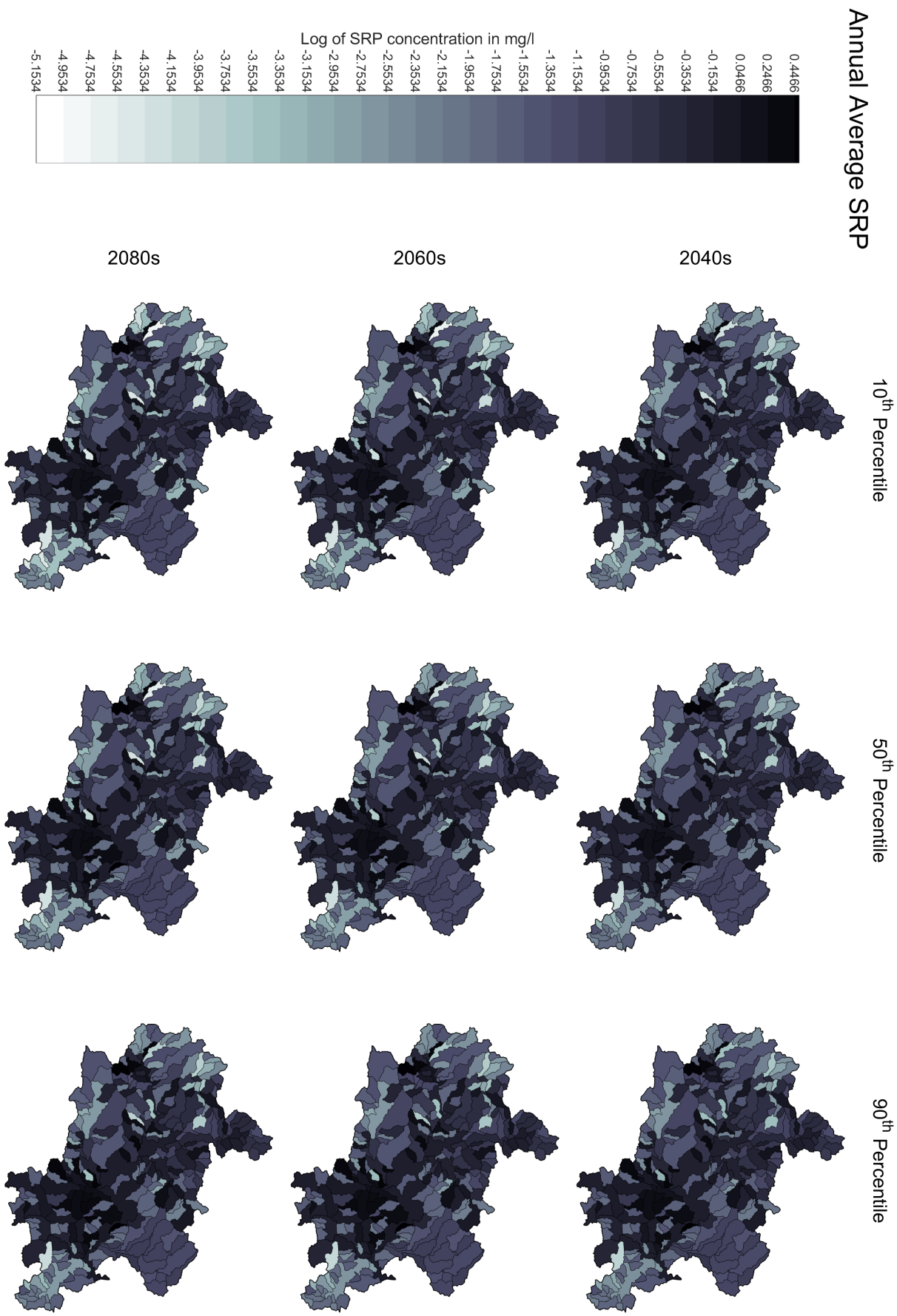


Figure 5-25: Thames Basin maps depicting the 10th, 50th and 90th percentile of log SRP concentrations for the UKCP09 projections for 2040s, 2060s and 2080s.

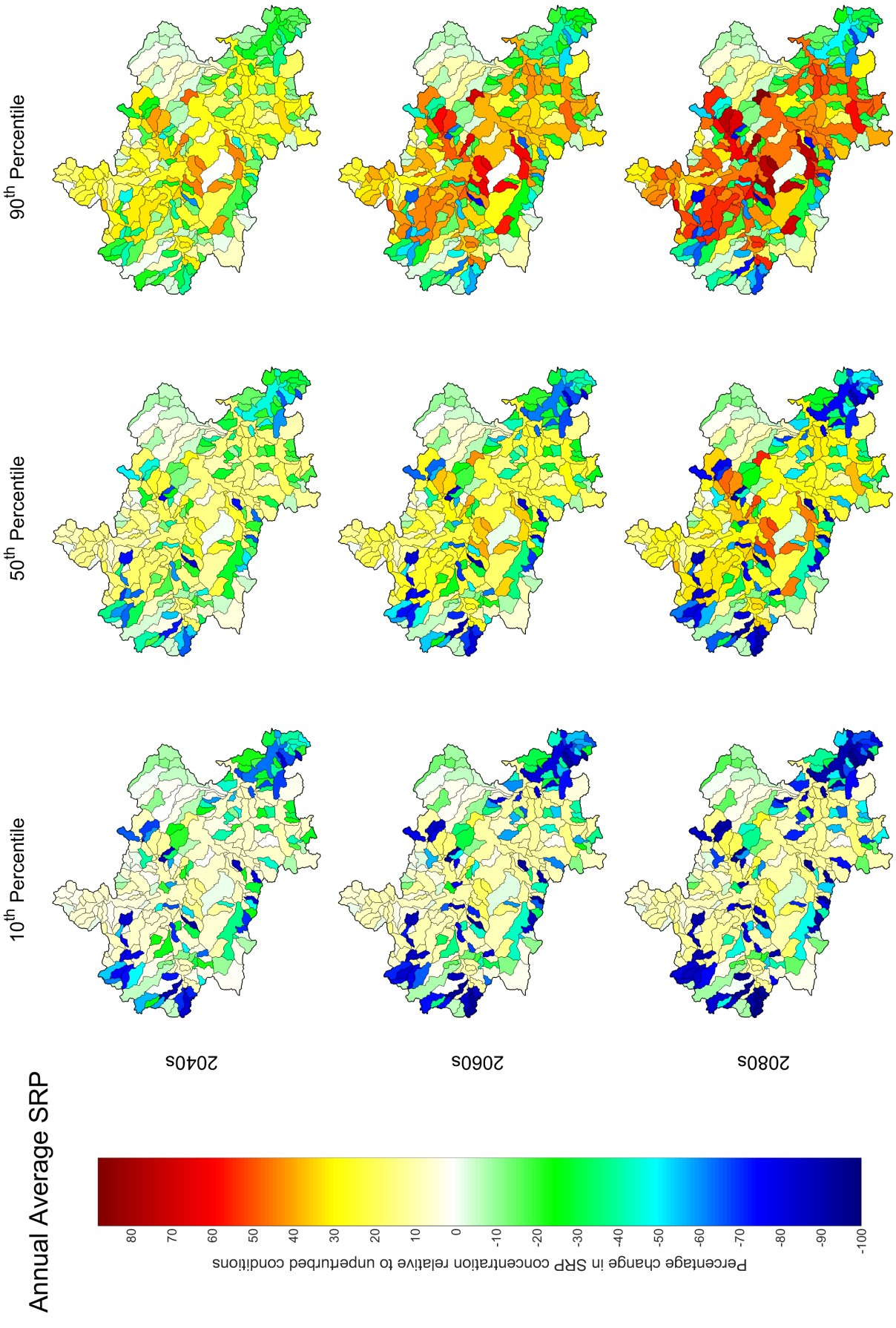


Figure 5-26: Thames Basin maps depicting the 10th, 50th and 90th percentile of percentage change in SRP concentrations for UKCP09 projections for 2040s, 2060s and 2080s over unperturbed conditions.

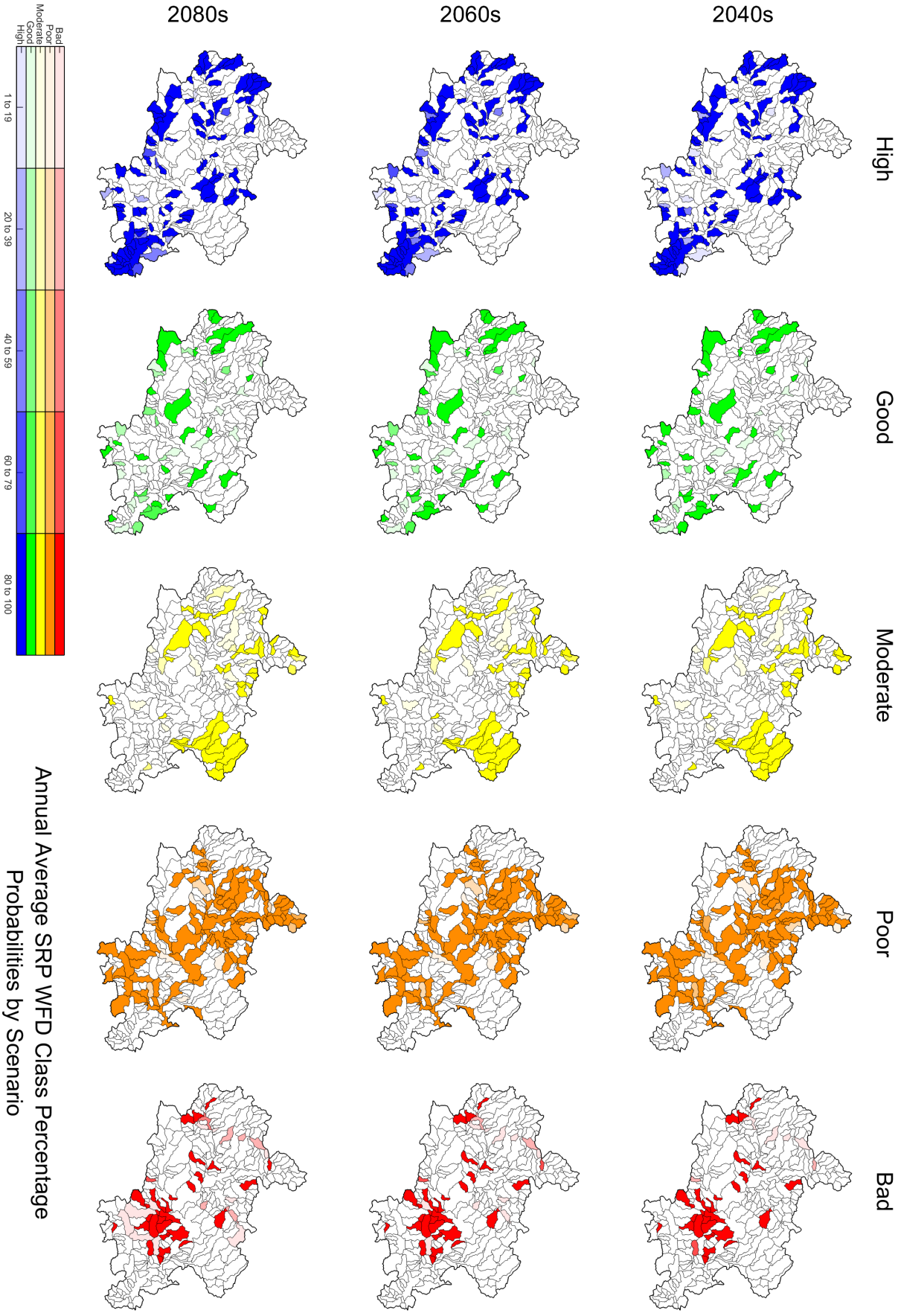


Figure 5-27: Thames Basin maps depicting the percentage likelihood of occurrence per WFD SRP class for the UKCP09 2040s, 2060s and 2080s projections.

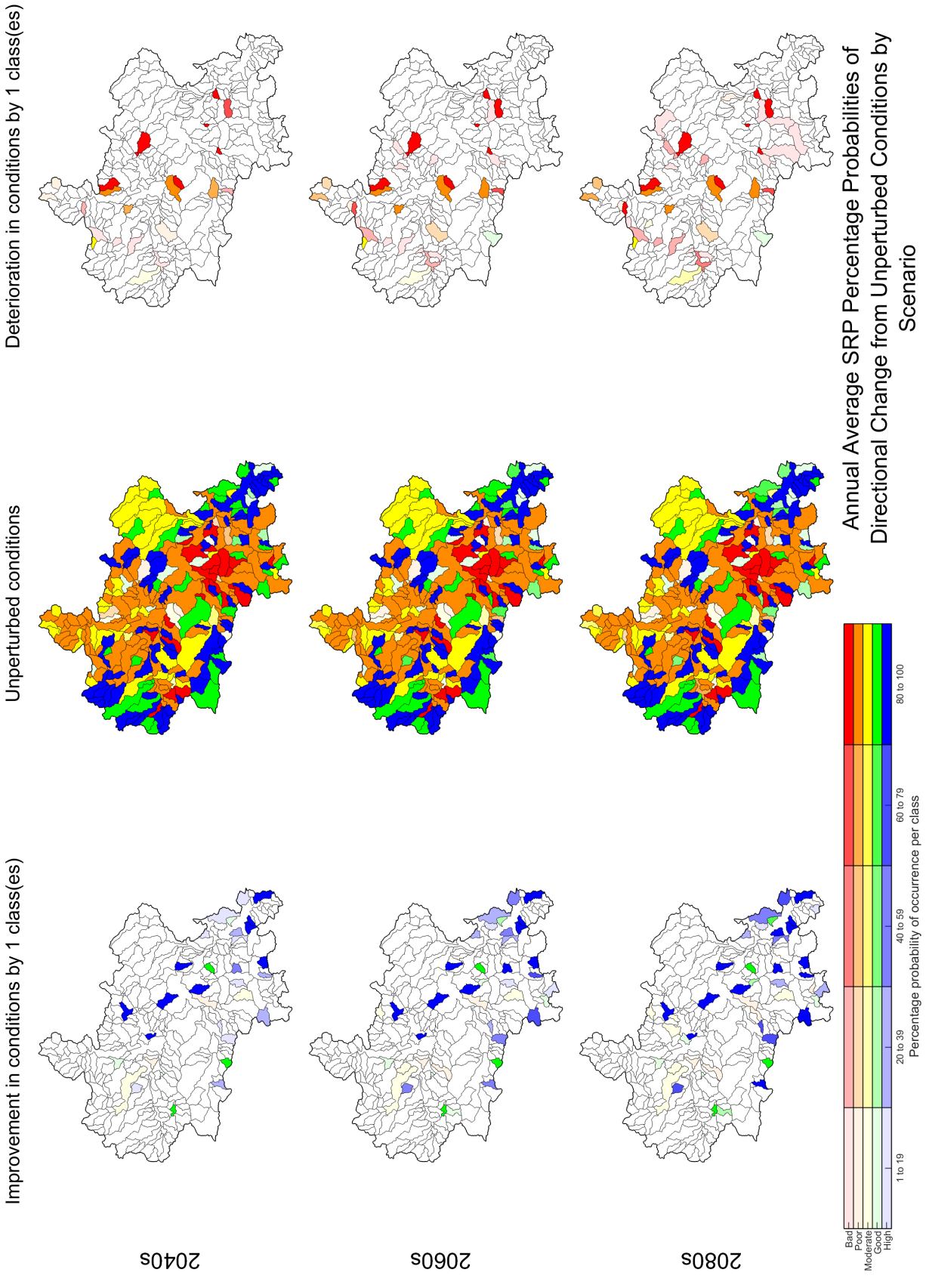


Figure 5-28: Thames Basin maps depicting the percentage likelihood of directional change in WFD SRP class for the UKCP09 2040s, 2060s and 2080s projections over unperturbed conditions.

5.4.3 AMMONIA

Figure 5-29 outlines the 10th, 50th and 90th percentiles of ammonia concentration throughout the Thames Basin for the 2040s, 2060s and 2080s. Ammonia concentrations have been log transformed to facilitate presentation of results using a single colour gradient. In similar fashion to SRP above, it is problematic to observe significant colour changes (and thus changes in ammonia concentration) within and between scenarios. There is, however, a basin-wide trend towards lighter shades (lower concentrations) from the 2040s to 2080s, suggesting a reduction in ammonia concentrations into the future across the Thames Basin. Furthermore, concentration values increase from the 10th to 90th percentile within scenarios, with the largest range occurring in the 2080s. This increase in the breadth of projected concentrations is indicative of the decrease in certainty associated with predicting further into the future.

A more informative and clearer representation of the changes occurring within and between scenarios is presented in Figure 5-30, which demonstrates the percentage change in ammonia concentrations for each catchment relative to unperturbed conditions. Evidently, significant change is projected to occur over unperturbed conditions both within and between scenarios across the entire Thames Basin. In the vast majority (281) of catchments, ammonia concentrations are predicted to decrease relative to unperturbed conditions across the entire distribution of all future scenarios. Notably, the Colne sub-basin consistently demonstrates the largest decrease in concentrations under all scenarios. Conversely, for a minority (11) of catchments, ammonia concentrations are projected to increase over unperturbed conditions by no more than 8% in any scenario. These catchments are typically associated with headwater streams located in the south of the Thames basin, except for the two most downstream catchments of the main stem of the Thames (Teddington and Staines). This is a particularly notable result, since these catchments respond in a manner contrary to the entire Thames basin that drains into them.

Specifically, the 2040s projects most of the Thames basin will experience a median decrease in ammonia concentrations of between -10% to -25% over unperturbed conditions. Furthermore, the

distribution of values in the 2040s appears relatively narrow, with little deviation occurring between the median values and outer limits of the distribution (10th and 90th percentiles). The 2060s demonstrates a trend towards more negative percentage change in ammonia concentrations over those of 2040s. Median values for the 2060s projects a decrease in ammonia concentrations of between -20% to -40% over unperturbed conditions for the majority of the Thames Basin. Furthermore, there is a more notable geographical clustering, with the largest decreases occurring in the northernmost (Colne, Cherwell and Cotswolds) and southernmost (Loddon, Mole and Wey). The distribution of data predicted in the 2060s is significantly broader than the 2040s, with more negative concentration change predicted across the Thames basin at the 10th percentile and less negative concentration change at the 90th percentile. The distribution is skewed towards more negative concentration changes, as the deviation from median values is far greater at the 10th percentile than the 90th. Finally, the 2080s demonstrates a further trend towards more negative percentage change in ammonia concentrations relative to unperturbed conditions, with median values of -25% to -55% projected for the majority of the Thames Basin. The geographical clustering first evident in the 2060s is predicted to be more pronounced in the 2080s, particularly in the upper reached of the Cotswolds, Cherwell and Colne. The 2080s project the broadest distribution of future values, with a similar skew towards more negative percentage concentration change at the 10th percentile. Due to this skew, the basin maps appear significantly more different between scenarios at the 10th percentile than either the median or 90th percentile.

Figure 5-31 presents the percentage probability per class for ammonia for each catchment within the whole Thames Basin under all three future scenarios. In a similar fashion to SRP, ammonia concentrations do vary with climatic alterations but rarely sufficiently to trigger a threshold change. When thresholds are exceeded, it is often extremes of the data distribution and so the degree of change is very small and therefore very unlikely to occur. As such, Figure 5-31 demonstrates that ammonia class maps appear very similar to each other across scenarios. However, there is a notable trend towards less severe ('High', 'Good') classes over time, reflecting the basin-wide decrease in ammonia concentrations predicted in Figure 5-29. The geographical distribution of ammonia classes

is worth noting and is consistent between scenarios. Due to the very low concentrations predicted across all scenarios, the vast majority of the Thames Basin is classified as 'High'. In addition to this, there are a notable number of catchments predicted as 'Good'. These catchments are in the most downstream sections of the main stem of the Thames and throughout the Loddon, Thame and South Chilterns and lower order streams of the Cherwell. Furthermore, a cluster (~10) of catchments classified as 'Moderate' is in the upper reaches of the Loddon. Finally, a very small number of catchments (4) are classified as either 'Poor' or 'Bad' and are in the higher order streams of the Maidenhead and Sunbury and Vale of the White Horse sub-basins.

The extent to which alterations in climate will impact upon ammonia classification throughout the Thames Basin, relative to unperturbed conditions, is presented in Figure 5-32. Most catchments throughout the Thames basin are predicted to experience no change in ammonia classification relative to unperturbed conditions under any future scenario. However, there are approximately 30 catchments whose classification is predicted to improve by one class under all future scenarios. These are distributed throughout the Thames Basin, with clusters occurring in the Loddon, Kennet and Pang, Thame and South Chilterns and the Wey sub-basins. The percentage probability of a change towards a more favourable class increases over time, with catchments in the 2080s demonstrating a 50% greater likelihood of occurring than those in the 2040s. This is similarly true for four catchments (located in the Loddon and Wey), that are predicted to improve by two classes over unperturbed conditions. These represent a significant improvement in ecological condition with reference to ammonia concentrations. Conversely, a single catchment (located in the upper reaches of the Mole sub-basin) is predicted to deteriorate by a single class from 'High' to 'Good'. In contrast to improvements in classification, the likelihood of this deterioration occurring is greatest in the 2040s and diminishes over time.

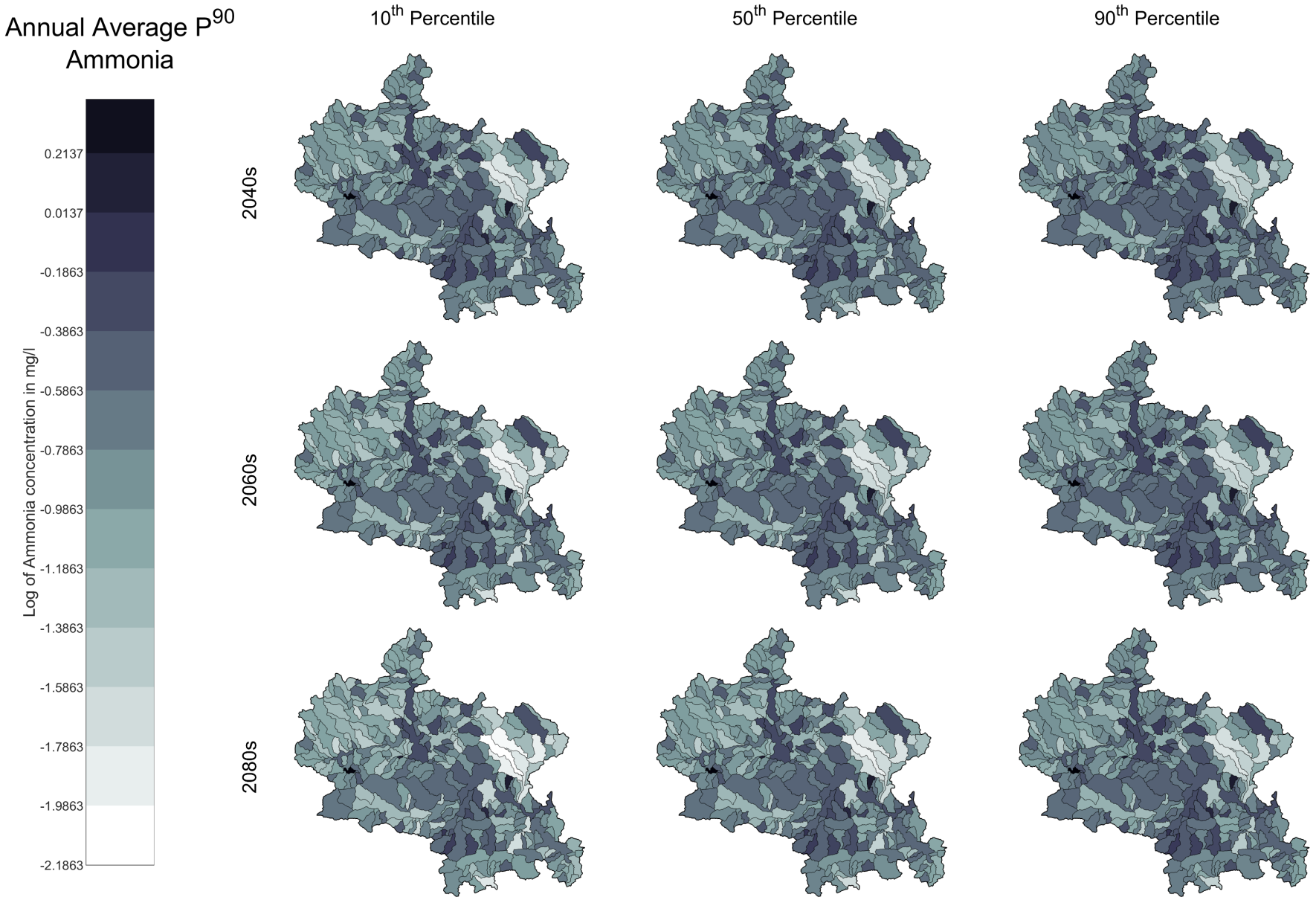


Figure 5-29: Thames Basin maps depicting the 10th, 50th and 90th percentile of log ammonia concentrations for the UKCP09 projections for 2040s, 2060s and 2080s.

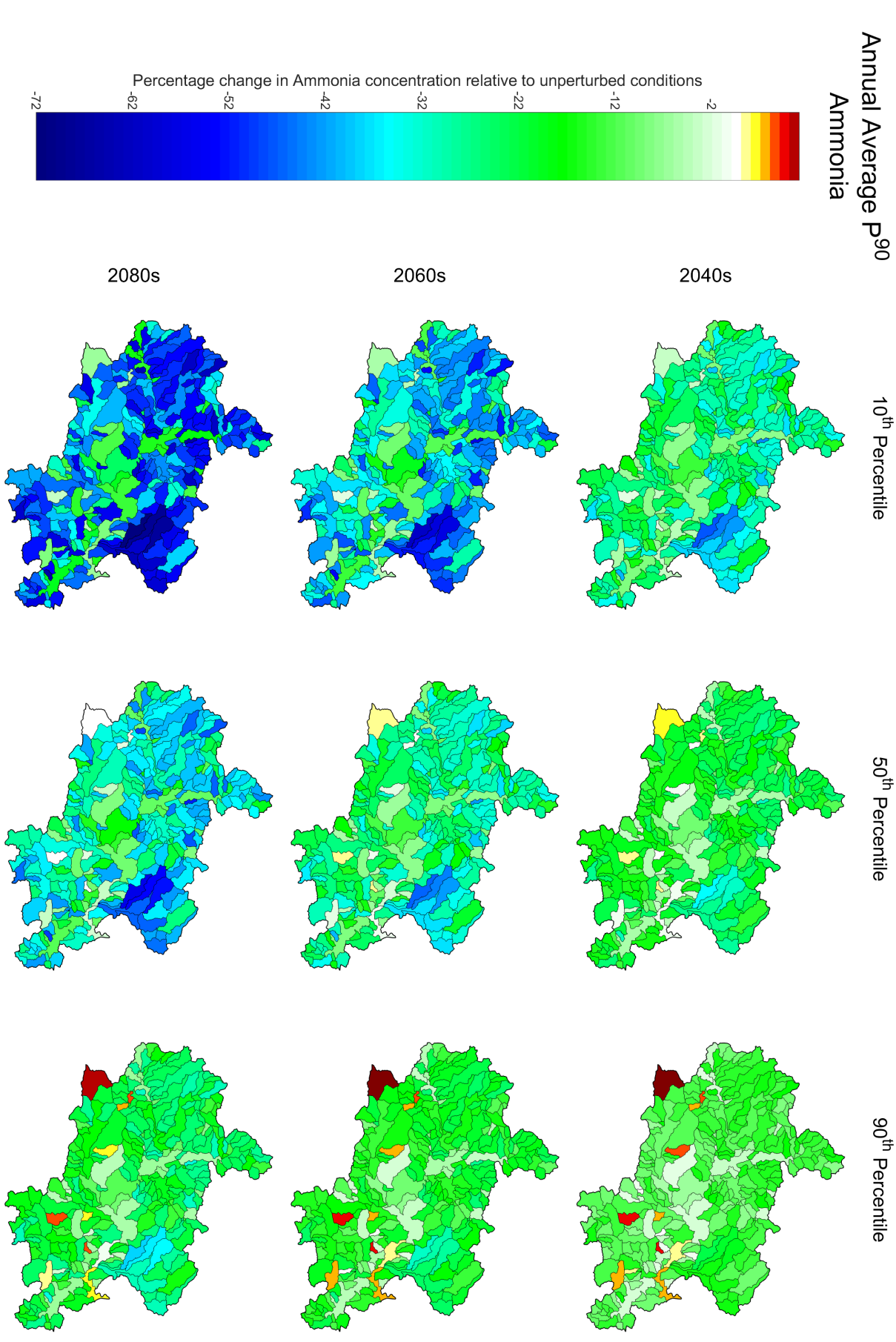


Figure 5-30: Thames Basin maps depicting the 10th, 50th and 90th percentile of percentage change in ammonia concentrations for UKCP09 projections for 2040s, 2060s and 2080s over unperturbed conditions.

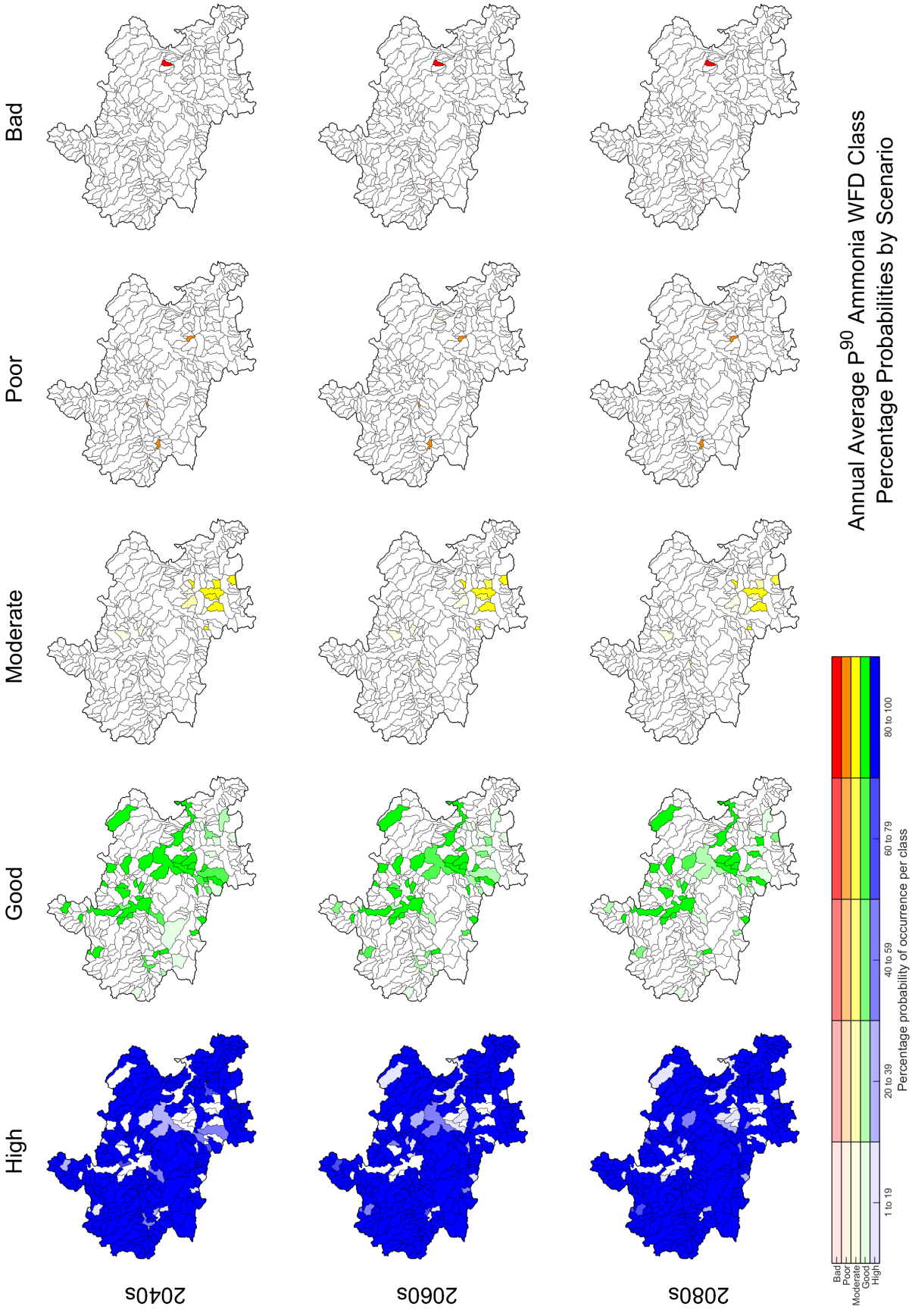


Figure 5-31: Thames Basin maps depicting the percentage likelihood of occurrence per WFD ammonia class for the UKCP09 2040s, 2060s and 2080s projections.

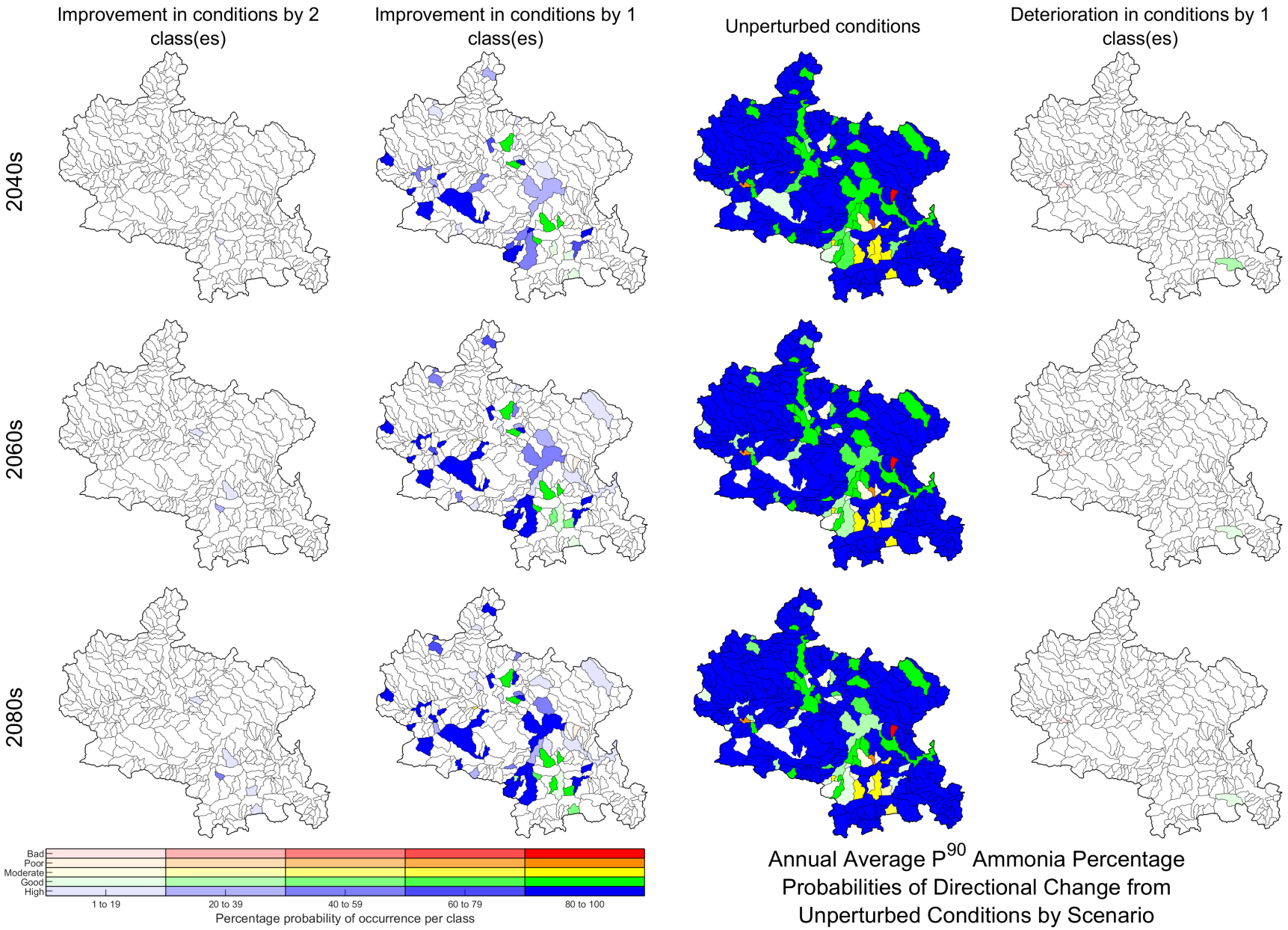


Figure 5-32: Thames Basin maps depicting the percentage likelihood of directional change in WFD ammonia class for the UKCP09 2040s, 2060s and 2080s projections over unperturbed conditions.

5.4.4 WATER TEMPERATURE

Figure 5-33 outlines the 10th, 50th and 90th percentiles of water temperature throughout the Thames Basin for the 2040s, 2060s and 2080s. Water temperature is strongly positively correlated with air temperature, with variations in temperature between catchments determined by elevation, latitude, land-use and in-stream processes. There is a clear, basin-wide trend in median maps towards darker shades (and therefore elevated temperatures) from the 2040s to 2080s, suggesting an increase in water temperature across the Thames Basin into the future. Typically, higher water temperatures are associated with lower-order (larger) rivers, normally associated with lower elevations. In contrast, higher-order (smaller) streams, particularly those at higher elevations, are associated with lower water temperatures. The distribution for the 2040s demonstrates a relatively narrow range of water temperatures (on average ~2.5°C) predicted for each catchment from the 10th to 90th percentiles. For the 2060s, this distributional range between upper and lower percentiles increases (on average ~3.5°C) over the 2040s. Finally, the 2080s demonstrates the broadest distribution of predicted water temperatures, with an average range of ~5°C between the 10th and 90th percentile. This increase in the breadth of projected water temperatures is indicative of the decrease in certainty associated with predicting further into the future.

Figure 5-34 presents the absolute change in water temperature for each catchment relative to unperturbed conditions. There is significant change projected to occur over unperturbed conditions both within and between scenarios across the entire Thames Basin. Water temperatures are only predicted to increase over unperturbed conditions, which correlate with increases in air temperature predicted over the Thames Basin. Specifically, the 2040s projects the Thames Basin will experience a homogeneous median increase in water temperature between 2.0°C to 2.5°C over unperturbed conditions. The distribution of values in the 2040s appears skewed towards higher increases in water temperature change. There is little reduction in water temperature occurring at the 10th percentile relative to the median, whereas there is a much greater increase relative to the median seen at the 90th percentile. Furthermore, at the upper extreme of the distribution for the 2040s (90th percentile), a clear geographical variation in temperatures becomes apparent. Due to the overlap in values

predicted across scenarios, the map of 90th percentile for the 2040s is almost identical to the median for the 2060s and the 10th percentile of the 2060s approximating that of the median for the 2040s; similarly, for the 2060s and 2080s. As highlighted about, the median map for the 2060s presents a clear geographical variation in temperature change throughout the Thames Basin than that of the 2040s. Temperature change is predicted to vary significantly across the Thames Basin, from ~2.0°C to ~4.5°C. Lower temperature change is typically predicted to occur in upper-order, high elevation catchments. Middling change is predicted to occur in the lower-order, low elevation catchments. Finally, the greatest temperature change is predicted to occur in higher-order streams that are at mid-to-low elevations. The distribution of values for the 2060s remains skewed towards greater temperature change, with a broader range of temperature change predicted to occur between the 10th and 90th percentiles than for the 2040s. Finally, the 2080s demonstrates a further trend towards greater temperature change relative to unperturbed conditions, with median values from ~3°C to ~6.5°C predicted throughout the Thames Basin. The geographical clustering first evident in the 2060s is similarly pronounced, with consistently elevated temperatures seen across all catchments in the Thames Basin. Finally, the distribution of the 2080s remains skewed towards greater temperature change and represents the broadest range of temperature change predicted across all scenarios (up to 8°C in some catchments at the 90th percentile).

Figure 5-35 presents the percentage probability per class for water temperature for each catchment within the whole Thames Basin under all three future scenarios. For many catchments within the Thames basin, the distribution of class percentage probability is split over several classes. In general, there is a shift in these catchment distributions towards higher probabilities of more severe water temperature class occurrence. For the 2040s, the majority of the Thames Basin is classified as ‘High’, with the highest percentage probability of class occurrence located in the Cotswolds and northern Kennet and Pang, and Mole sub-basins. Large numbers of catchments in the Colne, Cherwell, Vale of the White Horse and Wey sub-basins are distributed between both ‘High’ and ‘Good’ classes, with a skew towards a greater probability of ‘Good’ occurring in higher-order catchments. Furthermore, many catchments throughout the Thames Basin are also categorised as ‘Moderate’, with most of

these occurring in the upper reaches of the Cherwell, Vale of the White Horse, Thame and South Chilterns, southern Kennet and Pang, Mole and majority of Maidenhead and Sunbury sub-basins. Finally, a relatively small number of catchments are categorised as 'Poor', with even fewer classified as 'Bad'. These are distributed throughout the Thames Basin and in general have a low percentage probability of occurring in the 2040s. The basin maps for both the 2060s and 2080s demonstrate an increase in the probability of more severe classes (i.e. a deterioration) occurring in relation to the 2040s. By the 2060s, the majority of the Thames Basin has shifted towards a 'Good' classification, with an associated decrease in the percentage of occurrence of 'High' classification and increase of percentage occurrence in 'Moderate', 'Poor' and 'Bad' classes. This trend continues into the 2080s, with a marked increase in the number of catchments registering the most severe classifications of 'Poor' and 'Bad'. In certain catchments, predominantly associated higher-order streams, the most likely classification is 'Bad', demonstrating a significant deterioration from the 2040s.

While it is important to understand the likelihood of classes predicted under future scenarios, it is of ecological relevance to see how classification is likely to change relative to unperturbed conditions. Figure 5-36 demonstrates the degree of impact that alterations in climate will have on water temperature classification throughout the Thames Basin relative to unperturbed conditions. It is evident from the series of maps that there is a shift towards greater deterioration in classes relating to water temperature from the 2040s to 2080s. In the 2040s, most of the Thames basin is most likely not to deviate from unperturbed conditions. However, a significant number of higher-order catchments throughout the Thames (except for the Kennet and Pang sub-basin) will most likely deteriorate by a single class. Furthermore, a very small number of catchments are highly unlikely to deteriorate by two classes over unperturbed conditions. Following the trend outlined in the previous paragraph and noted in Figure 5-36, the percentage likelihood of class deterioration increases over time from the 2040s to 2080s. The spatial patterns of catchment classification observed in the 2040s shift towards most catchments in the Thames Basin deteriorating by a single class in the 2060s and 2080s (except for the Kennet and Pang sub-basin). In the 2080s, substantial proportions of upper-reach catchments within the Thames Basin are increasingly likely to deteriorate by two classes,

suggesting a significant shift in ecological conditions relating to water temperature in headwater streams. In extreme cases, there is a small likelihood for some of these catchments to deteriorate by three or even four classes.

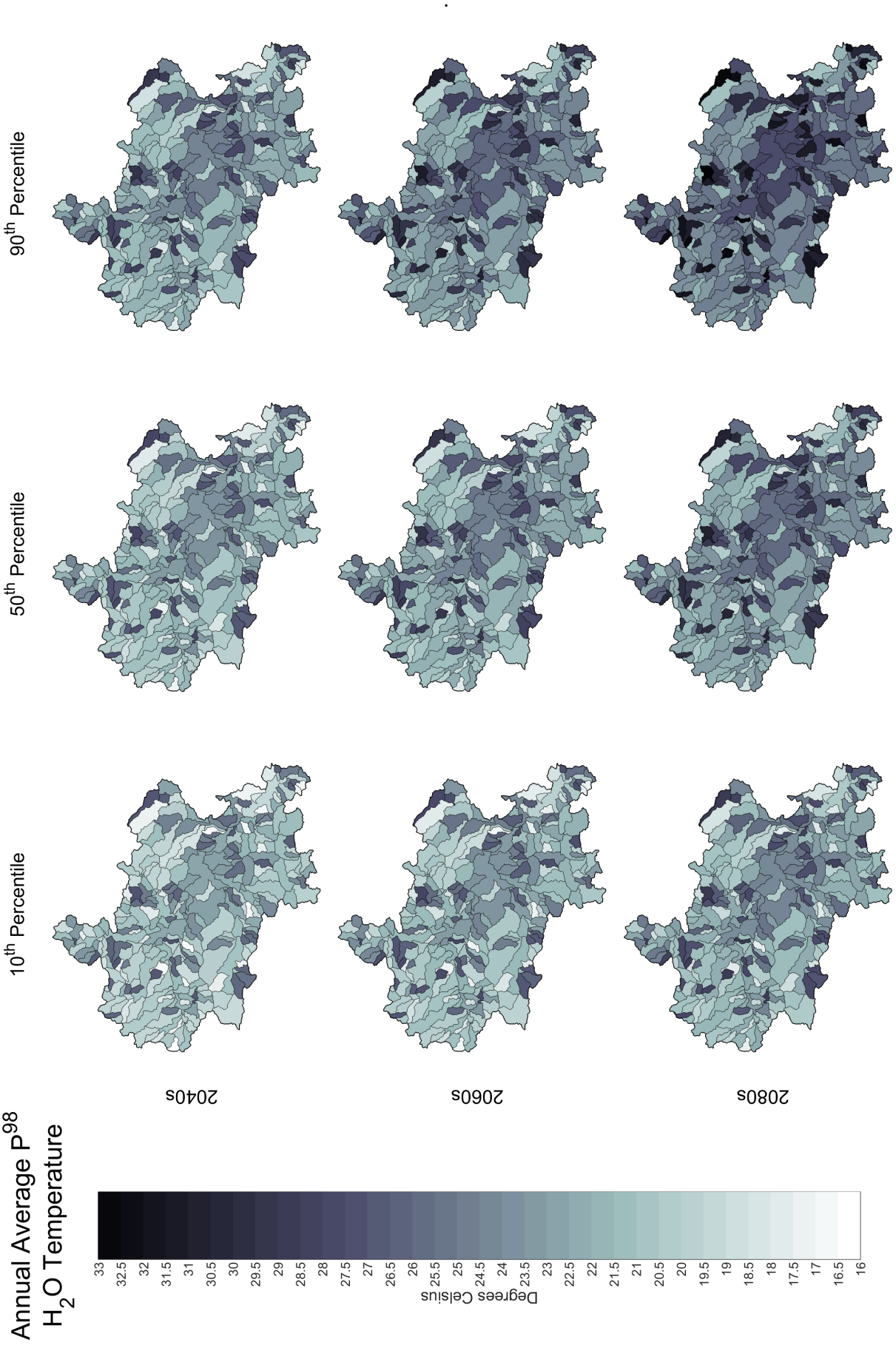


Figure 5-33: Thames Basin maps depicting the 10th, 50th and 90th percentile of water temperature (°C) for the UKCP09 projections for 2040s, 2060s and 2080s.

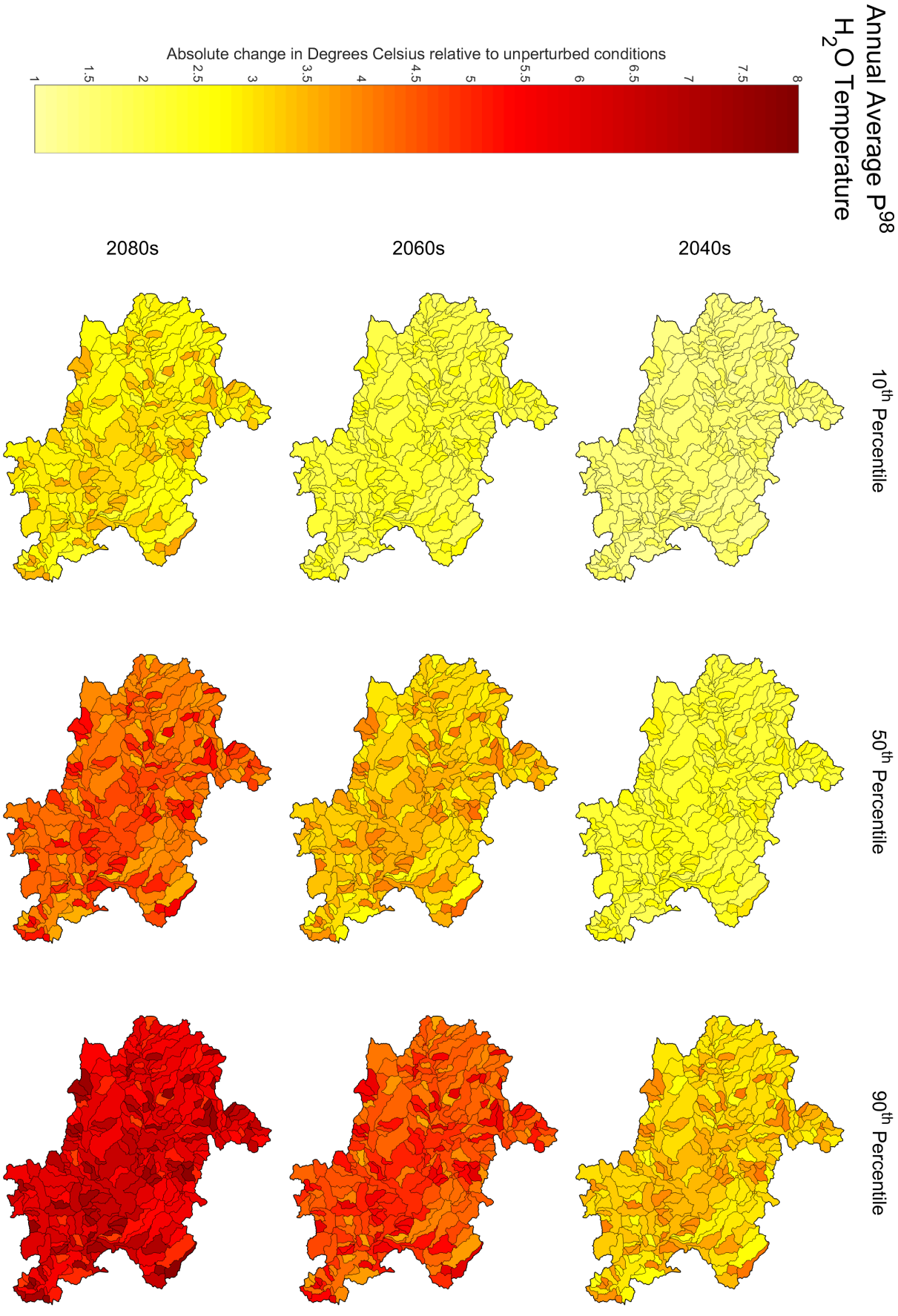


Figure 5-34: Thames Basin maps depicting the 10th, 50th and 90th percentile of absolute change in water temperature (°C) for the UKCP09 projections for 2040s, 2060s and 2080s over unperturbed conditions.

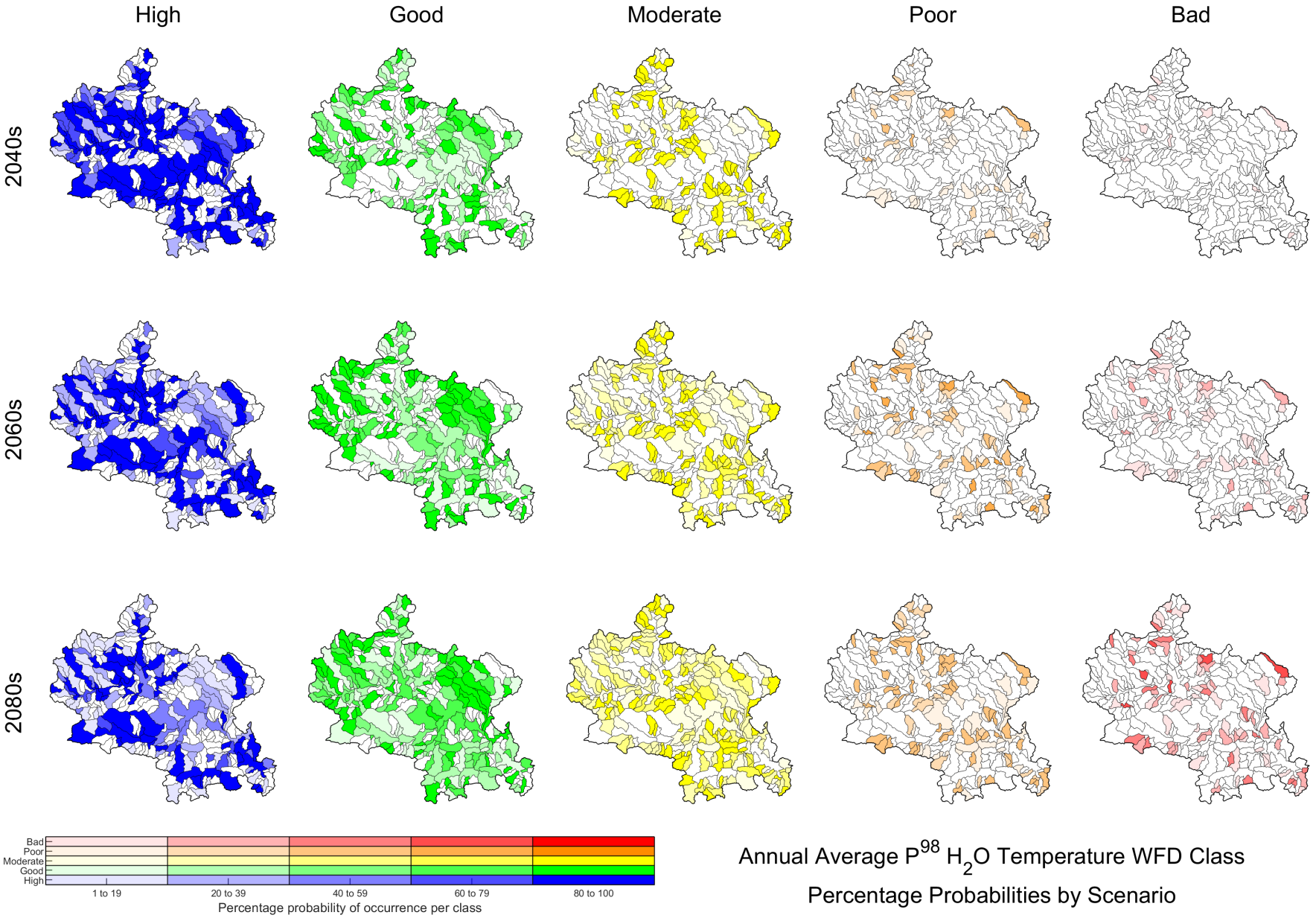


Figure 5-35: Thames Basin maps depicting the percentage likelihood of occurrence per WFD water temperature class for the UKCP09 2040s, 2060s and 2080s projections.

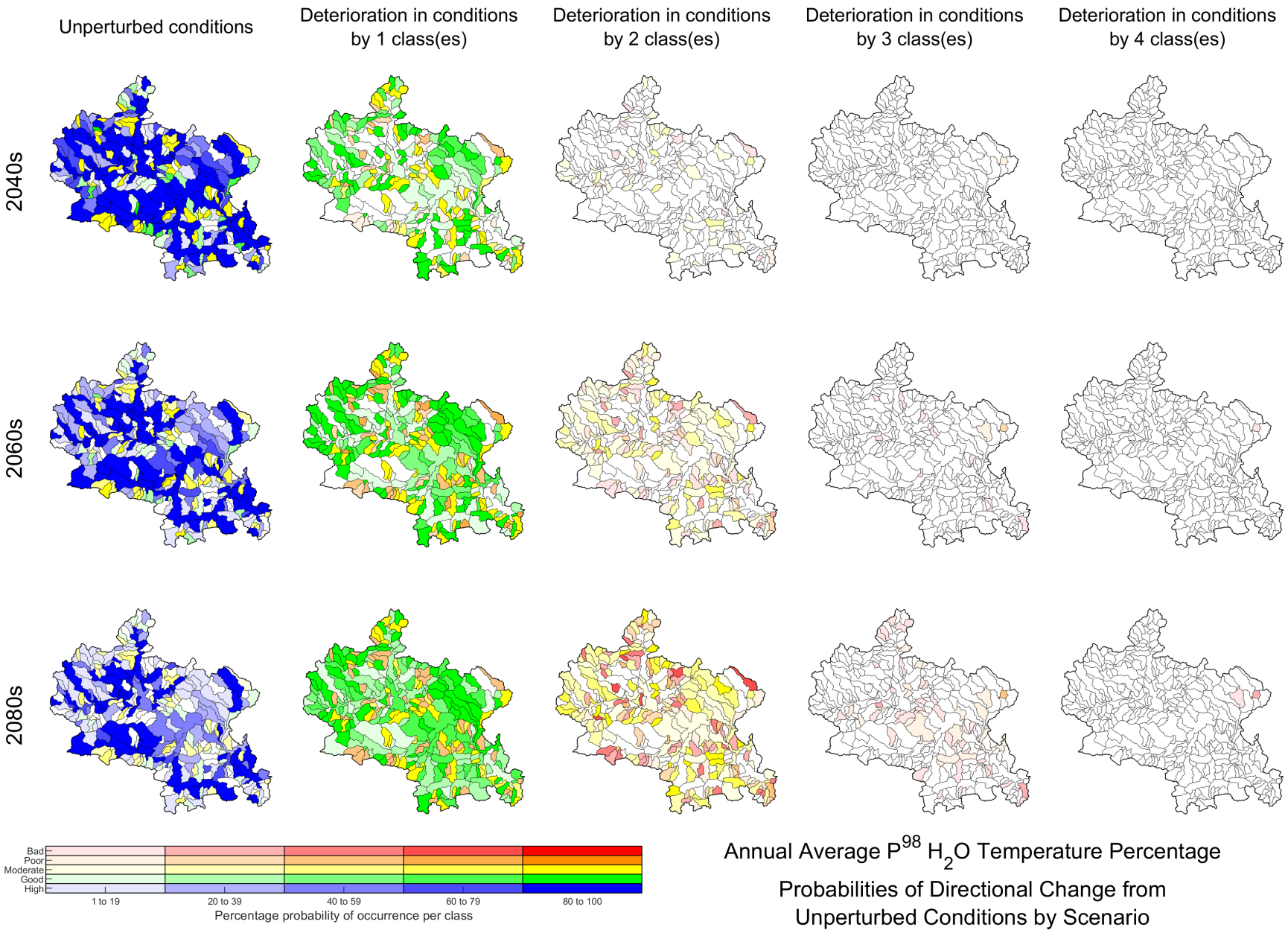


Figure 5-36: Thames Basin maps depicting the percentage likelihood of directional change in WFD water temperature class for the UKCP09 2040s, 2060s and 2080s projections over unperturbed conditions.

5.4.5 DHRAM

Figure 5-37 outlines the 10th, 50th and 90th percentiles of DHRAM scores throughout the Thames Basin for the 2040s, 2060s and 2080s. DHRAM is a methodology for determining alterations in key eco-hydrological indicators over naturalised conditions and linking this to a disturbance or hydrological quality score. Changes in annual average precipitation and temperature are likely to have a significant impact on the hydrological regime, and this should be reflected in DHRAM scores. There is a clear, basin-wide trend in median maps towards darker shades (and therefore higher DHRAM scores) from the 2040s to 2080s, suggesting an increase in DHRAM scores across the Thames Basin into the future. The geographical distribution of DHRAM scores is relatively homogeneous throughout the Thames Basin, apart from notably increased scores occurring in the upper-reaches of the Cherwell, Colne, Cotswolds, and Loddon sub-basins and throughout the Kennet and Pang, with decreased scores occurring throughout the Mole and Wey sub-basins. The distribution for the 2040s demonstrates a relatively narrow range of DHRAM scores (on average 0 to 5) predicted for each catchment from the 10th to 90th percentiles. For the 2060s, this distributional range between upper and lower percentiles increases (on average 0 to 8) with respect to the 2040s. Finally, the 2080s demonstrates the broadest distribution of predicted DHRAM scores, with an average range of 0 to 12 between the 10th and 90th percentiles. This increase in the breadth of projected DHRAM scores is indicative of the decrease in certainty associated with predicting further into the future.

Figure 5-38 presents the absolute change in DHRAM scores for each catchment relative to unperturbed conditions. There is significant change projected to occur over unperturbed conditions both within and between scenarios across the entire Thames Basin. DHRAM scores are predicted to primarily increase relative to unperturbed conditions, with increased scores associated with further deviation from naturalised conditions. However, a small number of catchments are predicted to decrease in score relative to unperturbed conditions, suggesting a return to more naturalised conditions. The 2040s project a relatively homogeneous increase in median DHRAM scores (1-2) across the majority of the Thames Basin. However, catchments in the upper-reaches of the Cotswolds and Wey sub-basins are predicted to increase in score by 5 to 7 over unperturbed

conditions. A further group of 10 catchments distributed throughout the lower-reaches of the Vale of the White Horse, Thame and South Chilterns, Colne, Kennet and Pang and Wey sub-basins are predicted to decrease in score by 1 or 2 over unperturbed conditions. Finally, a large portion of both the Wey and Mole sub-basins register no change in DHRAM score relative to unperturbed conditions. The distribution of scores in the 2040s appears relatively narrow, with scores typically varying by 2 between median values and outer limits of the distribution (10^{th} and 90^{th} percentiles). The median map for the 2060s suggests that DHRAM scores typically follow the same geographical pattern as those in the 2040s, with only slight increases in score (1 to 2) seen across the entire catchment. Notably, catchments that were demonstrating a reduction in DHRAM scores in the 2040s demonstrate no change over unperturbed conditions in the 2060s. The distribution of scores in the 2060s does appear skewed towards greater changes in scores over unperturbed conditions. Little reduction in scores is predicted to occur at the 10^{th} percentile relative to the median, yet a much greater increase in score relative to the median seen at the 90^{th} percentile. Finally, the 2080s demonstrates a further trend towards greater DHRAM score change relative to unperturbed conditions, with median scores typically 1-2 higher than those predicted in the 2060s. The geographical clustering first evident in the 2040s is similarly pronounced, except for a reduction in the number of catchments predicting a decrease in DHRAM scores relative to unperturbed conditions. Notably, in contrast to the 2040s and 2060s, the Wey and Mole sub-basins are predicted to increase in DHRAM score over unperturbed conditions. Finally, the distribution of the 2080s remains skewed towards greater DHRAM score change and represents the broadest range of score change predicted across all scenarios (up to 10 in some catchments at the 90^{th} percentile).

Figure 5-39 presents the percentage probability per class for DHRAM scores for each catchment within the whole Thames Basin under all three future scenarios. For most catchments within the Thames basin, the distribution of DHRAM class percentage probability is split between the ‘High’, ‘Good’ and ‘Moderate’ classes. Whilst the percentage of each class varies across scenarios, the majority of the Thames Basin is categorised as ‘Good’ for all scenarios. The percentage of catchments classified as ‘High’ decreases from the 2040s to the 2080s, with an associated increase in the

percentage probability of both 'Good' and 'Moderate' classes. The geographical distributions of these classes directly correlate with the DHRAM scores in Figure 5-37. For all scenarios, catchments within the Wey and Mole sub-basins typically display a higher probability towards 'High' classification than the remainder of the Thames Basin. Conversely, catchments in the upper reaches of the Cotswolds, Colne, Kennet and Pang, and Loddon all typically exhibit a higher probability than the remainder of the Thames Basin towards categorisation as 'Moderate'. For all scenarios, there are a very small number of scenarios that are most likely to classify as 'Poor'.

Figure 5-40 demonstrates the degree of impact that alterations in climate will have on DHRAM class distribution throughout the Thames Basin relative to unperturbed conditions. There is a general trend towards an increased probability of catchment class deterioration from the 2040s to the 2080s. It is evident that deviation in class from unperturbed conditions closely follows the geographical distribution highlighted in the previous paragraph. For the 2040s, there is a relatively high probability that a small number of catchments in the Colne, Cotswolds, Vale of the White Horse and Thame and South Chiltern sub-basins improve in DHRAM classification over unperturbed values. Most of the catchments within the Wey, Mole, Vale of the White Horse and southern Thame and South Chiltern sub-basins have a high probability of remaining the same class as unperturbed conditions. Thus, throughout the remaining catchments within the Thames Basin, deterioration by a single class is most likely. In both the 2060s and 2080s, there is a shift towards higher scores and, therefore, higher classes. This is reflected in the increased likelihood of deterioration in class occurring for any given catchment within the Thames Basin. By the 2080s, catchments in the upper reaches of the Cotswolds, Cherwell, and Kennet and Pang all suggest a significant likelihood towards deterioration in conditions by two classes, and in some cases three. This represents a major alteration to eco-hydrological indicators over naturalised conditions and a significant deviation from current, unperturbed conditions, which will likely result in substantial ecological and chemical degradation.

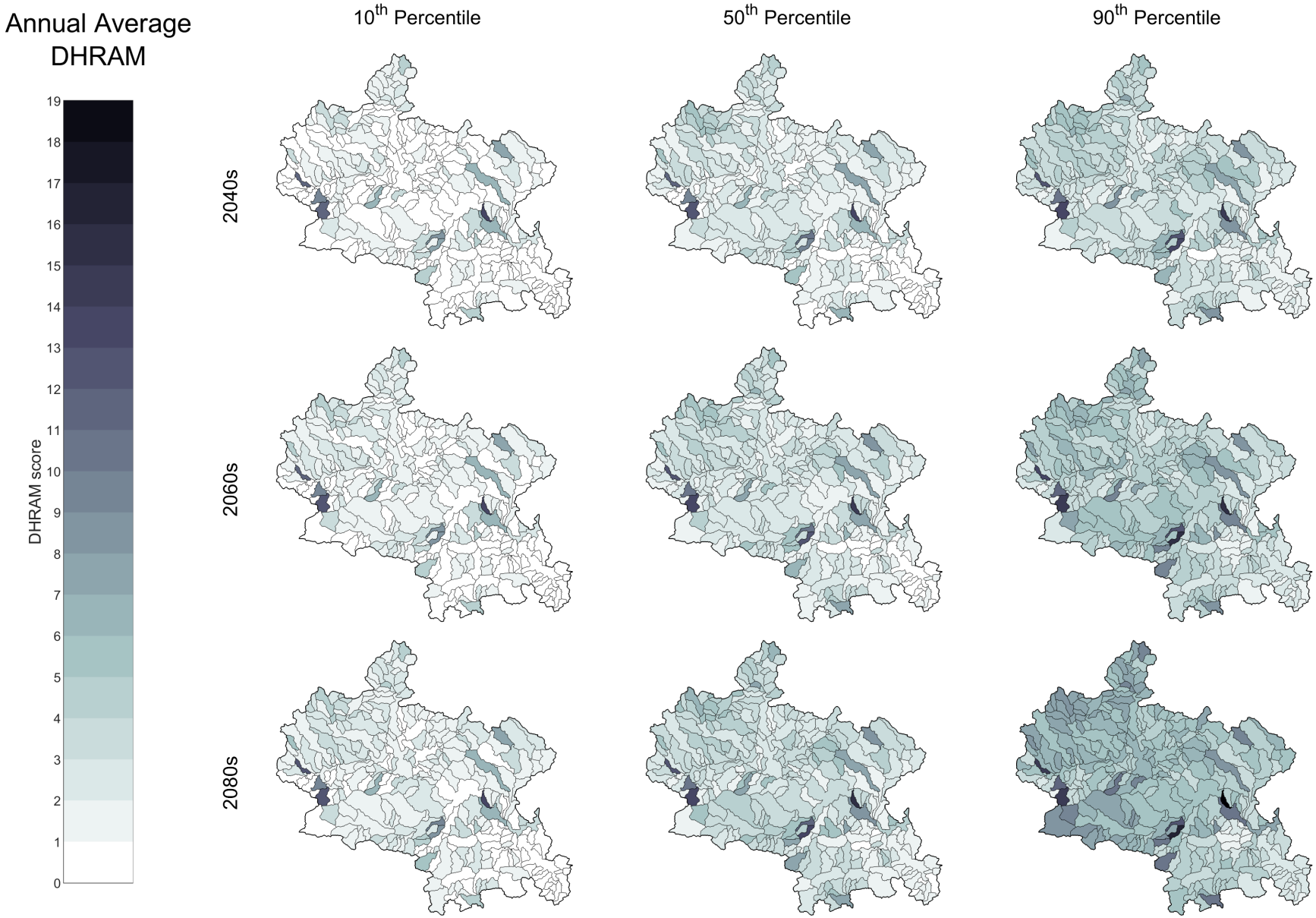


Figure 5-37: Thames Basin maps depicting the 10th, 50th and 90th percentile of DHRAM scores (maximum 30) for the UKCP09 projections for 2040s, 2060s and 2080s.

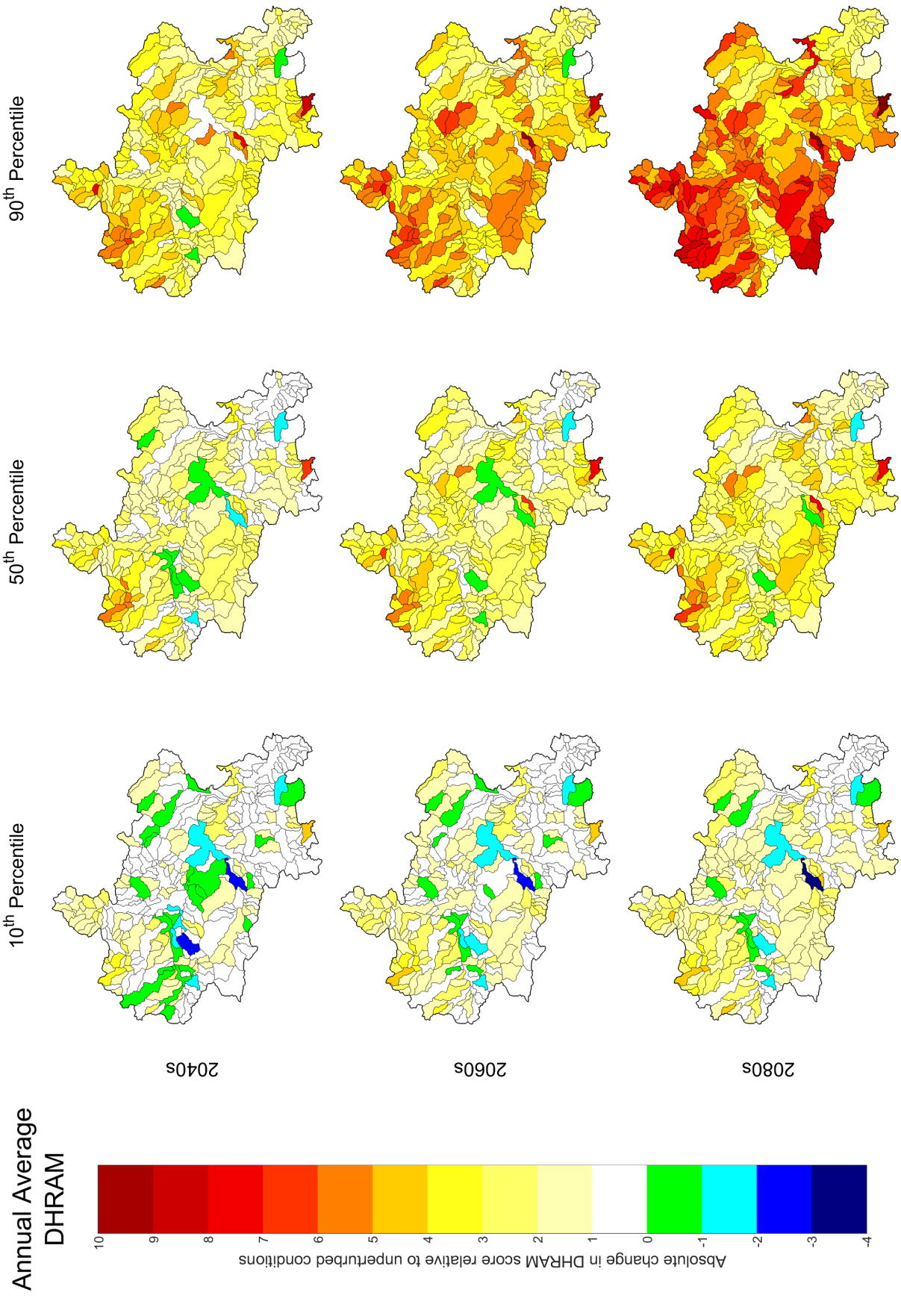


Figure 5-38: Thames Basin maps depicting the 10th, 50th and 90th percentile of absolute change in DHRAM scores for the UKCP09 projections for 2040s, 2060s and 2080s over unperturbed conditions.

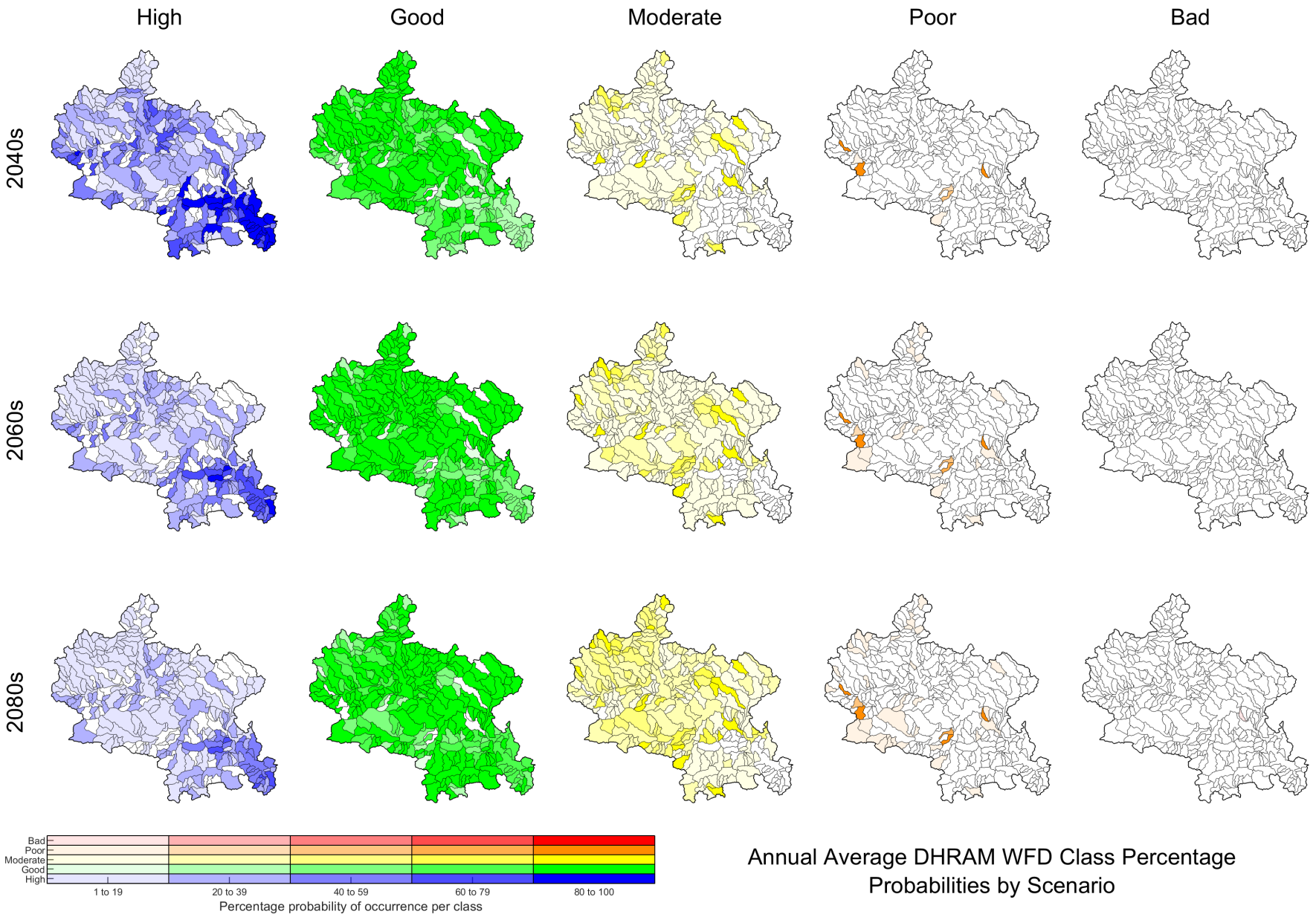


Figure 5-39: Thames Basin maps depicting the percentage likelihood of occurrence per WFD DHRAM class for the UKCP09 2040s, 2060s and 2080s projections.

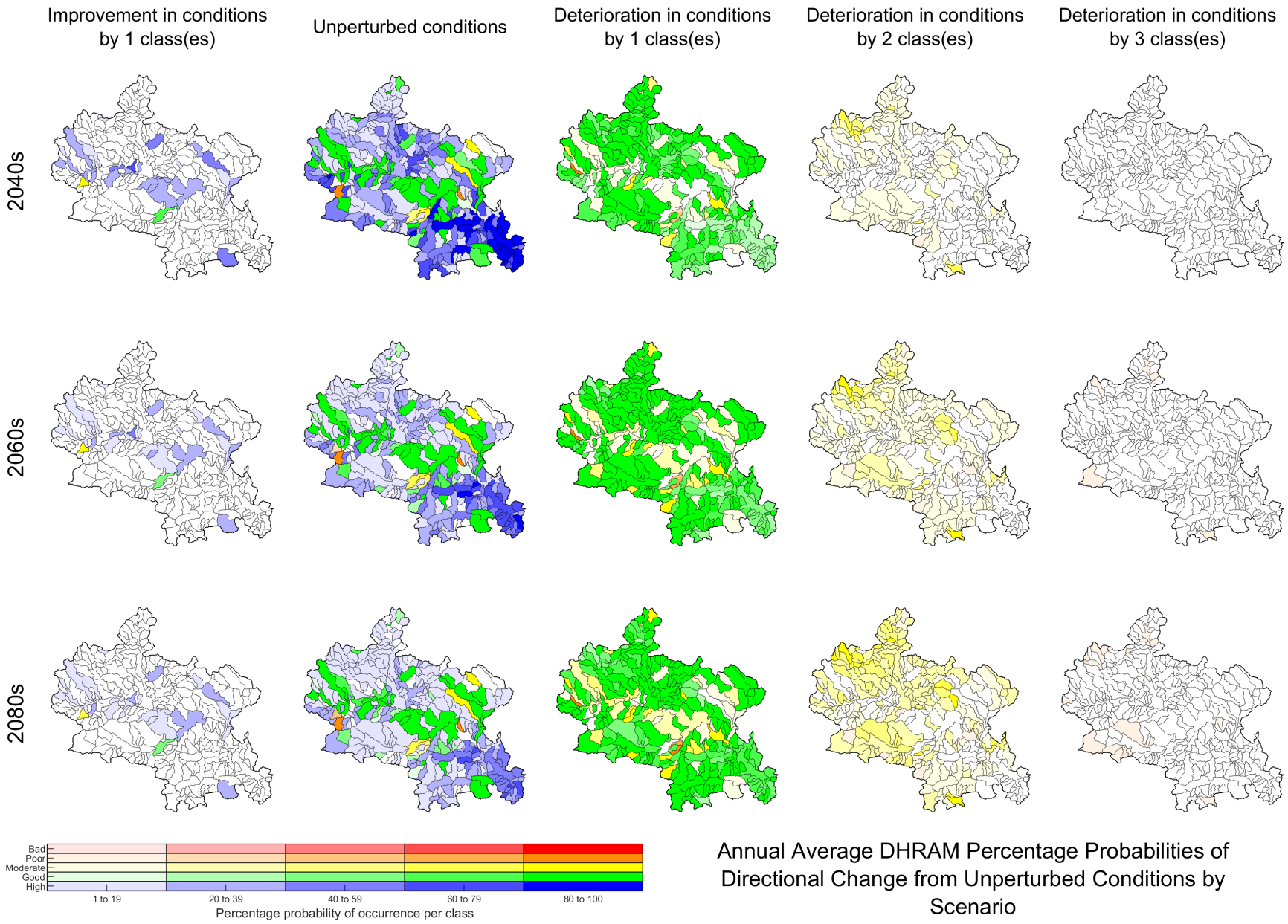


Figure 5-40: Thames Basin maps depicting the percentage likelihood of directional change in WFD DHRAM class for the UKCP09 2040s, 2060s and 2080s projections over unperturbed conditions.

5.5 QUANTIFYING CLIMATE RISK: THAMES BASIN SUMMARY MAPS

The potential risks of future impacts that are attributable to climate change were evaluated through the combination of each of the four variables assessed in this research using the methodologies outlined in section 4.7. Figure 5-41 combines the predicted class percentages for each of the four indicators (SRP, ammonia, water temperature and DHRAM) across scenarios to generate summary maps of potential impact due to climate change based on the order of magnitude risk associated with individual indicators. These summary maps provide a detailed and comprehensive overview of the whole Thames Basin, catchment by catchment. As discussed in section 4.7, base (4^2=16) was considered to be an appropriate order of magnitude for considering the combined impact of four variables, since this approach provides a balanced view of risk based on the predicted future classes of all contributing indicators. There is, as might be anticipated, a general trend toward an increase in risk throughout the whole Thames Basin from the 2040s to the 2080s. The Loddon exhibits the sub-basin with the greatest risk, with most catchments categorised as either 'High' or 'Very High'. The Cherwell, Vale of the White Horse, Thame and South Chilterns, Maidenhead and Sunbury, and Wey sub-basins all demonstrate 'High' levels of risk, with catchments also categorised as 'Moderate' or 'Very High'. The Colne sub-basin typically exhibits 'Moderate' risk and the Kennet and Pang and Cotswolds sub-basins both exhibit 'Low' levels of risk to the East, rising to 'Moderate' in the East. Finally, the Mole sub-basin exhibits the lowest risk, with catchments categorised as either 'None' to 'Low' levels of risk.

Figure 5-42 utilises the base (4^{12}) methodology, outlined in section 4.7, to provide a more conservative approach to assessing risk, like that currently employed by the Environment Agency. The assessment of risk is predominantly based on the single indicator projected to have the worst WFD classification i.e. 'Poor'. Therefore, the risk of impact seen in Figure 5-42 will always be more severe than in Figure 5-41, which takes a more balanced approach. Again, there is a general trend towards greater estimates of risk from the 2040s to 2080s. Similarly, the spatial patterns in distribution of the risk observed throughout the Thames Basin are very similar to Figure 5-41, since

both use the same four input indicators. However, the severity of risk is increased throughout the Thames, with all sub-basins exhibiting at least a 'low' risk to changes in hydro-ecological indicators under all UKCP09 scenarios. By the 2080s, the whole Thames Basin, except for the Mole, is projected to have at least a 'Moderate' risk of impact.

The spatial distribution of risk is explored further in the Chapter 6 and a critical assessment of the methodology provided. Furthermore, the risk that climate change impact outlined in Figure 5-41 and Figure 5-42 may have on protected areas within the Thames is discussed and recommendations are made for inclusion into future management plans for the Thames Basin.

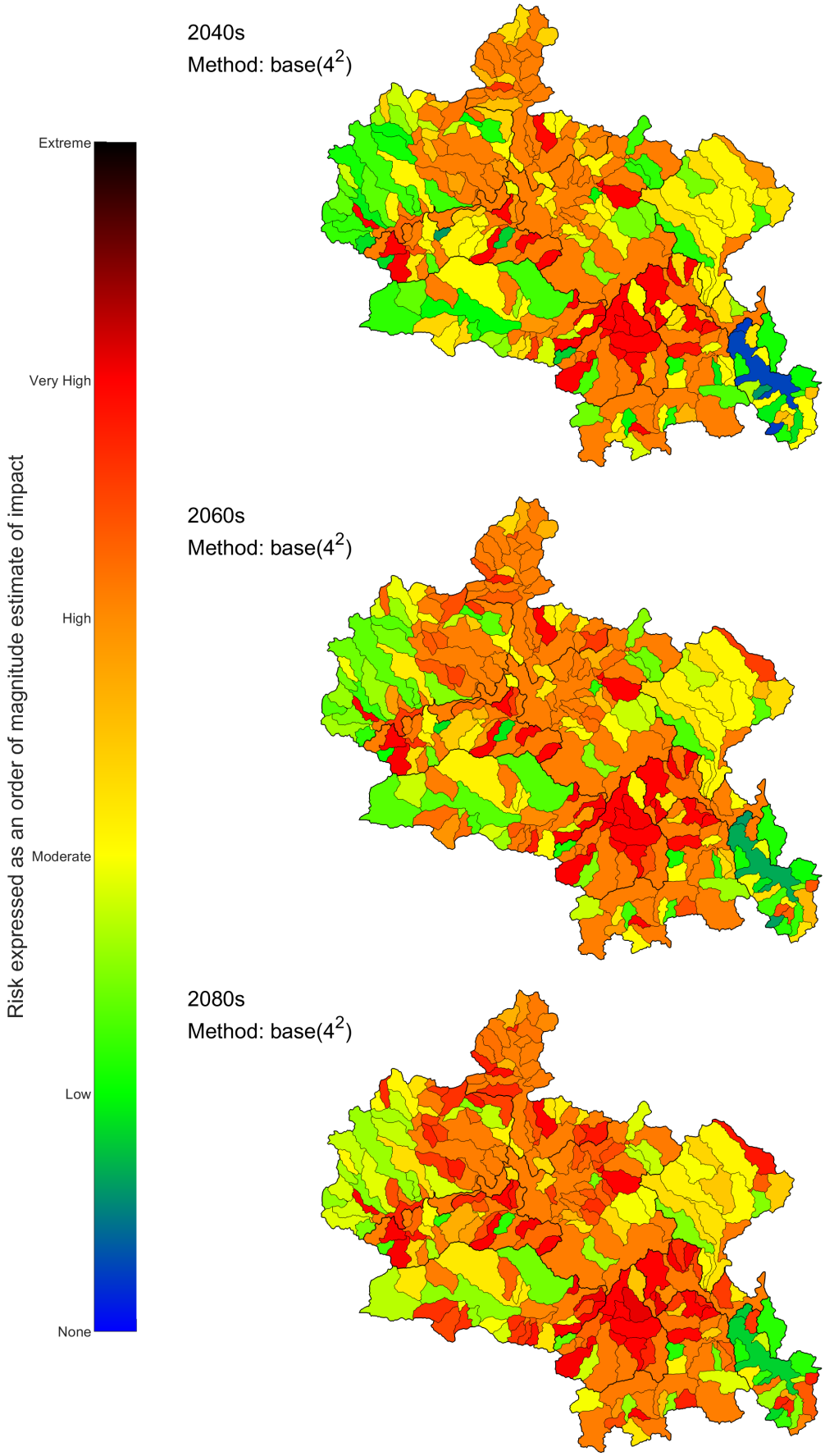


Figure 5-41: Thames Basin maps of risk of ecological impact under UKCP09 projections for the 2040s, 2060s and 2080s. The predicted class percentages for each of the four indicators (SRP, ammonia, water temperature and DHRAM) were combined using the base (4^2) method outlined in section 4.7. This method provides a balance across all indicators.

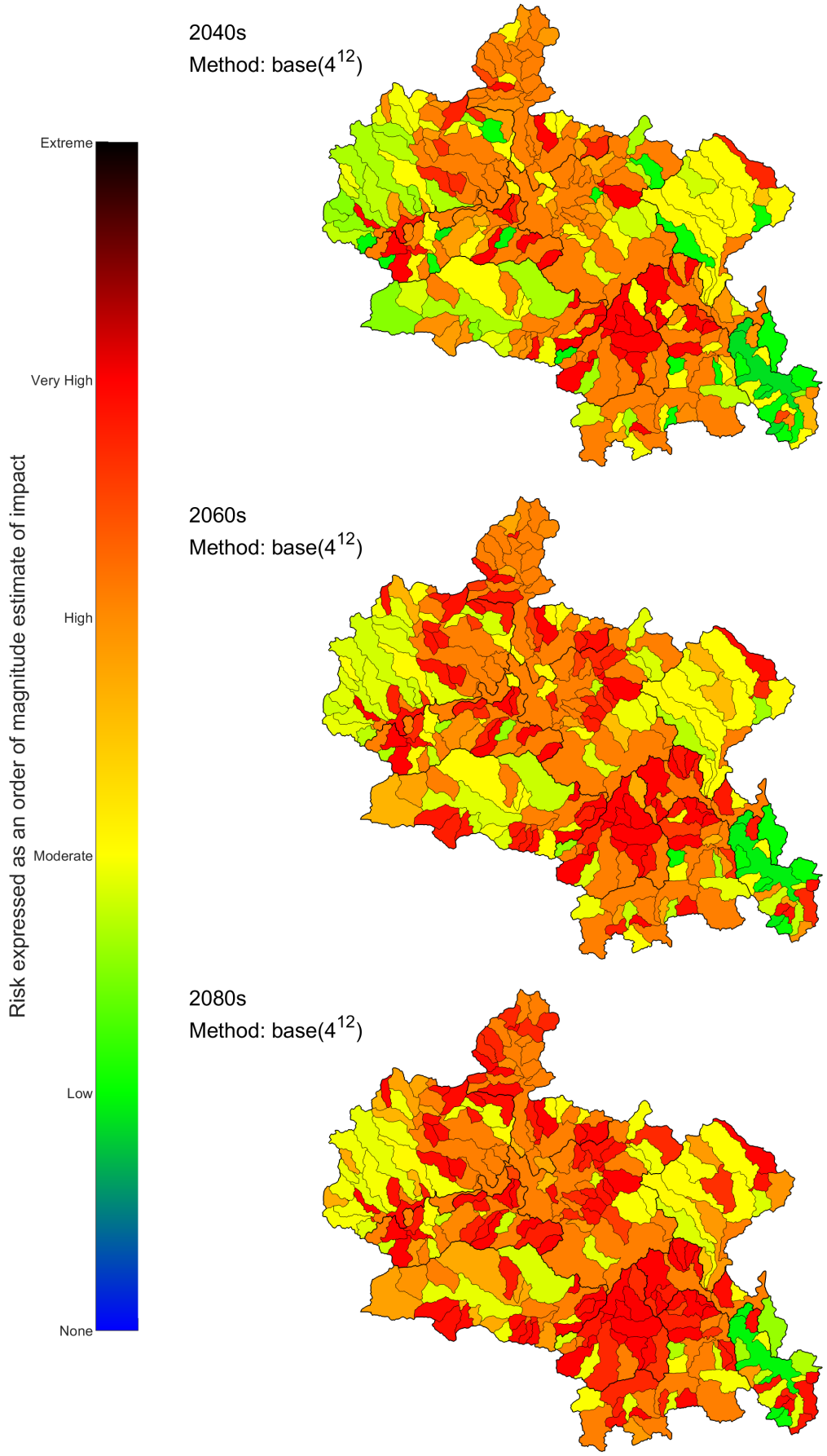


Figure 5-42: Thames Basin maps of risk of ecological impact under UKCP09 projections for the 2040s, 2060s and 2080s. The predicted class percentages for each of the four indicators (SRP, ammonia, water temperature and DHRAM) were combined using the base (4^{12}) method outlined in section 4.7. This conservative method places prominence on the most severe indicator.

Chapter 6 THAMES BASIN: DISCUSSION

The results presented in the previous chapter demonstrate that alterations in both mean annual precipitation and temperature affect macro-nutrient concentrations, water temperature and indicators of the flow regime to varying degrees for all 292 catchments within the Thames Basin. The exemplar catchments, chosen to demonstrate the response of different catchment typologies, demonstrate significant variation in their sensitivity to alterations in climate. Furthermore, applying Water Framework Directive (WFD) standards to the raw data response surfaces enabled a quantifiable metric for assessing the impact that climatic alterations may have on the ecological health of a catchment. The application of UKCP09 to variable response surfaces enabled the probability and risk of projected climate change to be elucidated for a time horizon (2040s, 2060s and 2080s in this research) for each key variable throughout the Thames Basin. Climate change, as projected using the HadCM3 probabilistic change factors, is demonstrated to have varying effects on both the magnitude and spatial distribution within and between response variables. The specifics of these variations and the overall ecological impact of climate change on each response variable are discussed below, along with notable model and methodological limitations.

6.1 CLIMATE CHANGE AND SOLUBLE REACTIVE PHOSPHORUS

The exemplar catchments for Soluble Reactive Phosphorus (SRP) show two different responses to alterations in precipitation and temperature. The response surfaces of those catchments with currently high SRP levels demonstrate SRP concentrations increasing with both increases in temperature and decreases in precipitation. Conversely, those catchments with current low levels of SRP demonstrate concentrations of SRP increasing with both decreases in temperature and increases in precipitation. These two responses may be explained using the follow principles that account for the phosphorus inputs to a catchment. Catchments with high levels of SRP are highly likely to contain a sewage treatment plant (STP) (see Figure 6-1). Higher temperatures increase evapotranspiration and, when coupled with decrease in precipitation, result in reduced river flow. Consequently, phosphorus concentrations in these catchments increase due to the associated reduction in river

flow used to dilute effluent from STPs. This is consistent with other studies in the Thames Basin that predict that the impact of climate change will be to enhance phosphorus concentration during low flows (Crossman et al., 2013a, 2013b, Bussi et al., 2016c). Conversely, lower temperatures reduce evapotranspiration from a river, which increases flow. When coupled with greater flow due to increased precipitation, there is greater run-off from agricultural land leading to increased phosphorus input to rivers. This contrasts with STPs, whose output of phosphorus via effluent is not dependent on changes in river flow. This dynamic of increased in-stream phosphorus loading has a disproportionate effect in catchments with currently low SRP concentrations, leading to increased SRP levels despite an increase in both the flow and volume of water in the river (Jarvie et al., 2002).

These two responses observed in the exemplar catchments are reflected in each of the Thames Basin maps for UKCP09 projections (Figure 5-25 and Figure 5-26). The conditions predicted using the HadCM3 probabilistic change factors range from an increase of 0.8-4.4°C and precipitation variation of -9% to 11% for the 2040s, to an increase of 1.3-6.3°C and precipitation variation of -10% to 13% for the 2060s and finally an increase of 1.8-8.3°C and precipitation variation of -12% to 16% for the 2080s. The spatial correlation between catchments with high concentrations of SRP and those containing STPs is clearly observed in Figure 6-1. These STPs are typically found throughout the Central and Eastern section of the Thames Basin (the most highly populated regions) in large-lowland catchments. Thus, there is a correlation with the WFD catchment typology used to identify exemplar catchments in-so-far as catchments types associated with low-land large and medium rivers typically have the larger number of STPs. The SRP concentrations in these catchments are all predicted to increase under all UKCP09 scenarios, with concentrations increasing from the 2040s through to the 2080s. Conversely, catchments without STPs are those with low SRP concentrations and are typically found in the upper-reaches of Thames (Western section) away from population centres. The SRP concentrations in these catchments are all predicted to decrease under all UKCP09 scenarios, with concentrations decreasing from the 2040s through to the 2080s. One notable exception is the Mole catchment in the lower reach of the Thames. However, this is likely to be an anomaly, as no sewage treatment plant effluent data were available for input into the INCA models, despite their presence

in the sub-basin (DEFRA, 2012). Therefore, SRP concentrations in the Mole sub-basin are likely to be underestimated. The spatial variation in the percentage of concentration change seen between catchments exhibiting the same response to climate change is predominantly due to river size. Smaller rivers (head-water streams) are seen to exhibit the greatest change in SRP concentrations, for both increased and decreased SRP concentrations. This is due to the proportional affect that flow alterations have on different river sizes, with reductions in flow having a greater impact in head-water streams than lower reaches (Poff et al., 1997). The buffering capacity of a large volume of water and multiple inputs ensures that changes in nutrient concentrations are less severe in low-land rivers than those in head-water streams, where flow is predominantly determined by the quantity of run-off from within the catchment area (Alexander et al., 2007).

This research aligns with the findings of existing studies within the Thames Basin (Crossman et al., 2013a, 2013b, Bussi et al., 2016c), as all catchments comprising the main stem of the Thames are predicted to increase in SRP concentration under all future scenarios. However, these previous studies divided the Thames Basin into 22 reaches (average drainage area of 439km^2) and modelled changes at points along the main stem of the Thames. This method necessitated the conglomeration of spatially explicit data throughout the Thames into average values used to model each large-scale reach. Therefore, the impact that the distribution of STPs has on catchment phosphorus levels and how this determines the sensitivity of response to climate change is limited, with only broad-scale increases in SRP concentration noted under climate change. This current research split the Thames Basin to a scale an order of magnitude (292; average drainage area of 33km^2) over existing studies, thus elucidating the both the spatial patterns and varying directions of response observed in Figure 5-25 and Figure 5-26. This level of detail, which is lacking in previous studies that conglomerate catchments at a coarser scale, represents greater differentiation at the basin scale and enables more tailored mitigation strategies to be developed.

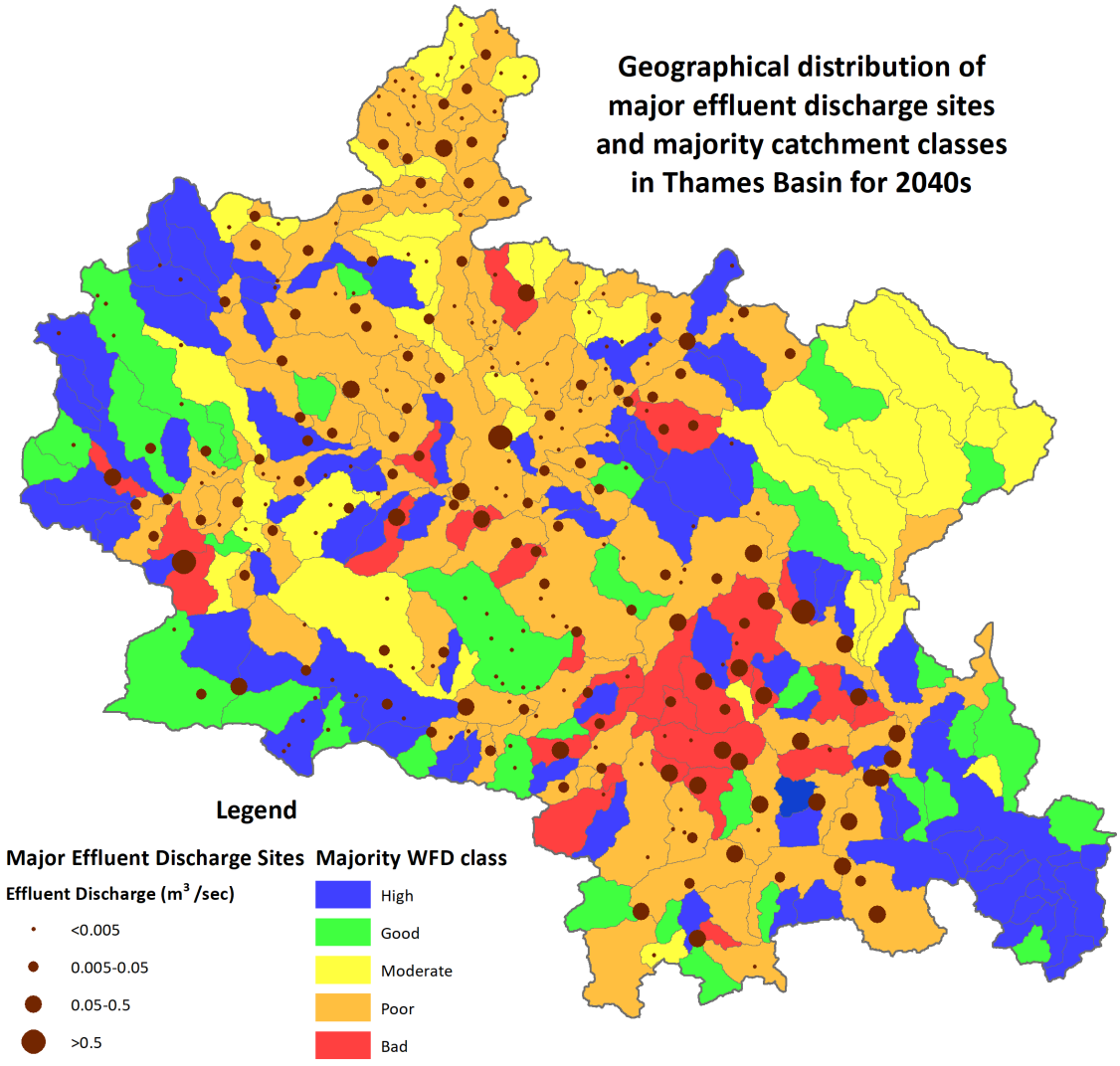


Figure 6-1: Map of the Thames Basin showing the spatial congruence of both the median SRP WFD classes for the 2040s and major effluent discharge sites.

Finally, when considering the impact of catchment-specific WFD thresholds, the distributions of WFD classes throughout the Thames Basin (Figure 5-27 and Figure 5-28) largely follow the same spatial patterns observed in the raw data (Figure 5-25 and Figure 5-26). Catchments classified as either 'High' and 'Good' are typically associated with head-water streams and those that do not contain STPs. Those classified as 'Moderate' to 'Bad' are typically associated with large to medium, low-land rivers, in catchments that contain STPs and near population areas. There is a general trend over the UKCP09 scenarios towards the extremes of WFD classification, with catchments associated with low phosphorus concentrations more probable to improve in classification over time and catchments with high phosphorus concentrations further increasingly probable to deteriorate over time (Figure

5-28). The overall ecological impact of climate change on changes in SRP classification over unperturbed conditions appears to be relatively minimal. A small, approximately equal, number of catchments are projected to both improve and deteriorate in WFD classification, with these changes occurring at both extremes of the classification system (i.e. 'Good' to 'High' and 'Poor' to 'Bad'), with changes in SRP classification limited to head-water catchments. The WFD standards for SRP represent an indicator of the health of a catchment based on the derivation of class thresholds from the tolerance of macrophytes and diatoms to phosphorus concentrations. Therefore, for most catchments, projected climate change alone will not significantly impact on phosphorus concentrations to which these taxa are sensitive.

6.2 Climate Change and Ammonia

The exemplar catchments for Ammonia show a singular response to alterations in mean annual temperature, with increase in temperature causing a decrease in ammonia concentrations across all catchments and vice versa. However, there are two contrasting responses to mean annual precipitation; some catchments exhibit increased ammonia concentration with increases in precipitation while others show the reverse, with a reduction in precipitation associated with an increase in ammonia concentrations. Alterations to the flow regime and temperature impact the nitrogen mineralisation process (Ferrier et al., 1995). Therefore, these variations in response can be attributed to spatially explicit alterations in temperature and flow regime and the associated impacts these have on the mineralisation of nitrogen in soil of individual reaches. Furthermore, STP effluent and agricultural run-off (i.e. fertilisers, pesticides) have a significant impact on in-stream ammonia concentrations (Jin et al., 2012). This is reflected in Figure 5-29, which presents the distribution of probable ammonia concentrations throughout the Thames Basin map for all UKCP09 projections. Those catchments with STPs typically have higher concentrations of ammonia than those without, reflecting the pattern noted for SRP concentrations. However, the variation in ammonia concentrations across the Thames Basin is significantly lower than that of SRP, as naturally higher levels of ammonia exist in rivers than those of SRP due to the integral role that microbes and plants

in the nitrogen cycle, particularly in forested streams (Meybeck, 1982, Arheimer et al., 1996). SRP is typically bound in more stable forms, typically in river-bed sediments, and therefore not as present naturally in the water column (Meybeck, 1982)

Climate change has been shown to trigger increased mineralisation of nitrogen in soils and reduce ammonia concentrations in rivers due to increased temperatures and decreased summer flows, both of which enhance the denitrification process (Ferrier et al., 1995). These changes are reflected in the basin-wide reductions in ammonia concentrations caused predicted by the UKCP09 projections of climate change in this research (Figure 5-30). Furthermore, ammonia concentrations are projected to continuously decrease throughout the Thames Basin from the 2040s through to the 2080s. These results broadly reflect those of Jin et al. (2012), who provide climate change impact estimates on nitrate concentrations in the River Thames using the INCA-N model and a 'top-down' assessment framework (coupling water quality model with climate change model projections). Furthermore, a more recent study by Bussi et al. (2017) utilised the same INCA-N model but adopted a scenario-neutral approach to assessing climate change, similar to the method used in this research. Both studies reported a similar response in nitrate concentrations within the Thames Basin to increases and decreases in precipitation, with increased river nitrate concentrations in winter and decreased concentrations in summer, following wetter winters and drier summers. The response of nitrate was modelled in this study and broadly agrees with these two studies. However, ammonia was presented as WFD standards exist for in-stream ammonia concentrations but not for nitrate.

The variation observed in the percentage reduction in ammonia concentrations may predominantly be attributed to the presence or absence of STPs. Smaller, head-water streams typically display a greater reduction in ammonia concentrations than those in the large, lower-reaches. The reduction in ammonia concentrations is more pronounced in these catchments, as most STPs are situated in the mid to lower-reaches of the Central-Eastern section of the Thames Basin. Therefore, without continuous effluent input from STPs, ammonia concentrations are predominantly dependent on both the temperature and precipitation sensitive nitrogen cycle processes and dynamic nature of

catchment run-off. As with SRP, no direct correlation with WFD catchment typology is observed, as the primary cause of variation is due to STP location. However, coincidental correlation does occur, since most small, higher elevation streams, regardless of geological type, see greater reductions in ammonia concentrations than large lowland rivers.

Figure 5-31 demonstrates that much of the Thames is projected to conform to 'High' WFD status under all UKCP09 projections, with an increase in probability from the 2040s to 2080s towards higher classifications. Catchments associated with 'Good' are predominantly associated with catchments containing major STPs, typically corresponding to large, lowland river types. Ammonia WFD standards are derived from ammonia concentrations associated with macro-invertebrate communities at 'High' and 'Good' status. Therefore, the change in classification of a catchment under climate change reflects the potential impact on macroinvertebrate community health and function with references to their sensitivity to in-stream ammonia concentrations. Climate change is unlikely to have a significant negative impact on the ecological-classification of many catchments within the Thames Basin (Figure 5-32). Conversely, for those impacted catchments, classifications are projected to improve over unperturbed conditions across all climate projections. As discussed above, many of these impacted catchments contain major STPs. Therefore, in certain catchments, it may be that climate change can help mitigate effluent outputs from STPs by lowering in-stream concentrations of ammonia.

6.3 Climate Change and Water Temperature

Air temperatures have directly proportional effects on water temperatures, which are observed in the singular response of water temperatures in the exemplar catchments to alterations in mean annual temperature; increased temperature causes increased water temperatures. The response surfaces indicate that water temperatures do not vary with alterations in mean annual precipitation. However, this is a product of the simplistic water temperature model used within INCA, rather than likely future outcomes. Given that both changes in air temperatures (through evapotranspiration) and precipitation drive river flow, a determinant of water temperature, it is expected that alterations

in precipitation would also cause variation in water temperatures (Bussi et al., 2017). However, the INCA model calculates water temperature as a linear function of air temperature and does not consider river flow in this process (Whitehead et al., 1998a).

There is a consistent trend towards increased water temperatures across the whole Thames Basin for all UKCP09 climate change projections, with water temperatures increasing from the 2040s to 2080s proportionally with air temperature (Figure 5-33). Spatially, temperatures are generally greater in the large, lowland rivers around the Central and Eastern region of the basin and lower temperatures are typically associated with head-water streams at higher elevations. Relative to unperturbed (current) conditions, these catchments in the upper-reaches (small, shallower streams) are likely to experience the greatest change (Figure 5-33). Conversely, large deeper rivers have absolute temperatures that are typically higher than those in the head-water streams yet demonstrate a reduced impact from climate change over unperturbed conditions (Figure 5-34). This is consistent with other studies (Wilby and Harris, 2006), since increases in air temperature have a proportionally greater impact on small, shallower rivers than larger, deeper rivers due to the volume of water present in the reach.

The spatial distribution of increase in water temperature are replicated in the derivation of WFD classifications throughout the Thames (Figure 5-35). There is a consistent trend towards an increased likelihood of deterioration in classification from the 2040s to 2080s. Water temperature WFD standards were developed using the temperature tolerances of fish species within the UK. Threshold standards are dependent on the composition of fish communities and typically vary with catchment type. Despite large, low-land rivers projected to have the highest raw temperatures under future scenarios, most are classified as achieving either ‘High’ or ‘Good’ status, reflecting the capacity of fish communities existing in these catchments to persist under elevated temperatures. Conversely, those catchments classified as ‘Moderate’ or worse are associated with head-water streams, reflecting the impact that elevated temperatures have on the fish communities in these catchments.

Much of Thames Basin is projected to deteriorate by a single classification relative to unperturbed conditions for all UKCP09 projections (Figure 5-36). Large, lowland rivers, forming the main stem of

the Thames and associated sub-basins, are least likely to deteriorate from current conditions. Mid-level streams become increasingly likely to deteriorate with time and head-waters are consistently likely to deteriorate across all scenarios. Finally, by the 2080s, catchments throughout the head-waters of the Thames Basin are highly likely to have deteriorated by two classifications over unperturbed (current) conditions. Therefore, it is probable that climate change will have a significantly detrimental impact on the ecological classification of water temperatures throughout the Thames Basin and associated impacts on fish communities in these reaches. These increased water temperatures are also highly likely to have detrimental, synergistic effects on many key ecosystem-processes (e.g. nutrient-cycling, flow-regime seasonality) (Gibson et al., 2005, Woodward et al., 2010) and biological composition and function (e.g. food-web synchrony, species phenology) (Kishi et al., 2005, Dallas and Ross-Gillespie, 2015).

6.4 Climate Change and changes to the flow regime (DHRAM)

The exemplar catchments demonstrate a sensitivity and singular response of DHRAM scores to alterations in both mean annual temperature and precipitation. The highest DHRAM scores are associated with both reduced temperatures/increased precipitation and increased temperatures/reduced precipitation. This is due to both precipitation and temperature driving river flow (Poff et al., 1997). Increased precipitation causes greater catchment run-off, resulting in increased river flow. Higher temperatures increase evapotranspiration and thus decrease river flow. The most extreme alterations to mean river flow are therefore observed when these two responses are inversely combined. As such, river flow is at its lowest with a decrease in precipitation and increase in temperature and at its highest with an increase in precipitation and a decrease in temperature. Both conditions are reflected in the DHRAM response surfaces, as the methodology identifies absolute alterations in river flow from ‘pristine’ conditions.

There is a general trend towards greater DHRAM scores throughout the whole Thames Basin for all UKCP09 climate change projections, with scores projected to consistently increase from the 2040s through to the 2080s (Figure 5-37). There is a significant spatial variation in scores, with the highest

DHRAM scores, and thus greatest alteration in eco-hydrological indicators, seen throughout the upper-reaches of the Thames Basin. This is expected, since small streams are more sensitive to flow alterations than larger rivers (Poff and Zimmerman, 2010, McCluney et al., 2014). This is due to the buffering capacity of a large volume of water and multiple upstream inputs in large rivers, which serve to mitigate alterations in precipitation and temperature (McCluney et al., 2014). Conversely, in head-water streams, flow is predominantly determined by the quantity of run-off from within the catchment area and therefore highly sensitive to alterations in both temperature and precipitation (McCluney et al., 2014). Relative to unperturbed (current) conditions, climate change is also expected to increase DHRAM scores throughout the Thames Basin, with scores increasing from the 2040s through to the 2080s (Figure 5-38). Reaches associated with high elevations (in the upper reaches of the Cotswolds catchment) are projected to demonstrate the largest increase in scores. However, DHRAM scores are projected to decrease for all UKCP09 scenarios relative to unperturbed conditions for several large, low-elevation rivers, suggesting a return to a more 'pristine' flow regime and improvement of current conditions.

The spatial distribution of increases in DHRAM scores are replicated in the derivation of classifications throughout the Thames Basin (Figure 5-39). There is a consistent trend towards an increased likelihood of deterioration in classification from the 2040s to 2080s for most catchments. DHRAM classifications were derived through categorisation of the total of key eco-hydrological indicators outlined by (Richter et al., 1996, 1998) for altered climates demonstrating sufficient deviation from unaltered, 'pristine' conditions (Black et al., 2005, Dyer et al., 2014). Most catchments throughout the Thames Basin experience enough flow regime alteration under climate change to classify as 'Good' under the proposed methodology outlined in this thesis. Notably, the Mole sub-basin is projected to achieve 'High' status for both the 2040s and 2060s, with probable shift to 'Good' classification in the 2080s.

Much of Thames Basin is projected to deteriorate by a single classification relative to unperturbed conditions for all UKCP09 projections (Figure 5-40). Mid-level streams become increasingly likely to

deteriorate from the 2040s to 2080s and head-waters are consistently likely to deteriorate across all scenarios. By the 2080s, catchments throughout the north-western region of the Thames Basin, and specifically the Kennet and Pang sub-basin, are most likely to have deteriorated by two classifications over unperturbed (current) conditions. Conversely, large lowland rivers forming the main stem of the Thames and associated sub-basins are likely to improve in DHRAM classification over current conditions. Climate change is therefore likely to have a significantly detrimental impact on the majority of the Thames Basin, through the further alteration of flow regimes over 'pristine' conditions. However, conversely, several catchments throughout the headwaters of the Thames Basin are more likely to improve under climate change, with a return to more 'pristine' flow regime. Since flow regime may be considered the primary determinant for sustaining biodiversity and ecological integrity in lotic systems (Poff et al., 1997), significant alterations to the magnitude, frequency and timing of the natural flow regime are likely to have profound ecological consequences (Arthington et al., 2006). The results presented in this thesis strongly indicate that climate change is highly likely to have a detrimental effect on ecological function in most catchments throughout the Thames, through further deviation from both the current and natural flow regime.

6.5 CLIMATE CHANGE AND MACROINVERTEBRATES

The impact that climate change may have on the macroinvertebrate model presented in this thesis was explored for the exemplar catchments. There was a variation in the sensitivity of response to climatic drivers seen across catchments, with the most responsive relating to catchment types associated with low elevation, head-water streams. This demonstrates that the macroinvertebrate model may be sensitive to alterations in mean annual precipitation and temperature; with a greater percentage likelihood of less severe classes occurring with decreases in temperature and increased precipitation and a greater percentage likelihood of more severe classes occurring at higher temperatures and reduced precipitation. As discussed previously, alterations in both precipitation and temperature change both the flow regime and water temperatures, and by extension, SRP and ammonia concentrations. Therefore, it is reasonable to assume that the patterns observed in the response surfaces of the macroinvertebrates may align with those of the variables outlined above, due to their inclusion as parameters in the joint macroinvertebrate model.

Comparison of the exemplar catchment response surfaces for each of the variables suggests a potential visual correlation between SRP concentrations and macroinvertebrate response. As such, SRP may be the dominant driver in determining macroinvertebrate model responses in this research. This is feasible, as the metric used to derive WFD standards for macroinvertebrates is the WHPT index, which is known to be sensitive to fluctuations in water quality (Paisley et al., 2014). However, a comprehensive assessment of the respective weight of each parameter in determining model outcomes was not performed in this research, and indeed not possible due to the use of principle component analysis in removing co-linearity from the parameter space. A more comprehensive study could be undertaken to better understand the sensitivity of parameters to model outputs through the application of differential sensitivity analysis (Hamby, 1994). This technique generates a sensitivity coefficient, defined as the ratio of the change in output to the change in input (singular perturbed parameter) while all other parameters remain constant (Hamby, 1994). The parameter with the greatest sensitivity coefficient is the most influential in determining model outputs. However, the application of such a model was beyond the scope of this thesis, particularly since the

macroinvertebrate model outputs were not considered in the final summary maps generated to consider the basin-wide impacts of climate change and potential effects on current conservation efforts.

Macroinvertebrate model outputs were not presented for the whole of the Thames Basin. This was predominantly due to the homogeneity of macro-invertebrate classes throughout the Thames and in part to the complexity of visualising the data in a spatially explicit format. This homogeneity is a result of the sensitivity of the macroinvertebrate model to changes in mean annual temperature and precipitation, rather than a reflection of the likely distribution of macroinvertebrate community conditions under climate change (Heino et al., 2003). This lack of sensitivity in the joint macro-invertebrate model is probably due to the paucity of modelled hydro-ecological parameters available and calibration of the model at the Thames Basin scale. Furthermore, the response variable, in this instance WHPT scores, could be altered. Studies have shown the Lotic-invertebrate Index for Flow Evaluation (LIFE) metric and pressure-sensitive index (PSI) to be sensitive to perturbations in both flow regime and general riverine degradation (Monk et al., 2007, Monk et al., 2008, Dunbar et al., 2010, Monk et al., 2012, Glendell et al., 2014). However, WFD standards have not been developed for these indices and thus were not used in the research, as the aim was to couple changes in ecological WFD standards to perturbations in climatic drivers.

Several complex local hydro-ecological parameters that have been shown to influence macroinvertebrate community structure and their response to river degradation were not available for use in the macroinvertebrate model. These include, but are not limited to, dissolved oxygen (Connolly et al., 2004), streambed porosity (Olsen and Townsend, 2003), stream alkalinity (Clements et al., 1989), organic matter abundance (Lepori and Malmqvist, 2007), local channel morphology (Crossman et al., 2011), heavy-metal concentrations and inter-predation (Clements, 1999). Furthermore, the temporal variability of these factors is an important element not considered in the current model, with macroinvertebrates shown to be particularly sensitive to changes in seasonal variations and extreme events of climatic drivers such as precipitation and temperature (Hussain and

Pandit, 2012). Model sensitivity could thus be improved through the introduction of such local hydro-ecological parameters and dynamic climatic drivers. However, this was beyond the scope of this research, as discussed previously, with further work required to accurately predict such localised parameters under projections of climate change.

Additionally, the joint macroinvertebrate model was calibrated using joint chemistry-flow-macroinvertebrate monitoring sites throughout the entire Thames Basin. These sites encompassed a significant variation in magnitude of parameters, not least SRP and ammonia concentrations, which ranged over several orders of magnitude. Therefore, the sensitivity of the macroinvertebrate model could be improved through cluster-analysis to isolate groups of catchments that respond similarly to climatic drivers. Thus, individual macroinvertebrate models could be calibrated and applied to each of these catchment clusters, reducing variation in model calibration and ensuring increased sensitivity to climatic drivers. Further work should be conducted to determine the sensitivity and predictive capacity of spatially differentiated models at the basin-scale.

6.6 RESILIENCE TO CLIMATE CHANGE AT THE BASIN-SCALE

Resilience to climate change was not considered in developing the summary maps of projected ecological impact. This is a key step in developing a more holistic view to the potential impacts of climate change and a core component of the vulnerability framework. At the basin scale, this resilience component may be considered through the application of specific management actions and strategies aimed at reducing sensitivities to likely exposures. For example, application of phosphorus removal strategies from STP effluent and agricultural run-off to reduce in-stream phosphorus concentrations (Whitehead et al., 2013) , or alternatively increase riparian vegetation in headwater streams to reduce the impacts of increases in temperature (reduce instream temperature in INCA) (Whitehead et al., 2006). Management strategies may be run independently for each of the 300 altered climates (e.g. phosphorus strategies in one run and increased riparian vegetation in headwaters in another run) and then combined to form an integrated strategy. This final output demonstrates how effectively an integrated catchment management plan can mitigate (increase

resilience) against the ecological impact of climate change over individual strategies and provides a basis for adopting management strategies in the Thames Basin. Furthermore, it is important when creating these independent management strategies to consider the final, integrated catchment plan and to account for upstream-downstream interactions. For example, if flow is reduced upstream, this will increase nutrient concentrations downstream and may negatively impact catchments downstream that are sensitive to nutrients (Olden et al., 2011). Additionally, management strategies devised by major users within the Thames Basin, i.e. Thames Water and the Environment Agency may be tested for their efficacy in achieving management targets. Specifically, Thames Water has developed a 25 year management plan (2010-2035) outlining major costs and developments in the region (Thames_Water, 2012) and the Environment Agency have developed a river basin management plan for the Thames that outlines progress towards key WFD targets (EA, 2015b). Incorporating resilience, in the form of management strategies, was beyond the scope of this research for both time and computational reasons yet represents a fascinating and important area for further work.

6.7 THE POTENTIAL IMPACTS OF CLIMATE CHANGE ON FRESHWATER CONSERVATION IN THE THAMES BASIN

The summary maps presented in section 5.5 demonstrate a novel approach to quantifying the risk of climate change due to relative percentage likelihood of WFD class occurrence in the contributing indicators. This was achieved through the inclusion of a nominal system of risk analysis for each WFD classification. If, for example, the ecological impact for one indicator is known to be substantially larger than all others, then a larger order of magnitude can be assigned to this indicator. This will be visually reflected in the associated map with colours that are most closely associated with a higher risk indicator. The current research assumes a weighting system reflecting the power-law i.e. each subsequently more severe class is assigned a power greater than the one before, as outlined in Table 4-17. Although this weighting is not formally enumerated, this system offers a novel method for assessing risk associated with quantifiable ecological-impact in the context of climate change.

Furthermore, the methodological process involved in parameter summation enables a range of assessments to be made; a balanced view of risk across all parameters (base N^2) or isolation of the most severely classified parameter (base N^{12}) (where N is the number of input parameters). Further work should be done to elucidate the relative ecological impact that changes in WFD status may have on a catchment, as it is unlikely to follow a power-law. This work would require experimental data focussed on the relative ecological function and health of a system under a range of perturbations at the local scale and was beyond the scope of this research.

Furthermore, this methodology could be used in a management context to assign a fiscal cost associated with improving a catchment from, say, 'Moderate' to 'Good' status. Such assessments would have to be carried out on a catchment-by-catchment scale and align with Integrated Water Resource Management (IWRM) plans that seek to balance the needs of ecological and human actors within a catchment (Heldt et al., 2017). This was beyond the scope of this current research, but could prove a valuable asset in determining the fiscal cost associated with meeting the Water Framework Directive of attaining 'Good' water body status for all catchments by 2021 (EA, 2014b). Figure 6-2 provides a demonstration of how catchment specific data may be applied to individual reaches within the Thames Basin. This digital, dendritic network is essential in the development of local catchment management plans and enables individual catchment scores to be placed in the context of the whole drainage basin. Downstream effects can be incorporated into the network, enabling the transmission of variables through the system. Additionally, all upstream reaches from a site or reach of interest may be elucidated, providing invaluable information on the cumulative impact of contributing upstream catchments.

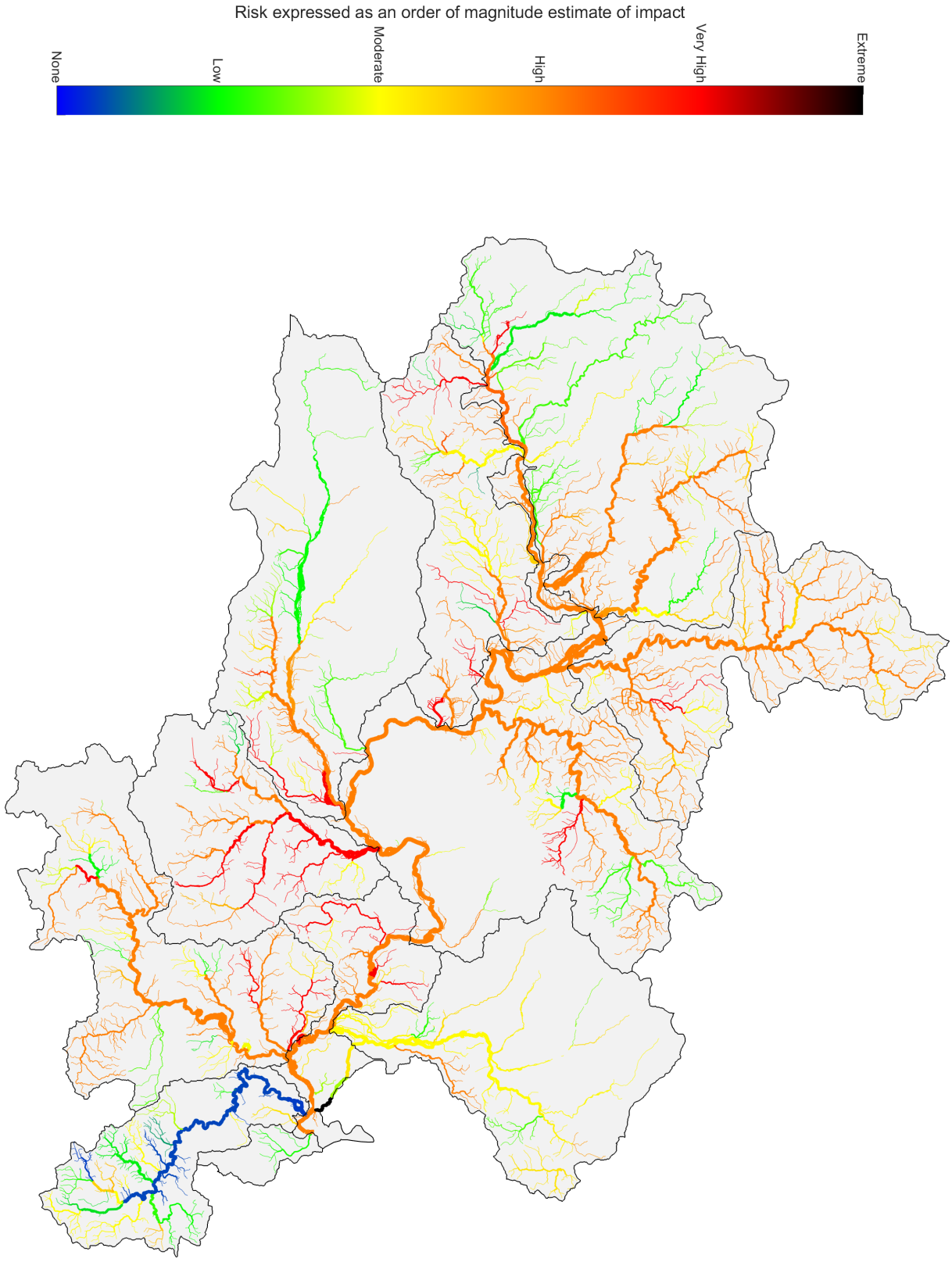


Figure 6-2: Map of the Thames Basin demonstrating the application of the catchment risk associated with ecological impact for the 2040s scenario (adopting the balanced approach to indicator aggregation (4^2) to a high resolution, dendritic river network.

The potential impact on current conservation efforts within the Thames Basin was briefly explored through the spatial congruence between both non-freshwater specific protected areas (Special Sites of Scientific Interest (SSSIs) and Special Conservation Areas (SCAs)) and freshwater specific priority areas and risk for the 2040s using the balanced aggregation method (base4[2]) (Figure 6-3). Through exploring these interactions, some general conclusions can be drawn about potential impacts on current conservation efforts in the Thames Basin. At present, protected areas within the United Kingdom typically aim to balance the requirements of site-specific species (i.e. Site of Special Scientific Interest (SSSI)) (JNCC, 1989) or broadly maintain vast cultural landscapes (i.e. Areas of Outstanding Natural Beauty (AONB)) (Dower, 1945). The former is of interest to this study, as the focus is more on the conservation of species, ecosystems and functional processes.

A Site of Special Scientific Interest (SSSI) is a formal conservation designation for an area that is of particular interest because of its fauna, flora or geological or physiological features, currently covering fewer than 7% of England (JNCC, 1989). Most of these sites are not specific to freshwaters and may encompass any presence of rare species or geological and physiological features deemed important to science. However, broadly speaking, the strict guidelines imposed at these sites may prove beneficial to riverine systems since direct human impact on the catchment is reduced (Christie and Rayment, 2012). Of relevance to this study are the rivers Kennet and Lambourn, both of which are designated as a SSSI. The priority river habitats and headwaters, identified for England by Natural England, are of far greater importance to conservation efforts in freshwaters. Priority river habitats were selected in England based on naturalness criteria (physical, hydrological, chemical and biological), capturing the most natural remaining examples (Natural_England, 2014). Similarly, priority headwaters were selected throughout England using naturalness criteria based on land-cover (Natural_England, 2014). The impact of climate change on non-freshwater specific protected areas was assessed in Figure 6-3a and in Figure 6-3b for freshwater specific priority areas. This was achieved by treating the protected areas layer as a mask and using Spatial Analyst toolset within ArcGIS© to extract the spatial congruence between these sites and the underlying maps developed during this thesis outlining the risk of ecological impact due to climate change.

Many of the SSSIs are in the Loddon, Maidenhead and Sunbury and Wey sub-basins regions, which are all predicted to have 'High' to 'Very High' risk of ecological impact under the 2040s scenario and forecast to become more severe from the 2060s to 2080s. Those in the North-Western area of the Thames Basin (Cotswolds, Cherwell, Kennet and Pang and Thame and South Chilterns) are typically associated with a 'Moderate' to 'High' risk of impact under climate change in the 2040s. The rivers Kennet and Lambourn correspond to 'low' to 'medium' risk, suggesting these freshwater-specific SSSIs have a lower risk of ecological impact due to climate change. However, the methodology devised in this research is of limited usefulness in assessing the risk of impact from climate change on the predominantly terrestrial SSSIs. Climate change impact on these SSSIs should thus be quantified through a primarily terrestrial based approach, with shifts in the composition of flora and fauna likely due to changes in species physiology, dispersal, phenology, predation and, ultimately, ecosystem structure, productivity and nutrient cycling (Walther et al., 2002). However, it is important to note the distribution of SSSIs throughout the Thames Basin, with the majority in the South-Eastern section identified as the most at risk to climate change impact in this research. Therefore, the integration of both terrestrial studies and the results presented in this research may provide a more holistic view of the implications of climate change on the protected areas network and restoration strategies in the UK.

The priority river habitats and headwaters do not represent formal protected areas, but instead highlight particularly important sites and areas for consideration within future management plans and protected area development within the UK. Since the Thames Basin is both highly urbanised and agricultural, there are comparatively few priority sites identified for the region. However, for those present, the headwaters in the Cotswolds, associated with mid-elevation, calcareous head-water streams, show the lowest potential risk under projected climate change in the 2040s ('Low' to 'Moderate'). Similarly, priority river habitats in the same region are likely to experience similar risks. Moving eastward, climate risk generally increases, with priority headwaters and river habitats in the Cherwell, Kennet and Pang, and Thame and South Chilterns projected to have 'Moderate' to 'High' risk of impact under climate change. The lone headwater in the Loddon catchment is the most

severe, with projections suggesting a 'Very High' risk of impact under climate change. Much of the risk associated with these catchments is due to elevated SRP concentrations throughout much of the central and eastern Thames Basin, with concentrations projected to increase under climate change (Figure 5-25). Strategies aimed at reducing nutrient enrichment of the Thames and tributaries through decreased agricultural run-off and reduced effluent concentrations would significantly reduce the risk of negative ecological impact under climate change. Furthermore, strategies aimed at facilitating the dispersal of species will go some way to mitigate the impacts of rising temperatures. In the context of the Thames, a heavily regulated river, this would involve the construction of fish-runs at locks and weirs to facilitate upstream movement (Gardiner, 1988).

The integration of these priority habitats and headwaters may prove essential in addressing the current paucity of freshwater protected areas within the Thames Basin, primarily due to the extensive degradation of natural river systems throughout the region (Natural_England, 2014). These sites represent the remnants of naturalised riverine systems and catchments and should be conserved through protection within specifically-designated protected areas (Abell et al., 2007, Natural_England, 2014). Furthermore, the presence of heavily degraded chalk springs within the Thames Basin is a priority for restoration of natural processes and re-introduction of lost species (Natural_England, 2014). The brief analysis conducted in this thesis highlights the potential ecological impact that climate change may have on this region under the UKCP09 scenarios. Further analysis and incorporation into a formalised conservation planning system would ensure priority conservation areas are identified that incorporate the dynamic threat posed by climate change (Pressey et al., 2007, Turak et al., 2011b). Such an analysis was beyond the scope of this current research, yet the outputs presented here were specifically designed for such an application. To this end, more specific details for further work are outlined in the subsequent chapter, alongside general conclusions from the both the regional and basin scale assessments of climate change impact conducted in this thesis.

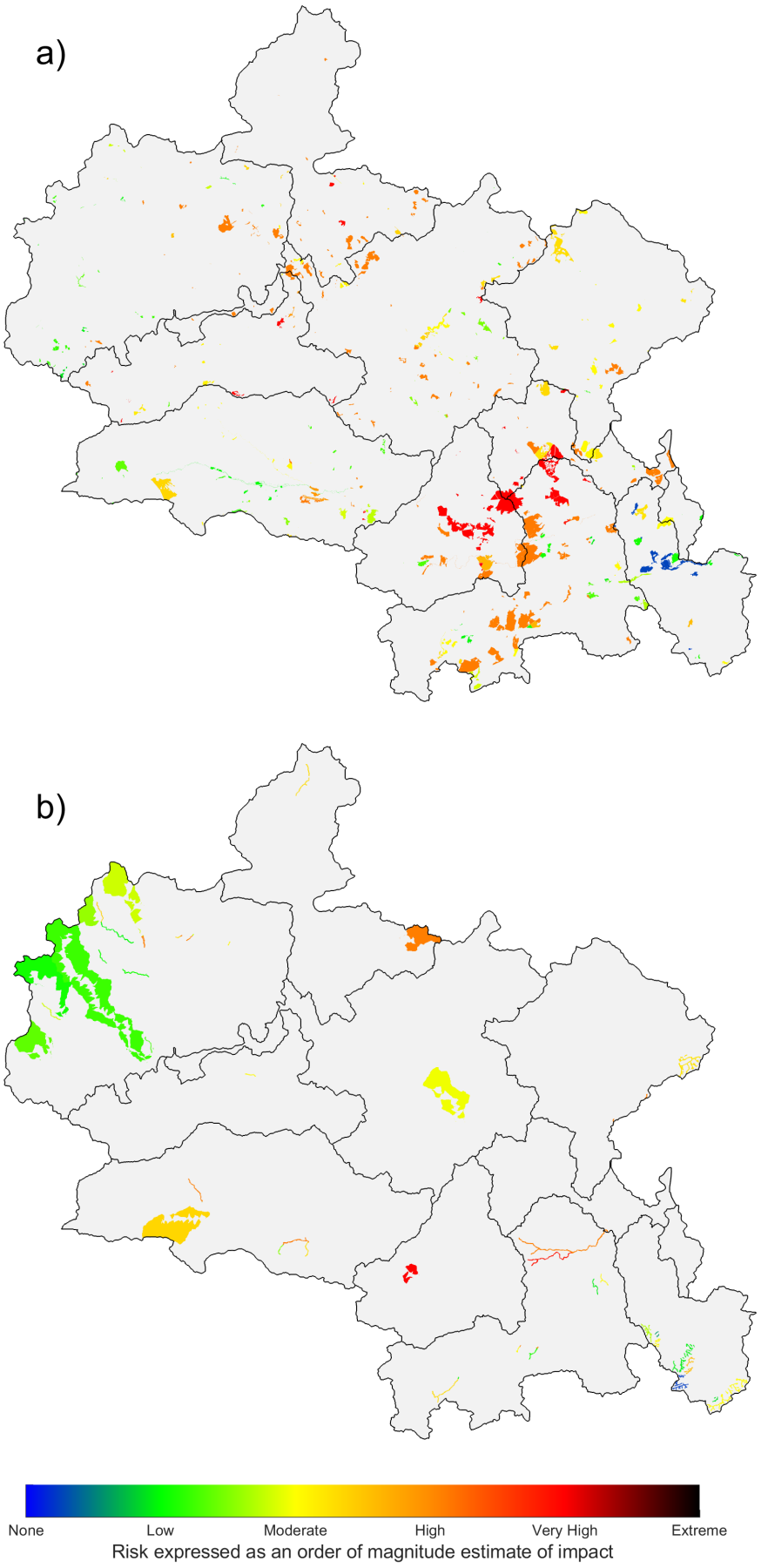


Figure 6-3: The projected risk for the 2040s (using the balanced aggregation method, 4^2) for both a) SSSIs and SPAs and b) Priority River Habitats and Headwaters within the Thames Basin

6.8 UNCERTAINTIES IN THE MODELLING PROCESS

It is necessary to outline the possible sources of uncertainty affecting the results of this research and summarise the limitations of the methods employed in generating results. The model structure used in this research (a cascade of three models: PERSiST, INCA and a macroinvertebrate model) can lead to the propagation of errors through each stage of the modelling chain. The uncertainties associated with both the PERSiST and INCA models used in this study have been addressed extensively in the existing literature, with 20-25 parameters identified as particularly influential in model accuracy (Raat et al., 2004, Rankinen et al., 2006, Dean et al., 2009, Futter et al., 2014, Whitehead et al., 2015, Bussi et al., 2016a). A sensitivity analysis of these key parameters enabled the calibration of both PERSiST and INCA models to observed results using a simulated-annealing algorithm of 10,000 randomly generated plausible parameter sets. The model results in this research for both PERSiST and INCA demonstrate a 'very high' level of model performance across all 11 sub-basins in reproducing observed flows following the model evaluation guidelines given by Moriasi et al. (2007) (see both Figure 3-9 and Table 3-5 in section 3.7). Similar approaches by Rankinen et al. (2006) and Dean et al. (2009) aimed to evaluate uncertainty in model results through the application of a generalised likelihood uncertainty estimation (GLUE) framework to the INCA-N and INCA-P model respectively. These studies suggested that experimental knowledge be incorporated into the calibration process of these models (Rankinen et al., 2006), and that uncertainty due to model structure and parametrisation was similar to uncertainty associated with measured values of total phosphorus in the river (Dean et al., 2009).

However, despite the very good model responses observed in this research, Table 3-5 demonstrates the presence of uncertainty in model predictions for each sub-basin through the application of a percentage bias (PBIAS) equation (Gupta et al., 1999). The average error across all models relative to observed values was 18.9%, -30.2% and 22.5% for flow, SRP and nitrate respectively. This indicates a tendency for the models to overestimate flow and nitrate values and underestimate values of SRP. Furthermore, similar to Crossman et al. (2013c), average errors in model flow, SRP and nitrate were found to be greater in the summer (22.4%, -32.6%, 27.1% respectively) than in the winter (15.4%, -

27.8%, 17.9%). This is most likely due to the singular value of SRP and nitrate inputs from STPs applied to each reach within INCA and the interaction with seasonal low and peak flow events. In reality, there is a temporal aspect to STP effluent in rivers, with effluent only released during high flows to facilitate dilution (DEFRA, 2012). Similarly, a singular value for abstraction was applied to each reach, whereas in reality there are stringent controls over the quantity of water abstracted under certain flow conditions (EA, 2014a). Incorporating these temporally dynamic parameters are, in theory, possible within the INCA models. However, time-series data for abstraction and effluent discharge were not available to the author for the Thames Basin and determining alternatives was beyond the scope of this research. This is reflected in the spatial distribution of sub-basin model uncertainties, with those in the Western part of the Thames away from STPs and population centres (Cotswolds, Vale of the White Horse and Cherwell) typically exhibiting lower PBIAS scores than those in the Central to Eastern sections (Maidenhead and Sunbury, Wey, Loddon, Kennet and Pang and Thame and South Chilterns). The derivation of observed temperature and precipitation time-series is also likely to impact on the quality of specific sub-basins, since the spatial variation in observed climate within the Thames Basin was not considered (average values were taken from across the entire Thames Basin). Therefore, these driving datasets are likely to better reflect the observed conditions in certain sub-basins than other.

Specifically, the main stem of the Thames represents the best calibrated sub-basin model, due to the simplicity of this model (11 catchments), quantity of observed data available for calibration of each catchment and close approximation of driving data to actual conditions. Notably, the absence of monitoring data available to this research (though requested) in both the Mole and Colne catchments ensured it was not possible to calibrate either nitrate or SRP against observed data in these sub-basins. Consequently, parameter sets from both the Loddon and Thame and South Chilterns were used to drive the Mole and Colne sub-basins respectively. Therefore, it may be assumed that the results presented for these catchments may have a greater degree of deviation from observed conditions, which should be considered when observing the impacts of climate change. Finally, the sensitivity analysis was performed using a variety of climatic conditions, from a

dry year (2010) to a very wet winter (2013), thus ensuring that the model can respond to a wide range of climatic conditions.

The parametric uncertainty of both the PERSiST and INCA models must be considered alongside the uncertainty associated with climate change scenarios, which is a particularly relevant source of uncertainty in climate change impact assessments (Wilby and Harris, 2006, Kay et al., 2009, Prudhomme and Davies, 2009a, Prudhomme and Davies, 2009b, Prudhomme et al., 2010). In the context of this research, climate models were not used in the model cascade but instead utilised by defining a 'probable area' of the response surfaces to generate future estimations the risk of climate change impacts. The UKCP09 projections were developed to include a very broad range of possible future climate outcomes, given the large uncertainty affecting climate model results (Bell et al., 2012, Christierson et al., 2012). The levels of uncertainty involved in these predictions are substantially greater than those demonstrated in the application of the PERSiST and INCA models to the Thames Basin. Therefore, in assessing the potential risk associated with climate change, uncertainty estimates for both future climate change and the modelling cascade are incorporated into observed outcomes in key eco-hydrological variables due to changes in mean, annual precipitation and temperature.

However, in considering these uncertainties, it is necessary to note that the output uncertainty of a modelling chain is typically less than the summed uncertainty in the input parameters (Skeffington et al., 2007). Therefore, in this research it is reasonable to assume that the final uncertainty of the modelling chain (PERSiST, INCA and UKCP09) is likely to be of a similar order of magnitude to the uncertainty of the individual models (Whitehead et al., 2009). This level of uncertainty is typically considered acceptable for climate change and land-use change analysis within the hydrological and water quality modelling community, in particular when reproducing highly uncertain processes (Jin et al., 2010, Crossman et al., 2013b, Bussi et al., 2016a). Finally, uncertain models may still provide useful information to inform management plans and climate mitigation strategies because the

factors of change in the variable(s) of interest are used rather than the absolute values of those variables (Christierson et al., 2012).

6.9 LIMITATIONS OF METHODOLOGY

The limitations of the methodology used in this research are outlined below. The scenario-neutral methodology utilised in this thesis uses mean annual precipitation and temperature to drive changes in water quality, temperature and flow regime. This approach does not consider alterations in the frequency or duration of extreme flow events or changes to the seasonality of flow regimes that are independent of changes in annual mean values. Since, alterations to the frequency and duration of extreme flow events are likely to cause severe disruption to ecological processes in lotic systems (Bell et al., 2012), incorporating other drivers of change should be considered. These could include the seasonality of precipitation (Prudhomme et al., 2010) or changes in extreme precipitation (Bussi et al., 2016b). However, since this research assessed changes in the long-term means of nutrient concentrations and water temperatures, it was reasonable to consider alterations in mean annual climatic drivers.

The feasibility of adding more drivers is directly related to both computational and storage constraints. Perturbation of multiple drivers generates a series of altered climates that is numerically dimensionally proportional to the number of drivers (i.e. 20 temperature steps, 15 precipitation steps; 300 altered climate sets used in this research). For example, the introduction of a third driver leads to an additional dimension of calculation. Only 15 steps for this third driver would generate 20x15x15, or 4,500, altered climates. This translates to 4,500 runs of 2 different types of INCA models for the 292 catchments in the Thames over a 30-year period, which is approximately equivalent to 28.77 billion daily time steps for a single variable. This is beyond the scope of this research and would require the adaption of current models to server or cloud-based solutions.

The application of WFD standards in the context of climate change is a novel approach to quantifying changes in climate to tangible ecological thresholds determined through experimental procedure and expert review. The current ecological health of a catchment is determined by a suite of

approximately 50 indicators across a broad spectrum of physio-chemical and biological parameters (UKTAG, 2014b). Since it was not possible to model all indicators, a select group were chosen that provided a representative sample of the breadth of biological, physical and chemical components of a river system. These corresponded to variables capable of being modelled by INCA and shown to be both robust in determining ecological health. Consequently, the principal aim of this research was not to generate precise projections of ecological condition under future conditions, but rather determine the sensitivity of strategic water quantity and quality attributes and respective WFD classifications to changes in climatic drivers. The application of the UKCP09 probabilistic projections enabled an envelope of climate risk to be ascertained for these key variables and likelihood of deviations in respective WFD standards. Therefore, the classification of variables using WFD standards adopts a probabilistic approach and, as such, may only inform management strategies as to the relative likelihood of occurrence under a set of given future conditions.

The limitations of this approach are in part determined by the limitations of WFD standards in replicating the sensitivity of an eco-hydrological variable to alterations in the health of a specific species or group of taxa. The three WFD standards used in this research (SRP, ammonia and water temperature) are predominantly determined by the correlation of reference sites classified as 'High' or 'Good' using species specific metrics throughout the UK (i.e. WHPT for benthic macroinvertebrate taxa) with known water quality data at these sites (UKTAG, 2014b). These WFD standards are then differentiated based on the UK catchment typology derived from altitude, river size and underlying geology. As such, these multivariate models may perform well at the UK scale, but are unable to replicate catchment specific responses to climatic variables at the basin scale. Moreover, the thresholds do not account for changes in climate, as they do not consider the temporal aspect of fluctuating biodiversity metrics and water quality at a site over time. It is important to note however, that these thresholds have been through several rounds of peer review and associated revisions and represents the current state of knowledge. They represent the state-of-the-art in determining ecological conditions from physio-chemical variables in the UK and align with current freshwater policy as directed by the EU Water Framework Directive (WFD).

Currently, a WFD standard does not exist to measure the ecological impact of alterations in flow regimes. Several indicators do exist that quantify abstraction allowances based on certain flow regime metrics (UKTAG, 2014b). However, these were not fit for purpose and so a suite of extensively applied eco-hydrological indicators (Richter et al., 1996, 1998) were utilised to quantify the sensitivity of the flow regime to alterations in climate. The Dundee Hydrological Regime Alteration Method (DHRAM), developed to assess the impact of hydrological alteration due to dams between unperturbed and altered conditions (Black et al., 2005), was used to relate changes in indicators to WFD classifications. This current research represents its first use in the context of sensitivity analysis to regime alterations and classification due to alterations in climatic variables (although the approach was previously adapted by Dyer et al. (2014) to address climate change in an Australian catchment). For consistency and simplicity, the existing DHRAM thresholds for combining individual indicator scores and generating classifications were applied in this research. This was justified, since many of the thresholds were analogous to those described by Laizé et al. (2014) and employed in the regional-scale assessment in section 2.2.4 of this thesis. However, further work should be undertaken to calibrate thresholds for application of the DHRAM methodology in both lowland-UK rivers and in a climate change context. One significant limitation, which was followed in this research, of using the DHRAM methodology to assess sensitivity to alterations in mean precipitation and temperatures is that the eco-hydrological indices used to identify changes in seasonality and the magnitude and frequency of extreme events does not vary between baseline and altered scenarios. This is because the scenario-neutral approach perturbs an observed precipitation and temperature time-series for the region of interest by applying a mean annual delta change to each daily data value. Thus, only alterations in mean annual precipitation and temperature are accounted for, with no consideration of seasonal fluctuations or changes in the magnitude and frequency of extreme events (both floods and droughts). This could be addressed through the inclusion of drivers of change associated with the temporal or extreme events aspect of the flow regime, such as seasonality of precipitation (Prudhomme et al., 2010) or changes in extreme precipitation (Bussi et al., 2016b).

Water temperature was incorporated into this assessment as a means of determining broad-scale impacts in catchments with reference to the thermal tolerances of fishes. However, INCA calculates water temperature in a simplistic manner (linearly correlated with air temperature), which may provide an inaccurate assessment of water temperature in a reach. This method does not account for localised variables contributing to water temperature in reaches, such as flow regime, riparian shading and river morphology (Hannah et al., 2008b, Hannah and Garner, 2015). It also does not account for alterations in temperature due to changes in elevation and influxes of groundwater. Therefore, the pattern of temperature change seen across the Thames basin is far more homogeneous than might be anticipated, with major alterations in classification attributed to the various class thresholds for different catchment types. It is likely that the local variables unaccounted for in this model (i.e. riparian shading), are likely to impact the water temperature of rivers (Woodward et al., 2010). Riparian shading probably mitigates rises in water temperature in the upper reaches (McGregor et al., 1995), but has limited impact on large, lowland rivers due to the small proportion of the river that is actually shaded (van Vliet et al., 2013). However, in the Thames Basin, the large-lowland rivers typically flow through regions dominated by chalk aquifers and thus there may be some mitigation of increased water temperatures due to the influx of cooler groundwater (Webb et al., 2008). Finally, the presence and size of sewage treatment plants are likely to increase localised in-stream temperatures, since the effluent is often several degrees warmer than the river into which it discharges (DEFRA, 2012). Despite these limitations, water temperatures will increase throughout the whole Thames basin in response to climate change and the results presented here are useful in visualising the increasing impact that rising temperatures may have over an extended time-frame.

Chapter 7 CONCLUDING REMARKS AND SUGGESTIONS FOR FURTHER WORK

The principal aim of this thesis was to assess the potential impacts of climate change on hydro-ecology at the regional and basin scale, with reference to the associated effects these may have on conservation efforts. Critically, the resulting outputs from this thesis should facilitate further studies that seek to incorporate climate change into freshwater conservation and management at multiple spatial scales. To this end, two contrasting methodologies were applied at both the regional (European HydroBasins; Chapter 2) and basin (Thames, UK Water Framework Directive waterbodies; Chapters 3 to 6) scale respectively. Both methodologies utilised a framework based on derivations of the vulnerability principle that consists of three core components: exposure, sensitivity and resilience. These methodologies, however, differed in their approach to assessing climate change impacts, predominantly because of the scale of the study region. The availability of data and appropriate models, alongside existing knowledge of the region, was critical in determining the methodological approach. The main differences of the two methodologies are further explored below, with reference made to important findings for each case-study. Moreover, general conclusions are drawn about the appropriateness of the approaches to achieving the objectives of this thesis and, where appropriate, suggestions for further work are outlined.

The use of a vulnerability framework is a robust method for assessing the potential impacts of climate change on a system, since the three core components of exposure, sensitivity and resilience provide a more holistic viewpoint than consideration of the components individually (Adger, 2006, Gallopín, 2006, Smit and Wandel, 2006). This approach has been widely used in prior climate change assessments (Pyne and Poff, 2017, Foden et al., 2013, Brown et al., 2012, Comer et al., 2012, Chin et al., 2010, Williams et al., 2008) and indeed is now the de-facto methodology considered by the International Panel on Climate Change (IPCC) (IPCC, 2014a). However, in this thesis, the way the vulnerability framework was applied varied between case studies, with differing emphasis and interpretation placed on each of the core components.

The exposure component of climate change assessments is a critical factor in determining results, as it represents the potential perturbation expected to occur in each locale. At the regional scale (European HydroBasins), exposure to climate change was defined using gridded monthly outputs from both General Climate Models (GCMs) and hydrological models generated by the European Union WATCH (Water and Global Change) project. A 'top-down' approach to climate assessment was thus employed, using these data to drive spatial variations in vulnerability throughout European HydroBasins. Exposure was greatest in the Ebro basin in Spain, Garonne in France, Pechora in Russia and catchments along the Adriatic coast and northern Scandinavia. Conversely, at the basin scale (Thames Basin), a 'scenario-neutral' approach to climate change assessment was employed. This approach considers exposure as an external component of vulnerability and was incorporated through the application of the UKCP09 projections to determine probabilistic outcomes from the quantified catchment responses of selected parameters to alterations in climatic variables. For the Thames Basin, Soluble Reactive Phosphorus concentrations were predicted to increase in those catchments with existing high levels and decrease in those with existing low levels. Ammonia concentrations were projected to decrease throughout the entire Thames Basin, whilst water temperature was observed to increase throughout the whole basin. Alterations in flow regime showed significant variation across the Thames Basin, but followed an increasing trend towards greater deviation from naturalised conditions. The approaches adopted in this study were entirely determined by the data available, which in turn is directly related to the scale of the region under investigation. For the European case-study, the author did not have access to a regional-scale, distributed hydrological model and was thus unable to adopt the preferred, 'scenario-neutral' approach used in the Thames case-study.

The definition of sensitivity to climate change also varied between case-studies, predominantly due to how exposure was considered in each methodological process. The regional-scale assessment used a species-based approach to identify specific traits relating to individual species and assemblages of species that may make them sensitive to climate change; examples include endemism and rarity. Consequently, species-rich catchments with high endemism and rareness (Lake

Ohrid in particular) were identified as those most sensitive to climate change. Conversely, the basin-scale assessment explored the sensitivity of four key hydro-ecological variables to perturbations in climatic drivers. The ecological health of these variables was defined through existing Water Framework Directive standards, enabling specific changes to be linked to quantified thresholds of ecological health. Species responses were considered (macroinvertebrates), but not incorporated into the final aggregated maps due to issues surrounding the sensitivity of the model to perturbations in climatic drivers, as outlined in more detail in section 6.5. As such, the regional scale provides generalised observations of potential ecological sensitivity to climate change, whereas the local scale approach can quantify the sensitivity of a catchment to ecological impact under altered climatic conditions.

Resilience was incorporated into the regional model through physical catchment characteristics, such as the loss of habitat connectivity due to dam presence and the complexity of river networks within the catchment. The extensive damming of rivers throughout Eastern Europe, and particularly along the Danube and its tributaries, suggests few opportunities for climatically-driven species migration towards cooler climates, thus indicating low resilience to climate change. The concept of resilience was not considered at the basin scale yet may be incorporated through the development of management strategies to mitigate climate change impacts (Whitehead et al., 2013, Bussi et al., 2016c). This was beyond the scope of this study, due to constraints imposed by time and computational power. However, the results presented in this thesis suggest that reducing phosphorus loadings in rivers through adoption of stricter sewage treatment protocols, reduced fertiliser application and introduction of buffer zones for nutrient leaching along headwaters could go some way to mitigating against the worst impacts of climate change (Whitehead et al., 2013).

Several novel methodologies were presented in this thesis aggregating the components into a cohesive estimation of vulnerability or risk of impact from climate change. The aggregation of these components is a complex, and often semi-quantitative, process involving weighting the importance of each component. Further work should be conducted to determine a method for assessing the

importance of each component, with techniques from risk analysis research presenting the most likely route (Ylhäisi et al., 2015).

For the European case-study, components were assigned equal weighting and accumulated into an overall vulnerability index using several methodologies to investigate spatial consensus of potential impacts. Vulnerability was found to be greatest in both the Balkan Lakes and Mediterranean islands. A gap analysis was conducted to identify the congruence between the existing protected area network in Europe and these catchments most highly vulnerable to climate change. Less than 25% of these most vulnerable catchments are currently included in the European protected area network, with protected areas rarely designed specifically to conserve freshwater ecosystems. Further work is necessary, with principles from Strategic Conservation Planning going some way to preserve the ecological functionality under climate change of these most vulnerable regions through incorporation into the existing European protected area network (Nel et al., 2011b, Markovic et al., 2014a). Furthermore, existing climate change policy and strategies for current protected areas containing climatically vulnerable catchments should be updated to better account for this serious and dynamic threat (Araújo et al., 2011).

The potential impact of climate change on the Thames Basin was quantified through the application of UKCP09 projections to explore the risk of potential ecological impact due to alterations in projected status of the Water Framework Directive through aggregation of all four variables. The greatest risk was observed in the central and eastern sub-basins of the Thames (Cherwell, Vale of the White Horse, Loddon, Wey, Thame and South Chilterns, Maidenhead and Sunbury), with medium impacts observed in the Cotswolds, Kennet and Pang, and Colne sub-basins. The lowest risk was observed in the Mole sub-basin. However, spatial patterns in aggregated risk were noted to correlate with the worst indicator status (Soluble Reactive Phosphorus in this instance). No sewage effluent data was available for the Mole despite the presence of sewage treatment plants in the catchment. Therefore, the Mole can be expected to present a higher risk of potential impact from climate change than that observed in this thesis, highlighting the importance of data availability in generating

accurate results. The potential impact that climate change may have on the current protected areas within the Thames Basin was explored through examination of the congruence between summary maps of risk with current protected areas. Furthermore, the maps were used to differentiate the likely ecological impact under climate change for priority river habitats and headwaters that are not yet designated as protected areas. These represent crucial sites for both conservation and restoration, and further work should be conducted to integrate these into the existing protect area network for the United Kingdom, given the knowledge of the dynamic threat posed by climate change outlined in this thesis.

In summary, the scale of the case-study determines the methodological approach adopted, primarily through the availability and quality of existing data in the region of interest. Moreover, the interpretation of results and potential application in future work similarly varies between approaches. The very recent completion of the large European Union 7th Framework Programme Managing Aquatic ecosystems and water Resources under multiple Stress (MARS) provides scope for integrating the results of this thesis into exciting new fields of freshwater science and policy. One key output from MARS Work Package 5 assessed the ecological status of waterbodies under multiple stressors, providing a percentage likelihood of meeting the WFD target of 'good' ecological status (Grizzetti et al., 2017). Incorporating this research into the regional scale case-study of European HydroBasins climate change vulnerability developed in this thesis and analysing the spatial congruence between the two datasets could provide a powerful tool in re-designing the European protected area network. Such an assessment would identify multiple catchment clusters, requiring different management strategies and priorities within a conservation planning framework, under a changing climate (i.e. catchments with high vulnerability to climate change and low probability of 'good' ecological status prioritised for inclusion in PA network and restoration). Furthermore, an explicit link could be drawn between conservation planning management targets and existing freshwater policy within the EU, facilitating a quicker and smoother transition towards a new planning framework.

The basin scale assessment of Thames WFD waterbodies generated summary maps of the risk of potential ecological change due to projected climate change and could be used as an exploratory management tool to determine the most effective restoration strategies in mitigating climate change within the Thames Basin. Furthermore, the identification of Priority River Habitats and Headwaters (outlined by Natural England) at highest risk of ecological change under climate change may see these areas prioritised for urgent mitigation and restoration strategies. This is in alignment with the latest policy developments from the 2020 European Commission biodiversity strategy and recent UK 25-year environment plan, both of which point towards an agenda based on restoration of habitats and ecosystems to a more natural state (restoring at least 15% of degraded ecosystems) (EC, 2011, HM_Government, 2018). Furthermore, the exploratory management tool developed in this thesis could be augmented through the application of research conducted within Work Package 6 of MARS, which calculated levels of stressor mitigation (MARS, 2018). Such quantification of the specific effort required to achieve management targets (i.e. cross the 'good' - 'moderate' threshold) would prove a powerful tool in estimating the cost and determining the efficacy of specific restoration strategies to mitigate the impacts of climate change.

One particularly promising line of future work could be to combine both approaches into determining the risk to potential changes to hydro-ecology for the United Kingdom. This could be achieved through the application of a fully-distributed hydrological model using the large number of high-resolution gridded datasets now available at the national scale, capturing the sensitivity of hydro-ecological parameters to climatic drivers throughout the UK (Prudhomme et al., 2012). Coupling this with a localised, reach-based model would enable the downscaling of broad changes in temperature and other parameters to account for localised variables (such as river morphology and riparian shading). Application of this methodology could facilitate the production of high-resolution projections of the potential risk posed by climate change for every river reach at the national scale. Such a resource would prove invaluable in generating a coherent strategy towards tackling the dynamic threat posed by climate change for river systems at the national scale.

REFERENCES

AAZAMI, J., ESMAILI SARI, A., ABDOLI, A., SOHRABI, H. & VAN DEN BRINK, P. J. J. E. M. 2015. Assessment of Ecological Quality of the Tajan River in Iran Using a Multimetric Macroinvertebrate Index and Species Traits. 56**,** 260-269.

ABELL, R., ALLAN, J. D. & LEHNER, B. 2007. Unlocking the potential of protected areas for freshwaters. *Biological Conservation,* 134**,** 48-63.

ABELL, R., THIEME, M. L., REVENGA, C., BRYER, M., KOTTELAT, M., BOGUTSKAYA, N., COAD, B., MANDRAK, N., BALDERAS, S. C., BUSSING, W., STIASSNY, M. L. J., SKELTON, P., ALLEN, G. R., UNMACK, P., NASEKA, A., NG, R., SINDORF, N., ROBERTSON, J., ARMIJO, E., HIGGINS, J. V., HEIBEL, T. J., WIKRAMANAYAKE, E., OLSON, D., LÓPEZ, H. L., REIS, R. E., LUNDBERG, J. G., SABAJ PÉREZ, M. H. & PETRY, P. 2008. Freshwater Ecoregions of the World: A New Map of Biogeographic Units for Freshwater Biodiversity Conservation. *BioScience,* 58**,** 403-414.

ABELLÁN, P., SÁNCHEZ-FERNÁNDEZ, D., VELASCO, J. & MILLÁN, A. 2007. Effectiveness of protected area networks in representing freshwater biodiversity: the case of a Mediterranean river basin (south-eastern Spain). *Aquatic Conservation: Marine and Freshwater Ecosystems,* 17**,** 361-374.

ADGER, W. N. 2006. Vulnerability. *Global Environmental Change,* 16**,** 268-281.

ADRIAENSSENS, V., GOETHALS, P. L. M., CHARLES, J. & DE PAUW, N. 2004. Application of Bayesian Belief Networks for the prediction of macroinvertebrate taxa in rivers. *Annales de Limnologie - International Journal of Limnology,* 40**,** 181-191.

ALBRECHT, C. & WILKE, T. 2009. Ancient Lake Ohrid: biodiversity and evolution. *In:* WILKE, T., VÄINÖLÄ, R. & RIEDEL, F. (eds.) *Patterns and Processes of Speciation in Ancient Lakes.* Springer Netherlands.

ALDOUS, A., FITZSIMONS, J., RICHTER, B. & BACH, L. 2011. Droughts, floods and freshwater ecosystems: evaluating climate change impacts and developing adaptation strategies. *Marine and Freshwater Research,* 62**,** 223-231.

ALEXANDER, R. B., BOYER, E. W., SMITH, R. A., SCHWARZ, G. E. & MOORE, R. B. 2007. The Role of Headwater Streams in Downstream Water Quality1. 43**,** 41-59.

ALLAN, J. D., ABELL, R., HOGAN, Z. E. B., REVENGA, C., TAYLOR, B. W., WELCOMME, R. L. & WINEMILLER, K. 2005. Overfishing of inland waters. *BioScience,* 55**,** 1041–1051.

ALLEY, R. B., MAROTZKE, J., NORDHAUS, W. D., OVERPECK, J. T., PETEET, D. M., PIELKE, R. A., PIERREHUMBERT, R. T., RHINES, P. B., STOCKER, T. F., TALLEY, L. D. & WALLACE, J. M. 2003. Abrupt Climate Change. *Science,* 299**,** 2005-2010.

ALVAREZ, D. & NICIEZA, A. G. 2005. Compensatory response 'defends' energy levels but not growth trajectories in brown trout, Salmo trutta L. *Proceedings of the Royal Society of London B: Biological Sciences,* 272**,** 601-607.

AMIS, M. A., ROUGET, M., LOTTER, M. & DAY, J. 2009. Integrating freshwater and terrestrial priorities in conservation planning. *Biological Conservation,* 142**,** 2217-2226.

ANGILLETTA, M. J. 2009. *Thermal adaptation : a theoretical and empirical synthesis,* Oxford, Oxford : Oxford University Press.

ARAÚJO, M. B., ALAGADOR, D., CABEZA, M., NOGUÉS-BRAVO, D. & THUILLER, W. 2011. Climate change threatens European conservation areas. *Ecology Letters,* 14**,** 484-492.

ARAÚJO, M. B. & WILLIAMS, P. H. 2001. The Bias of Complementarity Hotspots toward Marginal Populations. *Conservation Biology,* 15**,** 1710-1720.

ARHEIMER, B., ANDERSSON, L. & LEPISTÖ, A. 1996. Variation of nitrogen concentration in forest streams — influences of flow, seasonality and catchment characteristics. *Journal of Hydrology,* 179**,** 281-304.

ARNELL, N. W. 2011. Incorporating Climate Change Into Water Resources Planning in England and Wales1. 47**,** 541-549.

ARTHINGTON, A. H., BUNN, S. E., POFF, N. L. & NAIMAN, R. J. 2006. The challenge of providing environmental flow rules to sustain river ecosystems. *Ecological Applications,* 16**,** 1311-1318.

ARTHINGTON, A. H., NAIMAN, R. J., MCCLAIN, M. E. & NILSSON, C. 2010. Preserving the biodiversity and ecological services of rivers: new challenges and research opportunities. *Freshwater Biology,* 55**,** 1-16.

BAATTRUP-PEDERSEN, A., LARSEN, S. E., ANDERSEN, D. K., JEPSEN, N., NIELSEN, J. & RASMUSSEN, J. J. 2018. Headwater streams in the EU Water Framework Directive: Evidence-based decision support to select streams for river basin management plans. *Science of The Total Environment,* 613-614**,** 1048-1054.

BAE, D.-H., JUNG, I.-W. & LETTENMAIER, D. P. 2011. Hydrologic uncertainties in climate change from IPCC AR4 GCM simulations of the Chungju Basin, Korea. *Journal of Hydrology,* 401**,** 90-105.

BAGCHI, R., CROSBY, M., HUNTLEY, B., HOLE, D. G., BUTCHART, S. H. M., COLLINGHAM, Y., KALRA, M., RAJKUMAR, J., RAHMANI, A., PANDEY, M., GURUNG, H., TRAI, L. T., VAN QUANG, N. & WILLIS, S. G. 2013. Evaluating the effectiveness of conservation site networks under climate change: accounting for uncertainty. *Global Change Biology,* 19**,** 1236-1248.

BALIAN, E., SEGERS, H., LÉVÈQUE, C. & MARTENS, K. 2008. The Freshwater Animal Diversity Assessment: an overview of the results. *Hydrobiologia,* 595**,** 627-637.

BARTELS, R. H., BEATTY, J. C. & BARSKY, B. A. 1998. Hermite and cubic spline interpolation. *An Introduction to Splines for Use in Computer Graphics and Geometric Modelling***,** 9-17.

BASTOLA, S., MURPHY, C. & SWEENEY, J. 2011a. Evaluation of the transferability of hydrological model parameters for simulations under changed climatic conditions. *Hydrology and Earth System Sciences Discussions***,** 5891-5915.

BASTOLA, S., MURPHY, C. & SWEENEY, J. 2011b. The sensitivity of fluvial flood risk in Irish catchments to the range of IPCC AR4 climate change scenarios. *Science of The Total Environment,* 409**,** 5403-5415.

BATES, B., KUNDZEWICZ, Z. W., WU, S. & PALUTIKOF, J. 2008a. *Climate Change and Water. Technical Paper of the Intergovernmental Panel on Climate Change,* Geneva, Switzerland, Intergovernmental Panel on Climate Change (IPCC).

BATES, B. C., KUNDZEWICZ, Z. W., WU, S. & PALUTIKOF, J. P. 2008b. *Climate Change and Water. Technical Paper of the Intergovernmental Panel on Climate Change,* IPCC Secretariat, Geneva.

BEITINGER, T. L., BENNETT, W. A. & MCCAULEY, R. W. J. E. B. O. F. 2000. Temperature Tolerances of North American Freshwater Fishes Exposed to Dynamic Changes in Temperature. 58**,** 237-275.

BELL, V. A., KAY, A. L., COLE, S. J., JONES, R. G., MOORE, R. J. & REYNARD, N. S. 2012. How might climate change affect river flows across the Thames Basin? An area-wide analysis using the UKCP09 Regional Climate Model ensemble. *Journal of Hydrology,* 442-443**,** 89-104.

BENISTON, M., STEPHENSON, D. B., CHRISTENSEN, O. B., FERRO, C. A. T., FREI, C., GOYETTE, S., HALSNAES, K., HOLT, T., JYLHÄ, K., KOFFI, B., PALUTIKOF, J., SCHÖLL, R., SEMMLER, T. & WOTH, K. J. C. C. 2007. Future extreme events in European climate: an exploration of regional climate model projections. 81**,** 71-95.

BLACK, A., BRAGG, O., DUCK, R., JONES, A., ROWAN, J. & WERRITTY, A. J. A. U. M. I. T. D. H. R. A. M. S. R. S. 2000. Methods of assessing anthropogenic impacts on the hydrology of rivers and lochs. 1.

BLACK, A. R., ROWAN, J. S., DUCK, R. W., BRAGG, O. M. & CLELLAND, B. E. 2005. DHRAM: a method for classifying river flow regime alterations for the EC Water Framework Directive. *Aquatic Conservation: Marine and Freshwater Ecosystems,* 15**,** 427-446.

BLOOMFIELD, J. P., BRICKER, S. H. & NEWELL, A. J. 2011. Some relationships between lithology, basin form and hydrology: a case study from the Thames basin, UK. 25**,** 2518-2530.

BOCK, A. R., HAY, L. E., MCCABE, G. J., MARKSTROM, S. L. & ATKINSON, R. D. 2018. Do Downscaled General Circulation Models Reliably Simulate Historical Climatic Conditions? *Earth Interactions,* 22**,** 1-22.

BOISNEAU, C., MOATAR, F., BODIN, M. & BOISNEAU, P. 2008. Does global warming impact on migration patterns and recruitment of Allis shad (Alosa alosa L.) young of the year in the Loire River, France? *Hydrobiologia,* 602**,** 179-186.

BONDEAU, A., SMITH, P. C., ZAEHLE, S., SCHAPHOFF, S., LUCHT, W., CRAMER, W., GERTEN, D., LOTZE-CAMPEN, H., MÜLLER, C., REICHSTEIN, M. & SMITH, B. 2007. Modelling the role of agriculture for the 20th century global terrestrial carbon balance. *Global Change Biology,* 13**,** 679-706.

BOSCARINO, B. T., RUDSTAM, L. G., MATA, S., GAL, G., JOHANNSSON, O. E. & MILLS, E. L. 2007. The effects of temperature and predator—prey interactions on the migration behavior and vertical distribution of Mysis relicta. *Limnology and Oceanography,* 52**,** 1599-1613.

BREIMAN, L. 1996. Bagging predictors. *Machine Learning,* 24**,** 123-140.

BREIMAN, L., FRIEDMAN, J.H., OLSHEN, R.A., STONE, C.J. 1984. Regression Trees. *Classifciatoin and Regression Trees.* New York: Routledge.

BROWN, C., GHILE, Y., LAVERTY, M. & LI, K. 2012. Decision scaling: Linking bottom-up vulnerability analysis with climate projections in the water sector. *Water Resources Research,* 48**,** W09537.

BROWN, C. & WILBY, R. L. 2012. An alternate approach to assessing climate risks. *Eos, Transactions American Geophysical Union,* 93**,** 401-402.

BROWN, R. D. 2000. Northern Hemisphere Snow Cover Variability and Change, 1915–97. 13**,** 2339-2355.

BUSSI, G., DADSON, S. J., PRUDHOMME, C. & WHITEHEAD, P. G. 2016a. Modelling the future impacts of climate and land-use change on suspended sediment transport in the River Thames (UK).

BUSSI, G., DADSON, S. J., PRUDHOMME, C. & WHITEHEAD, P. G. 2016b. Modelling the future impacts of climate and land-use change on suspended sediment transport in the River Thames (UK). *Journal of Hydrology,* 542**,** 357-372.

BUSSI, G., JANES, V., WHITEHEAD, P. G., DADSON, S. J. & HOLMAN, I. P. 2017. Dynamic response of land use and river nutrient concentration to long-term climatic changes. *Science of the Total Environment,* 590**,** 818-831.

BUSSI, G., WHITEHEAD, P. G., BOWES, M. J., READ, D. S., PRUDHOMME, C. & DADSON, S. J. 2016c. Impacts of climate change, land-use change and phosphorus reduction on phytoplankton in the River Thames (UK). *Science of The Total Environment,* 572**,** 1507-1519.

CAISSIE, D. 2006. The thermal regime of rivers: a review. *Freshwater Biology,* 51**,** 1389-1406.

CAMPBELL GRANT, E. H., LOWE, W. H. & FAGAN, W. F. 2007. Living in the branches: population dynamics and ecological processes in dendritic networks. *Ecology Letters,* 10**,** 165-175.

CARLYLE, G. C. & HILL, A. R. 2001. Groundwater phosphate dynamics in a river riparian zone: effects of hydrologic flowpaths, lithology and redox chemistry. *Journal of Hydrology,* 247**,** 151-168.

CARRIZO, S. F., LENGYEL, S., KAPUSI, F., SZABOLCS, M., KASPERIDUS, H. D., SCHOLZ, M., MARKOVIC, D., FREYHOF, J., CID, N., CARDOSO, A. C. & DARWALL, W. 2017. Critical catchments for freshwater biodiversity conservation in Europe: identification, prioritisation and gap analysis. *Journal of Applied Ecology,* 54**,** 1209-1218.

CEH. 2015. *National River Flow Archive* [Online]. Available: http://nrfa.ceh.ac.uk/ [Accessed].

CHAO, B. F. 1995. Anthropogenic impact on global geodynamics due to reservoir water impoundment. *Geophysical Research Letters,* 22**,** 3529-3532.

CHIN, A., KYNE, P. M., WALKER, T. I. & MCAULEY, R. B. 2010. An integrated risk assessment for climate change: analysing the vulnerability of sharks and rays on Australia's Great Barrier Reef. *Global Change Biology,* 16**,** 1936-1953.

CHOW, V. T. 1959. *Open-channel hydraulics,* New York, McGraw-Hill.

CHRISTENSEN, J. H. & CHRISTENSEN, O. B. J. C. C. 2007. A summary of the PRUDENCE model projections of changes in European climate by the end of this century. 81**,** 7-30.

CHRISTIE, M. & RAYMENT, M. 2012. An economic assessment of the ecosystem service benefits derived from the SSSI biodiversity conservation policy in England and Wales. *Ecosystem Services,* 1**,** 70-84.

CHRISTIERSON, B. V., VIDAL, J.-P. & WADE, S. D. 2012. Using UKCP09 probabilistic climate information for UK water resource planning. *Journal of Hydrology,* 424-425**,** 48-67.

CLEMENTS, W. H. 1999. METAL TOLERANCE AND PREDATOR–PREY INTERACTIONS IN BENTHIC MACROINVERTEBRATE STREAM COMMUNITIES. 9**,** 1073-1084.

CLEMENTS, W. H., FARRIS, J. L., CHERRY, D. S. & CAIRNS, J. 1989. The influence of water quality on macroinvertebrate community responses to copper in outdoor experimental streams. *Aquatic Toxicology,* 14**,** 249-262.

COMER, P., YOUNG, B., SCHULZ, K., KITTEL, G., UNNASCH, B., BRAUN, D., HAMMERSON, G., SMART, L., HAMILTON, H. & AUER, S. 2012. Climate Change Vulnerability and Adaptation Strategies for Natural Communities: Piloting methods in the Mojave and Sonoran deserts. Report to the US Fish and Wildlife Service. NatureServe, Arlington, VA. *iii Table of Contents Executive Summary,* 1**,** 3.

COMTE, L., BUISSON, L., DAUFRESNE, M. & GRENOUILLET, G. 2013. Climate-induced changes in the distribution of freshwater fish: observed and predicted trends. *Freshwater Biology,* 58**,** 625-639.

CONNOLLY, N. M., CROSSLAND, M. R. & PEARSON, R. G. 2004. Effect of low dissolved oxygen on survival, emergence, and drift of tropical stream macroinvertebrates. *Journal of the North American Benthological Society,* 23**,** 251-270.

COX, P. & STEPHENSON, D. 2007. A Changing Climate for Prediction. *Science,* 317**,** 207-208.

CROSSMAN, J., BRADLEY, C., BOOMER, I. & MILNER, A. 2011. Water Flow Dynamics of Groundwater-Fed Streams and Their Ecological Significance in a Glacierized Catchment. *Arctic, Antarctic, and Alpine Research,* 43**,** 364-379.

CROSSMAN, J., FUTTER, M. N., ONI, S. K., WHITEHEAD, P. G., JIN, L., BUTTERFIELD, D., BAULCH, H. M. & DILLON, P. J. 2013a. Impacts of climate change on hydrology and water quality: Future proofing management strategies in the Lake Simcoe watershed, Canada. *Journal of Great Lakes Research,* 39**,** 19-32.

CROSSMAN, J., WHITEHEAD, P. G., FUTTER, M., JIN, L., SHAHGEDANOVA, M., CASTELLAZZI, M. & WADE, A. J. 2013b. The interactive responses of water quality and hydrology to changes in multiple stressors, and implications for the long-term effective management of phosphorus. *Science of the Total Environment,* 454**,** 230-244.

CROSSMAN, J., WHITEHEAD, P. G., FUTTER, M. N., JIN, L., SHAHGEDANOVA, M., CASTELLAZZI, M. & WADE, A. J. 2013c. The interactive responses of water quality and hydrology to changes in multiple stressors, and implications for the long-term effective management of phosphorus. *Science of The Total Environment,* 454–455**,** 230-244.

DALLAS, H. & ROSS-GILLESPIE, V. 2015. Sublethal effects of temperature on freshwater organisms, with special reference to aquatic insects. *Water SA,* 41**,** 712-726.

DATRY, T., LAMOUROUX, N., THIVIN, G., DESCLOUX, S. & BAUDOIN, J. M. 2015. Estimation of Sediment Hydraulic Conductivity in River Reaches and its Potential Use to Evaluate Streambed Clogging. *River Research and Applications,* 31**,** 880-891.

DAVY-BOWKER, J., CLARKE, R. T., CORBIN, T. A., VINCENT, H. M., PRETTY, J., HAWCZAK, A., MURPHY, J. F. & JONES, I. 2008. River Invertebrate Classification Tool. Edinburgh, Scotland.

DAWSON, T. P., JACKSON, S. T., HOUSE, J. I., PRENTICE, I. C. & MACE, G. M. 2011. Beyond Predictions: Biodiversity Conservation in a Changing Climate. *Science,* 332**,** 53-58.

DE ZWART, D., DYER, S. D., POSTHUMA, L. & HAWKINS, C. P. 2006. PREDICTIVE MODELS ATTRIBUTE EFFECTS ON FISH ASSEMBLAGES TO TOXICITY AND HABITAT ALTERATION. 16**,** 1295-1310.

DEAN, S., FREER, J., BEVEN, K., WADE, A. J. & BUTTERFIELD, D. 2009. Uncertainty assessment of a process-based integrated catchment model of phosphorus. *Stochastic Environmental Research and Risk Assessment,* 23**,** 991-1010.

DEFRA 2002. Waste water collection and treatment, and disposal of sewage sludge. London: Department for Environment, Food and Rural Affairs

DEFRA 2011. Fertiliser Manual RB209.

DEFRA 2012. Waste water treatment in the United Kingdom DEFRA.

DEFRA. 2015a. *Agricultural Census Database. University of Edinburgh;* [Online]. Available: http://edina.ac.uk/agcensus/description.html [Accessed].

DEFRA. 2015b. *Soil Nutrient Balances* [Online]. Available: https://www.gov.uk/government/uploads/system/uploads/attachment_data/file/447625/soilnutrientbalances-UK-2014-23jul15.pdf [Accessed].

DEFRA. 2015c. *UK deposition maps* [Online]. Available: http://pollutantdeposition.defra.gov.uk/image/tid/7 [Accessed].

DESMET, P. & COWLING, R. M. 2004. Using the species-area relationship to set baseline targets for conservation. *Ecology and Society* [Online], 9. Available: http://www.ecologyandsociety.org/vol9/iss2/art11/

DIERCKX, P. 1995. *Curve and surface fitting with splines*, Oxford University Press.

DÖLL, P., KASPAR, F. & LEHNER, B. 2003. A global hydrological model for deriving water availability indicators: model tuning and validation. *Journal of Hydrology,* 270**,** 105-134.

DOLLAR, E. S. J., NICOLSON, C. R., BROWN, C. A., TURPIE, J. K., JOUBERT, A. R. TURTON, A. R., GROBLER, D. F., PIENAAR, H. H., EWART-SMITH J. AND MANYAKA, S. M. 2010. Development of the South African Water Resource Classification System (WRCS): a tool towards the sustainable, equitable and efficient use of water resources in a developing country. *Water Policy,* 12**,** 479-499.

DOMISCH, S., ARAÚJO, M. B., BONADA, N., PAULS, S. U., JÄHNIG, S. C. & HAASE, P. 2013. Modelling distribution in European stream macroinvertebrates under future climates. *Global Change Biology,* 19**,** 752-762.

DOWER, J. 1945. Report to the Government on National Parks in England and Wales. The National Archives, Kew.

DRIVER, A., MAZE, K., ROUGET, M., LOMBARD, A. T., NEL, J., TURPIE, J. K., COWLING, R. M., DESMET, P., GOODMAN, P. & HARRIS, J. 2005. National Spatial Biodiversity Assessment 2004: priorities for biodiversity conservation in South Africa.

DUDGEON, D., ARTHINGTON, A. H., GESSNER, M. O., KAWABATA, Z.-I., KNOWLER, D. J., EACUTE, ECIRC, QUE, C., NAIMAN, R. J., PRIEUR-RICHARD, A.-H., EGRAVE, NE, SOTO, D., STIASSNY, M. L. J. & SULLIVAN, C. A. 2006. Freshwater biodiversity: importance, threats, status and conservation challenges. *Biological Reviews,* 81**,** 163-182.

DUNBAR, M. J., PEDERSEN, M. L., CADMAN, D., EXTENCE, C., WADDINGHAM, J., CHADD, R. & LARSEN, S. E. 2010. River discharge and local-scale physical habitat influence macroinvertebrate LIFE scores. *Freshwater Biology,* 55**,** 226-242.

DURANCE, I. & ORMEROD, S. J. 2007. Climate change effects on upland stream macroinvertebrates over a 25-year period. 13**,** 942-957.

DYER, F., ELSAWAH, S., CROKE, B., GRIFFITHS, R., HARRISON, E., LUCENA-MOYA, P. & JAKEMAN, A. 2014. The effects of climate change on ecologically-relevant flow regime and water quality attributes. *Stochastic Environmental Research and Risk Assessment,* 28**,** 67-82.

EA 2014a. Thames catchment abstraction licensing strategy. Environment Agency.

EA 2014b. WFD Surface Water Management Catchments Cycle 2. Environment Agency.

EA 2015a. National Evidence and Data Report. *Update to the river basin management plans in England.* Environment Agency.

EA 2015b. Thames river basin district river basin management plan. DEFRA.

EASDALE, M., AND CROAL, A. 2007. River Invertebrate Classification Tool – System Developments - Detailed Functional Specification. *SNIFFER project WFD72ci.*

EC 2011. Our life insurance, our natural capital: an EU biodiversity strategy to 2020. European Commission, Brussels.

EL-KHOURY, A., SEIDOU, O., LAPEN, D. R., QUE, Z., MOHAMMADIAN, M., SUNOHARA, M. & BAHRAM, D. 2015. Combined impacts of future climate and land use changes on discharge, nitrogen and phosphorus loads for a Canadian river basin. *Journal of Environmental Management,* 151**,** 76-86.

ELSER, J. J., BRACKEN, M. E. S., CLELAND, E. E., GRUNER, D. S., HARPOLE, W. S., HILLEBRAND, H., NGAI, J. T., SEABLOOM, E. W., SHURIN, J. B. & SMITH, J. E. 2007. Global analysis of nitrogen and phosphorus limitation of primary producers in freshwater, marine and terrestrial ecosystems. 10**,** 1135-1142.

ELSNER, J. B., KOSSIN, J. P. & JAGGER, T. H. 2008. The increasing intensity of the strongest tropical cyclones. *Nature,* 455**,** 92.

EU-STAR 2004a. Methods of biological sampling: guidance on hand-net sampling of aquatic benthic macro-invertebrates. *Water quality. Methods for biological testing.*

EU-STAR 2004b. Water quality. Sampling in deep water for macro-invertebrates. *Guidance on the use of colonization, qualitative and quantitative samplers*

EUROPEAN_COMMISSION 2012. United Kingdom. *Implementation of the Water Framework Directive (2000/60/EC) River Basin Management Plans.* Brussels: European Union.

EYLES, N. & YOUNG, G. M. 1994. Geodynamic controls on glaciation in Earth history. *In:* DOMACK, E. W., YOUNG, G. M., FAIRCHILD, I., MILLER, J. M. G., DEYNOUX, M. & EYLES, N. (eds.) *Earth's Glacial Record.* Cambridge: Cambridge University Press.

FAUSCH, K. D., TORGERSEN, C. E., BAXTER, C. V. & LI, H. W. 2002. Landscapes to riverscapes: bridging the gap between research and conservation of stream fishes. *BioScience,* 52**,** 483–498.

FEELY, R., DONEY, S. & COOLEY, S. 2009. *Ocean Acidification: Present Conditions and Future Changes in a High-CO2 World*.

FERRIER, R. C., WHITEHEAD, P. G., SEFTON, C., EDWARDS, A. C. & PUGH, K. 1995. Modelling impacts of land use change and climate change on nitrate-nitrogen in the River Don, North East Scotland. *Water Research,* 29**,** 1950-1956.

FERRIER, S. 2002. Mapping Spatial Pattern in Biodiversity for Regional Conservation Planning: Where to from Here? *Systematic Biology,* 51**,** 331-363.

FERRIER, S., PRESSEY, R. L. & BARRETT, T. W. 2000. A new predictor of the irreplaceability of areas for achieving a conservation goal, its application to real-world planning, and a research agenda for further refinement. *Biological Conservation,* 93**,** 303-325.

FODEN, W. B., BUTCHART, S. H. M., STUART, S. N., VIÉ, J.-C., AKÇAKAYA, H. R., ANGULO, A., DEVANTIER, L. M., GUTSCHE, A., TURAK, E., CAO, L., DONNER, S. D., KATARIYA, V., BERNARD, R., HOLLAND, R. A., HUGHES, A. F., O'HANLON, S. E., GARNETT, S. T., ŞEKERCIOĞLU, Ç. H. & MACE, G. M. 2013. Identifying the World's Most Climate Change Vulnerable Species: A Systematic Trait-Based Assessment of all Birds, Amphibians and Corals. *PLoS ONE,* 8**,** e65427.

FOOD & AGRICULTURE ORGANIZATION OF THE UNITED, N. 2002. The State of World Fisheries and Aquaculture 2002. *Rome: FAO Fisheries Department.*

FUTTER, M. N., ERLANDSSON, M. A., BUTTERFIELD, D., WHITEHEAD, P. G., ONI, S. K. & WADE, A. J. 2014. PERSiST: a flexible rainfall-runoff modelling toolkit for use with the INCA family of models. *Hydrol. Earth Syst. Sci.,* 18**,** 855-873.

GALLOPÍN, G. C. 2006. Linkages between vulnerability, resilience, and adaptive capacity. *Global Environmental Change,* 16**,** 293-303.

GARDINER, J., THOMSON, K. & NEWSON, M. 1994. Integrated watershed/river catchment planning and management: a comparison of selected Canadian and United Kingdom experiences. *Journal of Environmental Planning and Management,* 37**,** 53-67.

GARDINER, J. L. 1988. Environmentally sound river engineering: Examples from the thames catchment. *Regulated Rivers: Research & Management,* 2**,** 445-469.

GARDNER, C. M. K., COOPER, D. M. & HUGHES, S. 2002. Phosphorus in soils and field drainage water in the Thame catchment, UK. *Science of The Total Environment,* 282-283**,** 253-262.

GENTRY, L. E., DAVID, M. B., ROYER, T. V., MITCHELL, C. A. & STARKS, K. M. 2007. Phosphorus Transport Pathways to Streams in Tile-Drained Agricultural Watersheds. 36**,** 408-415.

GERGIS, J. & FOWLER, A. 2009. A history of ENSO events since A.D. 1525: implications for future climate change. *Climatic Change,* 92**,** 343-387.

GIBSON, C. A., MEYER, J. L., POFF, N. L., HAY, L. E. & GEORGAKAKOS, A. 2005. Flow regime alterations under changing climate in two river basins: implications for freshwater ecosystems. *River Research and Applications,* 21**,** 849-864 %U http://dx.doi.org/10.1002/rra.855.

GILLETT, N. P., FYFE, J. C. & PARKER, D. E. 2013. Attribution of observed sea level pressure trends to greenhouse gas, aerosol, and ozone changes. 40**,** 2302-2306.

GILLETT, N. P. & THOMPSON, D. W. J. 2003. Simulation of recent Southern Hemisphere climate change. *Science,* 302**,** 273-275.

GISTEMP 2018. GISS Surface Temperature Analysis (GISTEMP). NASA Goddard Institute for Space Studies.

GLENDELL, M., EXTENCE, C., CHADD, R. & BRAZIER, R. E. 2014. Testing the pressure-specific invertebrate index (PSI) as a tool for determining ecologically relevant targets for reducing sedimentation in streams. *Freshwater Biology,* 59**,** 353-367.

GORDON, C., COOPER, C., SENIOR, C. A., BANKS, H., GREGORY, J. M., JOHNS, T. C., MITCHELL, J. F. B. & WOOD, R. A. J. C. D. 2000. The simulation of SST, sea ice extents and ocean heat transports in a version of the Hadley Centre coupled model without flux adjustments. 16**,** 147-168.

GRIZZETTI, B., PISTOCCHI, A., LIQUETE, C., UDIAS, A., BOURAOUI, F. & VAN DE BUND, W. 2017. Human pressures and ecological status of European rivers. *Scientific Reports,* 7**,** 205.

GROOMBRIDGE, B. & JENKINS, M. D. 2002. *World atlas of biodiversity: Earth's living resources in the 21st century,* Berkeley, California; London, University of California Press.

GUO, D., WESTRA, S. & MAIER, H. R. 2018. An inverse approach to perturb historical rainfall data for scenario-neutral climate impact studies. *Journal of Hydrology,* 556**,** 877-890.

GUPTA, H., SOROOSHIAN, S. & YAPO, P. 1999. Status of Automatic Calibration for Hydrologic Models: Comparison with Multilevel Expert Calibration. *Journal of Hydrologic Engineering,* 4**,** 135-143.

GUSE, B., KAIL, J., RADINGER, J., SCHRÖDER, M., KIESEL, J., HERING, D., WOLTER, C. & FOHRER, N. 2015. Eco-hydrologic model cascades: Simulating land use and climate change impacts on hydrology, hydraulics and habitats for fish and macroinvertebrates. *Science of The Total Environment,* 533**,** 542-556.

HADDELAND, I., CLARK, D. B., FRANSSEN, W., LUDWIG, F., VOß, F., ARNELL, N. W., BERTRAND, N., BEST, M., FOLWELL, S., GERTEN, D., GOMES, S., GOSLING, S. N., HAGEMANN, S., HANASAKI, N., HARDING, R., HEINKE, J., KABAT, P., KOIRALA, S., OKI, T., POLCHER, J., STACKE, T., VITERBO, P., WEEDON, G. P. & YEH, P. 2011. Multimodel Estimate of the Global Terrestrial Water Balance: Setup and First Results. *Journal of Hydrometeorology,* 12**,** 869-884.

HAGEMANN, S., CHEN, C., HAERTER, J. O., HEINKE, J., GERTEN, D. & PIANI, C. 2011. Impact of a Statistical Bias Correction on the Projected Hydrological Changes Obtained from Three GCMs and Two Hydrology Models. *Journal of Hydrometeorology,* 12**,** 556-578.

HALL, J. W., WATTS, G., KEIL, M., DE VIAL, L., STREET, R., CONLAN, K., O'CONNELL, P. E., BEVEN, K. J. & KILSBY, C. G. 2012. Towards risk-based water resources planning in England and Wales under a changing climate. 26**,** 118-129.

HALL, M. H. P. & FAGRE, D. B. 2003. Modeled Climate-Induced Glacier Change in Glacier National Park, 1850–2100. *BioScience,* 53**,** 131-140.

HAMBY, D. M. 1994. A review of techniques for parameter sensitivity analysis of environmental models. *Environmental Monitoring and Assessment,* 32**,** 135-154.

HANNAH, D. M. & GARNER, G. 2015. River water temperature in the United Kingdom: Changes over the 20th century and possible changes over the 21st century. *Progress in Physical Geography: Earth and Environment,* 39**,** 68-92.

HANNAH, D. M., MALCOLM, I. A., SOULSBY, C. & YOUNGSON, A. F. 2008a. A comparison of forest and moorland stream microclimate, heat exchanges and thermal dynamics. *Hydrological Processes,* 22**,** 919-940.

HANNAH, D. M., WEBB, B. W. & NOBILIS, F. 2008b. River and stream temperature: dynamics, processes, models and implications. *Hydrological Processes,* 22**,** 899-901.

HARPER, M. P. & PECKARSKY, B. L. 2006. Emergence cues of a mayfly in a high-altitude stream ecosystem: Potential response to climate change. *Ecological Applications,* 16**,** 612-621.

HAWKESWORTH, D. L. & KALIN-ARROYO, M. T. 1995. Magnitude and distribution of biodiversity. *In:* HEYWOOD, V. H. & WATSON, R. T. (eds.) *Global biodiversity assessment.* Cambridge: Cambridge University Press.

HAY, L. E., WILBY, R. L. & LEAVESLEY, G. H. 2000. A comparison of delta change and downscaled GCM scenarios for three mountainous basins in the United States. *JAWRA Journal of the American Water Resources Association,* 36**,** 387-397.

HEIN, C. L., ÖHLUND, G. & ENGLUND, G. 2011. Dispersal through stream networks: modelling climate-driven range expansions of fishes. *Diversity and Distributions,* 17**,** 641-651.

HEINO, J., MUOTKA, T. & PAAVOLA, R. 2003. Determinants of macroinvertebrate diversity in headwater streams: regional and local influences. *Journal of Animal Ecology,* 72**,** 425-434.

HEINO, J., VIRKKALA, R. & TOIVONEN, H. 2009. Climate change and freshwater biodiversity: Detected patterns, future trends and adaptations in northern regions. *Biological Reviews,* 84**,** 39-54.

HELDT, S., RODRÍGUEZ-DE-FRANCISCO, J. C., DOMBROWSKY, I., FELD, C. K. & KARTHE, D. 2017. Is the EU WFD suitable to support IWRM planning in non-European countries? Lessons learnt from

the introduction of IWRM and River Basin Management in Mongolia. *Environmental Science & Policy,* 75**,** 28-37.

HERING, D., JOHNSON, R. K., KRAMM, S., SCHMUTZ, S., SZOSZKIEWICZ, K. & VERDONSCHOT, P. F. M. 2006. Assessment of European streams with diatoms, macrophytes, macroinvertebrates and fish: a comparative metric-based analysis of organism response to stress. 51**,** 1757-1785.

HERMOSO, V., FILIPE, A. F., SEGURADO, P. & BEJA, P. 2018. Freshwater conservation in a fragmented world: Dealing with barriers in a systematic planning framework. *Aquatic Conservation: Marine and Freshwater Ecosystems,* 28**,** 17-25.

HERON, S. F., EAKIN, C. M., DOUVERE, F., ANDERSON, K. L., DAY, J. C., GEIGER, E., HOEGH-GULDBERG, O., VAN HOOIDONK, R., HUGHES, T. & MARSHALL, P. 2017. Impacts of climate change on World Heritage coral reefs: A first global scientific assessment.

HICKLING, R., ROY, D. B., HILL, J. K. & THOMAS, C. D. 2005. A northward shift of range margins in British Odonata. *Global Change Biology,* 11**,** 502-506.

HIJMANS, R. J., CAMERON, S. E., PARRA, J. L., JONES, P. G. & JARVIS, A. 2005. Very high resolution interpolated climate surfaces for global land areas. *International Journal of Climatology,* 25**,** 1965-1978.

HM_GOVERNMENT 2018. UK 25-year environment plan. UK Government, London.

HOANG, T. H., LOCK, K., MOUTON, A. & GOETHALS, P. L. M. 2010. Application of classification trees and support vector machines to model the presence of macroinvertebrates in rivers in Vietnam. *Ecological Informatics,* 5**,** 140-146.

HOEGH-GULDBERG, O. & BRUNO, J. F. 2010. The Impact of Climate Change on the World's Marine Ecosystems. *Science,* 328**,** 1523-1528.

HOEGH-GULDBERG, O., HUGHES, L., MCINTYRE, S., LINDENMAYER, D. B., PARMESAN, C., POSSINGHAM, H. P. & THOMAS, C. D. 2008. Assisted Colonization and Rapid Climate Change. *Science,* 321**,** 345-346.

HOLLAND, R. A., DARWALL, W. R. T. & SMITH, K. G. 2012. Conservation priorities for freshwater biodiversity: The Key Biodiversity Area approach refined and tested for continental Africa. *Biological Conservation,* 148**,** 167-179.

HUSSAIN, Q. A. & PANDIT, A. K. 2012. Macroinvertebrates in streams: A review of some ecological factors. *International Journal of Fisheries and Aquaculture,* 4**,** 114-123.

IMHOLT, C., GIBBINS, C. N., MALCOLM, I. A., LANGAN, S. & SOULSBY, C. 2010. Influence of riparian cover on stream temperatures and the growth of the mayfly Baetis rhodani in an upland stream. *Aquatic Ecology,* 44**,** 669-678.

IMHOLT, C., MALCOLM, I. A., BACON, P. J., GIBBINS, C. N., SOULSBY, C., MILES, M. & FRYER, R. J. 2011. Does diurnal temperature variability affect growth in juvenile Atlantic salmon Salmo salar? *Journal of fish biology,* 78**,** 436-448.

IMPSON, N. D., BILLS, I. R. & CAMBRAY, J. A. 2002. A conservation plan for the unique and highly threatened freshwater fishes of the Cape Floral Kingdom. *Conservation of Freshwater Fishes: Options for the Future. Oxford: Fishing News Books, Blackwell Science***,** 432–440.

IPCC 2007. *Climate Change 2007 Synthesis Report: Contribution of Working Groups I, II and III to the Fourth Assessment Report of the Intergovernmental Panel on Climate Change,* Geneva, Switzerland, Intergovernmental Panel on Climate Change.

IPCC 2014a. *Climate Change 2014: Impacts, Adaptation, and Vulnerability. Part A: Global and Sectoral Aspects. Contribution of Working Group II to the Fifth Assessment Report of the Intergovernmental Panel on Climate Change [Field, C.B., V.R. Barros, D.J. Dokken, K.J. Mach, M.D. Mastrandrea, T.E. Bilir, M. Chatterjee, K.L. Ebi, Y.O. Estrada, R.C. Genova, B. Girma, E.S. Kissel, A.N. Levy, S. MacCracken, P.R. Mastrandrea, and L.L. White (eds.)],* Cambridge, United Kingdom and New York, NY, USA, Cambridge University Press.

IPCC 2014b. Summary for Policymakers. *In:* FIELD, C. B., BARROS, V. R., DOKKEN, D. J., MACH, K. J., MASTRANDREA, M. D., BILIR, T. E., CHATTERJEE, M., EBI, K. L., ESTRADA, Y. O., GENOVA, R. C., GIRMA, B., KISSEL, E. S., LEVY, A. N., MACCRACKEN, S., MASTRANDREA, P. R. & WHITE, L. L. (eds.) *Climate Change 2014: Impacts, Adaptation, and Vulnerability. Part A: Global and Sectoral Aspects. Contribution of Working Group II to the Fifth Assessment Report of the*

Intergovernmental Panel on Climate Change. Cambridge, United Kingdom, and New York, NY, USA: Cambridge University Press.

IUCN. 2014. Guidelines for Using the IUCN Red List Categories and Criteria. Version 11. Available: http://www.iucnredlist.org/documents/RedListGuidelines.pdf [Accessed 22nd April 2014].

JACKSON-BLAKE, L. A. & STARRFELT, J. 2015. Do higher data frequency and Bayesian auto-calibration lead to better model calibration? Insights from an application of INCA-P, a process-based river phosphorus model. *Journal of Hydrology,* 527**,** 641-655.

JAMES, A. B. W., DEWSON, Z. S. & DEATH, R. G. 2008. Do stream macroinvertebrates use instream refugia in response to severe short-term flow reduction in New Zealand streams? *Freshwater Biology,* 53**,** 1316-1334.

JARVIE, H. P., NEAL, C., WILLIAMS, R. J., NEAL, M., WICKHAM, H. D., HILL, L. K., WADE, A. J., WARWICK, A. & WHITE, J. 2002. Phosphorus sources, speciation and dynamics in the lowland eutrophic River Kennet, UK. *Science of The Total Environment,* 282-283**,** 175-203.

JARVIE, H. P., NEAL, C. & WITHERS, P. J. A. 2006. Sewage-effluent phosphorus: A greater risk to river eutrophication than agricultural phosphorus? *Science of The Total Environment,* 360**,** 246-253.

JARVIE, H. P., SHARPLEY, A. N., WITHERS, P. J. A., SCOTT, J. T., HAGGARD, B. E. & NEAL, C. 2013. Phosphorus Mitigation to Control River Eutrophication: Murky Waters, Inconvenient Truths, and "Postnormal" Science. 42**,** 295-304.

JENKINS, M. 2003. Prospects for biodiversity. *Science,* 302**,** 1175.

JENSEN, A. J. 2003. Atlantic salmon (Salmo salar) in the regulated River Alta: effects of altered water temperature on parr growth. *River Research and Applications,* 19**,** 733-747.

JIN, L., WHITEHEAD, P. G. & CHOVELON, G. Modelling flow and nitrogen dynamics in the River Thames: Implication of future climate induced water vulnerability in south-east England. Third International Symposium (BHS 2010) Conference Proceeding, 2010 Newcastle, United Kingdom. British Hydrological Society, 103-109.

JIN, L., WHITEHEAD, P. G., FUTTER, M. N. & LU, Z. 2012. Modelling the impacts of climate change on flow and nitrate in the River Thames: assessing potential adaptation strategies. *Hydrology Research,* 43**,** 902-916.

JNCC 1989. Guidelines for selection of biological SSSIs. Nature Conservancy Council.

JOHNSON, I., SOROKIN, N., ATKINSON, C., RULE, K. & HOPE, S. J. 2007. Proposed EQS for Water Framework Directive Annex VIII substances: ammonia (un-ionised). Environment Agency.

JONES, T., PHILLIPS, B., WILLIAMS, C., PITTOCK, J. & DAVIS, T. 2003. Conserving rivers: lessons from WWF's work for integrated river basin management. *World Wildlife Fund, Gland, Switzerland*.

KATZ, R. 2010. Statistics of extremes in climate change. *Climatic Change,* 100**,** 71-76.

KAY, A. L., DAVIES, H. N., BELL, V. A. & JONES, R. G. 2009. Comparison of uncertainty sources for climate change impacts: flood frequency in England. *Climatic Change,* 92**,** 41-63.

KAY, A. L. & JONES, R. G. J. C. C. 2012. Comparison of the use of alternative UKCP09 products for modelling the impacts of climate change on flood frequency. 114**,** 211-230.

KEITH, P. 2000. The part played by protected areas in the conservation of threatened French freshwater fish. *Biological conservation,* 92**,** 265–273.

KENNARD, M. J., PUSEY, B. J., OLDEN, J. D., MACKAY, S. J., STEIN, J. L. & MARSH, N. 2010. Classification of natural flow regimes in Australia to support environmental flow management. *Freshwater Biology,* 55**,** 171-193.

KERNAN, M., BATTARBEE, R. W. & MOSS, B. 2010. *Climate Change Impacts on Freshwater Ecosystems,* Oxford, Wiley-Blackwell.

KING, J., BROWN, C. & SABET, H. 2003. A scenario-based holistic approach to environmental flow assessments for rivers. *River Research and Applications,* 19**,** 619-639.

KINGSFORD, R. T. 2011. Conservation management of rivers and wetlands under climate change – a synthesis. *Marine and Freshwater Research,* 62**,** 217-222.

KINNIBURGH, J. H. & BARNETT, M. 2010. Orthophosphate concentrations in the River Thames: reductions in the past decade. 24**,** 107-115.

KISHI, D., MURAKAMI, M., NAKANO, S. & MAEKAWA, K. 2005. Water temperature determines strength of top-down control in a stream food web. *Freshwater Biology,* 50**,** 1315-1322.

KLEIN, C. J., CHAN, A., KIRCHER, L., CUNDIFF, A. J., GARDNER, N., HROVAT, Y., SCHOLZ, A., KENDALL, B. E. & AIRAMÉ, S. 2008. Striking a Balance between Biodiversity Conservation and Socioeconomic Viability in the Design of Marine Protected Areas. *Conservation Biology,* 22**,** 691-700.

KNOUFT, J. H. & FICKLIN, D. L. 2017. The Potential Impacts of Climate Change on Biodiversity in Flowing Freshwater Systems. *Annual Review of Ecology, Evolution, and Systematics,* 48**,** 111-133.

KOUTROULIS, A. G., PAPADIMITRIOU, L. V., GRILLAKIS, M. G., TSANIS, I. K., WYSER, K. & BETTS, R. A. 2018. Freshwater vulnerability under high end climate change. A pan-European assessment. *Science of The Total Environment,* 613-614**,** 271-286.

KUNDZEWICZ, Z. W., MATA, L. J., ARNELL, N. W., DÖLL, P., JIMENEZ, B., MILLER, K., OKI, T., ŞEN, Z. & SHIKLOMANOV, I. 2008. The implications of projected climate change for freshwater resources and their management. *Hydrological Sciences Journal,* 53**,** 3-10.

KUNDZEWICZ, Z. W. & STAKHIV, E. Z. 2010. Are climate models "ready for prime time" in water resources management applications, or is more research needed? *Hydrological Sciences Journal,* 55**,** 1085-1089.

LAIZÉ, C. L. R., ACREMAN, M. C., SCHNEIDER, C., DUNBAR, M. J., HOUGHTON-CARR, H. A., FLÖRKE, M. & HANNAH, D. M. 2014. Projected flow alteration and ecological risk for pan-european rivers. *River Research and Applications,* 30**,** 299-314.

LASSALLE, G., BÉGUER, M., BEAULATON, L. & ROCHARD, E. 2008. Diadromous fish conservation plans need to consider global warming issues: An approach using biogeographical models. *Biological Conservation,* 141**,** 1105-1118.

LAWRENCE, J. E., LUNDE, K. B., MAZOR, R. D., BÊCHE, L. A., MCELRAVY, E. P. & RESH, V. H. 2010. Long-term macroinvertebrate responses to climate change: implications for biological assessment in mediterranean-climate streams. 29**,** 1424-1440.

LAZAR, A. N., BUTTERFIELD, D., FUTTER, M. N., RANKINEN, K., THOUVENOT-KORPPOO, M., JARRITT, N., LAWRENCE, D. S. L., WADE, A. J. & WHITEHEAD, P. G. 2010. An assessment of the fine sediment dynamics in an upland river system: INCA-Sed modifications and implications for fisheries. *Science of The Total Environment,* 408**,** 2555-2566.

LEAF, S. 2018. Taking the P out of pollution: an English perspective on phosphorus stewardship and the Water Framework Directive. 32**,** 4-8.

LEOPOLD, L. B. & MADDOCK JR, T. 1953. The hydraulic geometry of stream channels and some physiographic implications. *Professional Paper.* - ed.

LEPORI, F. & MALMQVIST, B. 2007. Predictable changes in trophic community structure along a spatial disturbance gradient in streams. *Freshwater Biology,* 52**,** 2184-2195.

LÉVÊQUE, C. & BALIAN, E. 2005. Conservation of freshwater biodiversity: does the real world meet scientific dreams? *Hydrobiologia,* 542**,** 23-26.

LICENCE, O. G. 2015. Contains OS data © Crown copyright [50m DEM]

LIERMANN, C. R., NILSSON, C., ROBERTSON, J. & NG, R. Y. 2012. Implications of Dam Obstruction for Global Freshwater Fish Diversity. *BioScience,* 62**,** 539-548.

LINDSTRÖM, G., JOHANSSON, B., PERSSON, M., GARDELIN, M. & BERGSTRÖM, S. 1997. Development and test of the distributed HBV-96 hydrological model. *Journal of Hydrology,* 201**,** 272-288.

LINKE, S., NORRIS, R. H. & PRESSEY, R. L. 2008. Irreplaceability of river networks: towards catchment-based conservation planning. *Journal of Applied Ecology,* 45**,** 1486-1495.

LINKE, S., TURAK, E. & NEL, J. 2011. Freshwater conservation planning: the case for systematic approaches. *Freshwater Biology,* 56**,** 6-20.

LIRA-NORIEGA, A., AGUILAR, V., ALARCÓN, J., KOLB, M., URQUIZA-HAAS, T., GONZÁLEZ-RAMÍREZ, L., TOBÓN, W. & KOLEFF, P. 2015. Conservation planning for freshwater ecosystems in Mexico. *Biological Conservation,* 191**,** 357-366.

LUBCHENCO, J., PALUMBI, S. R., GAINES, S. D. & ANDELMAN, S. 2003. Plugging a hole in the ocean: the emerging science of marine reserves. *Ecological Applications,* 13**,** S3–S7.

LUCK, G. W., CHAN, K. M. A. & FAY, J. P. 2009. Protecting ecosystem services and biodiversity in the world's watersheds. *Conservation Letters,* 2**,** 179-188.

LUNDBERG, J. G., KOTTELAT, M., SMITH, G. R., STIASSNY, M. L. J. & GILL, A. C. 2000. So many fishes, so little time: an overview of recent ichthyological discovery in continental waters. *Annals of the Missouri Botanical Garden,* 87**,** 26–62.

MADSEN, H., WILSON, G. & AMMENTORP, H. C. 2002. Comparison of different automated strategies for calibration of rainfall-runoff models. *Journal of Hydrology,* 261**,** 48-59.

MALCOLM, J. R., LIU, C., NEILSON, R. P., HANSEN, L. & HANNAH, L. E. E. 2006. Global Warming and Extinctions of Endemic Species from Biodiversity Hotspots. *Conservation Biology,* 20**,** 538-548.

MALMQVIST, B. & RUNDLE, S. 2002. Threats to the running water ecosystems of the world. *Environmental Conservation,* 29**,** 134–153.

MANNING, R. 1891. On the flow of water in open channels and pipes. *Transactions of the Institution of Civil Engineers of Ireland,* 20**,** 161-207.

MANTYKA-PRINGLE, C. S., MARTIN, T. G., MOFFATT, D. B., UDY, J., OLLEY, J., SAXTON, N., SHELDON, F., BUNN, S. E. & RHODES, J. R. 2016. Prioritizing management actions for the conservation of freshwater biodiversity under changing climate and land-cover. *Biological Conservation,* 197**,** 80-89.

MARAUN, D., WETTERHALL, F., IRESON, A. M., CHANDLER, R. E., KENDON, E. J., WIDMANN, M., BRIENEN, S., RUST, H. W., SAUTER, T., THEMEßL, M., VENEMA, V. K. C., CHUN, K. P., GOODESS, C. M., JONES, R. G., ONOF, C., VRAC, M. & THIELE-EICH, I. 2010. Precipitation downscaling under climate change: Recent developments to bridge the gap between dynamical models and the end user. *Reviews of Geophysics,* 48.

MARGULES, C. R. & PRESSEY, R. L. 2000. Systematic conservation planning. *Nature,* 405**,** 243-253.

MARKOVIC, D., CARRIZO, S., FREYHOF, J., CID, N., LENGYEL, S., SCHOLZ, M., KASPERDIUS, H. & DARWALL, W. 2014a. Europe's freshwater biodiversity under climate change: distribution shifts and conservation needs. 20**,** 1097-1107.

MARKOVIC, D., CARRIZO, S., FREYHOF, J., CID, N., LENGYEL, S., SCHOLZ, M., KASPERIDUS, H. & DARWALL, W. 2014b. Europe's freshwater biodiversity under climate change: distribution shifts and conservation needs. *Diversity and Distributions***,** (in press).

MARKOVIC, D., CARRIZO, S. F., KÄRCHER, O., WALZ, A. & DAVID, J. N. W. 2017. Vulnerability of European freshwater catchments to climate change. 23**,** 3567-3580.

MARKOVIC, D., SCHARFENBERGER, U., SCHMUTZ, S., PLETTERBAUER, F. & WOLTER, C. 2013. Variability and alterations of water temperatures across the Elbe and Danube River Basins. *Climatic Change,* 119**,** 375-389.

MARS 2018. Managing Aquatic ecosystems and water Resources under multiple Stress: Final Report. European Union 7th Framework Programme.

MAXWELL, R. M. & KOLLET, S. J. 2008. Interdependence of groundwater dynamics and land-energy feedbacks under climate change. *Nature Geoscience,* 1**,** 665.

MCCLUNEY, K. E., POFF, N. L., PALMER, M. A., THORP, J. H., POOLE, G. C., WILLIAMS, B. S., WILLIAMS, M. R. & BARON, J. S. 2014. Riverine macrosystems ecology: sensitivity, resistance, and resilience of whole river basins with human alterations. *Frontiers in Ecology and the Environment,* 12**,** 48-58.

MCGREGOR, G., PETTS, G. E., GURNELL, A. M. & MILNER, A. M. 1995. Sensitivity of alpine stream ecosystems to climate change and human impacts. *Aquatic Conservation: Marine and Freshwater Ecosystems,* 5**,** 233-247.

MCMANUS, J. F., FRANCOIS, R., GHERARDI, J. M., KEIGWIN, L. D. & BROWN-LEGER, S. 2004. Collapse and rapid resumption of Atlantic meridional circulation linked to deglacial climate changes. *Nature,* 428**,** 834.

MEEHL, G. A., COLLINS, W. D., BOVILLE, B. A., KIEHL, J. T., WIGLEY, T. M. L. & ARBLASTER, J. M. 2000. Response of the NCAR Climate System Model to increased CO2 and the role of physical processes. *Journal of Climate,* 13**,** 1879-1898.

MEIGH, J. R., MCKENZIE, A. A. & SENE, K. J. 1999. A Grid-Based Approach to Water Scarcity Estimates for Eastern and Southern Africa. *Water Resources Management,* 13**,** 85-115.

MEYBECK, M. 1982. Carbon, nitrogen, and phosphorus transport by world rivers. 282**,** 401-450.

MICHENER, W. K., BLOOD, E. R., BILDSTEIN, K. L., BRINSON, M. M. & GARDNER, L. R. 1997. CLIMATE CHANGE, HURRICANES AND TROPICAL STORMS, AND RISING SEA LEVEL IN COASTAL WETLANDS. 7**,** 770-801.

MILNER, A. M. & PETTS, G. E. 1994. Glacial rivers: physical habitat and ecology. *Freshwater Biology,* 32**,** 295-307.

MOILANEN, A., LEATHWICK, J. & ELITH, J. 2008. A method for spatial freshwater conservation prioritization. *Freshwater Biology,* 53**,** 577-592.

MONK, W. A., WOOD, P. J., HANNAH, D. M., EXTENCE, C. A., CHADD, R. P. & DUNBAR, M. J. 2012. How does macroinvertebrate taxonomic resolution influence ecohydrological relationships in riverine ecosystems. *Ecohydrology,* 5**,** 36-45.

MONK, W. A., WOOD, P. J., HANNAH, D. M. & WILSON, D. A. 2007. Selection of river flow indices for the assessment of hydroecological change. *River Research and Applications,* 23**,** 113-122.

MONK, W. A., WOOD, P. J., HANNAH, D. M. & WILSON, D. A. 2008. Macroinvertebrate community response to inter-annual and regional river flow regime dynamics. *River Research and Applications,* 24**,** 988-1001.

MONK, W. A., WOOD, P. J., HANNAH, D. M., WILSON, D. A., EXTENCE, C. A. & CHADD, R. P. 2006. Flow variability and macroinvertebrate community response within riverine systems. 22**,** 595-615.

MONTGOMERY, D. R. 1999. Process domains and the river continuum. *JAWRA Journal of the American Water Resources Association,* 35**,** 397-410.

MORIASI, D. N., ARNOLD, J. G., LIEW, M. W. V., BINGNER, R. L., HARMEL, R. D. & VEITH, T. L. 2007. Model evaluation guidelines for systematic quantification of accuracy in watershed simulations. *Transactions of the ASABE,* 50**,** 885-900.

MOSS, B., HERING, D., GREEN, A. J., AIDOUD, A., BECARES, E., BEKLIOGLU, M., BENNION, H., BOIX, D., BRUCET, S., CARVALHO, L., CLEMENT, B., DAVIDSON, T., DECLERCK, S., DOBSON, M., VAN DONK, E., DUDLEY, B., FEUCHTMAYR, H., FRIBERG, N., GRENOUILLET, G., HILLEBRAND, H., HOBAEK, A., IRVINE, K., JEPPESEN, E., JOHNSON, R., JONES, I., KERNAN, M., LAURIDSEN, T. L., MANCA, M., MEERHOFF, M., OLAFSSON, J., ORMEROD, S., PAPASTERGIADOU, E., PENNING, W. E., PTACNIK, R., QUINTANA, X., SANDIN, L., SEFERLIS, M., SIMPSON, G., TRIGA, C., VERDONSCHOT, P., VERSCHOOR, A. M. & WEYHENMEYER, G. A. 2009. Climate Change and the Future of Freshwater Biodiversity in Europe: A Primer for Policy-Makers. *Freshwater Reviews,* 2**,** 103-130.

MURPHY, J. M., BOOTH, B. B. B., COLLINS, M., HARRIS, G. R., SEXTON, D. M. H. & WEBB, M. J. 2007. A methodology for probabilistic predictions of regional climate change from perturbed physics ensembles. 365**,** 1993-2028.

MYERS, N. 1993. Biodiversity and the Precautionary Principle. *Ambio,* 22**,** 74-79.

NAKICENOVIC, N., ALCAMO, J., DAVIS, G., DE VRIES, B., FENHANN, J., GAFFIN, S., GREGORY, K., GRUBLER, A., JUNG, T. Y., KRAM, T., LA ROVERE, E. L., MICHAELIS, L., MORI, S., MORITA, T., PEPPER, W., PITCHER, H. M., PRICE, L., RIAHI, K., ROEHRL, A., ROGNER, H.-H., SANKOVSKI, A., SCHLESINGER, M., SHUKLA, P., SMITH, S. J., SWART, R., VAN ROOIJEN, S., VICTOR, N. & DADI, Z. 2000. *Special Report on Emissions Scenarios : a special report of Working Group III of the Intergovernmental Panel on Climate Change,* Cambridge, UK, Cambridge University Press.

NAKICENOVIC, N. & SWART, R. 2000. *Emissions scenarios - special report of the Intergovernmental Panel on Climate Change*, Cambridge University Press, Cambridge (United Kingdom); %J.

NASH, J. E. & SUTCLIFFE, J. V. 1970. River flow forecasting through conceptual models part I — A discussion of principles. *Journal of Hydrology,* 10**,** 282-290.

NATURAL_ENGLAND 2014. Priority river habitat in England - mapping and targeting measures. Natural England.

NEAL, C., WILLIAMS, R. J., NEAL, M., BHARDWAJ, L. C., WICKHAM, H., HARROW, M. & HILL, L. K. 2000. The water quality of the River Thames at a rural site downstream of Oxford. *Science of The Total Environment,* 251–252**,** 441-457.

NEL, J. L., REYERS, B., ROUX, D. J. & COWLING, R. M. 2009a. Expanding protected areas beyond their terrestrial comfort zone: Identifying spatial options for river conservation. *Biological Conservation,* 142**,** 1605-1616.

NEL, J. L., REYERS, B., ROUX, D. J., DEAN IMPSON, N. & COWLING, R. M. 2011a. Designing a conservation area network that supports the representation and persistence of freshwater biodiversity. *Freshwater Biology,* 56**,** 106-124.

NEL, J. L., ROUX, D. J., ABELL, R., ASHTON, P. J., COWLING, R. M., HIGGINS, J. V., THIEME, M. & VIERS, J. H. 2009b. Progress and challenges in freshwater conservation planning. *Aquatic Conservation: Marine and Freshwater Ecosystems,* 19**,** 474-485.

NEL, J. L., ROUX, D. J., MAREE, G., KLEYNHANS, C. J., MOOLMAN, J., REYERS, B., ROUGET, M. & COWLING, R. M. 2007. Rivers in peril inside and outside protected areas: a systematic approach to conservation assessment of river ecosystems. *Diversity and Distributions,* 13**,** 341–352.

NEL, J. L., TURAK, E., LINKE, S. & BROWN, C. 2011b. Integration of environmental flow assessment and freshwater conservation planning: a new era in catchment management. *Marine and Freshwater Research,* 62**,** 290-299.

NERC 2011. LCM2007 © NERC (CEH) 2011. Contains Ordnance Survey data © Crown Copyright 2007. © third part licensors.

NICHOLLS, R. J. & CAZENAVE, A. 2010. Sea-Level Rise and Its Impact on Coastal Zones. 328**,** 1517-1520.

NILSSON, C. & BERGGREN, K. 2000. Alterations of riparian ecosystems caused by river regulation. *BioScience,* 50**,** 783–792.

NILSSON, C., REIDY, C. A., DYNESIUS, M. & REVENGA, C. 2005. Fragmentation and Flow Regulation of the World's Large River Systems. *Science,* 308**,** 405-408.

OLDEN, J. D., KENNARD, M. J., LAWLER, J. J. & POFF, N. L. 2011. Challenges and Opportunities in Implementing Managed Relocation for Conservation of Freshwater Species

Retos y Oportunidades para la Implementación de la Reubicación Controlada para la Conservación de Especies Dulceacuícolas. *Conservation Biology,* 25**,** 40-47.

OLDEN, J. D., KENNARD, M. J., LEPRIEUR, F., TEDESCO, P. A., WINEMILLER, K. O. & GARCÍA-BERTHOU, E. 2010. Conservation biogeography of freshwater fishes: recent progress and future challenges. *Diversity and Distributions,* 16**,** 496-513.

OLDEN, J. D. & POFF, N. L. 2003. Redundancy and the choice of hydrologic indices for characterizing streamflow regimes. 19**,** 101-121.

OLSEN, D. A. & TOWNSEND, C. R. 2003. Hyporheic community composition in a gravel-bed stream: influence of vertical hydrological exchange, sediment structure and physicochemistry. *Freshwater Biology,* 48**,** 1363-1378.

ORMEROD, S. J. 2009. Climate change, river conservation and the adaptation challenge. *Aquatic Conservation: Marine and Freshwater Ecosystems,* 19**,** 609-613.

PACIFICI, M., FODEN, W. B., VISCONTI, P., WATSON, J. E. M., BUTCHART, S. H. M., KOVACS, K. M., SCHEFFERS, B. R., HOLE, D. G., MARTIN, T. G., AKÇAKAYA, H. R., CORLETT, R. T., HUNTLEY, B., BICKFORD, D., CARR, J. A., HOFFMANN, A. A., MIDGLEY, G. F., PEARCE-KELLY, P., PEARSON, R. G., WILLIAMS, S. E., WILLIS, S. G., YOUNG, B. & RONDININI, C. 2015. Assessing species vulnerability to climate change. *Nature Climate Change,* 5**,** 215.

PAISLEY, M. F., TRIGG, D. J. & WALLEY, W. J. 2014. REVISION OF THE BIOLOGICAL MONITORING WORKING PARTY (BMWP) SCORE SYSTEM: DERIVATION OF PRESENT-ONLY AND ABUNDANCE-RELATED SCORES FROM FIELD DATA. *River Research and Applications,* 30**,** 887-904.

PAISLEY, M. F., WALLEY, W. J. & TRIGG, D. J. 2011. Identification of macro-invertebrate taxa as indicators of nutrient enrichment in rivers. *Ecological Informatics,* 6**,** 399-406.

PALMER, M. A., REIDY LIERMANN, C. A., NILSSON, C., FLÖRKE, M., ALCAMO, J., LAKE, P. S. & BOND, N. 2008. Climate change and the world's river basins: anticipating management options. *Frontiers in Ecology and the Environment,* 6**,** 81-89.

PARMESAN, C. 2006. Ecological and Evolutionary Responses to Recent Climate Change. *Annual Review of Ecology, Evolution, and Systematics,* 37**,** 637-669.

PEARCE, F. 2006. *When the rivers run dry: water, the defining crisis of the twenty-first century*, Beacon Pr.

PETIT, J.-R., JOUZEL, J., RAYNAUD, D., BARKOV, N. I., BARNOLA, J. M., BASILE, I., BENDER, M., CHAPPELLAZ, J., DAVIS, M. & DELAYGUE, G. 1999. Climate and atmospheric history of the past 420,000 years from the Vostok ice core, Antarctica. *Nature,* 399**,** 429.

PHILLIPS, A. 2007. A short history of the international system of protected area management categories. *WCPA Task Force on protected area categories*.

PIANI, C., WEEDON, G. P., BEST, M., GOMES, S. M., VITERBO, P., HAGEMANN, S. & HAERTER, J. O. 2010. Statistical bias correction of global simulated daily precipitation and temperature for the application of hydrological models. *Journal of Hydrology,* 395**,** 199-215.

PIELKE, R. A. & WILBY, R. L. 2012. Regional climate downscaling: What's the point? *Eos, Transactions American Geophysical Union,* 93**,** 52-53.

PITTOCK, J. & FINLAYSON, C. M. 2011. Australia's Murray–Darling Basin: freshwater ecosystem conservation options in an era of climate change. *Marine and Freshwater Research,* 62**,** 232-243.

PITTOCK, J., HANSEN, L. J. & ABELL, R. 2008. Running dry: Freshwater biodiversity, protected areas and climate change. *Biodiversity,* 9**,** 30-38.

POFF, N. L., ALLAN, J. D., BAIN, M. B., KARR, J. R., PRESTEGAARD, K. L., RICHTER, B. D., SPARKS, R. E. & STROMBERG, J. C. 1997. The Natural Flow Regime. *BioScience,* 47**,** 769-784.

POFF, N. L., ALLAN, J. D., PALMER, M. A., HART, D. D., RICHTER, B. D., ARTHINGTON, A. H., ROGERS, K. H., MEYER, J. L. & STANFORD, J. A. 2003a. River flows and water wars: emerging science for environmental decision making. *Frontiers in Ecology and the Environment,* 1**,** 298-306.

POFF, N. L., OLDEN, J. & STRAYER, D. 2012. Climate Change and Freshwater Fauna Extinction Risk. *In:* HANNAH, L. (ed.) *Saving a Million Species.* Washington: Island Press/Center for Resource Economics.

POFF, N. L., RICHTER, B. D., ARTHINGTON, A. H., BUNN, S. E., NAIMAN, R. J., KENDY, E., ACREMAN, M., APSE, C., BLEDSOE, B. P., FREEMAN, M. C., HENRIKSEN, J., JACOBSON, R. B., KENNEN, J. G., MERRITT, D. M., O'KEEFFE, J. H., OLDEN, J. D., ROGERS, K., THARME, R. E. & WARNER, A. 2010. The ecological limits of hydrologic alteration (ELOHA): a new framework for developing regional environmental flow standards. *Freshwater Biology,* 55**,** 147-170.

POFF, N. L. & ZIMMERMAN, J. K. H. 2010. Ecological responses to altered flow regimes: a literature review to inform the science and management of environmental flows. *Freshwater Biology,* 55**,** 194-205.

POFF, N. L. R., ALLAN, J. D., PALMER, M. A., HART, D. D., RICHTER, B. D., ARTHINGTON, A. H., ROGERS, K. H., MEYER, J. L. & STANFORD, J. A. 2003b. River flows and water wars: emerging science for environmental decision making. *Frontiers in Ecology and the Environment,* 1**,** 298–306.

POIANI, K. A., RICHTER, B. D., ANDERSON, M. G. & RICHTER, H. E. 2000. Biodiversity Conservation at Multiple Scales: Functional Sites, Landscapes, and Networks. *BioScience,* 50**,** 133-146.

PRESSEY, R. L. 1994. Ad Hoc Reservations: Forward or Backward Steps in Developing Representative Reserve Systems?

Reservaciones ad hoc: pasos adelante o atrás en el desarrollo de sistemas de reservas representativos? *Conservation Biology,* 8**,** 662-668.

PRESSEY, R. L., CABEZA, M., WATTS, M. E., COWLING, R. M. & WILSON, K. A. 2007. Conservation planning in a changing world. *Trends in ecology & evolution,* 22**,** 583-592.

PRUDHOMME, C., DADSON, S., MORRIS, D., WILLIAMSON, J., GOODSELL, G., CROOKS, S., BOELEE, L., DAVIES, H., BUYS, G., LAFON, T. & WATTS, G. 2012. Future Flows Climate: an ensemble of 1-km climate change projections for hydrological application in Great Britain. *Earth System Science Data,* 4**,** 143-148.

PRUDHOMME, C. & DAVIES, H. 2009a. Assessing uncertainties in climate change impact analyses on the river flow regimes in the UK. Part 1: baseline climate. *Climatic Change,* 93**,** 177-195.

PRUDHOMME, C. & DAVIES, H. 2009b. Assessing uncertainties in climate change impact analyses on the river flow regimes in the UK. Part 2: future climate. *Climatic Change,* 93**,** 197-222.

PRUDHOMME, C., WILBY, R. L., CROOKS, S., KAY, A. L. & REYNARD, N. S. 2010. Scenario-neutral approach to climate change impact studies: Application to flood risk. *Journal of Hydrology,* 390**,** 198-209.

PURVIS, A., JONES, K. E. & MACE, G. M. 2000. Extinction. *BioEssays,* 22**,** 1123-1133.

PYNE, M. I. & POFF, N. L. 2017. Vulnerability of stream community composition and function to projected thermal warming and hydrologic change across ecoregions in the western United States. *Global Change Biology,* 23**,** 77-93.

RAAT, K. J., VRUGT, J. A., BOUTEN, W. & TIETEMA, A. 2004. Towards reduced uncertainty in catchment nitrogen modelling: quantifying the effect of field observation uncertainty on model calibration. *Hydrology and Earth System Sciences,* 8**,** 751-763.

RANKINEN, K., KARVONEN, T. & BUTTERFIELD, D. 2006. An application of the GLUE methodology for estimating the parameters of the INCA-N model. *Science of The Total Environment,* 365**,** 123-139.

REVENGA, C., CAMPBELL, I., ABELL, R., DE VILLIERS, P. & BRYER, M. 2005. Prospects for monitoring freshwater ecosystems towards the 2010 targets. *Philosophical Transactions of the Royal Society B: Biological Sciences,* 360**,** 397-413.

REVENGA, C. & KURA, Y. 2003. Status and trends of biodiversity of inland water ecosystems. *Secretariat of the Convention on Biological Diversity, Montreal, Technical Series,* 11.

RICCIARDI, A. & RASMUSSEN, J. B. 1999. Extinction rates of North American freshwater fauna. *Conservation Biology,* 13**,** 1220–1222.

RICHTER, B., BAUMGARTNER, J., WIGINGTON, R. & BRAUN, D. 1997. How much water does a river need? *Freshwater Biology,* 37**,** 231-249.

RICHTER, B. D., BAUMGARTNER, J. V., BRAUN, D. P. & POWELL, J. 1998. A spatial assessment of hydrologic alteration within a river network. *River Research and Applications,* 14**,** 329-340.

RICHTER, B. D., BAUMGARTNER, J. V., POWELL, J. & BRAUN, D. P. 1996. A Method for Assessing Hydrologic Alteration within Ecosystems. *Conservation Biology,* 10**,** 1163-1174.

RICHTER, B. D., WARNER, A. T., MEYER, J. L. & LUTZ, K. 2006. A collaborative and adaptive process for developing environmental flow recommendations. *River Research and Applications,* 22**,** 297-318.

RICKETTS, T. H., DINERSTEIN, E., BOUCHER, T., BROOKS, T. M., BUTCHART, S. H. M., HOFFMANN, M., LAMOREUX, J. F., MORRISON, J., PARR, M., PILGRIM, J. D., RODRIGUES, A. S. L., SECHREST, W., WALLACE, G. E., BERLIN, K., BIELBY, J., BURGESS, N. D., CHURCH, D. R., COX, N., KNOX, D., LOUCKS, C., LUCK, G. W., MASTER, L. L., MOORE, R., NAIDOO, R., RIDGELY, R., SCHATZ, G. E., SHIRE, G., STRAND, H., WETTENGEL, W. & WIKRAMANAYAKE, E. 2005. Pinpointing and preventing imminent extinctions. *Proceedings of the National Academy of Sciences of the United States of America,* 102**,** 18497-18501.

ROBSON, A. J. & NEAL, C. 1997. A summary of regional water quality for Eastern UK rivers.

SALA, O. E., CHAPIN III, S. F., ARMESTO, J. J., BLOOMFIELD, J., DIRZO, R., HUBER-SANWALD, E., HUENNEKE, L. F., JACKSON, R. B., KINZIG, A., LEEMANS, R., LODGE, D. M., MOONEY, H. A., OESTERHELD, M. N., POFF, N. L., SYKES, M. T., WALKER, B. H., WALKER, M. & WALL, D. H. 2000. Global Biodiversity Scenarios for the Year 2100. *Science,* 287**,** 1770 -1774.

SAND-JENSEN, K. A. J. & PEDERSEN, N. L. 2005. Differences in temperature, organic carbon and oxygen consumption among lowland streams. *Freshwater Biology,* 50**,** 1927-1937.

SAUNDERS, D. L., MEEUWIG, J. J. & VINCENT, A. C. J. 2002. Freshwater Protected Areas: Strategies for Conservation. *Conservation Biology,* 16**,** 30-41 %U http://dx.doi.org/10.1046/j.1523-1739.2002.99562.x.

SCHINDLER, D. W. 1997. WIDESPREAD EFFECTS OF CLIMATIC WARMING ON FRESHWATER ECOSYSTEMS IN NORTH AMERICA. *Hydrological Processes,* 11**,** 1043-1067.

SCHOLZE, M., KNORR, W., ARNELL, N. W. & PRENTICE, I. C. 2006. A climate-change risk analysis for world ecosystems. *Proceedings of the National Academy of Sciences,* 103**,** 13116-13120.

SEBER, G. A. 2009. *Multivariate observations*, John Wiley & Sons.

SHARPLEY, A. N., BERGSTRÖM, L., ARONSSON, H., BECHMANN, M., BOLSTER, C. H., BÖRLING, K., DJODJIC, F., JARVIE, H. P., SCHOUMANS, O. F., STAMM, C., TONDERSKI, K. S., ULÉN, B., UUSITALO, R. & WITHERS, P. J. A. 2015. Future agriculture with minimized phosphorus losses to waters: Research needs and direction. *Ambio,* 44**,** 163-179.

SINGH, D., TSIANG, M., RAJARATNAM, B. & DIFFENBAUGH, N. S. 2014. Observed changes in extreme wet and dry spells during the South Asian summer monsoon season. *Nature Climate Change,* 4**,** 456.

SKEFFINGTON, R. A., WHITEHEAD, P. G., HEYWOOD, E., HALL, J. R., WADSWORTH, R. A. & REYNOLDS, B. 2007. Estimating uncertainty in terrestrial critical loads and their exceedances at four sites in the UK. *Science of The Total Environment,* 382**,** 199-213.

SMIT, B. & WANDEL, J. 2006. Adaptation, adaptive capacity and vulnerability. *Global Environmental Change,* 16**,** 282-292.

SMITH, V. H., JOYE, S. B. & HOWARTH, R. W. 2006. Eutrophication of freshwater and marine ecosystems. *Limnology and Oceanography***,** 351–355.

SMITH, V. H., TILMAN, G. D. & NEKOLA, J. C. 1999. Eutrophication: impacts of excess nutrient inputs on freshwater, marine, and terrestrial ecosystems. *Environmental Pollution,* 100**,** 179-196.

SOLOMON, S., PLATTNER, G.-K., KNUTTI, R. & FRIEDLINGSTEIN, P. 2009. Irreversible climate change due to carbon dioxide emissions. *Proceedings of the National Academy of Sciences,* 106**,** 1704-1709.

SOULSBY, C., TETZLAFF, D., RODGERS, P., DUNN, S. & WALDRON, S. 2006. Runoff processes, stream water residence times and controlling landscape characteristics in a mesoscale catchment: An initial evaluation. *Journal of Hydrology,* 325**,** 197-221.

STAKHIV, E. Z. 2011. Pragmatic Approaches for Water Management Under Climate Change Uncertainty1. *JAWRA Journal of the American Water Resources Association,* 47**,** 1183-1196.

STATZNER, B., BONADA, N. & DOLÉDEC, S. J. O. 2008. Predicting the abundance of European stream macroinvertebrates using biological attributes. 156**,** 65-73.

STEIN, B. A., STAUDT, A., CROSS, M. S., DUBOIS, N. S., ENQUIST, C., GRIFFIS, R., HANSEN, L. J., HELLMANN, J. J., LAWLER, J. J., NELSON, E. J. & PAIRIS, A. 2013. Preparing for and managing change: climate adaptation for biodiversity and ecosystems. *Frontiers in Ecology and the Environment,* 11**,** 502-510.

STIASSNY, M. L. J. 2002. Conservation of freshwater fish biodiversity: the knowledge impediment. *Verhandlungen der Gesellschaft für Ichthyologie,* 3**,** 7–18.

STROEVE, J. C., SERREZE, M. C., HOLLAND, M. M., KAY, J. E., MALANIK, J. & BARRETT, A. P. J. C. C. 2012. The Arctic's rapidly shrinking sea ice cover: a research synthesis. 110**,** 1005-1027.

SUMNER, N. R., MICK FLEMING, P. & C. BATES, B. 1997. Calibration of a modified SFB model for twenty-five Australian catchments using simulated annealing. *Journal of Hydrology,* 197**,** 166-188.

TANG, S. & DESSAI, S. 2012. Usable Science? The U.K. Climate Projections 2009 and Decision Support for Adaptation Planning. 4**,** 300-313.

TAYE, M. T., NTEGEKA, V., OGIRAMOI, N. P. & WILLEMS, P. 2011. Assessment of climate change impact on hydrological extremes in two source regions of the Nile River Basin. *Hydrol. Earth Syst. Sci.,* 15**,** 209-222.

THAMES_WATER 2012. Executive Summary. *Water Resources Managment Plan 2010-2035.* Thames Water.

THARME, R. E. 2003. A global perspective on environmental flow assessment: emerging trends in the development and application of environmental flow methodologies for rivers. *River Research and Applications,* 19**,** 397-441.

THIEME, M., LEHNER, B., ABELL, R., HAMILTON, S. K., KELLNDORFER, J., POWELL, G. & RIVEROS, J. C. 2007. Freshwater conservation planning in data-poor areas: An example from a remote Amazonian basin (Madre de Dios River, Peru and Bolivia). *Biological Conservation,* 135**,** 484-501.

TICKNER, D. P., ANGOLD, P. G., GURNELL, A. M. & MOUNTFORD, J. O. 2001. Riparian plant invasions: hydrogeomorphological control and ecological impacts. *Progress in Physical Geography,* 25**,** 22.

TURAK, E., FERRIER, S., BARRETT, T. O. M., MESLEY, E., DRIELSMA, M., MANION, G., DOYLE, G., STEIN, J. & GORDON, G. 2011a. Planning for the persistence of river biodiversity: exploring alternative futures using process-based models. *Freshwater Biology,* 56**,** 39-56.

TURAK, E. & KOOP, K. 2008. Multi-attribute ecological river typology for assessing ecological condition and conservation planning. *Hydrobiologia,* 603**,** 83-104.

TURAK, E. & LINKE, S. 2011. Freshwater conservation planning: an introduction. *Freshwater Biology,* 56**,** 1-5.

TURAK, E., MARCHANT, R., BARMUTA, L. A., DAVIS, J., CHOY, S. & METZELING, L. 2011b. River conservation in a changing world: invertebrate diversity and spatial prioritisation in south-eastern coastal Australia. *Marine and Freshwater Research,* 62**,** 300-311.

TURNER, B. L., KASPERSON, R. E., MATSON, P. A., MCCARTHY, J. J., CORELL, R. W., CHRISTENSEN, L., ECKLEY, N., KASPERSON, J. X., LUERS, A., MARTELLO, M. L., POLSKY, C., PULSIPHER, A. & SCHILLER, A. 2003. A framework for vulnerability analysis in sustainability science. *Proceedings of the National Academy of Sciences,* 100**,** 8074-8079.

TURNHOUT, E., HISSCHEMÖLLER, M. & EIJSACKERS, H. 2007. Ecological indicators: Between the two fires of science and policy. *Ecological Indicators,* 7**,** 215-228.

UKTAG 2008. UK Environmental Standards and Conditions. UK Technical Advisory Group on the Water Framework Directive.

UKTAG 2014a. Invertebrates (General Degradation): Whalley, Hawkes, Paisley & Trigg (WHPT) metric in River Invertebrate Classification Tool (RICT). *UKTAG River Assessment Method Benthic Invertebrate Fauna.* UK Technical Advisory Group for the Water Framework Directive.

UKTAG 2014b. Updated Recommendations on Environmental Standards. *River Basin Management (2015-21).* UK Technical Advisory Group on the Water Framework Directive.

UN 2015. World Statistics Pocketbook, 2015 edition New York, USA: United Nations.

VAN VLIET, M. T. H., FRANSSEN, W. H. P., YEARSLEY, J. R., LUDWIG, F., HADDELAND, I., LETTENMAIER, D. P. & KABAT, P. 2013. Global river discharge and water temperature under climate change. *Global Environmental Change,* 23**,** 450-464.

VAUGHAN, I. P. & ORMEROD, S. J. 2012. Large-scale, long-term trends in British river macroinvertebrates. 18**,** 2184-2194.

VERCRUYSSE, K., GRABOWSKI, R. C. & RICKSON, R. J. 2017. Suspended sediment transport dynamics in rivers: Multi-scale drivers of temporal variation. *Earth-Science Reviews,* 166**,** 38-52.

VOROSMARTY, C. J., MCINTYRE, P. B., GESSNER, M. O., DUDGEON, D., PRUSEVICH, A., GREEN, P., GLIDDEN, S., BUNN, S. E., SULLIVAN, C. A., LIERMANN, C. R. & DAVIES, P. M. 2010. Global threats to human water security and river biodiversity. *Nature,* 467**,** 555-561.

WADE, A. J., BUTTERFIELD, D., GRIFFITHS, T. & WHITEHEAD, P. G. 2007. Eutrophication control in river-systems: an application of INCA-P to the River Lugg. *Hydrology and Earth System Sciences Discussions,* 11**,** 584-600.

WADE, A. J., DURAND, P., BEAUJOUAN, V., WESSEL, W. W., RAAT, K. J., WHITEHEAD, P. G., BUTTERFIELD, D., RANKINEN, K. & LEPISTO, A. 2002a. A nitrogen model for European catchments: INCA, new model structure and equations. *Hydrol. Earth Syst. Sci.,* 6**,** 559-582.

WADE, A. J., RAAT, K., BUTTERFIELD, D. & WHITEHEAD, P. G. 2004. Effectiveness of eutrophication control by phosphorus reduction: development of the INCA-P model. Environment Agency.

WADE, A. J., WHITEHEAD, P. G. & BUTTERFIELD, D. 2002b. The Integrated Catchments model of Phosphorus dynamics (INCA-P), a new approach for multiple source assessment in heterogeneous river systems: model structure and equations. *Hydrol. Earth Syst. Sci.,* 6**,** 583-606.

WAGENHOFF, A., TOWNSEND, C. R. & MATTHAEI, C. D. 2012. Macroinvertebrate responses along broad stressor gradients of deposited fine sediment and dissolved nutrients: a stream mesocosm experiment. 49**,** 892-902.

WALLACE, J. B. & WEBSTER, J. R. 1996. The Role of Macroinvertebrates in Stream Ecosystem Function. *Annual Review of Entomology,* 41**,** 115-139.

WALLEY, W. J. & HAWKES, H. A. 1996. A computer-based reappraisal of the Biological Monitoring Working Party scores using data from the 1990 river quality survey of England and Wales. *Water Research,* 30**,** 2086-2094.

WALLEY, W. J. & HAWKES, H. A. 1997. A computer-based development of the Biological Monitoring Working Party score system incorporating abundance rating, site type and indicator value. *Water Research,* 31**,** 201-210.

WALTHER, G. R., POST, E., CONVEY, P., MENZEL, A., PARMESAN, C., BEEBEE, T. J. C., FROMENTIN, J. M., HOEGH-GULDBERG, O. & BAIRLEIN, F. 2002. Ecological responses to recent climate change. *Nature,* 416**,** 389–395.

WEBB, B. W., HANNAH, D. M., MOORE, R. D., BROWN, L. E. & NOBILIS, F. 2008. Recent advances in stream and river temperature research. *Hydrological Processes,* 22**,** 902-918.

WEEDON, G. P., GOMES, S., VITERBO, P., SHUTTLEWORTH, W. J., BLYTH, E., ÖSTERLE, H., ADAM, J. C., BELLOUIN, N., BOUCHER, O. & BEST, M. 2011. Creation of the WATCH Forcing Data and Its Use to Assess Global and Regional Reference Crop Evaporation over Land during the Twentieth Century. *Journal of Hydrometeorology,* 12**,** 823-848.

WEHRLY, K. E., WANG, L. & MITRO, M. 2007. Field-based estimates of thermal tolerance limits for trout: Incorporating exposure time and temperature fluctuation. *Transactions of the American Fisheries Society,* 136**,** 365-374.

WHITE, K. D., VADDEY, S. V., HAMLET, A. F., COHEN, S., NEILSEN, D. & TAYLOR, W. 2006. Integrating climate impacts in water resource planning and management. *Current Practices in Cold Regions Engineering.*

WHITEHEAD, P. G., BUSSI, G., BOWES, M. J., READ, D. S., HUTCHINS, M. G., ELLIOTT, J. A. & DADSON, S. J. 2015. Dynamic modelling of multiple phytoplankton groups in rivers with an application to the Thames river system in the UK. *Environmental Modelling & Software,* 74**,** 75-91.

WHITEHEAD, P. G., CROSSMAN, J., BALANA, B. B., FUTTER, M. N., COMBER, S., JIN, L., SKURAS, D., WADE, A. J., BOWES, M. J. & READ, D. S. 2013. A cost-effectiveness analysis of water security and water quality: impacts of climate and land-use change on the River Thames system. *Philosophical Transactions of the Royal Society A: Mathematical, Physical and Engineering Sciences,* 371.

WHITEHEAD, P. G., JIN, L., BAULCH, H. M., BUTTERFIELD, D. A., ONI, S. K., DILLON, P. J., FUTTER, M., WADE, A. J., NORTH, R., O'CONNOR, E. M. & JARVIE, H. P. 2011. Modelling phosphorus dynamics in multi-branch river systems: A study of the Black River, Lake Simcoe, Ontario, Canada. *Science of The Total Environment,* 412–413**,** 315-323.

WHITEHEAD, P. G., WADE, A. J. & BUTTERFIELD, D. 2009. Potential impacts of climate change on water quality and ecology in six UK rivers. *Hydrology Research,* 40**,** 113-122.

WHITEHEAD, P. G., WILBY, R. L., BUTTERFIELD, D. & WADE, A. J. 2006. Impacts of climate change on in-stream nitrogen in a lowland chalk stream: An appraisal of adaptation strategies. *Science of The Total Environment,* 365**,** 260-273.

WHITEHEAD, P. G., WILSON, E. J. & BUTTERFIELD, D. 1998a. A semi-distributed Integrated Nitrogen model for multiple source assessment in Catchments (INCA): Part I — model structure and process equations. *Science of The Total Environment,* 210-211**,** 547-558.

WHITEHEAD, P. G., WILSON, E. J., BUTTERFIELD, D. & SEED, K. 1998b. A semi-distributed integrated flow and nitrogen model for multiple source assessment in catchments (INCA): Part II — application to large river basins in south Wales and eastern England. *Science of The Total Environment,* 210–211**,** 559-583.

WILBY, R. L. 2010. Evaluating climate model outputs for hydrological applications. *Hydrological Sciences Journal,* 55**,** 1090-1093.

WILBY, R. L. & DESSAI, S. 2010. Robust adaptation to climate change. 65**,** 180-185.

WILBY, R. L. & HARRIS, I. 2006. A framework for assessing uncertainties in climate change impacts: Low-flow scenarios for the River Thames, UK. *Water Resources Research,* 42.

WILBY, R. L., ORR, H., WATTS, G., BATTARBEE, R. W., BERRY, P. M., CHADD, R., DUGDALE, S. J., DUNBAR, M. J., ELLIOTT, J. A., EXTENCE, C., HANNAH, D. M., HOLMES, N., JOHNSON, A. C., KNIGHTS, B., MILNER, N. J., ORMEROD, S. J., SOLOMON, D., TIMLETT, R., WHITEHEAD, P. J. & WOOD, P. J. 2010. Evidence needed to manage freshwater ecosystems in a changing climate: Turning adaptation principles into practice. *Science of The Total Environment,* 408**,** 4150-4164.

WILLIAMS, S. E., SHOO, L. P., ISAAC, J. L., HOFFMANN, A. A. & LANGHAM, G. 2008. Towards an Integrated Framework for Assessing the Vulnerability of Species to Climate Change. *PLoS Biol,* 6**,** e325.

WILLIS, K. J., JEFFERS, E. S. & TOVAR, C. 2018. What makes a terrestrial ecosystem resilient? 359**,** 988-989.

WITHERS, P. J. A. & LORD, E. I. 2002. Agricultural nutrient inputs to rivers and groundwaters in the UK: policy, environmental management and research needs. *Science of The Total Environment,* 282–283**,** 9-24.

WOODWARD, G., PERKINS, D. M. & BROWN, L. E. 2010. Climate change and freshwater ecosystems: impacts across multiple levels of organization. *Philosophical Transactions of the Royal Society B: Biological Sciences,* 365**,** 2093-2106.

WORRALL, T. P., DUNBAR, M. J., EXTENCE, C. A., LAIZÉ, C. L. R., MONK, W. A. & WOOD, P. J. 2014. The identification of hydrological indices for the characterization of macroinvertebrate community response to flow regime variability. *Hydrological Sciences Journal,* 59**,** 645-658.

WRIGHT, J. F., FURSE, M. T. & MOSS, D. 1998. River classification using invertebrates: RIVPACS applications. 8**,** 617-631.

WU, L., LONG, T.-Y., LIU, X. & GUO, J.-S. 2012. Impacts of climate and land-use changes on the migration of non-point source nitrogen and phosphorus during rainfall-runoff in the Jialing River Watershed, China. *Journal of Hydrology,* 475**,** 26-41.

XENOPOULOS, M. A. & LODGE, D. M. 2006. Going with the flow: using species-discharge relationships to forecast losses in fish biodiversity. *Ecology,* 87**,** 1907-1914.

XENOPOULOS, M. A., LODGE, D. M., ALCAMO, J., M\ÄRKER, M., SCHULZE, K. & VAN VUUREN, D. P. 2005. Scenarios of freshwater fish extinctions from climate change and water withdrawal. *Global Change Biology,* 11**,** 1557–1564.

YAZDIAN, H., JAAFARZADEH, N., ZAHRAIE, B. J. J. O. E. H. S. & ENGINEERING 2014. Relationship between benthic macroinvertebrate bio-indices and physicochemical parameters of water: a tool for water resources managers. 12**,** 30.

YIP, J. Y., CORLETT, R. T. & DUDGEON, D. 2004. A fine-scale gap analysis of the existing protected area system in Hong Kong, China. *Biodiversity and Conservation,* 13**,** 943–957.

YLHÄISI, J. S., GARRÈ, L., DARON, J. & RÄISÄNEN, J. 2015. Quantifying sources of climate uncertainty to inform risk analysis for climate change decision-making. *Local Environment,* 20**,** 811-835.

APPENDIX I

This appendix contains additional figures representing all the results from exposure, sensitivity and resilience components of the index, alongside results for all vulnerability assessment methodologies (VAM) and consensus approaches. Additional tables are also provided that summarise key statistics for all VAM and consensus methodologies. A description for each figure and table is provided in the captions.

Table A1: Summary statistics for the VAM_1 based vulnerability categories and the 'conservative' sensitivity assessment. No. catchments are the number of catchments in each vulnerability category ('low', 'medium', 'high' and 'very high'). Surface area denotes the percentage of the total study area (10,073,990 km^2), and protected area denotes the percentage of the surface area found within the European protected area networks (Natura 2000 and WDPA for IUCN categories I-IV). The mapping of the sensitivity, 1-resilience and exposure scores to vulnerability categories is provided in Table 2-2. Note that for 13 catchments the climate change vulnerability could not be estimated due to missing data on the resilience components. See Figure A5 for associated maps.

	Scenario/ category	2030s B1 dams	2030s A2 dams	2080s B1 dams	2080s A2 dams	2030s B1 no dams	2030s A2 no dams	2080s B1 no dams	2080s A2 no dams
No. catchments	low	0	0	0	0	20	17	0	0
	medium	5560	6739	719	366	10928	11596	6882	6026
	high	13166	11981	17884	18170	7789	7124	11794	12604
	very high	44	50	167	234	33	33	94	140
surface area [%]	low	0.0	0.0	0.0	0.0	0.1	0.1	0.0	0.0
	medium	33.1	38.5	4.3	2.1	60.3	62.7	39.5	34.9
	high	66.5	61.1	94.2	95.8	39.3	36.9	59.4	63.7
	very high	0.4	0.4	1.5	2.2	0.3	0.3	1.0	1.4
protected area [%]	low	0.0	0.0	0.0	0.0	18.0	16.2	0.0	0.0
	medium	9.1	9.3	11.6	14.6	9.7	9.7	8.5	8.1
	high	13.4	13.8	11.9	11.8	15.6	16.1	14.2	14.0
	very high	37.8	28.4	28.4	24.4	34.6	24.7	29.5	27.4

Table A2: Summary statistics for the VAM_2 based vulnerability categories using the 'standard' sensitivity assessment. No. catchments are the number of catchments in each vulnerability category ('low', 'medium', 'high' and 'very high'). Surface area denotes the percentage of the total study area (10,073,990 km^2), and protected area denotes the percentage of the surface area found within the European protected area networks (Natura 2000 and WDPA for IUCN categories I-IV). The mapping of the sensitivity, 1-resilience and exposure scores to vulnerability categories is provided in Table 2-2. Note that for 13 catchments the vulnerability to climate change could not be estimated due to missing data on the resilience components. See Figure A6 for associated maps.

	Scenario	2030s B1 dams	2030s A2 dams	2080s B1 dams	2080s A2 dams	2030s B1 no dams	2030s A2 no dams	2080s B1 no dams	2080s A2 no dams
No. catchments	low	105	136	2	0	4443	4743	1643	1571
	medium	12840	12844	12329	2751	11033	11563	9294	7966
	high	5816	5780	6398	15962	3286	2453	7795	9193
	very high	9	10	41	57	8	11	38	40
surface area [%]	low	0.6	0.7	0.0	0.0	25.1	26.8	8.9	9.0
	medium	67.0	67.1	64.9	15.7	56.2	58.5	51.9	45.1
	high	32.4	32.1	34.7	83.4	18.6	14.5	38.7	45.4
	very high	0.1	0.1	0.4	0.9	0.1	0.1	0.4	0.5
protected area [%]	low	15.1	13.4	63.2	0.0	8.4	8.9	12.1	10.0
	medium	10.0	10.1	10.0	9.6	11.9	11.8	10.0	10.4
	high	16.3	16.3	15.8	12.4	17.6	19.0	14.7	14.0
	very high	58.2	40.1	29.7	27.1	53.7	35.0	28.4	34.6

Table A3: Summary statistics for the VAM_3 based vulnerability categories using the 'standard' sensitivity assessment. No. catchments are the number of catchments in each vulnerability category ('low', 'medium', 'high' and 'very high'). Surface area denotes the percentage of the total study area (10,073,990 km^2), and protected area denotes the percentage of the surface area found within the European protected area networks (Natura 2000 and WDPA for IUCN categories I-IV). The mapping of the sensitivity, 1-resilience and exposure scores to vulnerability categories is provided in Table 2-2. Note that for 13 catchments the vulnerability to climate change could not be estimated due to missing data on the resilience components. See Figure A7 for associated maps.

	Scenario	2030s B1 dams	2030s A2 dams	2080s B1 dams	2080s A2 dams	2030s B1 no dams	2030s A2 no dams	2080s B1 no dams	2080s A2 no dams
No. catchments	low	1720	1947	1099	114	8434	9084	5321	4855
	medium	16430	16275	15543	15860	9834	9313	11997	12306
	high	611	538	2087	2739	494	362	1414	1569
	very high	9	10	41	57	8	11	38	40
surface area [%]	low	9.2	9.8	6.4	0.5	47.1	49.8	30.0	27.6
	medium	85.3	85.3	80.8	84.3	48.7	47.0	61.5	63.0
	high	5.4	4.8	12.3	14.3	4.2	3.1	8.1	8.9
	very high	0.1	0.1	0.4	0.9	0.1	0.1	0.4	0.5
protected area [%]	low	10.0	11.3	11.0	24.3	9.5	9.6	9.0	8.2
	medium	11.6	11.6	10.8	10.6	13.6	13.9	12.4	12.4
	high	23.0	22.8	20.8	19.5	23.7	25.6	20.6	20.8
	very high	58.2	40.1	29.7	27.1	53.7	35.0	28.4	34.6

Table A4: Summary statistics for the VAM$_4$ based vulnerability categories using the 'standard' sensitivity assessment. No. catchments are the number of catchments in each vulnerability category ('low', 'medium', 'high' and 'very high'). Surface area denotes the percentage of the total study area (10,073,990 km^2), and protected area denotes the percentage of the surface area found within the European protected area networks (Natura 2000 and WDPA for IUCN categories I-IV). The mapping of the sensitivity, 1-resilience and exposure scores to vulnerability categories is provided in Table 2-2. Note that for 13 catchments the vulnerability to climate change could not be estimated due to missing data on the resilience components. See Figure A8 for associated maps.

	Scenario	2030s B1 dams	2030s A2 dams	2080s B1 dams	2080s A2 dams	2030s B1 no dams	2030s A2 no dams	2080s B1 no dams	2080s A2 no dams
No. catchments	low	18480	18479	18479	18479	18498	18497	18497	18497
	medium	285	286	286	280	267	266	263	263
	high	5	5	4	10	5	7	9	9
	very high	0	0	1	1	0	0	1	1
surface area [%]	low	96.5	96.5	96.5	96.5	96.8	96.8	96.8	96.8
	medium	3.5	3.5	3.5	3.4	3.2	3.1	3.0	3.0
	high	0.0	0.0	0.0	0.1	0.0	0.1	0.1	0.1
	very high	0.0	0.0	0.0	0.0	0.0	0.0	0.0	0.0
protected area [%]	low	11.8	11.8	11.8	11.8	11.8	11.8	11.8	11.8
	medium	21.5	21.5	21.5	21.4	21.7	21.8	21.7	21.7
	high	51.5	51.5	48.2	27.6	51.5	29.9	27.4	27.4
	very high	0.0	0.0	73.2	73.2	0.0	0.0	73.2	73.2

Table A5: Summary statistics for the VAM_1, VAM_2, VAM_3 and VAM_4 consensus-based climate change vulnerability categories using the 'standard' sensitivity assessment. No. catchments are the number of catchments according to all vulnerability estimation methods (VAM_1, VAM_2, VAM_3 and VAM_4) in the vulnerability categories ('low to medium' and 'high to very high', with 'no consensus' denoting catchments where vulnerability estimation methods did not agree on the vulnerability category). Surface area denotes the percentage of the total study area (10,073,990 km^2), and protected area denotes the percentage of the surface area found within the European protected area networks (Natura 2000 and WDPA for IUCN categories I-IV). The mapping of the sensitivity, 1-resilience and the exposure scores to vulnerability categories is provided in Table 2-2. Note that for 13 catchments the vulnerability to climate change could not be estimated due to missing data on the resilience components. See Figure A9 for associated maps.

	Scenario	2030s B1 dams	2030s A2 dams	2080s B1 dams	2080s A2 dams	2030s B1 no dams	2030s A2 no dams	2080s B1 no dams	2080s A2 no dams
No. catchments	low to medium	11873	11606	5666	2054	14716	15517	10064	8620
	high to very high	5	5	5	11	5	7	10	10
	no consensus	6892	7159	13099	16705	4049	3246	8696	10140
surface area [%]	low to medium	64.3	62.3	34.8	11.9	78.3	82.2	56.3	49.2
	high to very high	0.0	0.0	0.0	0.2	0.0	0.1	0.1	0.1
	no consensus	35.6	37.7	65.1	88.0	21.6	17.7	43.5	50.7
protected area [%]	low to medium	9.7	9.5	8.9	8.5	10.5	10.5	10.1	9.8
	high to very high	51.5	51.5	51.5	28.7	51.5	29.9	28.5	28.5
	no consensus	16.5	16.5	13.8	12.6	18.0	19.7	14.6	14.3

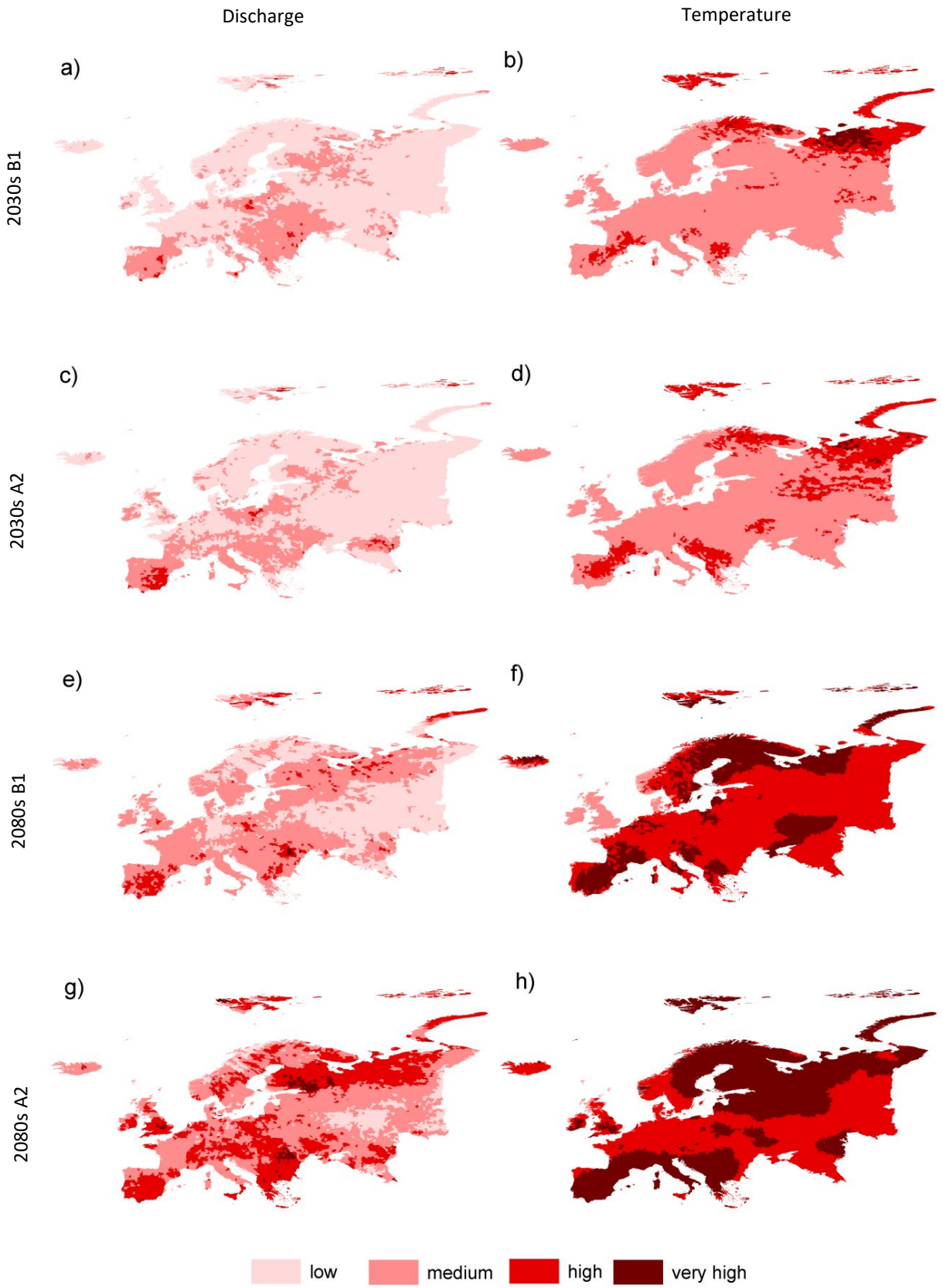


Figure A1: Individual components of exposure to climate change at the European catchment scale for the 2030s (a-d) and 2080s (e-h): a) 2030s, discharge indicators, B1 scenario; b) 2030s, temperature indicators, B1 scenario; c) 2030s, discharge indicators, A2 scenario; d) 2030s, temperature indicators, A2 scenario; e) 2080s, discharge indicators, B1 scenario; f) 2080s, temperature indicators, B1 scenario; g) 2080s, discharge indicators, A2 scenario; h) 2080s, temperature indicators, A2 scenario.

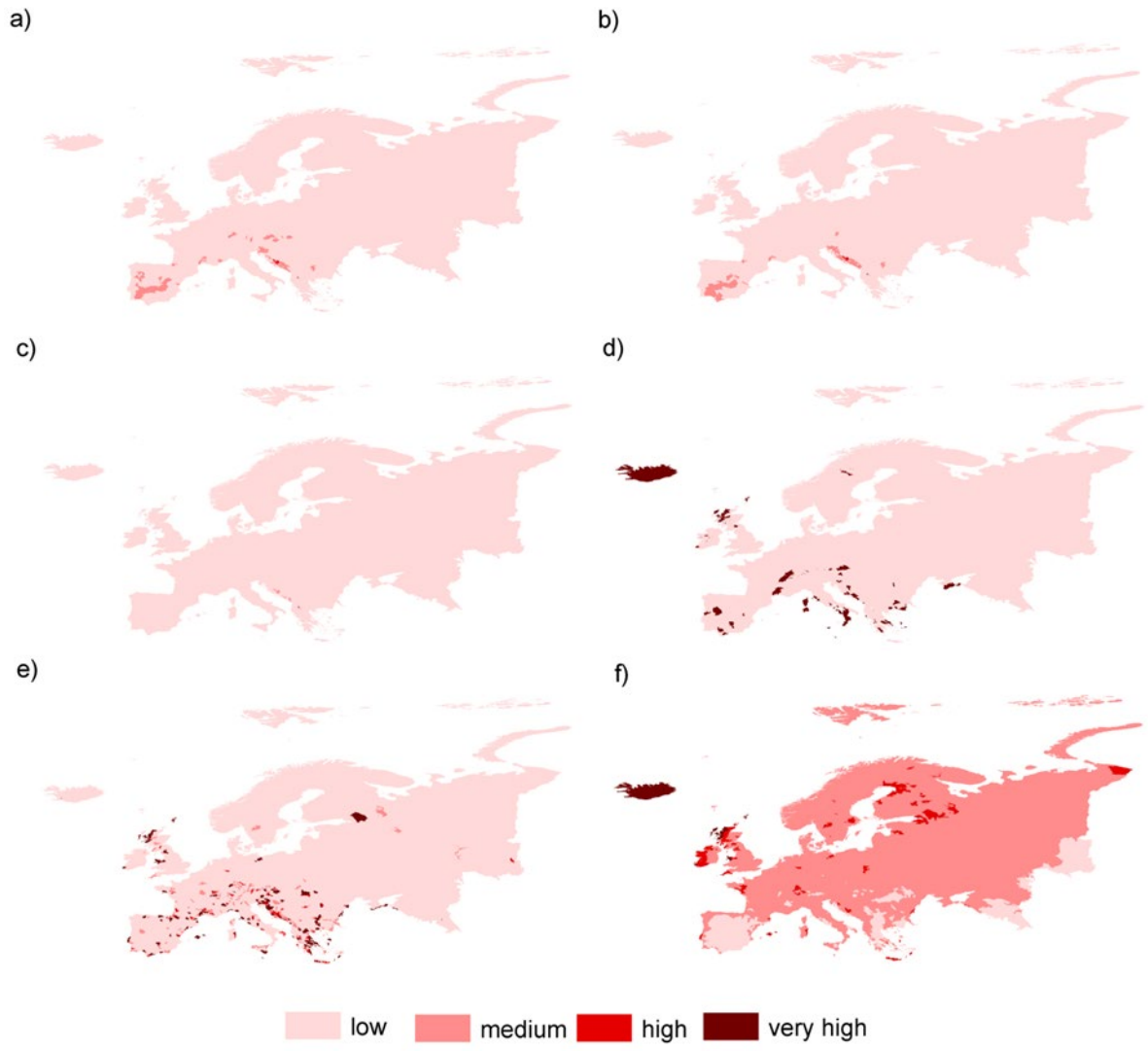


Figure A2: Individual attributes of sensitivity to climate change for freshwater ecosystems at the European catchment scale: a) presence of threatened species (Global Red List); b) presence of threatened species (European Red List); c) presence of species of restricted range; d) presence of species that are confined to a single freshwater ecoregion; e) irreplaceability of catchments and f) species' environmental tolerance breadths.

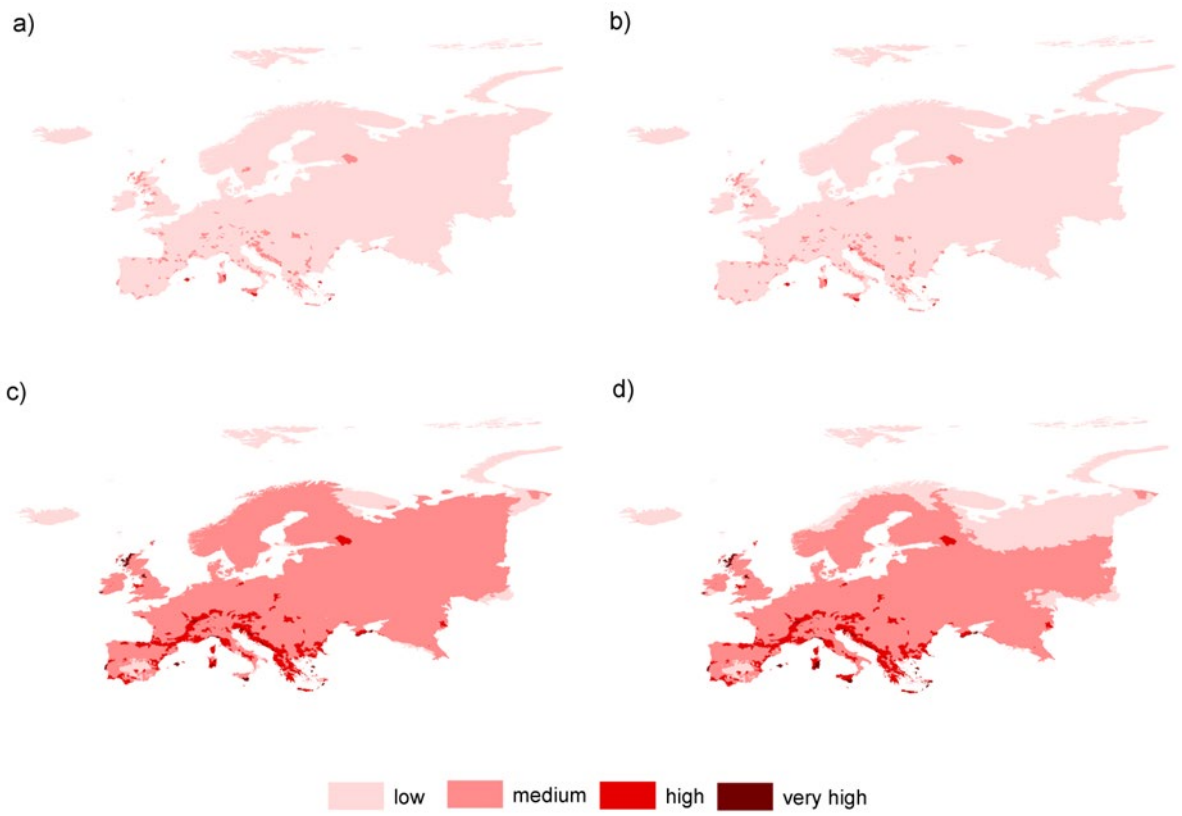


Figure A3: Sensitivity to Climate change for freshwater ecosystems at the European catchment scale. For a) and c) the sensitivity is based on the Global Red List of threatened species, whilst b) and d) show sensitivity estimates based on the European Red List. Within a) and b) the relative numbers of species that are either threatened or of restricted range were used (i.e. the 'standard approach'), whilst for c) and d) the presence of a single species in either category was enough to trigger classification as 'sensitive to climate change' (i.e. the 'conservative approach').

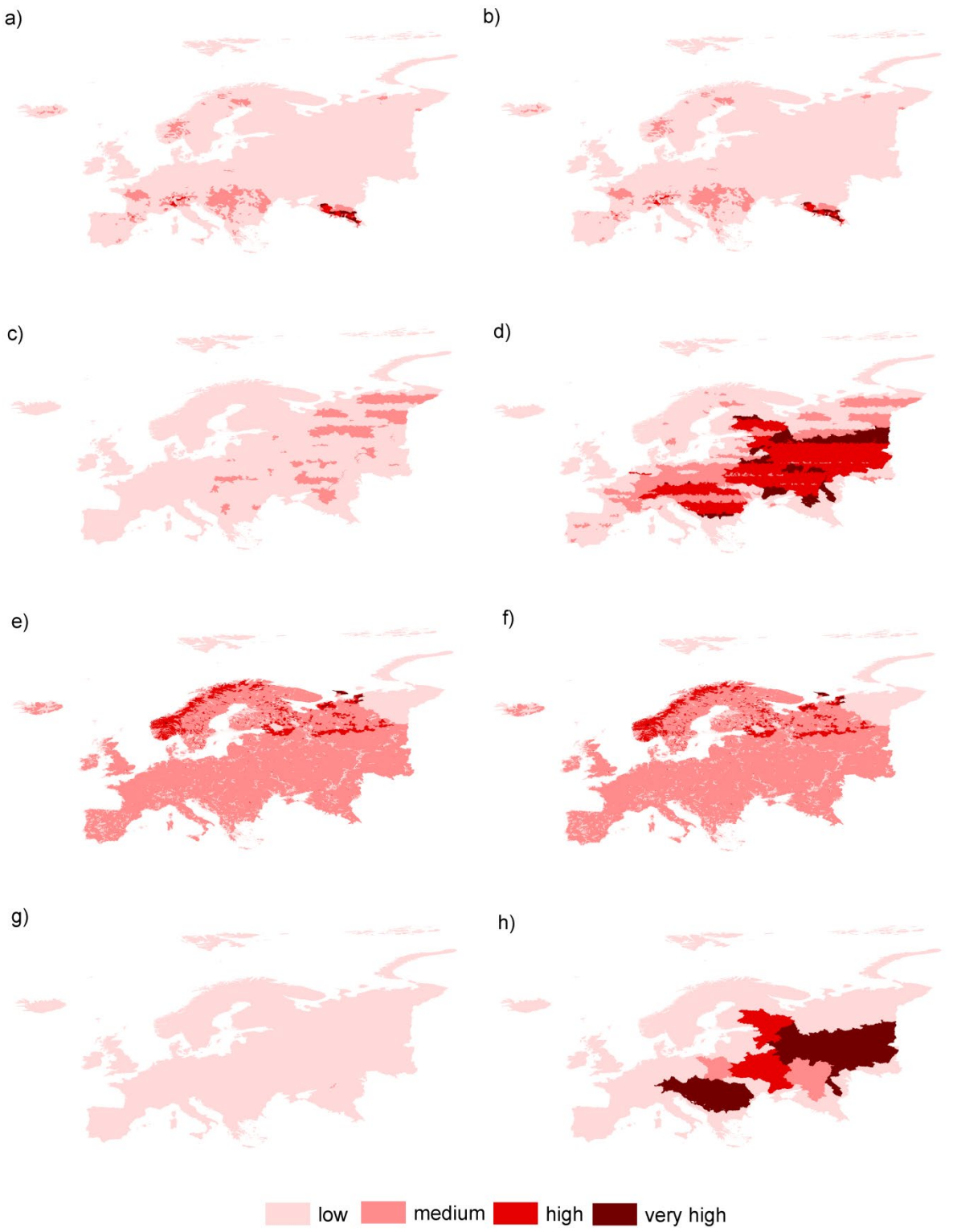


Figure A4: Individual attributes of resilience to climate change for freshwater ecosystems at the European catchment scale, considering dams and obstacles (left panel) and assuming no dams and obstacles (right panel): (a –b) altitudinal range; (c-d) latitudinal gradient; (e-f) network density; (g-h) network complexity. Note: the resilience values presented here are the inverse of exposure and sensitivity values (i.e. low values indicate low resilience potential to climate change). Resilience values used in vulnerability methods are the inverse of the values presented here (1-resilience), so that they are comparable to the exposure and sensitivity components.

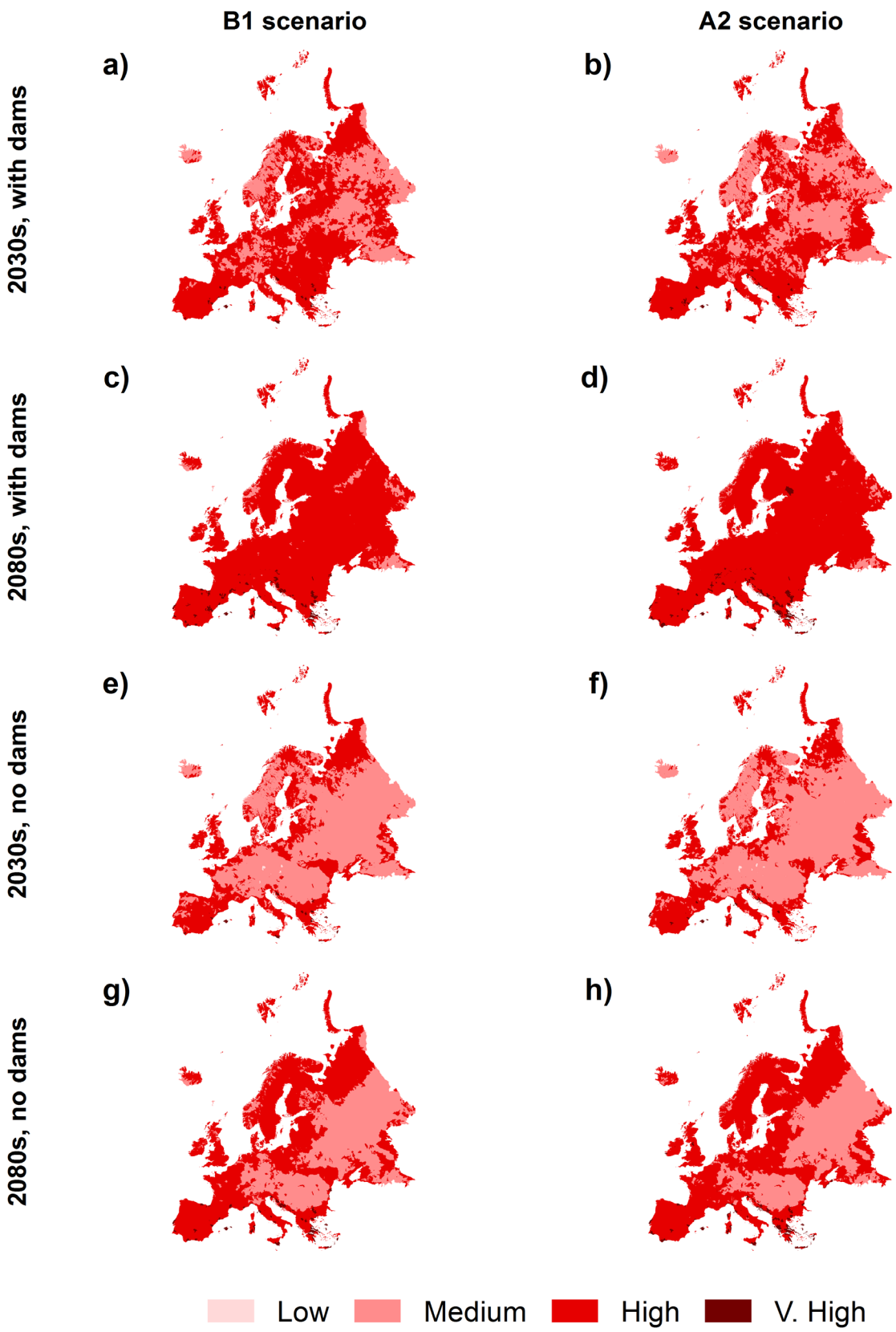


Figure A5: Vulnerability to climate change based on the method VAM_1 (see Table 2-2) for 2030s and 2080s exposure, conservative sensitivity estimates and 1-resilience calculation with dispersal dams (a-d) and without dispersal dams (e-h): a) 2030s exposure, B1 scenario, with dams; b) 2030s exposure, A2 scenario, with dams; c) 2080s exposure, B1 scenario, with dams; d) 2080s exposure, A2 scenario, with dams; e) 2030s exposure, B1 scenario, without dams; f) 2030s exposure, A2 scenario, without dams; g) 2080s exposure, B1 scenario, without dams; h) 2080s exposure, A2 scenario, without dams; The sensitivity dimension is based on the species Global Red List status. Summary statistics are provided in Table A1.

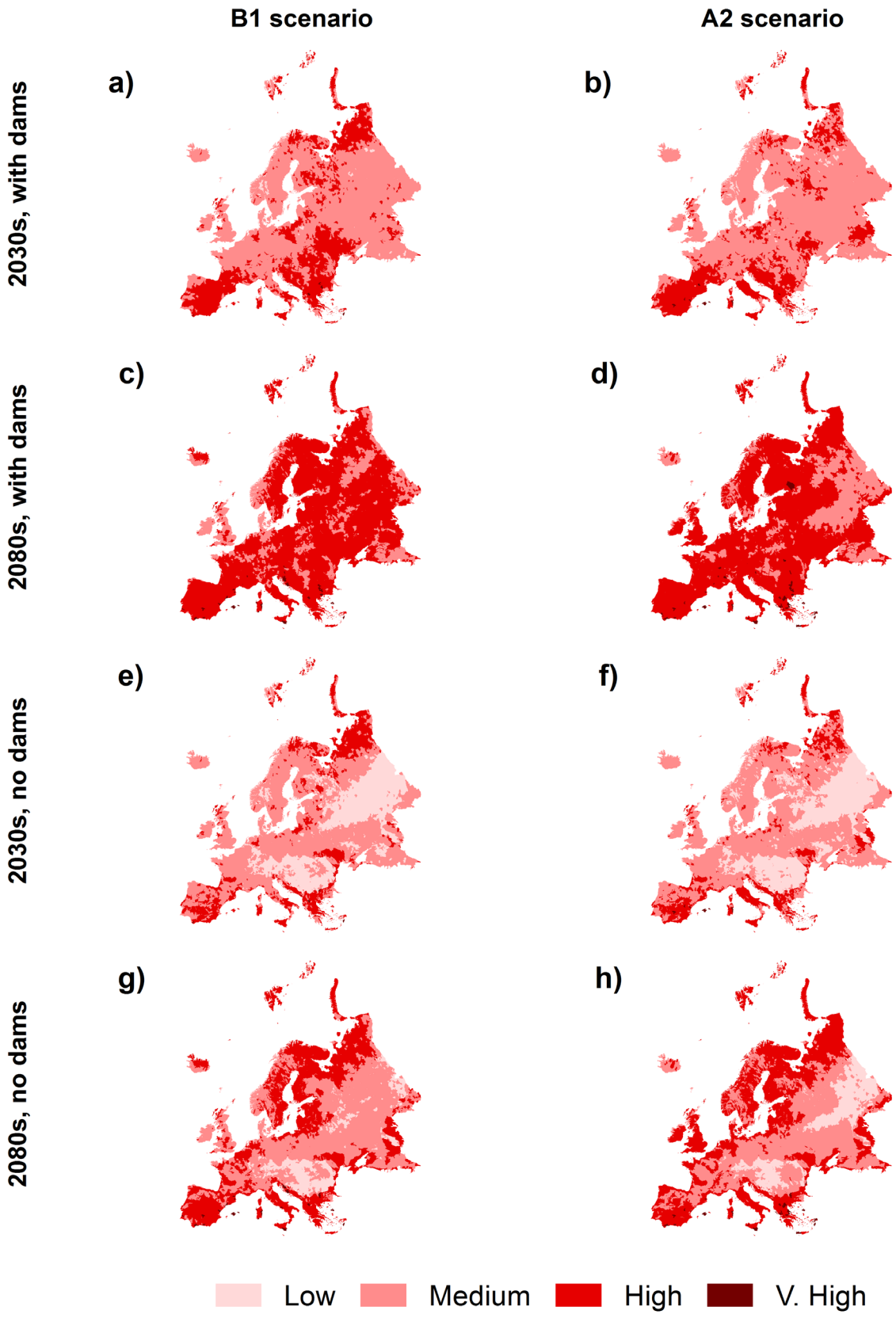


Figure A6: Vulnerability to climate change based on the method VAM_2 (see Table 2-2 Error! Reference source not found.**) for 2030s and 2080s exposure and 1-resilience calculation with dispersal dams (a-d) and without dispersal dams (e-h): a) 2030s exposure, B1 scenario, with dams; b) 2030s exposure, A2 scenario, with dams; c) 2080s exposure, B1 scenario, with dams; d) 2080s exposure, A2 scenario, with dams; e) 2030s exposure, B1 scenario, without dams; f) 2030s exposure, A2 scenario, without dams; g) 2080s exposure, B1 scenario, without dams; h) 2080s exposure, A2 scenario, without dams; The sensitivity dimension is based on the species Global Red List status. Summary statistics are provided in Table A2.**

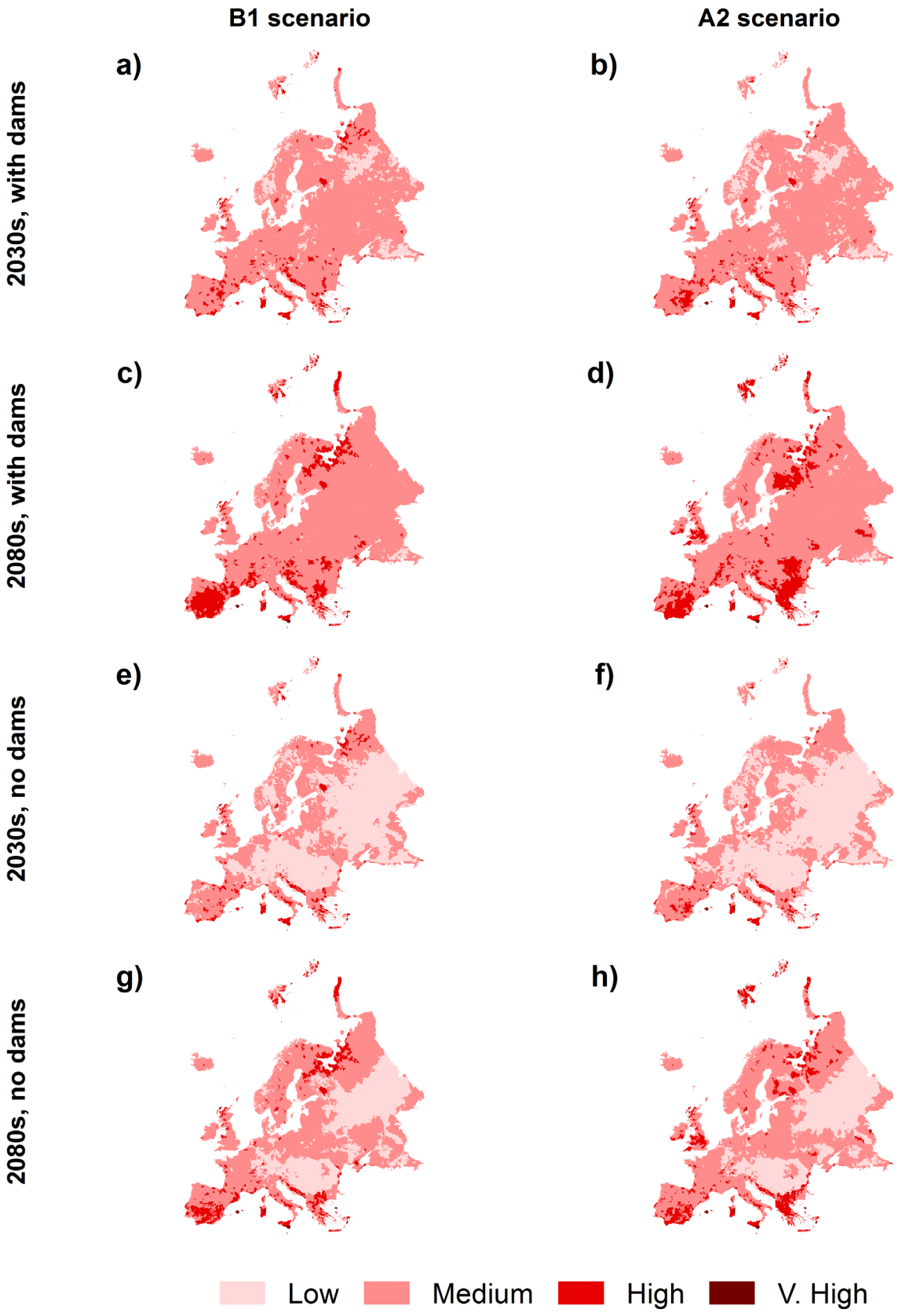


Figure A7: Vulnerability to climate change based on the method VAM_3 (see Table 2-2) for 2030s and 2080s exposure and 1-resilience calculation with dispersal dams (a-d) and without dispersal dams (e-h): a) 2030s exposure, B1 scenario, with dams; b) 2030s exposure, A2 scenario, with dams; c) 2080s exposure, B1 scenario, with dams; d) 2080s exposure, A2 scenario, with dams; e) 2030s exposure, B1 scenario, without dams; f) 2030s exposure, A2 scenario, without dams; g) 2080s exposure, B1 scenario, without dams; h) 2080s exposure, A2 scenario, without dams; The sensitivity dimension is based on the species Global Red List status. Summary statistics are provided in Table A3.

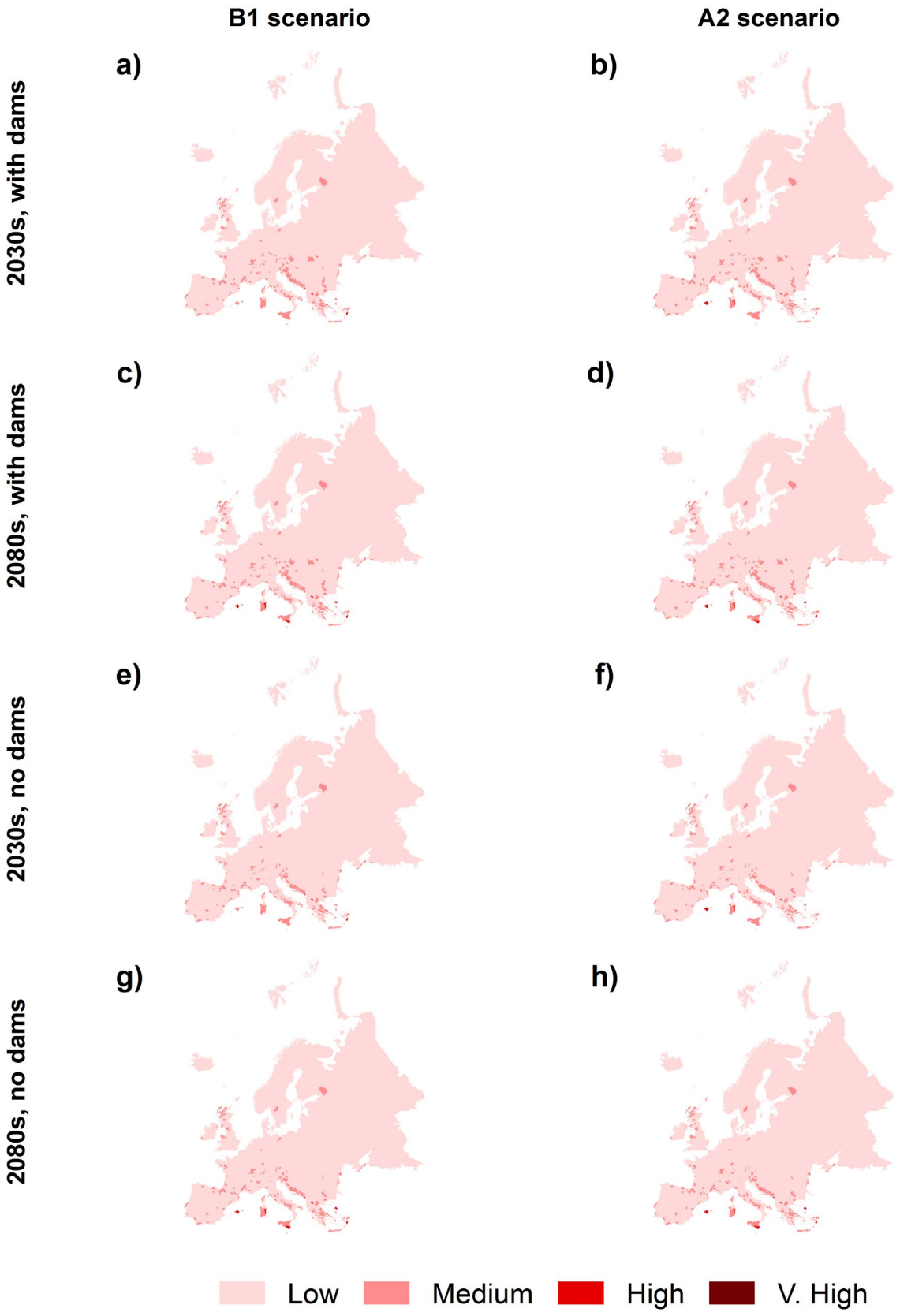


Figure A8: Vulnerability to climate change based on the method VAM_4 (see Table 2-2) for 2030s and 2080s exposure and 1-resilience calculation with dispersal dams (a-d) and without dispersal dams (e-h): a) 2030s exposure, B1 scenario, with dams; b) 2030s exposure, A2 scenario, with dams; c) 2080s exposure, B1 scenario, with dams; d) 2080s exposure, A2 scenario, with dams; e) 2030s exposure, B1 scenario, without dams; f) 2030s exposure, A2 scenario, without dams; g) 2080s exposure, B1 scenario, without dams; h) 2080s exposure, A2 scenario, without dams; The sensitivity dimension is based on the species Global Red List status. Summary statistics are provided in Table A4.



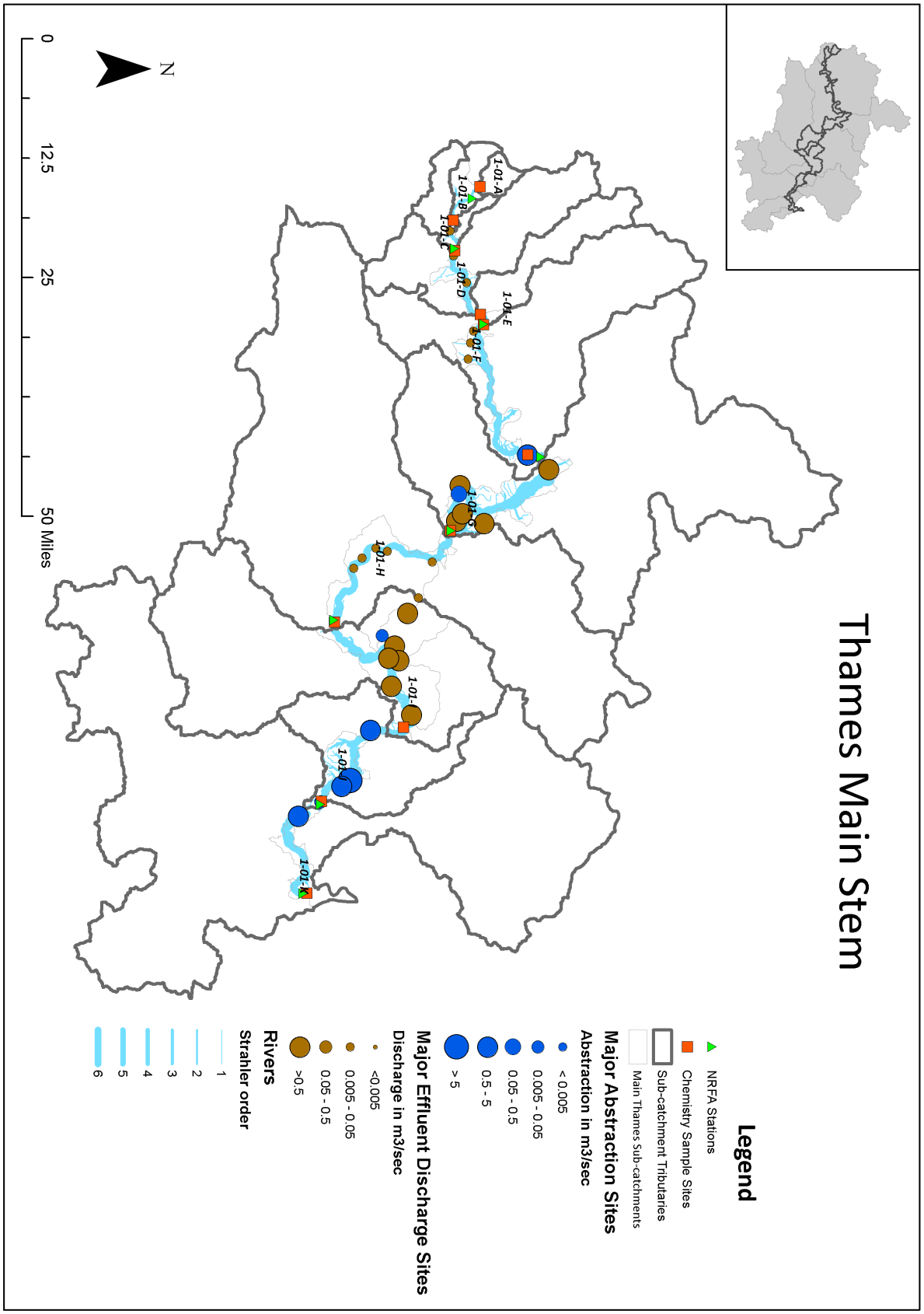
Figure A9: Consensus patterns for vulnerability to climate change based on VAM_1, VAM_2, VAM_3 and VAM_4 methods for: a) 2030s exposure, B1 scenario, with dams; b) 2030s exposure, A2 scenario, with dams; c) 2080s exposure, B1 scenario, with dams; d) 2080s exposure, A2 scenario, with dams; e) 2030s exposure, B1 scenario, without dams; f) 2030s exposure, A2 scenario, without dams; g) 2080s exposure, B1 scenario, without dams; h) 2080s exposure, A2 scenario, without dams. Within the consensus approach, a catchment was assigned the category 'low to medium' or 'high to very high' only if the same category was assigned for all four vulnerability estimations; otherwise it was assigned 'no consensus' (see Table 2-2 for details on vulnerability methods). Summary statistics are provided in Table A5.

APPENDIX II

Detailed catchment maps and calibration parameter values for all 11 major sub-basins within the Thames region.

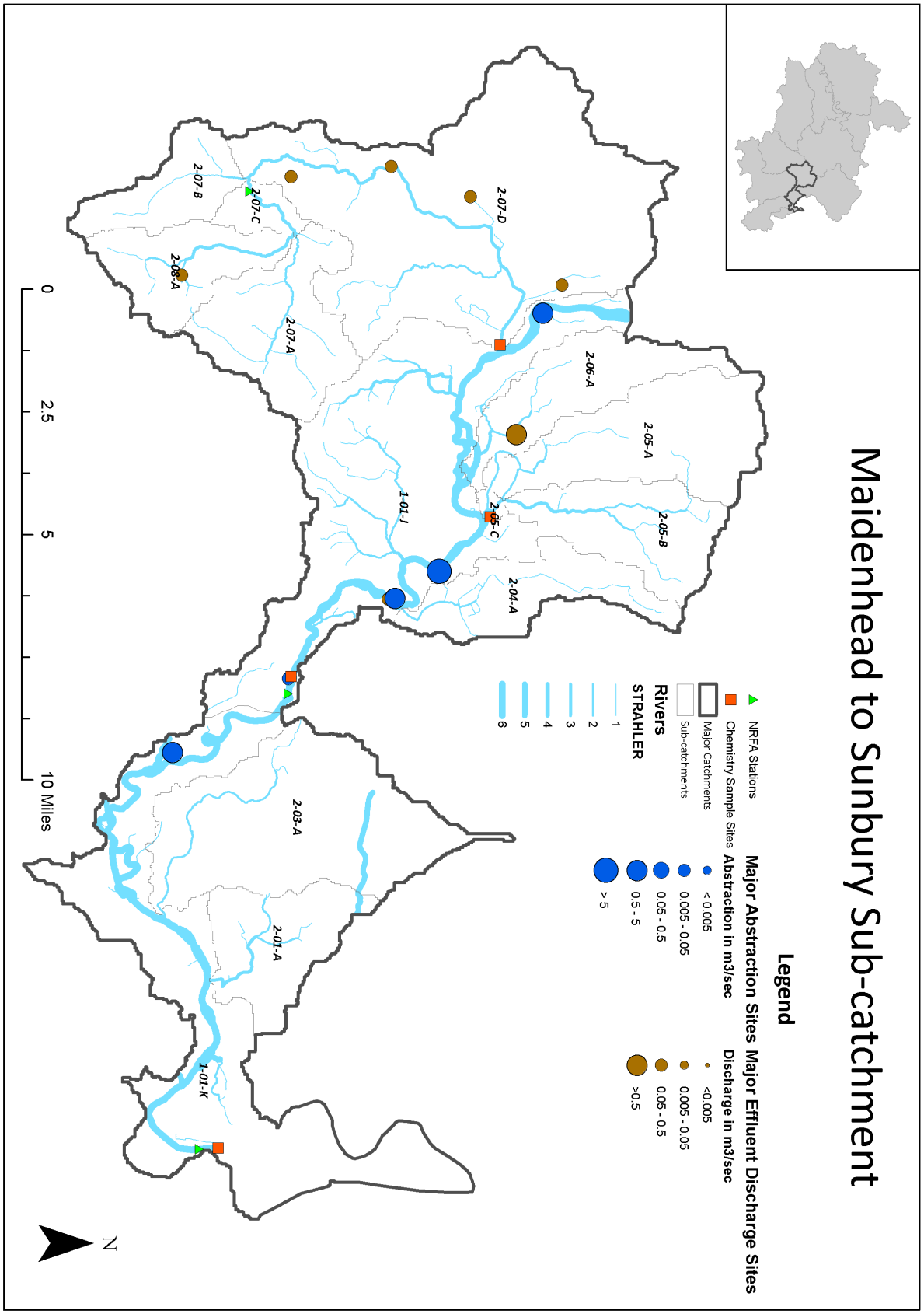
MAIN STEM OF THE THAMES

Sub-catchment	Name	River Typology	Strahler order	Area (km2)	Reach length (m)	Reach width (m)	*a* flow parameter	BFI	Urban	Intensive Agriculture	Non-intensive Agriculture	Wetlands	Forest
1-01-A	Thames (Source to Kemble)	Low, Small, Calcareous	1	33.16	1,098	5.2	0.151	0.64	0.53	46.67	23.81	0.08	28.91
1-01-B	Thames (Kemble to Waterhay Bridge)	Low, Small, Calcareous	2	34.09	12,236	5.7	0.143	0.64	3.57	58.51	23.16	11.44	3.33
1-01-C	Thames (Waterhaybridge to Cricklade) and Chelworth Brook	Low, Medium, Calcareous	3	8.36	5,447	9.0	0.190	0.68	5.12	8.94	74.30	10.10	1.54
1-01-D	Thames (Churn to Coln)	Low, Medium, Calcareous	5	28.72	24,883	10.9	0.055	0.57	5.33	55.93	35.98	0.64	2.12
1-01-E	Thames (Coln to Leach)	Low, Medium, Calcareous	5	6.92	3,229	18.9	0.052	0.71	8.60	54.44	34.11	0.87	1.99
1-01-F	Thames (Leach to Evenlode)	Low, Large, Calcareous	5	73.55	54,151	19.4	0.048	0.67	1.89	42.39	45.30	3.65	6.78
1-01-G	Thames (Evenlode to Thame)	Low, Large, Calcareous	6	123.79	66,078	23.8	0.047	0.64	17.05	39.12	29.25	3.87	10.70
1-01-H	Thames Wallingford to Caversham	Low, Large, Calcareous	6	187.94	41,653	40.4	0.017	0.64	12.67	40.47	30.26	1.41	15.19
1-01-I	Thames (Reading to Cookham)	Low, Large, Calcareous	6	215.73	41,648	43.3	0.043	0.70	9.56	30.28	37.24	2.94	19.98
1-01-J	Thames (Cookham to Egham)	Low, Large, Calcareous	6	65.74	31,136	42.0	0.038	0.66	25.21	16.02	36.95	4.30	17.52
1-01-K	Thames (Egham to Teddington)	Low, Large, Calcareous	6	58.00	32,908	37.3	0.016	0.63	48.81	3.08	30.91	8.13	9.08


Thames Main Stem
Legend
NRFA Stations
Chemistry Sample Sites
Sub-catchment Tributaries
Main Thames Sub-catchments
Major Abstraction Sites
Abstraction in m3/sec
< 0.005
0.005 - 0.05
0.05 - 0.5
0.5 - 5
> 5
Major Effluent Discharge Sites
Discharge in m3/sec
<0.005
0.005 - 0.05
0.05 - 0.5
>0.5
Rivers
Strahler order
1
2
3
4
5
6
1-01-A
1-01-B
1-01-C
1-01-D
1-01-E
1-01-F
1-01-G
1-01-H
1-01-I
1-01-J
1-01-K
N
0
12.5
25
50 Miles

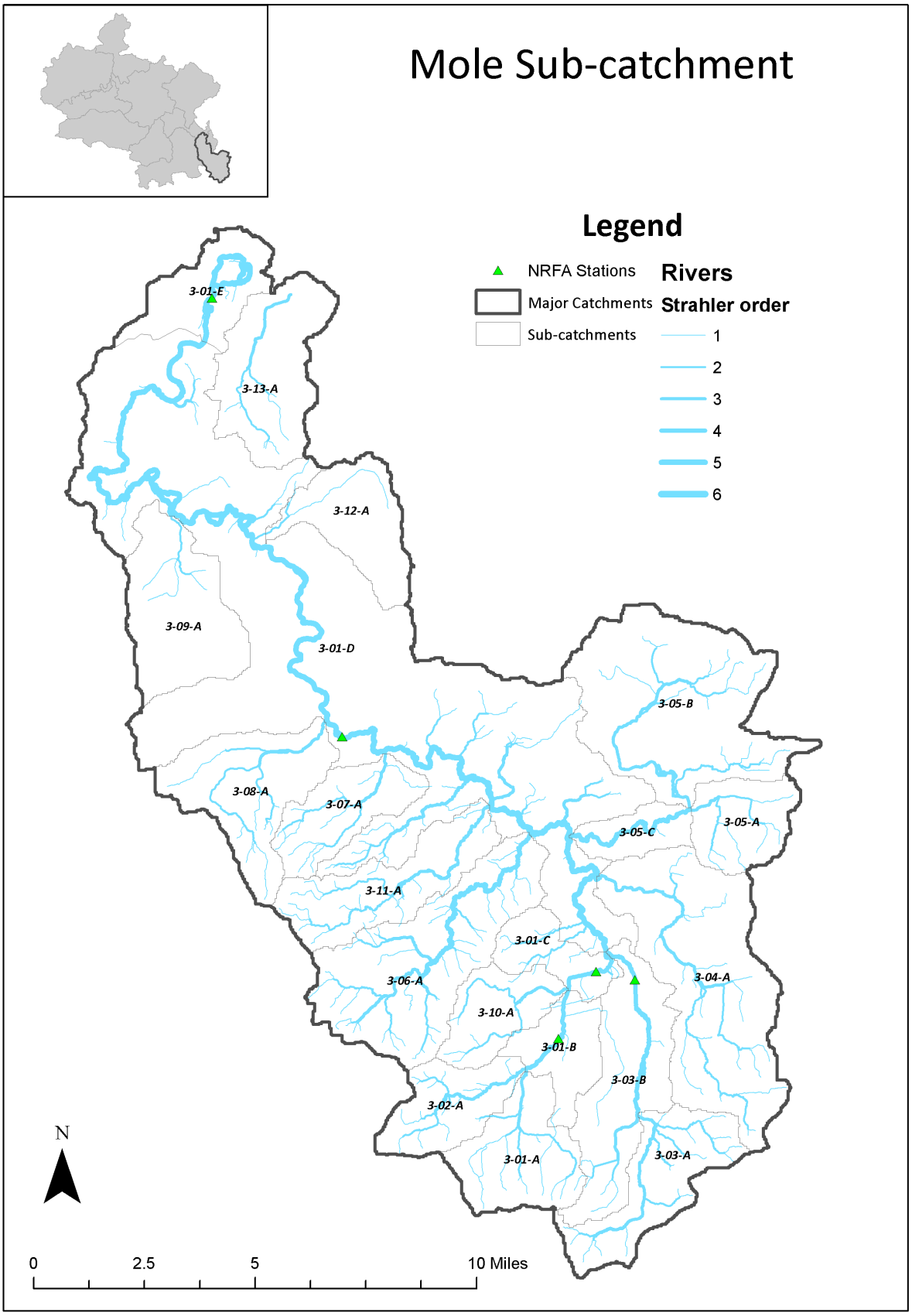
MAIDENHEAD TO SUNBURY

Sub-catchment	Name	River Typology	Strahler order	Area (km2)	Reach length (m)	Reach width (m)	*α* flow parameter	BFI	Urban	Intensive Agriculture	Non-intensive Agriculture	Wetlands	Forest
2-01-A	Port Lane Brook	Low, Small, Calcareous	1	15.99	2,166	9.8	0.104	0.63	67.73	0.00	28.62	1.43	2.23
2-02-A	Hogsmill	Low, Small, Calcareous	1	75.48	9,908	5.9	0.161	0.74	52.78	8.00	28.97	0.07	10.17
2-03-A	Ash & Stanwell brook	Low, Small, Calcareous	2	40.31	10,898	6.2	0.073	0.63	51.64	4.38	23.54	17.90	2.53
2-04-A	Datchet Common Brook	Low, Small, Calcareous	1	15.63	11,312	2.8	0.369	0.71	41.58	10.69	27.43	10.20	10.09
2-05-A	Chalvey Ditches at Slough	Low, Small, Siliceous	1	24.98	5,407	3.1	0.293	0.71	30.21	12.39	31.99	0.66	24.76
2-05-B	Salthill Stream	Low, Small, Siliceous	2	17.15	7,491	2.1	0.449	0.71	41.99	3.91	32.68	0.23	21.19
2-05-C	Chalvey Ditches (lower reaches to River Thames confluence)	Low, Small, Siliceous	3	0.75	506	4.0	0.154	0.71	12.87	13.79	58.64	1.66	13.04
2-06-A	Roundmoor Ditch and Boveney Ditch	Low, Small, Siliceous	1	16.04	6,394	3.2	0.373	0.70	22.13	25.33	38.37	3.94	10.23
2-07-A	Cut (Ascot to Bull Brook confluence at Warfield)	Low, Small, Calcareous	1	20.47	5,558	4.8	0.176	0.46	13.77	18.15	50.88	1.17	16.02
2-07-B	Cut at west Bracknell	Low, Small, Siliceous	1	10.80	5,265	0.8	0.569	0.46	60.99	5.47	10.17	1.00	22.37
2-07-C	Cut (Warfield to north Bracknell)	Low, Small, Calcareous	3	3.69	2,938	3.4	0.179	0.46	36.71	20.08	38.68	0.39	4.14
2-07-D	Cut (Binfield to River Thames confluence) and Maidenhead Ditch	Low, Medium, Calcareous	1	77.73	22,992	7.1	0.131	0.46	19.03	34.61	35.58	1.22	9.56
2-08-A	Bull Brook	Low, Small, Siliceous	1	13.65	5,157	2.6	0.254	0.46	37.76	4.07	10.86	1.69	45.62


Maidenhead to Sunbury Sub-catchment
Legend
NRFA Stations
Chemistry Sample Sites
Major Catchments
Sub-catchments
Major Abstraction Sites
Abstraction in m3/sec
< 0.005
0.005 - 0.05
0.05 - 0.5
0.5 - 5
> 5
Major Effluent Discharge Sites
Discharge in m3/sec
<0.005
0.005 - 0.05
0.05 - 0.5
>0.5
Rivers
STRAHLER
1
2
3
4
5
6
2-07-D
2-07-B
2-07-C
2-08-A
2-07-A
2-06-A
2-05-A
2-05-B
2-05-C
1-01-J
2-04-A
2-03-A
2-01-A
1-01-K
0
2.5
5
10 Miles
N

MOLE

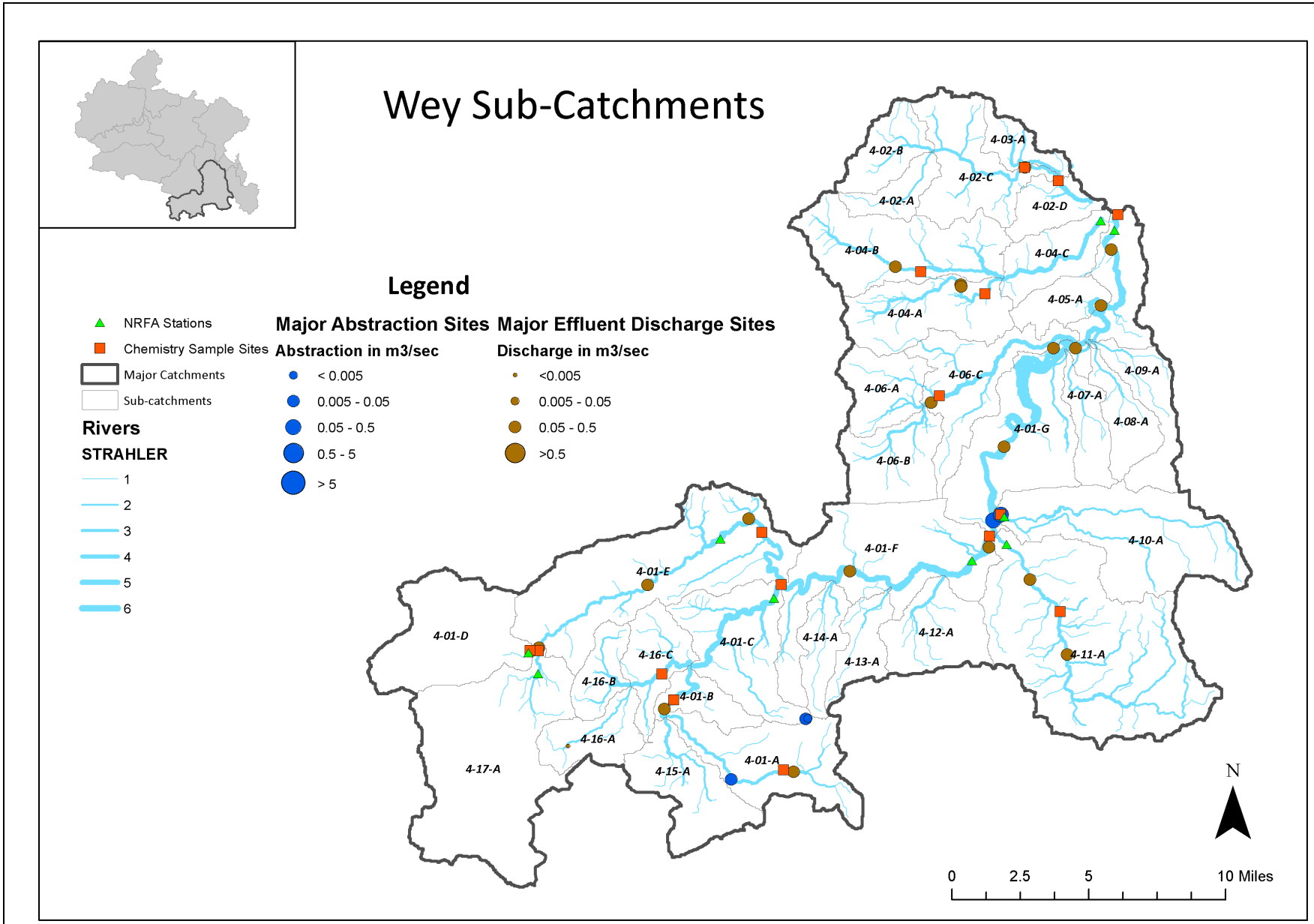
Sub-catchment	Name	River Typology	Strahler order	Area (km2)	Reach length (m)	Reach width (m)	*α* flow parameter	BFI	Urban	Intensive Agriculture	Non-intensive Agriculture	Wetlands	Forest
3-01-A	Ifield Brook	Low, Small, Calcareous	1	16.21	2,686	2.3	0.240	0.23	35.10	12.97	23.67	0.81	27.45
3-01-B	Mole (Crawley to Gatwick Airport)	Low, Small, Calcareous	4	9.69	4,406	3.5	0.250	0.23	43.21	11.06	36.83	0.00	8.90
3-01-C	Mole at Gatwick Airport	Low, Small, Calcareous	1	8.04	2,384	4.5	0.126	0.45	27.74	17.58	44.99	0.00	9.69
3-01-D	Mole (Horley to Hersham)	Low, Medium, Calcareous	5	147.56	62,008	13.9	0.096	0.42	19.38	15.20	38.17	0.49	26.77
3-01-E	Mole (Hersham to R. Thames conf at East Molesey)	Low, Medium, Calcareous	5	12.88	8,564	25.7	0.049	0.50	52.55	0.91	32.91	9.30	4.32
3-02-A	Baldhorns Brook	Low, Small, Calcareous	1	12.18	11,733	2.5	0.213	0.23	1.28	22.94	62.24	0.00	13.54
3-03-A	Stanford Brook	Low, Small, Siliceous	1	17.31	9,527	2.9	0.298	0.23	14.95	6.56	22.85	1.03	54.62
3-03-B	Tilgate Brook, Gatwick Stream and Crawters Brook at Crawley	Low, Small, Siliceous	1	22.26	8,194	3.0	0.323	0.61	56.50	6.29	16.90	0.98	19.32
3-04-A	Burstow Stream	Low, Small, Calcareous	1	40.77	17,318	2.6	0.228	0.61	16.36	18.68	45.17	0.33	19.46
3-05-A	Salfords Stream (Redhill Brook confluence upstream)	Low, Small, Calcareous	1	11.09	4,260	3.5	0.194	0.39	2.07	50.92	38.04	0.08	8.88
3-05-B	Redhill Brook	Low, Small, Calcareous	3	40.31	12,392	1.7	0.559	0.39	19.67	21.49	41.11	1.62	16.11
3-05-C	Salfords Stream (Salfords to River Mole confluence)	Low, Small, Calcareous	4	6.35	8,046	3.9	0.286	0.39	12.63	24.43	54.77	0.12	8.05
3-06-A	Deanoak Brook	Low, Small, Calcareous	1	33.77	12,687	4.9	0.135	0.39	2.34	17.91	63.05	0.97	15.73
3-07-A	Tanners Brook (Holmewood to River Mole confluence at Brockham)	Low, Small, Calcareous	1	12.69	2,477	2.8	0.237	0.42	9.72	24.82	35.60	0.38	29.48
3-08-A	Pipp Brook	Low, Small, Siliceous	1	20.95	12,007	2.2	0.363	0.42	17.80	13.90	37.17	0.87	30.26
3-09-A	Downside Ditches and Bookham Brook	Low, Small, Calcareous	1	21.20	4,642	3.8	0.239	0.42	17.92	19.12	37.88	0.52	24.57
3-10-A	Man's Brook (Charlwood to Gatwick Airport)	Low, Small, Calcareous	1	10.55	2,637	3.7	0.206	0.23	5.53	14.08	58.05	0.00	22.35
3-11-A	Leigh Brook	Low, Small, Calcareous	2	18.28	17,103	3.0	0.223	0.39	2.99	28.89	44.00	0.04	24.08
3-12-A	The Rye at Ashtead	Low, Small, Calcareous	1	14.47	1,977	1.4	0.420	0.93	37.84	4.92	29.03	0.00	28.22
3-13-A	Rythe	Low, Small, Calcareous	1	20.57	5,099	1.7	0.278	0.50	39.65	3.25	27.01	0.30	29.78


Mole Sub-catchment
Legend
NRFA Stations
Major Catchments
Sub-catchments
Rivers
Strahler order
1
2
3
4
5
6
3-01-E
3-13-A
3-12-A
3-09-A
3-01-D
3-05-B
3-08-A
3-07-A
3-05-C
3-05-A
3-11-A
3-01-C
3-06-A
3-04-A
3-10-A
3-01-B
3-03-B
3-02-A
3-01-A
3-03-A
N
0
2.5
5
10 Miles

WEY

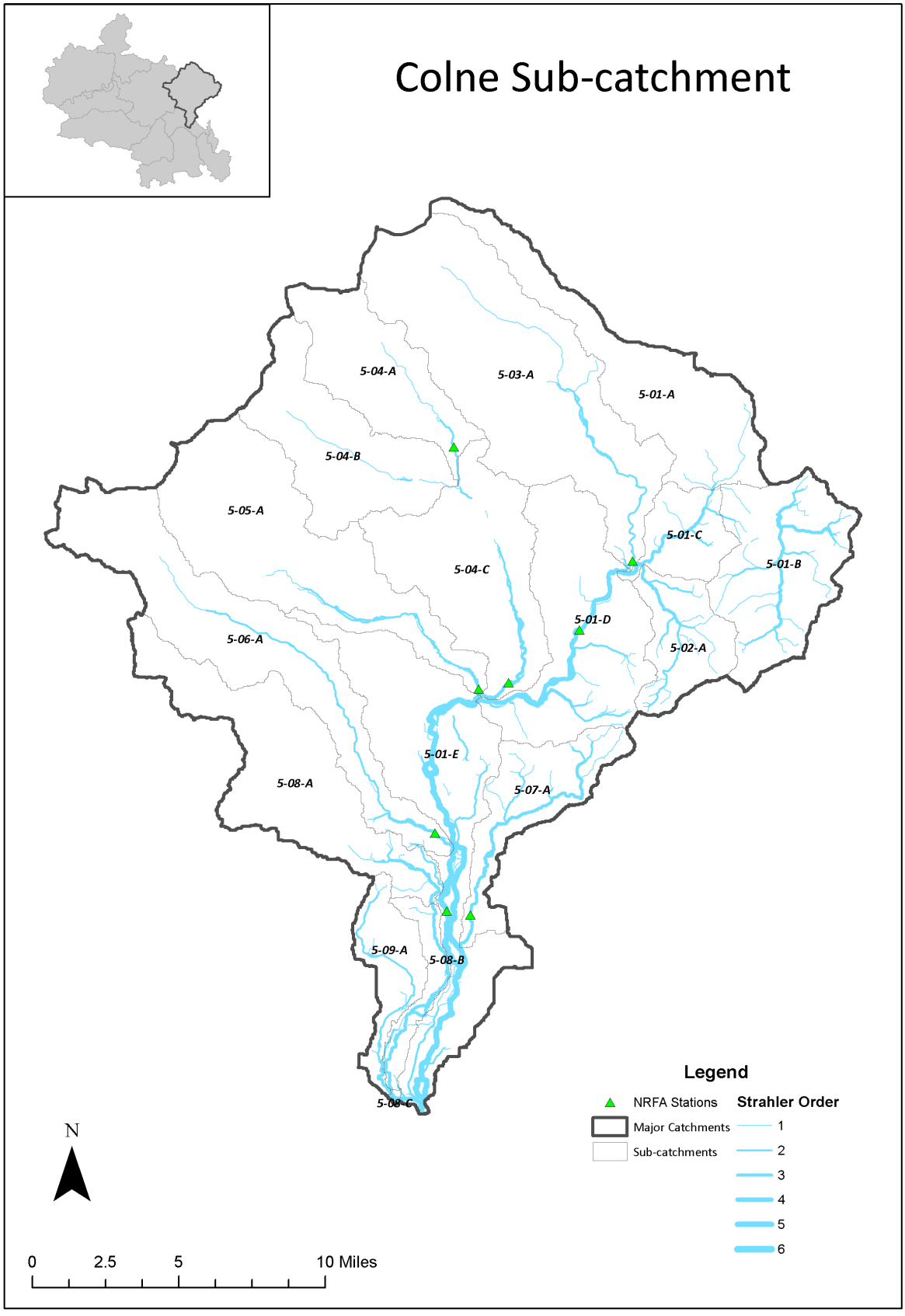
Sub-catchment	Name	River Typology	Strahler order	Area (km2)	Reach length (m)	Reach width (m)	*α* flow parameter	BFI	Urban	Intensive Agriculture	Non-intensive Agriculture	Wetlands	Forest
4-01-A	South Wey (Haslemere to Bordon)	Low, Small, Siliceous	3	40.49	17,234	4.1	0.277	0.72	17.05	4.43	23.83	4.71	49.98
4-01-B	South Wey (Bordon to River Slea confluence)	Low, Small, Siliceous	1	11.84	5,891	5.6	0.157	0.72	18.34	5.86	28.89	8.84	38.06
4-01-C	South Wey (River Slea confluence to Tilford)	Low, Medium, Siliceous	2	37.79	12,062	8.5	0.125	0.72	6.70	13.79	29.32	8.06	42.14
4-01-D	North Wey at Alton	Low, Small, Calcareous	1	45.85	2,311	2.6	0.372	0.88	6.72	49.06	29.58	0.15	14.49
4-01-E	North Wey (Alton to Tilford)	Low, Medium, Siliceous	1	82.51	31,734	5.9	0.199	0.73	14.28	39.07	26.24	1.48	18.93
4-01-F	Wey (Tilford to Shalford)	Low, Medium, Siliceous	5	65.23	23,488	12.2	0.136	0.67	10.23	20.58	31.77	4.63	32.79
4-01-G	Wey (Shalford to River Thames confluence at Weybridge)	Low, Medium, Siliceous	5	73.85	50,472	15.3	0.090	0.65	32.13	12.05	36.55	0.88	18.40
4-02-A	Chertsey Bourne (Sunningdale to Virginia Water)	Low, Small, Siliceous	1	10.80	7,667	1.9	0.322	0.46	23.88	5.06	27.12	1.49	42.45
4-02-B	Chertsey Bourne (Ascot to Virginia Water)	Low, Small, Siliceous	1	16.73	1,589	1.9	0.326	0.71	20.29	7.52	19.81	1.77	50.61
4-02-C	Chertsey Bourne (Virginia Water to Chertsey)	Low, Small, Siliceous	1	34.07	10,318	4.4	0.330	0.66	16.21	8.18	26.85	8.29	40.47
4-02-D	Chertsey Bourne (Chertsey to River Thames confluence)	Low, Small, Siliceous	1	13.15	4,322	5.7	0.246	0.67	29.51	6.66	41.37	0.61	21.85
4-03-A	The Moat at Egham	Low, Small, Siliceous	1	10.25	4,741	3.5	0.190	0.66	26.27	8.74	27.91	14.51	22.57
4-04-A	Addlestone Bourne (West End to Hale/Mill Bourne confluence at Mimbridge)	Low, Small, Siliceous	1	33.95	12,397	3.0	0.218	0.71	28.25	4.64	24.22	22.18	20.71
4-04-B	Hale/Mill Bourne (Bagshot to Addlestone Bourne confluence near Chobham)	Low, Small, Siliceous	1	46.32	15,621	2.7	0.239	0.67	15.12	6.96	30.43	9.54	37.96
4-04-C	Addlestone Bourne (Mill/Hale to Chertsey Bourne)	Low, Small, Siliceous	4	19.45	11,799	5.6	0.156	0.67	31.88	7.77	33.02	1.68	25.65
4-05-A	Wey Navigation (Pyrford reach)	Low, Small, Siliceous	1	12.28	3,832	13.9	0.059	0.67	59.29	1.67	24.13	0.12	14.80
4-06-A	Hoe Stream (Normandy to Pirbright)	Low, Small, Siliceous	1	19.94	5,511	2.0	0.322	0.71	6.16	4.54	17.26	29.57	42.47
4-06-B	Clasford Brook and Wood Street Brook	Low, Small, Siliceous	1	25.17	4,648	4.1	0.166	0.67	7.88	31.43	36.89	2.16	21.63
4-06-C	Hoe Stream (Pirbright to River Wey confluence at Woking)	Low, Small, Siliceous	1	33.92	14,517	5.8	0.166	0.67	30.28	5.66	34.55	2.25	27.26
4-07-A	East Clandon Stream	Low, Small, Calcareous	1	13.71	4,218	2.1	0.217	0.93	8.25	25.38	40.10	1.12	25.15
4-08-A	Guileshill Brook	Low, Small, Calcareous	1	15.53	3,889	7.6	0.136	0.93	6.26	30.48	40.77	0.00	22.50
4-09-A	Stratford Brook	Low, Small, Calcareous	1	19.58	3,094	2.8	0.228	0.93	13.68	11.20	28.55	0.04	46.53
4-10-A	Tillingbourne	Low, Small, Siliceous	2	61.44	24,122	4.2	0.168	0.89	4.56	13.19	37.49	0.85	43.91
4-11-A	Cranleigh Waters	Low, Medium, Calcareous	1	110.14	28,791	5.4	0.064	0.39	5.89	19.09	48.05	1.86	25.11

Sub-catchment	Name	River Typology	Strahler order	Area (km2)	Reach length (m)	Reach width (m)	*α* flow parameter	BFI	Urban	Intensive Agriculture	Non-intensive Agriculture	Wetlands	Forest
4-12-A	Ock	Low, Small, Siliceous	1	25.67	7,510	1.9	0.368	0.39	12.98	21.53	30.56	1.86	33.07
4-13-A	Royal Brook	Low, Small, Siliceous	2	14.25	3,584	2.4	0.274	0.72	2.00	14.63	26.76	10.63	45.98
4-14-A	Truxford Brook	Low, Small, Siliceous	1	14.89	2,590	3.0	0.276	0.72	3.40	9.90	18.36	29.01	39.33
4-15-A	Hollywater and Deadwater at Bordon	Low, Small, Siliceous	1	30.05	5,997	3.4	0.226	0.40	11.02	8.76	20.55	15.16	44.51
4-16-A	Oakhanger Stream	Low, Small, Calcareous	1	18.06	8,343	3.1	0.230	0.40	6.26	26.93	38.99	3.58	24.24
4-16-B	Kingsley Stream	Low, Small, Calcareous	1	12.80	873	3.8	0.160	0.40	0.49	40.03	37.69	1.66	20.12
4-16-C	Slea (Kingsley to Sleaford)	Low, Small, Calcareous	1	18.71	5,544	4.3	0.151	0.40	6.79	20.18	35.43	3.94	33.66
4-17-A	Caker Stream	Low, Small, Calcareous	1	87.79	5,567	2.8	0.137	0.40	3.07	48.87	34.32	0.19	13.54


Wey Sub-Catchments
Legend
NRFA Stations
Chemistry Sample Sites
Major Catchments
Sub-catchments
Rivers
STRAHLER
1
2
3
4
5
6
Major Abstraction Sites
Abstraction in m3/sec
< 0.005
0.005 - 0.05
0.05 - 0.5
0.5 - 5
> 5
Major Effluent Discharge Sites
Discharge in m3/sec
<0.005
0.005 - 0.05
0.05 - 0.5
>0.5
4-02-B
4-03-A
4-02-C
4-02-A
4-02-D
4-04-B
4-04-C
4-05-A
4-04-A
4-06-C
4-09-A
4-06-A
4-07-A
4-08-A
4-01-G
4-06-B
4-10-A
4-01-F
4-01-E
4-01-D
4-01-C
4-14-A
4-12-A
4-16-C
4-11-A
4-13-A
4-16-B
4-01-B
4-16-A
4-01-A
4-17-A
4-15-A
N
0
2.5
5
10 Miles

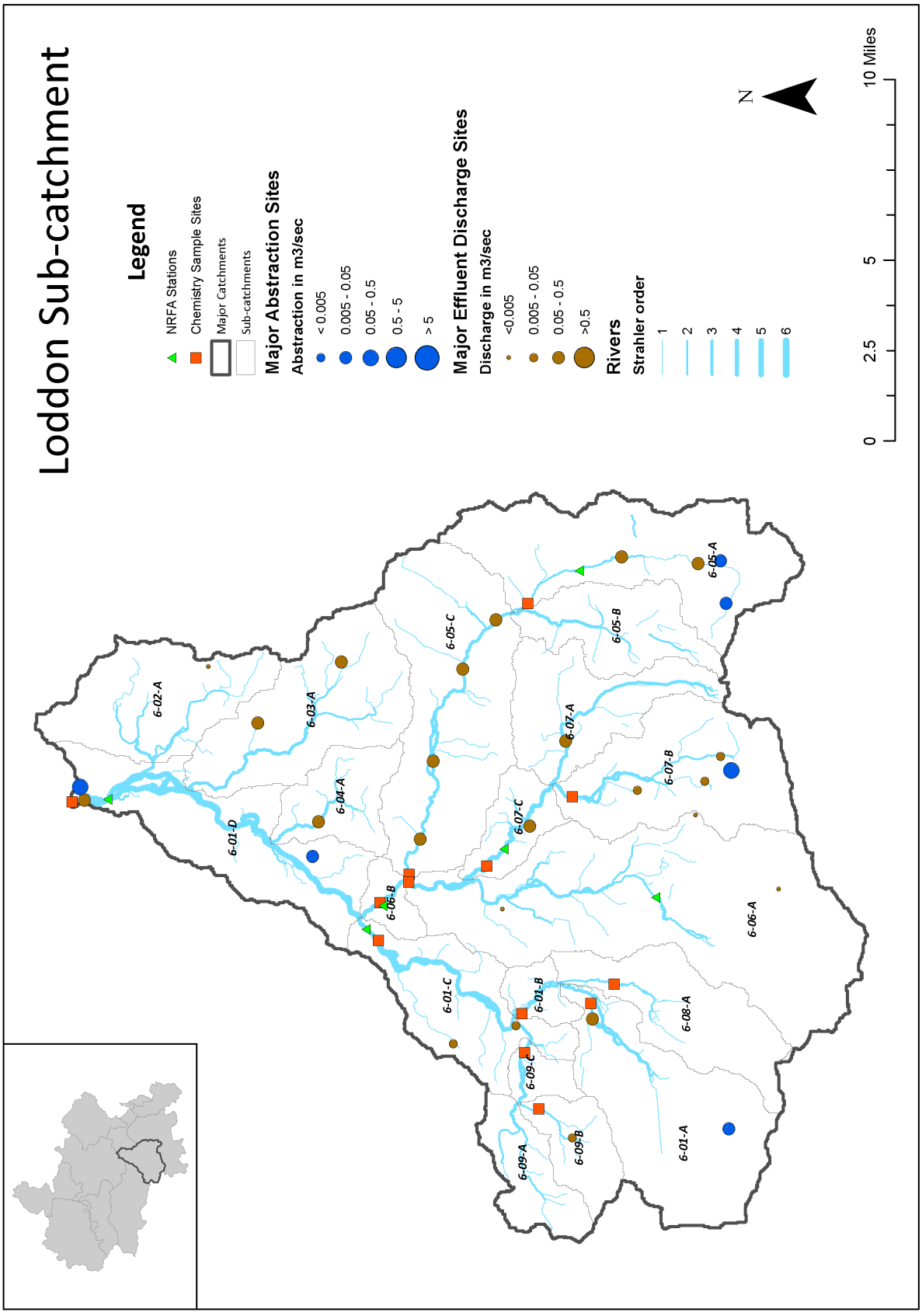
COLNE

Sub-catchment	Name	River Typology	Strahler order	Area (km2)	Reach length (m)	Reach width (m)	*α* flow parameter	BFI	Urban	Intensive Agriculture	Non-intensive Agriculture	Wetlands	Forest
5-01-A	Ellen Brook	Low, Small, Calcareous	1	66.72	3,762	3.0	0.219	0.91	23.15	42.85	25.05	0.78	8.16
5-01-B	Colne (upper east arm including Mimshall Brook)	Low, Small, Calcareous	1	61.21	24,303	2.8	0.272	0.88	17.06	33.98	35.71	0.14	13.11
5-01-C	Colne (upper stretch, Hatfield to confluence with Ver)	Low, Medium, Calcareous	1	21.74	10,521	6.9	0.078	0.88	17.39	41.05	31.01	1.83	8.72
5-01-D	Colne (from Confluence with Ver to Gade)	Low, Medium, Calcareous	4	77.79	20,653	7.4	0.100	0.68	39.22	20.10	27.08	1.10	12.51
5-01-E	Colne and GUC (from confluence with Chess to Ash)	Low, Medium, Calcareous	5	98.75	56,321	13.2	0.106	0.87	31.18	15.36	33.15	5.89	14.41
5-02-A	Tykeswater	Low, Small, Calcareous	1	28.79	7,859	2.7	0.274	0.88	34.11	11.77	40.41	1.22	12.49
5-03-A	Ver	Low, Medium, Calcareous	2	134.81	27,570	5.4	0.235	0.88	16.73	50.31	24.27	0.52	8.18
5-04-A	Gade (Upper stretch Great Gaddesden to confluence with Bulbourne / GUC)	Low, Small, Calcareous	1	48.61	10,253	10.7	0.088	0.83	5.80	35.02	36.32	0.12	22.74
5-04-B	Bulbourne	Low, Small, Calcareous	1	61.13	9,140	4.2	0.129	0.83	15.61	35.79	34.18	0.50	13.92
5-04-C	Gade (from confluence with Bulbourne to Chess)	Low, Medium, Calcareous	1	75.05	15,601	12.1	0.111	0.88	28.13	23.15	35.23	0.63	12.86
5-05-A	Chess	Low, Small, Calcareous	2	97.87	19,137	8.0	0.340	0.95	8.79	31.15	45.18	0.34	14.53
5-06-A	Misbourne	Low, Small, Calcareous	2	94.36	27,179	7.0	0.242	0.90	13.45	32.47	35.07	0.47	18.54
5-07-A	Pinn	Low, Small, Calcareous	1	38.78	19,826	2.6	0.101	0.21	57.02	0.84	27.10	0.41	14.62
5-08-A	Alderbourne	Low, Small, Calcareous	3	79.26	8,308	3.5	0.356	0.90	15.56	18.76	38.64	1.53	25.51
5-08-B	Colne Brook (from confluence with Alderbourne to confluence with Horton Brook)	Low, Small, Calcareous	3	13.38	14,912	9.4	0.106	0.21	19.06	23.55	30.78	17.00	9.62
5-08-C	Colne Brook (from confluence with Horton Brook to Thames)	Low, Small, Calcareous	3	0.43	974	8.0	0.140	0.66	39.10	8.87	25.87	18.02	8.14
5-09-A	Horton Brook	Low, Small, Calcareous	2	23.76	18,310	3.5	0.352	0.66	21.85	20.72	28.04	9.92	19.47


Colne Sub-catchment
5-04-A
5-03-A
5-01-A
5-04-B
5-05-A
5-01-C
5-01-B
5-04-C
5-01-D
5-06-A
5-02-A
5-01-E
5-08-A
5-07-A
5-09-A
5-08-B
5-08-C
Legend
NRFA Stations
Strahler Order
Major Catchments
1
Sub-catchments
2
3
4
5
6
N
0
2.5
5
10 Miles

LODDON

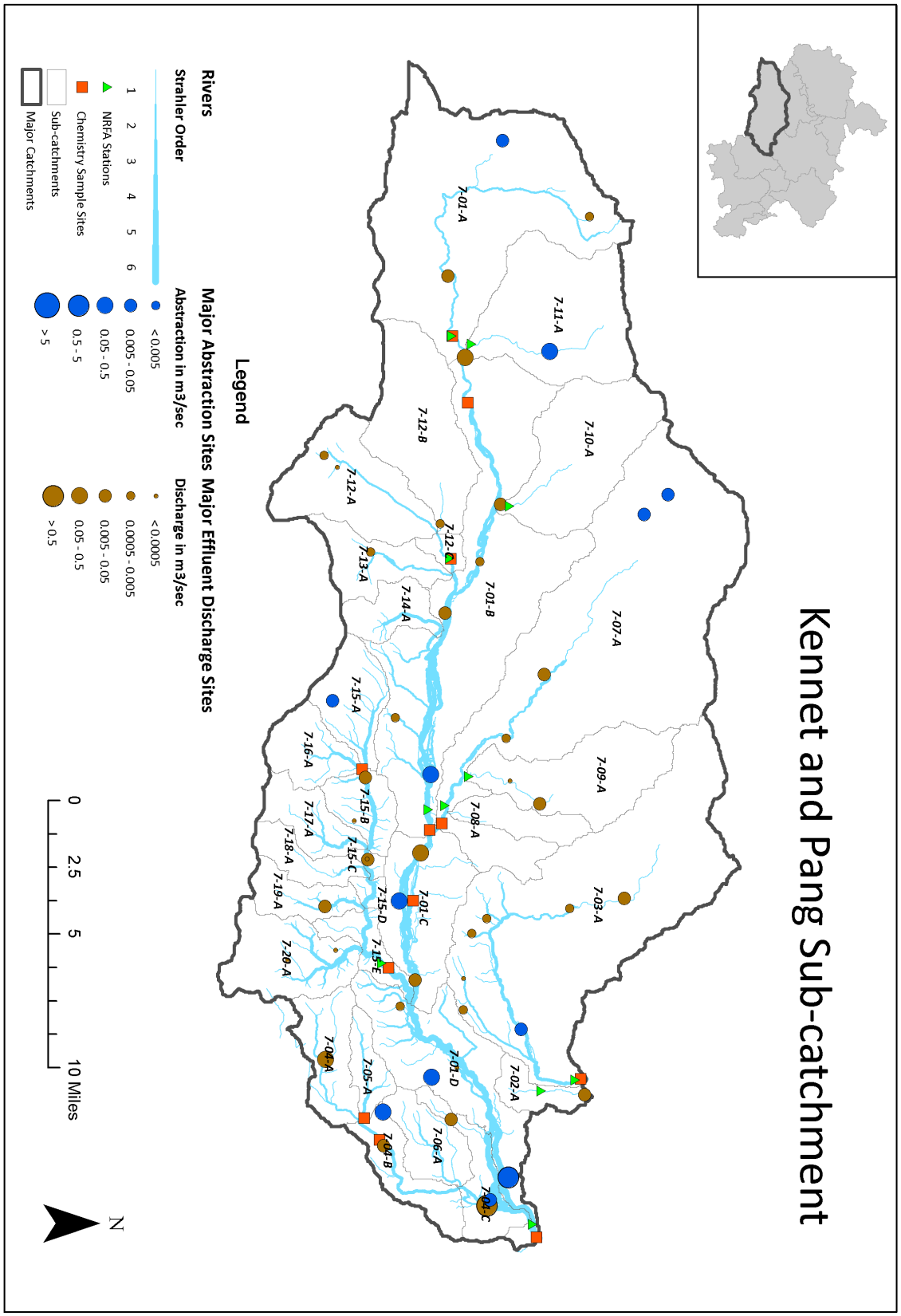
Sub-catchment	Name	River Typology	Strahler order	Area (km2)	Reach length (m)	Reach width (m)	*a* flow parameter	BFI	Urban	Intensive Agriculture	Non-intensive Agriculture	Wetlands	Forest
6-01-A	Loddon (Basingstoke to River Lyde confluence at Hartley Wespall)	Low, Small, Calcareous	1	55.71	11,559	6.2	0.296	0.94	42.66	30.41	17.30	0.27	9.36
6-01-B	Loddon (Hartley Wespall to Sherfield on Loddon)	Low, Small, Calcareous	3	6.96	5,699	8.1	0.246	0.64	1.98	34.72	48.64	0.19	14.48
6-01-C	Loddon (Sherfield on Loddon to Swallowfield)	Low, Medium, Calcareous	4	33.74	14,622	11.8	0.121	0.76	4.42	54.10	28.83	0.74	11.91
6-01-D	Loddon (Swallowfield to River Thames confluence)	Low, Medium, Calcareous	5	47.52	22,703	14.0	0.140	0.69	35.38	22.77	28.85	3.10	9.90
6-02-A	Twyford Brook	Low, Small, Calcareous	2	37.03	9,227	4.8	0.173	0.46	3.99	44.19	36.07	0.52	15.22
6-03-A	Emm Brook	Low, Small, Siliceous	1	47.36	14,566	3.1	0.300	0.46	30.99	16.95	24.87	3.13	24.05
6-04-A	Barkham Brook	Low, Small, Calcareous	1	18.40	6,903	2.9	0.286	0.67	16.54	20.45	45.58	1.97	15.45
6-05-A	Blackwater (Aldershot to Cove Brook confluence at Hawley)	Low, Small, Siliceous	1	60.11	16,641	4.1	0.101	0.71	44.32	11.00	13.37	9.41	21.90
6-05-B	Cove Brook	Low, Small, Siliceous	1	25.17	6,828	3.0	0.176	0.71	49.31	6.50	17.89	3.70	22.60
6-05-C	Blackwater (Hawley to Whitewater confluence at Bramshill)	Low, Medium, Calcareous	1	69.29	16,777	9.4	0.181	0.64	24.11	8.32	24.43	12.18	30.97
6-06-A	Whitewater	Low, Medium, Calcareous	1	111.01	19,628	7.4	0.232	0.94	5.99	47.42	27.24	1.01	18.34
6-06-B	Blackwater (Bramshill to River Loddon confluence at Swallowfield)	Low, Medium, Calcareous	4	6.46	2,905	11.9	0.101	0.67	4.56	46.56	36.96	0.40	11.53
6-07-A	Fleet Brook	Low, Small, Siliceous	1	32.28	16,041	2.2	0.296	0.71	22.62	12.24	13.77	8.94	42.43
6-07-B	Hart (Crondall to Elvetham)	Low, Small, Siliceous	1	47.32	10,889	3.4	0.246	0.73	13.07	47.52	19.43	0.63	19.35
6-07-C	Hart (Elvetham to Hartley Wintney)	Low, Small, Siliceous	1	12.58	7,859	5.7	0.115	0.64	4.78	18.14	27.05	12.37	37.66
6-08-A	Lyde	Low, Small, Calcareous	2	32.85	8,712	5.0	0.209	0.94	3.85	51.89	23.64	0.32	20.31
6-09-A	Bow Brook (Pamber End to Bramley)	Low, Small, Calcareous	2	17.06	14,311	3.0	0.290	0.52	1.52	47.12	33.35	0.74	17.27
6-09-B	Vyne Stream	Low, Small, Calcareous	1	14.24	7,313	3.2	0.228	0.52	4.86	53.40	23.17	1.82	16.76
6-09-C	Bow Brook (Pamber End to Sherfield Green)	Low, Small, Calcareous	3	6.12	3,726	4.9	0.228	0.94	6.93	25.22	30.39	0.31	37.15


Loddon Sub-catchment
Legend
NRFA Stations
Chemistry Sample Sites
Major Catchments
Sub-catchments
Major Abstraction Sites
Abstraction in m3/sec
< 0.005
0.005 - 0.05
0.05 - 0.5
0.5 - 5
> 5
Major Effluent Discharge Sites
Discharge in m3/sec
<0.005
0.005 - 0.05
0.05 - 0.5
>0.5
Rivers
Strahler order
1
2
3
4
5
6
N
0
2.5
5
10 Miles
6-01-A
6-01-B
6-01-C
6-01-D
6-02-A
6-03-A
6-04-A
6-05-A
6-05-B
6-05-C
6-06-A
6-06-B
6-07-A
6-07-B
6-07-C
6-08-A
6-09-A
6-09-B
6-09-C

KENNET AND PANG

Sub-catchment	Name	River Typology	Strahler order	Area (km2)	Reach length (m)	Reach width (m)	*α* flow parameter	BFI	Urban	Intensive Agriculture	Non-intensive Agriculture	Wetlands	Forest
7-01-A	Upper Kennet to Marlborough	Low, Medium, Calcareous	2	144.56	27,765	6.7	0.145	0.94	1.82	65.18	28.66	0.24	4.09
7-01-B	Middle Kennet (Marlborough to Newbury)	Low, Medium, Calcareous	3	147.63	87,096	11.9	0.118	0.93	5.99	49.47	30.46	0.44	13.64
7-01-C	Kennet (Lambourn confluence to Enborne confluence)	Low, Medium, Calcareous	4	41.12	17,188	15.0	0.093	0.52	16.58	29.22	33.19	4.93	16.08
7-01-D	Kennet and Holy Brook	Low, Large, Calcareous	5	57.94	31,029	10.5	0.055	0.88	18.58	22.22	34.18	6.69	18.34
7-02-A	Sulham Brook	Low, Small, Calcareous	1	10.40	5,861	5.0	0.114	0.61	6.81	40.13	35.58	0.35	17.14
7-03-A	Pang	Low, Medium, Calcareous	1	171.49	36,570	5.7	0.116	0.87	2.21	52.12	27.66	0.76	17.24
7-04-A	Foudry Brook (Source to WestEnd Brook)	Low, Small, Calcareous	1	23.15	11,060	2.7	0.324	0.52	16.48	31.85	27.02	1.19	23.47
7-04-B	Foudry Brook (West End Brook to M4)	Low, Small, Calcareous	3	19.50	9,986	4.1	0.260	0.76	10.34	49.10	32.78	0.32	7.46
7-04-C	Kennet and Foudry Brook and Clayhill Brook in Reading	Low, Small, Calcareous	5	18.52	15,573	13.3	0.072	0.64	39.30	20.23	20.36	12.79	7.32
7-05-A	West End Brook (tributary of Foudry Brook)	Low, Small, Calcareous	2	10.67	1,837	2.6	0.281	0.52	5.04	27.21	22.68	8.56	36.52
7-06-A	Burghfield Brook	Low, Small, Calcareous	1	18.17	6,782	7.5	0.173	0.88	9.16	37.03	33.36	3.23	17.22
7-07-A	Lambourn (Source to Newbury)	Low, Medium, Calcareous	2	205.37	32,228	10.5	0.116	0.97	2.35	61.92	27.78	0.30	7.65
7-08-A	Lambourn tributary (North of Newbury)	Low, Small, Calcareous	1	13.70	-	0.0	0.319	0.97	7.48	34.16	39.06	1.89	17.41
7-09-A	Winterbourne	Low, Small, Calcareous	1	45.02	7,128	2.5	0.215	0.96	0.55	72.32	19.07	0.15	7.92
7-10-A	Aldbourne	Low, Small, Calcareous	1	53.98	3,919	4.8	0.453	0.96	1.86	64.41	29.70	0.22	3.81
7-11-A	Og	Low, Small, Calcareous	1	65.17	3,111	6.8	0.193	0.95	1.18	61.62	34.89	0.16	2.15
7-12-A	Upper Dun	Low, Small, Calcareous	1	44.71	9,846	3.7	0.403	0.95	1.35	65.03	20.62	0.16	12.85
7-12-B	Froxfield Stream	Low, Small, Calcareous	1	51.23	3,422	3.5	0.251	0.94	0.33	47.88	20.43	0.04	31.31
7-12-C	Kennet and Avon Canal and Dun above Hungerford	Low, Small, Calcareous	2	4.56	3,725	6.1	0.381	0.95	0.42	59.67	28.52	0.70	10.68
7-13-A	Shalbourne (source to Kennet at Hungerford)	Low, Small, Calcareous	2	21.09	7,338	3.7	0.332	0.95	1.79	60.71	28.46	1.30	7.74
7-14-A	Inkpen Stream (source to Kennet)	Low, Small, Calcareous	1	14.99	3,624	8.0	0.238	0.95	0.54	47.37	33.64	2.52	15.92
7-15-A	Enborne (Source to downstream A34)	Low, Small, Calcareous	1	22.63	10,660	3.3	0.550	0.93	2.18	43.21	38.86	0.15	15.60
7-15-B	Enborne (downstream A34 to Burghclere Brook)	Low, Small, Calcareous	1	15.02	6,394	6.2	0.263	0.93	11.50	17.83	34.53	2.80	33.34
7-15-C	Enborne (Burghclere Brook to Ecchinswell Brook)	Low, Small, Calcareous	1	2.27	2,503	5.7	0.255	0.93	10.66	24.92	31.44	1.62	31.36
7-15-D	Enborne (Ecchinswell Brook to Kingsclere Brook)	Low, Small, Calcareous	1	3.14	3,367	5.7	0.287	0.52	2.65	29.08	37.88	2.25	28.14
7-15-E	Lower Enborne	Low, Medium, Calcareous	4	11.78	10,061	7.6	0.112	0.52	0.73	57.43	24.91	0.62	16.32
7-16-A	Hollingtonstand Milford Lake (source to Enborne)	Low, Small, Calcareous	1	18.91	2,473	3.2	0.476	0.93	5.56	28.94	28.30	1.08	36.12

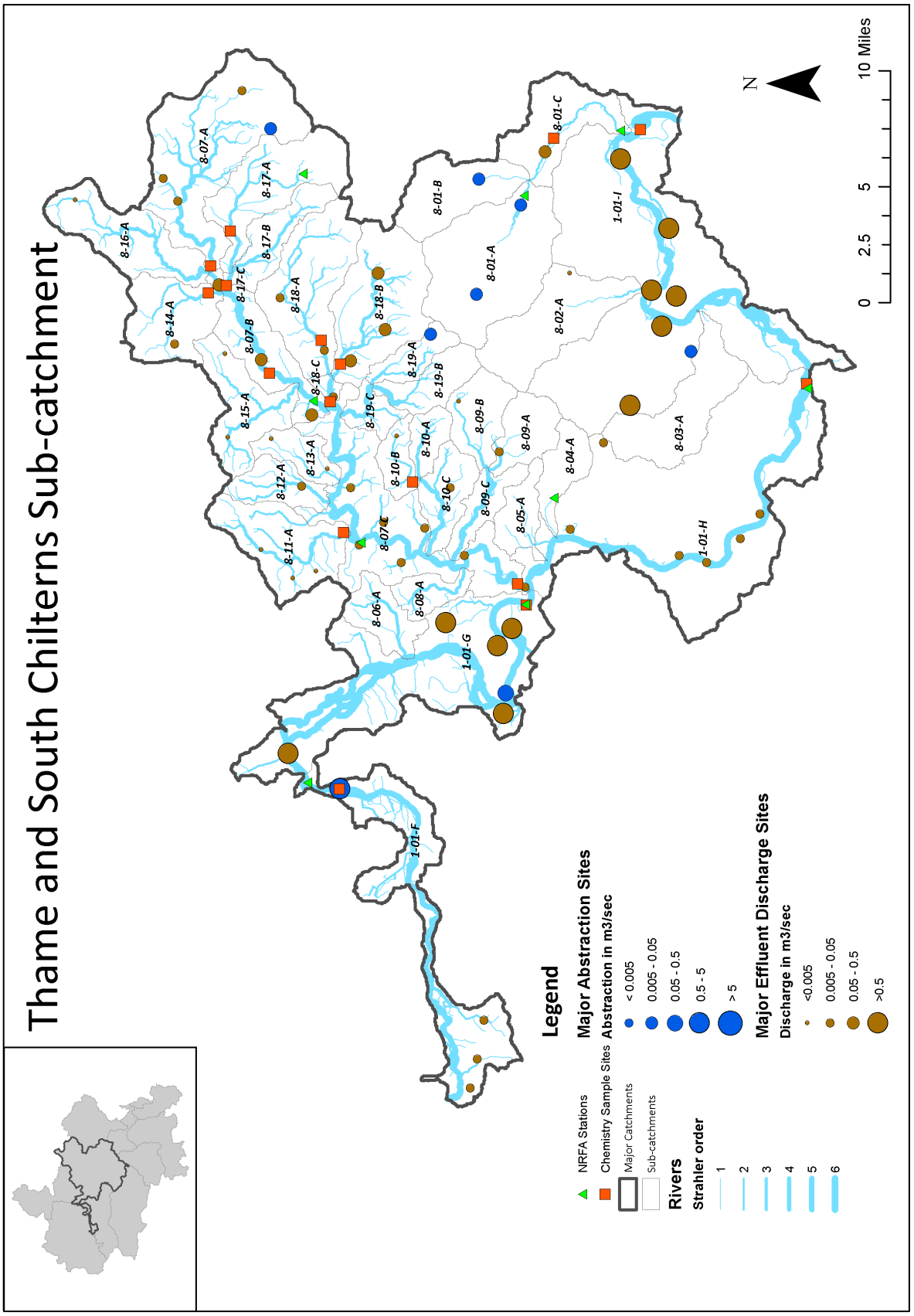
Sub-catchment	Name	River Typology	Strahler order	Area (km2)	Reach length (m)	Reach width (m)	*α* flow parameter	BFI	Urban	Intensive Agriculture	Non-intensive Agriculture	Wetlands	Forest
7-17-A	Earlstone Stream and Burghclere Brook (source to Enborne)	Low, Small, Calcareous	1	17.06	4,655	3.7	0.420	0.93	1.25	47.34	30.56	0.80	20.05
7-18-A	Ecchinswell Brook (source to Enborne)	Low, Small, Calcareous	1	13.19	7,127	4.3	0.394	0.93	0.93	42.30	40.43	0.32	16.02
7-19-A	Kingsclere Brook (Source to Enborne)	Low, Small, Calcareous	1	14.87	7,529	3.6	0.396	0.52	5.83	48.83	33.17	0.52	11.65
7-20-A	Baughurst Brook	Low, Small, Calcareous	1	33.92	6,578	3.4	0.449	0.52	1.41	51.61	24.75	0.65	21.58


Kennet and Pang Sub-catchment
7-01-A
7-11-A
7-10-A
7-12-B
7-12-A
7-13-A
7-12-C
7-01-B
7-14-A
7-07-A
7-15-A
7-16-A
7-09-A
7-08-A
7-15-B
7-17-A
7-18-A
7-15-C
7-19-A
7-01-C
7-15-D
7-20-A
7-15-E
7-03-A
7-04-A
7-05-A
7-01-D
7-02-A
7-06-A
7-04-B
7-01-E
Legend
Rivers
Strahler Order
1
2
3
4
5
6
NRFA Stations
Chemistry Sample Sites
Sub-catchments
Major Catchments
Major Abstraction Sites
Abstraction in m3/sec
< 0.005
0.005 - 0.05
0.05 - 0.5
0.5 - 5
> 5
Major Effluent Discharge Sites
Discharge in m3/sec
< 0.0005
0.0005 - 0.005
0.005 - 0.05
0.05 - 0.5
> 0.5
0
2.5
5
10 Miles
N

THAME AND SOUTH CHILTERNS

Sub-catchment	Name	River Typology	Strahler order	Area (km2)	Reach length (m)	Reach width (m)	*α* flow parameter	BFI	Urban	Intensive Agriculture	Non-intensive Agriculture	Wetlands	Forest
8-01-A	Wye (Source to High Wycombe fire station)	Low, Small, Calcareous	2	71.07	5,134	7.1	0.361	0.94	12.49	32.88	33.62	0.39	20.63
8-01-B	Hughenden Stream	Low, Small, Calcareous	1	32.56	3,628	1.8	0.345	0.94	11.55	23.77	44.40	0.04	20.25
8-01-C	Wye (High Wycombe fire station to Thames)	Low, Medium, Calcareous	1	34.18	12,067	5.5	0.056	0.93	38.18	17.42	30.35	0.59	13.46
8-02-A	Hamble Brook and Hambleden Stream	Low, Small, Calcareous	1	44.42	6,713	4.0	0.533	0.94	0.97	20.56	47.23	0.07	31.18
8-03-A	Harpsden Court Drain (West of Henley)	Low, Small, Calcareous	1	40.27	-	0.0	0.552	0.69	3.91	27.13	41.93	0.07	26.95
8-04-A	Ewelme Stream (Source to Thames)	Low, Small, Calcareous	1	15.65	3,376	3.0	0.376	0.98	4.14	58.31	24.50	0.38	12.66
8-05-A	Berrick Stream and Lady Brook	Low, Small, Calcareous	1	14.37	3,932	1.7	0.883	0.98	0.27	73.21	24.04	0.18	2.30
8-06-A	Northfield Brook (Source to Thames) at Sandford	Low, Small, Calcareous	1	17.97	1,784	7.7	0.299	0.54	34.95	32.86	24.61	0.30	7.28
8-07-A	Thame upstream of Aylesbury	Low, Small, Calcareous	1	84.89	24,613	3.9	0.201	0.96	6.71	39.03	46.94	1.72	5.60
8-07-B	Thame (Aylesbury to Scotsgrove Brook)	Low, Medium, Calcareous	5	30.82	18,215	8.8	0.083	0.53	3.24	41.35	52.42	0.39	2.60
8-07-C	Thame (Scotsgrove Brook to Thames)	Low, Medium, Calcareous	5	77.77	53,086	10.9	0.041	0.54	5.66	52.21	37.46	1.22	3.45
8-08-A	Baldon Brook (South of Oxford)	Low, Small, Calcareous	1	11.45	7,850	2.2	0.659	0.54	2.77	80.17	15.90	0.11	1.05
8-09-A	Chalgrove Brook at Watlington	Low, Small, Calcareous	1	18.41	2,830	2.7	0.673	0.98	3.33	55.72	29.55	0.05	11.35
8-09-B	Lewknor Brook	Low, Small, Calcareous	2	20.84	6,535	2.7	0.386	0.98	1.15	66.16	24.62	0.21	7.86
8-09-C	Chalgrove Brook (Watlington to Thame)	Low, Small, Calcareous	4	13.76	9,126	3.5	0.158	0.98	6.49	56.68	32.89	0.31	3.62
8-10-A	Haseley Brook (Upper reaches)	Low, Small, Calcareous	1	10.06	4,153	3.5	0.497	0.53	1.01	61.06	32.79	0.09	5.03
8-10-B	Latchford Brook at Tetsworth	Low, Small, Calcareous	1	10.88	5,898	2.3	0.698	0.53	1.44	60.18	36.42	0.19	1.78
8-10-C	Haseley Brook (Latchford Brook to Thame)	Low, Small, Calcareous	1	19.42	10,299	3.6	0.432	0.54	1.25	60.50	34.23	0.34	3.67
8-11-A	Holton Brook and tributaries	Low, Small, Calcareous	1	40.90	16,098	2.7	0.671	0.54	2.44	38.26	41.61	0.17	17.52
8-12-A	Worminghall Brook and tributaries	Low, Small, Calcareous	1	16.82	7,619	2.1	0.340	0.53	2.06	44.25	52.87	0.04	0.78
8-13-A	Peppershill and Shabbington Brooks	Low, Small, Calcareous	1	13.44	12,229	1.7	0.344	0.53	0.39	39.78	58.84	0.04	0.94
8-14-A	Fleet Marston Brook, Denham Brook, Pitchcott Brook west	Low, Small, Calcareous	2	32.23	8,071	3.3	0.135	0.16	1.88	40.29	54.72	0.02	3.09
8-15-A	Dorton, Chearsley and Waddesdon Brooks	Low, Small, Calcareous	1	32.31	11,545	3.1	0.242	0.53	0.27	34.96	60.20	0.09	4.48
8-16-A	Hardwick Brook (Source to Thame)	Low, Small, Calcareous	3	38.44	23,720	3.6	0.090	0.96	1.75	53.17	43.90	0.22	0.96
8-17-A	Bear Brook and Wendover Brook	Low, Small, Calcareous	1	43.12	21,788	3.3	0.426	0.96	23.68	28.10	34.89	0.52	12.82
8-17-B	Stoke Brook Aylesbury	Low, Small, Calcareous	1	19.60	8,682	2.0	0.452	0.96	22.13	37.79	36.89	0.19	3.00
8-17-C	Bear Brook, Hartwell Ditch, at west Aylesbury	Low, Small, Calcareous	3	1.31	2,668	3.8	0.295	0.96	40.55	16.17	41.98	0.29	1.00
8-18-A	Scotsgrove Brook (upstream Kingsey Cuttle Brook)	Low, Small, Calcareous	1	51.41	16,844	3.6	0.192	0.96	3.40	38.61	54.49	0.13	3.36

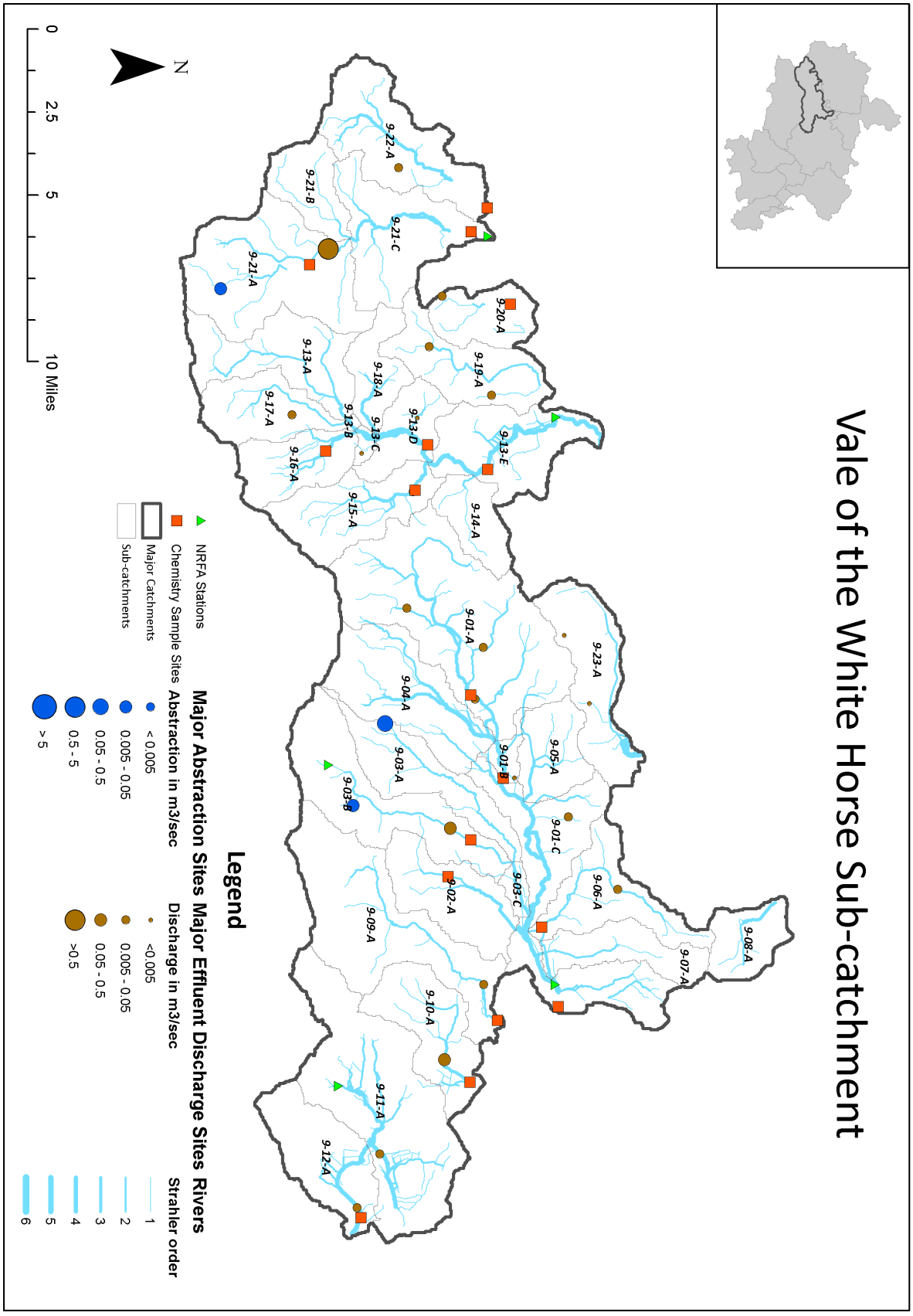
Sub-catchment	Name	River Typology	Strahler order	Area (km2)	Reach length (m)	Reach width (m)	*a* flow parameter	BFI	Urban	Intensive Agriculture	Non-intensive Agriculture	Wetlands	Forest
8-18-B	Kingsey Cuttle Brook and tributaries at Thame	Low, Small, Calcareous	1	54.12	24,074	3.1	0.262	0.53	6.58	43.50	43.34	0.21	6.36
8-18-C	Scotsgrove Brook (Kingsey Cuttle to Thame)	Low, Medium, Calcareous	4	2.91	3,383	5.4	0.193	0.53	0.32	37.12	60.45	0.13	1.97
8-19-A	Chinnor Brook and Upper Cuttle Brook	Low, Small, Calcareous	1	12.40	6,771	2.7	0.277	0.53	5.14	53.55	34.52	1.75	5.05
8-19-B	Upper Cuttle Brook and tributaries	Low, Small, Calcareous	3	17.72	2,856	2.8	0.313	0.53	1.57	52.90	38.02	0.29	7.22
8-19-C	Cuttle Brook (lower section) and tributaries at Thame	Low, Small, Calcareous	4	9.48	5,666	4.6	0.156	0.53	9.77	28.80	57.54	0.20	3.69


Thame and South Chilterns Sub-catchment
Legend
NRFA Stations
Chemistry Sample Sites
Major Catchments
Sub-catchments
Rivers
Strahler order
1
2
3
4
5
6
Major Abstraction Sites
Abstraction in m3/sec
< 0.005
0.005 - 0.05
0.05 - 0.5
0.5 - 5
> 5
Major Effluent Discharge Sites
Discharge in m3/sec
<0.005
0.005 - 0.05
0.05 - 0.5
>0.5
N
0
2.5
5
10 Miles
8-16-A
8-07-A
8-17-A
8-14-A
8-17-B
8-17-C
8-18-A
8-07-B
8-18-B
8-15-A
8-18-C
8-19-A
8-19-B
8-19-C
8-13-A
8-12-A
8-10-A
8-09-B
8-10-B
8-09-A
8-10-C
8-09-C
8-04-A
8-11-A
8-07-C
8-05-A
8-06-A
8-08-A
1-01-G
1-01-F
8-01-B
8-01-A
8-01-C
8-02-A
1-01-I
8-03-A
1-01-H

VALE OF THE WHITE HORSE

Sub-catchment	Name	River Typology	Strahler order	Area (km2)	Reach length (m)	Reach width (m)	*α* flow parameter	BFI	Urban	Intensive Agriculture	Non-intensive Agriculture	Wetlands	Forest
9-01-A	Ock (Source to Stutfield Brook) and tributaries	Low, Small, Calcareous	1	65.30	23,545	2.5	0.134	0.71	2.44	56.87	34.60	1.18	4.91
9-01-B	Gainfield Brook, Ock, Charney Wick Ditch at Charney Bassett	Low, Small, Calcareous	4	3.39	2,328	7.2	0.143	0.86	0.20	55.41	44.34	0.06	0.00
9-01-C	Ock and tributaries (Land Brook confluence to Thames)	Low, Medium, Calcareous	4	38.25	21,911	6.3	0.100	0.64	13.29	53.11	30.09	0.24	3.27
9-02-A	Cow Common Brook and Portobello Ditch	Low, Small, Calcareous	1	21.22	8,247	2.2	0.326	0.64	0.22	86.25	11.17	0.10	2.26
9-03-A	Childrey Brook and tributaries	Low, Small, Calcareous	2	20.08	15,461	2.4	0.379	0.80	4.24	60.69	33.74	0.16	1.16
9-03-B	Letcombe Brook	Low, Small, Calcareous	1	33.24	14,180	4.7	0.134	0.96	12.50	58.78	26.74	0.29	1.68
9-03-C	Childrey Brook and Norbrook at Common Barn	Low, Small, Calcareous	3	2.63	2,942	4.9	0.117	0.64	0.24	72.07	25.71	0.00	1.97
9-04-A	Stutfield Brook (source to Ock)	Low, Small, Calcareous	1	29.82	4,645	3.2	0.227	0.96	0.22	50.01	46.60	0.12	3.05
9-05-A	Cherbury Brook and associated tributaries	Low, Small, Calcareous	2	13.56	2,209	2.9	0.230	0.86	0.47	68.43	23.61	0.14	7.34
9-06-A	Frilford and Marcham Brook	Low, Small, Calcareous	2	20.99	13,857	2.7	0.295	0.64	3.70	34.92	46.64	0.49	14.25
9-07-A	Sandford Brook (source to Ock)	Low, Small, Calcareous	1	14.36	8,177	2.1	0.382	0.64	4.59	37.65	47.61	0.31	9.84
9-08-A	Filchhampstead Brook at Farmoor	Low, Small, Calcareous	1	11.63	4,106	2.7	0.273	0.66	10.46	43.10	23.98	6.01	16.46
9-09-A	Ginge Brook and Mill Brook	Low, Small, Calcareous	2	45.52	17,096	4.2	0.253	0.63	7.05	62.43	25.82	0.25	4.44
9-10-A	Moor Ditch and Ladygrove Ditch	Low, Small, Calcareous	1	21.69	7,505	2.0	0.742	0.63	27.51	49.98	18.01	1.85	2.65
9-11-A	Mill Brook and Bradfords Brook system, Wallingford	Low, Small, Calcareous	1	55.62	11,280	5.7	0.445	0.96	10.85	62.75	24.92	0.28	1.19
9-12-A	Cholsey Brook and tributaries	Low, Small, Calcareous	1	23.00	6,312	3.5	0.442	0.96	4.16	68.21	24.29	0.18	3.15
9-13-A	Cole and Dorcan Brook (Source to Liden Brook confluence)	Low, Small, Calcareous	2	24.39	6,048	3.3	0.302	0.57	41.56	25.99	27.42	1.43	3.59
9-13-B	Cole (Liden Brook to Lenta Brook)	Low, Small, Calcareous	1	0.40	865	4.6	0.163	0.52	0.00	27.50	64.53	6.41	1.56
9-13-C	Cole (Acorn Bridge to South Marston Brook)	Low, Small, Calcareous	4	1.52	1,135	5.6	0.159	0.52	1.57	70.18	26.52	0.12	1.61
9-13-D	Cole and tributaries at Sevenhampton	Low, Small, Calcareous	4	11.94	4,679	6.3	0.221	0.52	2.80	49.55	42.55	0.49	4.61
9-13-E	Cole (Bower Bridge to Thames) including Coleshill	Low, Medium, Calcareous	4	25.21	14,000	8.1	0.063	0.52	2.70	61.27	32.70	0.15	3.19
9-14-A	Waterloo Ditch (East of Coleshill)	Low, Small, Calcareous	1	11.18	5,258	2.2	0.367	0.71	0.92	59.50	35.58	0.00	4.01
9-15-A	Tuckmill Brook and tributaries	Low, Small, Calcareous	2	22.52	12,021	3.7	0.190	0.52	5.41	60.87	30.62	0.09	3.02
9-16-A	Lenta Brook, East of Swindon	Low, Small, Calcareous	1	15.38	6,757	3.0	0.182	0.52	2.20	62.67	34.03	0.00	1.10
9-17-A	Liden Brook, Swindon	Low, Small, Calcareous	2	16.71	8,062	2.4	0.299	0.95	11.16	48.95	37.99	1.21	0.69
9-18-A	South Marston Brook to Swindon	Low, Small, Calcareous	1	11.21	5,072	1.8	0.206	0.57	32.48	32.99	28.97	1.96	3.59
9-19-A	Bydemill Brook (Source to Thames)	Low, Small, Calcareous	1	21.59	16,843	2.5	0.185	0.52	6.00	50.14	39.57	0.29	3.99

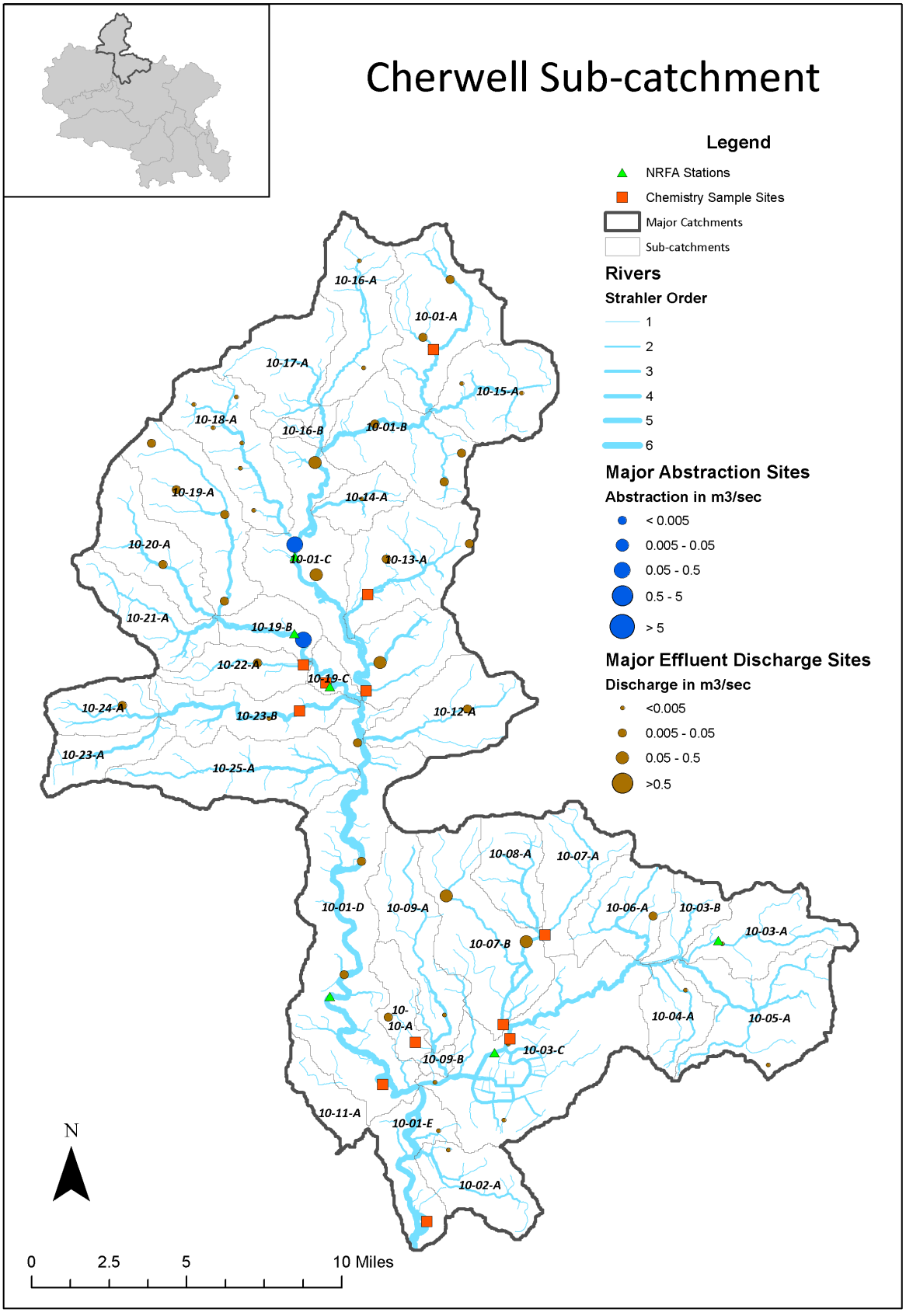
Sub-catchment	Name	River Typology	Strahler order	Area (km2)	Reach length (m)	Reach width (m)	*a* flow parameter	BFI	Urban	Intensive Agriculture	Non-intensive Agriculture	Wetlands	Forest
9-20-A	Share ditch	Low, Small, Calcareous	1	12.75	5,498	2.8	0.147	0.57	0.15	80.76	17.40	0.00	1.70
9-21-A	Ray (Wiltshire) source to Lydiard Brook	Low, Small, Calcareous	1	41.29	11,501	2.7	0.227	0.57	44.03	14.57	36.49	0.81	4.12
9-21-B	Lydiard and Shaw Brooks at Swindon	Low, Small, Calcareous	1	12.59	5,660	2.3	0.229	0.57	18.16	22.48	54.66	1.20	3.50
9-21-C	Ray (Wiltshire): Lydiard Brook to Thames	Low, Small, Calcareous	3	27.91	14,688	4.1	0.161	0.57	24.33	18.95	50.93	2.42	3.38
9-22-A	Key (Source to Thames)	Low, Small, Calcareous	1	29.98	10,448	3.7	0.198	0.68	3.29	12.30	76.99	0.68	6.73
9-23-A	Wadley Stream (Source to Thames at Duxford)	Low, Small, Calcareous	2	23.93	10,734	6.4	0.117	0.86	0.53	57.62	34.97	0.11	6.77


Vale of the White Horse Sub-catchment
N
0
2.5
5
10 Miles
9-22-A
9-21-B
9-21-C
9-21-A
9-20-A
9-19-A
9-13-A
9-18-A
9-17-A
9-13-B
9-13-C
9-13-D
9-13-E
9-16-A
9-15-A
9-14-A
9-01-A
9-23-A
9-04-A
9-03-A
9-01-B
9-05-A
9-03-B
9-01-C
9-06-A
9-03-C
9-02-A
9-09-A
9-08-A
9-07-A
9-10-A
9-11-A
9-12-A
Legend
NRFA Stations
Chemistry Sample Sites
Major Catchments
Sub-catchments
Major Abstraction Sites
Abstraction in m3/sec
< 0.005
0.005 - 0.05
0.05 - 0.5
0.5 - 5
> 5
Major Effluent Discharge Sites
Discharge in m3/sec
<0.005
0.005 - 0.05
0.05 - 0.5
>0.5
Rivers
Strahler order
1
2
3
4
5
6

CHERWELL

Sub-catchment	Name	River Typology	Strahler order	Area (km2)	Reach length (m)	Reach width (m)	*a* flow parameter	BFI	Urban	Intensive Agriculture	Non-intensive Agriculture	Wetlands	Forest
10-01-A	Cherwell (Source to Trafford Bridge)	Low, Small, Calcareous	1	35.52	20,881	2.6	0.249	0.40	2.94	56.84	37.08	0.29	2.85
10-01-B	Cherwell (Ashby Brook to Cropredy)	Low, Small, Calcareous	1	30.86	14,594	4.8	0.135	0.40	1.94	60.26	34.53	0.34	2.93
10-01-C	Cherwell (Cropredy to Nell Bridge)	Low, Medium, Calcareous	4	55.55	23,179	8.8	0.044	0.40	19.00	43.67	34.06	0.52	2.76
10-01-D	Cherwell Nell bridge to Ray confluence	Low, Medium, Calcareous	5	78.36	39,130	12.0	0.083	0.65	6.31	55.21	33.58	0.55	4.35
10-01-E	Cherwell (Ray to Thames) and Woodeaton Brook	Low, Medium, Calcareous	5	20.13	11,877	18.1	0.091	0.41	26.08	32.96	36.02	0.61	4.32
10-02-A	Bayswater Brook	Low, Small, Calcareous	1	19.76	2,586	3.3	0.460	0.41	17.01	52.68	21.27	0.27	8.76
10-03-A	Ray and tributaries NorthEast of Grendon Underwood	Low, Small, Calcareous	1	22.91	10,964	2.4	0.064	0.16	1.26	31.72	49.73	4.05	13.25
10-03-B	Gubbinshole and Broadmoor ditch to Ray (Oxon)	Low, Small, Calcareous	2	10.38	5,057	2.7	0.163	0.16	0.63	49.84	49.36	0.00	0.16
10-03-C	Oxon Ray (upstream A41 to Cherwell) including Otmoor	Low, Medium, Calcareous	1	65.89	22,039	7.8	0.254	0.41	4.09	33.17	55.51	0.89	6.34
10-04-A	Ludgershall Brook and Muswellhill Brook	Low, Small, Calcareous	1	14.59	4,984	3.8	0.214	0.16	0.80	16.35	81.01	0.05	1.79
10-05-A	Tetchwick Brook, Source to Ray and tribs	Low, Small, Calcareous	1	36.17	11,285	2.9	0.213	0.16	0.46	25.04	65.67	0.77	8.06
10-06-A	Summerstown Ditch and Launton and Cutters Brook	Low, Small, Calcareous	2	20.58	11,508	2.6	0.198	0.16	3.30	33.78	60.94	0.31	1.67
10-07-A	Langford Brook (source to downstream A41)	Low, Small, Calcareous	2	20.82	10,040	2.9	0.197	0.16	16.27	43.45	35.83	1.28	3.17
10-07-B	Langford Brook (Bicester to Ray inc Gagle Brook)	Low, Small, Calcareous	1	39.94	7,579	4.5	0.193	0.41	4.55	49.88	40.17	0.98	4.42
10-08-A	Town Brook at Bicester	Low, Small, Calcareous	1	16.66	3,412	1.9	0.411	0.65	21.50	55.32	18.75	0.51	3.92
10-09-A	Gallos Brook (Source to Bletchingdon Stream)	Low, Small, Calcareous	2	27.00	20,457	2.3	0.285	0.41	6.01	58.98	24.69	0.47	9.85
10-09-B	Gallos Brook (Bletchingdon Stream to Ray)	Low, Small, Calcareous	3	2.08	3,181	2.9	0.166	0.41	0.18	71.69	27.73	0.00	0.39
10-10-A	Bletchingdon Stream	Low, Small, Calcareous	1	10.32	2,985	1.3	0.270	0.41	1.61	56.05	33.19	0.76	8.40
10-11-A			1	10.79	-	0.0	0.414	0.65	11.57	49.77	31.22	0.69	6.74
10-12-A	Ockley Brook and Croughton Brook (Source to Cherwell)	Low, Small, Calcareous	1	26.89	13,998	2.9	0.311	0.74	2.55	64.77	26.73	0.54	5.41
10-13-A	Farthinghoe Stream (Source to Cherwell) and tributaries	Low, Small, Calcareous	1	31.94	11,843	3.9	0.258	0.74	3.37	59.41	34.42	0.36	2.44
10-14-A	Chacombe Brook (Source to Cherwell)	Low, Small, Calcareous	1	10.33	4,330	2.4	0.464	0.40	1.97	46.50	50.26	0.00	1.26
10-15-A	Ashby Brook (Source to Cherwell)	Low, Small, Calcareous	1	26.32	6,822	3.0	0.276	0.40	0.20	52.52	43.80	0.18	3.30
10-16-A	Highfurlong Brook (Source to Wormleighton Brook)	Low, Small, Calcareous	2	26.83	13,706	1.8	0.255	0.40	0.92	53.55	42.36	1.17	2.00
10-16-B	Highfurlong Brook (Wormleighton to Cherwell)	Low, Small, Calcareous	1	4.12	3,587	5.2	0.179	0.40	1.00	65.88	31.38	0.68	1.06
10-17-A	Clayton and Wormleighton Brook, Source to Highfurlong Brook	Low, Small, Calcareous	1	25.22	2,041	4.8	0.195	0.40	0.99	59.39	37.61	0.57	1.44

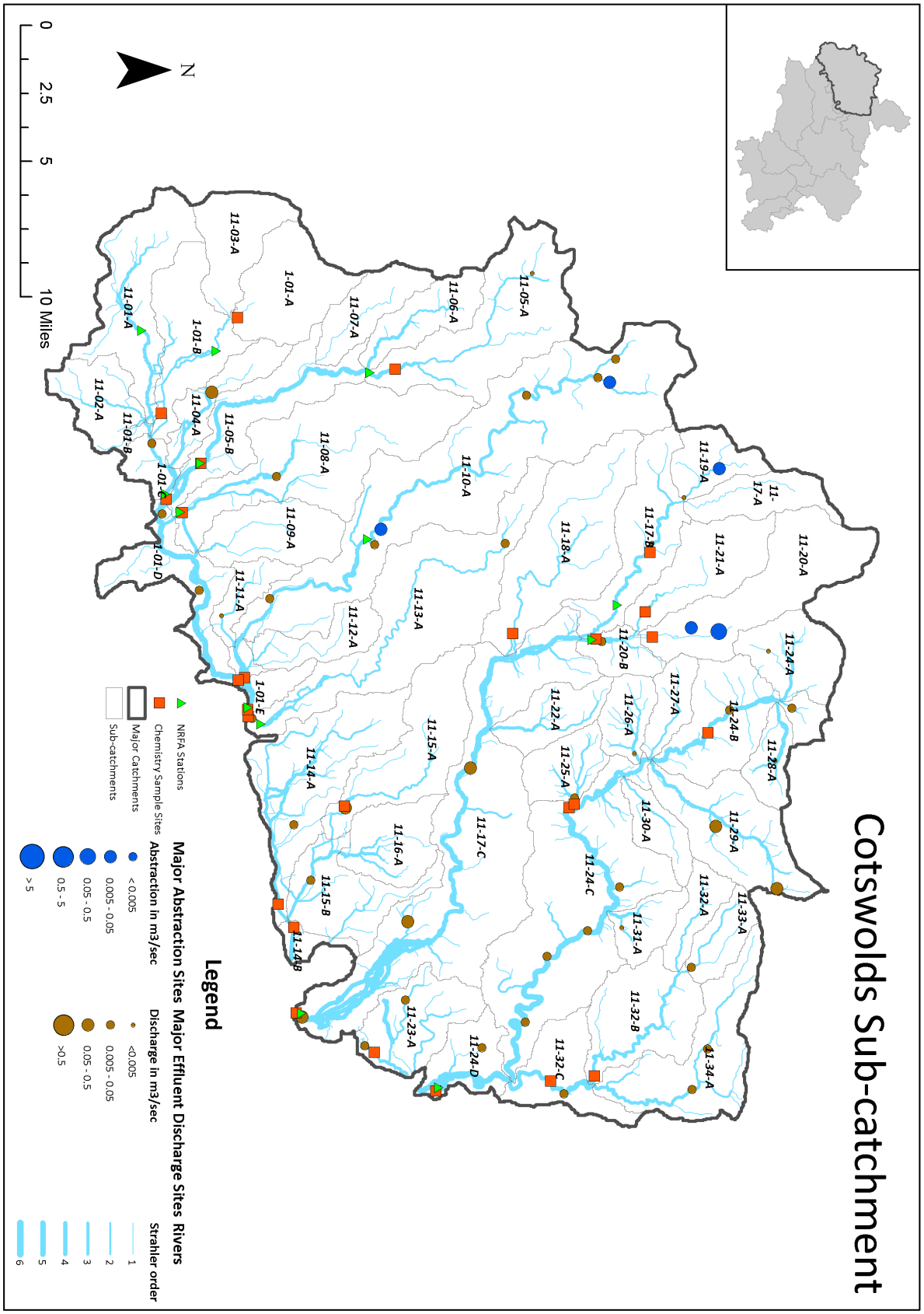
Sub-catchment	Name	River Typology	Strahler order	Area (km2)	Reach length (m)	Reach width (m)	*a* flow parameter	BFI	Urban	Intensive Agriculture	Non-intensive Agriculture	Wetlands	Forest
10-18-A	Hanwell Brook	Low, Small, Calcareous	1	29.04	16,685	2.7	0.303	0.40	2.79	64.36	29.50	0.40	2.94
10-19-A	Sor Brook (Source to Broughton)	Low, Small, Calcareous	1	33.60	18,115	2.9	0.329	0.40	1.23	67.14	28.39	0.15	3.09
10-19-B	Sor Brook (Broughton to Adderbury)	Low, Small, Calcareous	4	12.29	10,134	5.3	0.143	0.74	9.34	50.27	38.98	0.20	1.21
10-19-C	Sor Brook (Adderton to Cherwell)	Low, Medium, Calcareous	4	5.04	4,873	6.7	0.130	0.74	15.65	31.94	49.32	0.45	2.64
10-20-A	Shutford Stream (Source to Sor Brook)	Low, Small, Calcareous	1	24.70	6,400	2.9	0.292	0.40	0.34	52.91	44.03	0.19	2.54
10-21-A	Tadmarton Stream (Source to Sor Brook)	Low, Small, Calcareous	1	19.52	2,025	4.1	0.247	0.74	0.73	52.50	44.54	0.12	2.11
10-22-A	Bloxham Brook (Source to Sor Brook)	Low, Small, Calcareous	2	14.33	8,644	1.5	0.687	0.74	6.77	40.44	50.65	0.74	1.40
10-23-A	Upper Swere (Source to Wigginton)	Low, Small, Calcareous	1	13.55	8,774	5.0	0.262	0.74	0.28	64.71	29.72	0.24	5.04
10-23-B	Swere (Wigginton to Cherwell)	Low, Small, Calcareous	1	23.34	16,429	6.7	0.181	0.74	1.15	51.99	44.45	0.35	2.05
10-24-A	Hook Norton Brook (Source to Swere)	Low, Small, Calcareous	2	14.24	5,938	2.7	0.295	0.74	3.28	35.53	57.71	0.29	3.20
10-25-A	Deddington Brook (Source to Cherwell)	Low, Small, Calcareous	1	35.19	17,221	2.9	0.316	0.74	1.43	56.61	38.35	0.10	3.50


Cherwell Sub-catchment
Legend
NRFA Stations
Chemistry Sample Sites
Major Catchments
Sub-catchments
Rivers
Strahler Order
1
2
3
4
5
6
Major Abstraction Sites
Abstraction in m3/sec
< 0.005
0.005 - 0.05
0.05 - 0.5
0.5 - 5
> 5
Major Effluent Discharge Sites
Discharge in m3/sec
<0.005
0.005 - 0.05
0.05 - 0.5
>0.5
10-16-A
10-01-A
10-17-A
10-15-A
10-18-A
10-16-B
10-01-B
10-19-A
10-14-A
10-20-A
10-01-C
10-13-A
10-21-A
10-19-B
10-22-A
10-19-C
10-24-A
10-23-B
10-12-A
10-23-A
10-25-A
10-08-A
10-07-A
10-01-D
10-09-A
10-06-A
10-03-B
10-03-A
10-07-B
10-
10-A
10-04-A
10-05-A
10-03-C
10-09-B
10-11-A
10-01-E
10-02-A
N
0
2.5
5
10 Miles

COTSWOLDS

Sub-catchment	Name	River Typology	Strahler order	Area (km2)	Reach length (m)	Reach width (m)	*a* flow parameter	BFI	Urban	Intensive Agriculture	Non-intensive Agriculture	Wetlands	Forest
11-01-A	Swill Brook (source to Ashton Keynes)	Low, Small, Calcareous	1	43.39	14,820	5.6	0.120	0.36	1.08	47.16	45.90	2.33	3.53
11-01-B	Swill Brook and Thames (High Bridge to Waterhay Bridge)	Low, Small, Calcareous	3	1.09	1,026	7.8	0.087	0.83	0.00	13.99	83.83	2.18	0.00
11-02-A	Derry Brook and Leighfield Brook	Low, Small, Calcareous	1	20.90	8,573	3.4	0.166	0.36	1.50	20.29	73.06	0.08	5.06
11-03-A	Kemble Ditch at Kemble	Low, Small, Calcareous	1	24.69	1,300	2.0	0.271	0.64	1.13	78.21	16.39	0.08	4.19
11-04-A	Cerney Wick Brook (source to Thames)	Low, Small, Calcareous	1	16.90	6,244	3.5	0.134	0.83	6.10	48.75	23.19	18.54	3.42
11-05-A	Churn (source to Perrots Brook)	Mid, Small, Calcareous	1	58.91	16,628	3.8	0.180	0.88	0.54	35.33	43.94	0.54	19.64
11-05-B	Churn (Baunton to Cricklade)	Low, Medium, Calcareous	4	35.52	23,959	5.6	0.259	0.83	13.34	39.33	37.14	5.85	4.35
11-06-A	Elkstone Brook	Mid, Small, Calcareous	1	19.70	4,643	1.8	0.223	0.88	0.63	52.79	32.61	0.89	13.08
11-07-A	Daglingworth Stream (Source to Churn)	Low, Small, Calcareous	1	18.81	7,494	2.0	0.214	0.90	2.71	53.89	38.31	0.09	4.99
11-08-A	Ampney and Poulton Brooks (Source to Thames)	Low, Small, Calcareous	1	74.10	14,680	5.2	0.124	0.73	1.01	61.38	32.69	0.31	4.60
11-09-A	Marston Meysey Brook	Low, Small, Calcareous	1	26.49	7,847	3.7	0.139	0.93	2.33	75.08	20.37	0.07	2.16
11-10-A	Coln (Source to Thames)	Low, Medium, Calcareous	3	147.43	55,488	6.5	0.219	0.93	1.53	49.45	37.90	1.50	9.62
11-11-A	Dudgrove Brook	Low, Small, Calcareous	1	10.91	6,244	2.7	0.315	0.93	14.14	51.98	24.21	7.61	2.06
11-12-A	Thornhill Ditch and tributaries at Cotswolds Water Park	Low, Small, Calcareous	1	16.84	1,516	2.0	0.354	0.93	0.38	70.56	14.71	6.36	8.00
11-13-A	Leach (Source to Thames)	Low, Small, Calcareous	2	79.46	30,562	5.7	0.154	0.79	0.70	65.52	28.13	0.79	4.85
11-14-A	Broadwell Brook, Langford Brook, Kelmscott Brook, Radcot	Low, Small, Calcareous	1	53.89	21,001	4.5	0.284	0.79	1.25	64.30	31.70	0.18	2.57
11-14-B	Great brook (Shill Brook to Thames)	Low, Medium, Calcareous	1	5.38	2,691	10.9	0.089	0.86	0.00	78.53	19.55	1.15	0.77
11-15-A	Shill Brook and Kencot Brook at Carterton	Low, Small, Calcareous	2	41.57	16,552	4.0	0.254	0.82	4.05	61.24	31.26	0.07	3.39
11-15-B	Shill Brook, Highmoor Brook and Elm Bank Ditch	Low, Small, Calcareous	1	30.16	7,576	4.9	0.147	0.82	3.48	62.52	30.66	0.35	2.99
11-16-A	Highmoor Brook at Brize Norton	Low, Small, Calcareous	1	23.14	4,839	2.1	0.360	0.82	16.00	54.80	26.24	1.47	1.49
11-17-A	Windrush (Source to Slade Barn Stream)	Mid, Small, Calcareous	1	18.24	8,545	2.3	0.377	0.94	0.35	47.76	39.92	0.43	11.54
11-17-B	Windrush (Slade Barn Stream to Dikler)	Mid, Small, Calcareous	3	36.01	14,841	5.9	0.233	0.94	2.43	46.95	44.05	0.68	5.90
11-17-C	Windrush and tributaries (Little Rissington to Thames)	Low, Medium, Calcareous	4	128.19	69,080	8.6	0.195	0.82	5.95	53.76	30.99	3.34	5.97
11-18-A	Sherbourne Brook	Low, Small, Calcareous	1	60.04	6,953	9.2	0.153	0.94	0.46	56.86	34.80	0.32	7.56
11-19-A	Slade Barn Stream (Source to Windrush)	Mid, Small, Calcareous	1	15.70	6,031	2.7	0.317	0.94	0.25	43.05	39.97	0.35	16.37
11-20-A	Dikler (Source to Wyck Rissington)	Mid, Small, Calcareous	1	50.28	7,149	5.9	0.182	0.94	0.61	38.74	47.73	0.48	12.43
11-20-B	Dikler (Wyck Rissington to Windrush) and Lower Eye	Mid, Small, Calcareous	3	10.20	6,857	4.8	0.247	0.82	0.69	29.45	62.42	2.62	4.82

Sub-catchment	Name	River Typology	Strahler order	Area (km2)	Reach length (m)	Reach width (m)	*a* flow parameter	BFI	Urban	Intensive Agriculture	Non-intensive Agriculture	Wetlands	Forest
11-21-A	Eye (Source to Dikler)	Mid, Small, Calcareous	1	30.36	8,441	5.3	0.208	0.94	0.79	40.52	48.67	0.73	9.29
11-22-A	Taynton Stream (source to Windrush)	Low, Small, Calcareous	1	17.53	8,913	3.0	0.319	0.82	1.95	49.82	37.72	0.04	10.47
11-23-A	Chil and Limb Brooks (source to B4044)	Low, Small, Calcareous	1	28.95	11,698	3.4	0.245	0.66	3.85	55.68	29.96	0.60	9.91
11-24-A	Evenlode (Source to Four Shires S) and Longborough Stream	Low, Small, Calcareous	1	23.79	2,107	2.7	0.372	0.94	4.42	40.89	48.44	0.44	5.81
11-24-B	Evenlode (Compton Bk to Bledington Bk) & 4 Shires	Low, Small, Calcareous	1	38.95	16,287	4.6	0.274	0.94	1.62	42.58	48.77	0.33	6.69
11-24-C	Evenlode (Bledington to Glyme confluence)	Low, Medium, Calcareous	1	101.87	42,685	8.3	0.255	0.71	2.47	55.46	29.37	0.26	12.45
11-24-D	Evenlode (Glyme to Thames)	Low, Medium, Calcareous	5	17.67	10,561	11.0	0.065	0.71	5.82	48.16	33.63	0.40	11.99
11-25-A	Littlestock Stream to tributary of Evenlode at Shipton	Low, Small, Calcareous	1	16.41	4,293	2.5	0.302	0.82	2.62	70.79	22.20	0.00	4.40
11-26-A	Westcote Brook (source to Evenlode at Bledington)	Low, Small, Calcareous	1	13.26	6,120	3.3	0.308	0.82	0.60	53.48	38.12	0.15	7.65
11-27-A	Bledington Brook (Source to Evenlode)	Low, Small, Calcareous	1	11.63	6,832	3.0	0.273	0.82	3.41	40.66	53.12	0.11	2.70
11-28-A	Little Compton Brook and tributaries (Source to Evenlode)	Low, Small, Calcareous	1	11.55	6,908	1.6	0.428	0.94	0.31	47.41	49.50	0.87	1.92
11-29-A	Cornwell Brook and tributaries (Source to Evenlode)	Low, Small, Calcareous	1	40.20	21,249	2.7	0.328	0.82	4.19	62.06	29.43	0.30	4.02
11-30-A	Sars Brook (source to Evenlode downstream Bledington)	Low, Small, Calcareous	1	12.29	5,440	3.1	0.276	0.82	0.63	59.70	28.35	0.82	10.50
11-31-A	Coldron and Taston Brooks	Low, Small, Calcareous	1	12.43	2,753	2.9	0.318	0.82	0.16	76.80	18.85	0.10	4.09
11-32-A	Glyme (Source to Enstone)	Low, Small, Calcareous	2	11.96	5,025	2.0	0.388	0.65	1.17	60.10	35.11	0.17	3.46
11-32-B	Glyme (Enstone to Dorn)	Low, Small, Calcareous	3	36.03	16,310	6.9	0.122	0.65	1.04	58.04	25.38	0.86	14.68
11-32-C	Glyme (Dorn confluence to Evenlode)	Low, Medium, Calcareous	4	23.82	7,540	11.1	0.167	0.65	3.55	47.96	29.64	2.45	16.40
11-33-A	Heythorpe Stream and tributaries	Low, Small, Calcareous	2	13.30	5,316	2.0	0.361	0.74	0.71	53.64	30.61	0.49	14.54
11-34-A	Dorn (Source to Glyme)	Low, Small, Calcareous	1	45.10	17,802	4.3	0.242	0.65	1.17	66.31	26.84	0.34	5.34


Cotswolds Sub-catchment
N
0
2.5
5
10 Miles
Legend
NRFA Stations
Chemistry Sample Sites
Major Catchments
Sub-catchments
Major Abstraction Sites
Abstraction in m3/sec
< 0.005
0.005 - 0.05
0.05 - 0.5
0.5 - 5
> 5
Major Effluent Discharge Sites
Discharge in m3/sec
<0.005
0.005 - 0.05
0.05 - 0.5
>0.5
Rivers
Strahler order
1
2
3
4
5
6
11-03-A
1-01-A
11-01-A
1-01-B
11-07-A
11-06-A
11-05-A
11-02-A
11-01-B
11-04-A
11-05-B
11-08-A
11-10-A
11-19-A
11-17-A
11-20-A
1-01-C
11-09-A
11-18-A
11-17-B
11-21-A
1-01-D
11-11-A
11-12-A
11-13-A
11-20-B
11-24-A
1-01-E
11-22-A
11-26-A
11-27-A
11-24-B
11-28-A
11-14-A
11-15-A
11-25-A
11-30-A
11-29-A
11-16-A
11-17-C
11-24-C
11-32-A
11-33-A
11-15-B
11-31-A
11-14-B
11-32-B
11-23-A
11-24-D
11-32-C
11-34-A

APPENDIX III

Table of model correlation coefficients (R^2) for all sub-catchments with observed data (*n=136*).

Sub-catchment	Discharge (R^2)	SRP (R^2)	Nitrate (R^2)
1-01-A	-	0.56	0.36
1-01-B	0.58	0.57	0.44
1-01-C	0.59	0.26	0.55
1-01-D	-	0.68	0.73
1-01-E	-	0.66	0.34
1-01-F	0.72	0.34	0.40
1-01-G	0.73	0.51	0.61
1-01-H	0.78	0.38	0.34
1-01-I	0.81	0.36	0.63
1-01-J	0.80	0.69	0.74
1-01-K	0.80	0.64	0.55
2-02-A	0.37	-	-
2-05-C	-	0.35	0.34
2-07-C	0.42	-	-
2-07-D	-	0.28	0.52
3-01-B	0.56	-	-
3-01-C	0.45	-	-
3-01-D	0.42	-	-
3-01-E	0.55	-	-
3-03-B	0.39	-	-
4-01-A	-	0.37	0.62
4-01-B	-	0.69	0.45
4-01-C	0.56	-	-
4-01-D	0.82	0.51	0.69
4-01-E	0.63	0.43	0.33
4-01-F	0.25	0.52	0.71
4-01-G	0.62	0.46	0.39
4-02-C	-	0.34	0.47
4-02-D	-	0.49	0.61
4-04-A	-	0.64	0.40
4-04-B	-	0.48	0.58
4-04-C	0.44	-	-
4-06-C	-	0.42	0.45
4-10-A	0.53	0.28	0.45
4-11-A	0.31	0.33	0.54
4-16-C	-	0.57	0.37
4-17-A	0.50	0.59	0.71
5-01-D	0.65	-	-
5-01-E	0.74	-	-
5-03-A	0.78	-	-
5-04-A	0.75	-	-
5-04-C	0.76	-	-
5-05-A	0.79	-	-
5-06-A	0.78	-	-
5-07-A	0.25	-	-
6-01-A	-	0.67	0.37
6-01-B	-	0.51	0.57
6-01-C	0.62	0.30	0.32
6-01-D	0.36	0.62	0.74
6-05-A	0.49	0.57	0.64
6-05-C	-	0.59	0.52
6-06-A	0.57	0.34	0.34
6-06-B	0.63	0.69	0.59
6-07-B	-	0.56	0.35
6-07-C	0.56	0.40	0.61
6-08-A	-	0.28	0.35
6-09-B	-	0.69	0.71
6-09-C	-	0.35	0.42
7-01-A	0.76	0.68	0.33
7-01-B	0.83	0.59	0.60
7-01-C	-	0.28	0.68
7-01-D	0.79	0.48	0.41
7-02-A	0.52	-	-
7-03-A	0.87	0.39	0.44
7-04-B	-	0.69	0.43
7-07-A	0.85	0.62	0.65
7-09-A	0.83	-	-
7-10-A	0.83	-	-
7-11-A	0.79	-	-
7-12-C	0.80	0.35	0.35
7-15-E	0.48	0.47	0.49
8-01-A	0.83	-	-
8-01-C	0.83	0.66	0.67
8-04-A	0.87	-	-
8-07-A	-	0.41	0.33
8-07-B	-	0.44	0.61
8-07-C	0.68	0.26	0.64
8-10-B	-	0.62	0.54
8-11-A	-	0.45	0.32
8-14-A	-	0.63	0.33
8-17-A	0.66	0.31	0.65
8-17-C	-	0.43	0.60
8-18-A	-	0.31	0.46
8-18-B	-	0.58	0.45
8-18-C	-	0.60	0.35
9-01-A	-	0.38	0.52
9-01-B	-	0.50	0.37
9-01-C	0.61	0.38	0.34
9-03-B	0.79	0.38	0.46
9-06-A	-	0.68	0.49
9-09-A	-	0.59	0.59
9-10-A	-	0.37	0.75
9-11-A	0.86	-	-
9-12-A	-	0.30	0.64
9-13-E	0.53	0.54	0.73
9-15-A	-	0.55	0.37
9-16-A	-	0.39	0.53
9-20-A	-	0.57	0.61
9-21-A	-	0.67	0.64
9-21-C	0.42	0.62	0.44
9-22-A	-	0.28	0.64
10-01-A	-	0.58	0.46
10-01-C	0.49	0.32	0.68
10-01-D	0.69	0.52	0.41
10-01-E	-	0.39	0.55
10-03-A	0.30	-	-
10-03-C	0.46	0.45	0.43
10-07-A	-	0.66	0.47
10-07-B	-	0.58	0.40
10-10-A	-	0.27	0.55
10-13-A	-	0.55	0.40
10-19-B	0.69	-	-
10-19-C	-	0.51	0.36
10-22-A	-	0.37	0.46
10-23-B	-	0.52	0.33
11-01-A	0.42	-	-
11-05-A	0.75	0.70	0.51
11-05-B	0.74	0.41	0.75
11-08-A	0.53	0.64	0.73
11-10-A	0.65	0.49	0.36
11-13-A	0.73	0.63	0.60
11-14-A	-	0.64	0.32
11-14-B	-	0.63	0.32
11-15-A	-	0.49	0.63
11-17-B	0.81	0.47	0.66
11-17-C	0.78	0.69	0.71
11-18-A	-	0.51	0.61
11-20-B	0.73	0.55	0.42
11-21-A	-	0.66	0.34
11-23-A	-	0.55	0.61
11-24-B	-	0.46	0.61
11-24-C	-	0.47	0.68
11-24-D	0.70	0.63	0.62
11-25-A	-	0.49	0.72
11-32-B	-	0.43	0.42
11-32-C	-	0.28	0.68